Surviving as a Quantum Computer in a Classical World

Daniel Gottesman

March 31, 2026

Contents

Part I

Quantum Error Correcting Codes

Chapter 1

Know Your Enemy: Quantum Errors

In this book, you will learn how to seek out and destroy errors on quantum states. Quantum errors are nasty, unforgiving things. If you don't know what you are doing, a single misstep can result in the destruction of irreplaceable quantum information. Of course, nobody's perfect, and in part II, you will learn how to handle your own fallibility. (Short answer: very carefully.) For now, we will assume you don't make any mistakes, but that doesn't mean things will be easy. The quantum errors are still out there, hungering to consume quantum information. You need to get the errors before they get you.

The key to most error hunts is preparation. There are two forms of preparation. One is dressing your quantum information properly: that is, encoding it in an appropriate quantum error-correcting code. You will learn about that in the other chapters in part I. This chapter will focus on the other aspect of preparation: studying the habits of the errors you are hunting.

1.1 The Quantum Channel

The most common way of characterizing a source of errors in a quantum system is as a quantum channel. "Quantum channel" is a general term for an opportunity for the environment to introduce errors into your quantum system. Usually, we consider a situation as depicted in figure 1.1. Alice wants to send quantum information to Bob. Alice and Bob both have perfect quantum computers, but the connection between them is possibly imperfect: the quantum channel. (We will drop the assumption that Alice and Bob have perfect quantum computers in part II.) While the quantum information is in transit, the external world (the "environment") has a chance to interact with the system, thereby changing it in some way, introducing errors (or "noise") relative to the state that Alice sent.

A common example of a quantum channel is an optical fiber. Single photons can pass through the optical fiber, but they may be lost or altered en route. Other possibilities are sending a photon through the air, physically moving an atom with information encoded in the state of the electron or nuclear spin, successively swapping the states of neighboring qubits arranged on a line, or even using quantum teleportation to send

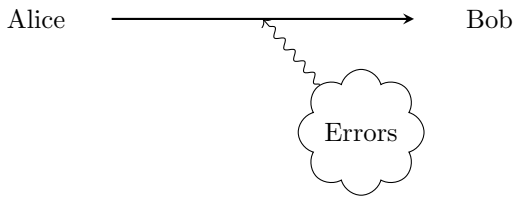

Figure 1.1: Alice, who has a perfect quantum computer, wants to send qubits to Bob, who also has a perfect quantum computer. However, the communications channel between them is *not* perfect.

a quantum state from Alice to Bob with classical communication and some sort of entangled state. This is not an exhaustive list. Indeed, any sort of communication, even a classical telephone call, can be considered as a quantum channel. If you try to send a qubit through a regular telephone connection, no amount of quantum error correction will allow you to recover the full quantum state afterwards, but that doesn't affect the telephone line's status as a quantum channel — it is simply a *very noisy* quantum channel.

Another common situation is when Bob is replaced by Alice's future self. In this case, we really want a "quantum memory": Alice wants to prepare some quantum information, go off and do other things, and then return and manipulate her stored quantum information again. If we assume that Alice's manipulations at the beginning and the end of the process are perfect, we can consider the "memory" portion, when the qubit is stored but subject to noise, as a quantum channel.

It is worth noting that the notion of a quantum channel only applies when we can look at a single communications link in isolation. That is, to have a quantum channel, the quantum state that exits the channel should only depend on the quantum state that goes into the channel. That may seem like a tautology, but it is not. Imagine that Alice has a quantum memory, and prepares a qubit to store in the memory at time 0. At time 1, she returns and fiddles some more with the stored system, then goes away again and comes back at time 2. The storage from time 0 to time 1 is a quantum channel (assuming Alice's initial preparation of the qubit is perfect), but the storage from time 1 to time 2 might not be. The problem is that the environment might remember what happened between time 0 and 1 (and more importantly, might remember something about the *state* that was stored between time 0 and 1) and use that to influence what it does to the state during the second time interval. The error now no longer depends only on what state is stored at time 1; it also depends on what state was stored at time 0. Of course, some environments have a very short memory, and in that case, it is a very good approximation to consider the time interval 1 to 2 to be independent of the time interval 0 to 1, and with that approximation, the second time interval *is* a quantum channel. When the environment has no memory, and every time interval is independent of any other non-overlapping time interval, the environment (or the error source) is called *Markovian*. When the environment does remember over time scales long enough to matter, it is a *non-Markovian* environment.

In part I, we only consider the case depicted in figure 1.1. There the environment has only one opportunity to attack the quantum information. While that opportunity may last for an extended period of time, because Alice and Bob do not do anything with the quantum information during that time, we can lump together everything the environment does to the state into a single transformation, and consider the whole communications line as a single quantum channel. The question of whether the environment is Markovian or non-Markovian then becomes moot. If we were to generalize this picture and allow noise during Alice and Bob's processing of the qubit, then the question arises again, since the environment then gets more than one shot at the quantum information, but don't worry about that situation until part II.

Now it is time to formally define a quantum channel:

Definition 1.1. A *quantum channel* is a completely positive trace-preserving (CPTP) map.

Wasn't that easy? At least, it is if you know what a CPTP map is. If not, you should refer to appendix A, where you will learn that a CPTP map is the most general physically possible transformation for an operation where the output depends only on the input, so this is the right definition. It is frequently convenient to consider the Kraus form of a CPTP map:

$$\mathcal{E}(\rho) = \sum_k A_k \rho A_k^\dagger. \tag{1.1}$$

We can think of this channel as a collection of possible errors A_k, where error A_k occurs with probability $\mathrm{tr}(A_k \rho A_k^\dagger)$. However, note that the probability of A_k occurring is not a single value but actually depends on the state ρ. Furthermore, remember that the decomposition into A_k operators is not unique and that $\sum_k A_k^\dagger A_k = I$.

Frequently, instead of dealing explicitly with a quantum channel, I will instead refer to the *set of possible errors*. One way to write this set is $\mathcal{E} = \{A_k\}$, but it is frequently convenient to rescale the errors, so more generally $\mathcal{E} = \{E_k\}$, where each $A_k = p_k E_k$ for some scalar p_k.

1.2 Single-Qubit Example Channels

1.2.1 Unitary Channels, Pauli Errors

Let us start by discussing some examples of channels acting on a single-qubit input. The simplest case is when there is only a single value of k in the Kraus decomposition:

$$\mathcal{E}(\rho) = A\rho A^\dagger. \tag{1.2}$$

Since $\sum_k A_k^\dagger A_k = I$, it follows that A is unitary. Typographically, I will usually represent a unitary channel the same way as a unitary matrix, e.g. $A(\rho)$ versus $A(|\psi\rangle)$, even though they formally act on different kinds of objects (density matrices versus state vectors). The one exception is that I will usually write the identity channel as $\mathcal{I}$, as opposed to the identity unitary I.

There are of course infinitely many unitary maps, but some are more interesting than others. One set that you will be particularly sick of by the end of this book are the Pauli matrices:

$$I = \begin{pmatrix} 1 & 0 \\ 0 & 1 \end{pmatrix}, \quad X = \begin{pmatrix} 0 & 1 \\ 1 & 0 \end{pmatrix}, \quad Y = \begin{pmatrix} 0 & -i \\ i & 0 \end{pmatrix}, \quad Z = \begin{pmatrix} 1 & 0 \\ 0 & -1 \end{pmatrix}. \tag{1.3}$$

I is, of course, the identity matrix — no error. X is probably the first thing you think of when you think of an error, a classical bit flip:

$$X|0\rangle = |1\rangle \tag{1.4}$$

$$X|1\rangle = |0\rangle. \tag{1.5}$$

However, since it is a quantum operator, it also acts sensibly on superpositions:

$$X(\alpha|0\rangle + \beta|1\rangle) = \alpha|1\rangle + \beta|0\rangle. \tag{1.6}$$

Z is the most basic kind of truly quantum error, a phase flip:

$$Z(\alpha|0\rangle + \beta|1\rangle) = \alpha|0\rangle - \beta|1\rangle. \tag{1.7}$$

Y is then just a combined bit flip and phase flip error:

$$Y = iXZ \tag{1.8}$$

$$Y(\alpha|0\rangle + \beta|1\rangle) = i\alpha|1\rangle - i\beta|0\rangle. \tag{1.9}$$

Recall that an *overall phase* — one that affects all states uniformly — has no physical significance, so Y and XZ are really the same channel. In the form presented above, all the Pauli matrices are Hermitian as well as unitary, which is sometimes useful.

In other contexts, the Pauli matrices are often written as σ_x, σ_y, and σ_z or σ_1, σ_2, and σ_3, but those are too much writing and less easy to read. I'll be using the Pauli matrices a *lot* in this book, so I'll use the more straightforward notation X, Y, and Z. In some of the earlier quantum error-correction literature, $Y = XZ$ instead of iXZ. There is not a huge difference, but I think this convention is somewhat nicer overall.

There are many more single qubit unitary errors, and some are even interesting. For instance, we can have phase rotation by an arbitrary angle:

$$R_\theta = \begin{pmatrix} e^{-i\theta} & 0 \\ 0 & e^{i\theta} \end{pmatrix} = e^{-i\theta} \begin{pmatrix} 1 & 0 \\ 0 & e^{2i\theta} \end{pmatrix}. \tag{1.10}$$

Again, we can ignore an overall phase, so R_θ is the same channel as $\mathrm{diag}(1, e^{2i\theta})$. The full set of physically distinct one-qubit unitary channels is the group $\mathsf{SU}(2)$.

In the Bloch sphere picture of the state space for a qubit, a unitary map is just a rotation of the sphere. X, Y, and Z are π rotations around the X, Y, and Z axes, as one might expect. R_θ is a rotation by angle 2θ around the Z axis. (I have defined R_θ this way in order to agree with the prevailing terminology for phase rotations, which results from talking about spin-1/2 particles.) Note that a reflection of the Bloch sphere is not a completely positive map. For instance, the transpose map is a reflection in the XZ plane, and when applied to part of an entangled state, the transpose gives something non-positive.

Figure 1.2: Bloch sphere transformation induced by a dephasing channel

1.2.2 Dephasing Channel

One very commonly-encountered channel is the dephasing channel.

Definition 1.2. A channel of the form

$$\mathcal{R}_p(\rho) = (1-p)\rho + pZ\rho Z^\dagger. \tag{1.11}$$

is a *dephasing channel*. When $p = 1/2$, we have the *completely dephasing channel*. We usually restrict attention to $p \leq 1/2$ since channels with $p > 1/2$ are related to channels with $p < 1/2$ by a Z operation.

The Kraus operators of a dephasing channel in this form are $\sqrt{1-p}I$ and $\sqrt{p}Z$. Since both are proportional to unitary maps, the probabilities of these two errors occurring do not depend on the input state. Thus, this channel corresponds to no error with probability $1-p$ and a phase flip with probability p. We can calculate how it acts on the density matrix in component form:

$$\mathcal{R}_p : \begin{pmatrix} a & b \\ c & d \end{pmatrix} \mapsto \begin{pmatrix} a & (1-2p)b \\ (1-2p)c & d \end{pmatrix}. \tag{1.12}$$

In other words, a dephasing channel shrinks the off-diagonal components of the density matrix. In the completely dephasing channel, the off-diagonal terms disappear completely.

An alternate Kraus decomposition is also edifying.

$$\mathcal{R}_p(\rho) = (1-2p)\rho + \frac{2p}{\pi}\int_0^\pi R_\theta \rho R_\theta^\dagger d\theta. \tag{1.13}$$

The dephasing channel is a channel for which, with probability $1-2p$, nothing happens to the state, and with probability $2p$, the phase between $|0\rangle$ and $|1\rangle$ is completely randomized. This seems to conflict with the decomposition into I and Z, where the state is left unchanged with probability $1-p$, not with probability $1-2p$. However, when the dephasing angle θ is chosen uniformly at random, there is a reasonable chance that θ is small and the state does not change very much. Of course, the probability that the angle θ is *exactly* zero is just $1-2p$, but using the magic of quantum mechanics, the small-θ cases cancel out just right so that if we break the channel up into I and Z, we find the probability of error is only p.

This example illustrates a rather disturbing principle: in quantum mechanics, the notion of "probability of error" is inherently somewhat subjective. When error correction is concerned, the decomposition into I and Z is the better choice for the dephasing channel, for reasons that will become clearer in chapter 2. However, there are many channels for which none of the decompositions is particularly favored, even for the specific application of quantum error correction.

In the Bloch sphere picture, a dephasing channel shrinks the sphere into an ellipsoid, leaving the Z axis unchanged, as in figure 1.2. A completely dephasing channel shrinks the Bloch sphere down to just the segment on the Z axis.

The dephasing channel is a physically very interesting channel. A dephasing channel occurs in any system where the environment learns about the qubit in the standard basis but does not otherwise interfere with the state. Even in a more realistic system where there are more complicated interactions between the system and the environment, there is frequently a large dephasing component to the noise. The prevalence of approximate dephasing channels is one of the reasons that the macroscopic world appears classical to us — a completely dephasing channel converts a qubit into a probabilistic classical bit.

We can make a simple model of a dephasing channel by having one environment qubit interact with the system qubit via a Hamiltonian $\mathcal{H} = \omega Z \otimes Z$. The environment qubit starts in the pure state $|+\rangle = (|0\rangle + |1\rangle)/\sqrt{2}$, and the system qubit starts in state $|\psi_0\rangle = \alpha|0\rangle + \beta|1\rangle$. Then, after a time t, the state of the two qubits is

$$e^{-i\omega t Z\otimes Z}|\psi_0\rangle \otimes |+\rangle = \frac{1}{\sqrt{2}}(\alpha e^{-i\omega t}|00\rangle + \alpha e^{+i\omega t}|01\rangle + \beta e^{+i\omega t}|10\rangle + \beta e^{-i\omega t}|11\rangle. \tag{1.14}$$

(Taking $\hbar = 1$.) Tracing over the second (environment) qubit, we find that the system qubit at time t is in an equal mixture of $R_{-\omega t}|\psi_0\rangle$ and $R_{+\omega t}|\psi_0\rangle$, giving it density matrix

$$\begin{pmatrix} |\alpha|^2 & \alpha\beta^* \cos(2\omega t) \\ \alpha^*\beta\cos(2\omega t) & |\beta|^2 \end{pmatrix}. \tag{1.15}$$

In other words, at time t, we have the dephasing channel $\mathcal{R}_{(1-\cos(2\omega t))/2}$. In this simple model, the system dephases at short times, but after a longer time $t = \pi/\omega$, it returns to its starting state.

In a more realistic system, there are many different environment qubits interacting with the system, and/or there are additional qubits interacting with the environment qubits. If we take a Markovian form of our simple model, and assume that the environment's internal interaction effectively resets the environment qubit after a very short time, phase coherence instead decays steadily:

$$\begin{pmatrix} |\alpha|^2 & \alpha\beta^* e^{-t/T_2} \\ \alpha^*\beta e^{-t/T_2} & |\beta|^2 \end{pmatrix}, \tag{1.16}$$

corresponding to a dephasing channel $\mathcal{R}_{(1-e^{-t/t_2})/2}$. The time constant T_2 of the exponential decay is known as the t_2 *time*. (Otherwise I probably would have used a different symbol.) One way to think about this behavior is that there is a constant probability $1/T_2$ per unit time that the phase is completely randomized as an instantaneous "quantum jump".

Another common source of dephasing is a varying energy difference between the $|0\rangle$ and $|1\rangle$ states. If $|a\rangle$ has energy E_a, after time t, $|a\rangle$ has evolved into $e^{-iE_a t}|a\rangle$. We can ignore the global phase, but there is still a relative phase difference $e^{-i(E_1-E_0)t}$ between $|0\rangle$ and $|1\rangle$. However, when E_0 and E_1 are known constants, we can generally ignore the relative phase too: if we keep track of the time t, the relative phase is known, and we can take it into account in any operation we want to perform. In some systems, there is a phase reference (such as the phase of a laser) which automatically compensates for the phase difference. However, when the energy difference varies unpredictably, we can no longer keep precise track of the relative phase, resulting in an uncompensated relative phase shift accumulating randomly over time. This results in dephasing. In some cases, the relative phase shift is not random, but is simply unknown, and more sophisticated techniques may be able to compensate.

Experimentally, the signature of dephasing is often a decay of coherent interference effects. In a Rabi oscillation experiment, the system cycles $\cos(\Omega_R t)|0\rangle + \sin(\Omega_R t)|1\rangle$. After time t, the system is measured to test if it is $|0\rangle$ or $|1\rangle$. If the system were perfect, if we were to plot the probability of 1 against the time, we would get a perfect oscillation $\sin^2(\Omega_R t)$ for all times. Instead, we get something more like figure 1.3, with oscillations decreasing in amplitude.

Let us imagine a Markovian environment, and assume that the T_2 time is much longer than the Rabi frequency Ω_R, so that we can assume the dephasing and oscillation are independent. If there is a quantum jump causing full dephasing at time t_0, the pure state $\cos(\Omega_R t_0)|0\rangle + \sin(\Omega_R t_0)|1\rangle$ becomes the mixed state with probability $\cos^2(\Omega_R t_0)$ of $|0\rangle$ and probability $\sin^2(\Omega_R t_0)$ of $|1\rangle$. Then $|0\rangle$ and $|1\rangle$ continue with their

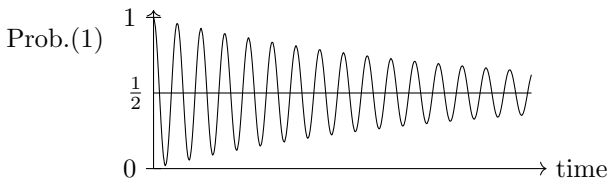

Figure 1.3: Decay of Rabi oscillations due to dephasing

own oscillations, but out of phase with each other. This mixture has density matrix

$$\begin{pmatrix} \cos^2(\Omega_R t_0)\cos^2(\Omega_R t') + \sin^2(\Omega_R t_0)\sin^2(\Omega_R t') & (\cos^2(\Omega_R t_0) - \sin^2(\Omega_R t_0))\sin(\Omega_R t')\cos(\Omega_R t') \\ (\cos^2(\Omega_R t_0) - \sin^2(\Omega_R t_0))\sin(\Omega_R t')\cos(\Omega_R t') & \cos^2(\Omega_R t_0)\sin^2(\Omega_R t') + \sin^2(\Omega_R t_0)\cos^2(\Omega_R t') \end{pmatrix} \tag{1.17}$$

$$= \begin{pmatrix} \sin^2(\Omega_R t_0) + \cos(2\Omega_R t_0)\cos^2(\Omega_R t') & \cos(2\Omega_R t_0)\sin(\Omega_R t')\cos(\Omega_R t') \\ \cos(2\Omega_R t_0)\sin(\Omega_R t')\cos(\Omega_R t') & \sin^2(\Omega_R t_0) + \cos(2\Omega_R t_0)\sin^2(\Omega_R t') \end{pmatrix} \tag{1.18}$$

$$= \sin^2(\Omega_R t_0) I + \cos(2\Omega_R t_0)\rho(t'), \tag{1.19}$$

where $t' = t - t_0$ and $\rho(t')$ is the density matrix of a Rabi oscillation running for time t'. We will still see Rabi oscillation, but with a reduced amplitude.

1.2.3 Depolarizing Channel and Pauli Channel

While the dephasing channel is perhaps the favorite (or least favorite, depending on your point of view) of experimentalists, it lacks a certain quantumness. It only involves one kind of non-trivial error, and indeed, in an appropriate choice of basis, it can be viewed as a purely classical noisy channel. Theorists are instead enamored of the depolarizing channel, which does experience the full range of quantum errors and is highly symmetric. It is not so common in the real world, which is less symmetric than theorists would prefer, but it is still extremely useful for exploring quantum error correction.

Definition 1.3. The *depolarizing channel* is the quantum channel

$$\mathcal{D}_p(\rho) = (1-p)\rho + \frac{p}{3}X\rho X^\dagger + \frac{p}{3}Y\rho Y^\dagger + \frac{p}{3}Z\rho Z^\dagger. \tag{1.20}$$

$\mathcal{D}_{3/4}$ is the *completely depolarizing channel*.

The depolarizing channel has an equal chance of an X, Y, or Z error, each with probability $p/3$. We can analyze what it does to the density matrix:

$$\mathcal{D}_p : \begin{pmatrix} a & b \\ c & d \end{pmatrix} \mapsto \begin{pmatrix} (1-2p/3)a + (2p/3)d & (1-4p/3)b \\ (1-4p/3)c & (1-2p/3)d + (2p/3)a \end{pmatrix}. \tag{1.21}$$

This is not particularly enlightening until you remember that $\operatorname{tr}\rho = 1$, in which case you can see that

$$\mathcal{D}_p(\rho) = (1-4p/3)\rho + (4p/3)(I/2). \tag{1.22}$$

In other words, with probability $1 - 4p/3$, the qubit is left alone, but with probability $4p/3$, it is replaced with the completely mixed state. It also should now be clear why I defined $p = 3/4$ as the completely depolarizing channel: in that case, the input state is always replaced with the maximally mixed state. As with the dephasing channel, there is some ambiguity as to what the "true" error rate is for the depolarizing channel, but the two representations can be reconciled by recognizing that the completely mixed state does contain a component of the original input state.

The other thing to notice about the second representation is that it is much more symmetric than the first one. The decomposition into Paulis has a certain amount of symmetry, treating X, Y, and Z on the

Figure 1.4: Bloch sphere transformation induced by a depolarizing channel

same footing, but the second decomposition has even more: there are no preferred bases or unitary operators at all appearing in it. This is the true beauty of the depolarizing channel — it can at once be considered as a simple mixture of the very basic Pauli errors, but also is invariant under any kind of unitary rotation. This symmetry property suggests a decomposition for the depolarizing channel akin to equation (1.13), and indeed there is one:

$$\mathcal{D}_p(\rho) = (1 - 4p/3)\rho + \frac{2p}{3\pi^2} \int_{\mathsf{SU}(2)} U\rho U^\dagger dU, \tag{1.23}$$

where the integral uses the Haar measure, the unitarily-invariant measure over $\mathsf{SU}(2)$.

We can generalize the depolarizing channel by giving up its symmetry but keeping its decomposition into Paulis:

Definition 1.4. A channel of the form

$$\mathcal{E}(\rho) = p_I\rho + p_X X\rho X^\dagger + p_Y Y\rho Y^\dagger + p_Z Z\rho Z^\dagger \tag{1.24}$$

is a *Pauli channel*.

A Pauli channel has potentially different probabilities for the four Pauli matrices I, X, Y, and Z. They don't *have* to be different — dephasing channels and depolarizing channels are both examples of Pauli channels — but once you've generalized to a Pauli channel, you might as well take advantage of the opportunity to have some variety among the Paulis. Naturally, $p_I + p_X + p_Y + p_Z = 1$ so that the total probability adds up to 1.

The depolarizing channel uniformly shrinks the Bloch sphere into a smaller sphere still centered on the origin, or to a single point (the maximally mixed state) if we have the completely depolarizing channel. A more general Pauli map shrinks the Bloch sphere into an ellipsoid centered on the origin.

1.2.4 Amplitude Damping Channel

Another physically motivated channel is the amplitude damping channel. It occurs, for instance, if $|0\rangle$ and $|1\rangle$ are the ground and excited state of a two-level atom, and the excited state can decay to the ground state by spontaneously emitting a photon. The amplitude damping channel also occurs for a photonic qubit where $|0\rangle$ is no photon and $|1\rangle$ is 1 photon — damping occurs when the photon escapes or is absorbed somewhere along the way. There should be 2 Kraus operators for the amplitude damping channel, one representing the cases when there is no emission (or loss), and one representing the "no-jump" case. It is worthwhile trying to figure out yourself what the form of the Kraus operators should be before looking at the definition below.

Definition 1.5. An *amplitude damping channel* has the following form:

$$\mathcal{A}_p(\rho) = A_0\rho A_0^\dagger + A_1\rho A_1^\dagger, \tag{1.25}$$

where

$$A_0 = \begin{pmatrix} 1 & 0 \\ 0 & \sqrt{1-p} \end{pmatrix}, \quad A_1 = \begin{pmatrix} 0 & \sqrt{p} \\ 0 & 0 \end{pmatrix}. \tag{1.26}$$

Figure 1.5: Bloch sphere transformation induced by an amplitude damping channel

Probably you were able to get the right form for A_1 (perhaps without the square root, which is a matter of convention depending on how we choose to parametrize amplitude damping channels). It represents the possibility that $|1\rangle$ can become $|0\rangle$. However, $|0\rangle$ never spontaneously gains energy in this idealized channel; even in the real world, it is fairly rare, since it requires that a stray photon of about the right energy be wandering by. Therefore the lower left corner of A_1 is 0.

A_0 might surprise you. (If not, then good work.) The most obvious guess is that since there is no decay, nothing should happen, and A_0 should be proportional to the identity. However, you won't be able to satisfy the constraint that $A_0^\dagger A_0 + A_1^\dagger A_1 = I$ if you choose A_1 as above and $A_0 \propto I$. Conceptually, the reason for this is that A_1 can only occur if the initial state was $|1\rangle$. Therefore, if A_1 *doesn't* happen, it means that the initial state was *more likely* to be $|0\rangle$, and A_0 reflects that, reducing the amplitude of $|1\rangle$ in the initial state. The same phenomenon can be found in classical probability theory, for instance in the "Monty Hall problem."

In the Bloch sphere picture, amplitude damping results in a uniform shrinkage to a smaller sphere. It differs from the depolarizing channel in that the center of the sphere is no longer fixed. Instead, the south pole (the $|0\rangle$ state) is fixed. In the limit $p = 1$, the whole sphere shrinks down to the south pole.

The characteristic decay time for a system undergoing continuous amplitude damping is the "T_1 time." (After all, there had to be a T_1 to go with T_2 for the dephasing time scale.)

1.2.5 Photon Loss Channels

Amplitude damping can occur due to photon loss from a photon channel when the presence or absence of a photon represents $|0\rangle$ or $|1\rangle$. However, this is not a particularly common encoding used for photonic qubits. More often, the qubit is stored in some other state of a single photon (such as the polarization), or by being in one of two modes (a "dual-rail encoding"), or some more complicated structure possibly involving multiple photons. When we use one of these encodings, loss of a photon is no longer represented by an amplitude damping channel.

Consider, for instance, a polarization encoding, with horizontal polarization being $|0\rangle$ and vertical polarization being $|1\rangle$. Now, photon loss can affect either $|0\rangle$ or $|1\rangle$, and what results if the photon does escape is neither of those states, instead being a third state $|\text{vacuum}\rangle$. Therefore, a photon loss channel for polarization encoding takes a qubit input but its output is a 3-dimensional *qutrit*. Assuming both polarizations have equal probability p to lose a photon, the channel is then very simple. There are three Kraus operators, corresponding to no photon loss, loss of a horizontally polarized photon, and loss of a vertically polarized photon:

$$A_0 = \sqrt{1-p}\begin{pmatrix} 1 & 0 \\ 0 & 1 \\ 0 & 0 \end{pmatrix}, A_1 = \sqrt{p}\begin{pmatrix} 0 & 0 \\ 0 & 0 \\ 1 & 0 \end{pmatrix}, \text{ and } A_2 = \sqrt{p}\begin{pmatrix} 0 & 0 \\ 0 & 0 \\ 0 & 1 \end{pmatrix}. \tag{1.27}$$

The same channel works for photon loss from a dual-rail encoding.

When the encoding involves multiple photons, there is still a sensible description as a quantum channel, but the analysis requires a bit more quantum optics, and is beyond the scope of this book.

1.2.6 Erasure Errors

The example of the photon loss qubit channel suggests another interesting kind of error. When a photon is not lost, the state is not changed at all. When a photon *is* lost, by monitoring the photon number (but not the polarization), we can, in principle, tell that a photon has been lost. In that case, we do not know what the original state of the system was, but at least we know that something has happened to it. Measuring the photon number without destroying the polarization state is technologically difficult, so for this particular example, this is more an issue of principle than of practice. There are, however, other systems where monitoring for loss of the qubit is easier.

Definition 1.6. A *qubit erasure error* is an error A acting on a single qubit which maps all qubit states to a third state $|\perp\rangle$ orthogonal to the qubit Hilbert space.

Erasure channels may seem to be difficult channels to correct, since the information is completely lost, but that's not the case. By measuring if the state is $|\perp\rangle$ is present (without collapsing superpositions of $|0\rangle$ and $|1\rangle$) — for instance, by measuring the number of photons — we can determine if an erasure error has occurred. Because erasure channels provide some classical information about which qubits underwent errors, erasure channels are actually easier to correct than more general channels.

1.3 Multiple-Qubit Channels

It's hard to do too much with only one qubit. Even if we have only one qubit of data, we'll need more than one qubit to create a real quantum error-correcting code. Therefore, we should also think some about channels acting on multiple qubits.

1.3.1 Pauli Channels

One route to defining multiple-qubit channels is to largely forgot about the tensor product structure and just pick some completely positive map acting on the Hilbert space as a whole. Such channels can be extremely complicated, since they act on a Hilbert space of dimension 2^n when there are n qubits. Sometimes this is necessary, as it reflects the actual physics of the system, but quantum computers are usually built out of systems that naturally break up into qubits, and many-qubit interactions are rare.

Mathematically, it is usually too difficult to deal with an arbitrary n-qubit channel, but the n-qubit generalization of the Pauli channel is sufficiently well-behaved to be sometimes useful.

Definition 1.7. A channel of the form

$$\mathcal{E}(\rho) = \sum_P p_P P \rho P^\dagger, \tag{1.28}$$

where the sum is taken over P which are tensor products of I, X, Y, and Z, is a *Pauli channel*.

In a Pauli channel, the operator P occurs with probability p_P. Pauli channels are a reasonable quantum analogue of classical channels. There is a definite probability of error, and the errors that occur are large and discrete. However, since we can have a mix of bit flip and phase errors, a Pauli channel does have enough quantum features to be interesting.

1.3.2 Independent/Memoryless Channels

The simplest way to create a channel on n qubits is to just treat each qubit separately.

Definition 1.8. An *independent* channel on n qudits (each of dimension q) has the form $\otimes_{i=1}^n \mathcal{E}_i$, where each $\mathcal{E}_i$ is a single-qudit channel.

A dimension-q qudit is a single system whose state space is a Hilbert space of dimension q, so for instance, $q = 2$ gives us a qubit, and for the moment, we will restrict attention to qubits. Often, we set all $\mathcal{E}_i$'s to be equal to $\mathcal{E}$, so that all qubits are treated equally.

As a simple example, we can consider $\mathcal{E} = \mathcal{R}_p$, the dephasing channel. Let us stick to $n = 3$ in order to be more explicit. There are a total of 8 possible Kraus operators for this channel, with the following probabilities:

Probability	Errors
$(1-p)^3$	$I \otimes I \otimes I$
$p(1-p)^2$	$Z \otimes I \otimes I$, $I \otimes Z \otimes I$, $I \otimes I \otimes Z$
$p^2(1-p)$	$Z \otimes Z \otimes I$, $Z \otimes I \otimes Z$, $I \otimes Z \otimes Z$
p^3	$Z \otimes Z \otimes Z$

The total probability of having a Z error on exactly one qubit is then $3p(1-p)^2$, and the probability of having two Z errors is $3p^2(1-p)$.

The chance of having at least one qubit with an error on it is therefore larger than the chance of having a single qubit by itself go wrong under the same dephasing channel $\mathcal{R}_p$. This makes sense, since there are more places for errors to occur. However, when p is small, most of the time, there will only be 0 or 1 Z error, and the other qubits will have I acting on them. This is the case we want to address through quantum error correction — errors are rare, but not negligibly so. In the case of this 3-qubit dephasing channel, we can make a good approximation by considering only the no-error or one-error possibilities, and ignoring the two- and three-qubit error cases.

1.3.3 Definition of t-Qubit Errors

More generally, we can define a t-qubit error to be one that acts on t qubits. However, there are two technical points in exactly how we want to define it:

Definition 1.9. We say that a linear operator A acting on n qubits has *weight* t if it is the tensor product of the identity on $n-t$ qubits with some matrix on the remaining t qubits. The weight of A is denoted wt A. We say that a weight t operator A has *support* on the t qubits on which it acts non-trivially. Generally (but not always), we cite the weight and support for the minimal set of qubits for which A acts non-trivially. A linear operator B acting on n qubits is a *t-qubit error* if it has the form

$$B = \sum_i B_i, \tag{1.29}$$

where each B_i has weight at most t, not necessarily with support on the same set of qubits for different i. An n-qubit quantum channel is a *t-qubit error channel* if it has a Kraus decomposition for which all Kraus operators are t-qubit errors. We can similarly define a *t-qubit error map* acting linearly on n-qubit density matrices but which may not be trace preserving.

Technical point number one is that even though a weight-t operator A acts non-trivially on only t qubits, it can act *arbitrarily* on those t qubits. In particular, it does not need to be a tensor product of errors on the separate qubits — it can entangle them however it likes. For instance, CNOT $\otimes I$ is a weight 2 operator acting on 3 qubits.

Technical point number two is that a t-qubit error B can be the sum of terms acting on different sets of t qubits. This naturally means that more than t qubits will be altered under the action of this error, but it turns out that they are altered in a way that is no more harmful than if we had a channel that had a possibility of altering each set of t qubits as separate Kraus operators. This point will be discussed in greater length in section 2.4.3, once we have a real quantum error-correcting code to examine.

We can also define t-qubit erasure errors. For instance, imagine we have many qubits each stored as the polarization of a photon, and each one undergoes a slight amount of photon loss.

Definition 1.10. A *t-qubit erasure error* is a weight t operator which is the tensor product of erasure errors on the qubits in its support. A *t-qubit erasure channel* is a quantum channel with a Kraus representation

where all Kraus operators are s-qubit erasure errors, with $s \leq t$. s can be different for different Kraus operators.

Note that here I am requiring that each Kraus operator has a specific set of qubits which can be erased, not a superposition of different sets of qubits. This reflects the idea that an erasure is in some sense a classical event, because the set of qubits that were erased can be measured.

1.3.4 Connection Between Independent Channel and t-Qubit Errors

An independent channel seems much more physically plausible (albeit still an approximation) than a t-qubit channel. However, it turns out to be more mathematically straightforward to design quantum error-correcting codes for t-qubit channels (or to correct a set of t-qubit errors) than for independent channels. Luckily, as suggested by the example of the 3-qubit dephasing channel, an n-qubit independent channel can be well approximated by a t-qubit channel (for some $t < n$) when the single-qubit channels making up the n-qubit channel are all close to the identity.

Theorem 1.1. *Let $\mathcal{I}$ be the 1-qubit identity channel and $\mathcal{E} = \otimes_{i=1}^{n} \mathcal{E}_i$ be an n-qubit independent channel, with $\|\mathcal{E}_i - \mathcal{I}\|_\diamond < \epsilon \leq \frac{t+1}{n-t-1}$, and $\epsilon \leq 1/3$ as well. Then*

$$\|\mathcal{E} - \tilde{\mathcal{E}}\|_\diamond < 5\binom{n}{t+1}[(4e+2)\epsilon]^{t+1} \tag{1.30}$$

for some t-qubit error map $\tilde{\mathcal{E}}$.

The significance of the theorem is that if we have a quantum error-correcting code which is designed to correct t-qubit error channels, it will automatically also correct independent channels where the single-qubit tensor factors are sufficiently close to the identity. Actually, that's not completely true: While the theorem does show that, this is not really the significance of the theorem, since there is much easier proof (which we will see in chapter 2) that a quantum error-correcting code that corrects t-qubit errors also corrects small independent error channels. Rather, this theorem provides a motivation for thinking about t-qubit error channels, which might otherwise seem rather bizarre.

When $\|\mathcal{E}_i - \mathcal{I}\|_\diamond < \epsilon$, we are getting about an ϵ chance of error per qubit, so with n qubits, we expect around ϵn errors. Therefore, we would not expect to be able to approximate $\mathcal{E}$ well by a t-qubit error map unless $t \gtrsim \epsilon n$, which is reflected in the bound on ϵ. The other detailed constants in the theorem shouldn't be taken too seriously, as the proof could likely be tightened considerably to get better constants. But if you do insist on taking those constants seriously, you might find, for example, that when $n = 5$ and $t = 1$, you would get $\|\mathcal{E} - \tilde{\mathcal{E}}\|_\diamond \lesssim 8286\epsilon^2$, which only gives a non-trivial bound when ϵ is less than about 0.01.

Two elements of equation (1.30) that *are* significant are the combinatorial factor $\binom{n}{t+1}$, which reflects the number of $(t+1)$-qubit subsets of the n qubits, and the exponent $t+1$ for ϵ, which tells us that the closeness of the approximation improves exponentially as we allow more qubits to have errors. In the limit of large n and any constant ratio t/n, the combination of the combinatorial factor and the exponent means that there will be a threshold value of ϵ below which we get a good approximation for all large n (and indeed, a better one as n gets larger).

Proof. We begin with a lemma on sums of error probabilities or amplitudes that will also be helpful later.

Lemma 1.2. *If $0 < t < n$, then*

a) For any $0 \leq \epsilon \leq 1$, $\sum_{j=t+1}^{n} \binom{n}{j} \epsilon^j (1-\epsilon)^{n-j} \leq \binom{n}{t+1} \epsilon^{t+1}$

b) When $0 \leq \epsilon \leq \frac{t+1}{n-t-1}$, then $\sum_{j=t+1}^{n} \binom{n}{j} \epsilon^j \leq \binom{n}{t+1} (e\epsilon)^{t+1}$

Proof of lemma. There are a number of ways to prove part a. One straightforward method is to interpret ϵ as a probability of some event (which is the main application we will have for this lemma). Then the sum is the probability that the event occurs at least $t+1$ times in n independent trials. We can upper bound

this probability by considering each subset of $t+1$ trials. The total probability of having the event occur in all trials in the subset, without regard to what happens on the other $n-t-1$ trials, is ϵ^{t+1}. There are $\binom{n}{t+1}$ subsets of size $t+1$, so by the union bound, the total probability of having some set of $t+1$ trials with the event is at most $\binom{n}{t+1}\epsilon^{t+1}$. Whenever the event occurs $j > t+1$ times, we have over-counted, since we included that probability as part of all $\binom{j}{t+1}$ sets of size $t+1$ which had the event.

For part b, note that

$$(1-\epsilon)^{n-t-1} \geq \left(1 - \frac{t+1}{n-t-1}\right)^{n-t-1} \geq e^{-(t+1)}. \tag{1.31}$$

Then

$$\sum_{j=t+1}^{n} \binom{n}{j}\epsilon^j = \sum_{j=t+1}^{n} \binom{n}{j}\epsilon^j(1-\epsilon)^{n-j}\frac{1}{(1-\epsilon)^{n-j}} \tag{1.32}$$

$$\leq \sum_{j=t+1}^{n} \binom{n}{j}\epsilon^j(1-\epsilon)^{n-j}\frac{1}{(1-\epsilon)^{n-t-1}} \tag{1.33}$$

$$\leq \binom{n}{t+1}\epsilon^{t+1}e^{t+1} \tag{1.34}$$

by part a and equation (1.31). □

As a warm-up to prove the theorem, let us consider the case when for all i, $\mathcal{E}_i$ has a Kraus operator $(1-\epsilon)I$. In this case, we can say that $\mathcal{E}_i$ has probability ϵ of having an error (one of the other Kraus operators), and a probability of $1-\epsilon$ of having no error. Part a of lemma 1.2 applies, so the probability of having at least $t+1$ errors is at most $\binom{n}{t+1}\epsilon^{t+1}$. In this case, the t-qubit error map $\mathcal{F}$ has all combinations of up to t "error" Kraus operators with the "good" Kraus operator $(1-\epsilon)I$ on the other qubits. The map $\mathcal{F}$ is completely positive, but is not trace preserving, since we have discarded the Kraus operators with more than t errors.

For the general case, first we need a better characterization of single-qubit channels $\mathcal{G}$ which are close to the identity.

Lemma 1.3. *If $\mathcal{E}$ is a quantum channel from $\mathcal{H}_D$ to $\mathcal{H}_D$ satisfying $\|\mathcal{E}-\mathcal{I}_1\|_\diamond < \epsilon \leq 1/3$, then $\mathcal{E}$ has a Kraus representation $\mathcal{E}(\rho) = \sum_k A_k\rho A_k^\dagger$ such that $\|A_0 - I\|_\infty < \sqrt{2D}\,(\epsilon+\epsilon^2) + (\epsilon/2+\epsilon^2)$ and $\sum_{k\neq 0}\|A_k\|_\infty^2 < D\epsilon(1/2+\epsilon)$.*

Proof of lemma. Using the Choi-Jamiolkowski isomorphism, the channel $\mathcal{E}$ corresponds to the entangled state $\Phi_\mathcal{E} = (I\otimes\mathcal{E})(|\Phi^+\rangle\langle\Phi^+|)$, with $|\Phi^+\rangle = \frac{1}{\sqrt{D}}\sum_a |aa\rangle$. (Note that I have normalized the state to make it easier to apply common identities, which is not always the convention used with the Choi-Jamiolkowski isomorphism.) Since $\|\mathcal{E}-\mathcal{I}_1\|_\diamond < \epsilon$,

$$\|\Phi_\mathcal{E} - |\Phi^+\rangle\langle\Phi^+|\|_1 < \epsilon \tag{1.35}$$

as well. Since the trace distance between these two states is small, the fidelity between them is high:

$$\langle\Phi^+|\Phi_\mathcal{E}|\Phi^+\rangle > 1-\epsilon/2. \tag{1.36}$$

Now, $|\Phi^+\rangle\langle\Phi^+|$ has one eigenvalue $+1$ and the remaining eigenvalues 0. Let us also write $\Phi_\mathcal{E}$ in terms of an eigenbasis,

$$\Phi_\mathcal{E} = \sum_{i=0}^{D^2-1}\lambda_i|\phi_i\rangle\langle\phi_i|. \tag{1.37}$$

$\Phi_\mathcal{E}$ is positive and has trace 1, so $\lambda_i \geq 0$ and $\sum_i \lambda_i = 1$. Now consider

$$|\langle\phi_i|\Phi^+\rangle\langle\Phi^+|\phi_j\rangle| = |\langle\phi_i|\left(\Phi_\mathcal{E} - |\Phi^+\rangle\langle\Phi^+|\right)|\phi_j\rangle| < \epsilon \tag{1.38}$$

for $i \neq j$. In addition,

$$\langle \Phi^+ | \Phi_{\mathcal{E}} | \Phi^+ \rangle = \sum_{i=0}^{D^2-1} \lambda_i |\langle \Phi^+ | \phi_i \rangle|^2 > 1 - \epsilon/2. \tag{1.39}$$

We can choose the phase of the eigenstates $|\phi_i\rangle$ to ensure that $\langle \Phi^+ | \phi_i \rangle$ is real and non-negative. Letting $a_i = \langle \Phi^+ | \phi_i \rangle$, we have $a_i \geq 0$, $\sum \lambda_i a_i^2 > 1 - \epsilon/2$, and $a_i a_j < \epsilon$ for $i \neq j$. Assume without loss of generality that a_0 is the largest of the a_is. Then $\sum \lambda_i a_i^2 \leq \sum \lambda_i a_0^2 = a_0^2$, so

$$a_0 > \sqrt{1 - \epsilon/2} \geq 1 - \epsilon/2. \tag{1.40}$$

Thus

$$a_i < \epsilon / a_0 < \frac{\epsilon}{1 - \epsilon/2} \tag{1.41}$$

for $i \neq 0$. Then

$$\sum_{i=0}^{D^2-1} \lambda_i a_i^2 \leq \lambda_0 + \sum_{i=1}^{D^2-1} \lambda_i \frac{\epsilon}{1 - \epsilon/2} \tag{1.42}$$

$$= \lambda_0 + (1 - \lambda_0) \frac{\epsilon}{1 - \epsilon/2} \tag{1.43}$$

$$= \frac{\epsilon + (1 - 3\epsilon/2)\lambda_0}{1 - \epsilon/2}, \tag{1.44}$$

since $\sum \lambda_i = 1$. Therefore,

$$\lambda_0 \geq \frac{(1 - \epsilon/2)^2 - \epsilon}{1 - 3\epsilon/2} \geq 1 - \epsilon/2 - \epsilon^2. \tag{1.45}$$

(assuming $\epsilon \leq 1/3$), which means

$$\sum_{i \neq 0} \lambda_i = 1 - \lambda_0 \leq \epsilon/2 + \epsilon^2 \tag{1.46}$$

for $i \neq 0$.

We have now bounded all the terms we need, but we'd like a tighter bound on a_0. We can do that by going back and plugging in the bound on $\sum \lambda_i$.

$$\| |\phi_0\rangle \langle \phi_0| - |\Phi^+\rangle \langle \Phi^+| \|_1 \leq (1 - \lambda_0) + \| \lambda_0 |\phi_0\rangle \langle \phi_0| - |\Phi^+\rangle \langle \Phi^+| \|_1 \tag{1.47}$$

$$\leq (1 - \lambda_0) + \| \sum_{i \neq 0} \lambda_i |\phi_i\rangle \langle \phi_i| \|_1 + \| \Phi_{\mathcal{E}} - |\Phi^+\rangle \langle \Phi^+| \|_1 \tag{1.48}$$

$$\leq 2\epsilon + 2\epsilon^2. \tag{1.49}$$

But the 1-norm distance between two pure states is just given by

$$\| |\phi_0\rangle \langle \phi_0| - |\Phi^+\rangle \langle \Phi^+| \|_1 = 2\sqrt{1 - |\langle \phi_0 | \Phi^+ \rangle|^2}, \tag{1.50}$$

meaning

$$\sqrt{1 - |\langle \phi_0 | \Phi^+ \rangle|} \leq \frac{\epsilon + \epsilon^2}{\sqrt{1 + |\langle \phi_0 | \Phi^+ \rangle|}} \leq \epsilon + \epsilon^2. \tag{1.51}$$

Thus, in the Choi-Jamiolkowski isomorphism form of the channel, the state has one large eigenvalue, for which the eigenstate is close to the maximally-entangled state, and the other eigenvalues are all small, with the eigenstates far from the maximally entangled state $|\Phi^+\rangle$. (Of course, they could be close to *other* maximally entangled states.) We can recover a set of Kraus operators for the channel by letting

$$A_k |a\rangle = \sqrt{D \lambda_k} \left(\langle a| \otimes I \right) |\phi_k\rangle \tag{1.52}$$

for basis states $|a\rangle$, extended linearly to the full Hilbert space $\mathcal{H}_D$. (Recall that $|\phi_i\rangle$ is a state in $\mathcal{H}_D \otimes \mathcal{H}_D$, so the right-hand side of equation (1.52) is in $\mathcal{H}_D$.) Then $\|A_k\|_1^2 \leq D\lambda_k$, so $\sum_{k\neq 0} \|A_k\|_\infty^2 \leq D\epsilon(1/2+\epsilon)$, as desired.

To get the bound on A_0, note that $A_0|\psi\rangle = \sqrt{D\lambda_0}\langle\psi^*|\phi_0\rangle$, where $|\psi^*\rangle$ is the complex conjugate of $|\psi\rangle$ in the basis $\{|a\rangle\}$. Furthermore, $|\psi\rangle = \sqrt{D}\langle\psi^*|\Phi^+\rangle$. Then

$$\|A_0 - \lambda_0 I\|_\infty = \max_{|\psi\rangle} |A_0|\psi\rangle - \lambda_0|\psi\rangle| \tag{1.53}$$

$$= \max_{|\psi\rangle} \sqrt{D\lambda_0}|\langle\psi^*|\phi_0\rangle - \langle\psi^*|\Phi^+\rangle| \tag{1.54}$$

$$= \sqrt{D\lambda_0}||\phi_0\rangle - |\Phi^+\rangle| \tag{1.55}$$

$$= \sqrt{D\lambda_0}\sqrt{2 - 2\,\mathrm{Re}\langle\Phi_+|\phi_0\rangle} \tag{1.56}$$

$$\leq \sqrt{2D}\,(\epsilon + \epsilon^2), \tag{1.57}$$

applying equation (1.51) in the last line, and recalling we have chosen $\langle\Phi_+|\phi_0\rangle$ to be real. Thus,

$$\|A_0 - I\|_\infty \leq \sqrt{2D}\,(\epsilon + \epsilon^2) + (\epsilon/2 + \epsilon^2) \tag{1.58}$$

□

For the case of qubits and applying $\epsilon \leq 1/3$, the lemma gives $\|A_0 - I\|_\infty \leq 7\epsilon/2$ and $\sum_{k\neq 0} \|A_k\|_1^2 \leq 5\epsilon/3$ for $k \neq 0$. We will round to $\|A_0 - I\|_1 < 4\epsilon$ and $\sum_{k\neq 0} \|A_k\|_1^2 \leq 2\epsilon$ for $k \neq 0$.

Given lemma 1.3, we can use a similar approach for the general case as we did for the warm-up, which was essentially classical. Channel $\mathcal{E}_i$ has Kraus operators A_k^i, with A_0^i close to the identity and A_k^i small for $k \neq 0$. The n-qubit independent channel $\mathcal{E}$ has Kraus operators which are all possible tensor products $\bigotimes_i A_{k_i}^i$. Let $\mathcal{F}$ be the map whose Kraus operators are all tensor products $\bigotimes_i A_{k_i}^i$ with at most t values of i for which $k_i \neq 0$. Then

$$\|\mathcal{F} - \mathcal{E}\|_\diamond \leq \sum_{r=t+1}^{n} \sum_{|S|=r} \prod_{i\in S} \sum_{k_i\neq 0} \|A_{k_i}^i\|_\infty^2. \tag{1.59}$$

The sum over r represents the number of values of i for which $k_i \neq 0$, and S is the set of indices for which $k_i \neq 0$. Since $\sum_{k_i\neq 0} \|A_{k_i}\|_\infty^2 \leq 2\epsilon$, we get

$$\|\mathcal{F} - \mathcal{E}\|_\diamond \leq \sum_{r=t+1}^{n} \binom{n}{r}(2\epsilon)^r \leq \binom{n}{t+1}(2e\epsilon)^{t+1} \tag{1.60}$$

by lemma 1.2.

Now $\mathcal{F}$ is not yet a t-qubit error map because the A_0 terms include some errors. However, the A_0 terms are all near I, so we can expand them as $A_0^i = I + \delta A^i$, with $\|\delta A^i\|_\infty < 4\epsilon$. Given a Kraus operator for $\mathcal{F}$ $A_{\{k_i\}} = \bigotimes_i A_{k_i}^i$ with r indices $k_i \neq 0$, expand all A_0^is in this way and form $A'_{\{k_i\}}$ by discarding all terms in the expansion with more than $t - r$ δA^i factors. The resulting Kraus operators are composed of sums of terms with weight at most t, of which r non-identity factors come from $k_i \neq 0$ terms, and the remaining come from δA^i components of $k_i = 0$ factors.

$$\|A'_{\{k_i\}} - A_{\{k_i\}}\|_\infty \leq \left(\prod_{j|k_j\neq 0} \|A_{k_j}\|_\infty\right) \sum_{s=t+1-r}^{n-r} \sum_{|S|=s} \prod_{i\in S} \|\delta A^i\|_\infty \tag{1.61}$$

$$\leq \left(\prod_{j|k_j\neq 0} \|A_{k_j}\|_\infty\right) \sum_{s=t+1-r}^{n-r} \binom{n-r}{s}(4\epsilon)^s \tag{1.62}$$

$$\leq \binom{n-r}{t+1-r}(4e\epsilon)^{t+1-r} \left(\prod_{j|k_j\neq 0} \|A_{k_j}\|_\infty\right). \tag{1.63}$$

Let ρ be an arbitrary pure state, possibly entangled between $\mathcal{H}_D$ and a reference system. Then

$$\|A'_{\{k_i\}}\rho(A'_{\{k_i\}})^\dagger - A_{\{k_i\}}\rho A^\dagger_{\{k_i\}}\|_1 \leq \|(A'_{\{k_i\}} - A_{\{k_i\}})\rho(A'_{\{k_i\}})^\dagger\|_1 + \|A_{\{k_i\}}\rho((A'_{\{k_i\}})^\dagger - A^\dagger_{\{k_i\}})\|_1 \tag{1.64}$$

$$\leq 2\left(\prod_{j|k_j\neq 0}\|A_{k_j}\|_\infty\right)\|A'_{\{k_i\}} - A_{\{k_i\}}\|_\infty \tag{1.65}$$

$$\leq 2\binom{n-r}{t+1-r}(4e\epsilon)^{t+1-r}\left(\prod_{j|k_j\neq 0}\|A_{k_j}\|^2_\infty\right). \tag{1.66}$$

I have omitted the $\otimes I$ terms affecting the reference system in the first line; the equation is complicated enough as is. In the second line, we have used the property that $\|A|\psi\rangle\| \leq \|A\|_\infty$ and bounded $\|A_{\{k_i\}}\|_\infty$ and $\|A'_{\{k_i\}}\|_\infty$ by the norm of just the terms with $k_j \neq 0$. If we sum over all $\{k_i\}$ with the same locations for which $k_j \neq 0$, we get

$$\sum \|A'_{\{k_i\}}\rho(A'_{\{k_i\}})^\dagger - A_{\{k_i\}}\rho A^\dagger_{\{k_i\}}\|_\infty \leq 2\binom{n-r}{t+1-r}(4e\epsilon)^{t+1-r}(2\epsilon)^r. \tag{1.67}$$

Finally, let $\mathcal{G}$ be the linear map with Kraus operators $A'_{\{k_i\}}$. In $\mathcal{G}$, we have eliminated all Kraus operators with more than t errors. Then we get a bound on $\|\mathcal{G} - \mathcal{F}\|_\diamond$ by applying them to ρ, and considering the 1-norm of the resulting state, which involves summing equation (1.66) over all possible values of $\{k_i\}$ with at most t indices $k_j \neq 0$ (those with more have already been excluded from $\mathcal{F}$). We get

$$\|\mathcal{G} - \mathcal{F}\|_\diamond \leq 2\sum_{r=0}^{t}\binom{n}{r}\binom{n-r}{t+1-r}(4e\epsilon)^{t+1-r}(2\epsilon)^r \tag{1.68}$$

$$= 2\sum_{r=0}^{t}\binom{n}{t+1}\binom{t+1}{r}(4e\epsilon)^{t+1-r}(2\epsilon)^r \tag{1.69}$$

$$\leq 2\binom{n}{t+1}[(4e+2)\epsilon]^{t+1}. \tag{1.70}$$

Combining this with equation (1.60), we get

$$\|\mathcal{G} - \mathcal{E}\|_\diamond \leq 3\binom{n}{t+1}[(4e+2)\epsilon]^{t+1}. \tag{1.71}$$

There is one final step needed. It is possible that $\mathcal{G}$ is no longer completely positive, since it could be that $\|A'_{\{k_i\}}\rho(A'_{\{k_i\}})^\dagger\|_1 > \|A_{\{k_i\}}\rho(A_{\{k_i\}})^\dagger\|_1$, which could result in $\operatorname{tr}\mathcal{G}(\rho) > 1$. We should therefore scale $\mathcal{G}$ down to $C\mathcal{G}$, for appropriately chosen constant C, to get a map that is guaranteed to be completely positive. $\mathcal{F}$ is trace non-increasing, though, so

$$\operatorname{tr}\mathcal{G}(\rho) \leq 1 + \|\mathcal{G} - \mathcal{F}\|_\diamond \leq 1 + 2\binom{n}{t+1}[(4e+2)\epsilon]^{t+1} = 1/C. \tag{1.72}$$

Then

$$\|C\mathcal{G} - \mathcal{E}\|_\diamond \leq 3\binom{n}{t+1}[(4e+2)\epsilon]^{t+1} + 1 - C \tag{1.73}$$

$$\leq 5\binom{n}{t+1}[(4e+2)\epsilon]^{t+1}. \tag{1.74}$$

□

1.4 A Peek Ahead: Errors During Computation

In part II, we'll consider more general types of errors. In particular, quantum gates will be able to go wrong in various ways, and errors will occur multiple times during a computation. As noted above, the quantum channel picture is no longer completely general then, since the noise might be non-Markovian. Mostly we'll stick to Markovian noise, but even then matters are much more complicated. Since our control is no longer reliable, we'll have to deal with errors occurring even while we're trying to fix them. However, there are various subtler difficulties to contend with as well.

For one thing, we don't know when an error occurs, so we can't assume we do error correction immediately after each error. In particular, an error might occur right before a gate that we had intended for some other purpose. Then even if the gate itself works perfectly, it can cause the error to propagate, infecting an additional qubit with the same error. In addition, the effect of the gate can change the type of error. For instance, a Z error that occurs before a Hadamard gate will change into a X error after the gate. This phenomenon makes it much more difficult to take advantage of information we know about the errors. For instance, suppose the noise source is largely dephasing noise. We might want to use a code that is particularly good at correcting dephasing noise, but if we use Hadamard gates in our circuit, some of the Z errors that occur will have become X errors by the time we get around to correcting them, and our code won't work anywhere near as well as expected. A particularly insidious form of this phenomenon occurs when errors happen *during* the implementation of a gate, which, after all, should take a non-zero time. Even if the completed gate does not change the type of error, depending on how the gate is being implemented, the partial gate may in fact alter the structure of the noise.

We'll return to all these issues in part II, and discuss how to design fault-tolerant quantum circuits that allow reliable error correction and computation on encoded states despite the complications.

Chapter 2

Redundancy Without Repetition: Basics Of Quantum Error Correction

Now we are ready to start designing quantum error-correcting codes. A natural place to start for inspiration is to look at the theory of classical error-correcting codes, and indeed it can give us some guidance. However, we'll rapidly see that there are some major differences between classical and quantum error correction.

The simplest classical error-correcting code is the repetition code:

$$0 \mapsto 000 \tag{2.1}$$

$$1 \mapsto 111. \tag{2.2}$$

If we send this 3-bit encoding through a 1-bit error classical channel, it is clear that we will be able to correct for any error that occurs on a single bit. If all three bits are the same, we know there hasn't been an error, while if one of the three is different, for instance 010, we know that the one that's different is the one that's wrong. By enforcing a boring conformity among the bits, we can recover the original state. Recall that if we use an independent channel instead of a 1-bit error channel, then there is some chance of 2 or 3 errors, which would fool us. If there are two errors, the one bit that we think is wrong is actually the only bit that's correct, and our well-meaning attempt to fix it will actually complete the error, making all three bits wrong. Luckily, the chance of two errors occurring is only $O(p^2)$ when the probability of an error on a single bit is p (see section 1.3.2). When p is small, the chance of the encoded state ending up wrong is less than the chance that an unencoded bit can make it unchanged through the channel.

Throughout this chapter, we'll assume we have a t-qubit error channel. This is justified by theorem 1.1, which tells us that if we actually have an independent channel, it is very close to a t-qubit channel, at least when the error rate per qubit is low. We will actually reprove a version of theorem 1.1 with an easier proof and better constants specifically applicable to quantum error-correctiong codes.

To make a quantum error-correcting code, we might want to imitate the classical repetition code, but that instantly runs into a few problems. We'll need to find a somewhat different way to protect our quantum information, one that adds redundancy without repeating the state.

2.1 Quantum Error Correction? Ridiculous!

Why am I so dead-set against a quantum repetition code? Perhaps we could encode

$$|\psi\rangle \mapsto |\psi\rangle|\psi\rangle|\psi\rangle. \tag{2.3}$$

If you've had much quantum information experience, you'll immediately see the problem with this encoding: it is forbidden by the No-Cloning Theorem.

1. No-cloning theorem prohibits repeating a quantum state.
2. Measuring the data while determining the error will destroy superpositions.
3. We must correct Y and Z errors in addition to X errors.
4. We must correct an infinite set of unitaries and also channels which decohere the state.

Table 2.1: Barriers to making a quantum error-correcting code.

Theorem 2.1 (No-Cloning Theorem)**.** *There is no quantum operation which maps an arbitrary state $|\psi\rangle$ to $|\psi\rangle|\psi\rangle$.*

Proof. The problem is linearity. Suppose

$$|0\rangle \mapsto |00\rangle \tag{2.4}$$
$$|1\rangle \mapsto |11\rangle. \tag{2.5}$$

Then, because quantum operations must be linear,

$$|\psi\rangle = \alpha|0\rangle + \beta|1\rangle \mapsto \alpha|00\rangle + \beta|11\rangle. \tag{2.6}$$

However, this is not equal to the cloned $|\psi\rangle$ state:

$$|\psi\rangle|\psi\rangle = \alpha^2|00\rangle + \beta^2|11\rangle + \alpha\beta(|01\rangle + |10\rangle). \tag{2.7}$$

□

Another problem has to do with how we correct errors for the repetition code. Given a 3-bit state coming out of the channel, we'd like to look at it and determine which of the three bits is different from the other two. However, when dealing with quantum states, looks really can kill. Or if not kill, at least decohere, destroying any superposition we have. And without the ability to be in a superposition, a qubit is no better than a classical bit. Somehow, to make a quantum error-correcting code, we'll need some way to correct errors without looking too closely at what we're doing.

Even if we can handle these problems, it's clear that quantum error correction will be more complicated than classical error correction. For a classical channel, basically all that can happen is a bit flip error, but quantum codes are going to need to handle phase flip errors as well, not to mention Y errors. While the 3-qubit repetition code is good at correcting bit flip errors, it doesn't do anything to help correct phase flips. Actually, it makes phase flip errors more common since there are now three qubits which could have phase flip errors instead of only one.

In addition to X, Y, and Z, we will also have to handle an infinite set of unitaries, such as the R_θ errors. Then there are more general channels, such as the dephasing channel or depolarizing channel, which turn pure states into mixed states. How can we come up with a correction operation that will turn the state from a mixed state back into a pure state?

At this point, the prospects for a quantum error-correcting code look bleak. The difficulties we've identified so far are listed in table 2.1. But don't worry — there are solutions to all of these problems. If there weren't, this book would be a lot thinner.

2.2 The 3-Qubit Code(s)

We won't try to handle all of these problems at once. Let's focus first on points 1 and 2. We'll try to make a quantum version of the three-bit repetition code. The quantum code will encode a qubit, but only protect against one kind of error, just like the classical three-bit code.

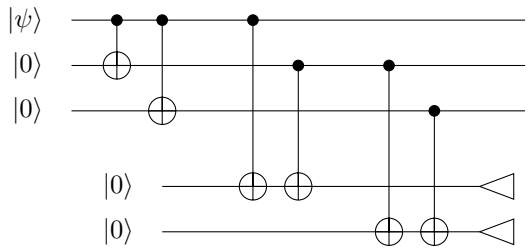

Figure 2.1: Encoding and syndrome measurement circuit for the 3-qubit bit flip correction code.

2.2.1 Correcting Bit Flips for Superposition States

Suppose we apply the classical repetition encoding to the basis states and extend to arbitrary superpositions by linearity:

$$\alpha|0\rangle + \beta|1\rangle \mapsto \alpha|000\rangle + \beta|111\rangle. \tag{2.8}$$

The first thing to notice is that this is an allowed encoding, and doesn't violate the no-cloning theorem. There is no rule against copying basis states — they act just like classical bits. The no-cloning theorem only kicks in if you try to copy superpositions as well. Rather than encoding a superposition $|\psi\rangle$ as three copies of $|\psi\rangle$ (which is impossible), we encode superpositions as *entangled* states. That takes care of difficulty 1.

Let's look at what happens to this state when there's been a bit flip error on the second qubit:

$$X_2(\alpha|000\rangle + \beta|111\rangle) = \alpha|010\rangle + \beta|101\rangle. \tag{2.9}$$

(In this book, I shall use the notation X_2 to indicate that the error X is acting on qubit 2. The same notation applies for gates. However, sometimes I shall omit the subscripts and instead write out a tensor product explicitly; in this case, that would be $I \otimes X \otimes I$.)

As with the classical repetition code, the error can be identified by noticing that the middle qubit is different from the first and third qubits. The critical point is that *this is true for both branches of the superposition.* It is therefore possible to measure the fact that the second qubit is different without measuring whether we have an encoded zero or an encoded one. If we don't measure the data that's encoded in the code, we don't destroy an encoded superposition. This is how we resolve the second barrier: we can measure the error without measuring the information we're trying to preserve.

2.2.2 Encoding Circuit and Error Syndrome Measurement

To understand this point in more detail, look at figure 2.1. The first part of the figure gives the encoding circuit for the 3-qubit code. We start with one qubit in an arbitrary unencoded state and add two additional qubits which become entangled with the first qubit. After the encoding, it is no longer particularly meaningful to ask which was the original data qubit and which are the ones we added. They are now all treated on an equal basis. The encoding of equation (2.8) is symmetric between all three qubits.

The second part of the circuit contains the error correction process. We wish to know whether one of the qubits is different from the other two, and if so, which one is different. We can break that down into two pieces: We ask whether the first two qubits are the same or different, and then we ask whether the second and third qubits are the same or different. In other words, we wish to know the *parity* of the first two qubits and the parity of the last two qubits. We will store the answers to these two questions on two more extra qubits. Extra qubits like these that are used for this or any other helpful purpose during a computation are known as *ancilla* qubits.

To tell whether two qubits are the same or different, the circuit in figure 2.1 uses two CNOT gates. If they are the same, either neither CNOT flips the corresponding ancilla, or both do; if they are different, exactly one of the CNOT gates flips the ancilla qubit. Thus, when we measure the ancilla qubit for one

of the parity measurements, the output we get is equal to the parity: 0 for same (even parity), and 1 for opposite (odd parity). Notice that the result does not depend at all on the encoded state, simply whether there is a bit flip error on the qubits we are measuring. That means the measurement can be done without disturbing a superposition of the encoded data.

Together, the measurement results for the two ancillas form a bit string known as the *error syndrome*. The error syndrome encapsulates all the information we have about the error. For instance, when the bit flip error is X_2, the error syndrome is 11 because both the first pair and the second pair of qubits are different. Similarly, error syndromes 10 and 01 correspond to the errors X_1 and X_3, respectively, and error syndrome 00 tells us that there is no error. Thus, every possible error for a one-qubit bit flip channel is accounted for. Once we know what the error is, we can simply correct it by performing another bit flip on the appropriate qubit.

Notice that the choice of error correction circuit and corresponding error syndrome is not unique. For instance, we could have measured the parity of the first and third qubits instead of measuring the parity of the second and third qubits. This would have given us the same information, but the correspondence between error syndromes and errors would have been shuffled. We could have measured the parities of all three pairs of qubits, but in that case the error syndrome (which would be 3 bits long) would be redundant: from any two error syndrome bits, we could deduce the third. It is not a coincidence that the number of syndrome bits we need is equal to the number of extra qubits we added to the data in order to perform the original encoding. This is a general property of quantum error-correcting codes, as discussed in chapter 3, although there are certain cases where we don't need all of the information encoded in the syndrome. (See section 18.3 for a description of that case.)

2.2.3 Phase Error Correction

The three-qubit code described above corrects a single bit flip error, but cannot correct any phase flip errors. It is also straightforward to make a code that works the other way: it corrects a single phase flip error, but cannot correct any bit flip errors.

The key to making this code is to notice that the Hadamard transform H switches the role of X and Z errors:

$$|0\rangle \leftrightarrow |+\rangle = \frac{1}{\sqrt{2}}(|0\rangle + |1\rangle) \tag{2.10}$$

$$|1\rangle \leftrightarrow |-\rangle = \frac{1}{\sqrt{2}}(|0\rangle - |1\rangle) \tag{2.11}$$

X acting on the $|0\rangle$, $|1\rangle$ basis is a bit flip, but in the $|+\rangle$, $|-\rangle$ basis, it maps

$$X|+\rangle = |+\rangle \tag{2.12}$$

$$X|-\rangle = -|-\rangle, \tag{2.13}$$

acting as a phase flip. Similarly, Z switches $|+\rangle$ and $|-\rangle$, so it acts as a bit flip in the Hadamard-rotated basis.

Therefore, we can make a three-qubit *phase* correcting code by just applying H to every qubit in the three-qubit bit flip correcting code:

$$|0\rangle \mapsto |\overline{0}\rangle = |+\rangle|+\rangle|+\rangle \tag{2.14}$$

$$|1\rangle \mapsto |\overline{1}\rangle = |-\rangle|-\rangle|-\rangle, \tag{2.15}$$

extended by linearity so that $\alpha|0\rangle + \beta|1\rangle \mapsto \alpha|\overline{0}\rangle + \beta|\overline{1}\rangle$. In this book, I shall use lines over a state or operator to indicate the encoded version of the object.

If there is a single phase flip error, for instance, Z_2, one of the three qubits will be different than the other two in the Hadamard basis. E.g., $Z_2|\overline{0}\rangle = |+\rangle|-\rangle|+\rangle$. We can locate the error in just the same way as before, except that now we should rotate the control qubits for the CNOTs in the error correction circuit by a Hadamard transform to work in the correct basis. The modified encoding and error correction circuit is pictured in figure 2.2.

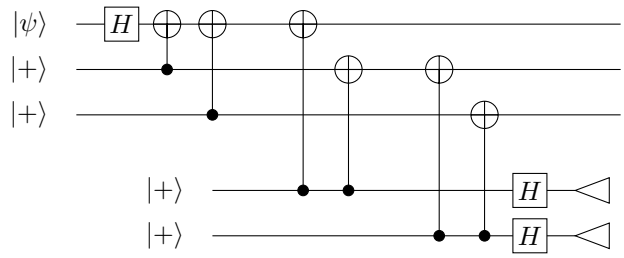

Figure 2.2: Encoding and syndrome measurement circuit for the 3-qubit phase correction code.

2.3 The 9-Qubit Code

The three-qubit codes resolve the first two barriers from table 2.1, but to address the third difficulty, we'll have to add more qubits. In order to make a code that corrects a bit flip error *or* a phase error, we'll encode one qubit into nine qubits, mixing together the encodings from both the bit and phase correcting three-qubit codes:

$$|0\rangle \mapsto |\overline{0}\rangle = \frac{1}{2\sqrt{2}}(|000\rangle + |111\rangle)(|000\rangle + |111\rangle)(|000\rangle + |111\rangle) \tag{2.16}$$

$$|1\rangle \mapsto |\overline{1}\rangle = \frac{1}{2\sqrt{2}}(|000\rangle - |111\rangle)(|000\rangle - |111\rangle)(|000\rangle - |111\rangle). \tag{2.17}$$

Again, we extend the encoding by linearity to work on superpositions. The 9-qubit code was discovered by Peter Shor and so is sometimes called the *Shor code*.

For the nine-qubit code, we will let the set of possible errors be $\{I, X_i, Y_i, Z_i | i = 1, \ldots, 9\}$, so we can have any single-qubit Pauli error. If we have an X error acting on a single qubit, that can be detected by looking at a single group of three qubits to see if one qubit is different from the other two in the standard basis. For instance,

$$X_5|\overline{0}\rangle = \frac{1}{2\sqrt{2}}(|000\rangle + |111\rangle)(|010\rangle + |101\rangle)(|000\rangle + |111\rangle), \tag{2.18}$$

and the error correction circuit of figure 2.1 applied to the middle set of three qubits will identify the error correctly. As before, once we identify the location of an X error, we can correct it by simply flipping the appropriate bit back to its original state. Also as before, the circuit tells us nothing about the encoded state.

If we have a Z error on a single qubit, matters are a little more complicated, but work basically the same way.

$$Z_5|\overline{0}\rangle = \frac{1}{2\sqrt{2}}(|000\rangle + |111\rangle)(|000\rangle - |111\rangle)(|000\rangle + |111\rangle). \tag{2.19}$$

Now we need to compare the three phases. Simply rotating into the Hadamard basis will not quite do it this time (although it gets us close), since we have to take into account the fact that the phase is distributed among a set of three qubits.

We will return to the nine-qubit code in chapter 3, and discuss exactly what to measure to find the error syndrome, but for now, let us just notice that it is possible in principle to make the desired measurement. The set of all correctly encoded states (the *code space*) forms a 2-dimensional subspace of the 2^9-dimensional Hilbert space of nine qubits. The two-dimensional subspace where the first phase is different from the other two (i.e., we have $-++$ or $+--$) is spanned by $Z_1|\overline{0}\rangle$ and $Z_1|\overline{1}\rangle$, and is orthogonal to the code space. Similarly, the subspaces where the second phase is different or the third phase is different are also orthogonal to the code space. Furthermore, these three erroneous code spaces are all orthogonal to each other. Thus, there is a measurement we can make that will distinguish them, and identify whether we have no phase error or one phase error, and if there is a phase error, on which set of three qubits it has occurred. Once we know the correct set of three, we can undo the phase error by applying Z to one of the qubits in that set of three.

A little consideration will show you that this argument applies to Y errors as well. The X and Z error correction procedures are essentially independent, and the argument that we can identify the block of three qubits with a Z error applies equally well if there is an X error on one of the nine qubits. Thus, the nine-qubit code can correct for both an X and a Z error. In particular, it can correct for a single-qubit Y error, which corresponds to having an X and a Z on the same qubit. In the set of possible errors, we only allowed single-qubit errors, but actually the code will still work if you extend the set of possible errors to allow one X error and one Z error on *any* pair of qubits.

2.4 Correcting General Errors

The nine-qubit code addresses problem 3, but it suggests that problem 4 might be troublesome. In order to correct a single bit-flip error, we needed 3 qubits, but to correct Y and Z errors as well, we went up to nine qubits. To solve problem 4 and correct general single-qubit errors, we'll need to handle an infinite set of errors. Does this mean we will have to use infinitely many qubits? Hopefully not.

2.4.1 Continuous Phase Rotation Example

Let's examine the specific case of the continuous phase rotation R_θ in more detail. We can rewrite

$$R_\theta = \begin{pmatrix} e^{-i\theta} & 0 \\ 0 & e^{i\theta} \end{pmatrix} = \cos\theta I - i\sin\theta Z. \tag{2.20}$$

Now suppose the usual nine-qubit code has experienced an error $(R_\theta)_i$ instead of the usual X, Y, or Z error, but imagine that we do not know that and use the usual error correction circuit for the nine-qubit code. We can figure out what happens to the state by again applying the linearity of quantum mechanics.

$$(R_\theta)_i|\overline{\psi}\rangle = \cos\theta I|\overline{\psi}\rangle - i\sin\theta Z_i|\overline{\psi}\rangle. \tag{2.21}$$

We know what happens to $I|\overline{\psi}\rangle$ and $Z_i|\overline{\psi}\rangle$ under the error correction circuit: First, we interact with some ancilla qubits and determine the error syndrome corresponding to these errors, then we measure the ancilla qubits. If $|I\rangle_{\text{syn}}$ and $|Z_i\rangle_{\text{syn}}$ are the error syndromes corresponding to the errors I and Z_i, when we interact with the ancillas, we get the following:

$$(R_\theta)_i|\overline{\psi}\rangle \mapsto \cos\theta I|\overline{\psi}\rangle|I\rangle_{\text{syn}} - i\sin\theta Z_i|\overline{\psi}\rangle|Z_i\rangle_{\text{syn}}. \tag{2.22}$$

Right now, we have an entangled state between the code qubits and the ancilla qubits. When we measure the ancilla register, we'll collapse the superposition, getting one of two results:

$$\text{Prob.}(\cos^2\theta): \ I|\overline{\psi}\rangle|I\rangle_{\text{syn}} \tag{2.23}$$

$$\text{Prob.}(\sin^2\theta): \ Z_i|\overline{\psi}\rangle|Z_i\rangle_{\text{syn}}. \tag{2.24}$$

Something miraculous has happened: now we have either an I error (i.e., no error at all) or a Z error, and the outcome of the error syndrome tells us which and where the error is. We can then correct it in the usual way. Somehow, by pretending that we had an I, X, Y, or Z error, we made it actually true that the error was one of those. It's a triumph of wishful thinking.

For the nine-qubit code, the same procedure works with arbitrary single-qubit unitaries, and actually works for any Kraus operator A_k. Indeed, this is not a property of just the nine-qubit code, but of quantum error-correcting codes in general: correcting I, X, Y, and Z errors is sufficient to correct general errors. At this point, we could easily prove this for the nine-qubit code, but it is worthwhile to prove the generalization. To do that, we will want to first define precisely what a quantum error-correcting code is.

2.4.2 Definition of a Quantum Error Correcting Code

Generally speaking, a quantum error-correcting code is a subspace of a larger Hilbert space. Typically, that subspace has been chosen in some complicated entangled way in order to have special properties when errors occur on states from the code space. Therefore, it is most sensible to define a quantum error-correcting code together with the set of errors it corrects. Also, we'll frequently want to consider the subspace as a Hilbert space encoding some quantum data, so we'll define the subspace as a map from a smaller Hilbert space into the big Hilbert space.

Definition 2.1. A *quantum error-correcting code* $(U, \mathcal{E})$ (or *QECC* for short) is a partial isometry $U : \mathcal{H}_K \to \mathcal{H}_N$ with the set of *correctable errors* $\mathcal{E}$ (consisting of linear maps $E : \mathcal{H}_N \to \mathcal{H}_M$) with the following property: $\exists$ quantum operation $\mathcal{D} : \mathcal{H}_M \to \mathcal{H}_K$ such that $\forall E \in \mathcal{E}$, $\forall |\psi\rangle \in \mathcal{H}_K$,

$$\mathcal{D}(EU|\psi\rangle \langle\psi|U^\dagger E^\dagger) = c(E, |\psi\rangle)|\psi\rangle \langle\psi|. \tag{2.25}$$

U is known as the *encoding* operation for the code (or the *encoder*), and $\mathcal{D}$ is the *decoding* map (or *decoder*). $\mathcal{D}$ is also known as the *recovery* operation. We say that the QECC *corrects* E if $E \in \mathcal{E}$.

Sometimes, we don't consider a specific encoding map, and refer to Image(U) (more precisely known as the *code space*) as the QECC. A *codeword* is any state in the code space. Often, a QECC is mentioned without an explicit set of correctable errors, which should be determined by context. Sometimes the error set simply does not matter. When it does matter but is not specified, the set of correctable errors is often the set of all t-qubit errors for the largest possible t; except sometimes it is instead the set of the most likely errors in the system. $\mathcal{H}_K$ is sometimes referred to as the *logical* Hilbert space and $\mathcal{H}_N$ is the *physical* Hilbert space. If $\mathcal{E}$ is the set of all t-qubit errors, we say that U (or Image(U)) is a *t-error correcting code*, or that it *corrects t errors*.

In the above definition (and elsewhere in the book), $\mathcal{H}_D$ is a Hilbert space of dimension D. A partial isometry is like a unitary in that it preserves inner products, but might not be invertible because it may map a Hilbert space to a Hilbert space of strictly larger dimension. Of course $\mathcal{D}$ actually maps matrices on $\mathcal{H}_M$ to matrices on $\mathcal{H}_K$. Since E can be a general linear map, not necessarily unitary, $EU|\psi\rangle$ might not be normalized properly, which is why we need the $c(E, |\psi\rangle)$ factor in equation (2.25). The definition explicitly allows $c(E, |\psi\rangle)$ to depend on $|\psi\rangle$, but it turns out that it does not (see section 2.5). It does depend on E, however.

To prove this, and in many other contexts, it is helpful to treat the decoding map as a unitary. This can be done via the Stinespring dilation, by purifying $\mathcal{D}$. To do so, we must add an ancilla register. Let the input ancilla to $\mathcal{D}$ be of dimension D and let the output ancilla have dimension D'. Then $\mathcal{H}_M \otimes \mathcal{H}_D \cong \mathcal{H}_K \otimes \mathcal{H}_{D'}$. $\mathcal{H}_{D'}$ plays the role of the error syndrome. Call the purification $V : \mathcal{H}_M \otimes \mathcal{H}_D \to \mathcal{H}_K \otimes \mathcal{H}_{D'}$. Now, $U|\psi\rangle = |\overline{\psi}\rangle$, and when the QECC corrects $E \in \mathcal{E}$,

$$V(E|\overline{\psi}\rangle_N \otimes |0\rangle_D) = \sqrt{c(E, |\psi\rangle)}\, |\psi\rangle_K \otimes |A(E, |\psi\rangle)\rangle_{D'} \tag{2.26}$$

I have put subscripts on the kets to help you keep track of which Hilbert spaces they belong to. There might be a phase on the RHS, but it can be absorbed into the ancilla state $|A(E, |\psi\rangle)\rangle$.

Proposition 2.2. *In definition 2.1, $c(E, |\psi\rangle)$ is independent of $|\psi\rangle$, as is $|A(E, |\psi\rangle)\rangle$ when we purify the decoder.*

Proof. Consider two codewords $|\overline{\psi}\rangle$ and $|\overline{\phi}\rangle$. Imagine we purify the decoder to the unitary V, so

$$VE|\overline{\psi}\rangle \otimes |0\rangle = \sqrt{c(E, |\psi\rangle)}\, |\psi\rangle \otimes |A(E, |\psi\rangle)\rangle \tag{2.27}$$

$$VE|\overline{\phi}\rangle \otimes |0\rangle = \sqrt{c(E, |\phi\rangle)}\, |\phi\rangle \otimes |A(E, |\phi\rangle)\rangle. \tag{2.28}$$

By linearity and the definition of a QECC applied to the superposition codeword $\alpha|\overline{\psi}\rangle + \beta|\overline{\phi}\rangle$,

$$VE(\alpha|\overline{\psi}\rangle + \beta|\overline{\phi}\rangle) \otimes |0\rangle = \alpha\sqrt{c(E, |\psi\rangle)}\, |\psi\rangle \otimes |A(E, |\psi\rangle)\rangle + \beta\sqrt{c(E, |\phi\rangle)}\, |\phi\rangle \otimes |A(E, |\phi\rangle)\rangle \tag{2.29}$$

$$= \sqrt{c(E, \alpha|\psi\rangle + \beta|\phi\rangle)}\, (\alpha|\psi\rangle + \beta|\phi\rangle) \otimes |A(E, \alpha|\psi\rangle + \beta|\phi\rangle)\rangle. \tag{2.30}$$

These two expressions can only be equal if $|A(E,|\psi\rangle)\rangle = |A(E,|\phi\rangle)\rangle = |A(E)\rangle$ (or the discarded ancilla will be entangled with the output state) and $c(E,|\psi\rangle) = c(E,|\phi\rangle) = c(E)$ (or the decoded state for the superposition will be wrong). The conceptual point here is that in order to preserve the coherent superposition in the decoder's output, there cannot be any information about the encoded state left in the ancilla, and the amplitudes (and thus norms) of different encoded states have to match, or the Hilbert space will get distorted. □

Note that the set of correctable errors is not a unique invariant property of an encoding map or code space, which is why I included it as part of the definition. The same code space could be used to correct different sets of errors. For instance, the 3-qubit phase correction code can correct the set $\mathcal{E} = \{I, Z_1, Z_2, Z_3\}$, but it also corrects the set $\mathcal{E} = \{I, Z_1Z_2, Z_1Z_3, Z_2Z_3\}$. In the former case, we interpret the non-zero error syndromes as caused by a single phase error, whereas in the latter case, we only consider two-qubit errors. Since Z_1 has the same error syndrome as Z_2Z_3 but they correspond to different logical states, we have to make a choice between them and cannot include both in the set of correctable errors at the same time. That is, $\mathcal{E} = \{I, Z_1, Z_2Z_3\}$ is *not* a possible set of correctable errors for the 3-qubit phase correction code.

There are many variations of the terms defined above. For instance, code space is sometimes coding space, code subspace, etc., and sometimes it is the encoded subspace. However, the encoded subspace also sometimes refers to $\mathcal{H}_K$, which can also be called the data or encoded data. As defined above, $\mathcal{D}$ incorporates both the error correction procedure and the "unencoding" process of returning the data to $\mathcal{H}_K$, but sometimes they are considered separately.

The decoder $\mathcal{D}$ incorporates whatever processing is necessary to correct and decode the state. For instance, it may incorporate a measurement of the error syndrome, and application of a correction operation conditional on the classical bits resulting from the syndrome measurement. The decoder $\mathcal{D}$ may not, however, be unique. Its behavior is completely determined on the subspace spanned by $E|\overline{\psi}\rangle$, where $E \in \mathcal{E}$ and $|\overline{\psi}\rangle$ is a codeword, but outside of that subspace, $\mathcal{D}$ can act arbitrarily, and the distinctions between different decoders can be important in a number of contexts, such as when studying the efficiency of the decoder, or its behavior on errors outside $\mathcal{E}$, or when considering fault tolerance.

Note that if we define a QECC just as a subspace instead of an encoding map, we haven't lost much information. In particular, the set of correctable errors is the same for all encoders:

Proposition 2.3. *Suppose we have two different encoders $U_1, U_2 : \mathcal{H}_K \to \mathcal{H}_N$ with* $\mathrm{Image}(U_1) = \mathrm{Image}(U_2)$. *Then $(U_1, \mathcal{E})$ is a QECC iff $(U_2, \mathcal{E})$ is a QECC.*

Proof. Because U_1 and U_2 are partial isometries with the same image, they can only differ by a unitary $V : \mathcal{H}_K \to \mathcal{H}_K$:

$$U_2 = U_1 V. \tag{2.31}$$

If we use decoder $\mathcal{D}_1$ for encoder U_1, then $V^\dagger \circ \mathcal{D}_1$ will serve as the decoding map for U_2:

$$\begin{aligned} V^\dagger \mathcal{D}_1(EU_2|\psi\rangle\langle\psi|U_2^\dagger E^\dagger)V &= V^\dagger \mathcal{D}_1(EU_1V|\psi\rangle\langle\psi|V^\dagger U_1^\dagger E^\dagger)V & (2.32)\\ &= V^\dagger(c(E,V|\psi\rangle)V|\psi\rangle\langle\psi|V^\dagger)V & (2.33)\\ &= c(E,|\psi\rangle)|\psi\rangle\langle\psi|. & (2.34)\end{aligned}$$

□

In the definition of a QECC, we have let the dimensions K, M, and N of the various Hilbert spaces involved be arbitrary, although $N \geq K$ or no QECC is possible. Nevertheless, there are some common restrictions. Frequently we assume $K = 2^k$ and $N = 2^n$, so there are k *logical qubits* (or *encoded qubits*) and n *physical qubits*. Sometimes we work with q-dimensional qudits instead of qubits, so $K = q^k$ and $N = q^n$. Occasionally we have even more general situations, where K and N might use different bases or not be powers at all. When there is a tensor factorization of the overall Hilbert space, but I don't want to be too specific about whether the individual factors are qubits, qudits, or maybe even different sizes from each other, I will refer to the *registers*, with each register being one tensor factor. A single error then affects a single register, whatever its size.

Most often $M = N$, so errors map the physical Hilbert space to itself. There is little lost by assuming this, since we can generally ignore any unused states in $\mathcal{H}_N$ or $\mathcal{H}_M$ without negative consequence. The main time when it matters is when errors occur repeatedly on the state before we perform error correction, as happens, for instance, in fault-tolerant quantum computation. In that case, you really need $M = N$, so that you can sensibly apply the same error over and over again.

One special case worth mentioning is that of erasure errors. Recall that an erasure error formally maps a qubit into a qutrit, so to treat erasure errors in the most precise way, we would take $N = 2^n$ and $M = 3^n$. However, most often we imagine that a "stop-leak" gate of some sort is performed before the decoder. The stop-leak gate will map the third $|\perp\rangle$ state of each qutrit to some state, perhaps a random one, of the corresponding qubit. Then we can consider an erasure error as mapping a qubit to a qubit, but with some additional classical information indicating that the qubit has undergone an error.

This is maybe a good place for an extremely important digression on the terminology of error correction. Specifically, I want to discuss the use of hyphens. Wait, did I say "important?" I meant "unimportant." But I am going to discuss hyphens anyway. In English, hyphens are occasionally used in compound nouns but not that frequently. Where they *are* used is to make compound adjectives. Thus, we have a hyphen in "error-correcting code" and "fault-tolerant computation" but not in "error correction" and "fault tolerance," unless one of the component words happens to get split between lines. (Notably, though, there is no hyphen for the "quantum" part, so "quantum error-correcting code.") Certainly, many scientists are not native speakers of English, so they have a good excuse for making this mistake. But you no longer have an excuse.

2.4.3 Linearity of Quantum Error Correction

Now we are ready to generalize the phenomenon we observed in section 2.4.1.

Theorem 2.4. *If $(U, \mathcal{E})$ is a QECC, then $(U, \mathcal{E}')$ is a QECC, where $\mathcal{E}' = \operatorname{span} \mathcal{E}$ is the linear span of $\mathcal{E}$.*

In other words, if a QECC can correct E and F, then it can also correct $\alpha E + \beta F$.

Proof. Basically, the idea is to duplicate the argument used in section 2.4.1 for the general case. We haven't defined the error syndrome for a general QECC, but we do have the decoding map to work with. We will purify it to V so that we can work with only unitary maps.

The QECC corrects $E, F \in \mathcal{E}$, so

$$V(E|\overline{\psi}\rangle_M \otimes |0\rangle_D) = c_E|\psi\rangle_K \otimes |s_E\rangle_{D'} \tag{2.35}$$

$$V(F|\overline{\psi}\rangle_M \otimes |0\rangle_D) = c_F|\psi\rangle_K \otimes |s_F\rangle_{D'}. \tag{2.36}$$

One difference from section 2.4.1 is that $|s_E\rangle$ and $|s_F\rangle$ don't need to be orthogonal. Also note that the c's from definition 2.1 would be the squares of c_E and c_F.

By linearity,

$$V[(\alpha E + \beta F)|\overline{\psi}\rangle_M \otimes |0\rangle_D] = \alpha c_E|\psi\rangle_K \otimes |s_E\rangle_{D'} + \beta c_F|\psi\rangle_K \otimes |s_F\rangle_{D'} \tag{2.37}$$

$$= |\psi\rangle_K \otimes (\alpha c_E|s_E\rangle_{D'} + \beta c_F|s_F\rangle_{D'}). \tag{2.38}$$

Tracing out $\mathcal{H}_{D'}$, we find that the decoder map is of the desired form, with

$$c(\alpha E + \beta F, |\psi\rangle) = \|\alpha c_E|s_E\rangle + \beta c_F|s_F\rangle\|^2. \tag{2.39}$$

□

2.4.4 Correcting Paulis Implies Correcting All Errors

As a corollary of theorem 2.4, we can simplify the condition for a code to correct t errors:

Corollary 2.5. *If a QECC set of correctable errors includes all tensor products of I, X, Y, and Z of weight t or less, it is a t-error correcting code.*

Proof. The set of all errors with support on a given set of t qubits is the set of $2^t \times 2^t$ matrices acting on those qubits. Tensor products of I, X, Y, and Z acting on those t qubits form a basis for this set of matrices. Therefore, an arbitrary weight t error can be written as the sum (with appropriate coefficients) of weight t tensor products of I, X, Y, and Z, and an arbitrary t-qubit error can be written as a sum weight t errors. The corollary then follows from theorem 2.4. □

As a consequence, we find that the nine-qubit code is a 1-error correcting code. Applying the definitions, we find that it encodes one logical qubit into nine physical qubits.

2.4.5 QECCs and Error Channels

We have finally answered all four objections to the existence of quantum error-correcting codes. However, it is worth thinking a little more carefully about what happens when we have a decoherent error that maps pure states to mixed states. For example, suppose that we have a dephasing channel with error probability p acting on qubit i. Then the pure codeword state $|\overline{\psi}\rangle$ becomes:

$$|\overline{\psi}\rangle\langle\overline{\psi}| \mapsto (1-p)I|\overline{\psi}\rangle\langle\overline{\psi}|I + pZ_i|\overline{\psi}\rangle\langle\overline{\psi}|Z_i, \tag{2.40}$$

which is a mixture of the pure states $|\overline{\psi}\rangle$ and $Z_i|\overline{\psi}\rangle$. Now, we know that the full error correction procedure corrects these two pure states:

$$|\overline{\psi}\rangle \mapsto |\overline{\psi}\rangle|I\rangle_{\text{syn}} \tag{2.41}$$

$$Z_i|\overline{\psi}\rangle \mapsto |\overline{\psi}\rangle|Z_i\rangle_{\text{syn}} \tag{2.42}$$

By the linearity of density matrices, that means that the final state after the dephasing channel followed by error correction is:

$$(1-p)|\overline{\psi}\rangle\langle\overline{\psi}| \otimes |I\rangle\langle I|_{\text{syn}} + p|\overline{\psi}\rangle\langle\overline{\psi}| \otimes |Z_i\rangle\langle Z_i|_{\text{syn}} = |\overline{\psi}\rangle\langle\overline{\psi}| \otimes \left[(1-p)|I\rangle\langle I|_{\text{syn}} + p|Z_i\rangle\langle Z_i|_{\text{syn}}\right]. \tag{2.43}$$

That is, the decoded logical qubit ends up as a pure state, but the overall state is still mixed: the randomness introduced by the error ends up in the error syndrome, or in the ancilla Hilbert space $\mathcal{H}_{D'}$ in the proof of theorem 2.4.

Recall that a t-qubit error channel is one for which there exists a Kraus decomposition where each Kraus operator is a sum of weight t linear operators. By theorem 2.4 and the argument above for the dephasing channel, any code that corrects arbitrary t-qubit linear errors will therefore also correct arbitrary t-qubit error channels.

What about independent channels?

Theorem 2.6. *Let $\mathcal{I}$ be the 1-qubit identity channel and $\mathcal{E} = \otimes_{i=1}^n \mathcal{E}_i$ be an n-qubit independent channel, with $\|\mathcal{E}_i - \mathcal{I}\|_\diamond < \epsilon \leq \frac{t+1}{n-t-1}$, and let U and $\mathcal{D}$ be the encoder and decoder for a QECC with n physical qubits that corrects t-qubit errors. Then*

$$\|\mathcal{D} \circ \mathcal{E} \circ U - \mathcal{I}\|_\diamond < 2\binom{n}{t+1}(e\epsilon)^{t+1}. \tag{2.44}$$

In other words, a QECC that can correct t-qubit errors also corrects small independent error channels up to a very good approximation. A similar statement immediately follows from theorem 1.1. This should thus be viewed as a specialization of theorem 1.1 with better constant factors and a much easier proof.

Proof. The strategy is straightforward: Expand $\mathcal{E}$ as a sum of a t-qubit error map (not normalized) and an additional small term. The t-qubit error map is corrected by the code due to linearity, and then we just have to bound the size of the additional term to prove the theorem.

Since $\|\mathcal{E}_i - \mathcal{I}\|_\diamond < \epsilon$, we can write $\mathcal{E}_i = \mathcal{I} + \delta\mathcal{E}_i$, with $\|\delta\mathcal{E}_i\|_\diamond < \epsilon$. Now,

$$\mathcal{E} = \mathcal{F} + \mathcal{G}, \tag{2.45}$$

where

$$\mathcal{F} = \sum_{r=0}^{t} \sum_{|S|=r} \bigotimes_{i \in S} \delta\mathcal{E}_i \tag{2.46}$$

$$\mathcal{G} = \sum_{r=t+1}^{n} \sum_{|S|=r} \bigotimes_{i \in S} \delta\mathcal{E}_i \tag{2.47}$$

are the sums over all tensor factors of $\leq t$ and $> t$ of the $\delta\mathcal{E}_i$s, respectively. (The tensor with $\mathcal{I}$ on other qubits is implicit.)

The first term $\mathcal{F}$ is a sum of terms acting on at most t qubits. Each term in the sum is not a completely positive map. In fact, $\delta\mathcal{E}_i$ is not even positive. However, $\delta\mathcal{E}_i$ is a difference of two completely positive maps, and therefore

$$\mathcal{F}(\rho) = \sum_k \alpha_k A_k \rho A_k^\dagger, \tag{2.48}$$

where the α_k coefficients can be either positive or negative real numbers and each A_k acts on at most k qubits. By theorem 2.4 (and the linearity of density matrices, as for the dephasing channel example), the QECC corrects $\mathcal{F}$.

By proposition 2.2, the scaling factor $c(E, |\psi\rangle)$ in definition 2.1, the definition of a QECC, does not depend on $|\psi\rangle$, which implies that

$$\mathcal{D} \circ \mathcal{F} \circ U = c\mathcal{I} \tag{2.49}$$

for some constant c.

Meanwhile,

$$\|\mathcal{G}\|_\diamond \leq \sum_{r=t+1}^{n} \sum_{|S|=r} \prod_{i \in S} \|\delta\mathcal{E}_i\|_\diamond \tag{2.50}$$

$$\leq \sum_{r=t+1}^{n} \binom{n}{r} \epsilon^r \tag{2.51}$$

$$\leq \binom{n}{t+1} (e\epsilon)^{t+1} = \delta \tag{2.52}$$

by lemma 1.2.

Now, $\mathcal{E}$, $\mathcal{D}$, and U are CPTP maps, so $\|\mathcal{D} \circ \mathcal{E} \circ U\|_\diamond = 1$. Thus,

$$1 - \delta \leq \|\mathcal{D} \circ \mathcal{E} \circ U\|_\diamond - \|\mathcal{D} \circ \mathcal{G} \circ U\|_\diamond \leq \|\mathcal{D} \circ \mathcal{F} \circ U\|_\diamond = \|c\mathcal{I}\|_\diamond = c \leq \|\mathcal{D} \circ \mathcal{E} \circ U\|_\diamond + \|\mathcal{D} \circ \mathcal{G} \circ U\|_\diamond \leq 1 + \delta. \tag{2.53}$$

That is, $|1 - c| \leq \delta$. Therefore,

$$\|\mathcal{D} \circ \mathcal{E} \circ U - \mathcal{I}\|_\diamond = \|\mathcal{D} \circ \mathcal{F} \circ U + \mathcal{D} \circ \mathcal{G} \circ U - \mathcal{I}\|_\diamond \tag{2.54}$$

$$= \|(c-1)\mathcal{I} + \mathcal{D} \circ \mathcal{G} \circ U\|_\diamond \tag{2.55}$$

$$\leq |c - 1| + \|\mathcal{G}\|_\diamond \tag{2.56}$$

$$\leq 2\delta. \tag{2.57}$$

□

2.5 The Quantum Error Correction Conditions

2.5.1 Sufficient Conditions (Non-degenerate Orthogonal Coding)

Recall the argument that we used to show that the nine-qubit code could correct phase errors. Very little about it was specific to the nine-qubit code. We said that phase errors generated subspaces which were orthogonal to the code space and to each other, and that therefore there was a measurement that distinguished

them. We can use this same argument to give a general sufficient condition to have a QECC: Suppose that $Q \subseteq \mathcal{H}_N$ is the code space, and let $E(Q)$ be the subspace formed by acting on Q with E. Then we want that for any pair of errors $E_1, E_2 \in \mathcal{E}$, the subspace $E_1(Q)$ is orthogonal to $E_2(Q)$. Then we will be able to make a measurement that identifies which subspace we are in and therefore identifies the error.

To be sure we have a QECC, we need a little bit more. After identifying the error, we need to be able to reverse it. That is only possible if $E|_Q$ is a unitary map from Q to $E(Q)$. $E|_Q$ is unitary iff $\langle\psi|E^\dagger E|\phi\rangle = \langle\psi|\phi\rangle$ for all $|\psi\rangle, |\phi\rangle \in Q$. Thus, we get the sufficient condition that $(Q, \mathcal{E})$ is a QECC if $\forall|\psi\rangle, |\phi\rangle \in Q$, $\forall E_a, E_b \in \mathcal{E}$,

$$\langle\psi|E_a^\dagger E_b|\phi\rangle = \delta_{ab}\langle\psi|\phi\rangle. \tag{2.58}$$

A code that satisfies this condition could be called a *non-degenerate orthogonal code*, although the term "orthogonal code" is not widely used.

2.5.2 The QECC Conditions

However, by looking at the nine-qubit code, we can already see that equation (2.58) is not a necessary condition. If $E_1 = Z_1$ and $E_2 = Z_2$, then equation (2.58) fails since $E_1|\overline{\psi}\rangle = E_2|\overline{\psi}\rangle$. We need to generalize slightly:

Theorem 2.7 (QECC Conditions)**.** *$(Q, \mathcal{E})$ is a QECC iff $\forall|\psi\rangle, |\phi\rangle \in Q$, $\forall E_a, E_b \in \mathcal{E}$,*

$$\langle\psi|E_a^\dagger E_b|\phi\rangle = C_{ab}\langle\psi|\phi\rangle. \tag{2.59}$$

Note that C_{ab} does not depend on $|\psi\rangle$ or $|\phi\rangle$.

Proof. $\Leftarrow$: Recalling theorem 2.4, we might as well pick a useful spanning set for $\mathcal{E}$ and restrict attention to that spanning set. Taking the adjoint of equation (2.59) and putting in $|\phi\rangle = |\psi\rangle$, we find that $C_{ab}^\dagger = C_{ba}^*$, i.e., the matrix C is Hermitian. Therefore C_{ab} is diagonalizable, and by choosing an appropriate spanning set $\{F_a\}$ for $\mathcal{E}$ we can actually diagonalize C_{ab}. (Note that it is not necessarily true that $F_a \in \mathcal{E}$, but that is not particularly relevant, it just means that the original set $\mathcal{E}$ is smaller than the maximal set of possible errors the code can correct.)

We have

$$\langle\psi|F_a^\dagger F_b|\phi\rangle = d_a\delta_{ab}\langle\psi|\phi\rangle. \tag{2.60}$$

This is almost equation (2.58), but the coefficient d_a can be different from 1. (d_a is an eigenvalue of C_{ab}, so it must be real.) However, it is still true that the different subspaces $F(Q)$ are orthogonal to each other, so we can make a measurement that determines which error F_a we have. It is not true that $F_a|_Q$ must be unitary, but if d_a is nonzero, $F_a|_Q$ can be written as a unitary followed by a uniform rescaling. The decoding then gives the original state rescaled by d_a. This is allowed by definition 2.1.

If d_a is zero, then $F_a|_Q$ cannot be inverted, since there is no state left. Formally, we are still OK, since in definition 2.1, we would just get that $c(F_a, |\psi\rangle) = 0$. Physically, this means that the error F_a *never occurs*. It has probability proportional to $\langle\psi|F_a^\dagger F_a|\psi\rangle$, which is 0.

Therefore, equation (2.59) gives sufficient conditions to have a QECC.

$\Rightarrow$: Recall that by proposition 2.2, $c(E, |\psi\rangle)$ and $|A(E, |\psi\rangle)\rangle$ don't depend on $|\psi\rangle$. More generally, if we purify the decoder to V, we get a unitary transformation, which preserves inner products:

$$\langle\overline{\psi}|E_a^\dagger E_b|\overline{\phi}\rangle = (\langle\overline{\psi}| \otimes \langle 0|)E_a^\dagger V^\dagger V E_b(|\overline{\phi}\rangle \otimes |0\rangle) \tag{2.61}$$

$$= \sqrt{c(E_a)c(E_b)}\,(\langle\psi| \otimes \langle A(E_a)|)(|\phi\rangle \otimes |A(E_b)\rangle) \tag{2.62}$$

$$= \sqrt{c(E_a)c(E_b)}\,\langle A(E_a)|A(E_b)\rangle\langle\psi|\phi\rangle. \tag{2.63}$$

This is equation (2.59) with $C_{ab} = \sqrt{c(E_a)c(E_b)}\langle A(E_a)|A(E_b)\rangle$.

□

2.5.3 Degenerate Codes

The difference between equation (2.58) and equation (2.59) consists in the fact that C_{ab} might not be δ_{ab}. When C_{ab} has maximum rank, this difference has no deep meaning, since we have just made a bad choice of basis errors. As in the proof of theorem 2.7, we can choose a different set of errors with the same span to diagonalize C_{ab}, and we can even rescale to make $C_{ab} = \delta_{ab}$.

When C_{ab} has non-maximal rank, we cannot do this. If the error set $\mathcal{E}$ is not linearly independent, C_{ab} cannot have maximal rank, since a linearly dependent set of errors will produce a linearly dependent set of rows in C_{ab}. The interesting case is when $\mathcal{E}$ is linearly independent. It is possible then to still have a QECC with non-maximal rank for C_{ab}. This is known as a degenerate code.

Definition 2.2. Suppose $(U, \mathcal{E})$ is a QECC and $\mathcal{E}$ is linearly independent. Then the code is *degenerate* if $\text{rank}(C_{ab}) < |\mathcal{E}|$. A code $(U, \mathcal{E})$ (for linearly dependent $\mathcal{E}$) is degenerate if $(U, \mathcal{E}')$ is degenerate, where $\mathcal{E}'$ is a minimal spanning set for $\mathcal{E}$. If a code is not degenerate, it is *non-degenerate*.

We have already seen an example of a degenerate code: the nine-qubit code. The essence of degeneracy is that different errors will produce the same result (or at least linearly dependent results) when acting on a codeword. In the nine-qubit code, any two Z errors acting on the same set of 3 qubits will produce the same result. For instance,

$$Z_1|\overline{0}\rangle = Z_2|\overline{0}\rangle = \frac{1}{2\sqrt{2}}(|000\rangle - |111\rangle)(|000\rangle + |111\rangle)(|000\rangle + |111\rangle) \tag{2.64}$$

$$Z_1|\overline{1}\rangle = Z_2|\overline{1}\rangle = \frac{1}{2\sqrt{2}}(|000\rangle + |111\rangle)(|000\rangle - |111\rangle)(|000\rangle - |111\rangle). \tag{2.65}$$

2.5.4 Distance

The most common situation when designing a QECC is to let the set of possible errors be all t-qubit errors. It is therefore worth examining theorem 2.7 more explicitly for a t-error correcting code. When E_a and E_b are both weight t errors, then $E_a^\dagger E_b$ is a weight $2t$ error.

Definition 2.3. Let $C \subseteq \mathcal{H}_N$ be a QECC. The *distance* of C is the minimum weight d of an error F such that

$$\langle\psi|F|\phi\rangle \neq c(F)\langle\psi|\phi\rangle, \tag{2.66}$$

where $|\psi\rangle$ and $|\phi\rangle$ run over all possible pairs of codewords of C.

Note that the notion of distance implies that the Hilbert space is broken up into qubits because weight is defined in terms of qubits. Naturally, we can easily generalize the distance to work with a code over qudits of dimension q by defining weight in terms of the number of qudits in the support of an operator.

We get the following corollary of theorem 2.7:

Corollary 2.8. *A distance d code corrects $\lfloor (d-1)/2 \rfloor$ errors.*

Inverting this formula, we find that to correct t errors, a code needs distance $2t + 1$. If the distance is even, the extra point is "wasted" for this application, but as we shall see in a moment, the extra point of distance can be helpful in alternative applications.

The three central properties of a QECC are the size of the logical subspace, the number of physical qubits, and the distance, so there is a notation encapsulating those properties.

Notation 2.4. A QECC which encodes $\mathcal{H}_K$ into $\mathcal{H}_{2^n}$ and has distance d is denoted as an $((n, K, d))$ code. If the physical Hilbert space is n qudits each of dimension q, it is an $((n, K, d))_q$ code. If the distance is unknown or irrelevant, it is an $((n, K))$ code or an $((n, K))_q$ code.

This notation is derived from an analogous one for classical error-correcting codes, which will be introduced in chapter 4. The classical notation uses single parentheses, and the double parenthesis indicates that we have a quantum error-correcting code.

Sometimes when we discuss a code we consider it to have a distance less than its true distance or to correct fewer errors than the maximum number it can correct. This is just a convenience indicating that we are ignoring some of the error-correcting capability of the code. However, the true distance of a QECC does give us the tightest estimate of the number of errors it can correct — that is, the converse of the corollary also holds. In order to get the definition of distance, we need F to run over all errors of weight $< d$, but the QECC conditions applied to a t-error correcting code only gives us equation (2.66) for errors of the form $E_a^\dagger E_b$, which does not include all possible weight $2t$ errors. However, equation (2.66) is linear in F, so it is sufficient to check the formula for a basis of the set of weight $2t$ errors, and the set of errors of the form $E_a^\dagger E_b$ does include such a basis.

By similar reasoning, you get the same notion of distance if you alter the definition of distance to use all d-qubit errors or just weight d tensor products of I, X, Y, and Z.

When describing a code without an explicit set of correctable errors, I said in the definition that you are supposed to determine the set of correctable errors by context. Typically, we will choose the error set to be the set of t-qubit errors, which makes the distance of a code one of its most critical properties. When the error set is given implicitly, we can define degeneracy in terms of the code's capability as a t-error correcting code.

Definition 2.5. Let $Q \subseteq \mathcal{H}_N$ be a QECC with distance $d = 2t + 1$. Then Q is *degenerate* if it is degenerate when the set of correctable errors is all t-qubit errors.

If the distance is even, $2t+2$, and there is no more structure, it makes the most sense to define degeneracy by also considering the set of correctable errors to be t-qubit errors, but for certain families of codes (such as stabilizer codes, discussed in chapter 3), we can do better.

2.5.5 Quantum Error Detection and Erasure Errors

The distance is useful information about a QECC partially because it tells you how many errors the code can correct, but also because it encapsulates some additional error-correction-related properties of the code. In particular, the distance also tells you about the code's ability to detect errors without correcting them and about the code's ability to correct erasure errors. These applications can take advantage of even distance codes, whereas correcting general t-qubit errors only needs odd distance codes.

Definition 2.6. An encoder U (defined as for a QECC) and a set of detectable errors $\mathcal{E}$ form a *quantum error-detecting code* if they have the following property: Let Π be the projector on the code space. Then $\Pi E|\psi\rangle = c(E, |\psi\rangle)|\psi\rangle$, for all $E \in \mathcal{E}$ and all codewords $|\psi\rangle$. The code space is defined as the image of U, as for a QECC, and we frequently refer to the code space as defining the error-detecting code instead of the encoder.

Based on the definition of an error-detecting code, the measurement $(\Pi, I - \Pi)$ will either project us back on the original state (with some probability $|c(E, |\psi\rangle)|^2$) or will identify that an error occurred. This condition can be easily rewritten in similar terms to the QECC conditions:

Theorem 2.9. *$(U, \mathcal{E})$ is a quantum error-detecting code iff*

$$\langle\psi|E|\phi\rangle = c(E)\langle\psi|\phi\rangle \tag{2.67}$$

for all codewords $|\psi\rangle$ and $|\phi\rangle$ and all $E \in \mathcal{E}$. A code with distance d detects arbitrary $(d-1)$-qubit errors.

Based on this theorem, we can understand the distance of the code as the minimum number of qubits on which we can act to produce an undetectable error, i.e., an error with a component taking a codeword to a *different* codeword. (An error taking a codeword to itself is considered "detectable" by the definition.)

Proof. $\Leftarrow$: We can write $\Pi = \sum |\psi_i\rangle \langle\psi_i|$ where the sum runs over a basis $|\psi_i\rangle$ for the code space Q. We can then calculate $\Pi E|\psi\rangle$ using equation (2.67) to see that we have a quantum error-detecting code.

$\Rightarrow$: Equation (2.67) follows immediately from the definition of a quantum error-detecting code if we can prove that $c(E, |\psi\rangle)$ does not depend on $|\psi\rangle$. This can be done by considering a superposition $\alpha|\psi_1\rangle + \beta|\psi_2\rangle$, as in proposition 2.2.

The definition of distance then shows that a distance d code detects $d-1$ errors. □

While I have presented quantum error-correcting codes and quantum error-detecting codes as different things, clearly there is a very close connection. A code able to correct t errors will also be able to detect $2t$ errors, and vice-versa. Detecting errors and correcting errors are really just two different applications for the same code, and henceforth, I won't make a distinction between a code designed to correct errors and one designed to detect errors. Both will be referred to as QECCs.

There is no unique maximal set of correctable errors for a QECC, but there is a unique maximal set of detectable errors. The quantum error-correction conditions involve a product of two errors, and there may be more than one set of errors that will run over all possibilities for the product. However, equation (2.67) is only linear in the error, so we can define a unique set of detectable errors.

Definition 2.7. Given a subspace Q, its set of *detectable errors* is

$$\{E \text{ s.t. } \langle\psi|E|\phi\rangle = c(E)\langle\psi|\phi\rangle \,\forall |\psi\rangle, |\phi\rangle \in Q\}. \tag{2.68}$$

If $\mathcal{E}_C$ is the set of correctable errors and $\mathcal{E}_D$ is the set of detectable errors for a code, then the QECC conditions can be rephrased as $\mathcal{E}_C^2 \subseteq \mathcal{E}_D$.

A code's ability to correct erasure errors can be understood just by applying the regular QECC conditions. The interesting twist in this case is that we can apply the side classical information we have about the location of the errors to correct twice as many errors:

Theorem 2.10. *A QECC with distance d can correct $d-1$ erasure errors.*

Proof. The best way to think about an erasure-correcting code is as a set of QECCs which all have the same encoder. Each code is associated with a different error set, depending on where the erasure errors took place. Since we don't know when doing the encoding where the errors are, we have to use the same encoder in all cases. When *decoding*, however, we know where the errors are (although not what kind of errors they are), so we can choose a decoder based on the actual error set — all possible errors on the actual set of qubits erased.

Therefore we need a single code space that satisfies the QECC conditions for any error set of the form $\mathcal{E}_S$, which is the set of all possible errors with support on the set S of at most t qubits. But $\mathcal{E}_S^2 = \mathcal{E}_S$ since the product of two errors with support on S still has support on S. For a distance d code, the set of detectable errors includes all $(d-1)$-qubit errors, so when $t \leq d-1$, all sets $\mathcal{E}_S$ are subsets of the set of detectable errors. □

2.5.6 Alternate Forms of the Quantum Error Correction Conditions

There are a number of variants of the QECC conditions which are useful in different contexts. You have just seen one relating a correctable set of errors with the set of detectable errors for a code. A few more appear in the following proposition:

Proposition 2.11. *The following are equivalent to the QECC conditions given in theorem 2.7:*

1. *For all codewords $|\psi\rangle$, all pairs $E_a, E_b \in \mathcal{E}$,*

$$\langle\psi|E_a^\dagger E_b|\psi\rangle = \mathrm{tr}(|\psi\rangle\langle\psi|E_a^\dagger E_b) = C_{ab}. \tag{2.69}$$

2. *If $\mathrm{span}(\mathcal{E}) = \mathcal{E}$: For any pair of codewords $|\psi\rangle, |\phi\rangle$, any error $E \in \mathcal{E}$,*

$$\langle\psi|E^\dagger E|\phi\rangle = C(E)\langle\psi|\phi\rangle. \tag{2.70}$$

3. If $\mathrm{span}(\mathcal{E}) = \mathcal{E}$*: For any codeword* $|\psi\rangle$*, any error* $E \in \mathcal{E}$*,*

$$\mathrm{tr}(|\psi\rangle\langle\psi|E^\dagger E) = C(E). \tag{2.71}$$

4. Let $\{|\psi_i\rangle\}$ *be a basis for the code space. For any* i *and* j *and for any pair* $E_a, E_b \in \mathcal{E}$*,*

$$\langle\psi_i|E_a^\dagger E_b|\psi_j\rangle = C_{ab}\delta_{ij}. \tag{2.72}$$

Proof. The QECC conditions from equation (2.59) immediately imply all four of these variant conditions, so we only need to show the reverse direction.

To show that the standard QECC conditions follow from the first variant above, pick arbitrary $|\phi_1\rangle$ and $|\phi_2\rangle$ in the code space and consider $|\psi\rangle = \alpha|\phi_1\rangle + \beta|\phi_2\rangle$ for different values of α and β. $|\phi_1\rangle$ and $|\phi_2\rangle$ may not be orthogonal, so we have

$$1 = |\alpha|^2 + |\beta|^2 + 2\,\mathrm{Re}(\alpha^*\beta\langle\phi_1|\phi_2\rangle). \tag{2.73}$$

Now, $|\psi\rangle$ is also in the code space, and

$$\begin{aligned} C_{ab} &= \langle\psi|E_a^\dagger E_b|\psi\rangle & (2.74)\\ &= |\alpha|^2\langle\phi_1|E_a^\dagger E_b|\phi_1\rangle + |\beta|^2\langle\phi_2|E_a^\dagger E_b|\phi_2\rangle + \alpha^*\beta\langle\phi_1|E_a^\dagger E_b|\phi_2\rangle + \alpha\beta^*\langle\phi_2|E_a^\dagger E_b|\phi_1\rangle & (2.75)\\ &= (|\alpha|^2 + |\beta|^2)C_{ab} + (\alpha^*\beta\langle\phi_1|E_a^\dagger E_b|\phi_2\rangle + \alpha\beta^*\langle\phi_2|E_a^\dagger E_b|\phi_1\rangle). & (2.76) \end{aligned}$$

If we first plug in $\alpha = \beta = 1/\sqrt{2(1 + \mathrm{Re}\langle\phi_1|\phi_2\rangle)}$, we find

$$\langle\phi_1|E_a^\dagger E_b|\phi_2\rangle + \langle\phi_2|E_a^\dagger E_b|\phi_1\rangle = C_{ab}(\langle\phi_1|\phi_2\rangle + \langle\phi_2|\phi_1\rangle). \tag{2.77}$$

Plugging in $\alpha = -i\beta = 1/\sqrt{2(1 - \mathrm{Im}\langle\phi_1|\phi_2\rangle)}$, we get

$$\langle\phi_1|E_a^\dagger E_b|\phi_2\rangle - \langle\phi_2|E_a^\dagger E_b|\phi_1\rangle = C_{ab}(\langle\phi_1|\phi_2\rangle - \langle\phi_2|\phi_1\rangle). \tag{2.78}$$

Putting these two equations together, we find

$$\langle\phi_1|E_a^\dagger E_b|\phi_2\rangle = C_{ab}\langle\phi_1|\phi_2\rangle, \tag{2.79}$$

as desired.

The second and third variants use a similar argument for E_a and E_b. The proof of the fourth version is left as an exercise. □

Applying a similar argument to definition of the set of detectable errors, we find that an operator E is detectable iff $\mathrm{tr}(\rho E)$ does not depend on the codeword ρ. This has an interesting interpretation: it says that an operator is detectable if and only if measurement of that operator reveals no information about the logical state of the code. Certainly, if measuring an operator does reveal information about the logical state, it will create errors in the encoded state. Two aspects of the condition are perhaps surprising: first, that some element of that error cannot be detected, and second, that revealing encoded information is the *only* thing that prevents an error from being detectable.

Another version of this insight appears when we apply the QECC conditions specifically to erasure errors.

Proposition 2.12. *Let* $\mathcal{E}$ *be a set of erasure errors, each one corresponding to a set of erased qubits (or qudits). Then* Q *corrects* $\mathcal{E}$ *iff* ρ_S *is the same for all logical states* $|\psi\rangle$ *whenever* $S \in \mathcal{E}$*. Here* S *is a subset of qubits that can be erased and* ρ_S *is the encoded state restricted to* S*.*

Note that the proposition just says that Q can correct for erasures on the set S iff the codeword on S has no information about the encoded state. Another interesting feature of this is that the ability to correct for erasures only refers to single sets, not pairs of sets, whereas more generally the QECC conditions refer to pairs of errors. This means that any QECC has a unique maximal set of erasure errors that it can correct, whereas, as I mentioned before, there is not a unique set of general errors that can be corrected — there is some tradeoff between correcting different kinds of errors.

Proof. As in the proof of theorem 2.10, we think of the code as a set of QECCs labelled after-the-fact by the set of erased qubits. We specialize to a single set $S \in \mathcal{E}$ and want to show that Q corrects erasures on S iff ρ_S is independent of the encoded state. Once we fix S, correcting erasures on S is equivalent to correcting arbitrary linear operators supported on S.

Let $E_a = |k\rangle\langle j|$ and $E_b = |k\rangle\langle i|$ where i, j, and k are bitstrings labelling basis vectors for the qubits just in S. We use variant 1 of the QECC conditions from proposition 2.11. Since E_a and E_b are always supported on S,

$$\begin{aligned} \operatorname{tr}(|\psi\rangle\langle\psi| E_a^\dagger E_b) &= \langle i|\rho_S|j\rangle\langle k|k\rangle & (2.80) \\ &= (\rho_S)_{ij}. & (2.81) \end{aligned}$$

As we let i and j vary over all possible basis states for S, equation (2.69) says that ρ_S does not depend on which codeword $|\psi\rangle$ we have, proving the forward direction of the proposition.

The reverse direction follows easily from variant 1 or variant 3 of proposition 2.11: If ρ_S is independent of $|\psi\rangle$, then taking the trace of ρ with operators on S will also give something independent of $|\psi\rangle$. □

2.6 What Makes a Good QECC?

Before we get any further in our discussion of quantum error-correcting codes, it is worth stopping to think about what we want out of a code. The first thing that comes to mind is that we want it to be good at correcting errors, so we want the set $\mathcal{E}$ of correctable errors to be large. When we're dealing with a t-error channel, we want the distance of the QECC to be large.

In order to correct errors, we have to add some extra qubits. For instance, to make the 9-qubit code, we had to add 8 extra qubits to encode 1. That 9 : 1 ratio seems pretty bad, so we'd like to find codes that use less overhead. In other words, we want k, the number of encoded qubits, to be large, and n, the number of physical qubits, to be small. Certainly we need $n > k$, but we'd like the *rate* k/n to be as close to 1 as possible. It's not clear a priori whether it's better to have a code with large k or small k, so we'd like good examples of codes for any value of k.

In general, if we fix t (the number of errors corrected) and let k get larger, we can make k/n larger too. However, this is rarely a sensible thing to do. As n gets larger, there are more opportunities for errors, so the expected number of errors gets larger. A better plan is to fix t/n when we vary n. In that scenario, there is a definite limit on the rate k/n that can be achieved, and we'd like to get as close to it as possible. We'd also like to know, theoretically, what the best possible rate is so that we know what to shoot for when designing codes. A family of codes that has both k/n and t/n as constants when n gets arbitrarily large is known as a *good* family of codes, and such code families are known.

The three parameters n, k, and d encapsulate the most interesting properties of a code, but not the only interesting ones. In part II, we'll talk about fault-tolerant quantum computation, and we'd like codes that are good for doing fault-tolerant protocols. We'd like a code that has a nice succinct classical description — describing even a single state on n qubits could require specifying 2^n amplitudes, and to specify a QECC we might need to list all 2^k states in a basis for the code subspace. Preferably, the n and k values of the code will be in the correct size range for the application we have in mind — we wouldn't want to have to add lots of extra logical qubits in order to use an otherwise nice code.

We'd also like the encoding and decoding operations to be implementable with a reasonable number of quantum gates. Frequently, when there is a short description of the code, the encoder can be performed with a small circuit. For instance, this is the case for the stabilizer codes which will be introduced in chapter 3. Ideally, the encoder would run in time $O(n)$ for a code with n physical qubits, and that is harder to achieve. (An arbitrary stabilizer code takes time $\Omega(n^2/\log n)$ to encode.) We might want additional properties, for instance that the encoding circuit can be implemented easily in a two-dimensional layout.

Decoding is a much more sticky problem. Even codes with a simple description may have a very difficult decoder. For the 9-qubit code, we had an error syndrome which identified the error. The error syndrome is not well-defined for all QECCs, but even if we restrict attention to codes with an error syndrome, we are faced with the *syndrome decoding problem* of determining the actual error given the error syndrome.

The syndrome decoding problem is NP-hard for most broad classes of codes. (This is true even for classical error-correcting codes.) When we come up with new codes, we'd like ones for which the decoding problem is not nearly as hard. Again, the ideal solution would be a code for which the syndrome decoding problem can be solved in linear time. Such codes exist, but they are somewhat rare.

This is a rather long wish list of properties we'd like out of a code. It's actually possible to satisfy many of them at the same time, but we don't currently know of any QECCs that are perfect in all respects. In other words, choosing a code is a matter of trade-offs. We'll want to use one code for some purposes and a different code for other purposes, depending on which property is most desirable for our current goal.

One thing to bear in mind when looking for a new code is that codes which look different may have pretty much the same properties. For instance, if you switch the first and second qubits of a code, you probably have a different subspace than you did before, but it doesn't really deserve the name of a new code. We capture this intuition with the notion of equivalent codes:

Definition 2.8. Two QECCs C and C' on n physical qubits are *equivalent* if C' can be produced from C by performing some set of single-qubit unitaries and by permuting the qubits.

The notion of equivalence can of course be extended to codes on a q^n-dimensional Hilbert space as well. Two equivalent codes have the same basic properties.

Proposition 2.13. *If C and C' are equivalent, then C and C' have the same number of logical qubits and the same distance.*

It's not necessarily true that C and C' correct exactly the same set of errors, since the local unitaries and permutations of the qubits can scramble up the errors. However, it's always true that an equivalence will map errors into errors of the same weight. It's also true that a fast decoding procedure for C will give a fast decoding procedure for C', so the codes don't differ in computational complexity either.

When you're looking for new codes, if you find a code that's equivalent to a known code, you probably shouldn't consider it to be new. It's not always straightforward to tell if two codes are equivalent, however. The safest thing is to find codes with new (hopefully better) parameters $((n, K, d))$ than preexisting codes.

Chapter 3

Will The Real Codeword Please Stand Still?: Stabilizer Codes

The treatment of QECCs in the last chapter was very general, but a bit unwieldy, particularly when it comes to finding new codes. We'd like a better method of discussing, manipulating, and finding QECCs, even if it comes at the cost of restricting somewhat the codes we can talk about. This chapter introduces the class of stabilizer codes, which have some nice properties and are much more tractable for most purposes than a general QECC. Stabilizer codes are built around a group of symmetries of the code that can distinguish between correct codewords and states with errors: The incorrect states will change under the action of the symmetry, while the correct ones will stay put.

3.1 The 9-Qubit Code Revisited

3.1.1 Error Syndrome Measurement for the 9-Qubit Code

The 9-qubit code is a stabilizer code, so I'll introduce the basic idea of a stabilizer code with some further examination of the nine-qubit code. Let's consider more carefully exactly what we measure when we measure the error syndrome for the nine qubit code. There are two parts to it: We measure each set of three qubits to see if one is different in the standard basis, and then we compare the three phases of the three sets of three qubits to see if one of the phases is different from the other two.

Recall that to determine if one of three qubits is different, we make two measurements. One measurement determines the parity of the first two qubits, and the other tells us the parity of the second and third qubits. Let us put that in a more quantum language: Determining the parity of two qubits is the same as measuring the eigenvalue of $Z \otimes Z$ on those qubits.

$$Z \otimes Z = \begin{pmatrix} +1 & 0 & 0 & 0 \\ 0 & -1 & 0 & 0 \\ 0 & 0 & -1 & 0 \\ 0 & 0 & 0 & +1 \end{pmatrix} \begin{matrix} 00 \text{ (even)} \\ 01 \text{ (odd)} \\ 10 \text{ (odd)} \\ 11 \text{ (even)} \end{matrix} \tag{3.1}$$

Eigenvalue $+1$ corresponds to even parity (syndrome bit 0) and eigenvalue -1 corresponds to odd parity (syndrome bit 1). Thus, within each set of three, to figure out if one qubit is different in the standard basis, we should measure $Z \otimes Z \otimes I$ and $Z \otimes I \otimes Z$.

We also need to determine whether two sets of three have the same phase or opposite phase. We'd like to phrase this as measurement of an eigenvalue. It should probably involve X, since the eigenvalues of X tell us the phase in $|0\rangle \pm |1\rangle$, but we actually have an entangled state. To determine the phase of $|000\rangle \pm |111\rangle$ we should instead measure the eigenvalue of $X \otimes X \otimes X$. To determine whether two sets of three have the same phase or opposite phase, we should thus measure the eigenvalue of the tensor product of six X's on

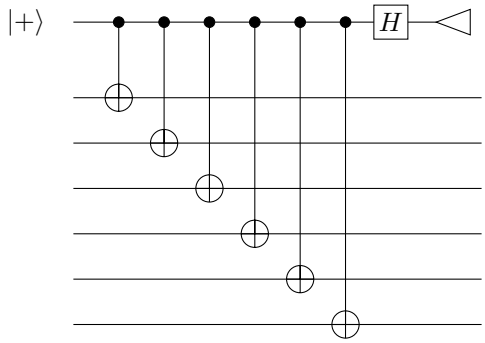

Figure 3.1: A non-fault-tolerant measurement procedure for $X \otimes X \otimes X \otimes X \otimes X \otimes X$.

Z	Z							
	Z	Z						
			Z	Z				
				Z	Z			
						Z	Z	
							Z	Z
X	X	X	X	X	X			
			X	X	X	X	X	X

Table 3.1: The generators of the stabilizer for the nine-qubit code. Blank spaces represent I operators.

the six relevant qubits. Remember, we want to learn whether the phases are the same or different without learning the actual value of each phase.

In case you're curious as to how one would actually measure this eigenvalue, you can look at figure 3.1. The question of how to measure the eigenvalue of a tensor product of arbitrary Paulis will be discussed in detail in section 12.1. Most of the focus of that section is on how to do the measurement fault-tolerantly, but it starts by discussing how to make a non-fault-tolerant measurement.

3.1.2 The Stabilizer for the 9-Qubit Code

The error syndrome for the 9 qubit code is 8 bits long: 2 bits for each set of three, identifying a bit flip error within that group of qubits, plus 2 additional bits telling us if and where a phase error has occurred. Putting together the list of all the operators whose eigenvalues give us those syndrome bits, we get the list in table 3.1. Each row corresponds to one operator, and the operator in column i indicates how that operator acts on qubit i. Blank spaces should be interpreted as I. Thus, the first row is the operator $Z \otimes Z \otimes I \otimes I \otimes I \otimes I \otimes I \otimes I \otimes I$. In other stabilizers, sometimes I will include the Is and sometimes omit them, whichever is most aesthetically appealing. (OK, maybe clarity plays a role too. And whimsy, definitely whimsy.)

As I mentioned in section 2.2, the choice of what qubits to measure for the error syndrome is not unique. For instance, we could have compared the parity of the first and third qubits. The parity would then be given by the eigenvalue of the operator $Z_1 Z_3$. Notice that $Z_1 Z_3$ is the product of the first two rows of table 3.1, and naturally the eigenvalue of the product will be the product of the eigenvalues. In general, we could use any product M of the operators listed in the table. The eigenvalue of M will tell us some information about the errors, but it won't be *new* information, since the eigenvalue of M can be determined from the eigenvalues of the operators used in the product.

Really, the operators we can measure to tell us about the error form a group, known as the *stabilizer* of

the nine-qubit code. The eight operators listed in table 3.1 are the *generators* of the stabilizer. Choosing a different way of defining the error syndrome of the code corresponds to choosing a different set of generators of the stabilizer.

Notice that we use tensor products of Zs to identify X (bit flip) errors, and we use tensor products of Xs to identify Z (phase flip) errors. The pattern here is that the errors anticommute with the stabilizer elements used to find them, and it is this property that makes stabilizers useful for discussing quantum error-correcting codes.

3.2 Pauli Group

I warned that you would be sick of the Pauli operators by the end of this book, and this chapter will get you started. Stabilizer codes are built around the Pauli operators, as you can perhaps see from the example of the nine-qubit code. It's therefore worth examining them in more detail.

Definition 3.1. The *Pauli group* P_n is composed of tensor products of I, X, Y, and Z on n qubits, with an overall phase of ± 1 or $\pm i$.

I will refer to elements of the n-qubit Pauli group as "Pauli operators," "Pauli errors," or just "Paulis" in the future; if I need to make a distinction between P_1 and P_n, I will do so explicitly.

The Pauli group, as its name suggests, is a group: It is closed under multiplication since $Y = iXZ$, and similarly, the product of any two of X, Y, and Z is equal to the third with an overall factor of $\pm i$. In addition, $X^2 = Y^2 = Z^2 = I$. Any tensor product of Paulis is its own inverse, i.e., it squares to I, and if there is an overall phase factor of $\pm i$, it instead squares to $-I$. (I use the one-qubit I and the n-qubit identity I interchangeably.)

The one-qubit Paulis anticommute with each other

$$XZ = -ZX \tag{3.2}$$

$$YZ = -ZY \tag{3.3}$$

$$XY = -YX. \tag{3.4}$$

Of course, I commutes with X, Y, and Z, and any Pauli commutes with itself. More general pairs (P, Q) of operators from P_n always either commute ($PQ = QP$) or anticommute ($PQ = -QP$). The difference from the single qubit case is that for P_1, only trivial pairs commute (when one Pauli is I or both are the same Pauli), but for $n > 1$, there are non-trivial commuting pairs. For instance, $X \otimes X$ commutes with $Z \otimes Z$. I will sometimes use the notation $[P, Q] = PQ - QP$ for the commutator and $\{P, Q\} = PQ + QP$ for the anticommutator.

P_n has 4^{n+1} elements since there are 4^n n-fold tensor products of I, X, Y, and Z, and 4 overall phases they could have. However, for many purposes, we can ignore the phase, giving us effectively 4^n distinct Paulis. If I wish to ignore the phase, I will refer to $\hat{\mathsf{P}}_n$. Thus, $\hat{\mathsf{P}}_n \cong \mathsf{P}_n / \{I, iI, -I, -iI\}$. The elements of $\hat{\mathsf{P}}_n$ are sets of 4 operators of the form $\{\pm P, \pm iP\}$, with P some n-qubit tensor product of I, X, Y, and Z. Each element of $\hat{\mathsf{P}}_n$ can thus be associated with an unsigned Pauli operator P, and it is more convenient by far to refer to elements of $\hat{\mathsf{P}}_n$ in terms of the associated Pauli rather than as a set of Paulis with signs.

Definition 3.2. Let $P \in \mathsf{P}_n$. Then $\hat{P} \in \hat{\mathsf{P}}_n$ is the element of $\hat{\mathsf{P}}_n$ corresponding to P. Similarly, if S is a subset of P_n, then $\hat{S}$ is the subset of $\hat{\mathsf{P}}_n$ consisting of $\hat{P}$ for all $P \in S$.

I have introduced these conventions separating P_n and $\hat{\mathsf{P}}_n$ in order to be mathematically precise. In some cases, we need to work with elements or subsets of P_n, and in some cases, to get the details completely correct, it is better to work with $\hat{\mathsf{P}}_n$. However, almost always, the distinction between the two is a small technical detail. My advice is to ignore the difference between P_n and $\hat{\mathsf{P}}_n$ unless you get confused.

Any Pauli operator has eigenvalues $+1$ and -1. Each eigenspace is exactly half the Hilbert space. That is, the $+1$ and -1 eigenspaces have dimension 2^{n-1}.

One feature of the Pauli group already mentioned is that P_n spans the space of all n-qubit linear operations. The weight t Paulis span the set of t-qubit errors. As discussed in corollary 2.5, this property means that to have a t-error correcting QECC, it suffices to correct all weight t Pauli operators.

This section has only discussed the most basic properties of the Pauli group. It has many more useful properties, some of which we will encounter in future sections of the book. Don't be surprised, however, if someday you are trying to solve a problem and discover a new property of the Paulis that is not mentioned in this book. In group theory, the Pauli group is an *extraspecial* group, and it truly deserves that name.

3.3 Stabilizer Codes

3.3.1 Definition and Basic Properties of the Stabilizer

Given a general quantum error-correcting code, we can define its stabilizer in more or less the same way as we did for the nine-qubit code:

Definition 3.3. Given a QECC $T \subseteq \mathcal{H}_{2^n}$, the *stabilizer* $\mathsf{S}(T)$ is

$$\mathsf{S}(T) = \{M \in \mathsf{P}_n | M|\psi\rangle = |\psi\rangle \ \forall |\psi\rangle \in T\}. \tag{3.5}$$

In other words, the stabilizer is composed of the Pauli operators for which all codewords are $+1$ eigenstates. In principle, one could define a stabilizer consisting of all unitaries which fix every codeword, but it turns out to be most useful to concentrate on the Pauli operators.

Proposition 3.1. *The stabilizer $\mathsf{S}(T)$ of a nonempty QECC T has three basic properties:*

a) $-I \notin \mathsf{S}(T)$

b) $\mathsf{S}(T)$ *is a group*

c) $\mathsf{S}(T)$ *is Abelian*

The property of being Abelian is the least obvious, but it makes sense since we want a set of operators which have the codewords as simultaneous eigenstates. Normally, for this to be possible, the operators should commute; in general, they only need to commute on a subspace, but for Pauli operators this is only possible if they truly commute.

Proof.

a) $-I$ has no $+1$ eigenstates, so it cannot be in the stabilizer.

b) If $M, N \in \mathsf{S}(T)$, it is clear that their product is also in $\mathsf{S}(T)$: For any $|\psi\rangle \in T$,

$$MN|\psi\rangle = M|\psi\rangle = |\psi\rangle. \tag{3.6}$$

c) By the argument for property 2, $MN|\psi\rangle = NM|\psi\rangle$ for any $|\psi\rangle \in T$, $M, N \in \mathsf{S}(T)$. Thus, $[M, N]$ annihilates the codewords. Paulis either commute or anticommute. If M and N anticommute, then $[M, N] = 2MN$, which is again an element of P_n, and therefore has no 0 eigenvalues. Therefore, the only option is that M and N commute.

□

It turns out to be most useful, when dealing with stabilizers, to work the other way around. We are given (or invent) a stabilizer with the properties we desire, and then use it deduce the code.

Definition 3.4. Let $\mathsf{S} \subseteq \mathsf{P}_n$ be an Abelian group, with $-I \notin \mathsf{S}$. Then define the code space corresponding to S by

$$\mathcal{T}(\mathsf{S}) = \{|\psi\rangle \text{ s.t. } M|\psi\rangle = |\psi\rangle \ \forall M \in \mathsf{S}\} \tag{3.7}$$

X	Z	Z	X	I
I	X	Z	Z	X
X	I	X	Z	Z
Z	X	I	X	Z

Table 3.2: The generators for the five-qubit code.

In general, $T \subseteq \mathcal{T}(\mathsf{S}(T))$, but when they are actually equal, the code has special properties.

Definition 3.5. If T is a QECC with $T = \mathcal{T}(\mathsf{S}(T))$, it is a *stabilizer code*.

Stabilizer codes are also sometimes known as *symplectic codes*, *additive codes*, or GF(4) *additive codes* for reasons that will be discussed in section 3.5 and section 5.2.

If we define a code from its stabilizer, then it is always a stabilizer code. In other words, a stabilizer code is one that could be defined just by giving its stabilizer. This is a consequence of the following proposition:

Proposition 3.2. $\mathsf{S} = \mathsf{S}(\mathcal{T}(\mathsf{S}))$.

I delay the proof until section 3.5 to keep you in suspense. Also, the proof will use a tool I won't introduce until then.

When dealing with stabilizer codes, I will frequently refer to the stabilizer S as the code instead of using the rather unwieldy phrase "stabilizer of the code $\mathcal{T}(\mathsf{S})$." When $M \in \mathsf{S}$, I will call M a "stabilizer element" or some variant of that phrase. However, many people seem to find that terminology unwieldy too, and just call M a "stabilizer." I do not approve of that usage, but I can't stop you if you want to say it.

Frequently we will want to pick a particular generating set $\{M_1, \ldots, M_r\}$ for the stabilizer, as we did for the nine-qubit code. In a minimal generating set no generator is a product of other generators. When we take a product of generators, the order does not matter since the generators commute. Also, note that since $-I \notin \mathsf{S}$, all elements of S must square to I, and any power of a generator greater than 1 can be reduced. Therefore, the elements of the stabilizer are uniquely determined by taking a product

$$M_{i_1,\ldots,i_r} = \prod_j M_j^{i_j}, \tag{3.8}$$

with $i_j \in \{0, 1\}$. This implies $|\mathsf{S}| = 2^r$.

Naturally, the set of generators is not unique, but when we do have a particular generating set to work with, I will talk about its elements as "stabilizer generators" or just "generators." When you describe a stabilizer, almost always the easiest way to do so is by listing one particular set of generators. The generators are enough to define the whole stabilizer, and it is much easier to list r generators than to list all 2^r elements of the stabilizer.

The code space of a stabilizer code is defined by requiring that all the eigenvalues be $+1$, but there is nothing magical about the $+1$ eigenstates. After all, a -1 eigenstate of M is a $+1$ eigenstate of $-M$, which is still in P_n. Given any set of generators $\{M_i\}$, we could define the code equally well by taking the -1 eigenstate, but switching M_i to $-M_i$. We *can't* arbitrarily change the eigenvalues associated with non-generators because the eigenvalues of the non-generators can be deduced from the eigenvalues of the generators. The generators are independent of each other, so we can pick their eigenvalues freely, but once we've done that, it defines the eigenvalues of all operators in the stabilizer. For more on this point, see section 3.5.

I'll conclude this subsection with a second example QECC to go with the nine-qubit code. This code has five physical qubits, and is, unsurprisingly, known as the "five-qubit code." The stabilizer for the five-qubit code is given in table 3.2. The code is cyclic: if you permute the qubits cyclically, you'll get the same stabilizer. You can almost see this from table 3.2. Shifting by one qubit for generators one through three gives you generators two through four. However, the fifth permutation $Z \otimes Z \otimes X \otimes I \otimes X$ is not one of the generators. Nevertheless, it is still in the stabilizer, as the product of all four generators given in the table.

Even though it's not a generator, it still has the same status in the code as the four operators that are listed. Indeed, we could have chosen any four of these five operators as a set of generators without changing the code.

3.3.2 Projection Operator on a Stabilizer Code Subspace

In order to convert back from the representation of a stabilizer code in terms of its stabilizer to one as a subspace of a larger physical Hilbert space, we have definition 3.4, but it is sometimes helpful to have something more concrete. In particular, we'd like a projection operator that defines the subspace.

The codewords are supposed to be $+1$ eigenvectors of every element of the stabilizer, although it is sufficient to check that they are $+1$ eigenvectors of the stabilizer generators. The projector on the $+1$ eigenspace of generator M_i is $(I + M_i)/2$. Therefore, the projector on the code space of S is

$$\Pi_{\mathsf{S}} = \frac{1}{2^r} \prod_{i=1}^{r} (I + M_i), \tag{3.9}$$

when the stabilizer has r generators. Only states that are codewords — $+1$ eigenvectors of all generators — will avoid being annihilated by Π_{S}, and any codeword will be left alone by Π_{S}, as desired. Note that the order of the generators in the product does not matter since they all commute.

We can rewrite the projector Π_{S} in an interesting way by multiplying out the product. We get a sum of terms, each of which consists of a distinct product of the generators $\{M_i\}$. Based on equation (3.8), the products of the generators give us all elements of the stabilizer:

$$\Pi_{\mathsf{S}} = \frac{1}{2^r} \sum_{M \in \mathsf{S}} M. \tag{3.10}$$

We can come up with actual codewords for the code by applying Π_{S} to states in the physical Hilbert space and renormalizing. We might get 0, if the state we started with is orthogonal to the code space, but frequently we'll get a real codeword. For instance, for the five-qubit code, we can apply the projector to $|00000\rangle$ and $|11111\rangle$ to get two orthogonal codewords which can serve as a basis for the code space:

$$\begin{aligned} |\overline{0}\rangle = {} & |00000\rangle + |10010\rangle + |01001\rangle - |11011\rangle + |10100\rangle - |00110\rangle - |11101\rangle - |01111\rangle \\ & + |01010\rangle - |11000\rangle - |00011\rangle - |10001\rangle - |11110\rangle - |01100\rangle - |10111\rangle + |00101\rangle \end{aligned} \tag{3.11}$$

$$\begin{aligned} |\overline{1}\rangle = {} & |11111\rangle + |01101\rangle + |10110\rangle - |00100\rangle + |01011\rangle - |11001\rangle - |00010\rangle - |10000\rangle \\ & + |10101\rangle - |00111\rangle - |11100\rangle - |01110\rangle - |00001\rangle - |10011\rangle - |01000\rangle + |11010\rangle. \end{aligned} \tag{3.12}$$

I got these codewords by working my way through all 16 elements of the stabilizer for the five-qubit code (products of the generators given in table 3.2) and applying them to the starting states. You need to be careful of the signs involved, but otherwise the process is straightforward if tedious.

3.3.3 Distance and Size of a Stabilizer Code

When a stabilizer code is given either as a subspace or via the stabilizer, the number of physical qubits n is immediately obvious. The other two central properties (number k of logical qubits and distance d) are not so obvious, but can be deduced directly from the stabilizer.

Proposition 3.3. *If the stabilizer S on n physical qubits has $|\mathsf{S}| = 2^r$ (i.e., S has r generators), then $\mathcal{T}(\mathsf{S})$ has dimension 2^{n-r}. That is, there are $k = n - r$ logical qubits.*

Intuitively the result is easy to understand. The first generator of the stabilizer divides the Hilbert space into a $+1$ eigenspace and a -1 eigenspace of equal size. The codewords live in the $+1$ eigenspace. Each additional generator divides the subspace available for codewords in half again, so the total available dimension is 2^{n-r}. Non-generators do not divide the space since their eigenvalues can be derived by looking

at the eigenvalues of the generators. This argument is not a proof, since we would need to show that the additional generators divide not just the full Hilbert space in half, but also all the smaller subspaces defined by the earlier generators. The actual proof is straightforward, but less intuitive:

Proof. The dimension of $\mathcal{T}(\mathsf{S})$ is equal to the trace of Π_{S}, the projection operator onto $\mathcal{T}(\mathsf{S})$. Now,

$$\operatorname{tr} \Pi_{\mathsf{S}} = \frac{1}{2^r} \sum_{M \in \mathsf{S}} \operatorname{tr} M. \tag{3.13}$$

However, $\operatorname{tr} P = 0$ for all Paulis P except for the identity. Thus,

$$\operatorname{tr} \Pi_{\mathsf{S}} = \frac{\operatorname{tr} I}{2^r} = \frac{2^n}{2^r}. \tag{3.14}$$

□

You can check the nine-qubit code in this formula: 9 physical qubits, 8 stabilizer generators, and 1 encoded qubit. For the five-qubit code, we have four generators, so again there should be 1 encoded qubit, with the basis codewords we saw above.

There's one special case which is not, strictly speaking, a QECC, but is interesting nonetheless. Yes, it's true, there are some things which are interesting other than quantum error correction. When the stabilizer has n generators on n qubits, proposition 3.3 would tell us we have 0 encoded qubits, which is a Hilbert space of dimension 1. That is, it is a single state, up to normalization.

Definition 3.6. A *stabilizer state* is the code space of a stabilizer with n generators on n qubits.

Since $r = n$ is the maximum number of generators you can have, a stabilizer state is an extreme limit of a QECC. Some constructions of QECCs will alter the number of encoded qubits from another code, and sometimes a stabilizer state can be the starting or ending point of such a construction. Also, stabilizer states are fairly common in the theory of quantum information, even discounting states arising from quantum error correction. For instance, the GHZ state $|000\rangle + |111\rangle$ and the Bell states $|00\rangle \pm |11\rangle$, $|01\rangle \pm |10\rangle$ are stabilizer states.

To understand how to deduce the distance of a stabilizer code, let us go back to the nine-qubit code and recall how it handled errors. The generators of the stabilizer were used to give us bits of the error syndrome. In particular, some generators were able to signal the presence of certain errors while missing other errors, but by looking at the full set of generators, we were able to identify all of the single-qubit errors.

I mentioned that the property responsible for determining whether a generator M is useful for an error E is anticommutation. Let us see how this works. Suppose $M \in \mathsf{S}$ and $E \in \mathsf{P}_n$ anticommutes with M. Then for any $|\psi\rangle \in \mathcal{T}(\mathsf{S})$,

$$M(E|\psi\rangle) = -EM|\psi\rangle = -E|\psi\rangle. \tag{3.15}$$

$|\psi\rangle$ was a $+1$ eigenvector of M — that is the definition of the code space — but $E|\psi\rangle$ is a -1 eigenvector.

Conversely, if E commutes with M then

$$M(E|\psi\rangle) = EM|\psi\rangle = E|\psi\rangle. \tag{3.16}$$

One advantage to dealing with the Pauli group is that these are the only choices. Either M and E commute or they anticommute. If we have an error that commutes with M, M retains a $+1$ eigenvalue, whereas if the error anticommutes with M, M's eigenvalue becomes -1, signaling that an error has occurred.

Definition 3.7. The *normalizer* $\mathsf{N}(\mathsf{S})$ of the stabilizer S is

$$\mathsf{N}(\mathsf{S}) = \{N \in \mathsf{P}_n | NM = MN \ \forall M \in \mathsf{S}\}. \tag{3.17}$$

If you know some group theory, you might recognize this as the definition of the *centralizer* of S (the set of things that commute with all elements of S) rather than the *normalizer* (the set of things that preserve S under conjugation), but because Paulis either commute or anticommute and $-I \notin \mathsf{S}$, they are the same thing for a stabilizer. I am choosing to call it the normalizer rather than the centralizer because the normalizer relates to logical operations, and this is an important function of $\mathsf{N}(\mathsf{S})$, as we shall see shortly in section 3.4.2.

Since the stabilizer is Abelian, $\mathsf{S} \subseteq \mathsf{N}(\mathsf{S})$ always. Indeed, $\mathsf{N}(\mathsf{S})$ also contains $-\mathsf{S}$ and $\pm i\mathsf{S}$. Since we worry about eigenvectors of S, changing the sign of an operator in the stabilizer is important, but $\mathsf{N}(\mathsf{S})$ is about errors, and global phase no longer matters. Therefore, we will usually want to work with $\hat{\mathsf{N}}(\mathsf{S})$.

The normalizer tells us which errors can be detected by the stabilizer code. If a Pauli E is outside the normalizer $\mathsf{N}(\mathsf{S})$, then $E|\psi\rangle$ has an eigenvalue -1 for some $M \in \mathsf{S}$, and thus is detected by measuring the eigenvalues of the stabilizer elements. Note that this is true for *any* codeword $|\psi\rangle$. Also note that it is sufficient to measure the generators of the stabilizer: If N commutes with M_1 and M_2, it also commutes with $M_1 M_2$. Thus, if N commutes with all generators of S, then $N \in \mathsf{N}(\mathsf{S})$.

When $E \in \mathsf{N}(\mathsf{S})$, then $E|\psi\rangle$ has eigenvalue $+1$ for all $M \in \mathsf{S}$, and therefore $E|\psi\rangle \in \mathcal{T}(\mathsf{S})$ for codewords $|\psi\rangle$. You might think that that means it is an undetectable error, but there is actually another class of Paulis that is "detectable" by definition 2.7. If $E \in \mathsf{S}$, then, while it's true that $E|\psi\rangle \in \mathcal{T}(\mathsf{S})$ for any codeword $|\psi\rangle$, it's also true that $E|\psi\rangle = |\psi\rangle$, so E is not actually an "error": it acts like the identity on the code space, leaving codewords unchanged. Ignoring global phases, we can say the same if $\hat{E} \in \hat{\mathsf{S}}$.

Putting this together, we get a characterization of the detectable errors for a stabilizer code.

Theorem 3.4. *The set of undetectable errors for a stabilizer code* S *is* $\hat{\mathsf{N}}(\mathsf{S}) \setminus \hat{\mathsf{S}}$. *The distance of* S *is* $\min\{\operatorname{wt} E | \hat{E} \in \hat{\mathsf{N}}(\mathsf{S}) \setminus \hat{\mathsf{S}}\}$.

The slanty line is a "set minus" operation. That is, $\hat{\mathsf{N}}(\mathsf{S}) \setminus \hat{\mathsf{S}}$ consists of those elements of $\hat{\mathsf{N}}(\mathsf{S})$ that are not in $\hat{\mathsf{S}}$.

Proof. We can prove the first statement directly from the definition of the set of detectable errors (definition 2.7). The second statement will then follow immediately from the definition of distance. We need to consider three cases for E. In cases 1 and 2, $|\psi\rangle$ and $|\phi\rangle$ are arbitrary codewords.

1. Case 1: $\hat{E} \in \hat{\mathsf{S}}$. Then for some choice of phase, $E \in \mathsf{S}$ and $E|\phi\rangle = |\phi\rangle$, so

$$\langle\psi|E|\phi\rangle = \langle\psi|\phi\rangle, \tag{3.18}$$

   and $c(E) = 1$. $\hat{E}$ is detectable.

2. Case 2: $\hat{E} \notin \hat{\mathsf{N}}(\mathsf{S})$. Then $\exists M \in \mathsf{S}$ such that $\{M, E\} = 0$ (for any choice of phase of E), so $M(E|\phi\rangle) = -E|\phi\rangle$, as per equation (3.15). Then

$$\langle\psi|E|\phi\rangle = \langle\psi|MEM|\phi\rangle = -\langle\psi|E|\phi\rangle = 0, \tag{3.19}$$

   since $M^2 = I$ for stabilizer elements. Thus $c(E) = 0$ and E is detectable.

3. Case 3: $\hat{E} \in \hat{\mathsf{N}}(\mathsf{S}) \setminus \hat{\mathsf{S}}$. Since $E \notin \mathsf{S}$, $\exists$ codeword $|\phi\rangle$ such that $E|\phi\rangle \neq |\phi\rangle$. Let $|\psi\rangle = E|\phi\rangle$. Since $E \in \mathsf{N}(\mathsf{S})$, $|\psi\rangle$ is also a codeword. However,

$$\langle\psi|E|\phi\rangle = 1 = \frac{1}{\langle\psi|\phi\rangle}\langle\psi|\phi\rangle, \tag{3.20}$$

   whereas

$$\langle\phi|E|\phi\rangle = \langle\phi|\psi\rangle = (\langle\phi|\psi\rangle)\langle\phi|\phi\rangle. \tag{3.21}$$

   Comparing equations (3.20) and (3.21) to definition 2.7 tells us that $\hat{E}$ is not detectable unless $|\langle\phi|\psi\rangle| = 1$, meaning $E|\phi\rangle = e^{i\theta}|\phi\rangle$. Furthermore, by equation (3.21), $\hat{E}$ is undetectable unless θ is the same for all $|\phi\rangle$. But that is not possible, since that would imply $\hat{E} \in \hat{\mathsf{S}}$.

X	X	X	X
Z	Z	Z	Z

Table 3.3: The stabilizer for the four-qubit code.

□

The key point here is that when $E \in \hat{\mathsf{N}}(\mathsf{S}) \setminus \hat{\mathsf{S}}$, then E maps some codewords to *different* codewords. That's the essence of an undetectable error, because the code has no way of knowing if a codeword is the original encoding of the state or the result of the action of the error on a different codeword.

Moving now to correcting errors, we find

Theorem 3.5. *The stabilizer code* S *corrects a set of errors* $\mathcal{E} \subseteq \mathsf{P}_n$ *iff* $\hat{E}^\dagger \hat{F} \notin \hat{\mathsf{N}}(\mathsf{S}) \setminus \hat{\mathsf{S}}$ *for all* $E, F \in \mathcal{E}$.

The theorem follows immediately from theorem 3.4 by comparing definition 2.7 with theorem 2.7. Recall that by the linearity of QECCs, and particularly corollary 2.5, it suffices to consider Pauli errors to understand the error-correcting capabilities of the code, at least when we are interested in correcting t-qubit errors.

For stabilizer codes, we have a slightly different notation than the more general $((n, K, d))$ notation that applies to arbitrary QECCs. Since the encoded subspace has a dimension that's always a power of 2, we write the code in terms of the number of encoded qubits k rather than the dimension $K = 2^k$ of the logical Hilbert space. We also use square brackets to indicate that we are dealing with a stabilizer code.

Notation 3.8. A stabilizer code with n physical qubits, k logical qubits, and distance d is denoted as an $[[n, k, d]]$ code. If the distance is unknown or irrelevant, it is an $[[n, k]]$ code.

We know that the nine-qubit code corrects a single-qubit error, so it must have distance at least 3. In fact, there are some 3-qubit Paulis (such as $X_1X_2X_3$) in $\hat{\mathsf{N}}(\mathsf{S}) \setminus \hat{\mathsf{S}}$ for the code, so the distance is exactly 3. Thus, the nine-qubit code is a $[[9, 1, 3]]$ code. The five-qubit code also turns out to have distance 3, so it is a $[[5, 1, 3]]$ code. Note that these codes are also $((9, 2, 3))$ and $((5, 2, 3))$ codes, but the more specific notation for a stabilizer code is generally used for them. As it happens, the five-qubit code is the smallest distance 3 code. You'll see the proof of that, as well as other techniques for proving limits on QECCs, in chapter 7.

You might wonder about distance 2 codes, since all the QECCs we have seen so far have distance 3. Distance 2 codes tend to be much simpler, but they can still be interesting. After all, a distance 2 code can detect one error or correct one erasure. The smallest distance 2 code is a $[[4, 2, 2]]$ code given in table 3.3. It is not hard to see that any one-qubit Pauli will anticommute with one or both of the two generators, but there are some two-qubit Paulis (e.g., $X \otimes X \otimes I \otimes I$) that commute with both. Thus, the code has distance 2.

3.3.4 Degeneracy and Stabilizer Codes

When is a stabilizer code degenerate? In the proof of theorem 3.4, we implicitly calculated the matrix C_{ab}. In particular, we found that $C_{ab} = 0$ if $E^\dagger F \notin \mathsf{N}(\mathsf{S})$ and $C_{ab} = 1$ if $E^\dagger F \in \mathsf{S}$. Any set of Paulis is linearly independent, so we just need to check if the resulting C_{ab} has maximum rank.

If $E_1^\dagger E_2 \in \mathsf{S}$, then $E_1^\dagger F \in \mathsf{S} \Leftrightarrow E_2^\dagger F \in \mathsf{S}$, so in this case the rows (or columns) of C_{ab} associated with E_1 and E_2 are the same. When $E_1^\dagger E_2 \notin \mathsf{S}$, then only one (or neither) of $E_1^\dagger F$ and $E_2^\dagger F$ can be in S, so in this case the rows associated with E_1 and E_2 cannot have 1s in the same column. Thus, we get the following proposition:

Proposition 3.6. *A stabilizer code* S *is degenerate for the error set* $\mathcal{E}$ *iff* $\exists E_1, E_2 \in \mathcal{E}$ *with* $E_1^\dagger E_2 \in \mathsf{S}$.

As with general QECCs, we can define degeneracy as a property of the code subspace without referring to specific set of errors by considering the distance. In the case of stabilizer codes, motivated by the above analysis, we can also sensibly define degeneracy when the code is used for error detection rather than error correction.

Definition 3.9. A stabilizer code S with distance d is *degenerate* if $\exists M \in \mathsf{S}$, $M \neq I$, with $\mathrm{wt}\, M < d$.

Note that this is slightly more general than the generic notion of a degenerate code. A stabilizer code with distance $d = 2t+2$ can be degenerate if S contains any elements of weight $2t+1$, but degeneracy wasn't defined for general non-stabilizer QECCs of even distance.

Looking once more at the stabilizer of the nine-qubit code (table 3.1), it is immediately obvious that it is a degenerate code. There are many generators of weight 2 and the code has distance 3. However, it is not always obvious from looking at the generators whether a stabilizer code is degenerate or not. It may be that the set of generators given to you all have high weight, but there is some product of the generators that does not. The five-qubit code is non-degenerate because all of the operators in the stabilizer have weight 4, but to see that you need to do some work.

3.4 Cosets and Error Syndromes

3.4.1 The Error Syndrome and the Stabilizer

For the nine-qubit code, we figured out the stabilizer by thinking about what we wanted to measure for the error syndrome. Each generator corresponded to a bit of the error syndrome. In fact, this is completely general:

Definition 3.10. Suppose S is a stabilizer code with generators $M_1, \ldots, M_r$ and $|\psi\rangle$ is an eigenvector (not necessarily with eigenvalue $+1$) of all $N \in \mathsf{S}$. The *error syndrome* of $|\psi\rangle$ is an r-bit string with ith bit 0 if $|\psi\rangle$ is a $+1$ eigenvector of M_i and ith bit 1 if $|\psi\rangle$ is a -1 eigenvector of M_i. The error syndrome $\sigma(E) : \mathsf{P}_n \to \mathbb{Z}_2^r$ is the error syndrome of $E|\phi\rangle$ for any codeword $|\phi\rangle$. When the stabilizer associated with a syndrome is in doubt, we will write $\sigma_{\mathsf{S}}(E)$.

If $P, Q \in \mathsf{P}_n$, then $c(P,Q) = 0$ if P and Q commute and $c(P,Q) = 1$ if they anticommute. ($c(P,Q) : \mathsf{P}_n \times \mathsf{P}_n \to \mathbb{Z}_2$.)

For a Pauli, bit i of the error syndrome is the same as $c(E, M_i)$. Note that the syndrome of E will be the same no matter what codeword $|\psi\rangle$ we choose to evaluate. This follows from equations (3.15) and (3.16) and means that Pauli errors map the code space, which is a subspace with $+1$ eigenvalue for all stabilizer elements, to a subspace that has a different set of eigenvalues, but for which each eigenvalue is still shared for all states in the subspace.

The subspaces derived this way are also error-correcting codes, but they are associated with different eigenvalues of the stabilizer. We can reinterpret them as traditional stabilizer codes (with all $+1$ eigenvalues) by replacing M_i with $-M_i$ whenever the ith syndrome bit is 1. Note that there are 2^r possible values of the error syndrome, and each subspace is isomorphic to the code space, which has dimension 2^k. When there are n physical qubits, $r = n - k$. Also, all the subspaces of different error syndromes are orthogonal to each other, since they have different eigenvalues. Thus, the full Hilbert space $\mathcal{H}_{2^n}$ decomposes as a direct sum of the 2^{n-k} subspaces associated with different syndromes.

Proposition 3.7. *The $c(P,Q)$ and $\sigma(E)$ functions have the following properties. In all cases, $+$ refers to binary addition.*

a) $c(P_1P_2, Q) = c(P_1, Q) + c(P_2, Q)$.

b) $c(P,Q) = c(Q,P)$.

c) $\sigma(EF) = \sigma(E) + \sigma(F)$.

These are straightforward to verify.

The various error syndromes are associated with different cosets of the normalizer in P_n.

Proposition 3.8. *Let $E, F \in \mathsf{P}_n$, and S be a stabilizer. Then F and E are in the same coset of $\mathsf{N}(\mathsf{S})$ iff E and F have the same error syndrome.*

Proof.

$\Rightarrow$: If E and F are in the same coset, then $F = EN$, with $N \in \mathsf{N}(\mathsf{S})$. Let $M \in \mathsf{S}$. Then $c(F, M) = c(E, M) + c(N, M)$. But $N \in \mathsf{N}(\mathsf{S})$, so $c(N, M) = 0$. Therefore the error syndromes of E and F are the same.

$\Leftarrow$: The argument works the other way too: Let $N = E^\dagger F$. If the error syndromes of E and F are the same, then $c(N, M) = 0$ for all $M \in \mathsf{S}$. Therefore, $N \in \mathsf{N}(\mathsf{S})$.

□

In much the same way as the full Hilbert space can be written as a direct sum of subspaces associated to different syndromes, the whole Pauli group can be partitioned into cosets of $\mathsf{N}(\mathsf{S})$, each associated with a different syndrome. All the cosets are the same size and there are 2^r of them. As a consequence, we know the size of the normalizer:

Proposition 3.9. $|\mathsf{N}(\mathsf{S})| = 4 \cdot 2^{n+k}$ *when* S *has* n *physical qubits and* k *logical qubits.*

3.4.2 Cosets inside the Normalizer

We can similarly analyze the cosets of S in $\mathsf{N}(\mathsf{S})$.

Proposition 3.10. *Let* $N_1, N_2 \in \mathsf{N}(\mathsf{S})$*. Then* N_1 *and* N_2 *are in the same coset of* S *iff* $N_1|\psi\rangle = N_2|\psi\rangle$ *for all codewords* $|\psi\rangle$*.*

Proof. $N_1|\psi\rangle = N_2|\psi\rangle$ iff $|\psi\rangle$ is a $+1$ eigenstate of $M = N_1^\dagger N_2$. This is true for all codewords $|\psi\rangle$ iff $M \in \mathsf{S}$. However, N_1 and N_2 are in the same coset of S iff $N_2 = N_1 M$ with $M \in \mathsf{S}$. □

Recall that when $N \in \mathsf{N}(\mathsf{S})$, then $N|\psi\rangle$ is a codeword for any input codeword $|\psi\rangle$. Thus, N is a *logical operation*: it always maps codewords to (possibly different) codewords. Since the different representatives of a coset of S act the same way on codewords, they are all different realizations of the *same* logical operation. Thus, the set $\mathsf{N}(\mathsf{S})/\mathsf{S}$ is of particular interest, since it consists of the distinct logical operations performed by the normalizer. (S is a normal subgroup of $\mathsf{N}(\mathsf{S})$ by definition, so we can take this quotient without any difficulties.)

Theorem 3.11. *Let* S *be a stabilizer with* n *physical qubits and* k *logical qubits. Then* $\mathsf{N}(\mathsf{S})/\mathsf{S} \cong \mathsf{P}_k$*.*

The quotient group $\mathsf{N}(\mathsf{S})/\mathsf{S}$ can be taken to be the *logical Pauli group*, performing Paulis on the encoded qubits. The proof of theorem 3.11 will be in section 3.5.

We can also look at cosets of S in the full Pauli group P_n, as in figure 3.2. Each coset of $\mathsf{N}(\mathsf{S})$ breaks up into cosets of S, so we can associate each coset of S in P_n with an error syndrome, inherited from the coset of $\mathsf{N}(\mathsf{S})$ which it sits within. If we pick a particular representative E of the coset of $\mathsf{N}(\mathsf{S})$, then we can again identify the coset of S with a logical operation $\overline{P} \in \mathsf{N}(\mathsf{S})/\mathsf{S}$; the interpretation of the coset is then a combination of the logical operation $\overline{P}$ and the error E.

When we perform decoding on a stabilizer code, we do just this. For each error syndrome s, we assign a particular error E_s with $\sigma(E_s) = s$. If our syndrome measurement gives s, we assume the error actually was E_s and correct that. If the error was actually some E' with the same syndrome, we hope that E_s and E' are in the same coset of S. If not, there has been a logical Pauli error, the one associated with the actual coset of S in which E' lies.

Theorem 3.12. *If* S *is a non-degenerate stabilizer code, the error syndromes of all errors in the correctable error set* $\mathcal{E}$ *are distinct. If* S *is a degenerate code,* E *and* F *have the same error syndrome iff* $\hat{E}^\dagger \hat{F} \in \hat{\mathsf{S}}$*.*

Proof. By proposition 3.8, two errors $E \neq F \in \mathcal{E}$ have the same error syndrome iff they are in the same coset of $\mathsf{N}(\mathsf{S})$, meaning $E^\dagger F \in \mathsf{N}(\mathsf{S})$. But both errors are correctable, and by theorem 3.5, $\hat{E}^\dagger \hat{F} \notin \hat{\mathsf{N}}(\mathsf{S}) \setminus \hat{\mathsf{S}}$, so $E^\dagger F \in \mathsf{N}(\mathsf{S})$ iff $\hat{E}^\dagger \hat{F} \in \hat{\mathsf{S}}$. Thus, the error syndromes of two correctable errors E and F are the same iff $\hat{E}^\dagger \hat{F} \in \hat{\mathsf{S}}$. If this ever occurs, the code is degenerate. □

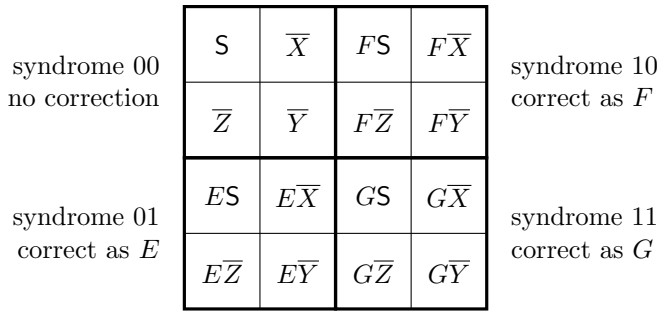

Figure 3.2: Cosets of the normalizer and stabilizer in the Pauli group. The errors E, F, and G are chosen as canonical errors for the syndromes 01, 10, and 11.

	X	Z	Z	X	I
	I	X	Z	Z	X
	X	I	X	Z	Z
	Z	X	I	X	Z
$\overline{X}$	X	X	X	X	X
$\overline{Z}$	Z	Z	Z	Z	Z

Table 3.4: The generators for the five-qubit code supplemented by representatives for logical Paulis.

Applying this theorem is one way to see that the five-qubit code has distance 3 and is non-degenerate. There are 15 possible one-qubit errors (X, Y, Z on each of five qubits), plus the identity. There are 4 generators, so there are 16 error syndromes. If you list the syndromes of the 16 errors, you'll find that each one is unique. There are no syndromes left over, so the five-qubit code is known as a *perfect* code.

It is frequently helpful to also pick representatives of the cosets of S in the normalizer. These representatives don't have an interpretation in error correction, but they do give us concrete realizations of the logical Pauli group, which is helpful in fault-tolerant computation. For now, they are simply convenient computational tools. We don't actually need to pick representatives for every coset of S. Since $\mathsf{N}(\mathsf{S})/\mathsf{S}$ has a group structure itself, it is sufficient to pick representatives of generators of $\mathsf{N}(\mathsf{S})/\mathsf{S}$ and let the generators of other cosets be determined by multiplication. In other words, we can pick representatives for $\overline{X}_i$ and $\overline{Z}_i$ for $i = 1, \ldots, k$. (The subscript i here means the operator acts on the ith logical qubit, not the ith physical qubit.) I have done this for the five-qubit code and the four-qubit code in tables 3.4 and 3.5. Then, for instance, you can get $\overline{Y}$ for the five qubit code to be $i\overline{X}\overline{Z} = Y \otimes Y \otimes Y \otimes Y \otimes Y$.

You need to be careful when assigning cosets to elements of the logical Pauli group. Remember, $\mathsf{N}(\mathsf{S})/\mathsf{S} \cong \mathsf{P}_k$, and we'd like to realize this through a choice of representatives for the generating cosets. This means that the commutation and anticommutation relationships of the logical Paulis must be realized through the coset representatives. For instance, the coset representatives for $\overline{X}_i$ and $\overline{Z}_i$ must anticommute, while the coset representative of $\overline{X}_i$ must commute with the representatives for $\overline{X}_j$ or $\overline{Z}_j$ ($j \neq i$).

We could in principle do the same thing for $\mathsf{P}_n/\mathsf{N}(\mathsf{S})$, choosing representative errors only for the basis error syndromes and deducing the other errors by multiplication. However, in most cases, this is not a good thing to do. If our goal is to correct t errors for the maximum possible t, what we'd like to do instead is choose the lowest weight error in each coset of $\mathsf{N}(\mathsf{S})$ as its representative. If we rely on multiplication to tell us the coset representatives, we'll frequently get errors of higher weight than necessary, and then there will be some lower weight errors that won't get corrected properly.

	X	X	X	X
	Z	Z	Z	Z
$\overline{X}_1$	X	X	I	I
$\overline{X}_2$	X	I	X	I
$\overline{Z}_1$	I	Z	I	Z
$\overline{Z}_2$	I	I	Z	Z

Table 3.5: The stabilizer for the four-qubit code supplemented by representatives for logical Paulis.

3.4.3 Maximum Likelihood Decoding

I'd like to depart briefly from the convention of most of this chapter, for which we had some fixed set $\mathcal{E}$ of errors that we'd like to correct, and we won't settle for anything less than correcting all of them. For the purposes of this subsection, assume we instead have some n-qubit Pauli channel, with $P \in \mathsf{P}_n$ occurring with probability p_P.

Given a stabilizer code S, we'd like to find a decoding procedure which minimizes the probability of error when the code goes through a Pauli channel. As discussed above, a decoding procedure can be understood as assigning to each error syndrome s a Pauli Q_s. When we measure s, we assume the actual error was Q_s and so perform the correction by inverting that error. If the actual error was something else, we may end up with the wrong state. In particular, if the true error P was in a different coset of S than Q_s was, we'll end up with some logical Pauli operation.

Thus, we can calculate the probability of logical error by summing over the cosets of S and $\mathsf{N}(\mathsf{S})$.

Proposition 3.13. *Let C_s be the coset of $\hat{\mathsf{N}}(\mathsf{S})$ with error syndrome s. $\hat{Q}_s\hat{\mathsf{S}}$ is the coset of $\hat{\mathsf{S}}$ containing the canonical error $\hat{Q}_s$ with syndrome s, so $\hat{Q}_s\hat{\mathsf{S}} \subseteq C_s$.*

a) The probability of error syndrome s (regardless of whether we correctly identify the error) is

$$p_s = \sum_{\hat{P} \in C_s} p_P. \tag{3.22}$$

b) The probability of having syndrome s and no logical error (i.e., error correction is successful) is

$$p_{s,\mathrm{OK}} = \sum_{\hat{P} \in \hat{Q}_s\hat{\mathsf{S}}} p_P. \tag{3.23}$$

c) The total probability of successfully decoding the state is

$$p_{\mathrm{OK}} = \sum_s \sum_{\hat{P} \in \hat{Q}_s\hat{\mathsf{S}}} p_P. \tag{3.24}$$

There is no interaction between the different error syndromes. If we change Q_s for one value of s, the only change to p_{OK} comes through the change to $p_{s,\mathrm{OK}}$. We can therefore treat each syndrome separately to maximize $p_{s,\mathrm{OK}}$. It doesn't matter which element of the coset $Q_s\mathsf{S}$ we choose, only which coset we choose within C_s.

In order to maximize the probability of successfully decoding, for each syndrome s, we should choose the coset $Q_s\mathsf{S}$ which maximizes $p_{s,\mathrm{OK}}$. As given by equation (3.23), that just means we look at each coset and add up the probability of all Paulis in the coset. Then we choose the coset with the highest value to be the representative coset for s.

The maximum likelihood decoder should be contrasted with the decoder that optimizes the distance, for which we choose the coset containing the lowest-weight Pauli. If we have an independent Pauli channel, the

two procedures frequently, but not always, give the same answer: When the probability of error per qubit is small, a specific low-weight error will have higher probability than a specific high-weight error. However, a coset which contains one low-weight error and a bunch of high-weight errors may be less likely than a coset which contains a large number of medium-weight errors.

Getting the *exactly* optimal decoder, in the sense of always picking the most likely coset, is usually a computationally challenging task. Often, therefore, we are willing to settle for a good approximate decoder that gets p_{OK} to be close to the optimal value but with a much smaller computational cost.

3.5 Binary Symplectic Representation

3.5.1 The Symplectic Representation of Paulis

One of the most useful techniques when dealing with stabilizer codes is to ignore the phases of Paulis and work with $\hat{\mathsf{P}}_n$ instead of P_n. We lose a couple of things by doing this. One is the ability to define the code space, which seems like a serious loss, but isn't really — as discussed above, the other eigenspaces of the stabilizer have the same error correction properties as the code space. The other missing thing is the ability to tell whether Paulis commute or anticommute, since $\hat{\mathsf{P}}_n$ is an Abelian group. This is a much greater loss, so we'll need to find a substitute.

The structure of $\hat{\mathsf{P}}_n$ is very straightforward. There are 4^n elements, and all pairs commute under multiplication. Therefore, $\hat{\mathsf{P}}_n \cong \mathbb{Z}_2^{2n}$. The group operation for $\mathbb{Z}_2^{2n}$ is usually written as addition. Conventionally, we choose to represent elements of $\hat{\mathsf{P}}_n$ as two n-bit binary vectors, one representing the "X" component and one representing the "Z" component.

Definition 3.11. The *binary symplectic representation* of $\hat{\mathsf{P}}_n$ is an isomorphism between $\hat{\mathsf{P}}_n$ and $\mathbb{Z}_2^n \times \mathbb{Z}_2^n$: $P \leftrightarrow v_P = (x_P|z_P)$. The ith component of x_P is 0 if P acts on qubit i as I or Z and 1 if P acts on qubit i as X or Y. The ith component of z_P is 0 if P acts on qubit i as I or X and 1 if P acts on qubit i as Y or Z. That is,

$$\begin{array}{cc} I & (0|0) \\ X & (1|0) \\ Y & (1|1) \\ Z & (0|1) \end{array} \quad \longleftrightarrow \quad \begin{array}{c} \\ \\ \\ \\ \end{array} \tag{3.25}$$

For instance, $X \otimes I \otimes Y \leftrightarrow (1\ 0\ 1|0\ 0\ 1)$. The "symplectic" refers to the substitute for commutativity/anticommutativity:

Definition 3.12. The *symplectic form* (or symplectic product) on $\mathbb{Z}_2^n \times \mathbb{Z}_2^n$ is $(x_1|z_1) \odot (x_2|z_2) = x_1 \cdot z_2 + x_2 \cdot z_1$, where the dot product is the usual scalar product in the vector space $\mathbb{Z}_2^n$ and addition is modulo 2.

Proposition 3.14. *$v_P \odot v_Q = c(P, Q)$ for $P, Q \in \mathsf{P}_n$.*

Proof. This can be checked exhaustively for a single qubit. For more than one qubit, note that both $\odot$ and $c(\cdot, \cdot)$ are equal to the parity of their single-qubit results. Therefore, since they are equal for single qubits, they are also equal for n qubits. □

Combining the symplectic form with the binary symplectic representation recovers the primary structure of the Pauli group. We can switch back and forth between the two representations to use whichever one is the most convenient at the moment. The conversion process is summarized in table 3.6. The one thing that is lost in the transition is the phase of a Pauli, so you must be careful whenever dealing with something that depends on that.

Some of the conversions need a little more explanation. There were three conditions for S to be a stabilizer: that $-I \notin \mathsf{S}$, that S is a group, and that S is Abelian. Since phase is lost when converting to the binary symplectic representation, the first condition is irrelevant. The second condition means that S becomes a linear subspace in $\mathbb{Z}_2^n \times \mathbb{Z}_2^n$, and the third means that $v \odot w = 0\ \forall v, w \in \mathsf{S}$. This analysis and the conversion of the normalizer prompts the following definition:

In the Pauli group	Binary symplectic representation
$P \in \mathsf{P}_n$	$v_P = (x_P \vert z_P) \in \mathbb{Z}_2^n \times \mathbb{Z}_2^n$
Multiplication	Addition
$c(P, Q)$	$v_P \odot v_Q$
Phase	No equivalent
Stabilizer S	Weakly self-dual subspace S
Normalizer $\mathsf{N}(\mathsf{S})$	Dual subspace $\mathsf{S}^\perp$ (under $\odot$)
Minimal set of generators for S	Basis for S

Table 3.6: Equivalence between the Pauli group and its binary symplectic representation.

$$\begin{array}{c} \\ \\ \\ \\ \overline{X} \\ \overline{Z} \end{array} \left(\begin{array}{ccccc|ccccc} 1 & 0 & 0 & 1 & 0 & 0 & 1 & 1 & 0 & 0 \\ 0 & 1 & 0 & 0 & 1 & 0 & 0 & 1 & 1 & 0 \\ 1 & 0 & 1 & 0 & 0 & 0 & 0 & 0 & 1 & 1 \\ 0 & 1 & 0 & 1 & 0 & 1 & 0 & 0 & 0 & 1 \\ \hline 1 & 1 & 1 & 1 & 1 & 0 & 0 & 0 & 0 & 0 \\ 0 & 0 & 0 & 0 & 0 & 1 & 1 & 1 & 1 & 1 \end{array}\right)$$

Table 3.7: The binary symplectic representation of the stabilizer and logical Pauli operators for the five-qubit code.

Definition 3.13. Let V be a linear subspace of $\mathbb{Z}_2^n \times \mathbb{Z}_2^n$. The *dual* of V (with respect to $\odot$) is $V^\perp = \{w \in \mathbb{Z}_2^n \times \mathbb{Z}_2^n | w \odot v = 0 \ \forall v \in V\}$. A subspace is *self-dual* if $V^\perp = V$. A subspace is *weakly self-dual* if $V \subseteq V^\perp$.

Table 3.7 gives the five-qubit code in binary symplectic representation, including the logical $\overline{X}$ and $\overline{Z}$ operators.

Conversion can go the other way too. For instance, it is convenient to define a notion of a set of Paulis being independent based on the standard definition for binary vector spaces:

Definition 3.14. A set of Paulis $\{P_1, \ldots, P_m\}$ is *independent* iff the vectors $\{v_{P_1}, \ldots, v_{P_m}\}$ are linearly independent.

A set of Paulis is independent unless one of them is a product of others; this is equivalent to saying that a set of $2n$-bit binary vectors is independent unless one of them is a sum of others. Since the binary vector space is $2n$-dimensional, the maximum number of independent Paulis is $2n$, which is equal to the number of generators of the Pauli group.

3.5.2 Linear Algebra Lemma

The power of the binary symplectic representation is that we can use standard results from linear algebra to prove a number of properties of the Pauli group and stabilizers. In particular, we have the following lemma:

Lemma 3.15. *Let $\{P_1, \ldots, P_m\}$ be an independent set of Paulis on n qubits, and let s be an m-bit vector with components s_i. Then $\exists Q \in \mathsf{P}_n$ with $c(P_i, Q) = s_i$. In fact, there are 2^{2n-m} such Paulis.*

Proof. Converting to the binary symplectic representation gives us m linearly independent vectors v_i, and we wish to find vector w such that $v_i \odot w = s_i$. Each of these conditions is a linear equation, and since the vectors v_i are independent, the system of linear equations is non-singular. There are m equations in a $2n$-dimensional vector space, so the space of solutions has dimension $2n - m$. It is a binary vector space, so that corresponds to 2^{2n-m} solutions. □

An important consequence of the lemma is that it tells us about the decomposition of the full physical Hilbert space into subspaces associated with the different error syndromes. I've already discussed this decomposition, but the missing piece is given by the following corollary of lemma 3.15:

Proposition 3.16. *Let* S *be a stabilizer with generators* $\{M_i\}$*. Then for any error syndrome* s*,* $\exists P \in \mathsf{P}_n$ *with* $\sigma(P) = s$*.*

That is, not only is every Pauli outside $\mathsf{N}(\mathsf{S})$ associated with an error syndrome, but every possible error syndrome is associated with some Pauli.

3.5.3 Consequences of the Lemma

Now it's time for some of the proofs I owe you. There is proposition 3.2, which claims $\mathsf{S} = \mathsf{S}(\mathcal{T}(\mathsf{S}))$, and theorem 3.11, which says $\mathsf{N}(\mathsf{S})/\mathsf{S} \cong \mathsf{P}_k$.

First, here is the proof that $\mathsf{N}(\mathsf{S})/\mathsf{S} \cong \mathsf{P}_k$:

Proof of theorem 3.11. The most straightforward way to show this is by sequentially picking coset representatives for the cosets corresponding to $\overline{X}_i$ and $\overline{Z}_i$. The Pauli group P_k is determined, like any finitely-presented group, by its generators and relations between them. In the case of the Pauli group, the relations are

$$c(X_i, X_j) = 0 \tag{3.26}$$
$$c(Z_i, Z_j) = 0 \tag{3.27}$$
$$c(X_i, Z_j) = \delta_{ij}. \tag{3.28}$$

It is sufficient to consider only the generating cosets, since we can let the representatives of a product of cosets be the product of the representatives, as discussed in section 3.4.2. Provided we can choose $\overline{X}_i$ and $\overline{Z}_i$ with the correct commutation relations, that gives us an injective map of P_k into $\mathsf{N}(\mathsf{S})/\mathsf{S}$. We know that $|\mathsf{N}(\mathsf{S})| = 4 \cdot 2^{n+k} = |\mathsf{S}||\mathsf{P}_k|$, so an injection has to be isomorphism.

Suppose we've chosen some independent set of $\overline{X}_i$'s and $\overline{Z}_i$'s with the correct commutation relations, and we wish to choose one more. The new logical Pauli must be in $\mathsf{N}(\mathsf{S})$, so in particular, it must commute with all generators of the stabilizer. Second, it has a defined commutation relation with the already chosen logical Paulis. By lemma 3.15, there exists a Pauli that satisfies all of these constraints.

The only remaining thing to check is that the new logical Pauli can be chosen to be independent of the prior ones. To simplify the analysis, let us first pick all the $\overline{X}_i$'s, then the $\overline{Z}_i$'s. When we are picking $\overline{Z}_j$, it satisfies different commutation relations than all previously selected logical Paulis. In particular, $\overline{Z}_j$ anticommutes with $\overline{X}_j$, unlike all the previous logical Paulis and all the stabilizer generators. Thus, $\overline{Z}_j$ must be independent.

When we pick $\overline{X}_j$, this argument doesn't apply, since the new one will commute with all stabilizer generators and all previous logical Paulis. However, there are $n-k$ stabilizer generators and at most $k-1$ logical Paulis already chosen, for a total of at most $n-1$ constraints. By lemma 3.15, there are thus at least 2^{n+1} possible solutions. The group generated by the stabilizer and previous logical Paulis contains only 2^{n-1} operators, so there are possible choices for $\overline{X}_j$ that are independent of the previous choices.

□

Finally, we can prove proposition 3.2, showing that $\mathsf{S} = \mathsf{S}(\mathcal{T}(\mathsf{S}))$:

Proof of proposition 3.2. If $M \in \mathsf{S}$, then certainly $M|\psi\rangle = |\psi\rangle$ for any $|\psi\rangle \in \mathcal{T}(\mathsf{S})$, so $\mathsf{S} \subseteq \mathsf{S}(\mathcal{T}(\mathsf{S}))$. We need to show that if $N \notin \mathsf{S}$, then $N \notin \mathsf{S}(\mathcal{T}(\mathsf{S}))$. If $N \notin \mathsf{N}(\mathsf{S})$ then $N|\psi\rangle$ (for any codeword $|\psi\rangle$) has a different eigenvalue for some $M \in \mathsf{S}$, and is therefore orthogonal to the code space, which in turn means $N \notin \mathsf{S}(\mathcal{T}(\mathsf{S}))$.

If S has n generators, that is all we need. Otherwise, if $r < n$, we still need to show that if $N \in \mathsf{N}(\mathsf{S}) \setminus \mathsf{S}$, then $\exists|\psi\rangle \in \mathcal{T}(\mathsf{S})$ such that $N|\psi\rangle \neq |\psi\rangle$. By lemma 3.15, we can choose a $M \in \mathsf{N}(\mathsf{S})\setminus\mathsf{S}$ such that $\{M, N\} = 0$. Consider the modified stabilizer S' formed by adding M to S as a new generator. S' has $r+1$ generators, so its code space has dimension 2^{k-1} (by proposition 3.3). Since $k \geq 1$, there is at least one state $|\psi\rangle$ (up to normalization) in the code space of S'. $|\psi\rangle$ is left fixed by all elements of S', and in particular by the elements

of $\mathsf{S} \subset \mathsf{S}'$. Thus, $|\psi\rangle \in \mathcal{T}(\mathsf{S})$. However, N anticommutes with M, which is in the stabilizer of $|\psi\rangle$. Therefore, $N|\psi\rangle$ has eigenvalue -1 for M, and in particular is orthogonal to $|\psi\rangle$. It follows that $N \notin \mathsf{S}(\mathcal{T}(\mathsf{S}))$, which proves the proposition.

□

Chapter 4

Maybe I Should Have Started Here: Classical Error Correction

In chapter 3, we saw the formalism of stabilizer codes, but we didn't see how to find new stabilizer codes. Indeed, finding new codes is a tricky topic. Already in the theory of classical error correction, it is quite difficult to find good new codes. Luckily, there are a few ways of taking already-discovered classical codes and turning them into quantum codes. That is not the subject of this chapter.

This chapter is instead about the theory of classical error-correcting codes. Naturally, I won't have time to go into complete detail on classical error correction, so I will focus on the particular points of the theory of classical error correction which have most relevance to QECCs. One purpose is to give you the background for chapter 5, which *is* about converting classical codes into quantum codes. The other reason is that it can give you a deeper understanding of the theory of QECCs and of stabilizer codes, since there are many parallels — and some critical differences — between the theories of classical and quantum error correction.

For those who are familiar with the theory of classical error correction, this chapter is likely to be somewhat boring, but I hope it won't be a complete waste of time. In particular, I will try to point out the parallels between classical coding theory and those aspects of quantum coding theory that we've seen so far. Some you may have already noticed yourself, but perhaps there are some parallels you missed.

4.1 Classical Error Correction in General

4.1.1 Abstract Description of a Classical Code

A general classical error-correcting code can be defined, much as we did for a QECC, as an encoding map.

Definition 4.1. A classical *error-correcting code* $(e, \mathcal{E})$ is a map $e : [1 \dots K] \to [1 \dots N]$ with a set of correctable errors $\mathcal{E}$ (consisting of maps $E : [1 \dots N] \to [1 \dots M]$) with the following property: $\exists$ map $d : [1 \dots M] \to [1 \dots K]$ such that $\forall E \in \mathcal{E}$, $\forall x \in [1 \dots K]$,

$$d(E(e(x))) = x. \tag{4.1}$$

The map d is the *decoder* for the code and e is the *encoder* for the code. Frequently, the code is just referred to as C, the image of the encoder e in $[1 \dots N]$.

I have written this to be completely analogous to the definition I gave for a QECC. The only real difference is that quantum states live in a Hilbert space, and maps between them should be quantum operations, or at least linear maps, whereas classically, we can consider states from any set and arbitrary functions between the sets as the encoder, decoder, and errors. But remember that classical codes are actually just a special case of quantum codes. The apparent extra constraint of linearity is really an extra freedom to include superpositions of basis states, whereas classical codes can only contain basis states.

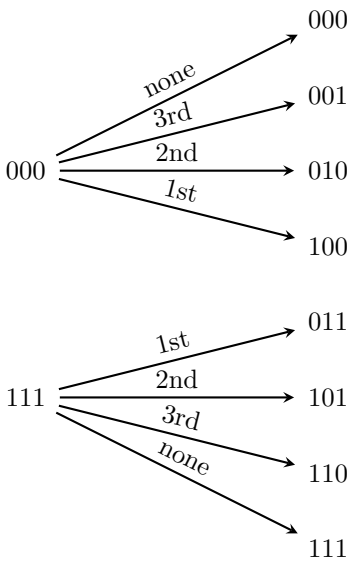

Figure 4.1: Codewords of the repetition code with errors on a single bit never get confused.

Ultimately, a classical error-correcting code is a just a set of objects (frequently bit strings), and the errors diversify those objects. The goal of the decoder is to get back to the original object. We have an uncorrectable error when two different logical objects x and y get confused: $E(e(x)) = F(e(y))$. If that never happens, a decoder exists: the sets $S_x = \{E(e(x))|E \in \mathcal{E}\}$ are all distinct, so we can define a function mapping all elements of S_x to x unambiguously.

This condition has no precise analogy for quantum codes. In some sense equation (2.58) is similar, if we interpret the correct quantum analogue of "different" as "orthogonal." Equation (2.58) says that orthogonal quantum states and different errors must produce orthogonal states, but for QECCs, that is only a sufficient condition, not a necessary one. From that point of view, QECCs seem somewhat more generous than classical error-correcting codes, since they don't require that it is possible to exactly determine the error. On the other hand, if you did exercise **??**, you saw a condition which can be broken up into two parts. When $i \neq j$, it says that we should never confuse different quantum states under an error; that seems analogous to the condition for classical error correction. But then there is an additional non-trivial condition for a QECC when $i = j$, which makes the quantum code seem more stringent than the classical one. The extra condition can be interpreted as saying that the environment should not learn anything about the logical subspace for a QECC. Classically, of course, it is harmless if the environment simply learns the encoded data, provided it doesn't change it. In the quantum case, learning about the data *necessarily* involves changing it.

4.1.2 Distance of a Classical Code

As with quantum codes, frequently we focus on codes where the encoded state N can be broken up into smaller pieces, $N = q^n$, and where $M = N$. We consider $[1 \ldots N]$ as the direct product of n copies of $[1 \ldots q]$. I will refer to each $[1 \ldots q]$ factor as a *register*, a *component*, or a *coordinate*. In the common case where $q = 2$, I may just refer to the ith bit (or physical bit) of the code. Sometimes I may even forget myself and accidentally refer to the ith qubit. In the quantum case, I'll use these same terms, but I try to avoid component since it also can refer to the component in some direction in the overall Hilbert space. In the classical case, the terminology comes from treating $[1 \ldots q^n]$ as an n-dimensional vector space over the finite field GF(q). We'll get back to that approach in section 4.2.

Also, we tend to focus on cases where $\mathcal{E}$ is composed of errors of weight t or less. The classical definitions

of *weight* and *support* are just the same as the quantum ones: the error E acts trivially on all but the coordinates in the support of E, and the weight of E is the size of the support. When we have a classical channel which causes errors independently on each coordinate with a small probability p, then the probability of having errors of weight $t+1$ or greater is $O(p^{t+1})$, much as in the quantum case. If we can find a code that simply corrects all errors of weight t or less, then with high probability, we'll get the correct state when we decode.

Definition 4.2. The *distance* of a classical error-correcting code $C \subseteq \mathbb{Z}_N$ (with $N = q^n$) is

$$\min\{\mathrm{wt}(E) | \exists x \neq y \in C, E(x) = y.\} \tag{4.2}$$

A classical code with distance d encoding K possible states in n registers of size q is an $(n, K, d)_q$ code. When $q = 2$, we just write (n, K, d).

In other words, the distance is the minimum number of coordinates that have to be changed to get from one codeword to another. The quantum distance can be understood in the same way, but there are more subtleties in the quantum case.

As with quantum codes, the distance tells us how many errors we can correct:

Proposition 4.1. *A classical code with distance d can:*

1. *correct general errors on up to $\lfloor (d-1)/2 \rfloor$ coordinates,*
2. *correct erasure errors on up to $d-1$ coordinates, or*
3. *detect errors on up to $d-1$ coordinates.*

4.2 Classical Linear Codes

General classical codes are unwieldy to deal with, just as are general quantum codes. The class of linear codes is very analogous to stabilizer codes — it is a much more tractable subclass of classical error-correcting codes, and many of the most interesting known codes are, in fact, linear codes.

For a linear code, we assume $N = q^n$, as above. For this section, I will further assume $q = 2$, and treat $[1 \ldots N]$ as an n-dimensional vector space over $\mathbb{Z}_2$. In section 4.4, I will return to the $q \neq 2$ case.

4.2.1 Generator Matrix and Parity Check Matrix

By considering $\mathbb{Z}_N = \mathbb{Z}_2^n$ as a vector space, we add an additional linear structure, and a linear code exploits that structure.

Definition 4.3. An error-correcting code $C \subseteq \mathbb{Z}_2^n$ is a *linear code* if $x, y \in C \Rightarrow x + y \in C$.

A linear code is thus a linear subspace of $\mathbb{Z}_2^n$. We can choose a basis $x_1, \ldots, x_k$ for the code, and all other vectors in the code will be linear combinations of the x_i's. Since $x + x = 0 \ \forall x \in \mathbb{Z}_2^n$, the only question is which subset of the basis vectors are added together to make a codeword. There are thus 2^k codewords in total and k encoded bits.

Definition 4.4. The *generator matrix* G_C of a linear code C is a matrix with row i equal to x_i.

The generator matrix can be used to define the encoder of C:

Proposition 4.2. *Let $C \subseteq \mathbb{Z}_2^n$ be a linear code with k encoded bits and generator matrix G. Then the linear map $v \in \mathbb{Z}_2^k \mapsto G^T v \in \mathbb{Z}_2^n$ is the encoder for C. In other words, x is a codeword of C iff $x = G^T v$ for some $v \in \mathbb{Z}_2^k$.*

In order to check for errors, we measure the parities of bits in the codeword.

Definition 4.5. Suppose the linear code C has generator G. A *parity check matrix* H_C for C is a matrix with row i equal to $y_i \in \mathbb{Z}_2^n$, where $Gy_i = 0\ \forall i$, and the set $\{y_i\}$ is a maximal linearly independent set with this property.

The parity check matrix of a code is not unique, but it is still frequently referred to as "the" parity check matrix. You can take any linear combinations of rows of the parity check matrix, and provided the new set of rows remains linearly independent, it will still function as a parity check matrix.

Theorem 4.3. *If C has k encoded bits and n physical bits, then G_C is a $k \times n$ matrix and H_C is an $(n-k)\times n$ matrix. $G_C {H_C}^T = 0$ and $H_C {G_C}^T = 0$.*

Proof. The only property which is not completely trivial is that H_C has $n-k$ rows. The constraints $G_C y_i = 0$ (which determine the rows of H_C) form a set of k non-singular linear equations on n bits, so the solution space has dimension $n-k$. Thus, a maximal set of $\{y_i\}$ will consist of $n-k$ of them. □

Using the linear structure of $\mathbb{Z}_2^n$, we can represent a set of bit flip errors as a vector $e \in \mathbb{Z}_2^n$, with 1 for those bits which have been flipped and 0 for those bits which have not been flipped. Under this convention, $\mathrm{wt}\, e$ is the weight of the error. If we start with bit string x and the error e occurs, we now have the bit string $x + e$.

The virtue of the parity check matrix is that it filters out the codewords and just tells us about the errors. Suppose $x \in C$ undergoes error e. Then, using linearity and proposition 4.2,

$$H_C(x+e) = H_C x + H_C e = H_C {G_C}^T v + H_C e = H_C e. \tag{4.3}$$

Definition 4.6. The *error syndrome* of an error e for linear code C is $H_C e$.

All of this probably sounds a bit familiar, since stabilizer codes and classical linear codes are closely related. The stabilizer of a stabilizer code is very analogous to the parity check matrix for a linear code, although the stabilizer also has some vague similarity to the generator matrix (in that the projector on the code space is formed from the stabilizer). In fact, linear codes are a special case of stabilizer codes, and the parity check matrix can be realized as the stabilizer:

Theorem 4.4. *Let C be a linear code with parity check matrix H, and let C correct the set of errors $\mathcal{E} \subseteq \mathbb{Z}_2^n$. Define a stabilizer code S to have stabilizer with binary symplectic representation $(0|H)$. Then S corrects the set of errors $\{(e|0)|e \in \mathcal{E}\}$ and for any $x \in \mathbb{Z}_2^n$, $x \in C$ iff $|x\rangle \in \mathsf{S}$.*

In other words, we form a stabilizer by replacing the 1s in H with Zs, with each row of the parity check matrix becoming a generator of the stabilizer. The resulting stabilizer code corrects the same errors as C and has the same basis codewords. The one difference is that the stabilizer code encodes a quantum state, so superpositions such as $|x_1\rangle + |x_2\rangle$ are also codewords of S, even though the combination is meaningless when considering a classical code. The proof of the theorem is straightforward, and is left as an exercise.

The non-uniqueness of the parity check matrix is just the same as the non-uniqueness of the generators of a stabilizer. Replacing a row of the parity check matrix with a linear combination of rows is equivalent to replacing a generator of the stabilizer with a product of generators.

The best analogy for the rows of the generator matrix are the logical Paulis in $\mathsf{N}(\mathsf{S})/\mathsf{S}$. For a stabilizer code, the coset representatives are non-unique, which is not an issue for classical codes. It is true that the generator matrix is not completely unique — we can take a different encoder, which corresponds to a different generator matrix. However, this is a different phenomenon, and corresponds to labeling the cosets in $\mathsf{N}(\mathsf{S})/\mathsf{S}$ with different logical Paulis rather than choosing different representatives of them.

4.2.2 Distance of a Linear Code

For a linear code, the distance has a somewhat nicer form than for a general classical error-correcting code.

Proposition 4.5. *The distance of a linear code C is* $\min\{\mathrm{wt}(e)|e \in C, e \neq 0\}$.

Proof. The general definition of distance is as $\min\{\operatorname{wt} e | x \neq y \in C, x+e=y\}$ (with the error rewritten from definition 4.2 to take advantage of linearity). But when $x, y \in C$, $e = x+y$ is also in C since C is linear. Any $e \in C$ can be realized this way by simply choosing any $x \in C$ and letting $y = x+e$, which will automatically be in C, again since C is linear. $x \neq y$ is equivalent to $e \neq 0$. □

Notation 4.7. An $(n, 2^k, d)$ linear code is denoted as an $[n, k, d]$ code.

For a linear code, the codewords themselves are the undetectable errors: adding a non-trivial codeword to another codeword results in a new codeword, and if you add a non-codeword to a codeword, you always get a non-codeword. For a set of errors to be correctable, any pair of errors must not add up to a codeword:

Theorem 4.6. *A linear code C corrects the error set $\mathcal{E}$ iff $e + f \notin C$ for all $e \neq f \in \mathcal{E}$. Equivalently, $H_C e \neq H_C f$ $\forall e \neq f \in \mathcal{E}$ (i.e., all errors in $\mathcal{E}$ have different error syndromes).*

Proof. If all errors in $\mathcal{E}$ have different error syndromes, than the code certainly can correct for $\mathcal{E}$ using the following procedure: Given an erroneous codeword $x + e$, apply the parity check matrix to get $H_C e$. Since the error syndromes are unique, we can identify e and then recover $x = (x + e) + e$.

If $e + f \in C$ then $H_C(e + f) = H_C e + H_C f = 0$. Conversely, if $e + f \notin C$, then $H_C(e + f) \neq 0$. This is true because the parity check matrix is formed from a *maximal* set of vectors annihilated by the generator matrix. When $e + f \notin C$, then the set of solutions of $G_C y_i = 0$ and of $(e + f) \cdot y_i = 0$ is only $n - k - 1$ dimensional, whereas the parity check matrix has $n - k$ rows. Thus, $e + f \notin C$ iff $H_C e \neq H_C f$.

Finally, if $e + f \in C$ for some pair $e \neq f \in \mathcal{E}$, then the code cannot correct $\mathcal{E}$. For instance, given $x \in C$, let $y = x + (e + f)$, which will also be in C. Then $x + e = y + f$, so if this string shows up, there is no way to tell whether it should be decoded to x (with error e) or y (with error f). □

The combination $e + f$ is reminiscent of the combination $E^\dagger F$ that appears in theorem 3.5 giving the set of correctable errors for a stabilizer code. Comparing further, you can see that for a classical code, $C \setminus \{0\}$ plays the role of $\hat{\mathsf{N}}(\mathsf{S}) \setminus \hat{\mathsf{S}}$ for a stabilizer code. Indeed, if you apply the transformation theorem 4.4 to code C to get stabilizer S, and then calculate $\hat{\mathsf{N}}(\mathsf{S}) \setminus \hat{\mathsf{S}}$, you find that it includes the conversion of $C \setminus \{0\}$. That's not all it contains, but it is a good exercise to work this out yourself.

Importantly, there is no good classical analogue to the concept of a degenerate quantum code. All classical codes are non-degenerate, and the presence of degenerate quantum codes complicates quantum coding theory.

4.2.3 Example: Hamming Codes

One example of a linear code is the repetition code $0 \mapsto 000$, $1 \mapsto 111$. It is linear because $000 + 000 = 000$, $000 + 111 = 111$, and $111 + 111 = 000$. The generator matrix is

$$G = \begin{pmatrix} 1 & 1 & 1 \end{pmatrix}, \tag{4.4}$$

and the parity check matrix is

$$H = \begin{pmatrix} 1 & 1 & 0 \\ 1 & 0 & 1 \end{pmatrix} \tag{4.5}$$

The three-bit repetition code (a $[3, 1, 3]$ code) can of course be generalized to d-bit repetition codes, which have parameters $[d, 1, d]$, but there is another interesting generalization, starting from the observation that in the parity check matrix for the three-bit repetition code, every column is different.

Supposing we want to correct only 1-bit errors. If $\operatorname{wt} e = 1$, with the only 1 in the ith coordinate, then for any parity check matrix H, He — the error syndrome of e — will be the ith column of H. Thus, if we pick all columns of H to be different, the error syndromes of all 1-bit errors will be different. We should not pick an all 0s column since we want the no error case ($e = 0$) to have error syndrome 0.

If we fix the number of rows of H to be r, we can choose up to $2^r - 1$ distinct columns by letting them run over all nonzero r-bit strings. This gives a Hamming code:

Definition 4.8. The $[2^r - 1, 2^r - r - 1, 3]$ Hamming code is the code whose $r \times (2^r - 1)$ parity check matrix has as columns all possible r-bit strings.

Notice that here we have defined the Hamming code by choosing a parity check matrix, much as for a stabilizer code, we choose the stabilizer to define the code. In this case, you can derive the set of actual codewords as $\{x|Hx = 0\}$. There are r linear constraints on $2^r - 1$ bits, so the linear space of solutions is $(2^r - r - 1)$-dimensional, giving the number of encoded qubits in the definition.

As a concrete example, when $r = 3$, we get a $[7, 4, 3]$ code. It has parity check matrix

$$\begin{pmatrix} 1 & 1 & 1 & 1 & 0 & 0 & 0 \\ 1 & 1 & 0 & 0 & 1 & 1 & 0 \\ 1 & 0 & 1 & 0 & 1 & 0 & 1 \end{pmatrix}, \tag{4.6}$$

and can be taken to have generator matrix

$$\begin{pmatrix} 1 & 1 & 1 & 1 & 1 & 1 & 1 \\ 1 & 1 & 1 & 1 & 0 & 0 & 0 \\ 1 & 1 & 0 & 0 & 1 & 1 & 0 \\ 1 & 0 & 1 & 0 & 1 & 0 & 1 \end{pmatrix}. \tag{4.7}$$

4.2.4 Example: Reed-Muller Codes

Looking at the generator matrix for the 7-bit Hamming code, it has a somewhat nice form. The form gets even nicer if you add an extra bit which is 1 for the first row and 0 for the others:

$$\begin{pmatrix} 1 & 1 & 1 & 1 & 1 & 1 & 1 & 1 \\ 1 & 1 & 1 & 1 & 0 & 0 & 0 & 0 \\ 1 & 1 & 0 & 0 & 1 & 1 & 0 & 0 \\ 1 & 0 & 1 & 0 & 1 & 0 & 1 & 0 \end{pmatrix}. \tag{4.8}$$

Now every codeword has weight 0, 4, or 8. This is an example of a Reed-Muller code, specifically $\mathcal{R}(1, 3)$. It is an $[8, 4, 4]$ code.

Definition 4.9. The *1st order Reed-Muller code* $\mathcal{R}(1, m)$ is a linear code with $n = 2^m$ physical bits. It has a generator matrix whose rows are the all-1s vector and the vectors v_i $(i = 1, \ldots, m)$, where the jth coordinate of v_i is equal to the ith bit of j (i.e., v_1 is the most significant bit), when j is expanded in binary (and assuming j runs from 0 to $n - 1$).

For instance, for $n = 4$, $v_1 = (0011)$ and $v_2 = (0101)$. The generator matrix is

$$\begin{pmatrix} 1 & 1 & 1 & 1 \\ 0 & 0 & 1 & 1 \\ 0 & 1 & 0 & 1 \end{pmatrix} \tag{4.9}$$

It is a $[4, 3, 2]$ code. Note that in equation (4.8), the order of the bits is reversed relative to this convention.

Theorem 4.7. *$\mathcal{R}(1, m)$ is a $[2^m, m + 1, 2^{m-1}]$ code.*

Proof. Each of the vectors v_i has weight exactly $n/2$ $(n = 2^m)$, as exactly half the numbers $0, \ldots, n - 1$ will be 1 in any given bit location. We can also easily show that any sum of $s > 0$ of the v_is will have weight exactly $n/2$: The sum will be 0 or 1 in the jth location iff the XOR of the corresponding bits of j is 0 or 1. For instance, for $v_1 + v_3$, take the XOR of the first and third bits of j. We then let j run over from $0, \ldots, n - 1$. As we do this, the set of bits we are looking at can take on every possible set of values, and furthermore, each set of values appears the same number of times, corresponding to every set of values for the other bits. In particular, any particular assignment of the s bits we are interested in shows up 2^{n-s}

times. For half of these assignments, the XOR will be 0, and for the other half, the XOR will be 1. Thus the weight of the sum we are looking at is exactly $n/2$.

The all-1s vector has weight n, and the all-1s vector added to any vector of weight $n/2$ is again a vector of weight $n/2$. Thus, the code has distance $n/2 = 2^{m-1}$.

This argument also shows that all the rows of the generator matrix are independent, since no linear combination gives 0. Therefore, the code has $m + 1$ encoded bits, the same as the number of rows.

□

Definition 4.10. The rth order Reed-Muller code $\mathcal{R}(r, m)$ has as rows of its generator matrix all products of up to r of the vectors v_i given in definition 4.9, where product means the bitwise product (1 in a coordinate iff all vectors in the product are 1 at that coordinate) The all-1s generator is also included. (It can be considered as the product of 0 of the v_i's.)

For instance, $\mathcal{R}(2, 2)$ has the additional generator $v_1 v_2 = (0001)$, giving the generator matrix

$$\begin{pmatrix} 1 & 1 & 1 & 1 \\ 0 & 0 & 1 & 1 \\ 0 & 1 & 0 & 1 \\ 0 & 0 & 0 & 1 \end{pmatrix} \tag{4.10}$$

$\mathcal{R}(2, 2)$ is a $[4, 4, 1]$ code, which actually means it contains all 4-bit vectors. $\mathcal{R}(2, 3)$ is more interesting, with generator matrix

$$\begin{pmatrix} 1 & 1 & 1 & 1 & 1 & 1 & 1 & 1 \\ 0 & 0 & 0 & 0 & 1 & 1 & 1 & 1 \\ 0 & 0 & 1 & 1 & 0 & 0 & 1 & 1 \\ 0 & 1 & 0 & 1 & 0 & 1 & 0 & 1 \\ 0 & 0 & 0 & 0 & 0 & 0 & 1 & 1 \\ 0 & 0 & 0 & 0 & 0 & 1 & 0 & 1 \\ 0 & 0 & 0 & 1 & 0 & 0 & 0 & 1 \end{pmatrix} \tag{4.11}$$

$\mathcal{R}(2, 3)$ is an $[8, 7, 2]$ code.

Theorem 4.8. *$\mathcal{R}(r, m)$ is a $[2^m, N(r, m), 2^{m-r}]$ code, where*

$$N(r, m) = 1 + \binom{m}{1} + \binom{m}{2} + \cdots + \binom{m}{r}. \tag{4.12}$$

Proof. We must show that the code has $N(r, m)$ encoded bits and has distance 2^{m-r}.

Number of encoded bits: $\mathcal{R}(r, m)$ is spanned by a product of vectors for each subset of up to r elements of the numbers $1, \ldots, m$. Counting them gives the formula for $N(r, m)$. However, we do need to show that these are linearly independent to see that this is also the number of encoded bits.

Consider the extreme case of $\mathcal{R}(m, m)$. The generator matrix for $\mathcal{R}(r, m)$ is contained in the top rows of that for $\mathcal{R}(m, m)$, so it is enough to show that the generator matrix for $\mathcal{R}(m, m)$ has full rank. $N(m, m) = 2^m = n$, so the rows are linearly independent iff they span the whole vector space.

We can imagine arbitrary vectors on 2^m bits as functions from m bits to one bit, as follows: for the jth bit of the vector, interpret j as the input of the function, with the output of the function given by the jth bit. (For instance, the vector 0110 is the function $f(00) = 0$, $f(01) = 1$, $f(10) = 1$, $f(11) = 0$.) In this interpretation, v_i is the function "take the ith bit of the input."

The product of multiple vectors $v_{i_1}, \ldots, v_{i_s}$ is the function "take the AND of bits $i_1, \ldots, i_s$ of the input," and the sum of products is the XOR of these ANDs. We can write an arbitrary function from m bits to 1 bit as the XOR of ANDs of up to all m bits, so all possible vectors are in the code $\mathcal{R}(m, m)$. Therefore all products of the v_is are linearly independent.

Distance: It is easy to see that the product of any r vectors v_i has weight $n/2^r = 2^{m-r}$, as the product is 1 in the jth location iff the AND of the corresponding bits of j is 1, which happens for only a fraction

$1/2^r$ of the possible values of j. We also have to check the distance, however, for the sums of these products, and it is not clear that taking the sum cannot cause the weight to decrease.

To show that the distance of $\mathcal{R}(r,m)$ is indeed 2^{m-r}, we perform induction on r and m. We have already calculated the distance for $\mathcal{R}(1,m)$ in theorem 4.7. As $m \geq r$, we also want as a base case to show it for a given r for the smallest possible value of m, namely $\mathcal{R}(r,r)$. In this case, there is nothing really to show, as the distance from the formula is 1, which is indeed the weight of the product of all r v_i vectors, and there is no possibility of having a shorter distance.

Claim 4.9. *Assume the distance of $\mathcal{R}(r-1,m)$ is 2^{m-r+1} and the distance of $\mathcal{R}(r,m)$ is 2^{m-r}. Then the distance of $\mathcal{R}(r,m+1)$ is 2^{m+1-r}.*

Proof of claim. We can consider any given sum of basis vectors, and break it up into a term where none of the products includes the vector v_1 and a term where all of the products include v_1. Now, if we restrict attention to the first 2^m coordinates, the second term is uniformly 0 and the first term is a vector from $\mathcal{R}(r,m)$, which we already know has weight at least 2^{m-r} unless it is the 0 vector.

If we restrict attention to the last 2^m coordinates, v_1 is always 1, so it can be ignored, and the second term is the sum of products of at most $r-1$ vectors, and is thus a vector from $\mathcal{R}(r-1,m)$. The first term is the same on the last 2^m coordinates as it was on the first 2^m coordinates, and is again a vector from $\mathcal{R}(r,m)$. But $\mathcal{R}(r-1,m) \subseteq \mathcal{R}(r,m)$, so the sum of a term from $\mathcal{R}(r-1,m)$ and a term from $\mathcal{R}(r,m)$ is in $\mathcal{R}(r,m)$, and therefore the last 2^m coordinates have weight at least 2^{m-r} by the inductive hypothesis unless the last 2^m coordinates are all 0.

If the first term is the 0 vector, we actually have a vector from $\mathcal{R}(r-1,m)$ on the last 2^m coordinates, which therefore has weight at least 2^{m-r+1} unless it is 0. To get 0 on the last 2^m coordinates, either both terms are 0 (in which case the whole vector is 0), or the first and second terms must cancel on the last 2^m coordinates. In order to cancel the second term, the first term must actually be a vector from $\mathcal{R}(r-1,m)$ on each half of the coordinates, which again means the vector on each half of the coordinates has weight 2^{m-r+1}.

That is, we have three cases (assuming the overall vector is not 0): In case one, the first term is 0, in which case the last 2^m coordinates have weight 2^{m-r+1}. In case two, the first and last 2^m coordinates will each have weight at least 2^{m-r}. In case three, the last 2^m coordinates have weight 0, but the first 2^m coordinates have weight 2^{m-r+1}. In all of these cases, we know that the overall vector has weight at least 2^{m+1-r}, completing the induction for the distance. □

If we have proven the formula for distance for $r-1$ and all m, then we can use induction on m. The base case is $\mathcal{R}(r,r)$ and we use the claim to prove the distance formula for this specific value of r and all m. This then allows us to use induction on r and the base case of $\mathcal{R}(1,m)$ to prove the distance formula for all values of r and m.

□

4.3 Dual Codes

4.3.1 Definition of a Dual Code

Definition 4.11. If C is a linear code, the *dual code* $C^\perp$ is

$$C^\perp = \{y \in \mathbb{Z}_2^n | x \cdot y = 0 \ \forall x \in C\}. \tag{4.13}$$

The dual code switches the role of the generator and parity check matrices: The generator matrix of $C^\perp$ is the parity check matrix of C and the parity check matrix of $C^\perp$ is the generator matrix of C. (Note that $(C^\perp)^\perp = C$.) It follows that the dual code of an $[n,k,d]$ code is an $[n,n-k,d']$ code. The distance d' does not in general have to be related to the distance d.

We also saw a definition of a dual code when discussing the binary symplectic representation of a stabilizer code. The dot product appears in this definition and the symplectic form appeared in that one, but otherwise they are the same.

We can also define *self-dual* codes and *weakly self-dual* codes in the same way as in section 3.5. That is, a self-dual code is equal to its dual, and a weakly self-dual code is contained in its dual.

4.3.2 Dual Codes for the Examples

For the 7-bit Hamming code, we've already worked out the generator and parity check matrices. Looking at the 8 vectors in the span of the rows of the parity check matrix of the 7-bit Hamming code, we see that all the nonzero vectors in the dual code have weight 4. The dual code of the $[7, 4, 3]$ is thus a $[7, 3, 4]$ code. We've already seen that the 7-bit Hamming code is related to a Reed-Muller code. The dual is too — if we take $\mathcal{R}(1, 3)$ and drop the all-1s vector, one bit is always zero. If we then discard that bit, we get the dual of the 7-bit Hamming code.

This is true in general:

Theorem 4.10. *Take $\mathcal{R}(1, m)$, remove the all-1s vector, and then* puncture *it: drop the bit that is always 0. The resulting $[2^m - 1, m, 2^{m-1}]$ code is the dual of the $[2^m - 1, 2^m - m - 1, 3]$ Hamming code.*

Proof. First, let us check the parameters of the punctured Reed-Muller code. Dropping the all-1s vector removes one encoded bit, leaving m logical bits. Removing codewords does not decrease the distance, and since the remaining vectors all have weight 2^{m-1}, it does not increase it in this case either. Dropping a bit that is always 0 also does not change the distance, giving the parameters $[2^m - 1, m, 2^{m-1}]$.

We are left with a generator matrix which has m rows $v_1, \ldots, v_m$. The jth bit of v_i is the ith bit of the binary representation of j, so the jth column of the generator matrix is exactly the binary representation of v_i. This was how we constructed the parity check matrix of the $[2^m - 1, 2^m - m - 1, 3]$ code, which is the generator of the dual. □

Naturally, this also means that the duals of the Reed-Muller codes $\mathcal{R}(1, m)$ are related to the Hamming codes. In the special case of $\mathcal{R}(1, 3)$, it was related both to the 7-bit Hamming code *and* to its dual. That is because $\mathcal{R}(1, 3)$ is a self-dual code. Most Reed-Muller codes are not self-dual, but $\mathcal{R}(1, 3)$ is not the only one that is. More importantly, the dual of every Reed-Muller code is another Reed-Muller code.

Theorem 4.11. *The dual of $\mathcal{R}(r, m)$ is $\mathcal{R}(m - r - 1, m)$ ($r \leq m - 1$).*

Proof. Let us take the dot product of two basis vectors $w \in \mathcal{R}(r, m)$ and $w' \in \mathcal{R}(r', m)$. The dot product is the parity of the pointwise product ww'. But w is the pointwise product of up to r of the v_i vectors, and w' is the pointwise product of up to r' of the v_i vectors, so ww' is the pointwise product of up to $r + r'$ of the v_i vectors. Suppose we eliminate redundant v_is that appear twice in the product, leaving us with $s \leq r + r'$ vectors v_i that appear in at least one of the two products w and w'. We already know from theorem 4.8 that such a product has weight exactly 2^{m-s}. Therefore the dot product of w and w' (the parity of the pointwise product) is 0 unless $s = m$, which is only possible if $r + r' \geq m$. Therefore, $\mathcal{R}(m - r - 1, m)$ is orthogonal to $\mathcal{R}(r, m)$, and is contained in its dual.

Now, $\mathcal{R}(r, m)$ encodes $N(r, m) = \binom{m}{0} + \binom{m}{1} + \cdots + \binom{m}{r}$ bits by theorem 4.8, so its dual encodes $2^m - N(r, m)$ bits. But $\mathcal{R}(m - r - 1, m)$ encodes

$$\binom{m}{0} + \binom{m}{1} + \cdots + \binom{m}{m - r - 1} = \binom{m}{m} + \binom{m}{m - 1} + \cdots + \binom{m}{r + 1} \tag{4.14}$$

bits. Therefore, $N(r, m) + N(m - r - 1, m) = 2^m$, and $\mathcal{R}(m - r - 1, m)$ is not only contained in the dual of $\mathcal{R}(r, m)$, it is the same size as the dual, and therefore equals the dual. □

Corollary 4.12. *When $m = 2r + 1$, the Reed-Muller code $\mathcal{R}(r, m)$ is self-dual. When $m \geq 2r + 1$, $\mathcal{R}(r, m)$ is weakly self-dual.*

4.4 Non-Binary Linear Codes

While binary codes, with the number of physical states $N = 2^n$, are the most common sort of error-correcting code, non-binary codes, which have other values of N, are also used. Some non-binary codes are quite important in the theory of quantum error correction, so we'll quickly cover the concepts here. We won't get to non-binary *quantum* codes until chapter 8, but we'll use some facts about non-binary classical codes even when discussing QECCs over qubits.

4.4.1 Linear Codes Over Finite Fields

When using the binary generalization of linear codes, we usually assume that $N = q^n$, and $q = p^m$ is a prime power. We want q to be a prime power because then there is a finite field GF(q) of size q, and we can consider $[1 \dots N]$ to be a vector space of dimension n over GF(q). (See appendix C for an introduction to finite fields.)

Definition 4.12. An error-correcting code $C \subseteq \mathrm{GF}(q)^n$ is a *linear code* if $x, y \in C \Rightarrow \alpha x + \beta y \in C$ for any $\alpha, \beta \in \mathrm{GF}(q)$. C is an *additive code* if $x, y \in C \Rightarrow x + y \in C$.

For binary linear codes, we only needed to worry about adding together codewords, but for non-binary linear codes, multiplication by scalars from the field GF(q) must also keep us within the code. If adding codewords gives a codeword but multiplication by scalars does not necessarily do so, then the code is merely *additive*. For bits, additive implies linear because the only scalars are 0 and 1, but for larger fields, there are more options.

We can again consider the possible errors to be vectors in $\mathrm{GF}(q)^n$. If an error e acts on a string x, the resulting state is $x + e$, as before. Bear in mind, however, that there are $q - 1$ different errors that can affect each register.

Non-binary linear codes have generator and parity check matrices defined in the same way as for binary codes, and the distance is also defined in the same way. We use the notation $[n, k, d]_q$ for a non-binary linear code with n physical registers, each of size q. The only difference in the basic properties of the code is that we now need to be careful of the distinction between addition and subtraction, which are the same for a binary code. In particular,

Theorem 4.13. *A non-binary linear code C corrects the error set $\mathcal{E}$ iff $e - f \notin C$ for all $e \neq f \in \mathcal{E}$. Equivalently, $H_C e \neq H_C f \ \forall e \neq f \in \mathcal{E}$ (i.e., all errors in $\mathcal{E}$ have different error syndromes).*

We can define the dual code for a non-binary code in just the same way as for a binary code using the dot product for a vector space over GF(q).

4.4.2 Example: Hamming Codes

The Hamming codes have a natural generalization to non-binary fields. Our goal in designing non-binary Hamming codes is again to choose the columns of the parity check matrix so that all single-qubit errors have different error syndromes. However, we need to be careful because there is now more than one possible single-bit error per register. If e_i is the error that is 1 in location i and 0 elsewhere, then e_i has syndrome equal to the ith column of the parity check matrix. When $\alpha \in \mathrm{GF}(q)$, αe_i has error syndrome equal to α times the ith column of the parity check matrix. Therefore, the correct generalization of the Hamming code is not to ensure just that all columns are different; instead, we want that no column of the parity check matrix is a scalar multiple of another for any scalar in GF(q).

For instance, GF(4) has 4 elements 0, 1, ω, and ω^2. Therefore, we have a $[5, 3, 3]$ Hamming code over GF(4) with the following parity check matrix:

$$\begin{pmatrix} 0 & 1 & 1 & 1 & 1 \\ 1 & 0 & 1 & \omega & \omega^2 \end{pmatrix} \tag{4.15}$$

Notice that we don't include columns $(0,\omega)$ or $(0,\omega^2)$ since they are scalar multiples of $(0,1)$, but that we include all columns of the form $(1,\alpha)$, since no two of them are scalar multiples. We don't, however, then need to include any columns (ω,α) or (ω^2,α).

Following this logic, we find the non-binary Hamming codes:

Theorem 4.14. *There exists a* $[(q^r-1)/(q-1),(q^r-1)/(q-1)-r,3]_q$ *code for any prime power* q *and any* $r>1$. *These codes are known as* Hamming codes.

Proof. There are r rows in the parity check matrix. We wish to choose $(q^r-1)/(q-1)$ columns so that none is a scalar multiple of another. Note that

$$(q^r-1)/(q-1) = 1+q+\cdots+q^{r-1}. \tag{4.16}$$

We will proceed by induction on r, the number of rows in the parity check matrix. If $r=1$, we just have the parity check matrix (1), which gives a $[1,0,1]_q$ code. It is a special case.

Next, we assume that we have a parity check matrix for $r-1$. For the r-row matrix, we can choose the first column to be all 0s except for the last row, which is 1. Then any column for which the first $r-1$ entries are 0 will be a scalar multiple of this column. The remaining columns are of the form (v,α), where v is a column of the parity check matrix for the Hamming code for q and $r-1$, and α is any element of GF(q). When $v\neq v'$ are two different columns of the $r-1$ Hamming code parity check matrix, than $v\neq\beta v'$, so it's certainly true that $(v,\alpha)\neq\beta(v',\alpha')$. Thus, we don't get columns which are scalar multiples that have different entries in the first $r-1$ entries. We should also compare (v,α) with (v,α'), but since the first r entries are not all 0, the only possible scalar factor between them is 1, which implies that $\alpha=\alpha'$. Thus, this scheme gives independent columns, as desired. We can pick $(q^{r-1}-1)/(q-1)$ columns of the $r-1$ Hamming code, and q entries for the last row in the column, plus we have the first column $(0,0,\ldots,0,1)$. The total number of columns is thus

$$1+q[(q^{r-1}-1)/(q-1)] = 1+q(1+q+\cdots+q^{r-2}) = 1+q+\cdots+q^{r-1} = (q^r-1)/(q-1), \tag{4.17}$$

as desired. □

4.4.3 Example: Reed-Solomon Codes

Reed-Solomon codes are a useful class of codes which are based on polynomials over finite fields.

Definition 4.13. Let $\alpha_1,\ldots,\alpha_n$ be n distinct elements of GF(q), and let $k\leq n$. A *Reed-Solomon code* is

$$\{(f(\alpha_1),\ldots,f(\alpha_n))|f \text{ is a polynomial of degree } <k\}. \tag{4.18}$$

The encoder for this code equates the input $(\beta_0,\ldots,\beta_{k-1})$ to the polynomial

$$f(x) = \beta_0+\beta_1 x+\beta_2 x^2+\cdots+\beta_{k-1}x^{k-1}. \tag{4.19}$$

Reed-Solomon codes are widely used for practical purposes, for instance to encode DVDs to protect against minor damage and in QR codes in case some part of the code can't be read. They are useful because they have a large distance and are easy to encode and decode. But who cares about that stuff? It's all very 20th-Century. The *real* reason Reed-Solomon codes are interesting is that they are useful for making quantum codes, although we won't see how until we discuss non-binary QECCs in chapter 8.

Theorem 4.15. *A Reed-Solomon code with* n *points from* GF(q) *and polynomials of degree at most* $k-1$ *is an* $[n,k,n-k+1]_q$ *code.*

Proof. Directly from the definition we can see that there are n physical registers and k logical registers. The distance is less obvious. The most straightforward way to see it is to consider correcting erasure errors.

Suppose that t registers have been erased. We are then left with $n-t$ registers, which are the values of the polynomial f evaluated at $n-t$ different points. We know that f has degree at most $k-1$, and

a degree $k-1$ polynomial is determined by its value at any k points. To be more concrete, given any k points, we have k different linear equations for the coefficients $\beta_0, \ldots, \beta_{k-1}$. The equations are defined by the Vandermonde matrix $V_{ij} = \alpha_i^{j-1}$. (I have assumed that the registers which are available correspond to the points $\alpha_1, \ldots, \alpha_k$ for notational simplicity.) The Vandermonde matrix is non-singular — it has determinant $\prod(\alpha_i - \alpha_j)$ — so the equations have a unique solution.

In short, provided $n - t \geq k$, we can reconstruct f and decode the code. Thus, the code corrects $n-k$ erasure errors, so it has distance $n-k+1$. The distance can't be higher than that, because if we have $n-k+1$ erasure errors, there are only $k-1$ points left, and there are multiple possible polynomials which go through those points since we could choose any value for a kth point and still reconstruct a valid polynomial. □

4.5 Hamming, Gilbert-Varshamov, and Singleton Bounds, MDS Codes

To conclude the discussion of classical codes, we'll discuss some basic limits on the existence of classical codes. I won't get to the quantum analogue of these bounds until chapter 7, but the bounds help to understand the example codes that we've discussed. As you'll see, the Hamming codes and Reed-Solomon codes are optimal codes, giving a maximal k and d for minimum n.

4.5.1 Hamming Bound, Perfect Codes

One can set a simple upper bound by taking advantage of the requirement that the states must be distinguishable after errors.

Theorem 4.16 (Hamming bound)**.** *An $(n, K, 2t+1)_q$ code must satisfy*

$$K \left(\sum_{j=0}^{t} (q-1)^j \binom{n}{j} \right) \leq q^n. \tag{4.20}$$

For large n,

$$(\log_q K)/n \leq 1 - (t/n)\log_q(q-1) - h_q(t/n), \tag{4.21}$$

where

$$h_q(x) = -x \log_q x - (1-x)\log_q(1-x). \tag{4.22}$$

Proof. Let x be a vector in the code C, and let S_x be the set of all vectors at distance at most t from x. (I.e., all strings that can be reached from x by altering up to t registers.) An error can take x to any string in S_x, so we need that $S_x \cap S_y = \emptyset$ when $x \neq y$. Otherwise, $z \in S_x \cap S_y$ can't be reliably decoded since it could have come from either x or y before the error.

Let us count the size of S_x. We break S_x into subsets $S_{x,j}$ which disagree with x on exactly $j \leq t$ registers. $S_{x,j}$ breaks down further into subsets which depend on which j registers disagree. There are $\binom{n}{j}$ possible sets of registers which disagree, and for a fixed set of registers, the strings in $S_{x,j}$ can take on any value except for the values in x. There are $q-1$ remaining choices for each of the j registers which disagree. Thus, the total size of $S_{x,j}$ is $(q-1)^j\binom{n}{j}$ and the total size of S_x is

$$\sum_{j=0}^{t} (q-1)^j \binom{n}{j}. \tag{4.23}$$

This is true for all x, and since $S_x \cap S_y = \emptyset$, the total number of strings in the union of all sets S_x is K times equation (4.23). This must be less than the total number of possible n-register strings, which is q^n, giving us equation (4.20).

To find the large n version of this equation, just take the logarithm base q. The h_q term comes from the log of the binomial coefficient (lemma 4.17), and only the largest value of $j = t$ contributes to the logarithm for large n. □

The formula for $h_q(x)$ is a fairly standard information-theoretic term, but it is sufficiently useful that I'll give a proof of it:

Lemma 4.17. *For large n,*

$$\log_q \binom{n}{j} = -j \log_q(j/n) - (n-j)\log_q(1-j/n) + o(n). \tag{4.24}$$

Proof.

$$\log \binom{n}{j} = \log(n!) - \log(j!) - \log[(n-j)!]. \tag{4.25}$$

(Assume everywhere that the base of the logarithm is q.)

Taking the logarithm of Stirling's formula and keeping only the terms at least linear in n, we have

$$\log(m!) = m \log m - m \log e. \tag{4.26}$$

Then

$$\log \binom{n}{j} = (n \log n - n \log e) - (j \log j - j \log e) - [(n-j)\log(n-j) - (n-j)\log e] \tag{4.27}$$

$$= j \log n + (n-j)\log n - j \log j - (n-j)\log(n-j) - [n - j - (n-j)]\log e \tag{4.28}$$

$$= -j \log(j/n) - (n-j)\log[(n-j)/n]. \tag{4.29}$$

□

The Hamming bound is also known as the *sphere-packing bound*. The name comes from the sets S_x, which can be viewed as "spheres" using the distance measure which counts the number of registers in which two strings differ. That metric is known as the *Hamming distance*. The spheres S_x are rather blocky for spheres, but that's what you get when you use a discrete distance.

The case when the Hamming bound is met exactly is somewhat interesting. First, it represents the best possible code you can have for a given n and $d = 2t + 1$. Second, when it is a linear code, it means that every error syndrome is used by an error of weight t or less.

Definition 4.14. A code which saturates the Hamming bound is *perfect*.

When $t = 1$, the condition for a perfect code is $K[1 + (q-1)n] = q^n$. Let us specialize to $K = q^k$. Then an $[n, k, 3]_q$ code is perfect if $(q-1)n = q^{n-k} - 1$. Letting $r = n - k$, we find that $n = (q^r - 1)/(q-1)$, $k = n - r$. These are exactly the parameters of the Hamming codes. The Hamming codes were designed to use up every error syndrome, so it's not surprising they are perfect codes, but now you can see that these parameters are the only ones possible for distance 3 perfect codes.

4.5.2 Gilbert-Varshamov Bound

The Hamming bound tells us that codes above a certain level of efficiency cannot exist — it is an *upper bound* on the efficiency of error-correcting codes. The Gilbert-Varshamov bound is a *lower bound*. It tells us that efficient codes do exist, provided we lower our standards a bit.

Theorem 4.18 (Gilbert-Varshamov bound)**.** *If n, K, and d satisfy*

$$K \left(\sum_{j=0}^{d-1} (q-1)^j \binom{n}{j} \right) \leq q^n, \tag{4.30}$$

then an $(n, K, d)_q$ code exists. For large n, a code exists if

$$(\log_q K)/n \leq 1 - (d/n)\log_q(q-1) - h_q(d/n), \tag{4.31}$$

with $h_q(x)$ given by equation (4.22).

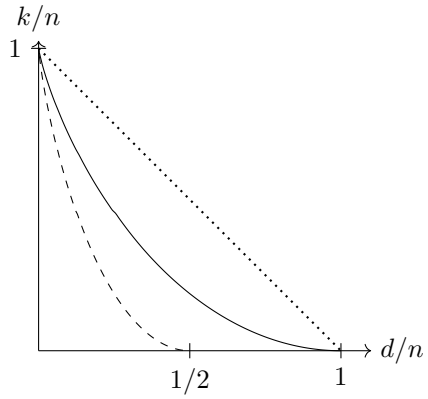

Figure 4.2: Classical Hamming bound (solid), Gilbert-Varshamov bound (dashed), and Singleton bound (dotted) for large n, $q = 2$

The difference between the upper bound given by the Hamming bound and the lower bound given by the Gilbert-Varshamov bound is replacing t (the number of correctable errors) with $d - 1$ (the number of detectable errors), which is $2t$. The asymptotic (large n) versions of the two bounds for $q = 2$ are plotted in figure 4.2, along with the Singleton bound (section 4.5.3). Of course, there may exist codes whose efficiency is in the region between the Hamming and Gilbert-Varshamov bounds, but this is not the generic case.

Proof. We will pick the codewords sequentially, thus showing the theorem by induction on K.

For the first codeword, pick any string x_1. Then exclude the Hamming sphere of radius $d-1$ around x_1, that is, the set S_{x_1} of all strings that are distance $d-1$ or less from x_1. Choose the second codeword x_2 to be any string outside S_{x_1}. x_2 has distance at least d from x_1, so the code $\{x_1, x_2\}$ has distance at least d.

In general, given any code $\{x_1, \ldots, x_{K-1}\}$ with distance at least d, exclude the radius $d-1$ Hamming spheres $S_{x_1}, \ldots, S_{x_{K-1}}$. Provided equation (4.30) is satisfied, there is at least one string not excluded. Choose it (at random if there is more than one) as the Kth codeword x_K. Then $\{x_1, \ldots, x_K\}$ also has distance at least d, since x_K is no closer than a Hamming distance d to any of the previous codewords. □

The proof can be strengthened to say not just that there exist codes with the parameters $(n, K, d)_q$, but actually that a *randomly chosen* (n, K) code has distance at least d (with high probability for large n). The Gilbert-Varshamov bound can also be improved to show the existence of codes with certain properties. For instance, when $K = 2^k$, there exists a linear code provided n, K, and d satisfy equation (4.30).

The proof of the Gilbert-Varshamov bound is sometimes referred to as *non-constructive*. Of course, in a literal sense it is constructive, since if we try all codes with the given parameters, we will eventually find one that works. In this context, the term means that it is not efficiently constructive in at least one of two ways. It can mean that picking a code according the algorithm implicitly given by the proof produces a code whose description is exponentially large in n. In this case, that is true, since $K = \exp(O(n))$ and each codeword has to be listed separately, but if we use the version of the Gilbert-Varshamov bound applying to linear codes, there is at least an efficient description of the resulting code in terms of the generator matrix. It could also mean that the algorithm for finding the code takes exponentially long in n. That is true both for the general version and linear code version of the Gilbert-Varshamov bound, since checking that a particular code has distance d takes exponentially long.

4.5.3 Singleton Bound

The Singleton bound is another upper bound, but it has a much simpler form than the Hamming bound. In particular, the form of the Singleton bound is the same for all register sizes q.

Theorem 4.19 (Singleton bound)**.** *If an* $(n, q^k, d)_q$ *code exists, then*

$$n - k \geq d - 1. \tag{4.32}$$

Proof. An $(n, q^k, d)_q$ code corrects $d-1$ erasure errors. For instance, if we discard the last $d-1$ registers, the remaining $n-(d-1)$ registers can still be used to reconstruct all k logical registers. This is only possible if $n-(d-1) \geq k$ since otherwise two different logical strings will be represented by the same string with $n-(d-1)$ components. □

Codes which saturate the Singleton bound have interesting properties, and therefore get their own name.

Definition 4.15. If an $(n, q^k, d)_q$ code satisfies $n = k + d - 1$, it is a *MDS* code.

"MDS" stands for "maximum distance separable." You can probably figure out the "maximum distance" part of the name. The "separable" part means that k coordinates of the codewords can be taken to be the logical registers when no errors are present. This is not a property that is possible for a quantum code, since it would violate the no-cloning theorem (if k qubits contain the logical state, then the remaining qubits contain no information about it, and would not be useful for error correction). I will still use the term "quantum MDS codes" for codes satisfying the analogous quantum Singleton bound.

Checking the parameters, you'll find that the Reed-Solomon codes are MDS codes. The repetition codes $[n, 1, n]$ are too. The Hamming codes with $r \geq 3$ are not — even though they are optimal for the Hamming bound, they do not saturate the Singleton bound.

4.5.4 Properties of MDS Codes

The dual code of an $[n, k, d]$ code is an $[n, n-k]$ code, but its distance might be bad. A remarkable property of MDS codes, and one that is very useful for making quantum codes, is that their duals also have good distance.

Theorem 4.20. *The dual of an MDS code is also an MDS code. In particular, the dual of an* $[n, k, n-k+1]$ *code is an* $[n, n-k, k+1]$ *code.*

Proof. We wish to show that any codeword from the dual code has weight greater than k. This will show that the distance of the dual code is at least $k+1$, but it cannot be any higher than that by the Singleton bound.

In terms of equations, we wish to show that if C is the original code and y is some string with $0 < \operatorname{wt} y \leq k$, then $\exists x \in C$ such that $y \cdot x \neq 0$. Recalling the proof of the Singleton bound, let us erase $d-1$ registers from an MDS code, leaving only k remaining registers, which are chosen to include the support of y. Call R the set of k registers we are considering. Since the logical state can be reconstructed from R, they must take on every possible value. That is, for any string x' with support within R, $\exists x \in C$ such that $x|_R = x'$. Let $y|_R = y'$. Since $y' \neq 0$, there certainly exists some x' such that $y' \cdot x' \neq 0$, and then $y \cdot x \neq 0$ whenever y has support on R. Since R was an arbitrary set of size k, this shows that if $y \in C^\perp$, then $\operatorname{wt} y > k$. □

Chapter 5

Combining The Old And The New: Making Quantum Codes From Classical Codes

Now that we've covered the basics of both classical and quantum error-correcting codes, we're ready to try combining them. By borrowing some codes from the old theory of classical error-correcting codes, we'll be able to make brand new quantum error-correcting codes, thus marrying quantum and classical error correction. But don't be blue, I'm sure there are still plenty of interesting quantum codes left to be discovered.

5.1 CSS Codes

5.1.1 CSS Construction and Parameters of a CSS Code

The first construction we'll discuss gives us a class of codes known as CSS codes after their inventors Calderbank, Shor, and Steane. The idea of CSS codes is to build on the observation that classical linear codes are a special case of stabilizer codes. In theorem 4.4, we made a stabilizer code by taking the parity check matrix for a classical linear code and replacing each 1 with a Z. The resulting stabilizer code corrects the same set of bit flip errors as the original classical code. If you instead replace the 1's in the parity check matrix with X's, you get a stabilizer code that corrects phase flip errors. In a CSS code, we do both: some of the stabilizer generators come from one classical linear code C_1 with the parity check matrix converted to Z's, and some generators come from a second linear code C_2 which is used to correct phase errors.

Definition 5.1. A stabilizer code is a *CSS code* if there is a choice of generators for which the stabilizer's binary symplectic representation is of the form

$$\left(\begin{array}{c|c} 0 & A \\ B & 0 \end{array}\right), \tag{5.1}$$

where A is a $r_1 \times n$ matrix and B is a $r_2 \times n$ matrix for some r_1, r_2. The generators of the form $(b|0)$ are X *generators* and the generators of the form $(0|a)$ are Z *generators*.

In other words, some generators for a CSS code are tensor products of only X and I and some are tensor products of only Z and I. This statement is of course dependent on the exact choice of generators. If you pick a different set of generators by multiplying some of the X generators with some of the Z generators, you will usually get generators which involve more than one of X, Y, and Z in the same operator. That doesn't mean the code is not a CSS code, only that you've picked a strange set of generators.

	Z	Z	Z	Z	I	I	I
	Z	Z	I	I	Z	Z	I
	Z	I	Z	I	Z	I	Z
	X	X	X	X	I	I	I
	X	X	I	I	X	X	I
	X	I	X	I	X	I	X
$\overline{X}$	X	X	X	X	X	X	X
$\overline{Z}$	Z	Z	Z	Z	Z	Z	Z

Table 5.1: The stabilizer and logical Paulis for the 7-qubit code.

The CSS construction allows us to take two classical codes and make a quantum code. As an example, let's form a 7-qubit code from the 7-bit Hamming code discussed in section 4.2.3. The second code will also be the 7-bit Hamming code. Take the three rows in its parity check matrix and convert the 1's to Z's, getting three generators of the stabilizer. Then take the rows a second time and convert the 1's to X's, getting three more generators. The resulting stabilizer is shown in table 5.1.

What is the distance of the 7-qubit code? Using the Z generators of the stabilizer, we can detect and identify any single-qubit bit flip error, since those generators are derived from a classical code which can do so. The first three bits of the error syndrome tell us where a bit flip error is. Using the same logic, the last three bits tell us where any single-qubit phase error has occurred. If there is a Y error, or indeed an X error on one qubit and a Z error on another, then the error will show up in both the first three bits and the last three bits of the error syndrome, identifying it as an error combining X and Z. Thus, the code can correct any single-qubit X, Y, or Z error, and has distance 3.

How many encoded qubits do we have? Using proposition 3.3, we have $n = 7$ physical qubits and 6 generators, so there should be 1 encoded qubit. But hold on a minute. In order to have *any* encoded qubits, we can't just take an arbitrary set of Paulis and call them the generators of a stabilizer. In particular, to have a stabilizer, we need to check that the generators we've written down commute with each other. The Z generators automatically commute with each other and the X generators commute with each other, so all we need to check is that every Z generator commutes with each X generator. In the case of the 7-qubit code, they do. Therefore, the 7-qubit code is well-defined as a $[[7, 1, 3]]$ code. The 7-qubit code is also known as the *Steane code*, since Steane first proposed it.

In the case of the 7-qubit code, we derived both the X and Z generators from the same code, the $[7, 4, 3]$ Hamming code. For a more general CSS code, we don't need to do that. We can use C_1 to correct bit flip errors and C_2 to correct phase errors.

Theorem 5.1. *Let C_1 be an $[n, k_1, d_1]$ classical linear code with parity check matrix H_1 and C_2 be an $[n, k_2, d_2]$ classical linear code with parity check matrix H_2. Suppose ${C_1}^\perp \subseteq C_2$. Let S be the CSS code with stabilizer*

$$\left(\begin{array}{c|c} 0 & H_1 \\ H_2 & 0 \end{array}\right). \tag{5.2}$$

Then S is an $[[n, k, d]]$ quantum code with $k = k_1 + k_2 - n$ and $d \geq \min\{d_1, d_2\}$.

There are a couple of things to notice about the statement of the theorem. You might think that the condition ${C_1}^\perp \subseteq C_2$ implies an asymmetry between C_1 and C_2, but that is not the case. Actually, the theorem treats them on an equal basis because ${C_1}^\perp \subseteq C_2 \Leftrightarrow {C_2}^\perp \subseteq C_1$. Also, observe that if $n > k_1 + k_2$, the theorem would predict a stabilizer code with a negative number of encoded qubits. That can't be right, and of course, it isn't. When $n > k_1 + k_2$, it is not possible that ${C_1}^\perp \subseteq C_2$.

While the theorem is phrased as just one way to make a CSS code, by comparing the theorem and the definition of a CSS code, you can see that it is actually the *only* way to make a CSS code. In the future, I'll refer to the codes C_1 and C_2 of a general CSS codes, indicating the classical codes that produce the Z generators and X generators, respectively. The choice of whether C_1 has the X generators or the Z

generators is an arbitrary convention, and you may find the other choice in the literature. Also, sometimes people will use the name "C_1" when they mean what I am calling "${C_1}^\perp$." Again, this is somewhat an arbitrary convention.

Proof. The main thing we need to check is that the X generators commute with the Z generators. Any X generator is of the form $(x|0)$, where $x \in {C_2}^\perp$. It is in the dual since it is derived from a row of the parity check matrix of C_2. Any Z generator is derived from the parity check matrix of C_1, so it has the form $(0|z)$, with $z \in {C_1}^\perp$. Then

$$(x|0) \odot (0|z) = x \cdot z, \tag{5.3}$$

with the usual binary inner product on the right. Thus, the stabilizer is Abelian iff $x \cdot z = 0$ for all $x \in {C_2}^\perp$, $z \in {C_1}^\perp$. Equivalently, we could say that if $z \in {C_1}^\perp$, then $z \in ({C_2}^\perp)^\perp$. Since $({C_2}^\perp)^\perp = C_2$, that produces the condition ${C_1}^\perp \subseteq C_2$.

Now let us determine the parameters of S. H_1 has $n - k_1$ rows and H_2 has $n - k_2$ rows, so the stabilizer has $2n - k_1 - k_2$ generators. Therefore, it has $n - (2n - k_1 - k_2) = k_1 + k_2 - n$ logical qubits. The code can detect up to $d_1 - 1$ bit flip errors using the Z generators, and it can detect up to $d_2 - 1$ phase errors using the X generators, and detecting bit flip errors does not in any way interfere with detecting phase errors. Any Pauli of weight less than $\min\{d_1, d_2\}$ can be written as a product PQ, with P a tensor product of X and I with weight $< d_1$ and Q a tensor product of Z and I with weight $< d_2$. The Pauli is non-trivial if at least one of P and Q is non-trivial, in which case it can be detected by looking at the appropriate bits of the error syndrome. Thus, the distance is at least $\min\{d_1, d_2\}$. □

From theorem 5.1, you can see why I made such a big deal about determining the duals of codes in chapter 4. The $[7, 4, 3]$ Hamming code contains its own dual, which is why we can use two copies of it to make the 7-qubit code. We can get other CSS codes by using the other example classical codes. For instance, let $r > m - r - 1$. Then $\mathcal{R}(r, m)^\perp = \mathcal{R}(m - r - 1, m) \subset \mathcal{R}(r, m)$, and we can make a CSS code with $C_1 = C_2 = \mathcal{R}(r, m)$. For instance, $\mathcal{R}(2, 4)$ is a $[16, 11, 4]$ code, and using it for C_1 and C_2, we get a $[[16, 6, 4]]$ CSS code.

We don't have to use the same code twice. For instance, we can let $C_1 = \mathcal{R}(2, 4)$ and $C_2 = \mathcal{R}(3, 4)$, which is a $[16, 15, 2]$ code. ${C_2}^\perp = \mathcal{R}(0, 4)$, which is just the 16-bit repetition code. $\mathcal{R}(0, 4) \subset C_1$, so we can make a CSS code, getting a $[[16, 10, 2]]$ code. Of course, this particular construction is not ideal if we're interested in a distance 2 code, since by taking $C_1 = C_2 = \mathcal{R}(3, 4)$, we get a $[[16, 14, 2]$ code, which has the same distance but more encoded qubits. Still, it might be useful if we want a code that detects any single-qubit phase error but can actually correct a bit flip error.

5.1.2 Degeneracy and CSS Codes

Theorem 5.1 says that the distance of S is greater than or equal to $\min\{d_1, d_2\}$. Why not just equal to? After all, since code C_1 has distance d_1, there is a bit flip error of weight d_1 that cannot be detected by code C_1 and therefore the corresponding Pauli error has 0 error syndrome for S. Similarly, C_2 has distance d_2, so there is also a Pauli with weight d_2 which is a tensor product of Z and I and has 0 error syndrome. But for a quantum code, 0 error syndrome is not enough to make an error undetectable. 0 error syndrome means that the error is in $\mathsf{N}(\mathsf{S})$. An error is undetectable only if it is in $\hat{\mathsf{N}}(\mathsf{S}) \setminus \hat{\mathsf{S}}$. That is, when a CSS code is degenerate, its distance could be greater than one might expect simply by examining the two classical codes that make it up.

For instance, the 9-qubit code is a degenerate CSS code. C_1 is composed of three copies of the repetition code. It has distance 3. However, C_2 has the following parity check matrix:

$$\begin{pmatrix} 1 & 1 & 1 & 1 & 1 & 1 & 0 & 0 & 0 \\ 0 & 0 & 0 & 1 & 1 & 1 & 1 & 1 & 1 \end{pmatrix}. \tag{5.4}$$

C_2 contains strings such as $(1, 1, 0, 0, 0, 0, 0, 0, 0)$ which have weight 2. Thus, C_2 has distance 2. (It is easy to check that any single-bit error will have nonzero error syndrome.) If we just took the distance to be $\min\{d_1, d_2\}$, we would think that the nine-qubit code had distance 2. However, the phase error formed from

the short codeword above is Z_1Z_2, which is in S. Similarly for all other weight 2 codewords of C_2. This is why the distance of the nine-qubit code can be 3.

5.1.3 Codewords of a CSS Code in Computational and Dual Basis

CSS codes also look nice when the codewords are written in the standard basis. The projector on the code space is a product of two projectors Π_1 and Π_2. Π_i is the projector on the $+1$ eigenspace of the generators derived from C_i. Π_1 thus projects on the subspace spanned by codewords of C_1. Π_2 can be written as a sum

$$\Pi_2 = \frac{1}{2^{n-k_2}} \left(\sum_{x \in {C_2}^\perp} P_x \right), \tag{5.5}$$

where P_x is the Pauli with binary symplectic representation $(x|0)$. The Paulis of this form (for $x \in {C_2}^\perp$) are the stabilizer elements formed from products of the generators derived from the parity check matrix of C_2.

Therefore, we can find the codewords of S by taking some codeword of C_1 (which is all that can pass Π_1) and applying Π_2. In general, we get something of the form

$$|u + {C_2}^\perp\rangle = \sum_{v \in {C_2}^\perp} |u + v\rangle, \tag{5.6}$$

for $u \in C_1$. Recall that ${C_2}^\perp \subseteq C_1$ and C_1 is linear, so $u + v \in C_1$.

When are two such codewords $|u + {C_2}^\perp\rangle$ and $|u' + {C_2}^\perp\rangle$ equal?

$$0 = |u + {C_2}^\perp\rangle - |u' + {C_2}^\perp\rangle = \sum_{v \in {C_2}^\perp} |u + v\rangle - \sum_{v' \in {C_2}^\perp} |u' + v'\rangle. \tag{5.7}$$

This is only possible if every term in the first sum is cancelled by a term in the second sum. That is, when $v \in {C_2}^\perp$, $u + v = u' + v'$ for some $v' \in {C_2}^\perp$. Thus, $u - u' = v' - v \in {C_2}^\perp$ since ${C_2}^\perp$ is linear. The states $|u + {C_2}^\perp\rangle$ only depend on cosets of ${C_2}^\perp$ within C_1, thus explaining the notation I chose to represent the basis states.

C_1 has 2^{k_1} codewords and ${C_2}^\perp$ has 2^{n-k_2} codewords, so $C_1/{C_2}^\perp$ has $2^{k_1+k_2-n}$ codewords, which is the same as the dimension of S. The codewords $|u + {C_2}^\perp\rangle$ form a basis for the code space of the CSS code.

I claimed that in the CSS construction, the two classical codes used were treated equally, but in this expansion, they certainly seem unequal. The solution lies in looking in the Hadamard rotated basis. The Hadamard transform switches the role of X and Z, so you might expect that it switches the role of C_1 and C_2. If you expected that, you are correct. Let's calculate it explicitly:

$$\begin{aligned}
H^{\otimes n}|u + {C_2}^\perp\rangle &= \sum_{v \in {C_2}^\perp} H^{\otimes n}|u + v\rangle && (5.8)\\
&= \sum_{v \in {C_2}^\perp} \sum_w (-1)^{(u+v)\cdot w}|w\rangle && (5.9)\\
&= \sum_w (-1)^{u\cdot w} \left(\sum_{v \in {C_2}^\perp} (-1)^{v\cdot w} \right) |w\rangle && (5.10)\\
&= \sum_{w \in C_2} (-1)^{u\cdot w}|w\rangle && (5.11)\\
&= \sum_{x \in C_2/{C_1}^\perp} (-1)^{u\cdot x} \sum_{y \in {C_1}^\perp} |x + y\rangle && (5.12)\\
&= \sum_{x \in C_2/{C_1}^\perp} (-1)^{u\cdot x}|x + {C_1}^\perp\rangle && (5.13)
\end{aligned}$$

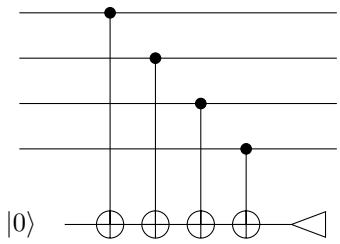

Figure 5.1: A circuit to measure the parity of 4 qubits.

To get the fourth line, observe that if $w \in C_2$, then $v \cdot w = 0$ always, but if $w \notin C_2$, then $v \cdot w = 0$ for half of the values of v and $v \cdot w = 1$ for the other half of the values of v. (It must be nonzero for some v since $w \notin C_2$. Call that v_0. Then if $v \in {C_2}^\perp$, so is $v + v_0$, but exactly one of $v \cdot w = 1$ and $(v + v_0) \cdot w = 1$. Thus we can pair the elements of ${C_2}^\perp$ such that within each pair one is orthogonal to w and one is not.)

In the next-to-last line, I have broken the sum over w into a sum over cosets of ${C_1}^\perp$ and a sum over elements of the cosets. This is a sensible thing to do because $u \cdot w$ only depends on which coset w lies in of ${C_1}^\perp$ in C_2: If $w' = w + y$, $y \in {C_1}^\perp$, then $u \cdot w' = u \cdot w + u \cdot y$, but $u \in C_1$, so $u \cdot y = 0$.

In particular, if we have associated the basis codewords $|u + {C_2}^\perp\rangle$ with logical basis codewords, then we recognize equation (5.13) as a Hadamard transform of the logical codewords, with the new basis codewords $|x + {C_1}^\perp\rangle$. In the standard basis, the CSS code consists of superpositions over cosets of ${C_2}^\perp$ in C_1, while in the Hadamard-rotated basis, it consists of superpositions over cosets of ${C_1}^\perp$ in C_2.

5.1.4 Error Correction for a CSS Code

CSS codes are stabilizer codes, so any general technique for performing error correction on stabilizer codes will work for CSS codes too. However, CSS codes have additional special structure which we can take advantage of to get better error correction procedures. In section 12.3, I'll discuss a fault-tolerant error-correction procedure that is designed for CSS codes, but for now, I'll just discuss a non-fault-tolerant scheme.

For a general stabilizer code, the bits of the error syndrome come from the eigenvalues of the stabilizer generators. For a CSS code, the stabilizer generators break up into two parts, one from the code C_1 and one from the code C_2. The first set of syndrome bits identifies bit flip errors, while the remaining syndrome bits identify phase errors.

In the standard basis, the codewords are superpositions of codewords of C_1, so we can measure the bit flip syndrome by measuring the parity checks of C_1. Of course, we must be careful to measure *only* the parity checks and nothing more, since we don't want to destroy any superposition of logical states. To measure a parity check, you can add a single ancilla qubit in the state $|0\rangle$ and perform CNOT gates from all the qubits involved in the parity check to the ancilla. Then measure the ancilla qubit and the outcome will be the desired parity. See figure 5.1 for an example.

The bit flip syndrome we get this way is exactly the syndrome of the classical code code C_1 if it underwent the same bit flip error. In order to decode the syndrome and learn the actual error, we can just invoke the classical procedure. If the code C_1 has an efficient syndrome decoding algorithm, then we get one for the bit flip errors of the CSS code also.

For the phase errors, we can simply rotate into the Hadamard basis. Now the codewords are superpositions of codewords of C_2, and the phase errors have become bit flip errors. If, after the Hadamard transform, we measure the parity checks of C_2, that is the same as measuring the phase error syndrome for the CSS code. The phase error syndrome is exactly the same as the error syndrome for C_2 if it underwent bit flip errors corresponding to the locations of the phase errors. Again, we can use the syndrome decoding algorithm for C_2 to identify the phase errors for the CSS code.

$+$	0	1	ω	ω^2
0	0	1	ω	ω^2
1	1	0	ω^2	ω
ω	ω	ω^2	0	1
ω^2	ω^2	ω	1	0

$\times$	0	1	ω	ω^2
0	0	0	0	0
1	0	1	ω	ω^2
ω	0	ω	ω^2	1
ω^2	0	ω^2	1	ω

Table 5.2: The addition and multiplication tables for GF(4).

5.2 GF(4) Codes and Stabilizer Codes

Now we'll return to more general stabilizer codes. CSS codes have many nice properties, but they are not perfect. For instance, general stabilizer codes can be more efficient than CSS codes — the 7-qubit code is the smallest CSS code that corrects 1 error, whereas the 5-qubit code, a stabilizer code, is the best QECC of any type that corrects 1 error. While there are some non-stabilizer codes known that are slightly better than any stabilizer code, the differences are small for codes correcting Pauli channels.

In this section, I'll therefore discuss a technique for adapting some classical codes to get stabilizer codes which are not CSS codes. In order to do so, we'll have to go to non-binary codes.

5.2.1 Correspondence Between GF(4) and the Pauli Group

The main "insight" of this particular technique is that the one-qubit Pauli group has 4 elements, and so does the finite field GF(4). Amazing, no?

Really, we're connecting $\hat{\mathsf{P}}_n$, the Pauli group sans phases, with an n-dimensional vector field over GF(4). For $n = 1$, we simply associate each element of the Pauli group with the elements of GF(4):

$$\begin{array}{ll} I \leftrightarrow 0 & X \leftrightarrow 1 \\ Z \leftrightarrow \omega & Y \leftrightarrow \omega^2 \end{array} \tag{5.14}$$

For n qubits, the ith tensor factor of $P \in \hat{\mathsf{P}}_n$ becomes the ith component of a vector over GF(4) using the rules in equation (5.14).

The conversion works much the same way as the conversion between $\hat{\mathsf{P}}_n$ and the binary symplectic representation of the Pauli group. Multiplication in $\hat{\mathsf{P}}_n$ becomes addition in GF(4). The full correspondence is summarized in table 5.3. It's also worth recalling the addition and multiplication tables for GF(4), which are given in table 5.2.

5.2.2 The GF(4) Symplectic Inner Product

As with the binary symplectic representation, we need to recover somehow the notation of commutation, and again we turn to a symplectic inner product. We want some map from GF(4) $\times$ GF(4) to $\mathbb{Z}_2$ which gives 0 when one input is 0 or both inputs are the same, and gives 1 otherwise. It turns out that the correct formula is $\mathrm{tr}(\overline{a}b)$. The $\overline{a}$ and trace operations are defined as follows for GF(4):

$$\begin{array}{llll} \overline{0} = 0 & \overline{1} = 1 & \mathrm{tr}\, 0 = 0 & \mathrm{tr}\, 1 = 0 \\ \overline{\omega} = \omega^2 & \overline{\omega^2} = \omega & \mathrm{tr}\, \omega = 1 & \mathrm{tr}\, \omega^2 = 1 \end{array} \tag{5.15}$$

You can check by trying all combinations that this formula works. The generalization to n-dimensional vectors is then straightforward:

$$a * b = \mathrm{tr}(\overline{a} \cdot b), \tag{5.16}$$

where $\cdot$ is just the usual dot product. In the classical coding literature, this inner product is sometimes known as the *trace-Hermitian inner product*.

In the Pauli group	In GF(4)
I	0
X	1
Z	ω
Y	ω^2
Multiplication	Addition
$c(P,Q)$	$a * b = \mathrm{tr}(\overline{a} \cdot b)$
Phase	No equivalent
No equivalent	Multiplication
Unitary T (see chapter 6)	Multiplication by ω
Stabilizer S	Weakly self-dual additive code S
Normalizer $\mathsf{N}(\mathsf{S})$	Dual $\mathsf{S}^\perp$ (under $*$)

Table 5.3: Equivalence between the Pauli group and GF(4).

5.2.3 Stabilizer Codes as GF(4) Codes

We can convert a stabilizer to sets of vectors over GF(4) just as we converted them to the binary symplectic representation. We'd like to interpret the resulting set as a classical error-correcting code over GF(4). Formally, there is no problem in doing so. However, what we get is not necessarily a linear code. Sometimes we do get a linear code, as in the example of the five-qubit code (converted to a GF(4) code in table 5.4), but it is not hard to come with stabilizer codes which don't produce linear GF(4) codes.

Because $P, Q \in \mathsf{S} \Rightarrow PQ \in \mathsf{S}$, the GF(4) code S which we get is additive (closed under addition). However, for it to be linear, S would also need to be closed under multiplication by ω, and that is not necessarily true. (It also needs to be closed under multiplication by ω^2, but that follows automatically if it is closed under multiplication by ω.)

The other condition we need to satisfy is that the stabilizer is Abelian. We can express this in terms of a dual with respect to the symplectic product $*$. The dual of an additive code is additive, and the dual of the GF(4) conversion of a stabilizer is the GF(4) conversion of the normalizer. An additive code corresponds to an Abelian group if it is weakly self-dual.

We now have the main components we need to convert GF(4) codes into stabilizer codes.

Theorem 5.2. *Suppose C is an additive code over* GF(4) *which is weakly self-dual under $*$. Then C can be converted to a stabilizer S with parameters $[[n, k, d]]$. n is the number of physical registers in C. If C contains $K = 2^r$ codewords, then $k = n - r$. The distance d of S is the smallest weight of a member of $C^\perp \setminus C$, and in particular, d is at least equal to the distance of $C^\perp$.*

Note that there are a number of peculiar things involved in the conversion. In some sense $C^\perp$ is more closely analogous to the quantum code we get, since the distance of S is at least equal to the distance of $C^\perp$. However, the number of encoded qubits is a formula that does not show up at all in classical coding theory (which is more interested in writing $K = 4^{r'}$ than $K = 2^r$), and of course the distance can be even larger than the distance of $C^\perp$ because of degeneracy. And it is important to bear in mind that the dual is taken with respect to the symplectic product $*$ rather than the usual inner product.

The upshot is that if we look at the most common classical GF(4) codes and try to convert them into quantum codes, we won't get the most general stabilizer code. But who cares about that? We only want good codes, and if we can get them by looking at existing GF(4) codes, that's good enough.

5.2.4 Linear GF(4) Codes

For linear GF(4) codes, the conditions in theorem 5.2 simplify somewhat. In particular, we have the following:

Proposition 5.3. *If C is a linear* GF(4) *code, then its dual with respect to the inner product $\overline{x} \cdot y$ is the same as the dual with respect to $*$.*

1	ω	ω	1	0
0	1	ω	ω	1
1	0	1	ω	ω
ω	1	0	1	ω

Table 5.4: The five-qubit code converted to a GF(4) code.

Proof. We wish to show that $\overline{x} \cdot y = 0 \ \forall y \in C$ iff $x * y = 0 \ \forall y \in C$. The forward direction is trivial, so we only need to show the backwards direction.

Suppose $\mathrm{tr}(\overline{x} \cdot y) = 0$, but $\overline{x} \cdot y = 1$. Then $\overline{x} \cdot (\omega y) = \omega$ and $x * (\omega y) = \mathrm{tr}(\overline{x} \cdot (\omega y)) = 1$. Therefore, since C is linear, if $x * y = 0 \ \forall y \in C$, then $\overline{x} \cdot y = 0 \ \forall y \in C$. □

This simplifies the procedure of checking for weakly self-dual codes because we can use the dual under the standard inner product and then take the conjugate rather than have to compute the dual under the unusual symplectic inner product $*$.

5.2.5 Example: Perfect Qubit Codes

Now let's look at some concrete examples of constructing stabilizer codes from GF(4) codes. It turns out that the GF(4) Hamming codes have the right properties, or rather their duals do.

Theorem 5.4. *The duals (with respect to the standard inner product) of the Hamming codes over* GF(4) *can be converted to stabilizer codes. The dual of the* $[(4^r - 1)/3, (4^r - 1)/3 - r, 3]_4$ *Hamming code becomes a* $[[(4^r - 1)/3, (4^r - 1)/3 - 2r, 3]]$ *qubit stabilizer code.*

Notice that the resulting stabilizer code encodes $(4^r - 1)/3 - 2r$ qubits whereas the Hamming code encodes $(4^r - 1)/3 - r$ GF(4) registers. This is a consequence of using a base of 2 instead of 4 to count registers, as mentioned in the discussion of theorem 5.2.

Proof. The Hamming codes are linear, so we need to show that a Hamming code contains its dual relative to $\overline{x} \cdot y$. Looking at the construction of the non-binary Hamming codes in the proof of theorem 4.14, we see that if we discard the last row of the parity check matrix, the first column is all 0, and then every other column is repeated four times. That means that the inner product of any two of these rows will be zero, since we end up adding the same thing four times.

Next, we should show that we also get 0 if we take the inner product of the last row with another row i. Since the first column of row i is 0, we can ignore the first column. The other columns break up into sets of four, within which row i has some value a repeated four times, while the last row runs over all the values in GF(4): 0, 1, ω, and ω^2. Whatever the value of a,

$$\overline{a}0 + \overline{a}1 + \overline{a}\omega + \overline{a}\omega^2 = \overline{a}(0 + 1 + \omega + \omega^2) = 0. \tag{5.17}$$

That proves that the parity check matrix of the Hamming code can be converted into a stabilizer. The number of encoded qubits follows from theorem 5.2.

The dual (with respect to $\overline{x} \cdot y$) of the dual (with respect to the standard inner product) of a Hamming code is just the conjugate of the Hamming code, produced by replacing x with $\overline{x}$ everywhere in the code. The conjugate of a code has the same distance as the code since taking the conjugate does not change the weight, and therefore, the stabilizer codes we have derived have distance at least 3. In fact, these codes are non-degenerate, so the distance is exactly 3. □

We get codes with parameters $[[5, 1, 3]]$, $[[21, 15, 3]]$, $[[85, 77, 3]]$, etc. The $[[5, 1, 3]]$ code produced this way (shown in table 5.5) is equivalent to the $[[5, 1, 3]]$ code we discussed before. Note that while the classical $[5, 3, 3]_4$ Hamming code has two rows in its parity check matrix, the quantum $[[5, 1, 3]]$ code has four generators of its stabilizer. The vectors v, ωv are considered linearly dependent for a code over GF(4), so we only need

					$I \quad X \quad X \quad X \quad X$
0	1	1	1	1	$I \quad Z \quad Z \quad Z \quad Z$
1	0	1	ω	ω^2	$X \quad I \quad X \quad Z \quad Y$
					$Z \quad I \quad Z \quad Y \quad X$

Table 5.5: The parity check matrix of the five-bit GF(4) Hamming code and the five-qubit code derived from it.

to include one of them in the parity check matrix, but they convert to Paulis which are independent when considered as operators on qubits, so we need to list them both in the stabilizer.

This family of quantum codes is interesting because, like the classical Hamming codes they are derived from, the codes in this family use up all of the error syndromes. The $[[(4^r-1)/3, (4^r-1)/3-2r, 3]]$ code has $2r$ stabilizer generators, so 4^r error syndromes. There are $3n+1 = 4^r$ zero and one-qubit errors, and the code is non-degenerate, so each syndrome is used exactly once.

It is unclear what the correct definition of a perfect degenerate QECC should be, but a non-degenerate quantum code is *perfect* if the number of correctable errors is exactly equal to the number of error syndromes. Thus, the QECCs derived from the GF(4) Hamming codes are perfect qubit codes.

Chapter 6

Symmetries Of Symmetries: The Clifford Group

When dealing with stabilizer codes, it is helpful to restrict attention to a set of quantum gates that is guaranteed to treat the code nicely. There exists a unitary operation that will take any subspace (for instance, a quantum error-correcting code) into any other subspace of the same dimension. Sometimes that's exactly what you want. However, if you've taken the effort to work with a code with a nice tractable description in terms of its stabilizer, you don't want your work ruined by using a poorly-thought-out unitary. In general, quantum gates will map the code space of a stabilizer code into some other code, which might not be a stabilizer code.

The Clifford group is a group of unitary gates that is specifically chosen so that it does not do this. If you start with a stabilizer code and perform a Clifford group gate, you will always have another stabilizer code. The key to this is using only unitary operations which can be thought of as permutations of the Pauli group. A Clifford group operation then just switches one stabilizer into another.

6.1 Definition of the Clifford Group

6.1.1 Motivation for the Clifford Group

Suppose we perform the unitary U on a state $|\psi\rangle$ from a stabilizer code S. What happens to the stabilizer? Suppose $M \in \mathsf{S}$, so $M|\psi\rangle = |\psi\rangle$. We want to find M' for which $U|\psi\rangle$ is a $+1$ eigenstate. It turns out the correct choice is $M' = UMU^\dagger$:

$$M'U|\psi\rangle = UMU^\dagger U|\psi\rangle = UM|\psi\rangle = U|\psi\rangle, \tag{6.1}$$

since U is unitary. Running over all M in the stabilizer, we find that $\mathsf{S}' = \{UMU^\dagger | M \in \mathsf{S}\}$ is a set of operators for which all states $U|\psi\rangle$ are $+1$ eigenstates (where $|\psi\rangle$ is any element of $\mathcal{T}(\mathsf{S})$).

We'd *like* to say that S' is the new stabilizer of the code, with code space $U(\mathcal{T}(\mathsf{S}))$. However, the catch is that without any additional constraint on U, S' might contain many non-Paulis, and the stabilizer is supposed to be a subset of P_n. In addition, the true stabilizer of the subspace $U(\mathcal{T}(\mathsf{S}))$ might contain additional Paulis that are not in S'. Furthermore, $U(\mathcal{T}(\mathsf{S}))$ might not be a stabilizer code — the Paulis in $\mathsf{S}(U(\mathcal{T}(\mathsf{S})))$ might be insufficient to specify the subspace. (Recall definition 3.4.)

The Clifford group is a set of unitaries that does not have these complications. It maps stabilizers to stabilizers. Fortunately, the Clifford group contains many interesting quantum gates; unfortunately, it is not enough for a universal quantum computer. The Clifford group is sufficient for encoding stabilizer codes, and gives a good start on fault-tolerant operations, but eventually we will need to go beyond it.

6.1.2 Definition of the Clifford Group and Variants

Definition 6.1. The *Clifford group* C_n on n qubits is the normalizer of P_n in the unitary group $\mathsf{U}(2^n)$. That is,

$$\mathsf{C}_n = \{U \in \mathsf{U}(2^n) | UPU^\dagger \in \mathsf{P}_n \ \forall P \in \mathsf{P}_n\}. \tag{6.2}$$

The name "Clifford group" is not particularly illuminating, perhaps. It is motivated by the idea that there might be a connection of some sort to Clifford algebras, but the connection is not very close. To add to the confusion, you might encounter the term "Clifford group" in the mathematics literature referring to a different group. In quantum information papers, Clifford group refers to definition 6.1 or one of its variants defined below. You might also encounter the terms "normalizer group," "symplectic group" (or operations), or sometimes "stabilizer operations" for C_n. None of these terms is completely satisfactory, and "Clifford group" is the most widespread, so I will use that.

The Clifford group contains all gates of the form $e^{i\theta}I$, and if $U \in \mathsf{C}_n$, then $e^{i\theta}U \in \mathsf{C}_n$. As with the Paulis, global phase is frequently not significant for Clifford group elements. Indeed, it is *less* likely to matter for the Clifford group. Anticommutation is less important in the Clifford group than it is in the Pauli group, so we will usually consider not the full Clifford group, but the Clifford group with phases removed.

By definition, the Pauli group P_n is a normal subgroup of C_n. Sometimes it is better to consider the Clifford group with the Pauli subgroup modded out. The Pauli group only contains the phases $\pm 1, \pm i$, so even once the Pauli group is gone, there are still additional phases to worry about. Typically, we will want to remove those as well.

Definition 6.2.

$$\hat{\mathsf{C}}_n = \mathsf{C}_n / \{e^{i\theta}I\} \tag{6.3}$$

$$\check{\mathsf{C}}_n = \hat{\mathsf{C}}_n / \hat{\mathsf{P}}_n. \tag{6.4}$$

I will refer to these variants as the "Clifford group," sometimes without specifying which one I mean. Usually it doesn't much matter, or can be deduced from context (or both).

6.1.3 Example Clifford Group Elements

Now let's look at some Clifford gates. We know the Pauli group is a subgroup of C_n, so that gives us one set of examples. The Cliffords are defined to act on P_n by conjugation, and, as you'll see shortly, the best way of characterizing an element of the Clifford group is usually by giving the action under conjugation. Suppose we have $P \in \mathsf{P}_n \subset \mathsf{C}_n$. What does it do to another Pauli Q under conjugation?

$$PQP^\dagger = (-1)^{c(P,Q)} QPP^\dagger = (-1)^{c(P,Q)} Q. \tag{6.5}$$

Thus, $Q \mapsto \pm Q$, with the sign determined by whether P and Q commute or anticommute. The effect of conjugating by a Pauli is to rearrange the signs of other Paulis without changing their identity. This is easy to square with what we know about stabilizers from chapter 3: Applying the error P will move us from the $+1$ eigenspace of Q to the -1 eigenspace of Q iff P and Q anticommute. Moving to the -1 eigenspace is equivalent to modifying the stabilizer to contain $-Q$ instead of Q, which is the way we understand the action of Clifford group elements.

Another gate in the Clifford group is the Hadamard transform H. As we've discussed, the Hadamard transform switches the role of X and Z. This can be made concrete by looking at the conjugation action of H. You can work it out by multiplying together the matrices, but I'll just tell you the answer:

$$HXH = Z \tag{6.6}$$

$$HYH = -Y \tag{6.7}$$

$$HZH = X. \tag{6.8}$$

$H^\dagger = H$, so I've skipped the adjoints in the above equations. As you can see, the action of H is indeed to switch X and Z. The effect on states is to switch Z eigenstates with X eigenstates:

$$|0\rangle \text{ (stabilizer } Z) \leftrightarrow |+\rangle = |0\rangle + |1\rangle \text{ (stabilizer } X) \tag{6.9}$$

$$|1\rangle \text{ (stabilizer } -Z) \leftrightarrow |-\rangle = |0\rangle - |1\rangle \text{ (stabilizer } -X) \tag{6.10}$$

While its action on Y is not as dramatic as its action on X and Z, H does not leave Y completely alone. Instead, it changes the sign of Y, so $+1$ eigenstates of Y get switched with -1 eigenstates of Y:

$$\frac{1}{\sqrt{2}}(|0\rangle + i|1\rangle) \leftrightarrow \frac{1}{2}[(1+i)|0\rangle + (1-i)|1\rangle] = \frac{e^{i\pi/4}}{\sqrt{2}}(|0\rangle - i|1\rangle). \tag{6.11}$$

The conjugation action doesn't tell us about the overall phase $e^{i\pi/4}$ introduced by H, but that has no physical significance anyway.

The other important thing about H's action on Y is that I didn't need to specify it. The action of H on Y can be deduced from its action on X and Z. Conjugation is a *group homomorphism* — the conjugate of the product is the product of the conjugates:

$$UPQU^\dagger = (UPU^\dagger)(UQU^\dagger). \tag{6.12}$$

In this case,

$$HYH = H(iXZ)H = i(HXH)(HZH) = iZX = -Y. \tag{6.13}$$

Equivalently, we could deduce the action of H on X from the action on Y and Z, or the action on Z from the action on X and Y. The action on I, of course, will always be trivial ($UIU^\dagger = I$).

The Hadamard switches X and Z, but only changes the phase of Y. There are also Clifford group elements that switch other pairs of Paulis. For instance, $R_{\pi/4} \in \mathsf{C}_n$:

$$R_{\pi/4} X R_{\pi/4}^\dagger = Y \tag{6.14}$$

$$R_{\pi/4} Y R_{\pi/4}^\dagger = -X \tag{6.15}$$

$$R_{\pi/4} Z R_{\pi/4}^\dagger = Z. \tag{6.16}$$

This is not 100% analogous to H, since Z really is left alone by $R_{\pi/4}$, but Y picks up a minus sign under H. However, by multiplying with a Pauli, we can take care of that sign issue:

$$(YR_{\pi/4}) X (YR_{\pi/4})^\dagger = Y \tag{6.17}$$

$$(YR_{\pi/4}) Y (YR_{\pi/4})^\dagger = X \tag{6.18}$$

$$(YR_{\pi/4}) Z (YR_{\pi/4})^\dagger = -Z. \tag{6.19}$$

You can deduce these equations by performing the conjugation action of $R_{\pi/4}$ and then following it with the conjugation action of Y, which switches the signs around. $R_{\pi/4}$ is often called the S gate — since it is a member of the Clifford group, it shows up with some frequency.

You might wonder if we can completely get rid of the minus sign, rather than simply switching it to another location, by choosing an appropriate Pauli. The answer is no: any Pauli will commute with one Pauli and anticommute with two of them. Thus, it switches the sign of two of the three one-qubit Paulis X, Y, and Z. We can go from one minus sign to three minus signs, but never to zero or two. What we *can* do is change the signs of the generators of P_1 (or P_n when dealing with n qubits) in any way we like. For instance, to change $X \mapsto -X$, $Z \mapsto Z$, conjugate by Z. The change in the sign of Y is determined by the change in the signs of X and Z.

Among two-qubit Clifford group elements, the most famous gate is the CNOT gate, which has the following conjugation action on the Paulis:

$$X \otimes I \mapsto X \otimes X \tag{6.20}$$
$$Z \otimes I \mapsto Z \otimes I \tag{6.21}$$
$$I \otimes X \mapsto I \otimes X \tag{6.22}$$
$$I \otimes Z \mapsto Z \otimes Z. \tag{6.23}$$

We are dealing with the two-qubit Pauli group, and I have taken advantage of the homomorphism property of conjugation to just list the action of CNOT on a generating set of four Paulis for P_2. For any other Pauli, you can deduce the conjugation action of CNOT by multiplying as described above for the Hadamard.

6.1.4 Determining Clifford Group Element From Action on Generating Paulis

Describing the conjugation action of Clifford group elements certainly tells us a lot about the unitary we are dealing with, but you might worry that some information is being lost. Indeed, if $U' = e^{i\theta}U$, then

$$U'PU'^{\dagger} = e^{i\theta}UPU^{\dagger}e^{-i\theta} = UPU^{\dagger}, \tag{6.24}$$

so the conjugation action tells us nothing about the global phase of the unitary. Of course, the global phase doesn't have any physical significance, so this is not a great loss. But perhaps there are more important properties not captured by the conjugation action? The next theorem tells us that there are not:

Theorem 6.1. *Suppose U and V are unitaries which have the same action by conjugation on P_n:*

$$UPU^{\dagger} = VPV^{\dagger} \tag{6.25}$$

for all $P \in \mathsf{P}_n$. Then $U = e^{i\theta}V$ for some θ.

The theorem does not apply only to Clifford group elements; U and V can be *any* unitary gates. When applied to the Clifford group, theorem 6.1 tells us that the conjugation action uniquely identifies elements of $\hat{\mathsf{C}}_n$. Consequently, we will be able to work with elements of $\hat{\mathsf{C}}_n$ using just the conjugation action.

Proof. Note that $V^{\dagger}U$ acts on the Pauli group trivially by conjugation ($P \mapsto P$), so it will be sufficient to consider the case of $V = I$ and show that $U = e^{i\theta}I$.

When $UPU^{\dagger} = P$ for all $P \in \mathsf{P}_n$, that means that U maps any stabilizer state to a state with the same stabilizer. For instance, the basis state $|j\rangle$ is a stabilizer state with stabilizer generated by $(-1)^{j_i}Z_i$, $i = 1, \ldots, n$ (where j_i is the ith bit of j). The only states with this stabilizer are $e^{i\theta_j}|j\rangle$. We conclude that U is diagonal

$$U = \begin{pmatrix} e^{i\theta_1} & 0 & \cdots & 0 \\ 0 & e^{i\theta_2} & \cdots & 0 \\ \vdots & & \ddots & \\ 0 & & \cdots & e^{i\theta_{2^n}} \end{pmatrix} \tag{6.26}$$

We still need to show that all θ_j are the same. Now consider stabilizer states with stabilizer generators X_1 and $(-1)^{j_{i-1}}Z_i$ for $i = 2, \ldots, n$. The eigenstates of those stabilizers are of the form $e^{i\phi_j}|+\rangle|j\rangle$. Applying equation (6.26) to $|+\rangle|j\rangle$, we find

$$e^{i\theta_j} = e^{i\theta_{2^{n-1}+j}} = e^{i\phi_j}. \tag{6.27}$$

Similarly, looking at stabilizers with X_i in place of X_1, we find that

$$e^{i\theta_j} = e^{i\theta_{2^{n-i}+j}}, \tag{6.28}$$

for any j such that the ith bit is 0. Applying all these equalities, we find that all $e^{i\theta_j}$ terms are equal, proving the theorem. □

Which permutations of P_n are allowed for a conjugation action by a Clifford group element? We know that conjugation is a group homomorphism. That means that there is no hope that we can freely choose images for any elements of P_n except for a generating set. In addition, conjugation will always take $-I$ to $-I$. That means that conjugation must preserve commutation and anticommutation:

$$U(PQ)U^\dagger = U[(-1)^{c(P,Q)}QP]U^\dagger = (-1)^{c(P,Q)}(UQU^\dagger)(UPU^\dagger) \tag{6.29}$$

$$= (UPU^\dagger)(UQU^\dagger) = (-1)^{c(UPU^\dagger, UQU^\dagger)}(UQU^\dagger)(UPU^\dagger). \tag{6.30}$$

Thus, $c(UPU^\dagger, UQU^\dagger) = c(P,Q)$.

The usual set of generators for $\hat{\mathsf{P}}_n$ is $\{X_i, Z_i\}$. To keep the right commutation relations, the images of X_i and Z_i must commute with the images of X_j and Z_j for $j \neq i$. However, the images of X_i and Z_i must anticommute with each other.

There is one additional constraint: Conjugation by U is an isomorphism, since it can be inverted by conjugating by $U^\dagger$. Therefore, the generators must map to an independent set of Paulis. However, this property actually follows from the commutation relations, so we don't need to impose it separately.

If these conditions are satisfied, a similar approach to the proof of theorem 6.1 gives a constructive method for finding the unitary corresponding to a given conjugation map. The same procedure applies even for conjugation by a non-Clifford unitary.

Procedure 6.1. Suppose the map $M : \mathsf{P}_n \to \mathsf{U}(2^n)$ is a group homomorphism, with $M(X_i) = \overline{X}_i$, $M(Z_i) = \overline{Z}_i$, such that

$$c(\overline{X}_i, \overline{X}_j) = c(\overline{Z}_i, \overline{Z}_j) = 0,$$
$$c(\overline{X}_i, \overline{Z}_j) = \delta_{ij}. \tag{6.31}$$

(When $\overline{X}_i$ and $\overline{Z}_j$ are outside the Pauli group, the definition of $c(\cdot,\cdot)$ is the same, and $c(P,Q)$ is undefined here if P and Q neither commute or anticommute.)

The following procedure finds the matrix representation in the standard basis of a U for which conjugation by U performs M:

1. Find the state $|\psi_0\rangle$ which is a $+1$ eigenstate of $\overline{Z}_i$ for all $i = 1, \ldots, n$.

2. Let b be any number from 0 to $2^n - 1$, and let b_i be the ith bit of b. Let

$$\overline{X}(b) = \prod_i (\overline{X}_i)^{b_i}. \tag{6.32}$$

3. Let $|\psi_b\rangle = \overline{X}(b)|\psi_0\rangle$.

4. Let

$$U_{ab} = \langle a|\psi_b\rangle. \tag{6.33}$$

Proof of the validity of procedure 6.1. M is a group homomorphism and $Z_i = Z_i^\dagger$, so it follows that $\overline{Z}_i = \overline{Z}_i^\dagger$ as well. All of the $\overline{Z}_i$ commute with each other, so $\Pi = \frac{1}{2^n}\prod_i (I + \overline{Z}_i)$ is a projector with trace 1. Thus, there is a unique state $|\psi_0\rangle$ (up to global phase) which is a $+1$ eigenstate of all $\overline{Z}_i$, as needed for step 1. The remaining steps of the procedure give a linear map $U|b\rangle = |\psi_b\rangle$.

I claim that $|\psi_b\rangle$ is an orthonormal basis, so U is unitary:

$$\langle\psi_b|\psi_{b'}\rangle = \langle\psi_0|(\overline{X}(b))^\dagger \overline{X}(b')|\psi_0\rangle \tag{6.34}$$

$$= \langle\psi_0| \prod_i (\overline{X}_i)^{b'_i - b_i} |\psi_0\rangle \tag{6.35}$$

using the fact that the $\overline{X}_i$ commute with each other. As with the $\overline{Z}_i$s, $\overline{X}_i = \overline{X}_i^\dagger$. Then since $|\psi_0\rangle$ is a $+1$ eigenstate of $\overline{Z}_i$,

$$\langle\psi_b|\psi_{b'}\rangle = \langle\psi_0|\prod_i(\overline{X}_i)^{b'_i+b_i}|\psi_0\rangle \tag{6.36}$$

$$= \langle\psi_0|\overline{Z}_j\prod_i(\overline{X}_i)^{b_i+b'_i}|\psi_0\rangle \tag{6.37}$$

$$= \prod_i(-1)^{(b_i+b'_i)c(\overline{Z}_j,\overline{X}_i)}\langle\psi_0|\prod_i(\overline{X}_i)^{b_i+b'_i}\overline{Z}_j|\psi_0\rangle \tag{6.38}$$

$$= (-1)^{b_i+b'_i}\langle\psi_0|\prod_i(\overline{X}_i)^{b_i+b'_i}|\psi_0\rangle \tag{6.39}$$

$$= (-1)^{b_i+b'_i}\langle\psi_b|\psi_{b'}\rangle. \tag{6.40}$$

It follows that if, for any j, $b_j \neq b'_j$, then $\langle\psi_b|\psi_{b'}\rangle = 0$ as desired. The states $|\psi_b\rangle$ we get from procedure 6.1 are normalized, so we have an orthonormal basis.

The last step is to prove that U acts by conjugation on the Pauli group according to M. Let us compute $UZ_iU^\dagger$ and $UX_iU^\dagger$:

$$UZ_iU^\dagger|\psi_b\rangle = UZ_i|b\rangle \tag{6.41}$$

$$= (-1)^{b_i}|\psi_b\rangle. \tag{6.42}$$

Now,

$$\overline{Z}_i|\psi_b\rangle = \overline{Z}_i\overline{X}(b)|\psi_0\rangle \tag{6.43}$$

$$= (-1)^{b_i}\overline{X}(b)\overline{Z}_i|\psi_0\rangle \tag{6.44}$$

$$= (-1)^{b_i}|\psi_b\rangle. \tag{6.45}$$

Since the $|\psi_b\rangle$ form a basis, $UZ_iU^\dagger = \overline{Z}_i$.

Similarly,

$$UX_iU^\dagger|\psi_b\rangle = UX_i|b\rangle \tag{6.46}$$

$$= |\psi_{b'}\rangle, \tag{6.47}$$

where b' is b with the ith bit flipped ($b'_i = b_i + 1$, $b'_j = b_j$ for $j \neq i$).

$$\overline{X}_i|\psi_b\rangle = \overline{X}_i\overline{X}(b)|\psi_0\rangle \tag{6.48}$$

$$= \overline{X}(b')|\psi_0\rangle \tag{6.49}$$

$$= |\psi_{b'}\rangle, \tag{6.50}$$

so $UX_iU^\dagger = \overline{X}_i$. □

If you apply procedure 6.1 to a mapping which does not preserve commutation or anticommutation, you will still get a linear map, but it won't be unitary. Furthermore, it may not realize the conjugation action you wanted, so there is no real reason to apply procedure 6.1 unless the map you are working with satisfies equation (6.31).

6.1.5 The Clifford Group and the Symplectic Group

The conditions on the conjugation map performed by a Clifford group operation become somewhat more straightforward if we consider them in terms of the binary symplectic representation. A group homomorphism of the Paulis becomes a linear map on $2n$-dimensional binary vectors. The requirement that the generators

map to independent Paulis just says that the linear map has maximum rank. The constraint that conjugation preserves the commutation relations just means that the linear map must preserve the symplectic inner product:

$$v \odot w = (Mv) \odot (Mw) \tag{6.51}$$

$$v^T J w = v^T M^T J M w, \tag{6.52}$$

with J the $2n \times 2n$ matrix

$$J = \left(\begin{array}{c|c} 0 & I \\ \hline I & 0 \end{array}\right). \tag{6.53}$$

Running over all values of v and w, we find

$$J = M^T J M. \tag{6.54}$$

M is a member of the symplectic group $\mathsf{Sp}(2n, \mathbb{Z}_2)$.

As usual, by going to the binary symplectic representation, we lose all information about the phases of Paulis in the stabilizer. An operation which only changes the phases of Paulis is always performed by conjugation by a Pauli:

Proposition 6.2. *If $UPU^\dagger = \pm P$ for all $P \in \mathsf{P}_n$, then $U = e^{i\theta} Q$ for $Q \in \mathsf{P}_n$ and some value of θ.*

Proof. I will show that any mapping $P \mapsto (-1)^{c_P} P$ which could possibly be performed by a unitary can also be performed by conjugation by some $Q \in \mathsf{P}_n$. Then the proposition follows from theorem 6.1.

For any unitary U, conjugation performs a group homomorphism, so

$$c_{PQ} = c_P + c_Q. \tag{6.55}$$

In particular, the mapping is completely determined by its action on X_i and Z_i for $i = 1, \ldots, n$. For any c_P consistent with equation (6.55), I claim there exists $Q \in \mathsf{P}_n$ that implements it. By equation (6.5), we need to find Q such that $c(Q, X_i) = c_{X_i}$ and $c(Q, Z_i) = c_{Z_i}$. By lemma 3.15, such a Q exists, though there is only one. Specifically,

$$Q = \bigotimes_{i=1}^{n} Q_i \tag{6.56}$$

with

$$Q_i = \begin{cases} I & \text{if } c_{X_i} = c_{Z_i} = 0 \\ X & \text{if } c_{X_i} = 0 \text{ and } c_{Z_i} = 1 \\ Y & \text{if } c_{X_i} = 1 \text{ and } c_{Z_i} = 1 \\ Z & \text{if } c_{X_i} = 1 \text{ and } c_{Z_i} = 0 \end{cases} \tag{6.57}$$

□

It follows from proposition 6.2 that elements of $\check{\mathsf{C}}_n = \hat{\mathsf{C}}_n / \hat{\mathsf{P}}_n$ correspond uniquely to symplectic operations. Indeed, $\check{\mathsf{C}}_n$ is *exactly* the symplectic group.

Theorem 6.3. $\check{\mathsf{C}}_n \cong \mathsf{Sp}(2n, \mathbb{Z}_2)$. *Equivalently, for every map $X_i \mapsto \overline{X}_i$, $Z_i \mapsto \overline{Z}_i$ with $\overline{X}_i, \overline{Z}_i \in \mathsf{P}_n$ and satisfying the correct commutation relations, there exists $U \in \mathsf{C}_n$ which performs that map under conjugation, and U is unique up to overall phase.*

Proof. Most of the pieces of this theorem are derived from theorem 6.1, equation (6.54), and proposition 6.2. The only remaining piece needed to complete the characterization is to show that every symplectic operation can be realized by a Clifford group operation. This is straightforward: Given any linear map from $\hat{\mathsf{P}}_n$ to $\hat{\mathsf{P}}_n$, we can lift it to a group homomorphism $M : \mathsf{P}_n \to \mathsf{P}_n$ by choosing arbitrary signs for the images of X_i and Z_i. When the original linear map is symplectic, M satisfies equation (6.31), so using procedure 6.1, we find a unitary U realizing M and thus realizing the symplectic map on the binary symplectic representation. U maps Paulis to Paulis under conjugation, so $U \in \mathsf{C}_n$. □

6.2 Classical Simulation of the Clifford Group

One of the most interesting and useful things about the Clifford group is also one of the most disappointing. If $U \in \mathsf{C}_n$, we can specify it by giving a global phase plus the images of $2n$ Paulis $X_1, Z_1, \ldots, X_n, Z_n$. Each image is also an n-qubit Pauli, so requires at most $2n+1$ bits to specify. Thus, a Clifford group element can be specified using only $(2n+1)(2n)$ bits plus a global phase. Contrast that with a general unitary $U \in \mathsf{U}(2^n)$, which needs 2^{2n} real parameters to specify. Clifford group elements have a much more succinct representation than general unitary gates.

Indeed, circuits made out of Clifford group gates have a much stronger property: they can be efficiently simulated on a classical computer. This is a very useful fact, since it makes working with even relatively large Clifford group circuits tractable. For instance, stabilizer codes are exactly those QECCs which can be encoded using a circuit composed of Clifford group gates. The ability to easily describe a stabilizer code via its stabilizer is one aspect of the efficient simulatability of the Clifford group gates which form its encoder. We'll also see in part II that this property plays a big role in helping us find fault-tolerant implementations of Clifford group gates.

However, there is a price to be paid. Because Clifford group gates can classically be simulated, it means that a circuit composed only of Clifford group gates cannot access the full power of quantum computation. (Presumably; as with most statements about computational power, this one relies on some unproven complexity-theoretic assumptions, in this case the assumption that quantum computers are computationally more powerful than classical computers.) When we get to fault tolerance, that means that we'll need to venture outside the Clifford group in order to get a universal set of fault-tolerant gates.

6.2.1 Simulation of a Unitary Circuit of Clifford Group Gates

If we have a unitary circuit consisting only of Clifford group gates, the simulation procedure is quite straightforward. Note that if $U, V \in \mathsf{C}_n$, and $U : P \mapsto Q$, $V : Q \mapsto R$, then $(VU) : P \mapsto R$. That's really all there is to the simulation.

Procedure 6.2. You are given a circuit consisting of a product $U = \prod_{i=m}^{1} U_i$, with $U_i \in \mathsf{C}_n$. (I.e., U_1 is the first gate performed, and U_m is the last gate to be performed.) Each U_i can be specified by its action on the generators of the Pauli group, $U_i : X_j \mapsto U_i(X_j)$, $U_i : Z_j \mapsto U_i(Z_j)$. Then the action of the overall circuit U on the Pauli group can be determined as follows:

1. Initialize $\overline{X}_j = X_j$ and $\overline{Z}_j = Z_j$.
2. Starting with $i = 1$, and stepping through i up to the last gate m, repeat the following steps:
   (a) Calculate $U_i(\overline{X}_j)$. This can be done by writing $\overline{X}_j$ as a product of single-qubit Xs and Zs and applying equation (6.12).
   (b) Let the new value of $\overline{X}_j$ be $U_i(\overline{X}_j)$.
   (c) Similarly, replace $\overline{Z}_j$ by $U_i(\overline{Z}_j)$.
3. The overall circuit U has the action $X_j \mapsto \overline{X}_j$, $Z_j \mapsto \overline{Z}_j$, using the final values of $\overline{X}_j$ and $\overline{Z}_j$.

When the circuit consists of only two-qubit gates, updating an $\overline{X}$ or $\overline{Z}$ operator only requires updating two qubits in the decomposition, since all qubits not affected by the gate retain the same Pauli values. Therefore, each gate can be updated in a total time $O(n)$ (since we need to update $2n$ $\overline{X}$ and $\overline{Z}$ operators). The simulation of the full circuit thus takes a time $O(nm)$.

As an example, consider the simple circuit given in figure 6.1. Following the above procedure, we find that this circuit has the following action on Paulis:

$$\begin{array}{lccccccc} \overline{X}_1: & X\otimes I & \to & X\otimes X & \to & Z\otimes X & \to & I\otimes X \\ \overline{Z}_1: & Z\otimes I & \to & Z\otimes I & \to & X\otimes I & \to & X\otimes Z \\ \overline{X}_2: & I\otimes X & \to & I\otimes X & \to & I\otimes X & \to & Z\otimes X \\ \overline{Z}_2: & I\otimes Z & \to & Z\otimes Z & \to & X\otimes Z & \to & X\otimes I. \end{array} \tag{6.58}$$

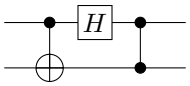

Figure 6.1: An example 2-qubit circuit made of Clifford group gates.

6.2.2 Simulation of a Unitary Circuit on a Stabilizer Subspace

Another interesting case is when we have some constraints on the input state of the circuit. For instance, the circuit may involve some ancillas, or it may be intended to be performed on a state encoded in a QECC. It may even be that the full input state of the circuit is specified, and we wish to determine the exact output state of the circuit. When the input state is a stabilizer state or lies within a stabilizer code, there still exists an efficient simulation procedure.

If the initial state is completely specified as a stabilizer state, we can keep track of the behavior of the generators $M_1, \ldots, M_n$ of the stabilizer. As before, we step through gates, updating the stabilizer generators at each step just as we updated $\overline{X}$ and $\overline{Z}$ before. When M_j is a generator of the stabilizer before we perform gate U_i, $U_i(M_j)$ is a generator of the stabilizer after the gate, so this procedure allows us to learn the stabilizer of the output state of the circuit. The are only two small differences from the case without a constraint. First of all, we need keep track of only n generators instead of $2n$ Paulis. The other difference is that the generators of the stabilizer are not unique, so after performing any gate, if it is convenient to do so, we may choose a new set of generators of the current stabilizer. There is no requirement to do so; only do it if it is clearly going to simplify the computation.

When the input state is only partially specified by a stabilizer code, we keep track both of the stabilizer, which now has $n-k$ generators, and of $2k$ logical $\overline{X}$ and $\overline{Z}$ operators. The case with $k = n$ is the "no constraint" case of the previous subsection, and the case with $k = 0$ is the stabilizer state case just discussed. Again, the stabilizer generators are non-unique, so at any step, we may choose a new set of generators. The logical $\overline{X}$ and $\overline{Z}$ operators are also now non-unique, so at any step we may multiply them by elements of the stabilizer, which means we are choosing a different coset representative.

Procedure 6.3. You are given a circuit consisting of a product $\prod_{i=m}^{1} U_i$, with $U_i \in \mathsf{C}_n$, which is to be performed on an arbitrary input state from stabilizer code S. S encodes k qubits ($0 \leq k \leq n$), has generators $M_1, \ldots, M_{n-k}$, and has logical Pauli operators $\overline{X}_j$, $\overline{Z}_j$, $j = 1, \ldots, k$. Each U_i can be specified by its action on the generators of the Pauli group, $U_i : X_j \mapsto U_i(X_j)$, $U_i : Z_j \mapsto U_i(Z_j)$. Then the action of the overall circuit on the stabilizer code can be determined as follows:

1. Initialize variables $N_j = M_j$ ($j = 1, \ldots, n-k$), $\overline{X}'_j = \overline{X}_j$ and $\overline{Z}'_j = \overline{Z}_j$ ($j = 1, \ldots, k$) to be the values given by the stabilizer code input.
2. Starting with $i = 1$, and stepping through i up to the last gate m, repeat the following steps:
   (a) Calculate $U_i(\overline{X}'_j)$ for $j = 1, \ldots, k$. This can be done by writing $\overline{X}'_j$ as a product of single-qubit Xs and Zs and applying equation (6.12).
   (b) Let the new value of $\overline{X}'_j$ be $U_i(\overline{X}'_j)$ for $j = 1, \ldots, k$.
   (c) Similarly, replace $\overline{Z}'_j$ by $U_i(\overline{Z}'_j)$ for $j = 1, \ldots, k$.
   (d) Replace N_j by $U_i(N_j)$ for $j = 1, \ldots, n-k$.
   (e) The current stabilizer T is generated by $\langle N_1, \ldots, N_{n-k} \rangle$
   (f) If desired, choose a new set of generators for T.
   (g) If desired, rewrite $\overline{X}'_j = N\overline{X}'_j$ or $\overline{Z}'_j = N\overline{Z}'_j$ with $N \in \mathsf{T}$.
3. The output state lies in a stabilizer code with generators equal to the final values of N_j, $j = 1, \ldots, n-k$. The encoded state has undergone the Clifford group operation given by the transformation $\overline{X}_j \mapsto \overline{X}'_j$, $\overline{Z}_j \mapsto \overline{Z}'_j$.

An important special case is when some qubits are completely specified (e.g., to be $|0\rangle$), and the remaining qubits are completely unconstrained. In that case, the stabilizer is the stabilizer of the ancilla qubits, and the initial logical operators $\overline{X}$ and $\overline{Z}$ are the Paulis on the unconstrained input qubits.

As an example of the expanded procedure, let us consider the circuit in figure 6.1 again, but this time with the second qubit initially in the state $|0\rangle$. We now begin with $M_1 = I \otimes Z$, $\overline{X}_1 = X \otimes I$, and $\overline{Z}_1 = Z \otimes I$. Using the same analysis as before, we find that the final value of the stabilizer and logical operators are:

$$N_1 = X \otimes I \tag{6.59}$$

$$\overline{X}'_1 = I \otimes X \tag{6.60}$$

$$\overline{Z}'_1 = X \otimes Z. \tag{6.61}$$

We can choose a new coset representative for $\overline{Z}'_1$: $I \otimes Z = (X \otimes I)(X \otimes Z)$. Then we can see that the overall transformation performed is to move the input qubit from the first qubit to the second qubit. In the output state, the first qubit is fixed to be $|0\rangle + |1\rangle$.

6.2.3 Measurement of Paulis

The final step is to add measurements to our simulation. I will phrase this in the most general way, where we measure the eigenvalue of an arbitrary Pauli operator on n qubits, but it would be equivalent to just consider measurement of single qubits in the standard basis. This is because measurement of any Pauli can be implemented via single-qubit measurements plus Clifford group operations. For simplicity, we restrict attention to Paulis with overall phase ± 1, so the eigenvalues are ± 1.

The analysis of measurements is somewhat more complicated than the analysis of unitary gates. For one thing, there are three separate cases to consider. The first case is when the Pauli P we wish to measure is in the current stabilizer T up to a phase: $\pm P \in \mathsf{T}$. In that case, the measurement outcome is just ± 1 ($+1$ if $P \in \mathsf{T}$ and -1 if $-P \in \mathsf{T}$), and the state does not change, since the state being measured is an eigenstate of P.

The second case is when $P \in \hat{\mathsf{N}}(\mathsf{T}) \setminus \hat{\mathsf{T}}$. Now, measurement of P constitutes a measurement of some of the encoded data. We must rewrite P as a product of the logical Paulis $\overline{X}$ and $\overline{Z}$, which determines that P corresponds to some logical Pauli $\overline{Q}$. The measurement output distribution of P is the same as the measurement output distribution of Q on the original input qubit. We must also update the encoded state for the effects of the measurement. Finally, the measurement has outcome ± 1, so we know that the post-measurement state is a $+1$ eigenstate of $\pm P$. In other words, $\pm P$ has joined the stabilizer.

The third case, when $P \notin \mathsf{N}(\mathsf{T})$, is the most complicated. Since $P \notin \mathsf{N}(\mathsf{T})$, $\exists M \in \mathsf{T}$ s.t. $\{P, M\} = 0$. Suppose $|\psi\rangle \in \mathcal{T}(\mathsf{T})$, so $M|\psi\rangle = |\psi\rangle$. The expectation value of a measurement of P on $|\psi\rangle$ is

$$\begin{aligned} \langle\psi|P|\psi\rangle &= \langle\psi|PM|\psi\rangle && (6.62)\\ &= \langle\psi|M(-P)|\psi\rangle && (6.63)\\ &= -\langle\psi|P|\psi\rangle && (6.64)\\ &= 0. && (6.65) \end{aligned}$$

(since $M^2 = I$, meaning $M = M^\dagger$). Thus, the probability of a $+1$ outcome and a -1 outcome for the measurement are both $1/2$.

We can also calculate the residual state. If the measurement has outcome $(-1)^b$, the state afterwards is $|\psi'\rangle = (1/\sqrt{2})(I + (-1)^b P)|\psi\rangle$ (taking into account normalization). If $N \in \mathsf{T}$ commutes with P, then $|\psi'\rangle$ is

still a $+1$ eigenstate of N:

$$N|\psi'\rangle = \frac{1}{\sqrt{2}} N(I + (-1)^b P)|\psi\rangle \tag{6.66}$$

$$= \frac{1}{\sqrt{2}} (I + (-1)^b P) N|\psi\rangle \tag{6.67}$$

$$= \frac{1}{\sqrt{2}} (I + (-1)^b P)|\psi\rangle = |\psi'\rangle. \tag{6.68}$$

$|\psi'\rangle$ is also a $+1$ eigenstate of $(-1)^b P$. That means that it is *not* an eigenstate of any M with $\{M, P\} = 0$, even if $M \in \mathsf{T}$. Define a stabilizer T' generated by $(-1)^b P$ plus all $N \in \mathsf{T}$ s.t. $[N, P] = 0$. The stabilizer of the remaining state after the measurement certainly contains T'. As we will see in a moment, that is all it contains.

How big is T'? To answer this, we need to know how many elements of T commute with P.

Proposition 6.4. *Let S be a stabilizer, and let $P \notin \mathsf{N}(\mathsf{S})$ be a Pauli that does not commute with every element of S. Then exactly half of the elements of S commute with P. Furthermore, for any coset $\overline{Q} \in \mathsf{N}(\mathsf{S})/\mathsf{S}$, exactly half the elements of $\overline{Q}$ commute with P.*

Proof. If $P \notin \mathsf{N}(\mathsf{S})$, let $M \in \mathsf{S}$ be an element of the stabilizer that anticommutes with P, $\{M, P\} = 0$. Then we can pair all elements of S:

$$N \leftrightarrow MN. \tag{6.69}$$

Note that $MN^2 = M$, so each element of S is a member of only one pair. The reason for doing this pairing is that N commutes with P iff MN anticommutes with P:

$$c(MN, P) = c(M, P) + c(N, P) = 1 + c(N, P). \tag{6.70}$$

Thus, the number of elements of S that commute with P is equal to the number of elements that anticommute with P.

Similarly, we can pair elements of the cosets representing logical Paulis, $N \leftrightarrow MN$, using the same $M \in \mathsf{S}$. Both N and MN are in the same coset $\overline{Q}$, and again, exactly one of them commutes with P and one anticommutes with P. Thus, half of the coset $\overline{Q}$ commutes with P. □

Corollary 6.5. $|\mathsf{T}'| = |\mathsf{T}|$.

The subspace of post-measurement states for a given measurement outcome can be no larger than the space of possible pre-measurement states, but it could potentially be smaller if multiple states collapse in the measurement to the same final state. However, as another corollary of proposition 6.4, we find that this cannot happen. If the code space of T contains k logical qubits, one possible basis for the code space is the set of 2^k codewords which are eigenstates of $\overline{Z}_1, \ldots, \overline{Z}_k$. Each of these codewords is a stabilizer state with stabilizer generated by $\mathsf{T}, \pm\overline{Z}_1, \ldots, \pm\overline{Z}_k$. By proposition 6.4 and the analysis preceding it, the stabilizer of the post-measurement state is generated by T' and by $\pm\overline{Z}_1, \ldots, \pm\overline{Z}_k$, with the same eigenvalues. However, we must make certain that each coset is represented by an element that commutes with P; such an element always exists by proposition 6.4. Since each of the 2^k basis states gets mapped to a distinct stabilizer state, the code space after the measurement also has dimension 2^k. This implies that T' is the actual stabilizer post-measurement, as claimed.

Furthermore, this logic also tells us that the T-coset of the logical $\overline{Z}_i$ operator gets replaced by the T'-coset which contains an element of the original $\overline{Z}_i$ that commutes with P. The same reasoning tells us how to find the new versions of the other logical Paulis. In short, we now know how to update both the stabilizer and the logical Paulis after measurement of a Pauli operator.

Theorem 6.6. *Suppose our system is a codeword of the stabilizer code T, with generators $N_1, \ldots, N_{n-k}$ and logical Paulis $\overline{X}_i$ and $\overline{Z}_i$ ($i = 1, \ldots, k$), and we measure the eigenvalue of Pauli $P \notin \mathsf{N}(\mathsf{T})$. Then, conditioned on outcome $(-1)^b$, the stabilizer and logical Paulis of the system after the measurement can be determined as follows:*

1. *Find generator $M \in \mathsf{T}$ such that $\{M, P\} = 0$. If necessary, reorder the generators so that $M = N_1$.*
2. *For each generator N_i, $i > 1$, if $[N_i, P] = 0$, let $N_i' = N_i$. If $\{N_i, P\} = 0$, let $N_i' = N_i M$.*
3. *Let $N_1' = (-1)^b P$.*
4. *The new stabilizer T' is generated by $N_1', \ldots, N_{n-k}'$.*
5. *Pick a representative $\overline{Z}_i$ for each of the logical Z operators for T. If $[\overline{Z}_i, P] = 0$, let $\overline{Z}_i' = \overline{Z}_i$; otherwise let $\overline{Z}_i' = \overline{Z}_i M$. $\overline{Z}_i'$ is a representative for the new logical Z_i operator.*
6. *Similarly, pick a representative $\overline{X}_i$ for each of the logical X operators for T. If $[\overline{X}_i, P] = 0$, let $\overline{X}_i' = \overline{X}_i$; otherwise let $\overline{X}_i' = \overline{X}_i M$. $\overline{X}_i'$ is a representative for the new logical X_i operator.*

One interesting twist on this system is that we can essentially control the measurement outcome. In particular, suppose we measure $P \notin \mathsf{N}(\mathsf{T})$ and get outcome -1. In theorem 6.6, we identify an element M from the old stabilizer T which anticommutes with P. However, M commutes with generators 2 through $n-k$ of T', since they are also elements of T. M also commutes with the standard coset representatives for $\overline{X}_i'$ and $\overline{Z}_i'$. Thus, if we perform M on the post-measurement state, we transform the stabilizer (according to procedure 6.3) only by changing $N_1' = -P$ to $+P$. The logical operators are unchanged. This is exactly the same state as we would have gotten (according to theorem 6.6) if the original measurement outcome had been $+1$.

Putting everything together, we get the following procedure for simulating Clifford group gates and Pauli measurements on either a fixed initial stabilizer state or a partially specified state with some free (logical) qubits:

Procedure 6.4. You are given a circuit consisting of a m-element sequence of unitary Clifford group gates and Pauli measurements. At step number i, the circuit calls for either Clifford group gate $U_i \in \mathsf{C}_n$ (specified by its action on Paulis $U_i : Q \mapsto U_i(Q)$) or measurement of the eigenvalue of $P_i \in \mathsf{P}_n$ (assuming P_i has eigenvalues ± 1, not $\pm i$). The initial state of the circuit is given by stabilizer S, which encodes k qubits ($0 \leq k \leq n$), has generators $M_1, \ldots, M_{n-k}$, and has logical Pauli operators $\overline{X}_j$, $\overline{Z}_j$, $j = 1, \ldots, k$.

1. Initialize variables $k' = k$, $N_j = M_j$ ($j = 1, \ldots, n-k$), $\overline{X}_j' = \overline{X}_j$ and $\overline{Z}_j' = \overline{Z}_j$ ($j = 1, \ldots, k$) to be the values given by the stabilizer code input. Let the variable state $|\overline{\psi}\rangle$ be the initial encoded state of the system, corresponding to the logical state $|\psi\rangle$.
2. Perform the following procedure for each step i in order, for $i = 1, \ldots, m$:
   (a) If at step i, the circuit calls for Clifford gate U_i:
      i. Calculate $U_i(\overline{X}_j')$ for $j = 1, \ldots, k'$. This can be done by writing $\overline{X}_j'$ as a product of single-qubit Xs and Zs and applying equation (6.12).
      ii. Let the new value of $\overline{X}_j'$ be $U_i(\overline{X}_j')$ for $j = 1, \ldots, k'$.
      iii. Similarly, replace $\overline{Z}_j'$ by $U_i(\overline{Z}_j')$ for $j = 1, \ldots, k'$.
      iv. Replace N_j by $U_i(N_j)$ for $j = 1, \ldots, n-k'$.
      v. The current stabilizer T is generated by $\langle N_1, \ldots, N_{n-k'} \rangle$
      vi. If desired, choose a new set of generators for T.
      vii. If desired, rewrite $\overline{X}_j' = N\overline{X}_j'$ or $\overline{Z}_j' = N\overline{Z}_j'$ with $N \in \mathsf{T}$.
   (b) If at step i, the circuit calls for measurement of P_i, determine whether $\pm P_i$ is in T, if $P_i \in \mathsf{N}(\mathsf{T}) \setminus \mathsf{T}$, or if P_i is not in $\mathsf{N}(\mathsf{T})$, as follows:
      i. Determine if P_i commutes with all generators N_j of the current stabilizer T. If not, then $P_i \notin \mathsf{N}(\mathsf{T})$.

ii. If P_i does commute with all generators, determine if $\pm P_i \in \mathsf{T}$. This can be done by writing P_i and the generators N_j in their binary symplectic representations and seeing if v_{P_i} is in the linear span of the v_{N_j}.

iii. If P_i commutes with all generators but is not in T, then $P_i \in \mathsf{N}(\mathsf{T}) \setminus \mathsf{T}$.

(c) If at step i, the circuit calls for measurement of P_i with $\pm P_i \in \mathsf{T}$:

i. Evaluate whether $+P_i \in \mathsf{T}$ or $-P_i \in \mathsf{T}$. This can be done using linear algebra and the binary symplectic representations of P_i and N_j to write $P_i = \pm \prod_{j=1}^{n-k'} N_j^{s_j}$.

ii. If $+P_i \in \mathsf{T}$, return measurement result $+1$. If $-P_i \in \mathsf{T}$, return measurement result -1.

(d) If at step i, the circuit calls for measurement of P_i with $P_i \in \mathsf{N}(\mathsf{T}) \setminus \mathsf{T}$:

i. Write $P_i = \prod_{j=1}^{n-k'} N_j^{s_j} \prod_{j'=1}^{k} \overline{X}_j'^{t_j} \overline{Z}_j'^{u_j}$, with $s_j, t_j, u_j \in \{0,1\}$. This can be done using linear algebra and the binary symplectic representations of the Paulis.

ii. Let $Q = \prod_{j'=1}^{k} X_j^{t_j} Z_j^{u_j}$.

iii. Perform a measurement of Q on the current logical state $|\psi\rangle$. Return the measurement result $(-1)^b$, and update $|\overline{\psi}\rangle$ accordingly. Note that this step may not be efficient, depending on the current state $|\psi\rangle$.

iv. Reduce k' by 1, and add $(-1)^b P_i$ to the stabilizer as a new generator $N_{n-k'+1}$. Update T accordingly, and if desired, choose a new set of generators for T.

v. Update the logical operators $\overline{X}_j'$ and $\overline{Z}_j'$ to relate to the new $|\overline{\psi}\rangle$. Again, this step may not be efficient.

(e) If at step i, the circuit calls for measurement of P_i with $P_i \notin \mathsf{N}(\mathsf{T})$:

i. Choose a uniformly random bit b and return measurement result $(-1)^b$.

ii. Find generator $M \in \mathsf{T}$ such that $\{M, P_i\} = 0$. If necessary, reorder the generators so that $M = N_1$.

iii. For each generator N_j, $j > 1$, if $[N_j, P_i] = 0$, leave N_j unchanged. If $\{N_j, P_0\} = 0$, replace N_j by $N_j M$.

iv. Replace N_1 by $(-1)^b P_i$.

v. Update the stabilizer T with the revised generators. If desired, choose new generators for the revised T.

vi. Pick a representative $\overline{Z}_j'$ for each of the logical Z operators for T. If $[\overline{Z}_j', P_i] = 0$, leave $\overline{Z}_j'$ unchanged; otherwise replace $\overline{Z}_j'$ by $\overline{Z}_j' M$. The updated $\overline{Z}_j'$ is a representative for the new logical Z_j operator; choose a new representative using the updated T if desired.

vii. Similarly, pick a representative $\overline{X}_j'$ for each of the logical X operators for T. If $[\overline{X}_j', P] = 0$, leave $\overline{X}_i'$ unchanged; otherwise replace $\overline{X}_j'$ by $\overline{X}_j' M$. The updated $\overline{X}_j'$ is a representative for the new logical X_j operator; choose a new representative using the updated T if desired.

3. The output state lies in a stabilizer code with generators equal to the final values of N_j, $j = 1, \ldots, n-k'$. The encoded state has had $k - k'$ logical qubits measured, and has undergone the transformation $\overline{X}_j \mapsto \overline{X}_j'$, $\overline{Z}_j \mapsto \overline{Z}_j'$ on the remaining qubits.

Generally, for this sort of simulation, we only consider circuits where measurement of $P_i \in \mathsf{N}(\mathsf{T}) \setminus \mathsf{T}$ does not occur, so that the simulation is an efficient one. For instance, if the circuit contains no measurements, this is not an issue, or equally if it contains no logical qubits (so $\mathsf{N}(\mathsf{T}) = \mathsf{T}$). In part II, we will see circuits that have measurements and some logical qubits, but they have been specially designed to avoid the troublesome case.

Theorem 6.7 (Gottesman-Knill)**.** *Given a circuit starting from an initial stabilizer state, followed by a sequence of Clifford group operations and Pauli measurements, which may depend on classical computations performed on previous measurement results, there is an efficient classical simulation of the circuit.*

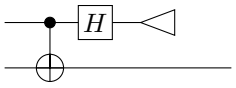

Figure 6.2: One-qubit teleportation: an example of a 2-qubit circuit made of Clifford group gates and measurement.

If you follow procedure 6.4, you will find a time of $O(n^3m)$ is needed to do the simulation, taking into account all the linear algebra manipulations needed to process measurement. However, by keeping track of slightly more information, this can be reduced to $O(n^2m)$.

To illustrate the measurement procedure, let us consider a variation of the example circuit from figure 6.1 which has some measurements in it. The revised circuit is given in figure 6.2. The first few steps are as before. After the Hadamard, we have the following stabilizer and logical Paulis:

$$\begin{array}{lrcl} N_1: & I\otimes Z & \rightarrow & X\otimes Z \\ \overline{X}: & X\otimes I & \rightarrow & Z\otimes X \\ \overline{Z}: & Z\otimes I & \rightarrow & X\otimes I. \end{array} \tag{6.71}$$

Then we measure $P = Z \otimes I$. In this case, there is only one element of the stabilizer, and it anticommutes with P. Suppose we get measurement outcome $+1$. By theorem 6.6, replace N_1 with P. $\overline{X}$ commutes with P, so its representative need not change. However, we can choose a new coset representative to take advantage of the new stabilizer: $(Z \otimes X)(Z \otimes I) = I \otimes X$. $\overline{Z}$ anticommutes with P, so we *must* choose a new coset representative

$$\overline{Z}N_1 = (X \otimes I)(X \otimes Z) = I \otimes Z. \tag{6.72}$$

After the measurement, the stabilizer and logical Paulis are thus

$$N_1 : Z \otimes I \tag{6.73}$$

$$\overline{X} : I \otimes X \tag{6.74}$$

$$\overline{Z} : I \otimes Z \tag{6.75}$$

The input qubit has been moved to the second qubit for the output, and the output value of the first qubit is $|0\rangle$.

In the case where the measurement result is -1, the stabilizer is $-P$ instead of P. The new representative for $\overline{X}$ also acquires this minus sign, so the final state is as follows:

$$N_1 : -Z \otimes I \tag{6.76}$$

$$\overline{X} : -I \otimes X \tag{6.77}$$

$$\overline{Z} : I \otimes Z \tag{6.78}$$

The output state of the first qubit is $|1\rangle$, and the output state of the second qubit is the input data qubit, but with a phase flip (Z) performed on it.

6.3 Generators of the Clifford Group

In section 6.1.3, we saw three common gates which are also elements of the Clifford group: H, $R_{\pi/4}$ and CNOT. In a sense, they are the *only* elements of the Clifford group, because they generate the Clifford group. That is:

Theorem 6.8. *Any gate in the n-qubit Clifford group* C_n *can be written as a product of* $e^{i\theta}I$, H_i, $R_{\pi/4,i}$, *and* $\mathrm{CNOT}_{i,j}$, *with* $i, j = 1, \ldots, n$ *and* $\theta \in [0, 2\pi)$.

Figure 6.3: a) Clifford group circuit for the SWAP gate. b) Clifford group circuit for the $\mathrm{C}-\mathrm{Z}$ gate.

$\mathrm{CNOT}_{i,j}$ means CNOT with qubit i as the control and qubit j as the target.

Proof. First, note that the Pauli group is inside the group generated by H and $R_{\pi/4}$: $Z = (R_{\pi/4})^2$, and $X = HZH$. Second, global phases are covered by the gates $e^{i\theta}I$. To finish the proof, we thus need only to prove that the symplectic representations of H, $R_{\pi/4}$ and CNOT generate $\check{\mathsf{C}}_n$.

It will be helpful to also use two additional gates: SWAP and $\mathrm{C}-\mathrm{Z}$. Both are in the Clifford group, and can easily be performed as a product of H, $R_{\pi/4}$, and CNOT, so we can use them freely without explicitly adding them to the generating set. In particular, SWAP is the product of 3 CNOT gates with alternating directions, and $\mathrm{C}-\mathrm{Z} = (I \otimes H)\mathrm{CNOT}(I \otimes H)$.

We can take advantage of theorem 6.3. The symplectic representation of H is

$$\left(\begin{array}{c|c} 0 & 1 \\ \hline 1 & 0 \end{array}\right), \tag{6.79}$$

the symplectic representation of $R_{\pi/4}$ is

$$\left(\begin{array}{c|c} 1 & 0 \\ \hline 1 & 1 \end{array}\right), \tag{6.80}$$

and the symplectic representation of CNOT is

$$\left(\begin{array}{cc|cc} 1 & 0 & 0 & 0 \\ 1 & 1 & 0 & 0 \\ \hline 0 & 0 & 1 & 1 \\ 0 & 0 & 0 & 1 \end{array}\right). \tag{6.81}$$

Additional qubits will modify these matrices by adding a direct sum with the identity matrix. For instance, when we have 3 qubits, $\mathrm{CNOT}_{2,3}$ is

$$\left(\begin{array}{ccc|ccc} 1 & 0 & 0 & 0 & 0 & 0 \\ 0 & 1 & 0 & 0 & 0 & 0 \\ 0 & 1 & 1 & 0 & 0 & 0 \\ \hline 0 & 0 & 0 & 1 & 0 & 0 \\ 0 & 0 & 0 & 0 & 1 & 1 \\ 0 & 0 & 0 & 0 & 0 & 1 \end{array}\right). \tag{6.82}$$

In general, if we have a symplectic matrix

$$U = \left(\begin{array}{c|c} A & B \\ \hline C & D \end{array}\right), \tag{6.83}$$

representing the Clifford group gate U, then left multiplication by another symplectic matrix representing the gate V gives us the matrix for VU whereas right multiplication gives us UV. The effects of left and right multiplication by H, $R_{\pi/4}$, CNOT, $\mathrm{C}-\mathrm{Z}$, and SWAP are summarized in table 6.1. As you can see, left multiplication gives us a set of row operations and right multiplication gives us a set of column operations. We can't exactly do standard Gaussian elimination, but we can do something very similar. In particular,

Gate	Left multiplication	Right multiplication
H_i	Switches the ith rows of $(A\|B)$ and $(C\|D)$	Switches the ith columns of $\left(\frac{A}{C}\right)$ and $\left(\frac{B}{D}\right)$
$R_{\pi/4,i}$	Adds the ith row of $(A\|B)$ to the ith row of $(C\|D)$	Adds the ith column of $\left(\frac{B}{D}\right)$ to the ith column of $\left(\frac{A}{C}\right)$
$\mathrm{CNOT}_{i,j}$	Adds the ith row of $(A\|B)$ to the jth row of $(A\|B)$, and adds the jth row of $(C\|D)$ to the ith row of $(C\|D)$	Adds the jth column of $\left(\frac{A}{C}\right)$ to the ith column of $\left(\frac{A}{C}\right)$, and adds the ith column of $\left(\frac{B}{D}\right)$ to the jth column of $\left(\frac{B}{D}\right)$
$\mathrm{C-Z}_{i,j}$	Adds the ith row of $(A\|B)$ to the jth row of $(C\|D)$, and adds the jth row of $(A\|B)$ to the ith row of $(C\|D)$	Adds the jth column of $\left(\frac{B}{D}\right)$ to the ith column of $\left(\frac{A}{C}\right)$, and adds the ith column of $\left(\frac{B}{D}\right)$ to the jth column of $\left(\frac{A}{C}\right)$
$\mathrm{SWAP}_{i,j}$	Swaps the ith rows of A, B, C, and D with the jth rows of A, B, C, and D	Swaps the ith columns of A, B, C, and D with the jth columns of A, B, C, and D

Table 6.1: The effects of left and right multiplication by H, $R_{\pi/4}$, CNOT, $\mathrm{C-Z}$, and SWAP on a symplectic matrix.

given an arbitrary symplectic matrix U, we will find a sequence of H, $R_{\pi/4}$, and CNOT to multiply by on the left and right to transform U into the identity:

$$\left(\prod_{k=1}^{g_L} V_{L,k}\right) U \left(\prod_{k=1}^{g_R} V_{R,k}\right) = I, \tag{6.84}$$

with $V_{L,k}$ and $V_{R,k}$ drawn from $\{H_i, R_{\pi/4,i}, \mathrm{CNOT}_{i,j}\}$. Then

$$U = \left(\prod_{k=g_L}^{1} V_{L,k}^\dagger\right)\left(\prod_{k=g_R}^{1} V_{R,k}^\dagger\right), \tag{6.85}$$

proving the theorem.

In equation (6.83), let a_i, b_i, c_i, and d_i be the ith columns of A, B, C, and D, respectively, and a_{ij}, b_{ij}, c_{ij}, and d_{ij} be the i,jth entries of A, B, C, and D. Because U is symplectic, we can apply equation (6.54) to get the following properties:

1. U has full rank.
2. $C^T A + A^T C = 0$; i.e., $(a_i|c_i) \odot (a_j|c_j) = 0$.
3. $C^T B + A^T D = I$; i.e., $(a_i|c_i) \odot (b_j|d_j) = \delta_{ij}$.
4. $D^T A + B^T C = I$, which is the same as the previous property.
5. $D^T B + B^T D = 0$; i.e., $(b_i|d_i) \odot (b_j|d_j) = 0$.

These properties all remain true if we multiply U on the left or right by other symplectic matrices.

To find a sequence of the form equation (6.84), we can use the following steps:

Procedure 6.5.

1. Since U has maximum rank, somewhere in the first column of A or C is a 1. Using left multiplication by H and SWAP, we can put this 1 in the upper left corner.
2. Do column reduction on the first column of A: Use left multiplication by CNOT to add the 1 in the upper left corner of A to any other row of A with a 1 in the first column.
3. Do row reduction on the first row of A: Use right multiplication by CNOT to add the 1 in the upper left corner of A to any other column of A with a 1 in the first row.
4. Using left multiplication by $R_{\pi/4}$ and/or $\mathrm{C-Z}$, we can similarly make the first column of C to be all 0s.
5. At this point, we find that the first row of C has also become all 0s. This must be the case since
$$0 = (a_1|c_1) \odot (a_j|c_j) = a_1 \cdot c_j + c_1 \cdot a_j = c_{1j} + 0. \tag{6.86}$$
6. Repeat steps 1 to 5 on the second row and column of A and C to make them all 0 except for a_{22}, which is 1. Continue with all other rows and columns in sequence, until we have $A = I$ and $C = 0$.
7. At this point it follows that $D = I$:
$$\delta_{ij} = (a_i|c_i) \odot (b_j|d_j) = a_i \cdot d_j + c_i \cdot b_j = d_{ij}. \tag{6.87}$$
Also, B is symmetric:
$$0 = D^T B + B^T D = B + B^T. \tag{6.88}$$

8. Right multiply by H for every qubit, switching A and B, and switching C and D, so now $B = C = I$, $D = 0$, and A is symmetric.

9. Right multiply by $R_{\pi/4}$ as needed to eliminate the diagonal of A. Right multiply by C − Z to eliminate all other elements of A, leaving $A = 0$. Since $D = 0$, these operations do not change C.

10. Right multiply by H for every qubit, switching the left and right halves back again. We are left with $A = D = I$, $B = C = 0$.

□

It is worth counting just how many gates from the generating set are needed in this procedure. To eliminate all the 1s in a single row and column of A and C takes $O(n)$ gates. Doing this for all n rows and columns thus requires $O(n^2)$ gates. Steps 8 and 10 only require $O(n)$ gates, but step 8 could require one gate for each element of A, which is again $O(n^2)$. Thus, the overall number of gates used in the procedure is $O(n^2)$. It turns out that this can be slightly improved, allowing an arbitrary element of the Clifford group to be written as a product of $O(n^2/\log n)$ generators.

6.4 Encoding Circuits for Stabilizer Codes

Any stabilizer code can be encoded with a Clifford group gate. Therefore, techniques useful for decomposing a Clifford group unitary into a detailed quantum circuit are also useful for deriving encoding circuits for stabilizer codes. The main difference between encoding a stabilizer code and finding a circuit for a Clifford group operation is that there is more freedom in choosing the encoder for a stabilizer code. When you are given a full Clifford group operation, it tells you exactly what unitary you must perform (up to global phase, perhaps), whereas for a stabilizer code, you have an additional freedom to perform unitaries which leave the code space unchanged.

The procedures discussed in this section are boring but necessary. However, it is sometimes possible to come up with clever codes with more exciting encoding circuits. The most general stabilizer code uses $O(n^2)$ gates in its encoding circuit, which is not too bad, but for a big code, we'd really like an encoding circuit with only $O(n)$ gates. Some such codes exist. It's not possible to do better than that for any sensible code, since with $o(n)$ gates, you can't even touch every qubit in the code with a gate. Some qubits will end up either unprotected or unused, maybe even unloved.

The true bottleneck, however, is the *decoding* circuit, and in particular, the syndrome decoding problem. Recall that the error syndromes correspond to cosets of $\mathsf{N}(\mathsf{S})$ in P_n, and that we assign a coset representative Q_s to each error syndrome s to serve as the "correct" way to correct a state with syndrome s. However, in general, it is quite difficult (NP-hard) to compute Q_s as a function of s. Efficient codes for which syndrome decoding can be performed efficiently are precious things, and one of the main points of coding theory is to find them. Even better is an efficient code for which encoding and syndrome decoding can both be done in time $O(n)$. In general, syndrome decoding, efficient or not, will use gates outside of the Clifford group, but is most often done on a classical computer since it is basically a classical problem.

6.4.1 Encoding a Stabilizer Code with Unspecified Logical Paulis

The most straightforward case is when the stabilizer is given, but not the logical Paulis. In this case, there is an additional freedom to perform unitaries within the code space, provided we do not mix codewords with non-codewords. In other words, we can use any set of logical Paulis that is convenient for us.

If the original state, pre-encoding, is $|0\rangle^{\otimes(n-k)} \otimes |\psi\rangle$ (where $|\psi\rangle$ is a k-qubit state), its initial stabilizer is generated by $Z_1, Z_2, \ldots, Z_{n-k}$. The final stabilizer S, post-encoding, also has $n - k$ generators $M_1, M_2, \ldots, M_{n-k}$. The choice of generators is not unique, of course, so we may pick any set of generators for S that we like. Then we must simply find some Clifford group circuit that maps $Z_i \mapsto M_i$ for $i = 1, \ldots, n - k$.

We can do this using a simplified version of procedure 6.5. There are two ways we can simplify: First, we don't really care what happens to Z_i for $i > n-k$ or to X_i. Thus, we need only concern ourselves with the first $n-k$ columns of A and C. Second, the choice of generators of the stabilizer is not unique. Therefore, we may permute columns and add columns to each other within A and C without using any actual gates. We are left with the following procedure:

Procedure 6.6. Generate a list of gates using the steps given below.

1. Write the generators $M_1, \ldots, M_{n-k}$ of S as binary symplectic vectors. Produce the first $n-k$ columns of a symplectic matrix as follows: The ith column of A is $a_i = x_{M_i}$. The ith column of C is $c_i = z_{M_i}$.

2. $(a_1|c_1)$ is a non-zero vector, so there is a 1 somewhere in the first column. Using left multiplication by H and SWAP, we can put this 1 in the upper left corner.

3. Do column reduction on the first column of A: Use left multiplication by CNOT to add the 1 in the upper left corner of A to any other row of A with a 1 in the first column.

4. Using left multiplication by $R_{\pi/4}$ and/or $\mathrm{C-Z}$, we can similarly make the first column of C to be all 0s.

5. Do row reduction on the first row of A: Replace generators of the stabilizer to add the 1 in the upper left corner of A to any other column of A with a 1 in the first row. (It does not matter much if this step is performed before or after the previous step.)

6. At this point, we find that the first row of C has also become all 0s. This must be the case since
$$0 = (a_1|c_1) \odot (a_j|c_j) = a_1 \cdot c_j + c_1 \cdot a_j = c_{1j} + 0. \tag{6.89}$$

7. Repeat the previous steps on the second row and column of A and C to make them all 0 except for a_{22}, which is 1. Continue with all other rows and columns in sequence up to column number $n-k$.

8. Perform H on qubits 1 through $n-k$ to switch A and C.

Take the inverse of this product of gates. The resulting Clifford group circuit will encode in some coset of S; that is, the stabilizer will be almost correct, except that we may have some error syndrome different from the correct trivial syndrome. (Also note that the choice of stabilizer generators may be different from that which was originally given to us.) Calculate the action of the encoding circuit on Z_i for $i = 1, \ldots, n-k$. If for any i, the resulting generator M_i has the wrong sign, add X_i to the beginning of the encoding circuit.

As an example, let us find an encoding circuit for the five-qubit code as given in table 3.2. We begin (step 1) with the matrix

$$\begin{array}{cccc} 1 & 0 & 1 & 0 \\ 0 & 1 & 0 & 1 \\ 0 & 0 & 1 & 0 \\ 1 & 0 & 0 & 1 \\ 0 & 1 & 0 & 0 \\ \hline 0 & 0 & 0 & 1 \\ 1 & 0 & 0 & 0 \\ 1 & 1 & 0 & 0 \\ 0 & 1 & 1 & 0 \\ 0 & 0 & 1 & 1 \end{array}. \tag{6.90}$$

Step 2 is unnecessary, as there is already a 1 for a_{11}. We can perform steps 3 and 4 using $\mathrm{CNOT}_{1,4} \cdot \mathrm{C-Z}_{1,2} \cdot \mathrm{C-Z}_{1,3}$. Be careful: you must perform the correct transformations on the full rows, not just the first column. Then, in step 5, we can clear out the first row of A by adding the first column to the

third column; this corresponds to replacing the third generator M_3 with M_1M_3. We now have the following matrix:

$$\begin{array}{cccc} 1 & 0 & 0 & 0 \\ 0 & 1 & 0 & 1 \\ 0 & 0 & 1 & 0 \\ 0 & 0 & 1 & 1 \\ 0 & 1 & 0 & 0 \\ \hline 0 & 0 & 0 & 0 \\ 0 & 0 & 1 & 0 \\ 0 & 1 & 1 & 0 \\ 0 & 1 & 1 & 0 \\ 0 & 0 & 1 & 1 \end{array}. \tag{6.91}$$

We can clear out the second column using $\mathrm{CNOT}_{2,5} \cdot \mathrm{C}-\mathrm{Z}_{2,3} \cdot \mathrm{C}-\mathrm{Z}_{2,4}$, then reduce the second row of A by replacing M_4 with M_2M_4. The third column requires slightly more care. First column reduce the third column of A using $\mathrm{CNOT}_{3,4}$. Then use $\mathrm{C}-\mathrm{Z}_{3,4} \cdot \mathrm{C}-\mathrm{Z}_{3,5}$ to eliminate the third column of C. The caution is necessary because $\mathrm{CNOT}_{3,4}$ and $\mathrm{C}-\mathrm{Z}_{3,4}$ do not commute; in this case, however, the difference is only Z, which will not affect the binary symplectic representation. Then we finish with the fourth column, using $\mathrm{CNOT}_{4,5}$ followed by $\mathrm{C}-\mathrm{Z}_{4,5}$. We then conclude by performing H on qubits 1 through 4. These gates give us the following sequence of matrices:

$$\begin{array}{cccc} 1 & 0 & 0 & 0 \\ 0 & 1 & 0 & 0 \\ 0 & 0 & 1 & 0 \\ 0 & 0 & 1 & 1 \\ 0 & 0 & 0 & 1 \\ \hline 0 & 0 & 0 & 0 \\ 0 & 0 & 0 & 0 \\ 0 & 0 & 1 & 1 \\ 0 & 0 & 1 & 1 \\ 0 & 0 & 1 & 1 \end{array} \rightarrow \begin{array}{cccc} 1 & 0 & 0 & 0 \\ 0 & 1 & 0 & 0 \\ 0 & 0 & 1 & 0 \\ 0 & 0 & 0 & 1 \\ 0 & 0 & 0 & 1 \\ \hline 0 & 0 & 0 & 0 \\ 0 & 0 & 0 & 0 \\ 0 & 0 & 0 & 0 \\ 0 & 0 & 0 & 1 \\ 0 & 0 & 0 & 1 \end{array} \rightarrow \begin{array}{cccc} 1 & 0 & 0 & 0 \\ 0 & 1 & 0 & 0 \\ 0 & 0 & 1 & 0 \\ 0 & 0 & 0 & 1 \\ 0 & 0 & 0 & 0 \\ \hline 0 & 0 & 0 & 0 \\ 0 & 0 & 0 & 0 \\ 0 & 0 & 0 & 0 \\ 0 & 0 & 0 & 0 \\ 0 & 0 & 0 & 0 \end{array} \rightarrow \begin{array}{cccc} 0 & 0 & 0 & 0 \\ 0 & 0 & 0 & 0 \\ 0 & 0 & 0 & 0 \\ 0 & 0 & 0 & 0 \\ 0 & 0 & 0 & 0 \\ \hline 1 & 0 & 0 & 0 \\ 0 & 1 & 0 & 0 \\ 0 & 0 & 1 & 0 \\ 0 & 0 & 0 & 1 \\ 0 & 0 & 0 & 0 \end{array} \tag{6.92}$$

Taking the inverses of these gates in reverse order, we get the following sequence of gates for the encoding circuit:

$$\begin{aligned} &\mathrm{CNOT}_{1,4} \cdot \mathrm{C}-\mathrm{Z}_{1,2} \cdot \mathrm{C}-\mathrm{Z}_{1,3} \cdot \mathrm{CNOT}_{2,5} \cdot \mathrm{C}-\mathrm{Z}_{2,3} \cdot \mathrm{C}-\mathrm{Z}_{2,4} \cdot \mathrm{CNOT}_{3,4} \\ &\quad \cdot \mathrm{C}-\mathrm{Z}_{3,4} \cdot \mathrm{C}-\mathrm{Z}_{3,5} \cdot \mathrm{CNOT}_{4,5} \cdot \mathrm{C}-\mathrm{Z}_{4,5} \cdot H_1 \cdot H_2 \cdot H_3 \cdot H_4 \end{aligned} \tag{6.93}$$

Now calculate the effect of these gates on $Z_1, \ldots, Z_4$:

$$Z_1 \rightarrow X \otimes Z \otimes Z \otimes X \otimes I \tag{6.94}$$
$$Z_2 \rightarrow I \otimes X \otimes Z \otimes Z \otimes X \tag{6.95}$$
$$Z_3 \rightarrow -I \otimes Z \otimes Y \otimes Y \otimes Z \tag{6.96}$$
$$Z_4 \rightarrow -Z \otimes I \otimes Z \otimes Y \otimes Y. \tag{6.97}$$

Since

$$I \otimes Z \otimes Y \otimes Y \otimes Z = +(X \otimes Z \otimes Z \otimes X \otimes I)(X \otimes I \otimes X \otimes Z \otimes Z) \tag{6.98}$$
$$Z \otimes I \otimes Z \otimes Y \otimes Y = +(I \otimes X \otimes Z \otimes Z \otimes X)(Z \otimes X \otimes I \otimes X \otimes Z), \tag{6.99}$$

the signs of Z_3 and Z_4 need to be corrected, so we start the encoding circuit with X_3X_4. The final encoding circuit is given in figure 6.4.

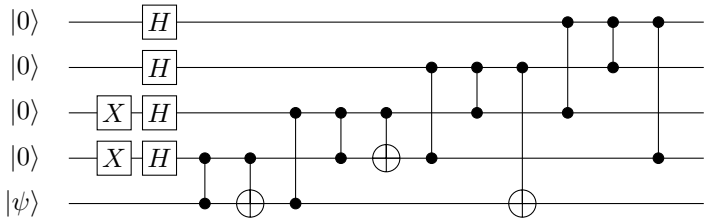

Figure 6.4: Encoding circuit for the five-qubit code derived in the text.

6.4.2 Encoding a Stabilizer Code with Specified Logical Paulis

If we are given a specific choice of logical Paulis, encoding becomes slightly more complicated. However, the same sort of techniques will work. There are two straightforward options.

Option 1 is to just use procedure 6.5, with fewer simplifications. The desired Clifford group operation maps $Z_i \to M_i$ for $i = 1, \ldots, n-k$, $Z_{n-k+j} \to \overline{Z}_j$ for $j = 1, \ldots, k$, and $X_{n-k+j} \to \overline{X}_j$ for $j = 1, \ldots, k$. Again, it is more convenient to perform the Hadamard on every qubit so that A and C of the desired symplectic matrix are full $n \times n$ matrices. Column operations which add the first $n-k$ columns of A and C to something can be done just by changing generators of the stabilizer or representatives of the logical Pauli cosets, but column operations involving the last k columns in either the right or left must be done with real gates.

Option 2 is to take advantage of the simplified procedure 6.6 to find an encoding circuit for a stabilizer without specified logical Paulis and see what actual logical Paulis $\overline{P}'$ it produces. Determine the logical Clifford group operation that maps $\overline{P}'$ to the desired logical Pauli $\overline{P}$. Use procedure 6.5 on k qubits to find a circuit performing that Clifford group operation. Perform this circuit on qubits $n-k+1, \ldots, n$, followed by the encoding circuit given by procedure 6.6. The resulting circuit will then encode the code with the correct logical Paulis.

For instance, in the previous subsection, we found an encoding circuit for the five-qubit code. Let us determine what logical Paulis it gives:

$$X_5 \to Z \otimes I \otimes I \otimes Z \otimes X \tag{6.100}$$

$$Z_5 \to Z \otimes Z \otimes Z \otimes Z \otimes Z. \tag{6.101}$$

In this encoding, $\overline{Z}$ is correct. However,

$$\overline{X} = Z \otimes I \otimes I \otimes Z \otimes X = -(X \otimes I \otimes X \otimes Z \otimes Z)(Z \otimes X \otimes I \otimes X \otimes Z)(X \otimes X \otimes X \otimes X \otimes X). \tag{6.102}$$

Therefore, we need the Clifford $X \to -X$, $Z \to Z$. This is just the gate Z, so we can correct the circuit of figure 6.4 by beginning with a Z_5 gate.

6.5 Extending the Clifford Group to a Universal Gate Set

Since the Clifford group can be simulated classically, to do any really interesting quantum algorithms, we will need some gates outside the Clifford group. How many gates and which ones suffice? It turns out *any* single gate will do it.

Theorem 6.9. *Let $G \subseteq \mathsf{SU}(2^n)$ be a group of quantum gates such that $\hat{\mathsf{C}}_n \subset G$ but $G \neq \hat{\mathsf{C}}_n$. Then G is dense in $\mathsf{SU}(2^n)$.*

That is, for any $U \in \mathsf{SU}(2^n)$ and any $\epsilon > 0$, $\exists V \in G$ such that $\|U - V\| < \epsilon$. Thus, we can approximate all quantum gates to any desired degree of accuracy using G, even if G is generated by just the Clifford group, plus any additional gate.

People frequently pick a somewhat nice gate to use as the extra gate. Two popular choices are the Toffoli gate Tof (also known as the controlled-controlled-NOT gate) $|a\rangle|b\rangle|c\rangle \mapsto |a\rangle|b\rangle|c \oplus ab\rangle$ and the $\pi/8$ phase rotation $R_{\pi/8}$, more commonly known today as the T gate. These gates are useful extra gates because they have comparatively straightforward fault-tolerant implementations using common QECCs, as you'll see in chapter 13.

The proof of theorem 6.9 is complicated and involves some more advanced concepts. I hope to include an accessible version of it in a later draft of this book.

Chapter 7

Tighter, Please: Upper And Lower Bounds On Quantum Codes

As I've told you, the three most important properties of a quantum code are the number n of logical qubits (or qudits), the dimension K of the encoded subspace, and the distance d of the code. Together, the parameters $((n, K, d))$ tell us about the trade-off between the rate at which we can send quantum information and the tolerance we gain against errors. Ideally, we'd like to know for any given set $((n, K, d))$ whether a QECC exists with those parameters.

Unfortunately, we can't answer that question. It seems to be extremely hard. However, we can set some bounds, which set limits on where we can hope to find interesting QECCs. On the one hand, there are lower bounds, saying that codes definitely exist with certain parameters. They can be *constructive* (specifying a particular code) or *non-constructive* (proving that codes with the parameters exist without giving an efficient method of specifying one). Then we have the upper bounds. There are many different methods used for proving upper bounds, but they are uniformly destructive: they tell us there are no codes with certain parameters.

The most attractive bounds are the tightest, with the upper bounds hugging as closely as possible to the lower bounds. Occasionally we can actually make the upper and lower bounds touch, but more often there is some space between. Unfortunately, in many instances, our bounds are rather baggy and shapeless, leaving a lot of room, which may or may not contain actual QECCs, between the upper and lower bounds.

7.1 The Quantum Gilbert-Varshamov Bound

We'll start with a lower bound, the quantum Gilbert-Varshamov bound. As you might guess from the name, it is a quantum analogue of the classical Gilbert-Varshamov lower bound discussed in section 4.5. The main difference from the classical Gilbert-Varshamov bound is that there are more quantum errors that occur on a qubit than there are classical errors that can occur on a bit.

Theorem 7.1 (Quantum Gilbert-Varshamov bound)**.** *Suppose*

$$2^k \left(\sum_{j=0}^{d-1} 3^j \binom{n}{j} \right) \leq 2^n. \tag{7.1}$$

Then there exists a $((n, 2^k, d))$ QECC. For large n, a code exists if

$$k/n \leq 1 - (d/n) \log 3 - h(d/n), \tag{7.2}$$

with $h(x) = h_2(x)$ given by equation (4.22).

Actually, the theorem will show that a stabilizer code with these parameters $[[n, k, d]]$ exists. It even can be made a little bit tighter than the statement of the theorem indicates, but it is usually phrased this way to be the closest analogue of the classical Gilbert-Varshamov bound. The proof is non-constructive. In this case, as with the classical Gilbert-Varshamov bound, that means that, while the proof specifies a procedure to find a code with these parameters, the procedure is exponentially long as a function of n, so it's not useful in practice. Since we get a stabilizer code, the code we produce can be described efficiently, but that is small consolation if we can't get all the way through the procedure to find it.

One can also prove a version of the quantum Gilbert-Varshamov bound for qudits, at least for prime power dimensions. The proof is analogous, using the idea of a qudit stabilizer code, which I'll discuss in chapter 8.

Proof. Imagine making a long list of all $[[n, k]]$ stabilizer codes. We are going to run through all possible errors of weight up to $d - 1$. For each error E, we can check which codes can detect that error and which cannot, and cross off the list any code that can't detect E. Once we finish running through all the errors, we know that any code that remains must have distance at least d. We'll prove that there must be at least one code to survive, giving us the desired $[[n, k, d]]$ code.

For any given error E, we need to count how many codes cannot detect it. For any two errors $E, F \in \mathsf{P}_n \setminus \{I\}$, there exists some Clifford group element U with $U(E) = F$. Furthermore, if stabilizer code S is a code that doesn't detect E, then $U(\mathsf{S})$ is a stabilizer code that doesn't detect F. That is, U will permute the list of stabilizer codes and their sets of undetectable errors. Thus, the number of codes that cannot detect E must be the same as the number of codes that cannot detect F. That is, all non-identity errors in the Pauli group are undetectable for the same number C of $[[n, k]]$ stabilizer codes.

Suppose there are N stabilizer codes with parameters $[[n, k]]$. (We can evaluate N exactly if we like, but it is not necessary for this argument.) The code S detects the errors outside $\hat{\mathsf{N}}(\mathsf{S}) \setminus \hat{\mathsf{S}}$, which contains $2^{n+k} - 2^{n-k}$ elements. If we consider a bigger list of pairs (S, E) for any pair for which $E \in \hat{\mathsf{N}}(\mathsf{S}) \setminus \hat{\mathsf{S}}$, we can count the number of elements on the list two ways: as the number of errors times the number of codes that cannot detect each error, or as the number of codes times the number of errors that each code cannot detect. There are $4^n - 1$ non-identity errors, and I never appears in $\hat{\mathsf{N}}(\mathsf{S}) \setminus \hat{\mathsf{S}}$, so we have that

$$(4^n - 1)C = N(2^{n+k} - 2^{n-k}). \tag{7.3}$$

Now let us go back to crossing codes off our list of stabilizer codes. We work our way through the set of errors of weight up to $d - 1$. For any non-identity error E with weight less than d, there are C codes which do not detect it, so we can cross those codes off the list. Some of them may have already been eliminated because they fail to detect a previous error, but certainly we cannot eliminate more than C new codes from the list of $[[n, k]]$ QECCs. There are a total of $B - 1$ non-identity errors of weight less than d, with

$$B = \sum_{j=0}^{d-1} 3^j \binom{n}{j} \tag{7.4}$$

(not including the identity since all codes detect it). By the time we finish going through all errors of weight less than d, we have therefore crossed off at most $(B - 1)C$ codes. If $(B - 1)C < N$, then at least one code remains.

Plugging in equation (7.3) to eliminate C, the condition we get is

$$\frac{2^{n+k} - 2^{n-k}}{4^n - 1}(B - 1)N < N, \tag{7.5}$$

or

$$2^{n-k}(B - 1) < \frac{4^n - 1}{4^k - 1}. \tag{7.6}$$

This is the tightest version of the quantum Gilbert-Varshamov bound, but notice that

$$\frac{4^n - 1}{4^k - 1} > \frac{4^n}{4^k} = 4^{n-k}, \tag{7.7}$$

so if

$$2^{n-k}B \leq 4^{n-k}, \tag{7.8}$$

then equation (7.6) is satisfied too. Equation (7.8) is just what we wanted to prove. □

7.2 The Quantum Hamming Bound

We'll now move on to an upper bound of sorts. It is an analogue of the classical Hamming bound, so is called the quantum Hamming bound.

Theorem 7.2 (Quantum Hamming bound)**.** *If a non-degenerate* $((n, K, 2t+1))_q$ *code exists, then*

$$K\left(\sum_{j=0}^{t}(q^2-1)^j\binom{n}{j}\right) \leq q^n. \tag{7.9}$$

The big catch in the statement of the quantum Hamming bound is that while it provides an upper bound, the upper bound *only holds for non-degenerate codes.* Here is where we start to see very concretely how the existence of degenerate codes makes the quantum case more complicated than the classical case. Insisting that a code be degenerate is potentially a big limitation, yet it is easier to prove bounds on the existence of non-degenerate codes. Indeed, while we don't know how to prove that the quantum Hamming bound applies to degenerate codes as well as non-degenerate codes, we also don't know any $((n, K, 2t+1))$ codes that violate it.

Proof. The proof is a straightforward exercise in counting dimensions, and is very analogous to the proof of the classical Hamming bound. Because the code is non-degenerate, we know that in the QECC conditions, the matrix

$$C_{ab} = \langle\psi|E_a^\dagger E_b|\psi\rangle \tag{7.10}$$

(for any codeword $|\psi\rangle$) has maximum rank when $E_a^\dagger$ and E_b run over any basis for the space of $\leq t$-qubit errors. In particular, this means that the states $E_a|\psi\rangle$ are all linearly independent. Furthermore, if $|\psi\rangle$ and $|\phi\rangle$ are two orthogonal codewords, then the QECC conditions tell us that

$$\langle\psi|E_a^\dagger E_b|\phi\rangle = 0, \tag{7.11}$$

so $E_a|\psi\rangle$ and $E_b|\phi\rangle$ are orthogonal for any a, b.

Thus, if we let $\{|\psi_i\rangle\}$ be a basis for the code space, the set of states $\{E_a|\psi_i\rangle\}$ (over all a, i) are linearly independent. The codespace has dimension K and there are q^2-1 one-qudit non-identity errors, so there are a total of

$$B = \sum_{j=0}^{t}(q^2-1)^j\binom{n}{j} \tag{7.12}$$

linearly independent errors of weight up to t. Thus, we have a set of KB linearly independent vectors, which we must fit into a Hilbert space of n qudits. Therefore,

$$KB \leq q^n \tag{7.13}$$

□

Looking at this proof, you'll see that the quantum Hamming bound does not make essential use of the qudit structure of the space, or the fact that we are dealing with t-qudit errors. In general, if we have a non-degenerate QECC with a K-dimensional code space living in an N-dimensional physical Hilbert space, and the code can correct $\mathcal{E}$, a set of linearly independent errors, then $K|\mathcal{E}| \leq N$.

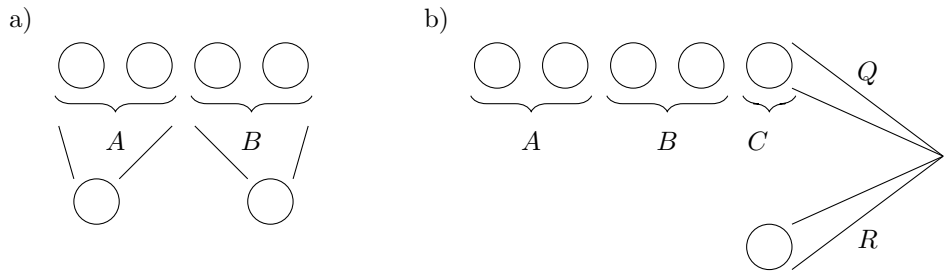

Figure 7.1: a) Dividing n registers into one set A of size $d-1$ and one set B of size $n-(d-1)$ for the proof of lemma 7.4. If $n-(d-1) \leq d-1$, we can decode each set separately to clone the encoded qubit. b) System Q is maximally entangled with system R. Q is then encoded into n registers, which are split into three sets for the proof of the quantum Singleton bound: sets A and B of size $d-1$ and set C of size $n-2(d-1)$.

7.3 The Quantum Singleton Bound

The quantum Singleton bound has a similar form to the classical Singleton bound, but is significantly harder to prove. The quantum Singleton bound is also known as the Knill-Laflamme bound, after the first people to state it. The quantum Singleton bound is a real upper bound, applying to non-degenerate codes as well as degenerate ones, and to both stabilizer and non-stabilizer codes over qubits or qudits.

Theorem 7.3 (Quantum Singleton bound)**.** *If an $((n, q^k, d))_q$ QECC exists, then*

$$n - k \geq 2(d-1). \tag{7.14}$$

As you can see by comparing with theorem 4.19, the quantum bound is more restrictive on the distance by a factor of 2. The reason for this factor of 2 turns out to be the No-Cloning Theorem! You may recall that our very first objection in section 2.1 to the possibility of a quantum error-correcting code was that classical codes seemed to use repetition of information as a key component. We circumvented that difficulty by using entanglement to spread out quantum information without repeating it. The quantum Singleton bound can be viewed as a way of codifying just how well information can be spread around without accidentally repeating anything. For instance, the bound immediately tells us that there can be no complete quantum analogue of the classical $(3, 2, 3)$ repetition code, since a $((3, 2, 3))$ QECC would violate the quantum Singleton bound.

Proof. We'll start by studying the $k = 1$ case, which is an immediate consequence of the No-Cloning Theorem:

Lemma 7.4. *If an $((n, q, d))_q$ QECC exists, then*

$$n - 1 \geq 2(d-1). \tag{7.15}$$

Proof of lemma. If a code has distance d, then it can correct $d-1$ erasure errors. We can imagine dividing the n registers of the code into two sets, a set A with $d-1$ registers and a set B with $n-(d-1)$ registers, as pictured in figure 7.1a. Set B has experienced $d-1$ erasures, so using just those registers, it is possible to reconstruct the original encoded state $|\psi\rangle$.

Now suppose that $n-1 < 2(d-1)$. Then $n-(d-1) \leq d-1$, and therefore set A has also experienced at most $d-1$ erasure errors. We would then be able to reconstruct a second copy of $|\psi\rangle$ using just the registers in set A. We could then use this code to clone the state $|\psi\rangle$ via the following procedure: Encode $|\psi\rangle$ using the QECC, split up the registers into the sets A and B, and then reconstruct $|\psi\rangle$ independently for each set. We know this isn't possible, leading to a contradiction and proving the lemma.

□

Now we can move on to the general case. When $k > 1$, we split the n registers into three sets, as pictured in figure 7.1b. Sets A and B will each have $d-1$ registers, and set C will have $n-2(d-1)$ registers. If an

$((n, q^k, d))_q$ code exists for $k \geq 1$, then a $((n, q, d))_q$ code also exists, as we can just ignore the extra logical codewords. We therefore know from the lemma that $n > 2(d-1)$, and set C is non-empty.

Now imagine taking a $2k$-qudit maximally entangled state between two registers R and Q, each with dimension q^k, and encode Q in the QECC. Then divide up the registers of the QECC into the sets A, B, and C, giving us a total of 4 sets (R, A, B, C). Globally, we now have a pure state, so $S(RABC) = 0$. If we split our sets into two groups, the entropy of the two groups is equal, e.g.

$$S(RA) = S(BC) \tag{7.16}$$
$$S(RB) = S(AC). \tag{7.17}$$

We also know that the code has distance d, so we can detect any erasure error restricted to just set A or to just set B (but not necessarily errors involving both sets). Applying the alternate QECC conditions of section 2.5.6, we see that this means that any operator we measure on set A will give us the same result for all possible logical codewords. Thus, the density matrix ρ_A of set A is the same for all logical codewords, and we find that the density matrix for R and A combined is of the form

$$\sum_{i=0}^{q^k-1} |i\rangle \langle i|_R \otimes \rho_A. \tag{7.18}$$

R and A are in a tensor product state, so $S(RA) = S(R) + S(A)$. Similarly, $S(RB) = S(R) + S(B)$. We also note that $S(R) = k \log q$.

Now, $S(RA) = S(BC)$, and by subadditivity of the entropy, $S(BC) \leq S(B) + S(C)$. Therefore,

$$k \log q + S(A) = S(RA) = S(BC) \leq S(B) + S(C), \tag{7.19}$$

or

$$k \log q \leq S(C) + [S(B) - S(A)]. \tag{7.20}$$

Applying subadditivity to $S(AC)$, we also find that

$$k \log q \leq S(C) + [S(A) - S(B)]. \tag{7.21}$$

Adding together these last two equations, we find that

$$k \log q \leq S(C). \tag{7.22}$$

However, $S(C) \leq \log \dim(C) = [n - 2(d-1)] \log q$. Therefore, we find

$$k \leq n - 2(d-1). \tag{7.23}$$

□

As an immediate application of the quantum Singleton bound, we find that the five-qubit code is optimal. Not only can there be no $((3, 2, 3))$ code, but there can also be no $((4, 2, 3))$ QECC. The five-qubit code exactly saturates the quantum Singleton bound; it is a *quantum MDS code*. We can also saturate the quantum Singleton bound with $d = 2$. There are $[[n, n-2, 2]]$ stabilizer codes for any even n (but not for odd n). As we go to more encoded qubits or to greater distances, it is no longer possible to exactly saturate the quantum Singleton bound with qubit codes. A similar phenomenon occurs classically, and as in the classical case, we get more MDS codes as we let the dimension of the registers increase. In section 8.3, we'll see a large family of such codes.

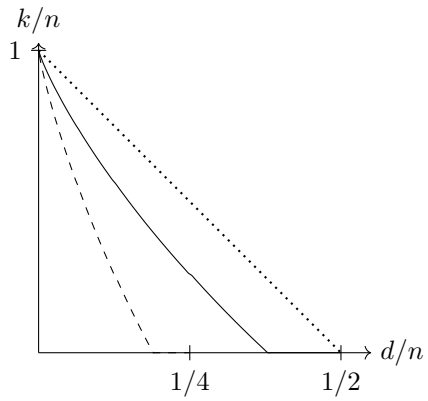

Figure 7.2: Quantum Hamming bound (solid), quantum Gilbert-Varshamov bound (dashed), and quantum Singleton bound (dotted) for large n, $q = 2$

7.4 Linear Programming Bounds

The quantum Singleton bound does provide us with some definite limits on the existence of QECCs since, unlike the quantum Hamming bound, it applies to degenerate codes too. Still, it doesn't tell us much. Figure 7.2 shows the lower bound provided by the quantum Gilbert-Varshamov bound along with the upper bound given by the quantum Singleton bound, both plotted for codes using qubits. I've also shown the quantum Hamming bound so you can see that even if we were able to prove it applied to degenerate codes, there would still be a lot of room where we don't know about the existence of codes. The quantum Singleton bound is much worse. There's no way we can be satisfied with that.

In order to do better, we'll need more powerful techniques. The main ones are known as *linear programming bounds*. A linear programming bound provides a set of linear inequalities that a QECC with a given set of parameters $((n, K, d))_q$ must satisfy. If we can prove that the set of inequalities has no solutions for a given n, K, and d, then we know that a QECC with those parameters cannot exist. If there *is* a solution, then a QECC may or may not exist, but the linear programming solution gives us a number of constraints about the structure of any possible code with those parameters, so provides a good hint as to what to look at to find a code.

In this section, I'll discuss the main linear programming bounds, but only for codes over qubits. These bounds can be generalized to apply to qudits, and it's possible to come up with more linear programming bounds, which could narrow down the set of possible codes even further.

7.4.1 Weight Enumerator and Dual Weight Enumerator

The primary tools used in coming up with linear programming bounds are known as *weight enumerators*. There are many different kinds of weight enumerators, but we'll start with the simplest, which gets no additional adjectives in its name. Weight enumerators are polynomials that encode information about the properties of a QECC.

To motivate the definition of weight enumerator, let's first consider the case of a stabilizer code. The stabilizer S consists of Pauli operators. Some of those Pauli operators are large, with high weight, and some are small, with low weight. Indeed, S always contains I, which has weight 0. We'll count up the number of elements of each weight; let A_j be the number of Paulis $M \in S$ with weight j. The A_js are integers which tell us about the structure of the stabilizer, although they don't tell us everything. How can we get similar information about more general QECCs?

Definition 7.1. Let Π be the projector onto the code subspace of some $((n, K))$ QECC Q. Let

$$A_j = \frac{1}{K^2} \sum_{P \in \hat{\mathsf{P}}_n \,|\, \mathrm{wt}(P)=j} |\mathrm{tr}(P\Pi)|^2 . \tag{7.24}$$

The *weight enumerator* of Q is the degree n polynomial

$$A(x) = \sum_{j=0}^{n} A_j x^j . \tag{7.25}$$

The motivation for defining the weight enumerator as a polynomial instead of just working with the individual coefficients will become clearer in the next subsection, where I'll discuss the quantum MacWilliams identity, which deals with the polynomial as a whole.

Proposition 7.5. *When Q is a stabilizer code with stabilizer S,*

$$A_j = |\{M \in \mathsf{S} |\, \mathrm{wt}\, M = j\}| . \tag{7.26}$$

Proof. For a stabilizer code, $K = 2^k$, and we have an explicit description of the projector onto the code:

$$\Pi = \frac{1}{2^{n-k}} \sum_{M \in \mathsf{S}} M. \tag{7.27}$$

Now, $\mathrm{tr}\, Q = 0$ if $Q \in \hat{\mathsf{P}}_n \setminus \{I\}$ and $\mathrm{tr}\, I = 2^n$. Thus,

$$|\,\mathrm{tr}(PM)| = \begin{cases} 2^n & \text{if } P = M \\ 0 & \text{if } P \neq M. \end{cases} \tag{7.28}$$

We will consider Paulis in $\hat{\mathsf{P}}_n$, so depending on what representatives we pick, it could actually be that $\mathrm{tr}(PM) = -2^n$ or $\pm i 2^n$. However, since we immediately take the absolute value, all of these give the same result.

Applying the general definition of A_j, we find

$$A_j = \frac{1}{2^{2k}} \sum_{P \in \hat{\mathsf{P}}_n \,|\, \mathrm{wt}(P)=j} \left| \frac{1}{2^{n-k}} \sum_{M \in \mathsf{S}} \mathrm{tr}(PM) \right|^2 \tag{7.29}$$

$$= \frac{1}{2^{2k}} \sum_{P \in \hat{\mathsf{P}}_n \,|\, \mathrm{wt}(P)=j} \left| \frac{1}{2^{n-k}} \sum_{M \in \mathsf{S}} 2^n \delta_{P,M} \right|^2 \tag{7.30}$$

$$= \frac{1}{2^{2k}} \sum_{P \in \hat{\mathsf{P}}_n \,|\, \mathrm{wt}(P)=j} 2^{2k} \chi_{\mathsf{S}}(P) \tag{7.31}$$

$$= |\{M \in \mathsf{S} |\, \mathrm{wt}\, M = j\}| . \tag{7.32}$$

In the third line, $\chi_{\mathsf{S}}(P)$ is the indicator function, which is 1 when $P \in \mathsf{S}$ and 0 when $P \notin \mathsf{S}$.

□

Similarly, we can define a dual weight enumerator. For a stabilizer code, it is built out of B_js which give the weight distribution of the *normalizer* of S. In general, we have the definition

Definition 7.2. Let Π be the projector onto the code subspace of some $((n, K))$ QECC Q. Let

$$B_j = \frac{1}{K} \sum_{P \in \hat{\mathsf{P}}_n \,|\, \mathrm{wt}(P)=j} \mathrm{tr}(P\Pi P^\dagger \Pi). \tag{7.33}$$

The *dual weight enumerator* of Q is the degree n polynomial

$$B(x) = \sum_{j=0}^{n} B_j x^j. \tag{7.34}$$

Again, the general definition reduces to the description given for stabilizer codes:

Proposition 7.6. *When Q is a stabilizer code with stabilizer S,*

$$B_j = \left| \{ N \in \hat{\mathsf{N}}(\mathsf{S}) | \operatorname{wt} N = j \} \right|. \tag{7.35}$$

Proof. Again, we have

$$\Pi = \frac{1}{2^{n-k}} \sum_{M \in \mathsf{S}} M, \tag{7.36}$$

and we see that

$$P \Pi P^\dagger = \frac{1}{2^{n-k}} \sum_{M \in \mathsf{S}} (-1)^{c(P,M)} M. \tag{7.37}$$

Note that when $P \in \mathsf{N}(\mathsf{S})$, then $P \Pi P^\dagger = \Pi$. However, when $P \notin \mathsf{N}(\mathsf{S})$, then $P \Pi P^\dagger$ will be the projector on the subspace given by a different error syndrome of S. That subspace is orthogonal to the code space, so we have that $P \Pi P^\dagger \Pi = 0$ when $P \notin \mathsf{N}(\mathsf{S})$. This is also straightforward to prove through direct computation:

$$\begin{aligned} P \Pi P^\dagger \Pi &= \frac{1}{2^{2(n-k)}} \sum_{M,N \in \mathsf{S}} (-1)^{c(P,M)} MN & (7.38) \\ &= \frac{1}{2^{2(n-k)}} \sum_{N' \in \mathsf{S}} \left(\sum_{M \in \mathsf{S}} (-1)^{c(P,M)} \right) N' & (7.39) \\ &= \frac{1}{2^{2(n-k)}} \sum_{N' \in \mathsf{S}} 2^{n-k} \chi_{\mathsf{N}(\mathsf{S})}(P)\, N' & (7.40) \\ &= \chi_{\mathsf{N}(\mathsf{S})}(P)\, \Pi, & (7.41) \end{aligned}$$

where $\chi_{\mathsf{N}(\mathsf{S})}(P)$ is the indicator function for $\mathsf{N}(\mathsf{S})$ and line three follows because if $P \notin \mathsf{N}(\mathsf{S})$, then P anticommutes with exactly half of S.

Thus, applying the general definition of B_j, we find

$$\begin{aligned} B_j &= \frac{1}{2^k} \sum_{P \in \hat{\mathsf{P}}_n | \operatorname{wt}(P) = j} \operatorname{tr}(\Pi) \chi_{\mathsf{N}(\mathsf{S})}(P) & (7.42) \\ &= \left| \{ N \in \mathsf{N}(\mathsf{S}) | \operatorname{wt} N = j \} \right|. & (7.43) \end{aligned}$$

□

The coefficients A_j and B_j of the weight enumerator and dual weight enumerator are always integers for a stabilizer code, but can be non-integer for general QECCs.

For a stabilizer code, the dual weight enumerator tells us about the structure of the normalizer, which in turn tells us something about which errors we can detect. If B_j is non-zero, it means there are some Paulis of weight j in the normalizer, which worries us if j is small. Actually, though, we are interested in the number of elements of $\hat{\mathsf{N}}(\mathsf{S}) \setminus \hat{\mathsf{S}}$, which is given by $B_j - A_j$. If *that* is non-zero, then we actually have some errors of weight j that are undetectable, giving us a bound on the distance of the code. While this argument does not hold for general QECCs, the intuition and result about A_j and B_j does carry over:

Theorem 7.7. *Let Q be a QECC with weight enumerator $A(x) = \sum A_j x^j$ and dual weight enumerator $B(x) = \sum B_j x^j$. Then*

a) $A_0 = B_0 = 1$

b) $B_j \geq A_j \geq 0$

c) Q has distance d iff $A_j = B_j$ *for* $j < d$.

Proof.

a) There is only one Pauli of weight 0: the identity. Thus,

$$A_0 = \frac{1}{K^2} \left|\mathrm{tr}(\Pi)\right|^2 = 1 \tag{7.44}$$

$$B_0 = \frac{1}{K} \mathrm{tr}(\Pi^2) = \frac{1}{K} \mathrm{tr}(\Pi) = 1. \tag{7.45}$$

b) From the definition of A_j, we can immediately see that $A_j \geq 0$.

Let $\{|a\rangle\}$ be a basis for the code space of Q. Then

$$\Pi = \sum_a |a\rangle \langle a|, \tag{7.46}$$

so

$$A_j = \frac{1}{K^2} \sum_{P|\,\mathrm{wt}(P)=j} \left| \sum_a \langle a|P|a\rangle \right|^2, \tag{7.47}$$

$$B_j = \frac{1}{K} \sum_{P|\,\mathrm{wt}(P)=j} \sum_{a,b} \left|\langle a|P|b\rangle\right|^2. \tag{7.48}$$

Our next step is to apply the Cauchy-Schwarz inequality, which says that for two complex vectors $\vec{x}$ and $\vec{y}$,

$$|\vec{x} \cdot \vec{y}|^2 \leq |\vec{x}|^2 |\vec{y}|^2. \tag{7.49}$$

Let $\vec{x}$ be the K^2-dimensional complex vector with entries $\langle a|P|b\rangle$ (running over pairs (a,b)), and let $\vec{y}$ be the K^2-dimensional vector with entries equal to $(1/K)\delta_{ab}$ (again running over pairs (a,b)). Then we have

$$|\vec{x} \cdot \vec{y}|^2 = \left| \frac{1}{K} \sum_{a,b} \langle a|P|b\rangle \delta_{ab} \right|^2 \tag{7.50}$$

$$= \frac{1}{K^2} \left| \sum_a \langle a|P|a\rangle \right|^2 \tag{7.51}$$

$$\leq |\vec{x}|^2 |\vec{y}|^2 \tag{7.52}$$

$$= \left(\sum_{a,b} \left|\langle a|P|b\rangle\right|^2 \right) \left(\sum_{ab} \frac{1}{K^2} \delta_{ab} \right) \tag{7.53}$$

$$= \frac{1}{K} \sum_{a,b} \left|\langle a|P|b\rangle\right|^2. \tag{7.54}$$

Plugging into equations (7.47) and (7.48), we find that $A_j \leq B_j$.

c) From the definition of distance, equation (2.66), if the code has distance d, then for $\mathrm{wt}(E) < d$,

$$\langle \psi|E|\phi\rangle = c(E) \langle \psi|\phi\rangle \tag{7.55}$$

for any codewords $|\psi\rangle$ and $|\phi\rangle$. Applying equations (7.47) and (7.48) for $j < d$, we get

$$A_j = \frac{1}{K^2} \sum_{E|\,\mathrm{wt}\,E=j} K^2 |c(E)|^2 \tag{7.56}$$

$$B_j = \frac{1}{K} \sum_{E|\,\mathrm{wt}\,E=j} K |c(E)|^2, \tag{7.57}$$

and $A_j = B_j$.

For the converse, looking at the proof of part b, the equality condition for the Cauchy-Schwarz inequality is that $\vec{x}$ is proportional to $\vec{y}$. Thus, $A_j = B_j$ implies that

$$\langle a|E|b\rangle = C(E)\delta_{ab} \tag{7.58}$$

whenever $\mathrm{wt}\,E = j$. This is one of the alternate forms of the QECC conditions.

□

The classical theory of weight enumerators is similar, except that for classical codes, $A_j = B_j = 0$ for $j < d$. The difference is essentially a manifestation of the phenomenon of degeneracy. Let's think about the special case of stabilizer codes. In a non-degenerate stabilizer code S, there are no elements of $\mathsf{N}(\mathsf{S})$ with weight less than d. Therefore $B_j = 0$ for $j < d$. In a degenerate stabilizer code, $\mathsf{N}(\mathsf{S})$ can have elements with weight less than d, but those elements must also be in S. Thus, $B_j = A_j > 0$ for some $j < d$.

This intuition almost carries over to general QECCs, but it turns out to be a slightly different concept.

Definition 7.3. An $((n, K, d))$ QECC with weight enumerators $A(x)$ and $B(x)$ is *pure* if $A_j = B_j = 0$ for $j < d$. A code that is not pure is *impure*.

The argument above shows that for stabilizer codes, pure is the same as non-degenerate. However, for more general codes, the property of being pure is more stringent than the property of being non-degenerate. In other words, a code can be impure without being degenerate, but if it's degenerate, it is definitely impure.

The possibility of impure codes complicates the application of the linear programming bounds to quantum codes. Some results which are known for classical codes have not yet been adapted for quantum codes because of the additional difficulty created by dealing with impure codes.

7.4.2 Quantum MacWilliams Identity

Theorem 7.7 gives us one set of inequalities constraining the coefficients A_j and B_j. However, these inequalities by themselves are not yet enough to rule out any codes, since for any set of parameters $((n, K, d))$, we can easily come up with a set of A_j and B_j that satisfy theorem 7.7. In order to get actual upper bounds on codes this way, we'll need a stronger relation between $A(x)$ and $B(x)$.

In the case of a stabilizer code, the weight enumerator $A(x)$ encapsulates properties of the stabilizer S and the dual weight enumerator $B(x)$ captures properties of $\mathsf{N}(\mathsf{S})$. Since $\mathsf{N}(\mathsf{S})$ is completely determined by S, it's perhaps not too surprising that there is some relationship between $A(x)$ and $B(x)$ as well. What *is* remarkable is that even though the full description of S contains a lot more information than is contained in $A(x)$, the weight enumerator by itself is enough to completely determine $B(x)$. Moreover, this relationship also holds for non-stabilizer codes.

Theorem 7.8 (Quantum MacWilliams identity)**.** *Suppose we have an $((n, K))$ QECC with weight enumerator $A(x)$ and dual weight enumerator $B(x)$. Then*

$$B(x) = \frac{K}{2^n}(1+3x)^n A\left(\frac{1-x}{1+3x}\right) \tag{7.59}$$

The quantum MacWilliams identity above is phrased in terms of codes over qubits, but like the other bounds we've discussed, it can also be generalized to codes over qudits.

Proof. Let's eliminate the projector Π that appears in the definitions of A_j and B_j in favor of Paulis. We can do this by using the fact that $\hat{\mathsf{P}}_n$ gives a basis for the space of $2^n \times 2^n$ matrices, so

$$\Pi = \sum_{Q \in \hat{\mathsf{P}}_n} c_Q Q. \tag{7.60}$$

The coefficients $c_Q = \operatorname{tr}(Q^\dagger \Pi)/2^n$.

Then

$$A_j = \frac{1}{K^2} \sum_{P \in \hat{\mathsf{P}}_n \,|\, \operatorname{wt}(P)=j} \left| \sum_{Q \in \hat{\mathsf{P}}_n} c_Q \operatorname{tr}(PQ) \right|^2 \tag{7.61}$$

$$= \frac{4^n}{K^2} \sum_{P \in \hat{\mathsf{P}}_n \,|\, \operatorname{wt}(P)=j} |c_P|^2, \tag{7.62}$$

and

$$B_j = \frac{1}{K} \sum_{P \in \hat{\mathsf{P}}_n \,|\, \operatorname{wt}(P)=j} \sum_{Q,R \in \hat{\mathsf{P}}_n} c_Q c_R^* \operatorname{tr}(PQP^\dagger R^\dagger) \tag{7.63}$$

$$= \frac{1}{K} \sum_{P \in \hat{\mathsf{P}}_n \,|\, \operatorname{wt}(P)=j} \sum_{Q,R \in \hat{\mathsf{P}}_n} c_Q c_R^* (-1)^{c(P,Q)} \delta_{Q,R} 2^n \tag{7.64}$$

$$= \frac{2^n}{K} \sum_{Q \in \hat{\mathsf{P}}_n} \left[\sum_{P \in \hat{\mathsf{P}}_n \,|\, \operatorname{wt}(P)=j} (-1)^{c(P,Q)} \right] |c_Q|^2. \tag{7.65}$$

In the first line for B_j, I've used $\Pi^\dagger$ in one place instead of Π (they are the same, after all) to finesse issues about using Paulis with the overall sign modded out. We can see that A_j and B_j both involve a sum over $|c_Q|^2$, but with two differences: In A_j, we only sum over Paulis of weight j whereas for B_j we sum over all Paulis, and in B_j we have an additional sum with alternating signs which depend on the commutation relations.

Let's take some Q with weight i and try to count how many Paulis of weight j commute with it, which we'll call C_{ij}, and how many anticommute, A_{ij}. Then we will have

$$B_j = \frac{2^n}{K} \sum_{Q \in \hat{\mathsf{P}}_n} (C_{\operatorname{wt}(Q),j} - A_{\operatorname{wt}(Q),j}) |c_Q|^2. \tag{7.66}$$

First of all, we know that there are a total of

$$3^j \binom{n}{j} \tag{7.67}$$

Paulis of weight j. Also note that the answer won't depend on exactly what Q we take, only its weight i, because single-qubit Clifford group operations and permutations of the qubits can relate any two Paulis of weight i, and those operations won't change the commutation relations or weights of Paulis.

Let's break up the counting problem into counting Paulis P that overlap with Q on exactly m qubits (i.e., the intersection of their supports is m qubits), and determining how many commute (C_{ij}^m) and how many anticommute (A_{ij}^m). P has total weight j, so it acts on exactly $j-m$ qubits outside the support of Q. There are thus

$$3^{j-m} \binom{n-i}{j-m} \tag{7.68}$$

ways of choosing the action of P outside the support of Q. Within the support of Q, there are $\binom{i}{m}$ ways of choosing which qubits P acts on non-trivially.

We now wish to find how many weight m Paulis commute and anticommute with a fixed Pauli of weight m, which can assume without loss of generality to be $Z^{\otimes m}$. That is, it suffices to find C^m_{mm} and A^m_{mm}, and then we know that

$$C^m_{ij} = 3^{j-m}\binom{n-i}{j-m}\binom{i}{m}C^m_{mm} \tag{7.69}$$

$$A^m_{ij} = 3^{j-m}\binom{n-i}{j-m}\binom{i}{m}A^m_{mm}. \tag{7.70}$$

Now, $C^1_{11} = 1$ and $A^1_{11} = 2$. We can use induction to determine C^m_{mm} and A^m_{mm} for all m:

$$C^m_{mm} = C^{m-1}_{(m-1)(m-1)} + 2A^{m-1}_{(m-1)(m-1)} \tag{7.71}$$

$$A^m_{mm} = 2C^{m-1}_{(m-1)(m-1)} + A^{m-1}_{(m-1)(m-1)}. \tag{7.72}$$

Actually, what we're really interested in is $C^m_{ij} - A^m_{ij}$, and we see that

$$C^m_{mm} - A^m_{mm} = -C^{m-1}_{(m-1)(m-1)} + A^{m-1}_{(m-1)(m-1)} = (-1)^{m-1}\left(C^1_{11} - A^1_{11}\right) = (-1)^m. \tag{7.73}$$

Putting all of this together, we find that

$$B_j = \frac{2^n}{K}\sum_{Q\in\hat{\mathsf{P}}_n}(C_{\mathrm{wt}(Q),j} - A_{\mathrm{wt}(Q),j})|c_Q|^2 \tag{7.74}$$

$$= \frac{2^n}{K}\sum_{i=0}^{n}\sum_{Q\in\hat{\mathsf{P}}_n\,|\,\mathrm{wt}\,Q=i}\left[\sum_{m=0}^{\min(i,j)}\left(C^m_{ij} - A^m_{ij}\right)\right]|c_Q|^2 \tag{7.75}$$

$$= \frac{2^n}{K}\sum_{i=0}^{n}\sum_{Q\in\hat{\mathsf{P}}_n\,|\,\mathrm{wt}\,Q=i}\left[\sum_{m=0}^{\min(i,j)}(-1)^m 3^{j-m}\binom{n-i}{j-m}\binom{i}{m}\right]|c_Q|^2 \tag{7.76}$$

$$= \frac{K}{2^n}\sum_{i=0}^{n}\left[\sum_{m=0}^{\min(i,j)}(-1)^m 3^{j-m}\binom{n-i}{j-m}\binom{i}{m}\right]A_i. \tag{7.77}$$

$$\tag{7.78}$$

The function

$$P_j(z;n) = \sum_{m=0}^{\min(z,j)}(-1)^m 3^{j-m}\binom{n-z}{j-m}\binom{z}{m} \tag{7.79}$$

is known as a Krawtchouk polynomial, and

$$(1+3x)^{n-z}(1-x)^z = \sum_j P_j(z;n)x^j, \tag{7.80}$$

as can be verified by expanding the left-hand side. That tells us

$$B(x) = \sum_{j=0}^{n} B_j x^j \tag{7.81}$$

$$= \frac{K}{2^n} \sum_{i=0}^{n} \sum_{j=0}^{n} P_j(i;n) A_i x^j \tag{7.82}$$

$$= \frac{K}{2^n} \sum_{i=0}^{n} (1+3x)^{n-i} (1-x)^i A_i \tag{7.83}$$

$$= \frac{K}{2^n} (1+3x)^n \sum_{i=0}^{n} \left(\frac{1-x}{1+3x} \right)^i A_i \tag{7.84}$$

$$= \frac{K}{2^n} (1+3x)^n A\left(\frac{1-x}{1+3x} \right) \tag{7.85}$$

□

The quantum MacWilliams identity combined with theorem 7.7 puts a number of restrictions on the possible values of $((n, K, d))$ for a code, enough to rule out many more possibilities than the quantum Singleton bound. However, we can set even tighter bounds by adding another weight enumerator known as the quantum shadow enumerator.

7.4.3 Quantum Shadow Enumerator

The quantum shadow enumerator has a somewhat stranger definition than the weight enumerator and dual weight enumerator. The weight enumerator and dual weight enumerator treat all Paulis of a given weight on an equal footing. The quantum shadow enumerator does not:

Definition 7.4. Suppose Π is the projector onto the code subspace of some $((n, K))$ QECC Q. Let

$$Sh_j = \frac{1}{K} \sum_{P \in \hat{\mathsf{P}}_n \,|\, \mathrm{wt}\, P = j} \mathrm{tr}(P \Pi P^\dagger Y^{\otimes n} \Pi^* Y^{\otimes n}). \tag{7.86}$$

The *shadow enumerator* of Q is

$$Sh(x) = \sum_{j=0}^{n} Sh_j x^j. \tag{7.87}$$

Π^* is the complex conjugate of the projector Π. The definition of the shadow enumerator is heavily basis-dependent, both for defining the Paulis and for defining the complex conjugate of an operator.

Theorem 7.9. *Suppose we have an $((n, K))$ QECC with weight enumerator $A(x)$ and shadow enumerator $Sh(x) = \sum Sh_j x^j$. Then*

a) $Sh_j \geq 0 \ \forall j$

b) $Sh(x)$ can be determined from $A(x)$:

$$Sh(x) = \frac{K}{2^n} (1+3x)^n A\left(\frac{x-1}{1+3x} \right). \tag{7.88}$$

Notice that the relation between $A(x)$ and $Sh(x)$ differs from the quantum MacWilliams identity only in that there is an $x - 1$ in the numerator of the argument of A instead of $1 - x$.

Proof.

a) We can write $\Pi = \sum_a |a\rangle\langle a|$, for $|a\rangle$ a basis of the code space. Note that this basis might be different from the basis in which the shadow enumerator is defined, so we let $|a^*\rangle$ be the complex conjugate of $|a\rangle$ in the defining basis. Then

$$Sh_j = \frac{1}{K} \sum_{P \in \hat{\mathsf{P}}_n | \, \mathrm{wt}\, P = j} \sum_{a,b} \mathrm{tr}(P|a\rangle \langle a|P^\dagger Y^{\otimes n}|b^*\rangle \langle b^*|Y^{\otimes n}) \tag{7.89}$$

$$= \frac{1}{K} \sum_{P \in \hat{\mathsf{P}}_n | \, \mathrm{wt}\, P = j} \sum_{a,b} \langle b^*|Y^{\otimes n} P|a\rangle \langle a|P^\dagger Y^{\otimes n}|b^*\rangle \tag{7.90}$$

$$\geq 0 \tag{7.91}$$

since $Y = Y^\dagger$.

b) The proof proceeds similarly to that for the quantum MacWilliams identity. We again write

$$\Pi = \sum_{Q \in \hat{\mathsf{P}}_n} c_Q Q, \tag{7.92}$$

and find

$$Sh_j = \frac{1}{K} \sum_{P \in \hat{\mathsf{P}}_n | \, \mathrm{wt}(P) = j} \sum_{Q, R \in \hat{\mathsf{P}}_n} c_Q c_R^* \, \mathrm{tr}(PQP^\dagger Y^{\otimes n} R^* Y^{\otimes n}) \tag{7.93}$$

$$= \frac{1}{K} \sum_{P \in \hat{\mathsf{P}}_n | \, \mathrm{wt}(P) = j} \sum_{Q, R \in \hat{\mathsf{P}}_n} c_Q c_R^* (-1)^{c(P,Q)} \, \mathrm{tr}(QY^{\otimes n} R^* Y^{\otimes n}). \tag{7.94}$$

Now, $X^* = X$ and $Z^* = Z$, but $Y^* = -Y$, so $R^* = \pm R$, with the sign determined by whether there are an even or an odd number of Ys in the tensor decomposition of R. Furthermore,

$$Y^{\otimes n} R^* Y^{\otimes n} = (-1)^{c(R, Y^{\otimes n})} R^*. \tag{7.95}$$

$c(R, Y^{\otimes n})$ is 1 if the number of Xs plus Zs in the tensor decomposition of R is odd, and 0 if it is even. Thus,

$$\mathrm{tr}(QY^{\otimes n} R^* Y^{\otimes n}) = (-1)^{\mathrm{wt}(R)} \delta_{Q,R} 2^n. \tag{7.96}$$

The sign follows because if the number of Ys and the number of Xs plus Zs in R are both even or both odd, we get an overall factor of $+1$, whereas if one of them is odd and one is even, we get a factor of -1.

We therefore have

$$Sh_j = \frac{1}{K} \sum_{P \in \hat{\mathsf{P}}_n | \, \mathrm{wt}(P) = j} \sum_{Q, R \in \hat{\mathsf{P}}_n} c_Q c_R^* (-1)^{c(P,Q) + \mathrm{wt}(R)} \delta_{Q,R} 2^n \tag{7.97}$$

$$= \frac{2^n}{K} \sum_{Q \in \hat{\mathsf{P}}_n} \left[\sum_{P \in \hat{\mathsf{P}}_n | \, \mathrm{wt}(P) = j} (-1)^{c(P,Q)} \right] (-1)^{\mathrm{wt}(Q)} |c_Q|^2. \tag{7.98}$$

The evaluation of the sum over P is just the same as before. We again get a Krawtchouk polynomial, to find

$$Sh(x) = \frac{K}{2^n} \sum_{j=0}^{n} \sum_{i=0}^{n} (-1)^i P_j(i; n) A_i x^j \tag{7.99}$$

$$= \frac{K}{2^n} \sum_{i=0}^{n} (1+3x)^{n-i} (1-x)^i (-1)^i A_i \tag{7.100}$$

$$= \frac{K}{2^n} (1+3x)^n \sum_{i=0}^{n} \left(\frac{x-1}{1+3x} \right)^i A_i \tag{7.101}$$

$$= \frac{K}{2^n} (1+3x)^n A \left(\frac{x-1}{1+3x} \right). \tag{7.102}$$

□

7.4.4 Example: There Is No $((3,2,2))$ Code

OK. We have these three weight enumerators, but what do we do with them? How can we put together the constraints we have to find out if certain parameters of codes are possible or not? One approach is to make approximations and use properties of the Krawtchouk polynomials to prove non-existence of certain solutions. This approach gives another method of proving the quantum Singleton bound, and can also give tighter bounds on the existence of QECCs.

Another approach is to apply the linear programming method. The procedure is to treat the parameters A_j, B_j, and Sh_j as unknown variables, and write down all the equations we have above:

$$A_0 = 1 \tag{7.103}$$
$$B_0 = 1 \tag{7.104}$$
$$B_j = A_j \text{ (for } j < d) \tag{7.105}$$
$$B_j \geq A_j \text{ (for } j \geq d) \tag{7.106}$$
$$A_j \geq 0 \tag{7.107}$$
$$Sh_j \geq 0 \tag{7.108}$$
$$B(x) = \frac{K}{2^n}(1+3x)^n A\left(\frac{1-x}{1+3x}\right) \tag{7.109}$$
$$Sh(x) = \frac{K}{2^n}(1+3x)^n A\left(\frac{x-1}{1+3x}\right) \tag{7.110}$$

Of course, many of the lines actually represent groups of equations, running over values of j. Notice that all the equations, even the last two groups, are linear in A_j, B_j, and Sh_j. Some are equalities and some are inequalities. The question of whether a solution exists or not is a linear programming problem, which is a common task. There are standard computer packages for solving linear programming problems, and so the usual method is to put the equations corresponding to the desired parameters $((n,K,d))$ of a code into such a package, and see whether it says a solution is possible. If not, we know no code can exist with those parameters. If so, we learn the solution(s) of the linear programming problem, which doesn't tell us whether a code exists or not, but does at least tell us possible values for the code's weight enumerator if it does exist, and therefore something about the structure of the code.

For large parameters, this is certainly best done by a computer, but to show you how the procedure works, I'll do a small example here explicitly, showing that there is no $((3,2,2))$ QECC. It is easy to show that there is no $[[3,1,2]]$ stabilizer code, but for more general codes, we need a more powerful method, and the linear programming bounds will suffice. The code is allowed by the quantum Singleton bound, and indeed, you'll see a $((3,3,2))_3$ code over qutrits in chapter 8.

Let us start by writing down the equations produced by the quantum MacWilliams identity:

$$B(x) = \frac{2}{2^3}(1+3x)^3 A\left(\frac{1-x}{1+3x}\right) \tag{7.111}$$
$$= \frac{1}{4}\left[(1+3x)^3 A_0 + (1+3x)^2(1-x)A_1 + (1+3x)(1-x)^2 A_2 + (1-x)^3 A_3\right] \tag{7.112}$$

Collecting the coefficients of x^j for $j = 0,\ldots,3$, we find

$$4B_0 = A_0 + A_1 + A_2 + A_3 \tag{7.113}$$
$$4B_1 = 9A_0 + 5A_1 + A_2 - 3A_3 \tag{7.114}$$
$$4B_2 = 27A_0 + 3A_1 - 5A_2 + 3A_3 \tag{7.115}$$
$$4B_3 = 27A_0 - 9A_1 + 3A_2 - A_3. \tag{7.116}$$

We also know that $A_0 = B_0 = 1$, $B_1 = A_1 \geq 0$, $B_2 \geq A_2 \geq 0$, and $B_3 \geq A_3 \geq 0$. Combining these equations, we find

$$A_1 + A_2 + A_3 = 3 \tag{7.117}$$
$$A_1 + A_2 - 3A_3 = -9 \tag{7.118}$$
$$3A_1 - 9A_2 + 3A_3 \geq -27 \tag{7.119}$$
$$-9A_1 + 3A_2 - 5A_3 \geq -27 \tag{7.120}$$

From equations (7.117) and (7.118), we find $A_3 = 3$, so $A_1 + A_2 = 0$. Since $A_1, A_2 \geq 0$, this means that $A_1 = A_2 = 0$. This solution also satisfies equations (7.119) and (7.120). Using only the quantum MacWilliams identity, we cannot rule out a $((3, 2, 2))$ code, but we know that if one exists, it must have weight enumerator $A(x) = 1 + 3x^3$ and dual weight enumerator $B(x) = 1 + 9x^2 + 6x^3$.

We now invoke the shadow enumerator. Let us write down the relation between $A(x)$ and $Sh(x)$, and plug in the above value for $A(x)$:

$$Sh(x) = \frac{1}{4}\left[(1+3x)^3 A_0 + (1+3x)^2(x-1)A_1 + (1+3x)(x-1)^2 A_2 + (x-1)^3 A_3\right] \tag{7.121}$$
$$= \frac{1}{4}\left[(1+3x)^3 + 3(x-1)^3\right] \tag{7.122}$$
$$= \frac{1}{4}\left(-2 + 18x + 18x^2 + 30x^3\right). \tag{7.123}$$

However, we see that $Sh_0 < 0$, which is not allowed. Thus, a $((3, 2, 2))$ code is not possible.

Chapter 8

Bigger Can Be Better: Qudit Codes

Computers seem to like base 2, even when they are quantum computers. Consequently, it may seem natural to stick to bits and qubits when dealing with error correcting codes, classical or quantum. Indeed, I've gone to a lot of effort in the previous chapters to build the mathematical structure of stabilizer codes and the Clifford group, all of which depends on the basic registers of our quantum computer being qubits. The problem is that there are lots of interesting codes that don't quite fit into this structure. Instead, they fit into similar structures associated to higher-dimensional registers — qudits.

The phenomenon also occurs in the theory of classical error correction, where it's helpful to work with linear codes over arbitrary finite fields rather than just binary linear codes. That's why I introduced non-binary codes in chapter 4. Now we'll see how to do the same for quantum codes. Quantum codes with bigger registers can generally correct more errors and send quantum data with a higher rate than qubit codes.

Based on the last sentence, this may appear a clear-cut case of bigger being better, but it's not quite that straightforward. You can't compare an error on a single qubit with an error on a 32-dimensional qudit on an even basis. I wouldn't say you are comparing apples to oranges; rather, you are comparing apples to boxes of apples. A 32-dimensional qudit could be written using 5 qubits, so a single error on a 32-dimensional error could be 5 single-qubit errors, and a single-qudit gate in 32 dimensions might need many one- and two-qubit gates to achieve the same transformation. Nevertheless, some qudit codes are sufficiently interesting, in terms of efficiency or other properties, to be worthwhile even once you take the size difference of the registers into account.

8.1 Qudit Pauli Group

A *qudit* is a generic term for a q-dimensional Hilbert space, considered as a fundamental unit of the overall Hilbert space of dimension q^n in much the same way that a qubit is a fundamental unit of a 2^n-dimensional Hilbert space. A 2^n-dimensional Hilbert space has many possible factorizations into two-dimensional tensor factors, but one factorization is considered physically favored, and that factorization gives us the physical qubits making up the full Hilbert space. (The *logical* qubits encoded in a quantum error-correcting code make up part of a different factorization.) Similarly, a q^n-dimensional Hilbert space is generally assumed to have some physically favored tensor product decomposition, producing the physical qudits comprising the code.

The word "qudit" for a q-dimensional Hilbert space seems to have mostly won out in the literature, but in some of the older literature you can find a variety of other terms, such as "qupit" (which usually assumes the dimension is a prime p). You can also find, in papers young and old, occasional terms referring to a qudit for a dimension of a specific size. "Qutrit" is the most common, for $D = 3$. Beyond that, you may have to delve into the word's Latin or Greek roots to figure out the dimension. For instance, a 4-dimensional qudit might be a "ququart", a 5-dimensional one might be a "ququint" or a "qupent" or some such, and for $D = 6$, you might even get lucky with a "qusext."

The first step in building quantum error-correcting codes for qudits, by whatever name, is to come up with the correct generalization of the Pauli group. As for qubits, the qudit Pauli group will play a role both in describing the types of errors we face and as a structural element for the qudit generalization of stabilizer codes. We're going to make heavy use of the machinery of finite fields in this chapter, so if you're not already familiar with it, you may want to go through appendix C first.

8.1.1 Qudit Pauli Group for Prime Dimension

The case where the qudit dimension p is prime is the simplest, so we'll start there.

Definition 8.1. The single-qudit *Pauli group* $\mathsf{P}_1(p)$ for prime $p > 2$ consists of elements $\{\omega^a X^b Z^c\}$, where

$$\omega = e^{2\pi i/p} \tag{8.1}$$

$$X|j\rangle = |(j+1) \bmod p\rangle \tag{8.2}$$

$$Z|j\rangle = \omega^j |j\rangle, \tag{8.3}$$

and a, b, c can be anywhere from 0 to $p-1$. The n-qudit *Pauli group* $\mathsf{P}_n(p) = \mathsf{P}_1(p)^{\otimes n}$; it consists of tensor products of n terms, each of the form $X^b Z^c$, with an overall phase factor of ω^a. $\hat{\mathsf{P}}_n(p) = \mathsf{P}_n(p)/\{\omega^a I\}$ is the qudit Pauli group without phases.

That is, ω is a pth root of unity, X is "add one mod p", and Z is a phase shift by a pth root of unity. We can write X and Z as matrices, of course:

$$X = \begin{pmatrix} 0 & 0 & \dots & 0 & 1 \\ 1 & 0 & \dots & 0 & 0 \\ 0 & 1 & \dots & 0 & 0 \\ \vdots & & \ddots & & \vdots \\ 0 & 0 & \dots & 1 & 0 \end{pmatrix} \qquad Z = \begin{pmatrix} 1 & 0 & \dots & 0 & 0 \\ 0 & \omega & \dots & 0 & 0 \\ \vdots & & \ddots & & \vdots \\ 0 & 0 & \dots & \omega^{p-2} & 0 \\ 0 & 0 & \dots & 0 & \omega^{p-1} \end{pmatrix} \tag{8.4}$$

You can see that X and Z are still unitary but are no longer Hermitian. I'd still like to talk about measuring X or Z; for any traditionalists reading this who prefer to measure only Hermitian operators, just imagine measuring a Hermitian operator that has the same eigenbasis as X or Z. For instance, $\sum_j j|j\rangle\langle j|$ works instead of Z, and outcome j corresponds to the ω^j eigenvalue of Z.

We can calculate the commutation relations between elements of the Pauli group. We find

$$ZX = \omega XZ. \tag{8.5}$$

It follows that

$$(X^a Z^b)(X^c Z^d) = \omega^{bc-ad}(X^c Z^d)(X^a Z^b). \tag{8.6}$$

Since ω is a pth root of unity, we might as well calculate $bc - ad$ using arithmetic modulo p. We can define a new function $c(P,Q) : \mathsf{P}_n(p) \times \mathsf{P}_n(p) \to \mathbb{Z}_p$ by

$$PQ = \omega^{c(P,Q)} QP. \tag{8.7}$$

We no longer are choosing between commuting and anti-commuting Paulis; now commutation is measured by an integer modulo p, which describes the phase factor that appears when we move P past Q as a power of ω.

A very important difference when p is an odd prime rather than 2 is that we only need the phases to be powers of ω; we don't get the annoying factor of i that shows up for qubits. This is because all elements of

$\mathsf{P}_n(p)$ have order p, regardless of overall phase:

$$(\omega^a X^b Z^c)^p = \omega^{ap}(X^b Z^c)(X^b Z^c)^{p-1} \tag{8.8}$$
$$= \omega^{bc} X^{2b} Z^{2c} (X^b Z^c)^{p-2} \tag{8.9}$$
$$= \omega^{bc+2bc} X^{3b} Z^{3c} (X^b Z^c)^{p-3} \tag{8.10}$$
$$\ldots = \omega^{bc+2bc+\cdots(p-1)bc} X^p Z^p \tag{8.11}$$
$$= \omega^{bcp(p-1)/2} \tag{8.12}$$
$$= 1, \tag{8.13}$$

since p is odd. This also means that the eigenvalues of all elements of the qudit Pauli group are of the form ω^j for integer j. While the qudit Pauli group is more complicated than the qubit Pauli group in a variety ways, in this one way, at least, it is simpler.

There are alternate representations of the qudit Pauli group, just as for the qubit Pauli group. For instance, we can define a $\mathbb{Z}_p$ symplectic representation of the qudit Pauli group by

$$P = \bigotimes_{j=1}^{n} X^{a_j} Z^{b_j} \mapsto v_P = (x_P | z_P), \tag{8.14}$$

with x_P and z_P being n-component vectors over $\mathbb{Z}_p$. x_P has entries a_j, and z_P has entries b_j. As with qubits, the overall phase of P is lost when moving to the symplectic representation.

Suppose we have v_P as defined in equation (8.14) and v_Q, with

$$Q = \bigotimes_{j=1}^{n} X^{c_j} Z^{d_j}. \tag{8.15}$$

We can define a symplectic inner product between v_P and v_Q as

$$v_P \odot v_Q = \sum_j (b_j c_j - a_j d_j), \tag{8.16}$$

with arithmetic taken mod p. With this definition, we have the following result:

Proposition 8.1. *Let $P, Q \in \mathsf{P}_n(p)$. Then $c(P,Q) = v_P \odot v_Q$.*

In other words, commutation in the qudit Pauli group corresponds to the symplectic inner product.

We can also map the qudit Pauli group to $\mathrm{GF}(p^2)$. However, the procedure is a bit more complicated than for qubits. We should think of $\mathrm{GF}(p^2)$ as a 2-dimensional vector space over $\mathrm{GF}(p)$ with basis $\{1, \alpha\}$. α can be any element of $\mathrm{GF}(p^2)$ that is not in the $\mathrm{GF}(p)$ subfield. We can write arbitrary $\beta \in \mathrm{GF}(p^2)$ as

$$\beta = a + b\alpha, \tag{8.17}$$

with $a, b \in \mathrm{GF}(p)$. We then map

$$X^a Z^b \mapsto a + b\alpha. \tag{8.18}$$

So far, so good. All is the same as for qubits. We lose the overall phase just as before. If we start with an element of $\hat{\mathsf{P}}_n(p)$, we end up with an n-component vector over $\mathrm{GF}(p^2)$ (with each element written as a 2-component vector over $\mathrm{GF}(p)$).

The complication comes in when we look at the generalization of the symplectic inner product. We wish to define it using multiplication within $\mathrm{GF}(p^2)$, and we want it to output an element of $\mathrm{GF}(p)$. The latter condition could be achieved by using the trace function (see appendix C for a discussion), but it turns out we don't want to do that in this case. For the former condition, the answer is not at all obvious, and historically took some time to find. It turns out that the inner product we want is given by the following definition:

Definition 8.2. Suppose a, b are n-dimensional vectors over $\mathrm{GF}(p^2)$. Let

$$a * b = \frac{a \cdot b^p - b \cdot a^p}{\alpha - \alpha^p}, \tag{8.19}$$

where a^p and b^p are the n-dimensional vectors whose entries are the pth power of the entries of a and b, and $\cdot$ represents the usual dot product between vectors.

Notice that the symplectic product we define (also called a *trace-alternating* inner product) depends explicitly on the specific element $\alpha \in \mathrm{GF}(p^2)$ that we used to give the mapping from $\hat{\mathsf{P}}_1(p)$ to $\mathrm{GF}(p^2)$. That wasn't the case for qubits because there were only two elements of GF(4) which are outside GF(2), namely ω and ω^2, but in $\mathrm{GF}(p^2)$ there are more choices for the pair (α, α^p).

I don't know of a better way to motivate this formula than by just calculating, but it turns out that it does work:

Theorem 8.2. *Suppose $P, Q \in \hat{\mathsf{P}}_n(p)$ correspond to vectors a, b over $\mathrm{GF}(p^2)$ according to equation (8.18). Then*

$$a * b = c(P, Q). \tag{8.20}$$

Proof. Let us calculate. We have

$$P \mapsto a = x + \alpha z \tag{8.21}$$
$$Q \mapsto b = x' + \alpha z'. \tag{8.22}$$

Now,

$$(x + \alpha z)^p = x^p + \alpha^p z^p = x + \alpha^p z, \tag{8.23}$$

since the field has characteristic p and x, z are vectors over $\mathrm{GF}(p)$. Then

$$a \cdot b^p = (x + \alpha z) \cdot (x' + \alpha z')^p \tag{8.24}$$
$$= x \cdot x' + \alpha z \cdot x' + \alpha^p x \cdot z' + \alpha^{p+1} z \cdot z' \tag{8.25}$$
$$b \cdot a^p = x \cdot x' + \alpha z' \cdot x + \alpha^p x' \cdot z + \alpha^{p+1} z \cdot z'. \tag{8.26}$$

Thus,

$$a \cdot b^p - b \cdot a^p = \alpha(z \cdot x' - x \cdot z') + \alpha^p(x \cdot z' - z \cdot x') \tag{8.27}$$
$$= (\alpha - \alpha^p)(x|z) \odot (x'|z') \tag{8.28}$$
$$= (\alpha - \alpha^p) c(P, Q). \tag{8.29}$$

□

8.1.2 Qudit Pauli Group for Prime Power Dimensions

The next most complicated case is when each qudit has dimension $q = p^m$, with p a prime. For these dimensions, the most straightforward thing to do is to let $\mathsf{P}_n(q) = \mathsf{P}_m(p)^{\otimes n}$. In other words, we consider each q-dimensional qudit as broken up into m p-dimensional qudits.

That's fine, as far as it goes, but we'd like to put more structure on the Hilbert space. In particular, we'd like to consider each q-dimensional qudit as an element of $\mathrm{GF}(q)$. Since Galois fields are involved, you can call these "Galois qudits." To fully take advantage of that structure, we'd like to also involve $\mathrm{GF}(q)$ in our understanding of $\mathsf{P}_n(q)$. We can do so as follows:

Definition 8.3. Suppose $\beta \in \mathrm{GF}(q)$. Let X^β and Z^β be defined as

$$X^\beta |\gamma\rangle = |\gamma + \beta\rangle \tag{8.30}$$
$$Z^\beta |\gamma\rangle = \omega^{\mathrm{tr}(\beta\gamma)} |\gamma\rangle, \tag{8.31}$$

where $\gamma \in \mathrm{GF}(q)$, $\omega = \exp(2\pi i/p)$ is a pth root of unity and tr is the $\mathrm{GF}(q)$ trace function which maps elements of $\mathrm{GF}(q)$ to elements of $\mathrm{GF}(p)$. Then $\mathsf{P}_n(q)$ consists of elements of the form

$$\eta\omega^a \bigotimes_{j=1}^{n} X^{\beta_j} Z^{\gamma_j}, \tag{8.32}$$

where $a \in \mathrm{GF}(p)$, $\beta_j, \gamma_j \in \mathrm{GF}(q)$. For odd q, η is always 1. For even q, η can be 1 or i. As usual, $\hat{\mathsf{P}}_n(q) = \mathsf{P}_n(q)/\{\omega^a I\}$ (for odd p) or $\hat{\mathsf{P}}_n(q) = \mathsf{P}_n(q)/\{i^a I\}$ (for $p = 2$).

Note that

$$Z^\gamma X^\beta = \omega^{\mathrm{tr}(\gamma\beta)} X^\beta Z^\gamma. \tag{8.33}$$

Now let us examine how this definition plays out given a particular way of breaking up each q-dimensional register into m p-dimensional ones. Suppose we consider $\mathrm{GF}(q)$ as an m-dimensional vector space over $\mathrm{GF}(p)$, so

$$\gamma = \sum_{i=0}^{m-1} a_i \alpha_i, \tag{8.34}$$

with $\gamma \in \mathrm{GF}(q)$, $a_i \in \mathrm{GF}(p)$, and the α_i's elements of $\mathrm{GF}(q)$ which are linearly independent vectors when considered over $\mathrm{GF}(p)$. It is most common to take $\alpha_i = \alpha^i$, with α some primitive element of $\mathrm{GF}(q)$. Note that with this choice, $\alpha_0 = 1$.

We can immediately see how equation (8.34) corresponds to breaking the qudit up into pieces: $|\gamma\rangle \leftrightarrow |a_0\rangle \otimes |a_1\rangle \otimes \cdots \otimes |a_{m-1}\rangle$. X^{α_i} then has a natural interpretation as the p-dimensional X applied to the ith tensor factor:

$$X^{\alpha_i}|\gamma\rangle = |\gamma + \alpha_i\rangle = |\sum_j (a_j + \delta_{ij})\alpha_i\rangle. \tag{8.35}$$

If we apply $X^{\sum b_i \alpha_i}$ instead, that corresponds to performing X^{b_i} in the ith tensor factor. That is, to understand the action of X^β, we expand β in the same basis used for the standard basis decomposition, and apply the appropriate power of X on each factor.

The interpretation of Z^β is a little trickier. It hinges on the notion of a *dual basis* (sometimes called a *complementary basis*): The set $\{\alpha_i\}$ forms a basis for $\mathrm{GF}(q)$ considered as an m-dimensional vector space over $\mathrm{GF}(p)$, and for any basis, there exists a dual basis $\{\beta_j\}$ with the property:

$$\mathrm{tr}(\alpha_i \beta_j) = \delta_{ij}. \tag{8.36}$$

Then

$$Z^{\beta_j}|\gamma\rangle = \omega^{\mathrm{tr}(\beta_j \sum_i a_i \alpha_i)} \bigotimes_{i=0}^{m-1} |a_i\rangle = \omega^{a_j} \bigotimes_{i=0}^{m-1} |a_i\rangle, \tag{8.37}$$

since trace is linear over $\mathrm{GF}(p)$. That is, Z^{β_j} corresponds to performing the p-dimensional Z on the jth tensor factor. To understand the action of Z^β in general, we simply then expand β in the dual basis to the one used for the standard basis. The choice of the dual bases $\{\alpha_i\}$ and $\{\beta_j\}$ thus specifies an isomorphism $\mathsf{P}_n(q) \cong \mathsf{P}_{mn}(p)$.

For some fields (and in particular for $q = 2^m$, which is the most interesting case), it is possible to simplify the decomposition by choosing the basis $\{\alpha_i\}$ to be *self-dual*, i.e., $\beta_i = \alpha_i$. In that case, X^{α_i} and Z^{α_i} simply represent the Pauli matrices acting on the ith tensor factor of the q-dimensional register. Not all finite fields have self-dual bases, unfortunately, so for some values of q, we have to pick different decompositions for the exponents of X and Z. Alternatively, we could abandon definition 8.3, but the advantages of that notation greatly outweigh the inconvenience of having a slightly more complicated decomposition into p-dimensional qudits.

For either odd or even characteristic, when we drop phases from the Pauli group, we get vectors on a symplectic space:

$$P = \bigotimes_{j=1}^{n} X^{\eta_j} Z^{\gamma_j} \mapsto v_P = (x_P|z_P), \tag{8.38}$$

with x_P an n-dimensional vector over GF(q) with entries η_j and z_P an n-dimensional vector with entries γ_j. The symplectic inner product between v_P and v_Q (with $Q = \bigotimes X^{\eta'_j} Z^{\gamma'_j}$) is

$$v_P \odot v_Q = \sum_j \mathrm{tr}(\gamma_j \eta'_j - \eta_j \gamma'_j). \tag{8.39}$$

Multiplication now is the GF(q) multiplication rule, and we take the trace to end up with an element of GF(p). Once more proposition 8.1 applies.

You probably can guess the next step: We wish to map the q-dimensional Pauli group into GF(q^2). The procedure is similar to that for GF(p); we pick an element $\alpha \in \mathrm{GF}(q^2) \setminus \mathrm{GF}(q)$, and map

$$(x|z) \mapsto x + \alpha z. \tag{8.40}$$

The correct symplectic inner product in this case is

$$a * b = \mathrm{tr}_{q/p}\left(\frac{a \cdot b^q - b \cdot a^q}{\alpha - \alpha^q}\right). \tag{8.41}$$

There are two differences from equation (8.19): We use the exponent q instead of p, and we use the trace function to give us an element of GF(p) for the answer. Note that we are using the trace of GF(q) over GF(p), *not* the trace of GF(q^2). This is because the term in parentheses already gives an element of GF(q).

Theorem 8.3. *Suppose $P, Q \in \hat{\mathsf{P}}_n(q)$ correspond to vectors a, b over* GF(q^2) *according to equation (8.40). Then*

$$a * b = c(P, Q). \tag{8.42}$$

The proof is essentially the same as theorem 8.2. We just need to add one final step where we take the trace to get the GF(q) symplectic product.

8.1.3 Qudit Pauli Group for Other Dimensions

If the dimension q of the register is not a prime power, there are two sensible ways to generalize the above approaches to define a Pauli group. One idea is to break q up into its prime factorization $q = \prod p_i^{m_i}$, and treat each prime power factor as a separate sub-register of size $p_i^{m_i}$ with its own Pauli group.

The second approach is to directly generalize the Pauli group used for prime dimensions, by letting

$$\omega = e^{2\pi i/q} \tag{8.43}$$

$$X|j\rangle = |(j+1) \bmod q\rangle \tag{8.44}$$

$$Z|j\rangle = \omega^j |j\rangle. \tag{8.45}$$

As usual, the n-qubit Pauli group consists of products of the form $\omega^a \bigotimes X^b Z^c$ for odd q. For even q, we must include a possible overall factor of i as well. This version of the Pauli group is also known as the *Heisenberg-Weyl group*.

It is also possible to use the Heisenberg-Weyl group in place of the usual Pauli group for prime power dimensions. These groups are different: For instance, in the $q = 9$ Heisenberg-Weyl group, X has order 9, whereas all elements of the usual $q = 9$ Pauli group have order 3. There are some applications where this is a sensible thing to do, but the cost of using the Heisenberg-Weyl group is that we lose the field structure we normally have in prime power dimensions. To distinguish the two choices of Pauli group, it is helpful to refer to qudits using the Heisenberg-Weyl group as "modular qudits," vs. the Galois qudits, which use GF(q).

Because the mathematical structure of the Heisenberg-Weyl group is more complicated than the Pauli groups for prime dimension or prime-power dimension, the standard techniques of coding theory don't work as well. The basic structure of a stabilizer code still exists, but codes based on the Heisbenberg-Weyl group lack some of the usual properties of stabilizer codes.

8.1.4 Nice Error Bases

Indeed, we can generalize even further and still have a stabilizer code structure. The most important features are that the elements of our generalized Pauli group form a group, are independent, and span the set of possible errors. This is codified by the definition of a nice error basis:

Definition 8.4. In a q-dimensional Hilbert space, let $\mathcal{E} = \{E_1, \ldots, E_{q^2}\}$ be a set of unitary operators satisfying $E_1 = I$ and $\operatorname{tr} E_i^\dagger E_j = q\delta_{ij}$. The set $\mathcal{E}$ is a *nice error basis* if $E_i E_j = \omega_{ij} E_{f(i,j)}$ for all i, j and some phases ω_{ij}.

For instance, for a single qubit, the usual Pauli operators $\{E_1 = I, E_2 = X, E_3 = Y, E_4 = Z\}$ form a nice error basis, with $\omega_{ij} \in \{\pm 1, \pm i\}$. To get a generalized Pauli group from a nice error basis, we take elements of the form ωE_i, ω is a product of ω_{ij}s.

Because there are exactly q^2 independent elements in a nice error basis, they form a basis for the space of $q \times q$ matrices. In this sense, they can act like the Pauli matrices — we can take any error on the q-dimensional register and expand it as a sum of elements from the nice error basis. It is thus sufficient for a QECC to correct all errors in a nice error basis to correct arbitrary errors on the register. This justifies the "error basis" part of the name.

Proposition 8.4. *The indices i of the errors in a nice error basis form a group under multiplication given by the binary operation $f(i, j)$.*

Proof. By the definition of a nice error basis, the set of indices is closed under the group operation. Associativity follows from the associativity of operator multiplication:

$$E_i E_j E_k = \omega_{ij} E_{f(i,j)} E_k = \omega_{ij} \omega_{f(i,j)k} E_{f(f(i,j),k)} \tag{8.46}$$

$$= \omega_{jk} E_i E_{f(j,k)} = \omega_{jk} \omega_{if(j,k)} E_{f(i,f(j,k))}. \tag{8.47}$$

Since the E_is are orthogonal, it follows that $f(f(i, j), k) = f(i, f(j, k))$, the statement of associativity.

The group identity is $i = 1$ since $E_1 = I$:

$$\omega_{1i} E_{f(1,i)} = I E_i = E_i. \tag{8.48}$$

To establish the existence of inverses, first note that if $f(i, j) = f(i, j')$, then

$$E_i E_{j'} = \omega_{ij'} \omega_{ij}^{-1} E_i E_j, \tag{8.49}$$

implying $E_{j'} = \omega E_j$ for some phase ω. Since the E_is are orthogonal, it follows that $j = j'$. Therefore, the function $j \mapsto f(i, j)$ is one-to-one, and since the domain and range both have size q^2, it must be onto as well. In particular, for all i, there must exist i^{-1} such that $f(i, i^{-1}) = 1$, and i^{-1} is the inverse of i. □

Definition 8.5. The group of indices $\{i\}$ under group operation $f(i, j)$ is called the *index group* of the nice error basis.

The index group can also be obtained by taking the Pauli group generated by the nice error group and modding out overall phase. For the usual qubit Pauli group, the index group is therefore isomorphic to $\mathbb{Z}_2 \times \mathbb{Z}_2$. For the Heisenberg-Weyl group in dimension q, the index group is $\mathbb{Z}_q \times \mathbb{Z}_q$, and for the prime power Pauli group, the index group is $\mathrm{GF}(q) \times \mathrm{GF}(q)$ under addition. All of these are fairly straightforward Abelian groups, but for large q, there exist error groups with more exotic index groups, including non-Abelian ones.

8.2 Qudit Stabilizer Codes

Now we are ready to talk about actual QECCs using qudits as registers. After going to all that effort to find qudit analogs of the Pauli group, you might guess that I'm now going to define a qudit analog of stabilizer codes. If you guessed that, you'd be correct.

8.2.1 Definition and Properties of Qudit Stabilizer Codes

The basic definition of a stabilizer and a stabilizer code is the same as for qubits. When q is a non-prime-power or when we are using a nice error group more exotic than the standard $\mathsf{P}_n(q)$, it is still possible to define a stabilizer code, but there are some complications to the theory. I'll just stick to the simpler cases.

The definition of a stabilizer is the same as for qubits:

Definition 8.6. Let $q = p^m$ be a prime power, $\mathsf{P} = \mathsf{P}_n(q)$, and let Q be a subspace of the Hilbert space $\mathcal{H}_q^{\otimes n}$ (i.e., consisting of n qudits). The GF(q) *stabilizer of* Q is the set

$$\mathsf{S}(Q) = \{M \in \mathsf{P} || \psi\rangle \text{ is an eigenvector of } M \text{ with eigenvalue } +1 \ \forall |\psi\rangle \in Q\}. \tag{8.50}$$

Let S be a subgroup of P. We say S is a GF(q) *stabilizer*, or just stabilizer when the GF(q) is clear from context, if it is Abelian and if $e^{i\phi} I \notin \mathsf{S}$ for any phase $\phi \neq 0$. The *code space* of a GF(q) stabilizer S is the subspace

$$\mathcal{T}(\mathsf{S}) = \{|\psi\rangle \text{ s.t. } M|\psi\rangle = |\psi\rangle \ \forall M \in \mathsf{S}\}. \tag{8.51}$$

The code Q is a GF(q) *stabilizer code* iff $Q = \mathcal{T}(\mathsf{S}(Q))$. The *normalizer* $\mathsf{N}(\mathsf{S})$ of the stabilizer S is

$$\mathsf{N}(\mathsf{S}) = \{N \in \mathsf{P} | NM = MN \ \forall M \in \mathsf{S}\}. \tag{8.52}$$

The only real differences from the qubit definition are the use of $\mathsf{P}_n(q)$ instead of P_n and forbidding $e^{i\phi}$ for all non-zero phases ϕ, which is needed because there are more phases in $\mathsf{P}_n(q)$ than just $\pm i, \pm 1$.

Note that a GF(q) stabilizer automatically gives a GF(p) stabilizer when $q = p^m$ when we reinterpret $\mathsf{P}_n(q)$ as $\mathsf{P}_{mn}(p)$ as discussed insection 8.1.2. Indeed, using the same isomorphism, we can interpret a GF(p) stabilizer on mn qudits as a GF(p^m) stabilizer on n qudits. The difference between them is the definition of weight (and thus distance of a code), which counts the number of non-trivial p-dimensional qudits in an operator for a GF(p) stabilizer but the number of non-trivial q-dimensional qudits for a GF(q) stabilizer. Thus, a Pauli which has weight t for GF(q) might have weight up to mt for GF(p), but there are also Paulis which have the same weight for GF(p) and GF(q).

Usually, although this is not required by definition 8.6, we deal with GF(q) stabilizer codes that have an additional property:

Definition 8.7. Let $P \in \mathsf{P}_n(q)$ have GF(q) symplectic representation $(x_P|z_P)$. Let S be a GF(q) stabilizer, with symplectic representation $\hat{\mathsf{S}}$. Then we say S is a *true* GF(q) *stabilizer* if $(x_P|z_P) \in \hat{\mathsf{S}}$ implies $(\gamma x_P|\gamma z_P) \in \hat{\mathsf{S}}$ as well for all $\gamma \in \mathrm{GF}(q)$.

That is, for a true GF(q) stabilizer code, the symplectic representation of the stabilizer is a GF(q)-linear space. Note that if q is prime, any GF(q) stabilizer code is a true GF(q) stabilizer code since $P \in \mathsf{S}$ implies $P^i \in \mathsf{S}$ as well, and

$$(x_{P^i}|z_{P^i}) = i(x_P|z_P). \tag{8.53}$$

However, when $q = p^m$ with $m > 1$, then there are some elements of GF(q) which are not numbers, so it is possible to have stabilizer codes which are not true GF(q) stabilizer codes.

GF(q) stabilizer codes have the same properties we are familiar with from qubit stabilizer codes.

Proposition 8.5. *If Q is a non-trivial subspace of the Hilbert space, then $\mathsf{S}(Q)$ is a* GF(q) *stabilizer (not necessarily a true* GF(q) *stabilizer). If S is a* GF(q) *stabilizer, then $\mathsf{S}(\mathcal{T}(\mathsf{S})) = \mathsf{S}$.*

The proof is almost identical to the qubit case. For prime qudit dimension p, we also get analogues of proposition 3.3 and theorem 3.4.

Theorem 8.6. *Let p be prime and let S be a* GF(p) *stabilizer for the code $\mathcal{T}(\mathsf{S})$, which has n physical qudits. If $|\mathsf{S}| = p^r$ (i.e., S has r generators), then $\dim \mathcal{T}(\mathsf{S}) = p^{n-r}$, so $\mathcal{T}(\mathsf{S})$ encodes $k = n - r$ physical qudits. The set of undetectable errors for S is $\hat{\mathsf{N}}(\mathsf{S}) \setminus \hat{\mathsf{S}}$. The distance of S is* $\min\{\mathrm{wt}\, E | E \in \hat{\mathsf{N}}(\mathsf{S}) \setminus \hat{\mathsf{S}}\}$.

The proofs are closely analogous to the qubit case, so I omit the details. The main notable difference is that $\frac{1}{2}(I+M)$ is *not* the projection operator on the $+1$ eigenspace of M. Instead, the projector on the $+1$ eigenspace of M is $\frac{1}{p}\sum_{j=0}^{p-1} M^j$. The projector on the codespace can be written as

$$\Pi_{\mathsf{S}} = \frac{1}{p^r} \sum_{M \in \mathsf{S}} M. \tag{8.54}$$

(Note that the normalization is p^{-r} instead of 2^{-r}.) The other difference is that in the case where the error $E \notin \mathsf{N}(\mathsf{S})$, there is a phase ω^a instead of -1, but that does not really alter the proof.

For prime power dimensions, there is a complication due to the fact that all Paulis have order p rather than q. It is most helpful to think of a GF(q) staibilizer of n qudits as a GF(p) stabilizer on mn qudits, in which case we can apply theorem 8.6. Considered as a GF(p) stabilizer, a stabilizer with r generators has p^r elements and encodes a p^{mn-r}-dimensional Hilbert space, the straightforward analog of the qubit result. If you insist on thinking of it as a GF(q) stabilizer, the same stabilizer still has r generators and p^r elements and encodes a Hilbert space of dimension $p^{mn-r} = q^{n-r/m}$ (it is, after all, the same code). In particular, a GF(q) stabilizer does not need to encode an integer number of q-dimensional qudits. However, a *true* GF(q) stabilizer code always has a number of generators which is a multiple of m, so does encode an integer number of q-dimensional qudits.

The other subtlety in prime power dimensions is the definition of distance, and indeed, this is the only property for which it really makes a difference whether we think of the code as a GF(p) code or a GF(q) code. It is still the case, of course, that the set of undetectable errors is $\hat{\mathsf{N}}(\mathsf{S}) \setminus \hat{\mathsf{S}}$. The distance is again the minimum weight of a Pauli in $\hat{\mathsf{N}}(\mathsf{S}) \setminus \hat{\mathsf{S}}$. However, when we think of it is a GF(q) code, we should use weight as defined by the decomposition into q-dimensional qudits (i.e., the number of q-dimensional registers with non-trivial Paulis). If we instead want to think of the code as a GF(p) code, the weight would be the number of non-trivial Paulis in the decomposition into p-dimensional qudits. The GF(p) weight of a Pauli could be equal to the GF(q) weight, but it could also be as high as m times the GF(q) weight. Also note that the lowest-weight operator in $\hat{\mathsf{N}}(\mathsf{S}) \setminus \hat{\mathsf{S}}$ using the GF(q) weight might even be a different operator than the lowest-weight operator using the GF(p) weight.

Notation 8.8. A stabilizer code with n physical qudits of dimension q, k logical qudits (also of dimension q), and distance d is denoted as an $[[n,k,d]]_q$ code.

Compare the notation $((n,K,d))_q$ for a qudit code that is not necessarily a stabilizer code and $[[n,k,d]]$ for a qubit stabilizer code. This way of listing the properties of a qudit stabilizer code is an obvious hybrid.

8.2.2 Examples: Distance 2 Code, 5-Qudit Code

Let us start to explore the world of qudit stabilizer codes by looking at qudit versions of some specific qubit codes. First, we can derive distance 2 codes. Again, we will choose one generator to detect Z errors on any qudit and one generator to detect X errors on any qudit. For prime qudit dimension p, this leads to a stabilizer of the form

$$M_1 = \bigotimes_{i=1}^{n} X^{a_i} \tag{8.55}$$

$$M_2 = \bigotimes_{i=1}^{n} Z^{b_i}. \tag{8.56}$$

We need the generators to commute, so we must pick the exponents so that $\sum a_i b_i = 0$ using GF(p) arithmetic. For instance, when n is even, it suffices if $a_i = 1$ (for all i) and $b_i = 1$ for half of the values of i and $b_i = -1$ for the other half. Note that it does *not* work to take all powers equal to 1 unless $n = 0 \bmod p$. It has distance 2 if all a_i and b_i are non-zero because

$$c(X_i^c Z_i^d, M_1) = d a_i \tag{8.57}$$

$$c(X_i^c Z_i^d, M_2) = -c b_i. \tag{8.58}$$

$M_1 =$	X	Z	Z^{-1}	X^{-1}	I
$M_2 =$	I	X	Z	Z^{-1}	X^{-1}
$M_3 =$	X^{-1}	I	X	Z	Z^{-1}
$M_4 =$	Z^{-1}	X^{-1}	I	X	Z

Table 8.1: The generators for the five-qudit code.

On the other hand, $X_1^{b_2} \otimes X_2^{-b_1}$ commutes with both generators, so we can see that the code is only distance 2. Notice also that, whereas for qubits, the smallest distance 2 code has 4 physical qubits, for larger qudits, it is possible to do it with just 3 qudits. For instance, for $p = 3$ (qutrits), there is the straightforward $[[3, 1, 2]]_3$ code with generators $X \otimes X \otimes X$ and $Z \otimes Z \otimes Z$.

For prime power qudits, the above construction does not give a distance 2 code. For instance,

$$c(Z_i^\delta, M_1) = \operatorname{tr} \delta a_i, \tag{8.59}$$

and for any a_i, there exists a γ for which $\operatorname{tr} \gamma a_i \neq 0$. The problem here is that X on a single dimension-q qudit does not detect Z^δ for all δ, basically because a single qudit is really m separate p-dimensional qudits. No matter what power X^α we choose, we will have the same problem, since there will be some decomposition (not necessarily the standard one) which will lead X^α to act only on a single p-dimensional tensor factor of the full q-dimensional qudit.

Luckily, we can easily fix this by making the minimal modification needed to get a true GF(q) stabilizer code, repeating the same operators on all the tensor factors of a qudit. Let S be the smallest stabilizer containing

$$M_1(\gamma) = \bigotimes_{i=1}^{n} X^{\gamma\alpha_i} \tag{8.60}$$

$$M_2(\gamma) = \bigotimes_{i=1}^{n} Z^{\gamma\beta_i}, \tag{8.61}$$

for all γ and any particular choice of (α_i, β_i) such that $\sum \alpha_i\beta_i = 0$ in GF(q). Note that $M_1(1)$ and $M_2(1)$ commute if $\sum \operatorname{tr}(\alpha_i\beta_i) = 0$, but that is not sufficient to make sure that all $M_1(\gamma)$ commute with all $M_2(\gamma)$. With these extra elements added to the stabilizer, the code is now distance 2. For instance, consider again the example Z_i^δ:

$$c(Z_i^\delta, M_1(\gamma)) = \operatorname{tr}(\delta\gamma\alpha_i). \tag{8.62}$$

While this will certainly be 0 for some specific γ, $\operatorname{tr}(\delta\gamma\alpha_i)$ can only be 0 for all γ if $\delta\alpha_i = 0$ in GF(q).

The operators $M_1(\gamma)$ are not independent for all γ. Since the number of generators for S is best determined by thinking of it as a GF(p) code, we should represent each γ as an m-dimensional vector over GF(p). (It is m-dimensional since $q = p^m$.) It's not hard to see that $M_1(\gamma)M_1(\eta) = M_1(\gamma+\eta)$ and $[M_1(\gamma)]^a = M_1(a\gamma)$ for $a \in$ GF(p). A set $\{M_1(\gamma)\}$ is thus independent for a subset of possible γ's if the corresponding GF(p) vectors are linearly independent, which means that S has a total of m generators of the form $M_1(\gamma)$. Similarly, it has m generators of the form $M_2(\gamma)$. When we go back to thinking of it as a GF(q) code, we get an $[[n, n-2, 2]]_q$ code. As a GF(p) code, this would be a $[[mn, m(n-2), 2]]_p$ code; this is a case where the distance is the same over GF(p) and GF(q).

For the next example, I will look at a 5-qudit code which is the qudit generalization of the 5-qubit code. Again beginning with prime dimension, consider the stabilizer given in table 8.1. You can check directly that it is Abelian. It is a bit harder (though still not that hard) to see that it has distance 3, but trust me, it does. Thus, this is a $[[5, 1, 3]]_p$ code. We could also have used the same stabilizer as for the qubit version of the code (table 3.2), but this version has the minor advantage that it is cyclic, just like the 5-qubit code, whereas table 3.2 would give us a non-cyclic $[[5, 1, 3]]_p$ code. While the 5-qubit code is unique up to a tensor product of single-qubit unitary rotations, there are multiple inequivalent 5-qudit codes for qudit dimension

$p \geq 3$. Another difference is that the 5-qubit code is perfect (number of errors equals number of syndromes), whereas the 5-qudit codes are not (more syndromes than single-qudit errors).

Moving to prime power qudits, this 5-qudit code has the same problem as the distance 2 codes — it does not detect or correct errors on the additional tensor factors of a qudit. We can solve it in the same way. Add to the stabilizer all operators of the form $M_i(\gamma)$, with each Pauli raised to the power $\pm\gamma$ instead of ± 1. For instance, $M_1(\gamma) = X^\gamma \otimes Z^\gamma \otimes Z^{-\gamma} \otimes X^{-\gamma} \otimes I$. The result is a true GF(q) stabilizer code with parameters $[[5, 1, 3]]_q$.

8.3 Qudit CSS Codes

We can use some of the same methods to make qudit codes that we used for qubit codes. As discussed in section 8.1, we can map the q-dimensional qudit Pauli group (for either prime or prime power dimension) to vectors over GF(q^2). This lets us interpret qudit stabilizer codes as GF(q^2) additive codes using the symplectic inner product (8.19) or (8.41) to determine commutation. Note that GF(q^2) linear codes which are weakly self-dual under the sympletic inner product are equivalent to true GF(q) stabilizer codes with an additional symmetry, just as linear GF(4) codes give qubit stabilizer codes with an extra symmetry (see exercise **??**).

Alternatively, by writing Paulis in the GF(q) symplectic form (an n-qudit Pauli written as a $2n$-component vector over GF(q)), we can use the CSS construction. You'll notice that the example distance 2 codes in the last section had some generators that were all Z's and some generators that were all X's, whereas the 5-qudit code had a mix of X and Z in each generator. This is because those distance 2 codes are qudit CSS codes, whereas the 5-qudit code is not.

8.3.1 The CSS Construction for Qudits

For prime dimension, the CSS construction is basically the same as for qubits. Generate a stabilizer code of the form

$$\left(\begin{array}{c|c} 0 & H_1 \\ H_2 & 0 \end{array}\right), \tag{8.63}$$

from the parity check matrices of two classical linear codes C_1 and C_2. In order to define a stabilizer code, the stabilizer must commute, so use the symplectic inner product (8.16) to test that. Again we find the condition that, if $x \in C_2^\perp$ and $z \in C_1^\perp$, $x \cdot z = 0$, so in order to get a valid stabilizer code, it must be the case that ${C_1}^\perp \subseteq C_2$. The distance and number of encoded qudits are given by the same formulas as for qubits. The only difference from the qubit case is that the arithmetic to determine commutation is mod p instead of mod 2.

For prime power qudits, we'd like to do the same construction, but we must be a bit more careful. Given two classical linear GF(q) codes C_1 and C_2, let's define the stabilizer S to be the smallest group containing all $\bigotimes_j Z^{\gamma_j}$ and $\bigotimes_j X^{\eta_j}$, where γ runs over elements of $C_1^\perp$ and η runs over elements of $C_2^\perp$. Note that it is *not* sufficient to look at the group generated in this way for basis vectors γ and η of $C_1^\perp$ and $C_2^\perp$. This is because if $\gamma \in C_1^\perp$, then GF(q) linearity implies that $\xi\gamma \in C_1^\perp$ as well for any $\xi \in$ GF(q), but $\bigotimes_j Z^{\gamma_j} \in \mathsf{S}$ is not sufficient to imply that $\bigotimes_j Z^{\xi\gamma_j} \in \mathsf{S}$. This contrasts with the GF(p) case, where

$$\bigotimes_j Z^{ab_j} = \Big(\bigotimes_j Z^{b_j}\Big)^a, \tag{8.64}$$

and since S must be closed under multiplication, it must also be closed under integer exponentiation. Exponentiation by $\xi \in$ GF(q) doesn't make any sense, and this is responsible for the difference between GF(p) and GF(q) stabilizer codes (including CSS codes).

Theorem 8.7. *Let C_1 and C_2 be two classical linear codes over* GF(q) *with parameters $[n, k_1, d_1]_q$ and $[n, k_2, d_2]_q$ and satisfying $C_1^\perp \subseteq C_2$. Then there exists a true* GF(q) *stabilizer code with stabilizer given as above with parameters $[[n, k_1 + k_2 - n, d]]_q$, $d \geq \min(d_1, d_2)$.*

Proof. The first consideration is whether the stabilizer given above is well-defined. We need to check that $M = \bigotimes_j Z^{\gamma_j}$ and $N = \bigotimes_j X^{\eta_j}$ commute when $\gamma \in C_1^\perp$ and $\eta \in C_2^\perp$. By equation (8.39),

$$c(M, N) = \sum_j \operatorname{tr} \gamma_j \eta_j = \operatorname{tr} \gamma \cdot \eta \tag{8.65}$$

(using the GF(q) dot product). Since $C_1^\perp \subseteq C_2$, $\gamma \in C_2$, so $\gamma \cdot \eta = 0$, and $c(M, N) = 0$ as desired.

Therefore, we have a well-defined GF(q) stabilizer code. The elements of the stabilizer have symplectic representations of the form $(\eta|\gamma)$ for $\eta \in C_2^\perp$ and $\gamma \in C_1^\perp$. Since C_1 and C_2 are GF(q) linear, so are $C_1^\perp$ and $C_2^\perp$. Thus, the code is a true GF(q) stabilizer code.

The next question is to determine how many logical qudits there are in this code. Each basis vector of $C_1^\perp$ or $C_2^\perp$ gives us m independent elements of S ($q = p^m$ as usual) for the reasons noted above (exponentiation by $\xi \in$ GF(q) does not make sense). Thus, there are $m(n - k_1)$ generators of S derived from C_1 and $m(n - k_2)$ generators derived from C_2. Thought of as a GF(p) code, the number of logical qudits is thus $mn - m(n - k_1) - m(n - k_2) = m(k_1 + k_2 - n)$. Thought of as a GF($q$) code again, we have $k_1 + k_2 - n$ logical qudits.

Finally, the distance can be determined just as for a usual binary CSS code. □

It might appear at first sight that it is possible to have GF(q) CSS codes that don't satisfy the condition $C_1^\perp \subseteq C_2$ since we actually only need $\operatorname{tr} \gamma \cdot \eta = 0$ for all γ and η. However, because C_1 and C_2 are *linear* GF(q) codes, $\operatorname{tr} \gamma \cdot \eta = 0$ for all γ and η iff $\gamma \cdot \eta = 0$ is.

As with binary CSS codes, the basis codewords have a straightforward form when written out in the standard basis:

$$|\gamma + {C_2}^\perp\rangle = \sum_{\eta \in {C_2}^\perp} |\gamma + \eta\rangle, \tag{8.66}$$

for $\gamma \in C_1$. This works for both prime dimension and prime power dimension. Indeed, we could just take it as the definition of a CSS code in any dimension.

8.3.2 Polynomial Codes

One particularly interesting family of qudit CSS codes is the family of *polynomial codes*, which are CSS codes derived from classical Reed-Solomon codes or their variants. Let us pick the code C_1 as a Reed-Solomon code by choosing n distinct points $(\alpha_1, \ldots, \alpha_n)$ from GF(q) $\setminus \{0\}$ ($n < q$) and a number $k_1 \leq n$. We'll use polynomials with degree up to $k_1 - 1$. We also pick a second number $0 \leq k_2 \leq k_1$ which will determine the size of C_2.

Definition 8.9. The basis codewords of the polynomial code over GF(q) with (n, k_1, k_2) are

$$|\overline{\beta_0, \ldots, \beta_{k_2-1}}\rangle = \sum_{(\beta_{k_2}, \ldots, \beta_{k_1-1}) \in \mathrm{GF}(q)} \bigotimes_{i=1}^{n} |\beta_0 + \beta_1 \alpha_i + \beta_2 \alpha_i^2 + \cdots + \beta_{k_1-1} \alpha_i^{k_1-1}\rangle. \tag{8.67}$$

The polynomial code is the span of these basis codewords.

That is, the basis codewords are indexed by k_2 values, the lowest-order coefficients of the polynomials being used. We then take the superposition over polynomials for all possible coefficients of x^{k_2} and higher, up to the maximum degree x^{k_1-1}. A particularly interesting special case is when $k_2 = 1$ so there is just one encoded qudit. Note that if $k_2 = 0$, the polynomial code can still be defined, but it is only a single state.

Clearly a polynomial code is a qudit CSS code, since the basis codewords have the correct form. However, instead of choosing both C_1 and C_2 to be Reed-Solomon codes (which wouldn't work, since they are not precisely dual to each other), we have chosen ${C_2}^\perp$ to be a modified Reed-Solomon code. In particular, ${C_2}^\perp$ is the code made up of vectors $(f(\alpha_1), \ldots, f(\alpha_n))$, where $f(x)$ runs over degree $k_1 - 1$ or lower polynomials for which the lowest nonzero term is the x^{k_2} power or higher. With this choice, it is manifestly true that ${C_2}^\perp \subseteq C_1$ and that the code encodes k_2 qudits. What is not clear is the distance of the resulting polynomial code.

Theorem 8.8. *The* GF(q) *polynomial code with parameters* (n, k_1, k_2) *is a non-degenerate true* $[[n, k_2, d]]_q$ *stabilizer code with* $d = \min(n - k_1 + 1, k_1 - k_2 + 1)$.

Proof. The code C_1 is used to correct bit flip errors. By theorem 4.15, the distance of C_1 is $n - k_1 + 1$. To prove the formula for distance, we thus need to show that C_2 has distance $k_1 - k_2 + 1$ and that the code is non-degenerate. The fact that it is a true GF(q) code follows from theorem 8.7.

The dual code ${C_2}^\perp$ has basis vectors $(\alpha_1^j, \ldots, \alpha_n^j)$ for $j = (k_2, \ldots, k_1 - 1)$. These form the rows of the parity check matrix H_2. A vector orthogonal to all rows of H_2 (i.e., a vector in C_2) corresponds to a linear dependence among the columns of H_2, so the distance of C_2 is the minimum number of columns of H_2 that are linearly dependent. There are $k_1 - k_2$ rows, so certainly no more than $k_1 - k_2$ columns can be linearly independent.

Let us look at the matrix formed by any set of $k = k_1 - k_2$ columns, say the first k. The matrix entries are $V_{ij} = \alpha_i^{k_2+j-1}$. This is not a Vandermonde matrix, but is clearly closely related. The columns of the matrix are linearly independent iff the rows are, and we can think of a linear combination of the rows as a polynomial with degree $k_1 - 1$ and all coefficients below degree k_2 being 0; that is, an element of ${C_2}^\perp$. The ith entry of the linear combination is the polynomial evaluated at α_i. A linear dependence of the rows is thus a polynomial that evaluates to 0 on all the points $\alpha_1, \ldots, \alpha_k$. Because the lowest degree term of the polynomial is x^{k_2}, the polynomial also has a 0 at $x = 0$ with multiplicity k_2. That gives a total of $k_2 + k = k_1$ zeros for the polynomial, which is too many for a degree $k_1 - 1$ polynomial; thus, for this to be true, the polynomial must be uniformly 0 everywhere (not just on $\alpha_1, \ldots, \alpha_k$). In other words, there is no linear dependence of the rows and the matrix V_{ij} is non-singular. Thus, any k columns are independent. Since any $k + 1$ columns are linearly dependent, the code C_2 has distance $k + 1$.

The only remaining thing to show is that the code is non-degenerate, from which it follows that it has distance exactly $\min(n - k_1 + 1, k_1 - k_2 + 1)$ and not a greater distance. We wish to show that there exists some non-trivial logical Pauli that has this weight. I will show that there is a logical $\overline{X}$ with weight exactly $n - k_1 + 1$ and a logical $\overline{Z}$ with weight exactly $k_1 - k_2 + 1$.

For a CSS code (over either qubits or qudits), the logical $\overline{X}$ operators can be taken to be products of physical Xs, $\overline{X} = \bigotimes X^{\eta_i}$. Moreover, the vectors (η_i) must be in C_1 to commute with the Z stabilizer generators. Since the distance of C_1 is exactly $n - k_1 + 1$, there is a vector of this weight. That is, there is a non-trivial polynomial f of degree $k_1 - 1$ or less such that $\eta_i = f(\alpha_i)$ is 0 for exactly $k_1 - 1$ values of α_i. Thus $\operatorname{wt} \overline{X} = n - k_1 + 1$. But since f has degree $k_1 - 1$, if it has more than $k_1 - 1$ zeros, then it will be uniformly zero. In particular, $f(0) \neq 0$. Now,

$$\overline{X}|\overline{0}\rangle = \sum_{g \in {C_2}^\perp} \bigotimes_{i=1}^{n} |(f + g)(\alpha_i)\rangle. \tag{8.68}$$

But the x^0 coefficient of g is 0 (since $g \in {C_2}^\perp$) and the x^0 coefficient of $f + g$ is *not* zero, so $\overline{X}|\overline{0}\rangle \neq |\overline{0}\rangle$ and $\overline{X} \notin \mathsf{S}$.

Similarly, the logical $\overline{Z}$ operators are products of physical Zs, $\overline{Z} = \bigotimes_i Z^{\gamma_i}$. The vectors (γ_i) must be in C_2, which means there is such a vector with weight exactly $k_1 - k_2 + 1$. This gives us $\overline{Z}$ with $\operatorname{wt} \overline{Z} = k_1 - k_2 + 1$. Now,

$$\overline{Z}|\overline{f}\rangle = \overline{Z} \sum_{g \in {C_2}^\perp} \bigotimes_{i=1}^{k+1} |(f + g)(\alpha_i)\rangle \tag{8.69}$$

$$= \sum_{g \in {C_2}^\perp} \omega^{\sum_i \operatorname{tr} \gamma_i (f+g)(\alpha_i)} \bigotimes_i |(f + g)(\alpha_i)\rangle \tag{8.70}$$

$$= \sum_{g \in {C_2}^\perp} \omega^{\operatorname{tr} \sum_i \gamma_i f(\alpha_i) + \operatorname{tr} \sum_i \gamma_i g(\alpha_i)} \bigotimes_i |(f + g)(\alpha_i)\rangle. \tag{8.71}$$

Since $(\gamma_i) \in C_2$ and $g \in {C_2}^\perp$, $\sum_i \gamma_i g(\alpha_i) = 0$.

But I claim there exists some $f \in C_1$ such that $\operatorname{tr} \sum_i \gamma_i f(\alpha_i) \neq 0$. We can assume without loss of generality that γ_i is non-zero only for $i = 1, \ldots, k_1 - k_2 + 1$. Consider polynomials $f_j(x) = x^j$ for $j = 0, \ldots, k_1 - k_2$. The matrix $V_{ij} = \alpha_i^j = g_j(\alpha_i)$ *is* a Vandermonde matrix, so the vectors $(f_j(\alpha_1), \ldots, f_j(\alpha_{k_1-k_2+1}))$ are linearly independent. They are vectors in a $(k_1 - k_2 + 1)$-dimensional vector space, so there is no non-zero vector that is orthogonal to all of them. In particular, the vector (γ_i) must have non-trivial overlap with at least one of the vectors $(f_j(\alpha_i))$: $\sum_i \gamma_i f_j(\alpha_i) = \xi \neq 0$. It is possible that $\operatorname{tr} \xi = 0$, but if we instead use the polynomial $f'(x) = \eta f_j(x)$, then $\sum_i \gamma_i f_j(\alpha_i) = \xi\eta$. η is arbitrary, so we just need to pick some η such that $\operatorname{tr}(\xi\eta) \neq 0$ to prove the claim.

Consequently, $\overline{Z}|\overline{0}\rangle = |\overline{0}\rangle$ but $\overline{Z}|\overline{f}'\rangle \neq |\overline{f}'\rangle$. Thus, $\overline{Z}$, which has weight $k_1 - k_2 + 1$, is a non-trivial logical operation. This proves the polynomial code is non-degenerate and thus the distance is exactly $\min(n - k_1 + 1, k_1 - k_2 + 1)$. □

If we choose the distances of the bit flip code and the phase code to be equal, then $n - k_1 = k_1 - k_2$, or $2k_1 = n - k_2$. In this case, $2d = n - k_1 + 1 + k_1 - k_2 + 1 = n - k_2 + 2$. Since k_2 is the number of encoded qudits, a polynomial code with these parameters saturates the quantum Singleton bound and is a quantum MDS code. For instance, we can have a $[[5, 1, 3]]_q$ polynomial code for $q > 5$. (There is also a variant with $q = 5$.) Note that this code is not equivalent to the $[[5, 1, 3]]_q$ stabilizer in table 8.1. This code is a CSS code, unlike the previous one, but it does not work for $q = 2$, 3, or 4, whereas the code of table 8.1 works for any prime or prime power dimension.

8.4 Qudit Clifford Group

Although I've spent a number of pages discussing qudit stabilizer codes, ultimately they are not that different than qubit stabilizer codes. They're not identical, to be sure, which is why I've gone through them in detail, but the differences are small. When we get to the qudit Clifford group, however, larger differences start to appear. The same general principles hold as for the qubit case, but there is a significant divergence at the level of details. I will focus on the case of prime dimension; for prime powers, simply consider the $q = p^m$-dimensional qudit as m p-dimensional qudits.

We start the same way as for qubits:

Definition 8.10. Let p be a prime. The *qudit Clifford group* is

$$\mathsf{C}_n(p) = \{U \in \mathsf{U}(p^n) | UPU^\dagger \in \mathsf{P}_n(p)\ \forall P \in \mathsf{P}_n(p)\}. \tag{8.72}$$

As with qubits, $\mathsf{P}_n(p)$ is a normal subgroup of $\mathsf{C}_n(p)$. We can also define

$$\hat{\mathsf{C}}_n(p) = \mathsf{C}_n(p)/\{e^{i\phi} I\} \tag{8.73}$$

$$\check{\mathsf{C}}_n(p) = \hat{\mathsf{C}}_n(p)/\hat{\mathsf{P}}_n(p). \tag{8.74}$$

It is still the case that $\check{\mathsf{C}}_n(p) \cong \mathsf{Sp}(2n, \mathbb{Z}_p)$ and that there exists a unitary in $\mathsf{C}_n(p)$ that performs any transformation of the Paulis that preserves commutation relations. It is also possible to efficiently simulate the behavior of the qudit Clifford group, including Pauli measurements, with a classical computer using essentially procedure 6.4. The main difference in the simulation is when measuring P_i with $P_i \notin \mathsf{N}(\mathsf{T})$. The measurement outcome is a uniform random value b from 0 to $p - 1$ rather than 0 or 1. We still find a generator M of the stabilizer to replace with $\omega^b P_i$, but we choose M that has a factor of ω when commuting past P_i rather than anticommuting with it. By taking the appropriate power r of M, we can ensure that NM^r commutes with P for stabilizer generators or logical operators N; we replace the original N with the appropriate NM^r.

The biggest difference with the qubit Pauli groups comes when comparing the actual elements of the Clifford group. Some of the elements are very closely analogous. For instance, the discrete Fourier transform over $\mathbb{Z}_p$ is the generalization of the Hadamard transform (which is the discrete Fourier transform over $\mathbb{Z}_2$):

$$\mathcal{F}|a\rangle = \frac{1}{\sqrt{p}} \sum_b \omega^{ab} |b\rangle. \tag{8.75}$$

Working out the conjugation action on the Paulis, we find that Fourier does not precisely swap X and Z, but does so adding an inverse:

$$X \mapsto Z \tag{8.76}$$
$$Z \mapsto X^{-1}. \tag{8.77}$$

There is also a two-qubit SUM gate which is the direct analogue of the qubit CNOT gate:

$$\text{SUM}|a\rangle|b\rangle = |a\rangle|a + b \bmod p\rangle \tag{8.78}$$
$$X \otimes I \mapsto X \otimes X \tag{8.79}$$
$$Z \otimes I \mapsto Z \otimes I \tag{8.80}$$
$$I \otimes X \mapsto I \otimes X \tag{8.81}$$
$$I \otimes Z \mapsto Z^{-1} \otimes Z. \tag{8.82}$$

Again there is an extra inverse in one of the images in the conjugation action. The inverse powers are needed to ensure that the Clifford group gate preserves commutation relations among the Paulis. For instance, $Z \otimes Z$ does not commute with $X \otimes X$, but $Z^{-1} \otimes Z$ does.

From here, though, we start to see a bigger divergence. There are operators in $\mathsf{C}_n(p)$ which don't have any qubit analog, such as scalar multiplication by $c \in \mathbb{Z}_p \setminus \{0\}$:

$$S_c|a\rangle = |ca\rangle \tag{8.83}$$
$$X \mapsto X^c \tag{8.84}$$
$$Z \mapsto Z^{c^{-1}}. \tag{8.85}$$

The power of Z is c^{-1}, the multiplicative inverse of c in $\mathbb{Z}_p$. For instance, for $p = 7$, $2^{-1} = 4$ since $2 \cdot 4 = 8 \equiv 1 \bmod 7$. There is also no precise qudit analog of $R_{\pi/4}$. The closest is a quadratic phase gate which has a similar action on Paulis:

$$B|a\rangle = \omega^{a(a-1)/2}|a\rangle \tag{8.86}$$
$$X \mapsto XZ \tag{8.87}$$
$$Z \mapsto Z. \tag{8.88}$$

Theorem 8.9. *The gates $\mathcal{F}$, B, and* SUM *along with global phase $e^{i\theta}I$ generate $\mathsf{C}_n(p)$.*

Proof. First, we can show that $\mathcal{F}$, B, SUM, S_c (for all $c \neq 0$), $\mathsf{P}_n(p)$ and $e^{i\theta}I$ generate $\mathsf{C}_n(p)$ using essentially procedure 6.5. In the algorithm, we can replace H with $\mathcal{F}$, CNOT with SUM, and $R_{\pi/4}$ with B. SWAP can be realized as

$$\text{SWAP}_{i,j} = S_{-1\,i}\text{SUM}_{i,j}\text{SUM}^{-1}{}_{j,i}\text{SUM}_{i,j}. \tag{8.89}$$

The analog of C − Z is $(I \otimes \mathcal{F})\text{SUM}(I \otimes \mathcal{F}^{-1})$. The symplectic matrices of these gates are quite similar to the qubit versions, but there are some additional minus signs that appear (when the power is an inverse). In the procedure, we will have to use some of them multiple times in order to cancel out terms. For instance, in step 2, we wish to eliminate entries in the first column of A. To do so, use left multiplication by SUM $p - a_{1j}$ to eliminate entry a_{1j}. We also add in S_c, which has the effect of multiplying rows or columns by c or c^{-1}. This is useful in step 1: we can use SWAP to move a non-zero entry into the upper left corner, but we then need S_c to make that entry 1.

The next step is to show that we don't need S_c. I claim that gates of this form can be generated using only $\mathcal{F}$, B, and $\mathsf{P}_1(p)$. Let $Q = \mathcal{F}B\mathcal{F}^{-1}$. Then

$$Q : X \mapsto X \tag{8.90}$$
$$Z \mapsto ZX^{-1}. \tag{8.91}$$

The action of $B^r Q^s B^m Q^n$ is then

$$X \mapsto \omega^a X^{1-ms} Z^{m+r-rms} \tag{8.92}$$

$$Z \mapsto \omega^b X^{-n-s+mns} Z^{1-(m+r)n+(mn-1)rs} \tag{8.93}$$

The powers a and b don't matter because we can get rid of the powers of ω using an appropriate element of $\mathsf{P}_1(p)$. Let $r = -c^{-1}$, $s = 1 - c$, $m = 1$, and $n = 1 - c^{-1}$, so $rs = rms = n = m + r$. Then

$$X \mapsto X^c \tag{8.94}$$

$$Z \mapsto Z^{c^{-1}}. \tag{8.95}$$

We also don't need the Paulis. $\mathcal{F}^2 = S_{-1}$, i.e. $\mathcal{F}^2|a\rangle = |-a\rangle$. Then

$$\mathcal{F}^2 B \mathcal{F}^2 B^{-1}|a\rangle = \mathcal{F}^2 B \omega^{-a(a-1)/2}|-a\rangle = \omega^{-a(-a-1)/2-a(a-1)/2}|a\rangle = \omega^a|a\rangle. \tag{8.96}$$

Thus, $Z = \mathcal{F}^2 B \mathcal{F}^2 B^{-1}$, and $X = \mathcal{F}^{-1} Z \mathcal{F}$, which then can be used to generate the full Pauli group. □

Chapter 9

Now, What Did I Leave Out?: Other Things You Should Know About Quantum Error Correction

By now, you know (or should, if you've been paying attention) quite a lot about quantum error-correcting codes. However, there's still a lot more to learn. Some topics, such as topological codes or channel capacity, deserve a chapter or more of their own, and those will be covered in part III. However, there are plenty of other things about QECCs which I don't want to get into at length, but are still interesting or important to know. Since many of them don't fit well into the structure of the previous chapters, I've put them here. Consequently, this chapter is a grab-bag of stuff about QECCs left out of the first 8 chapters. These topics are not really dependent on each other, and only a few of them are essential to later parts of the book. Concatenated codes (section 9.1) will play an important role in the discussion of fault tolerance in part II, and the coherent information (section 9.3) will be need in chapter 19. The rest of this chapter is optional, consisting of various stand-alone topics.

9.1 Concatenated Codes

9.1.1 Basic Properties

If one quantum error-correcting code is good, two codes must be better. That's the philosophy behind a concatenated code. To make a concatenated code, take your quantum data and encode using one code Q, then take each of the physical registers of Q and encode it again using R, as depicted in figure 9.1. The resulting concatenated code generally has a greater distance than either Q or R, albeit at the cost of more physical qudits for the same number of logical qudits. If concatenating once is not enough, you can add a third layer of concatenation, or a fourth, or however many it takes to satisfy your hunger for error correction.

More precisely, a concatenated code can be defined as follows:

Definition 9.1. Let Q be an $((n_1, K, d_1))_{q_1}$ code with encoder $\mathcal{E}_1$ and R be a $((n_2, q_1, d_2))_{q_2}$ code with encoder $\mathcal{E}_2$. The *concatenated code* formed from Q and R is an $((n_1 n_2, K))_{q_2}$ code with encoder $\mathcal{E}_2^{\otimes n_1} \circ \mathcal{E}_1$. Q is known as the *inner code* and R is the *outer code*.

Notice that a concatenated code gets the size of its logical Hilbert space from Q and the size of the physical registers from R, whereas the number of registers n is the product of n_1 and n_2. The register size from Q must match the logical Hilbert space size for R so that $\mathcal{E}_2$ can be applied to each register of Q.

It is easy to compute a bound on the distance of a concatenated code:

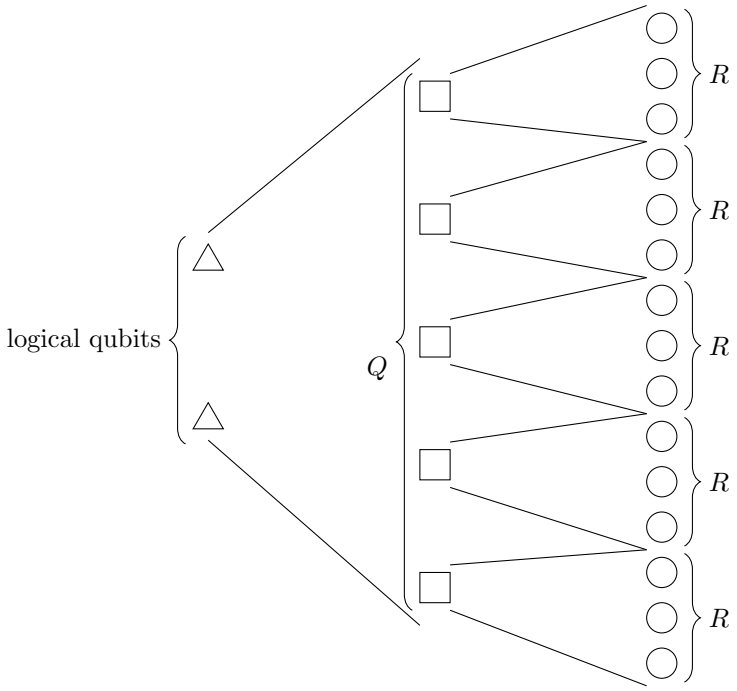

Figure 9.1: In a concatenated code, two codes are combined to produce a larger code. k_1 logical qubits (triangles) are encoded in the n_1 physical qubits of the inner code (squares), which are in turn individually encoded into the outer code, each using n_2 physical qubits (circles).

Proposition 9.1. *The concatenated code formed from a distance d_1 inner code and a distance d_2 outer code has distance $d \geq d_1 d_2$.*

Proof. Consider detecting errors with the code. If there are fewer than d_2 errors on any block of R involved in the concatenated code, we will detect the error using that that code alone. With at least d_2 errors on a single block, however, it may be possible to have an error that is undetectable by R alone. Formally, if $\operatorname{wt} E < d_2$, then $\Pi_R E|\psi\rangle = c(E)|\psi\rangle$ for all codewords $|\psi\rangle$, where Π_R is the projector on R. On the other hand, there must exist some E with $\operatorname{wt} E = d_2$ and some codeword $|\psi\rangle$, such that $\Pi_R E|\psi\rangle \neq c(E)|\psi\rangle$.

But that process only changes a single register of Q, which by itself would be detected using the properties of Q (provided $d_1 > 1$). In particular, let $F = \mathcal{D}_2 \Pi_R E$ be an error acting on a register of Q, where $\mathcal{D}_2$ is the decoder for R. From above, if $\operatorname{wt} E < d_2$, then $F \propto I$, whereas if $\operatorname{wt} E \geq d_2$, it is possible that $F \not\propto I$.

Suppose now that we have some error of weight w acting on the concatenated code as a whole. Break it up into a tensor product of errors, with E_i acting on the ith block of R. (We may assume the overall error is a tensor product or even a Pauli, by corollary 2.5.) Let $F_i = \mathcal{D}_2 \Pi_R E_i$. No matter how we divide the errors between blocks of R, there can be at most $\lfloor w/d_2 \rfloor$ blocks with d_2 or more errors per block, so at most $\lfloor w/d_2 \rfloor$ of the F_i are not proportional to the identity. That is, the error $F = \bigotimes_{i=1}^{n_1} F_i$ has weight at most $\lfloor w/d_2 \rfloor$

F is an error acting on Q when it is considered without concatenation. If $\operatorname{wt} F < d_1$, then Q by itself can detect F. In order to fool Q, therefore, we need an error acting on the concatenated code with $w/d_2 \geq d_1$. Therefore, the concatenated code can detect any error of weight $d_1 d_2 - 1$ or less, so by theorem 2.9, the distance of the concatenated code is at least $d_1 d_2$. □

Note that it is possible for the concatenated code to have distance greater than one would expect from proposition 9.1. For instance, the 9-qubit code can be thought of as the concatenation of an inner 3-qubit code correcting phase errors with an outer 3-qubit code correcting bit flip errors. Each of the 3-qubit codes by itself has distance 1 since it can only detect or correct one kind of error, but together they form a 9-qubit code with distance 3.

A common situation is when the inner code and the outer code are the same, which requires that the register size equal the encoded Hilbert space size. Therefore, we can concatenate a $((n, q, d))_q$ code with itself to get a $((n^2, q, d^2))_q$ code. We can repeat this process to get bigger and bigger codes.

Definition 9.2. Let $Q_1 = Q$ be a $((n, q, d))_q$ code, and let Q_k be the $((n^k, q, d^k))_q$ code obtained by concatenating Q_{k-1} as the inner code with Q as the outer code. We say that Q_k is a code involving k *levels* of concatenation. The physical qudits form *level* 0 qudits, the outer code for Q_k is *level* 1 of concatenation, and its logical qudits are *level* 1 qudits. The logical qudits for the outer code of the Q_ℓ that appears in the recursive definition of Q_k are *level* $k - \ell + 1$ qudits and the logical qudits for the overall code are *level* k qudits.

9.1.2 Concatenated Stabilizer Codes

If we concatenate two qubit stabilizer codes, the resulting code is a stabilizer code as well, with the stabilizer constructed in a particular way.

Procedure 9.1. Let the inner code be an $[[n_1, 1, d_1]]$ code with stabilizer S_1, and let the outer code be an $[[n_2, k, d_2]]$ code with stabilizer S_2 and logical Paulis $\overline{P}$. Then the stabilizer S of the concatenated code formed from these two codes is given as follows:

1. For each generator $M \in \mathsf{S}_2$, include in S the Pauli M_i consisting of M acting on the ith block of n_2 qubits in the code tensored with the identity on all other blocks.

2. For each generator $M \in \mathsf{S}_1$, replace each single-qubit Pauli P_i in its tensor product decomposition (i.e., acting on the ith physical qubit) with $\overline{P}_i$, the corresponding logical Pauli from the *outer* code acting on the ith block of n_2 qubits in the concatenated code. Take the tensor product of all the $\overline{P}_i$ operators for a single $M \in \mathsf{S}_1$ and include that in S.

	X	Z	Z	X	I	I	I	I	I	I	I	I	I	I	I	I	I	I	I	I	I	I	I
	I	X	Z	Z	X	I	I	I	I	I	I	I	I	I	I	I	I	I	I	I	I	I	I	I
	X	I	X	Z	Z	I	I	I	I	I	I	I	I	I	I	I	I	I	I	I	I	I	I	I
	Z	X	I	X	Z	I	I	I	I	I	I	I	I	I	I	I	I	I	I	I	I	I	I	I
	I	I	I	I	I	X	Z	Z	X	I	I	I	I	I	I	I	I	I	I	I	I	I	I	I
	I	I	I	I	I	I	X	Z	Z	X	I	I	I	I	I	I	I	I	I	I	I	I	I	I
	I	I	I	I	I	X	I	X	Z	Z	I	I	I	I	I	I	I	I	I	I	I	I	I	I
	I	I	I	I	I	Z	X	I	X	Z	I	I	I	I	I	I	I	I	I	I	I	I	I	I
	I	I	I	I	I	I	I	I	I	I	X	Z	Z	X	I	I	I	I	I	I	I	I	I	I
	I	I	I	I	I	I	I	I	I	I	I	X	Z	Z	X	I	I	I	I	I	I	I	I	I
	I	I	I	I	I	I	I	I	I	I	X	I	X	Z	Z	I	I	I	I	I	I	I	I	I
	I	I	I	I	I	I	I	I	I	I	Z	X	I	X	Z	I	I	I	I	I	I	I	I	I
	I	I	I	I	I	I	I	I	I	I	I	I	I	I	I	X	Z	Z	X	I	I	I	I	I
	I	I	I	I	I	I	I	I	I	I	I	I	I	I	I	X	Z	Z	X	I	I	I	I	I
	I	I	I	I	I	I	I	I	I	I	I	I	I	I	X	I	X	Z	Z	I	I	I	I	I
	I	I	I	I	I	I	I	I	I	I	I	I	I	I	Z	X	I	X	Z	I	I	I	I	I
	I	I	I	I	I	I	I	I	I	I	I	I	I	I	I	I	I	I	I	X	Z	Z	X	I
	I	I	I	I	I	I	I	I	I	I	I	I	I	I	I	I	I	I	I	I	X	Z	Z	X
	I	I	I	I	I	I	I	I	I	I	I	I	I	I	I	I	I	I	I	X	I	X	Z	Z
	I	I	I	I	I	I	I	I	I	I	I	I	I	I	I	I	I	I	I	Z	X	I	X	Z
	X	X	X	X	X	Z	Z	Z	Z	Z	Z	Z	Z	Z	X	X	X	X	X	I	I	I	I	I
	I	I	I	I	I	X	X	X	X	X	Z	Z	Z	Z	Z	Z	Z	Z	Z	Z	X	X	X	X	X
	X	X	X	X	X	I	I	I	I	I	X	X	X	X	X	Z	Z	Z	Z	Z	Z	Z	Z	Z	Z
	Z	Z	Z	Z	Z	X	X	X	X	X	I	I	I	I	I	X	X	X	X	X	Z	Z	Z	Z	Z
$\overline{X}$	X	X	X	X	X	X	X	X	X	X	X	X	X	X	X	X	X	X	X	X	X	X	X	X	X
$\overline{Z}$	Z	Z	Z	Z	Z	Z	Z	Z	Z	Z	Z	Z	Z	Z	Z	Z	Z	Z	Z	Z	Z	Z	Z	Z	Z

Table 9.1: The stabilizer for the $[[25, 1, 9]]$ code formed by concatenating the 5-qubit code with itself.

3. Form the group generated by the elements described in the previous steps.

One can also determine the logical Paulis for the concatenated code by the same process as in step 2: take a logical Pauli for S_1 and replace each Pauli in its tensor product decomposition with the corresponding logical Pauli for S_2.

An example of a concatenated stabilizer code is the $[[25, 1, 9]]$ code formed by concatenating the 5-qubit code with itself. The resulting stabilizer is given in table 9.1. Note that the 25-qubit code is degenerate. Indeed, a quick consideration of procedure 9.1 should convince you that concatenated stabilizer codes will frequently be degenerate: The stabilizer of a concatenated code contains many elements that are drawn from a single copy of the stabilizer of the outer code. These elements of S have weight bounded by n_2, which can easily be lower than the distance $d_1 d_2$ of the concatenated code.

Another interesting case is when the outer code is a qubit code, because then the resulting concatenated code is a qubit code as well. For instance, suppose the outer code is an $[[n_2, k_2, d_2]]_2$ code. Then the inner code should work with registers of size $q_1 = 2^{k_2}$. This is a prime power, so we are dealing with a code over $\mathrm{GF}(2^{k_2})$. For instance, we can use an $[[n_1, k_1, d_1]]_{2^{k_2}}$ code to get a $[[n_1 n_2, k_1 k_2, d_1 d_2]]_2$ code. (It has k_1 logical qudits of size 2^{k_2}, which corresponds to $k_1 k_2$ logical qubits.) This can be a useful way to find large qubit stabilizer codes with reasonable parameters.

9.1.3 Decoding Concatenated Codes

Given the structure of a concatenated code, one natural approach to decoding is to treat the inner code and the outer code separately. For each block of the outer code R, perform error correction via whichever

algorithm is appropriate to that code. Now each block of n_2 qudits is a valid codeword for R, but the logical state of each block may have been changed by the errors. If we decode each block, we are left with Q with some errors on it, and can perform the usual decoding procedure for it.

The advantage of this procedure is that it is efficient if the decoding algorithms used for Q and R are. It's also quite straightforward. The disadvantage is that it doesn't take advantage of the full error correction capability of the concatenated code. For instance, consider the 125-qubit code formed by concatenating the 25-qubit code of table 9.1 with the 5-qubit code. If a block of the outer 5-qubit code has 2 errors on it, the correction procedure on that block will fail, leaving an error on the logical qubit. However, the inner code can only correct four errors, so if five blocks of the outer code are wrong, which can happen with 10 errors in total, than this decoding procedure will make a mistake. The 125-qubit code has distance 27, so it should be able to correct 13 errors. The difference arises because when we correct the inner code and outer codes separately, we throw away some information that would be useful. For instance, if a single block of the five-qubit outer code has non-trivial syndrome, it is more likely the corresponding qubit of the inner code has an error on it. This means that if there are only two errors in any given 5-qubit block, the errors on the inner code act like *erasure* errors, allowing us to correct more of them. Of course, it's also possible that there are 3 errors on a 5-qubit code block, which could produce a logical error with no error syndrome advertising it, so the decoding process is not necessarily straightforward.

Notice that as we concatenate the same code many times, the fractional distance d/n decreases — with k levels of concatenation of an $[[n_0, 1, d_0]]$ code, $n = n_0^k$ and $d = d_0^k$. Thus, in a very meaningful sense, the code gets worse at correcting errors as we concatenate many times. However, this is only true if we insist on correcting the *worst case* error. For typical errors, the concatenated code does well. For instance, suppose we consider a depolarizing channel with total error probability p for each qubit (i.e., $p/3$ chance of each of X, Y, and Z errors). The probability that a single block of the $[[n_0, 1, d_0]]$ code fails and has a logical error is roughly

$$p_1 \approx \binom{n_0}{t+1} p^{t+1} = p_T (p/p_T)^{t+1}, \tag{9.1}$$

where $t = \lfloor (d-1)/2 \rfloor$, $p_T = \binom{n_0}{t+1}^{-1/t}$, and I have assumed that p is small, so that we can neglect terms of order p^{t+2} and higher, and that the code always fails when there are $t+1$ errors. If the code can correct some weight $t+1$ errors, the logical error rate will be lower.

Now, if we concatenate the $[[n_0, 1, d_0]]$ code with itself, and decode using the simple level-by-level scheme (which, as noted above, is sub-optimal), the probability of the concatenated code having a logical error is

$$p_2 \approx p_T (p/p_T)^{(t+1)^2}, \tag{9.2}$$

and we can show by induction that with k levels of concatenation, the probability of having a logical error is

$$p_k \approx p_T (p/p_T)^{(t+1)^k}. \tag{9.3}$$

When $p < p_T$, the logical error rate rapidly converges to 0 with k. Note that the typical case now has $pn_0^k \gg t^k$ errors occurring in the code. There will be cases where a small number of errors can cause the code to fail, but those are very rare.

9.2 Convolutional Codes

A *convolutional code*, as opposed to a *block code*, does not involve a fixed number of physical qubits. Instead, it is a family of arbitrarily large codes with the property that new logical qubits can be added on to the end. Convolutional codes frequently have a periodic structure, with the same stabilizer generators repeated shifted by a few qubits, although this is not required.

The main motivation for a classical convolutional code is to handle data provided in a streaming fashion — that is, logical bits appear one at a time and should be encoded promptly, without too much delay, and then the corresponding physical bits can be sent on their way. However, convolutional codes often have

other substantial advantages. In particular, the size of the encoding circuit for a convolutional code is usually linear in the number of logical bits, and there is a natural linear-time decoding algorithm as well for many convolutional codes.

In return, convolutional codes generally give up a bit of error protection, as logical bits are effectively localized, meaning an error affecting a small number of bits can change a logical bit. However, a well-designed convolutional code should also have the property that a local error only changes a few logical bits. This is in contrast to block codes, where all the logical bits are typically spread out over all the physical bits. This means a large physical error is necessary to cause a logical error, but when a logical error does occur, there is no protection against the error changing all of the logical bits.

The situation for quantum convolutional codes is more complicated. Unfortunately, it turns out not to be possible to make quantum convolutional codes with all the desireable properties of classical convolutional codes. Nevertheless, we can achieve some of the nice properties described above.

9.2.1 Basics of Quantum Convolutional Codes

A classical convolutional code is simply one in which the encoding of each logical bit depends only on itself and the previous bits. In particular, it does not depend on the subsequent bits. However, a quick consideration reveals that this definition does not make sense for quantum codes: Any non-trivial two-qubit gate alters *both* of the qubits, whereas a gate between bits can alter one bit conditionally while leaving the other unchanged.

However, most often, classical convolutional codes have an additional constraint — namely, a finite memory. Thus, each physical bit depends on only t bits of information about the previous logical bits, no matter how many bits have been encoded. This is a property that carries over sensibly to the quantum regime. We can thus define a quantum convolutional code as follows:

Definition 9.3. A qubit *quantum convolutional code* is a family of $((n_i, 2^{k_i}))$ quantum error-correcting codes Q_i ($i \in \mathbb{Z}^+$) with the properties

1. r, s, t are positive integers with $s \leq r \leq t$,
2. $n_i = n_{i-1} + r$, $k_i = k_{i-1} + s$ for $i > 1$,
3. There exist t-qubit unitaries U_i and V_i ($i \geq 2$) and n_1-qubit unitary W such that the encoding circuit for Q_i is $V_i(\prod_{j=i}^{2} U_j)W$. Here, U_i acts on qubits $n_i - t + 1$ to n_i and takes as input the last $t - r$ outputs of U_{i-1}, the s logical qubits $k_{i-1} + 1$ to k_i, and $r - s$ $|0\rangle$ ancilla qubits. V_i also acts on qubits $n_i - t + 1$ to n_i and takes as input the output qubits of U_i, and W acts on qubits 1 through n_1 and takes as input the logical qubits 1 to k_1 and $n_1 - k_1$ $|0\rangle$ ancilla qubits.

The *rate* of a quantum convolutional code is s/r.

The unitaries V_i and W are used to start and end the code block, to make the stream of qubits of finite length. The real meat of the convolutional code is in the unitaries U_i, which accumulate as the code gets longer and longer. Figure 9.2 illustrates the structure of the encoding circuit for a convolutional code, and it is evident from the figure that the encoder only relies on a finite memory for past qubits. Any qubits beyond the most recent t (including new logical qubits and ancillas) can be sent down the channel before encoding step U_i is performed, and are never needed again in the encoder. The rate of the convolutional code is the limiting rate k_i/n_i as $i \to \infty$. For finite i, the rate of the specific code Q_i might slightly differ from the asymptotic rate, but convolutional codes are usually considered in the limit of large i, so the asymptotic behavior is the dominant one.

Most often, the unitaries U_i and V_i are the same up to shifts. That is, $U_i = I^{\otimes(n_i - t)} \otimes U$ and $V_i = I^{\otimes(n_i - t)} \otimes V$. Moreover, we usually deal with stabilizer convolutional codes, for which U_i, V_i, and W are all Clifford group operations. It is also possible, of course, to define qudit quantum convolutional codes in the same way.

The stabilizer of a convolutional code consists of sets $\mathcal{S}_i$ of $r - s$ generators. The generators in $\mathcal{S}_i$ are of the form $I^{\otimes(n_i - t)} \otimes M_{i,j}$, with $j = 1, \ldots, r - s$. When the encoder is shift-invariant, so are the generators, so

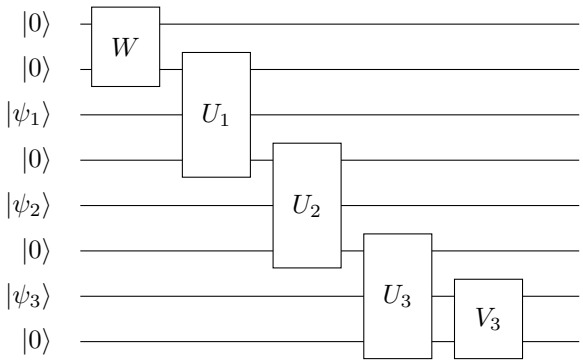

Figure 9.2: Encoding circuit for a convolutional code.

$M_{i,j} = M_j$ except perhaps for the largest and smallest values of i (due to the terminating unitaries V_i and W). Moreover, in many examples of convolutional codes (though not all), the weight of M_j is finite. Thus, the stabilizer of a large member of the convolutional code family can be described simply via $r - s$ finite-size Paulis which are then shifted systematically to give the full stabilizer of the code. For the remainder of this subsection, I will specialize to codes that have all of these properties (shift-invariant stabilizer convolutional codes with finite-weight stabilizer generators). I will also largely ignore the termination complication on the last few qubits, focusing instead on the main part of the code far from the end.

Since the shift transformation is so important in the description of convolutional codes, it is useful to have some specific notation for it. I will write D for the operation "shift by r qubits". Then, for instance, $M_{i,j} = D^{i-1} M_{1,j}$. We can also form polynomials out of D, of the form $\sum_i \alpha_i D^i$ with $\alpha \in \mathbb{Z}_2$. We can then define

$$\left(\sum_i \alpha_i D^i \right) (M_{1,j}) = \prod_i M_{i+1,j}^{\alpha_i}. \tag{9.4}$$

This is also an element of the stabilizer, since it is a product of generators. Indeed, we don't have to restrict to just finite-degree polynomials. Even an infinite-degree polynomial in D, also known as a formal *Laurent series*, gives us an element of the stabilizer in the limiting case where the code continues forever and never terminates.

Two examples of convolutional codes are given in tables 9.2 and 9.3. The first is based on the 5-qubit code, and has $r = 5$ and $s = 1$. Its rate is 1/5. The second example is not related to any standard block code, and has $r = 3$ and $s = 1$, with rate 1/3. By looking at the logical Paulis, you can see that both codes have distance 3. However, note that if there is only one error in each block of 5 (for the code of table 9.2) or 6 (for the code of table 9.3), then the syndrome will uniquely identify the error since it uniquely identifies that part of the error on each block. The generators M_0 and (for the second code) M_0' are produced by W and are not part of the repeated generators $\mathcal{S}_i$.

Since both of these codes have a finite extent to both the stabilizer generators and logical Paulis, we can deduce t by looking at the number of qubits involved in each block. For instance, in the case of the code in table 9.2, if we pick $t = 7$, we have enough room to make the 4 new generators and logical Paulis on the 1 new logical qubit have the correct commutation relations with each other and the old generators and logical

$$
\begin{array}{lccccccccccc}
M_0 & Z & X & & & & & & & & & \\
M_1 & X & Z & Z & X & & & & & & & \\
M_2 & & X & Z & Z & X & & & & & & \\
M_3 & & & X & Z & Z & X & & & & & \\
M_4 & & & & X & Z & Z & X & & & & \\
DM_1 & & & & & X & Z & Z & X & & & \\
DM_2 & & & & & & X & Z & Z & X & & \\
DM_3 & & & & & & & X & Z & Z & X & \\
DM_4 & & & & & & & & X & Z & Z & X \\
\vdots & & & & & & & & & & \ddots &
\end{array}
$$

$$
\begin{array}{lccccccccccc}
\overline{X}_1 & & X & X & X & X & X & & & & & \\
\overline{Z}_1 & & X & & Z & & X & & & & & \\
\overline{X}_2 & & & & & & & X & X & X & X & X \\
\overline{Z}_2 & & & & & & & X & & Z & & X \\
\vdots & & & & & & & & & & \ddots &
\end{array}
$$

Table 9.2: A convolutional code with period 5 and rate 1/5.

$$
\begin{array}{lccccccccccc}
M_0 & X & X & Z & Y & & & & & & & \\
M_0' & Z & Z & Y & X & & & & & & & \\
M_1 & & X & X & X & X & Z & Y & & & & \\
M_2 & & Z & Z & Z & Z & Y & X & & & & \\
DM_1 & & & & & X & X & X & X & Z & Y & \\
DM_2 & & & & & Z & Z & Z & Z & Y & X & \\
\vdots & & & & & & & & & \ddots & &
\end{array}
$$

$$
\begin{array}{lccccccccccc}
\overline{X}_1 & & X & Y & Z & & & & & & & \\
\overline{Z}_1 & & Z & X & Y & & & & & & & \\
\overline{X}_2 & & & & & X & Y & Z & & & & \\
\overline{Z}_2 & & & & & Z & X & Y & & & & \\
\vdots & & & & & & & & \ddots & & &
\end{array}
$$

Table 9.3: A convolutional code with period 3 and rate 1/3.

Paulis. In particular, we can let U_i transform Paulis as follows:

$$X \otimes I \otimes I \otimes I \otimes I \otimes I \otimes I \mapsto X \otimes I \otimes I \otimes I \otimes I \otimes I \otimes I \tag{9.5}$$
$$Z \otimes X \otimes I \otimes I \otimes I \otimes I \otimes I \mapsto Z \otimes X \otimes I \otimes I \otimes I \otimes I \otimes I \tag{9.6}$$
$$I \otimes I \otimes I \otimes X \otimes I \otimes I \otimes I \mapsto I \otimes X \otimes X \otimes X \otimes X \otimes X \otimes I \tag{9.7}$$
$$I \otimes I \otimes I \otimes Z \otimes I \otimes I \otimes I \mapsto I \otimes X \otimes I \otimes Z \otimes I \otimes X \otimes I \tag{9.8}$$
$$I \otimes I \otimes I \otimes Z \otimes I \otimes I \otimes I \mapsto X \otimes Z \otimes Z \otimes X \otimes I \otimes I \otimes I \tag{9.9}$$
$$I \otimes I \otimes I \otimes I \otimes Z \otimes I \otimes I \mapsto I \otimes X \otimes Z \otimes Z \otimes X \otimes I \otimes I \tag{9.10}$$
$$I \otimes I \otimes I \otimes I \otimes I \otimes Z \otimes I \mapsto I \otimes I \otimes X \otimes Z \otimes Z \otimes X \otimes I \tag{9.11}$$
$$I \otimes I \otimes I \otimes I \otimes I \otimes I \otimes Z \mapsto I \otimes I \otimes I \otimes X \otimes Z \otimes Z \otimes X \tag{9.12}$$

The action on the other independent Paulis can be anything with the right commutation relations. This Clifford will then leave the generators and logical Paulis created by the previous U_{i-1} unchanged while encoding the new $\overline{X}$, $\overline{Z}$, and 4 new stabilizer generators into their final form. Similarly, we can pick $t = 6$ for the code of table 9.3.

As you can see from the examples, the stabilizer generators typically act on a stretch of qubits longer than r, but we can still describe each stabilizer element with a shorthand over r "qubits" by using D. In particular, a generator can be expressed as a tensor product of r polynomials in D with coefficients from $\{I, X, Y, Z\}$. I will denote the tensor product of polyonomials corresponding to P by $P(D)$. Thus, in the code of table 9.2, the polynomials for the generators of $\mathcal{S}_1$ are

$$M_1(D) = X \otimes Z \otimes Z \otimes X \otimes I \tag{9.13}$$
$$M_2(D) = I \otimes X \otimes Z \otimes Z \otimes X \tag{9.14}$$
$$M_3(D) = XD \otimes I \otimes X \otimes Z \otimes Z \tag{9.15}$$
$$M_4(D) = ZD \otimes XD \otimes I \otimes X \otimes Z \tag{9.16}$$

The polynomials for the generators of $\mathcal{S}_1$ for the code in table 9.3 are

$$M_1(D) = YD \otimes X \otimes X \otimes X \otimes X \otimes Z \tag{9.17}$$
$$M_2(D) = XD \otimes Z \otimes Z \otimes Z \otimes Y \otimes X. \tag{9.18}$$

To find the versions of these generators shifted by r, just multiply by D.

When the set of stabilizer generators acts on more than r qubits, it will overlap with the same set of generators shifted by D. Thus, in order to determine if a purported stabilizer for a quantum convolutional code actually commutes, it is necessary to compare not just generators within the same set $\mathcal{S}_i$, but also ones in different sets. Using the shorthand provides a natural criterion:

Proposition 9.2. *$D^i P$ and $D^j Q$ commute for all i, j iff*

$$v_{P(D)} \odot v_{Q(D^{-1})} = x_{P(D)} \cdot z_{Q(D^{-1})} + z_{P(D)} \cdot x_{Q(D^{-1})} = 0. \tag{9.19}$$

Proof. Suppose we write $v_{P(D)} = \sum_i v_{P_i} D^i$ and $v_{Q(D^{-1})} = \sum_j v_{Q_j} D^{-j}$. Then

$$v_{P(D)} \odot v_{Q(D^{-1})} = \sum_{i,j} v_{P_i} \odot v_{Q_j} D^{i-j} \tag{9.20}$$
$$= \sum_{k=-\infty}^{+\infty} \sum_i v_{P_i} \odot v_{Q_{i-k}} D^k. \tag{9.21}$$

The coefficient of D^0, $\sum_i v_{P_i} \odot v_{Q_i}$, we can recognize immediately as $v_P \odot v_Q = c(P, Q)$. Similarly, the coefficient of D^k is

$$\sum_i v_{P_i} \odot v_{Q_{i-k}} = c(P, D^k Q). \tag{9.22}$$

Thus, $v_{P(D)} \odot v_{Q(D^{-1})} = 0$ as polynomials iff P and $D^k Q$ commute for all k. Since $c(D^i P, D^j Q) = c(P, D^{j-i} Q)$, this proves the proposition. □

9.2.2 Decoding of Convolutional Codes

One advantage of quantum convolutional codes is that by definition they have linear-time encoding algorithms. Note that this is true even for non-stabilizer codes, since each U_j, V_i, and W act on a constant number of qubits. Even for a stabilizer convolutional code, an $O(n)$ encoder is a signficant improvement over the $O(n^2/\log n)$ size of the encoding circuit for a generic stabilizer code.

Even more dramatic, and not as obvious, is that convolutional codes often have a linear-time decoding algorithm as well. Since general stabilizer codes could take exponential time to decode, this is a big deal. The algorithm is known as the *quantum Viterbi algorithm*. The Viterbi algorithm (classical or quantum) is an example of *dynamic programming*. The trick to it is to work in chunks of size r and try to figure out the most likely error up to qubit n_i. What we'd like to do then is to move to the next block of r qubits and try to figure out the most likely error up to qubit $n_{i+1} = n_i + r$. Ideally, we would just say, "Oh, the most likely error on n_{i+1} qubits is just the most likely error on the first n_i qubits followed by the most likely error on the next r qubits." Then we could just systematically work our way through each set of r qubits picking the most likely errors and get a decoding algorithm running in $O(n)$ time. Well, we could *say* that, but sometimes we'd be wrong. The problem is that (for a stabilizer code), there may be stabilizer generators that act on the first n_i qubits but also act on later qubits. These generators are not as helpful as they might be when determining the most likely error on the first n_i qubits because there will be multiple different choices of error on the next r qubits that get the error syndrome right. The problem is that some choices of error on the next r qubits might be extremely unlikely, but to know that, we would need to look at the error syndrome on more generators, which means involving even more qubits, and so on.

The solution is not to pick the *single* most likely error, but instead the most likely error ending in each possible way. That is, we need to consider all the different ways the error on the first n_i qubits might affect any stabilizer generators that continue into the next set of r qubits. Here's where we need to make an assumption: specifically, we will assume we have a convolutional code with finite-weight stabilizer generators, all bounded by a constant w. (Note that w might or might not be the same as t in general.) That means that the stabilizer generators in $\mathcal{S}_{i+1}$ only touch the last $w-r$ qubits out of the first n_i qubits. That's important, because it means that if we want to find an error that satisfies generators only in sets $\mathcal{S}_1$ through $\mathcal{S}_i$, there are only a constant number of ways, specifically 4^{w-r}, that the error can end. To extend to the most likely error satisfying the syndrome for $\mathcal{S}_{i+1}$ and ending in a particular way, we try out all the different ways an error on n_i qubits can end matched with all the compatible errors on the next r qubits and pick the most likely combination.

Putting this together, we get the following algorithm to find the most likely or lowest-weight error consistent with the measured error syndrome for all generators:

Algorithm 9.2 (quantum Viterbi algorithm)**.** Let $\{Q_i\}$ be a stabilizer quantum convolutional code with stabilizer generators $I^{\otimes(n_i-w)} \otimes M_{i,j}$, with $j = 1, \ldots, r-s$, $\mathrm{wt}\, M_{i,j} \leq w$, $r \leq w$. Given an error syndrome for some particular instance of the code with n total physical qubits, use the following algorithm to determine the most likely (or lowest-weight) error:

1. Create a table of all possible Pauli errors on $w-r$ qubits, with two entries (N_P, p_P) for each Pauli P. Initialize by simply letting $N_P = P$ and putting the probability (or weight) of P as p_P. If there are any stabilizer generators with support on just the first $w-r$ qubits, set the probability of any Pauli incompatible with the error syndrome to 0, or set the weight to ∞.

2. Set $n_0 = w - r$ and $i = 0$.

3. Until $n_i \geq n$, repeat the following steps:

   (a) For each Pauli P on qubits $n_{i+1} - (w-r) + 1$ to n_{i+1}, run through all possibilities for Q on qubits $n_i - (w-r) + 1$ to n_i and R on qubits $n_i + 1$ through $n_{i+1} - (w-r)$. (If $w - r \geq r$, we don't need to run over R and we only consider Q which is consistent with P on qubits $n_{i+1} - (w-r) + 1$ through n_i.) If $N_Q \otimes R \otimes P$ has the correct error syndrome for all generators $M_{i+1,j}$ $(j = 1, \ldots, r-s)$, calculate the probability (or weight) of $N_Q \otimes R \otimes P$ by multiplying the probability p_Q times the

probability of $R \otimes P$ (or by adding the weights p_Q and wt R+wt P). Choose Q and R such that the probability is highest or the weight is the lowest. Create an updated table with $N'_P = N_Q \otimes R \otimes P$ and p_P is the probability or weight of N'_P. If no Q and R gives the correct error syndrome, set p'_P to probability 0 or weight ∞.

(b) Switch the updated table (N'_P, p'_P) into the main table (N_P, p_P), increase i by 1 and let $n_{i+1} = n_i + r$.

4. Look through the table, running over all P, to find the value for which the probability p_P is a maximum or the weight is a minimum. Output that corresponding entry N_P as the most likely (or lowest-weight) error for this error syndrome.

Convolutional codes are looking pretty good right now: they have a non-zero asymptotic rate, a linear-time encoder, and can also have a linear-time decoder. Unfortunately, there is one big problem: they cannot have more than a constant distance. This is true for *any* quantum convolutional code, regardless of whether the U_i repeat, or whether it is a stabilizer code, or if the stabilizer generators have finite extent. This issue arises because qubits are not spread out enough by the encoding circuit. In particular, there is a small bottleneck, the finite memory of the encoder, which prevents too much information about old logical qubits from being involved in the later physical qubits.

Proposition 9.3. *Let $\{Q_j\}$ be a quantum convolutional code (not necessarily a stabilizer code). Then the distance of Q_j is less than c for all j, where c is the constant $c = r\lceil (3t + r)/s \rceil$.*

Proof. When the unitaries U_j and V_j are t-qubit unitaries, choose i to be an arbitrary value at least $\lceil t/r \rceil$, so U_{i+1} does not act on the first n_1 qubits. Also, U_i does not act on qubit $n_i + 1$ or any later qubit. Let $i' > i$ be such that $k_{i'} - k_i > 3t + r$, and let $i'' = i' + \lceil t/r \rceil$, so $U_{i''+1}$ does not act on the first $n_{i'}$ qubits. Finally, pick any $i''' \geq i''$. We can write the encoder as $U_C U_B U_A$, where $U_A = (\prod_{j=i}^{1} U_j)W$, $U_B = \prod_{j=i''}^{i+1} U_j$, $U_C = V_k(\prod_{j=i'''}^{i''+1} U_j)$.

Consider code $Q_{i'''}$. It has encoding circuit $U_C U_B U_A$. We will imagine fixing all logical qubits less than or equal to k_i and greater than $k_{i'}$ while varying the logical qubits $k_i + 1$ to $k_{i'}$. For instance, we can let the fixed qubits be all $|0\rangle$. Since U_A does not act on physical qubits $n_i + 1$ or later, it does not involve the varying logical qubits. Let $|\psi\rangle = U_A|0 \dots 0\rangle$. Now let us consider erasure errors E acting only on the physical qubits from $n_i + 1$ to $n_{i'}$. For the QECC conditions to hold, we must have, for $x \neq y$ basis states for logical qubits $k_i + 1$ through $k_{i'}$,

$$0 = \langle \overline{0 \dots 0x0 \dots 0} | E | \overline{0 \dots 0y0 \dots 0} \rangle \tag{9.23}$$

$$= \langle 0 \dots 0x0 \dots 0 | U_A^\dagger U_B^\dagger U_C^\dagger E U_C U_B U_A | 0 \dots 0y0 \dots 0 \rangle \tag{9.24}$$

$$= \langle 0 \dots 0x0 \dots 0 | U_A^\dagger U_B^\dagger E U_B U_A | 0 \dots 0y0 \dots 0 \rangle \tag{9.25}$$

$$= (\langle \psi | \otimes \langle x0 \dots 0 |) U_B^\dagger E U_B (|\psi\rangle \otimes |y0 \dots 0\rangle), \tag{9.26}$$

since U_C acts only on qubits not involved in E and U_A acts only logical qubits before k_i. Now, $|\psi\rangle$ could be an entangled state between those qubits which are acted on by U_B and those which are not, but even if it is maximally entangled, the Schmidt rank is at most t, since that is the largest number of qubits that U_B could act on. In particular, there exists unitary V acting only on qubits not acted on by U_B such that $V|\psi\rangle = |0 \dots 0\rangle \otimes |\psi'\rangle$, with $|\psi'\rangle$ a $2t$-qubit state, and with U_B not acting on the first tensor factor. We thus have

$$0 = (\langle \psi | \otimes \langle x0 \dots 0 |) U_B^\dagger E U_B (|\psi\rangle \otimes |y0 \dots 0\rangle) \tag{9.27}$$

$$= (\langle \psi | \otimes \langle x0 \dots 0 |) V^\dagger U_B^\dagger E U_B V (|\psi\rangle \otimes |y0 \dots 0\rangle) \tag{9.28}$$

$$= (\langle \psi' | \otimes \langle x0 \dots 0 |) U_B^\dagger E U_B (|\psi'\rangle \otimes |y0 \dots 0\rangle). \tag{9.29}$$

Moreover, only qubits up to $n_{i''}$ can be involved here too, since U_B cannot act on qubits $n_{i''} + 1$ or greater. Thus, equation (9.29) only involves $2t + r(i'' - i)$ qubits.

Finally, consider the case where $E = |0\ldots0\rangle\langle 0\ldots0|$ on qubits $n_i + 1$ through $n_{i'}$, a total of $n_{i'} - n_i = r(i' - i)$ physical qubits. Equation (9.29) then becomes an inner product

$$\langle \phi_x | \phi_y \rangle = 0, \tag{9.30}$$

where $|\phi_x\rangle$ is defined by $|\phi_x\rangle \otimes |0\ldots0\rangle = |0\ldots0\rangle\langle 0\ldots0|U_B(|\psi'\rangle \otimes |x0\ldots0\rangle)$.

$|\phi_x\rangle$ involves $2t + r(i'' - i') = 2t + r\lceil t/r \rceil < 3t + r$ qubits, and all the different $|\phi_x\rangle$ must be orthogonal. But the number of different such states is $k_{i'} - k_i > 3t + r$. This is a contradiction, so we have found an erasure error of weight $r(i' - i)$ for which the QECC conditions are not satisfied. Since $k_{i'} - k_i = s(i' - i)$, we have shown that the distance of the convolutional code is at most $r\lceil (3t + r)/s \rceil$. □

Basically, convolutional codes can only correct errors that do not cluster too much. Even randomly placed errors will have occasional clusters of size larger than c, so convolutional codes also are not good against them. Nevertheless, convolutional codes can still be useful if we're willing to settle for something less than correcting all errors. Typically, we restrict attention to codes which are *non-catastrophic*, meaning that a uncorrectable error confined to a region only affects logical qubits near that region, while logical qubits far away remain OK. Non-catastrophic convolutional codes do allow errors to happen, but they successfully quarantine them, limiting the damage.

Definition 9.4. Suppose the decoder for a stabilizer convolutional code $\{Q_i\}$ assigns Pauli P_σ to syndrome σ. Then for any error Q, $R_Q = P^\dagger_{\sigma(P)}Q$ is a logical Pauli operator. The decoder is *catastrophic* if there exists some finite-weight Pauli Q such that R_Q has unbounded weight as $i \to \infty$. A stabilizer convolutional code is catastrophic if all decoders for it are catastrophic.

9.3 Information-Theoretic Approach to QECCs

The QECC conditions (theorem 2.7) and their variants give us a nice algebraic set of conditions for determining if a subspace is a QECC. It is helpful to also have a different criterion based on information theory, which will basically say that the amount of quantum information in the encoded state stays constant.

One big difference in the information-theoretic approach compared to the algebraic approach of theorem 2.7 is that the information-theoretic approach requires us to specialize to a specific quantum channel for the noise, whereas the QECC conditions instead work with a list of possible errors. The advantage of the latter approach is that we don't need to know precisely what is going on with the noise, just the list of possible things that could happen to our data. The information-theoretic approach, on the other hand, is much more natural when we know that some types of error are substantially more likely than others. In the algebraic approach, our only option was to say "these errors are negligible, so we will ignore them." The information-theoretic approach lets us weight each error by its actual prevalence.

The algebraic approach is also useful for proving more algebraic properties of codes, such as the fact that the distance tells us about the code's ability to correct both general errors (corollary 2.8) and erasure errors (theorem 2.10) or the Eastin-Knill theorem (theorem 11.7) in fault tolerance. These types of things are tougher in the information-theoretic approach, which is more natural when dealing with information-theoretic properties like the quantum channel capacity, which I will discuss in chapter 19.

The big payoff of the information-theoretic approach is that it generalizes very naturally to approximate quantum error-correcting codes (section **??**), which don't recover the state perfectly but only to some good approximation. The algebraic QECC conditions don't work well for approximate codes, with a large (dimension-dependent) factor between the necessary and sufficient conditions, whereas the obvious generalization of the information-theoretic condition we will derive works straightforwardly. This is another reason to use the information-theoretic approach with the channel capacity, since it deals with the case of infinitely-many qubits, where the error is non-zero but asymptotes to zero.

9.3.1 Coherent Information

So, we want to quantify the amount of quantum information in a system Q. Information should be *about* something, which we can represent by an additional system R, known as a *reference system*. To make the

information quantum, we should allow for the possibility of entanglement between Q and R. However, the joint system of Q and R might not be pure, so we could also consider an environment E, as in the final state of figure 9.3. We might as well consider the whole universe outside of Q and R to be the environment; that is, we can let the joint state of RQE be a pure state. We imagine that R (being an idealized system) has remained isolated so that all its entanglement is with Q, but Q has not, so it may be entangled with E.

If Q and R are maximally entangled, it makes sense to say that the amount of quantum information is n when each system has n qubits, so Q has n qubits of quantum information "about" R. If ρ_{QR} is an arbitrary pure state, the amount of quantum information in Q about R should then just be the entanglement entropy between the two, $S(Q)$ (which I am using as shorthand for $S(\rho_Q)$).

Another case where the answer is obvious is when Q can be decomposed into a tensor product between a subsystem Q_1 which is entangled only with R and a second subsystem Q_2 which is entangled only with E. In that case, the amount of quantum information in Q about R is just

$$S(Q_1) = S(Q) - S(E). \tag{9.31}$$

This will turn out to be the correct answer more generally, and it makes sense. $S(E)$ is the amount of information that E "knows" about Q and if the environment knows about the state of a system, it can't be quantum. (For instance, because a measurement on the environment could collapse the logical state.)

We'd like to phrase our formula without talking about E so that it is just a property of the state of Q and R. Since the global state is pure, $S(E) = S(RQ)$. Then we have the following definition to quantify the amount of quantum information in a system.

Definition 9.5. Given a quantum system Q entangled with a reference system R in the state ρ_{RQ}, the *coherent information* in Q is

$$I_c(\rho_{RQ}) = S(\rho_Q) - S(\rho_{RQ}). \tag{9.32}$$

Let $\mathcal{E}$ be a quantum channel taking system L into Q. The initial state of L and R is a pure state ρ. Then the coherent information of $\mathcal{E}$ for ρ is

$$I_c(\mathcal{E}, \rho) = S(\mathcal{E}(\rho_L)) - S((\mathcal{I} \otimes \mathcal{E})(\rho)). \tag{9.33}$$

The channel set-up realizes the situation we discussed above: R remains isolated and does not go through the channel $\mathcal{E}$ or interact with the environment E, but Q does and therefore may lose some coherence to E. The coherent information of $\mathcal{E}$ on ρ then quantifies (as we will see shortly) how much quantum information about R remains in Q.

This suggests that it is helpful to consider not just the state of Q after the channel, but also the state of E. The channel that maps L to E is one that tells us a lot about error correction properties of $\mathcal{E}$:

Definition 9.6. Let $\mathcal{E}$ be a quantum channel taking system L into Q which can be purified into U using an environment E. Then the channel produced by performing U on L and discarding Q maps L to E. It is written $\hat{\mathcal{E}}$ and is called the *complementary channel*.

If you're familiar with classical information-theoretic quantities, you may recognize the formula for coherent information as the negative of a conditional entropy $I_c(\rho_{RQ}) = -S(R|Q)$. The conditional entropy is a quantification of the amount of uncertainty remaining in R once Q is specified. From a classical point of view, it is very peculiar to consider a negative conditional entropy: The coherent information can never be positive for a classical system! But from a quantum perspective, negative uncertainty actually makes a certain kind of perverse sense — negative uncertainty means that you are *more* certain about the state than would be allowed classically, which doesn't seem so dissimilar to entanglement providing stronger correlations than are possible classically, as happens with Bell inequalities.

One property of coherent information is that putting the state through a channel cannot increase it. This makes it suitable for the various applications we have in mind for it, since quantum information, once lost, should be gone for good. (Error correction does not replace lost quantum information, it protects it and spreads it out so that it is not destroyed in the first place.)

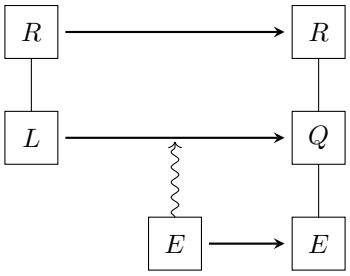

Figure 9.3: System L is entangled with reference system R. L goes through a noisy channel to become system Q after interacting with environment E.

Theorem 9.4 (Quantum data processing inequality)**.** *Let ρ be a mixed state on reference system R and quantum system L, and let $\mathcal{E}$ be a quantum channel mapping L to Q. Then*

$$I_c(\mathcal{E}, \rho) \leq I_c(\rho). \tag{9.34}$$

Equivalently, if $\mathcal{E}$ maps L to Q and $\mathcal{F}$ maps Q to Q', then

$$I_c(\mathcal{F} \circ \mathcal{E}, \rho) \leq I_c(\mathcal{E}, \rho). \tag{9.35}$$

Proof. I will only prove the first version, since the second is essentially identical. Let E be the environment used to purify the initial state ρ. $\mathcal{E}$ does not act on E; instead, it uses a new environment E'. $\mathcal{E}$ also does not act on R. Then

$$I_c(\rho) = S(L) - S(RL) = S(RE) - S(E) \tag{9.36}$$
$$I_c(\mathcal{E}, \rho) = S(Q) - S(RQ) = S(REE') - S(EE'). \tag{9.37}$$

Applying the strong subadditivity property of entropy to R, E, and E', we find

$$S(REE') + S(E) \leq S(RE) + S(EE') \tag{9.38}$$
$$I_c(\mathcal{E}, \rho) \leq I_c(\rho). \tag{9.39}$$

□

9.3.2 Coherent Information and QECCs

The data processing inequality immediately tells us that in order for a QECC to function, the coherent information must not decrease under the action of the error, since otherwise we cannot recover the lost coherent information and therefore cannot possibly get back to where we started. Thus, coherent information staying constant is a necessary condition for quantum error correction. It turns out that it is also a sufficient condition.

What is the condition, precisely? The coherent information is state-dependent, and we need it to be constant for any input codeword. It's simpler to phrase the condition by simply saying the coherent information remains constant for any input state, but then apply the condition not to the noise channel $\mathcal{E}$ by itself but to the composition of the encoder U followed by $\mathcal{E}$.

Theorem 9.5. *Let $\mathcal{F} : L \to Q$ be a quantum channel. Let R be a reference system, which must have a dimension at least as large as L. There exists a decoding CPTP map $\mathcal{G}$ with the property $\mathcal{G} \circ \mathcal{F} = \mathcal{I}$ iff $I_c(\mathcal{F}, \rho) = S(\rho_L)$ for all pure states ρ on $R \otimes L$.*

When we let $\mathcal{F} = \mathcal{E} \circ U$, where U is a partial isometry from the logical Hilbert space L to a larger physical Hilbert space, then the condition that $\exists\, \mathcal{G}$ such that $\mathcal{G} \circ \mathcal{F} = \mathcal{I}$ is immediately equivalent to the definition of a QECC for the case where the set of possible errors is just the set of Kraus operators of the channel $\mathcal{E}$. The normalization gets taken care of automatically because all of the channels U, $\mathcal{E}$, and $\mathcal{G}$ are trace preserving. Therefore, theorem 9.5 gives us the desired information-theoretic version of the QECC conditions.

Proof. Note that $I_c(\rho) = S(\rho_L)$ since ρ is a pure state, so there is no initial environment. Since $I_c(\mathcal{I}, \rho) = I_c(\rho)$, the forward direction follows immediately from the data processing inequality, as noted above.

Now suppose $I_c(\mathcal{F}, \rho) = S(\rho_L)$ for all ρ. Let us consider the purification of $\mathcal{F}$ to V, mapping L to $Q \otimes E$, and let $\sigma = \mathcal{I} \otimes V(\rho)$. Since the global state σ of RQE is a pure state, that means that

$$I_c(\mathcal{F}, \rho) = S(Q) - S(RQ) = S(RE) - S(E) \tag{9.40}$$

and since the initial state ρ is a pure state, $S(L) = S(R)$. Therefore,

$$S(RE) = S(E) + S(R), \tag{9.41}$$

which is true only when $\sigma_{RE} = \sigma_R \otimes \sigma_E$. This is true for all ρ, and in particular it is true when ρ is a maximally entangled state for RL.

When ρ is a maximally entangled state, we can prepare arbitrary pure states $|\psi\rangle_L$ on L by performing different projections on R. Since V doesn't act on R, projections on R commute with the channel. If we perform a projection on R for the final state σ, the state σ_E is unaffected, since $\sigma_{RE} = \sigma_R \otimes \sigma_E$. Thus the state of E is σ_E regardless of which pure state $|\psi\rangle_L$ was initially prepared for L.

Now, the effect of $\mathcal{F}$ is to do V, getting state σ, and then to discard E. Let us think of V as the encoding map of a QECC and discarding E as an erasure error that happens to this code. One version of the QECC conditions (proposition 2.12) says that we can correct for the erasure of E iff the state σ_E is independent of $|\psi\rangle_L$. That is true in this case, so there exists a recovery operation $\mathcal{G}$ for which $\mathcal{G} \circ \mathcal{F} = \mathcal{I}$. (Here, $\mathcal{F}$ combines both the encoding V and the error, an erasure of E, and recall that normalization automatically follows because $\mathcal{F}$ is trace preserving.) □

It's worth noting that in the proof, all we really need is for $I_c(\mathcal{F}, \rho) = S(\rho_L)$ for a maximally entangled state ρ. We don't actually need to check this condition for all ρ, but it follows from the proof that if it's true for a maximally entangled state, then it is true for all ρ.

Part II

Fault-Tolerant Quantum Computation

Chapter 10

Everyone Makes Mistakes: Basics Of Fault Tolerance

We've now discussed extensively the notion of quantum error correction. However, there's a flaw in the basic model we've been considering. Or rather, there is a *lack* of flaws: We've been assuming that the encoding and decoding circuits needed for error correction can be performed perfectly, and that errors only occur between these two steps. This might not be a bad idealization if you're mainly concerned about transmission over a noisy communications channel or storage for long amounts of time. These are cases where the errors introduced by mistakes in the encoding and decoding steps may be much rarer than errors occurring in the period in between. However, in practice, errors in gates are far from negligible and are likely to remain so for the forseeable future, so neglecting errors during the encoding and decoding circuits is a poor approximation. If we want to put together millions or more gates to perform a large quantum computation, the prospect of getting through the whole circuit without errors is vanishingly unlikely.

To protect quantum computations against errors, we need something more than a quantum error-correcting code, we need a *fault-tolerant protocol*, which allows us to perform unitary gates on encoded states despite errors occurring during the computation. Part II is devoted to developing the theory of fault-tolerant quantum computation, culminating in the *threshold theorem*, which says that arbitrarily long quantum computations are possible provided the error rate per physical gate and time step is below some constant threshold value. In this chapter, I'll introduce the basic concepts of fault tolerance. We'll learn what it means to compute in a world where no component can be taken for granted, where everyone — every qubit, every gate — can make a mistake.

10.1 The Fault-Tolerant Scenario

As discussed in chapter 1, there are many possible errors that can afflict a quantum state. In part I, the errors only had one shot at the quantum state: we encode, the errors do their thing (although we might wish they didn't), and then we decode and correct the state. For fault tolerance, we will need to deal with more pervasive errors. Errors can occur between gates or during gates, and even worse, the errors keep happening. Every time we do another gate, or even if we simply leave a qubit by itself for a little while, a new error can occur. Dealing with the full range of possible errors is a daunting task, so for the purposes of developing the theory and analyzing fault-tolerant protocols, we normally work with a simplified model, which I'll discuss in this section. We'll actually need to add another complication to this model before proving the threshold theorem in chapter 14, and we'll discuss fault tolerance for even more general error models in chapter 15.

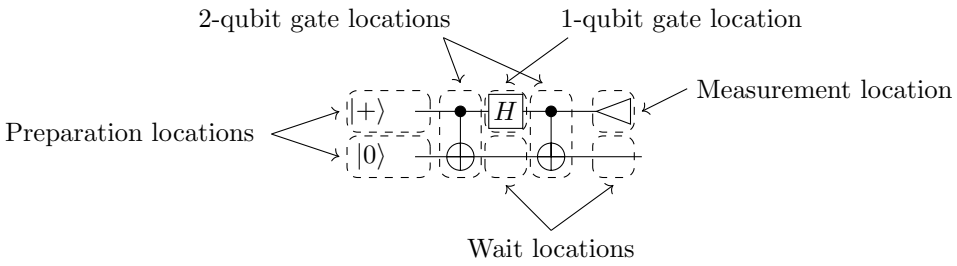

Figure 10.1: A sample circuit broken down into locations. Note that a 2-qubit gate location is a single location on 2 qubits. Thus, this sample circuit has a total of 8 locations.

10.1.1 Basic Model for Fault Tolerance (Independent Stochastic Errors)

Any quantum circuit, fault-tolerant or not, is composed of the same basic components. We perform gates on qubits, we may prepare new qubits and introduce them to the circuit, and sometimes we measure qubits and perhaps perform a classical computation on the outcome. Sometimes measurement occurs in the middle of the computation, in which case later actions may depend on the measurement outcomes, and sometimes measurement is delayed until the end of the computation. Each basic action that we can perform is called a *location*. We'll consider circuits which can perform gates in parallel, since we'll want to simultaneously correct errors in different parts of the computer.

Definition 10.1. Consider a quantum circuit, arranged into time steps. Each qubit can be involved in at most one action per time step, but multiple actions can be performed in a single time, provided they involve different qubits. A *location* is a single indivisible action in the circuit. We may consider the following different types of locations:

1. A *preparation location*: The preparation of a single qubit in a particular state, frequently $|0\rangle$. Sometimes we distinguish between different types of preparation locations based on the state prepared. Occasionally we may want a preparation location to encompass the creation of a multiple-qubit entangled state.

2. A *gate location*: A single gate from the universal gate set used to describe the circuit. Sometimes we may want to distinguish different types of gate location based on the kind of gate appearing (e.g., a CNOT location or a H location). If the gate is a multiple-qubit gate, the location encompasses all the qubits involved in the gate, but still just counts as a single location. Usually, we only consider unitary gates to produce gate locations, but one could also consider gate locations for more general quantum channels.

3. A *wait location* or *storage location*: A single qubit is stored for a unit time with no gate performed on it.

4. A *measurement location*: A single qubit is measured with a von Neumann measurement, usually in the standard basis $|0\rangle$, $|1\rangle$. The measurement outcome is captured as classical information. Occasionally we may want locations corresponding to other kinds of measurements, including possibly multiple-qubit entangled measurements.

5. A *classical computation location*: In the basic model for fault tolerance, we omit locations corresponding to classical computations. We assume that classical computation can be performed instantaneously (and flawlessly) on the outcomes of measurements, including combining the results of multiple measurement locations. The outcomes of the classical computations may later be used to control any other locations later in the circuit.

Remember, we are just developing the basic model for fault tolerance most often used in analyzing protocols. Because we're currently concerned with the task of manipulating quantum states, even giving ourselves unlimited classical computational power doesn't make this task trivial. Of course, we shouldn't abuse the privilege. For instance, it is definitely cheating to scrap the quantum circuit altogether, and solve the problem we are interested in using an inefficient classical algorithm — but note that even such a blatant cheat doesn't let us store an unknown quantum state indefinitely in the presence of noise. We'll discuss the assumption of perfect classical computation along with other deviations from the basic model in chapter 15.

Next, we want to add errors. In the basic model for fault tolerance, we consider that errors at different locations are independent, and furthermore consider a simplified model for the errors. We still want to include the possibility that any location can go bad.

Definition 10.2. Consider a quantum circuit C divided into locations, as above. An *independent error model* on the quantum circuit C is a circuit $\widetilde{C}$ where every preparation location, gate location, storage location, and measurement location is replaced by a separate quantum channel, arranged in the same way as the original circuit. In an *independent stochastic error model*, the quantum channel corresponding to a particular location L of C performs the correct action for L with probability $1 - p_L$ and does something else with the same input and output Hilbert space dimensions as L with probability p_L. I.e., the channel for a $|0\rangle$ preparation location L will prepare $|0\rangle$ with probability $1 - p_L$ and prepare some other single-qubit state (possibly mixed) with probability p_L. The quantum channel corresponding to L is still called a *location* and may be referred to as $\widetilde{L}$, or just L if the distinction between the two is not needed. p_L is called the *error probability* or *error rate* of location L.

The circuit $\widetilde{C}$ is called a *noisy* implementation of C. In any particular realization of a noisy circuit $\widetilde{C}$ with an independent stochastic error model, for some locations the correct action L is performed, while for other locations the wrong action is performed. The locations where the wrong thing happens are called *faulty*, or they are said to have a *fault*. We frequently say of a faulty location that a preparation error, gate error, storage error, or measurement error has occurred, depending on the type of location.

In an *independent Pauli error model*, a faulty location always performs the correct action followed by a Pauli channel. In a Pauli error model, a faulty measurement location will flip the measurement outcome bit with some probability.

A *fault path* is a set of locations in C. A *Pauli fault path* is a fault path with a Pauli error associated with each location in the fault path.

There are a number of things to point out about the independent stochastic error model. The error model is "independent" because the quantum channels for different locations are separate. In the stochastic version, we can consider that errors occur with a certain probability p_L. Then the probability of having faults at two specific locations L and M is $p_L p_M$.

Note, however, that (unless we are dealing with a Pauli error model) we make no prescription for what happens at faulty locations. In particular, multiple-qubit locations, such as a CNOT gate location, can have errors which involve both qubits, including errors which entangle the qubits in the wrong way. This still is considered to have probability p_L. The independence only applies to separate locations. This is an essential part of the error model, since errors that occur during the performance of a gate will generally affect all the qubits involved in the gate.

Another perhaps suprising observation is that, according to the definition, a faulty location might behave correctly! The identity is a possible matrix, even for a Pauli channel, so that "error" might turn out not to be one. In this case, we are essentially overcounting the number of faults, which generally means we are just being more conservative than we need to, and our conclusions will be correct. (There are occasional cases where having an identity "error" is actually worse than a real error, for instance if the error would cancel another previous error, but that just means that we are correct in thinking of the identity "error" location as a fault.)

The notion of fault path is useful when discussing and computing error rates, particularly (though not exclusively) for independent stochastic channels. The fault path represents the locations where errors occur in a particular realization of the circuit. A Pauli fault path adds in additional information about the type of error occurring at each location, under the assumption that the errors are Pauli errors.

Definition 10.3. A *basic model for fault tolerance* is as follows: An ideal circuit C is physically realized as a noisy circuit $\widetilde{C}$, according to an independent stochastic error model. The error model has the property that all locations of a given type have the same error probability. In other respects, the quantum channels used in the error model are arbitrary, and may be incompletely specified. A basic error model can therefore be summarized in terms of four error probabilities: p_P (the error probability for a preparation location), p_G (the error probability for a gate location), p_S (the error probability for a storage location), and p_M (the error probability for a measurement location).

Frequently the basic model is simplified even further, either by using an independent Pauli error model or by making some or all of the four error probabilities equal, or both. Sometimes the basic model is slightly elaborated by considering different error rates for different types of gate, for instance by letting the error rate for two-qubit gates be higher than the error rate for one-qubit gates.

Basic models for fault tolerance capture the main effects that are important in developing the theory of fault tolerance. While a particular physical realization for quantum computation may not fulfill precisely the assumptions of a basic model, provided it does not violate the assumptions too much, we expect fault-tolerant protocols to work more or less according to the analysis done for the basic model. We'll discuss in detail in chapter 15 what happens when we change the assumptions behind the basic model.

Conversely, if we attempt to simplify the basic model by leaving out parts of it, the analysis can fail badly for realistic systems. For instance, if we assume the storage error rate is 0, so wait locations are perfect, we might come up with a circuit that is very sensitive to storage errors and thus fails badly when the storage error rate becomes non-zero. Nevertheless, it is sometimes interesting to consider models that do include such simplifications, either because they represent the qualities of a particular physical system of interest or because they may give us insight into particular aspects of the theory of fault tolerance.

10.1.2 Error Propagation

Building fault-tolerant circuits that still work when subjected to independent stochastic errors is challenging because of two problems beyond those we solved to make QECCs. First, we can no longer count on any circuit or gate to do exactly what we intended it to do, since any gate can fail with probability p_G. Second, once errors appear, they don't stay put. Instead, they spread through the qubits of our computer like a disease being transmitted by sick air travellers. Even a portion of a circuit that has no faults in it can still cause problems by contributing to error propagation.

To see how this works, consider the CNOT gate. Assume it acts correctly, but that the initial state is wrong. Suppose instead of $|\psi\rangle$, the CNOT acts on $E|\psi\rangle$. Then

$$\text{CNOT}(E|\psi\rangle) = (\text{CNOT } E \text{ CNOT})\text{CNOT}|\psi\rangle. \tag{10.1}$$

The correct final state is $\text{CNOT}|\psi\rangle$, so the true final state has an error CNOT E CNOT on it, much as we saw for the analysis of the Clifford group in chapter 6. For example, suppose $E = X \otimes I$. Then CNOT E CNOT $= X \otimes X$, so a bit flip error spreads from the control qubit to the target qubit of the CNOT. Whereas only one qubit had an error before the CNOT, now two qubits have errors, even though the gate itself functioned perfectly. This is clearly a problem for a QECC which is designed to correct only a small number of errors — an error in one qubit, initially something the code could correct, might spread quickly to affect more qubits than the code is designed to handle.

Now consider $E = I \otimes Z$. We have CNOT E CNOT $= Z \otimes Z$, meaning the phase flip error has spread from the target qubit to the control qubit. While a classical CNOT can spread errors from control to target, the quantum CNOT can also spread errors the other way. This means that error propagation, already a challenge for classical fault-tolerant computers, is even more pervasive in a quantum computer. In general, any two-qubit entangling gate will cause errors to propagate in both directions through the gate. (The SWAP gate is an interesting exception in that it causes errors to switch between the two qubits without directly causing them to spread. But then, the SWAP gate doesn't really entangle the two qubits involved in the gate either.)

10.1.3 Example Transversal Gate

Single-qubit gates don't cause error propagation, so circuits composed of single-qubit gates will behave much better than general circuits involving multiple-qubit gates. For instance, consider the seven-qubit code. It turns out that the Hadamard transform applied to all 7 qubits of the code will perform the logical Hadamard transform:

$$H^{\otimes 7}|\overline{0}\rangle = \frac{1}{\sqrt{2}}(|\overline{0}\rangle + |\overline{1}\rangle) \tag{10.2}$$

$$H^{\otimes 7}|\overline{1}\rangle = \frac{1}{\sqrt{2}}(|\overline{0}\rangle - |\overline{1}\rangle) \tag{10.3}$$

(You can check this yourself, if you like.) Imagine we have a codeword $|\psi\rangle = \alpha|\overline{0}\rangle + \beta|\overline{1}\rangle$, and consider what happens if there is a single-qubit error on the codeword, say a bit flip on qubit 3. Then, as above, we find that the state post-Hadamard is

$$(H^{\otimes 7} X_3 H^{\otimes 7}) H^{\otimes 7}|\psi\rangle = Z_3 H^{\otimes 7}|\psi\rangle. \tag{10.4}$$

The single-qubit Hadamard transforms have changed the *type* of error from a bit flip to a phase flip, but crucially, it is still a single-qubit error. Before the Hadamard transforms, the code could correct the error, and the code can still correct the error after the Hadamard transforms.

This is the key idea that takes us a long way towards fault tolerance. The tensor product of 7 Hadamard transforms is an example of a *transversal gate*, a concept that we'll explore in much more detail in chapter 11. Of course, single-qubit gates alone won't get us very far, so we'll also see how to design multiple-qubit transversal gates. These gates will cause some error propagation, but the error propagation will be carefully controlled to be of a form we can handle. It turns out that even multiple-qubit transversal gates are still not enough to provide a universal set of gates on the encoded qubits, so we'll need to add some additional techniques discussed in chapter 13 to have a full range of control.

10.1.4 Starting and Ending Encoded

There is an additional pitfall to starting or ending a fault-tolerant computation. One natural approach is to start with unencoded qubits given to you by someone else, then to encode them in a QECC. Once it is encoded, perform the fault-tolerant quantum computation, then decode, leaving unencoded qubits once more. However, this approach leaves the qubits vulnerable to errors at the beginning and end of the computation. Even if we discount errors occurring before we're given the qubits or after we finish with them, there is always the possibility of errors early in the encoding circuit, before we've had time to develop any error correction capability, or late in the decoding circuit. Techniques exist to minimize the period of vulnerability, but it cannot be completely eliminated. Therefore, any quantum computation performed this way has a minimum error probability (derived from the error rates p_G, etc.) which cannot be reduced by using more powerful quantum error-correcting codes. The logical error rate during the main part of the computation can be reduced arbitrarily far via the threshold theorem, meaning the encoding and decoding error will dominate the error rate, regardless of how big a computation we are performing.

This is unsatisfactory. Luckily, there is a simple solution. Most of the time, we are interested in solving a problem with a classical description, and getting a classical answer out at the end of the computation. Then we can start our quantum computation in a standard encoded state, such as $|\overline{00\ldots0}\rangle$, which can be reliably created via fault-tolerant state preparation. At the end of the computation, we take the state, still encoded, and measure it using fault-tolerant measurement, getting a classical answer. Indeed, the classical answer is also encoded in some classical error-correcting code at this point, perhaps just the repetition code, or perhaps something more complicated. Then classical processing is used to extract the output of the computation. Since the basic model for fault-tolerance assumes classical computation is noiseless, it is safe to decode the classical data. In this way, the logical error rate can be made arbitrarily low, using the techniques we'll discuss in the following chapters.

If we have a quantum computation which takes qubits as input and also outputs qubits, this won't work. If possible, we should demand to be given qubits which are already encoded, and insist on outputting encoded qubits as well. Possibly we'll want to switch codes to do our fault-tolerant computation using a different QECC than the one provided to us, but fault-tolerant techniques exist for switching between codes. If the code used for input and output qubits is not a very good code (e.g., small distance), there may still be some unavoidable error in the process of switching into and out of the better code used for fault tolerance, but the error will likely be less than if the input and output qubits were completely unencoded.

Some years ago, I was at a conference where a skeptic about quantum error correction tried to explain what he thought was a problem with QECCs by making an analogy. He pointed out the unavoidable error due to encoding and decoding, as described above, and said it was like getting out of a car in the rain — there is not enough space to open your umbrella in the car, so you must get a least a little bit wet while simultaneously getting out and opening the umbrella. The solution of starting and ending encoded was already known (the skeptic was behind the times), so I pointed out that there is an analogous solution to avoid getting wet: If you always make sure to park in a covered lot, you can get out of the car and open the umbrella where there is more space while still being protected from the rain. Once the umbrella is open, you can safely leave the covered area and walk around under the protection of the umbrella. Fault-tolerant protocols work the same way. Of course, you might have to walk a bit further if the covered lot is not right where you want to park, but there is indeed a cost to fault tolerance.

10.1.5 Fault Tolerant Simulations and the Components of a Fault Tolerant Circuit

So, putting this together, what do we want out of a fault-tolerant protocol? The basic idea is this: We are given a circuit, broken down into a universal set of gates. We'd like to replace the qubits of the circuit with the logical qubits of a QECC. Then we'd like to perform a sequence of gates on the qubits, without ever leaving the protection of the code, that transforms the logical qubits with the same unitary transformation as the original ideal circuit we were given. And we'd like the sequence of gates we use to be fault tolerant, in the sense that errors on a small but constant fraction of the gates do not interfere with the getting the correct outcome for the logical qubits.

We can describe what we want as a *fault-tolerant simulation* of the circuit. We replace each location in the original circuit with a fault-tolerant *gadget* that does the same thing to logical qubits as the location is supposed to do in the ideal circuit.

Definition 10.4. Given a particular type L of location, specified precisely (e.g., not just that it is a gate location, but also the type of gate), a *gadget for* L is a QECC Q coupled with a circuit G_L, such that if the qubits involved in L are encoded into Q, then subjected to the circuit G_L, then decoded, all without errors, the effect is the same as if L were performed directly. The circuit G_L may involve adding and/or discarding physical qubits, which may or may not also be encoded in Q.

In other words, a gadget for a specific function is supposed to perform that function on the encoded state. If the encoder for Q is $\mathcal{E}$ and the decoder is $\mathcal{D}$, then

$$\mathcal{D} \circ G_L \circ \mathcal{E} = L. \tag{10.5}$$

Definition 10.4 does not guarantee that the gadget is in any sense fault-tolerant; I'll discuss in section 10.2 what is needed for a gadget to be fault-tolerant. In the simplest examples, the QECC used in a fault-tolerant protocol has only one encoded qubit, and in the definitions below, I will assume that. If the location involves multiple qubits but each code block only encodes one logical qubit, each logical qubit should be encoded in a separate block of the QECC, and the gadget circuitry will interact the different blocks as required. Another option for dealing with multiple qubits per block is to distinguish between locations which interact qubits encoded in the same block and locations which interact qubits encoded in different blocks. Then we'll need different kinds of gadgets to deal with these two different kinds of locations, even when the gate involved is otherwise the same.

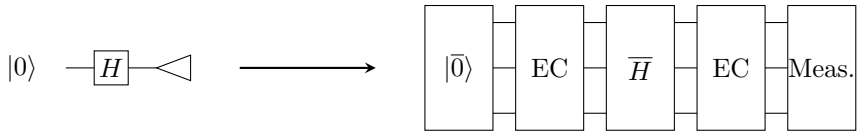

Figure 10.2: The fault-tolerant simulation of a circuit replaces each location with the corresponding gadget and puts error correction gadgets between each pair of other gadgets.

Gadgets can also be defined for other tasks, not directly corresponding to a location. In that case, the gadget is simply a QECC with a circuit. The proper functioning of the gadget has to be defined separately. The most useful sort of gadget that doesn't correspond to a location is an error-correction gadget. Obviously, an error-correction gadget is supposed to use the QECC to correct any errors pre-existing in the code, and a fault-tolerant error-correction gadget is supposed to do so even while new errors are occurring. The formal definition of a fault tolerant error-correction gadget is given in section 10.2.

Definition 10.5. A *fault-tolerant protocol* consists of a QECC Q along with the following types of gadgets:

- State preparation gadget for at least one type of state
- Measurement gadget for at least one type of measurement
- Gate gadgets for a universal set of gates
- Storage gadget
- Error correction gadget

The protocol may contain more than one gadget for a given type of location, and may contain some additional gadgets as well. All gadgets should satisfy some fault-tolerance criteria such as those given in section 10.2. Normally all gadgets associated with a given protocol use the same QECC; in cases where they do not, the protocol should also contain a code switching gadget that changes the QECC in which one or more logical qubits are encoded.

We don't usually bother explicitly describing a storage gadget, since a storage gadget can always be implemented by just putting a wait location for all physical qubits in the code. In principle, though, a fault-tolerant protocol could contain a different storage gadget involving non-trivial gates.

How do we put together gadgets in order to make a fault-tolerant circuit? Since each gadget for a location is supposed to perform the function of the location on the encoded state, obviously what we want to do is to replace each location in the original circuit with a corresponding gadget. However, that's not sufficient. In a noisy circuit, errors will occur, and in a large circuit, those errors will build up over time unless we are constantly performing error correction to eliminate them. The most common approach is to do a round of error correction as often as possible, namely between every adjacent pair of locations.

Definition 10.6. Let C be a circuit, broken down into locations as in definition 10.1. Then $FT(C)$, the *ideal fault-tolerant simulation of* C associated with a given fault-tolerant protocol, is the circuit created as follows: Take each location in C and replace it with the corresponding gadget of the fault-tolerant protocol, in the process replacing each qubit of C with a block of the QECC Q. After each state preparation gadget, gate gadget, or storage gadget, place an error correction gadget on each of the blocks of Q involved in the gadget. The *fault-tolerant simulation of* C is then $\widetilde{FT(C)}$. The *circuit size overhead* of $FT(C)$ is the number of locations of $FT(C)$ divided by the number of locations in C. The *space overhead* or *qubit overhead* is the ratio of the number of physical qubits involved in $FT(C)$ to the number of qubits involved in C, and the *depth overhead* or *time overhead* is the ratio of the depth of $FT(C)$ to the depth of C.

Note that we place error correction gadgets after the storage gadgets as well as after gate gadgets, since storage errors can occur even in wait locations. We don't need error correction gadgets after measurement gadgets, because the output of a measurement gadget is just classical information, and we are assuming that classical circuits don't suffer errors.

If the QECC used in the fault-tolerant protocol encodes $k > 1$ qubits per block, the fault-tolerant simulation must divide up the qubits of C into groups of k and encode them that way. The fault-tolerant protocol will probably then contain multiple different gadgets for a single two-qubit gate U, depending on whether U acts between qubits in the same block or between qubits in different blocks.

10.2 Formal Definition of Fault Tolerance

Now let us consider what we require for a fault-tolerant simulation to successfully simulate a low-noise logical computation using noisy physical gates. The definition of a gadget, definition 10.4, only requires that the gadget act correctly in the absence of errors. For a fault-tolerant protocol to truly tolerate faults, we'll need the gadgets to degrade gracefully in the presence of noise. If there are too many errors, we don't expect the gadget to work right, but if there aren't, there are two conditions we require: it should still behave correctly on the logical state, and it shouldn't propagate errors too badly.

The definitions in this section represent the most common notion of fault tolerance, but weaker or stronger definitions are possible as well, and have their place. Some protocols may need additional properties, requiring stronger definitions. On the other hand, when put together properly, gadgets satisfying weaker definitions can still achieve fault tolerance on the protocol as a whole.

10.2.1 Ideal Decoder and r-Filter

In order to define precisely what it means for a gadget to be fault tolerant, we'll need to talk about the logical state encoded in a QECC, and about the number of errors present in a noisy codeword. However, by just looking locally at a circuit, there is no way to tell what the "correct" encoded state is supposed to be. Luckily, we don't need to discuss that to define fault tolerance. A gadget is given some encoded state, which may be right or may be wrong, and it does something to that; we must check if the "something" is what we intended to do or not.

To talk about the number of errors in a state, we therefore only consider the number of errors relative to *some* codeword, not necessarily the "correct" one, since we don't know what the correct codeword is supposed to be. We can codify this by thinking of a projector:

Definition 10.7. The *r-filter* for the QECC Q is the projector on the subspace spanned by states of the form $E|\psi\rangle$, where $|\psi\rangle \in Q$ and E is an error of weight at most r. Pictorially, I will draw an r-filter as:

(10.6)

The doubled horizontal lines in this picture represent a block of the QECC Q rather than single physical qubits.

When we apply an r-filter to some state, we get a state which contains only errors of weight less than or equal to r. Thus, any codeword passes through the r-filter unchanged. Components of the state with more errors on them are dropped. The r-filter is thus a test we can apply to see if there are many errors on the state (relative to any codeword). If

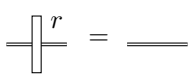

(10.7)

then the input state has r or fewer errors on it.

To talk about the logical state of a code, we should decode it. To do so, we would need to correct errors, and using a real circuit, the attempt at decoding would have a chance of introducing additional errors, and

the state we end up with might not be the same logical state as we had before we tried to decode. However, we're only *talking* about the logical state; we don't actually have to produce it. Therefore, we can imagine decoding using an ideal decoder that does not have any faults.

Definition 10.8. The *ideal decoder* for the QECC Q is the quantum channel that takes a state (possibly with errors) encoded in Q, corrects the errors, and then decodes the logical state, discarding all ancilla qubits. I will draw an ideal decoder as follows:

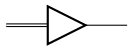

(10.8)

The doubled horizontal line on the left of the picture represents a block of Q. The single horizontal line on the right of the picture is the logical qubit after decoding.

For now, it is sufficient for the decoder to keep only the logical qubit. Later on, we'll also want to consider decoders that keep the syndrome information they extracted during error correction.

10.2.2 Fault-Tolerant Gate Properties

We're now ready to define what it means for a gate gadget to be fault tolerant. Using the pictorial language we started to develop above, we'll be able to draw two pictures that define properties that a fault-tolerant gate gadget must satisfy. For the purposes of these definitions, we can include storage gadgets as gate gadgets. Just think of them as performing the identity gate.

Definition 10.9. The picture to represent a noisy gate gadget with exactly s faults is

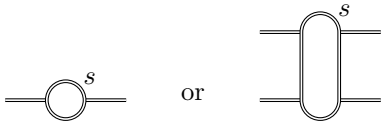

(10.9)

-for one- and two-qubit gates, respectively. Each doubled horizontal line represents a single block of the QECC.

The picture to represent an ideal gate performed on unencoded qubits without noise is

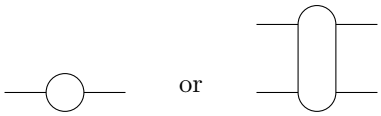

(10.10)

for one- and two-qubit gates, respectively. Each single horizontal line represents a single unencoded qubit.

In an independent stochastic noise model, these pictures can be interpreted as completely positive maps. For some particular realization of the noisy gate gadget circuit, there are some number s of faults specified by a fault path S. Replacing the locations in S with the CP maps corresponding to faults in the noise model (usually we will want to rescale to make the maps trace-preserving, if possible) gives a linear map corresponding to the picture. The picture for a gadget with s faults thus represents many different maps, depending on the exact locations which are faulty and on the precise error model.

The ideal decoder and r-filter are also CP maps; the decoder is trace preserving, but the r-filter is not. We can compose them with the CP map corresponding to a realization of a gate gadget to get more CP maps, and the properties for fault tolerance will be defined as equations relating CP maps derived this way. We can thus represent such equations simply as pictures.

Definition 10.10 (FT Gate Error Propagation Property)**.** Suppose we have a gate gadget associated with a QECC with distance $2t + 1$ (i.e., it corrects t errors). If it is a single-qubit gate gadget, it satisfies the *FT Gate Error Propagation Property*, abbreviated *GPP*, if, whenever $r + s \leq t$,

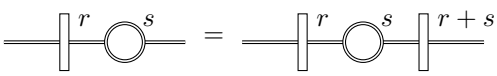

(10.11)

A two-qubit gate gadget satisfies the GPP if, whenever $r_1 + r_2 + s \leq t$,

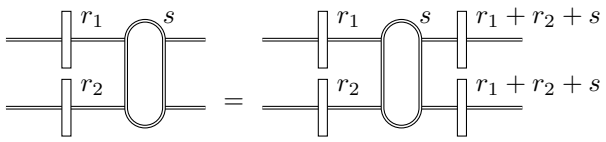

(10.12)

For both equations, the faulty locations on both sides of the equation have the same fault path and error maps substituted in.

These equations use filters on the left to ensure that the input state to the CP maps can be considered to be at most r errors away from a codeword. The equations then demand that, given such an input state, the state exiting the gadget be at most $r + s$ or $r_1 + r_2 + s$ errors away from a codeword. In the case of the two-qubit gate gadget, we allow errors to propagate between the two blocks of the code. Thus, even if $s = 0$, so the gadget itself is faulty, the number of errors in a block may increase as a result of error propagation. However, we insist that the number of errors ending up in a single block is limited by the total number of errors $r_1 + r_2$ input in the two blocks plus the number s of new faults. This is the sense in which this property limits the error propagation.

Note that for the two-qubit gate gadget, the condition uses *separate* filters on the two blocks of the code involved in the gadget. Thus, the final state of the two blocks taken together might have a total of $2(r_1 + r_2 + s)$ errors on it.

For the Gate Error Propagation Property, we only impose the equations when the total number of errors on input states plus faults in the gadget is at most t. When there are more than t total errors floating around, we don't in general insist that our gadgets have to work correctly. In many cases, fault-tolerant gate constructions do continue to satisfy these equations even when there are more errors, but that is an additional property not required by the basic definition.

Definition 10.11 (FT Gate Correctness Property)**.** Suppose we have a gate gadget associated with a QECC with distance $2t+1$. If it is a single-qubit gate gadget, it satisfies the *FT Gate Correctness Property*, abbreviated *GCP*, if, whenever $r + s \leq t$,

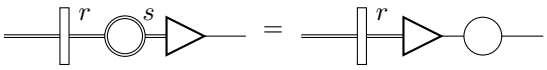

(10.13)

A two-qubit gate gadget satisfies the Gate Correctness Property if, whenever $r_1 + r_2 + s \leq t$,

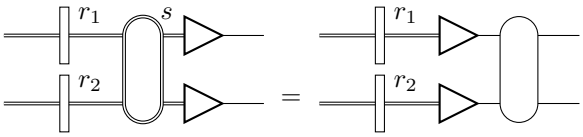

(10.14)

These equations must hold for any choice of CP maps substituted in for the faulty locations on the left-hand side.

What do these conditions mean? They say that if we perform the noisy gate gadget and then decode, we get the same thing as if we decode and then perform the gate gadget. The combination

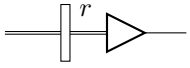

(10.15)

extracts the logical state of the input after limiting the number of errors. The RHS of each equation thus outputs the state we should get by doing an ideal gate on the logical state. The LHS is the state we actually get. The Gate Correctness Property thus ensures that a noisy gate gadget performs the correct operation on the encoded state, generalizing the definition of a gadget to the case in which there are errors.

Again, we only insist that the condition hold when the total number of errors floating around is at most t. In this case, that is usually all we can hope for. That is because if there is any arrangement of errors that allows all $r_1 + r_2 + s$ errors to concentrate in a single block, on the LHS, the concentration will happen, possibly giving a logical error which is not corrected by the ideal decoder, whereas on the RHS, all the errors are corrected immediately before there is any opportunity for propagation.

10.2.3 Fault-Tolerant Preparation and Measurement Properties

The properties for fault-tolerant state preparation and measurement gadgets are similar:

Definition 10.12. The picture for a single-qubit state preparation gadget with exactly s faults is

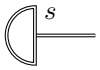

(10.16)

The picture for a single-qubit measurement gadget with exactly s faults is

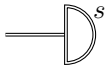

(10.17)

In both cases, the doubled horizontal lines represent encoded blocks of the QECC. The measurement gadget outputs classical information, generally a single bit.

The pictures for ideal preparation of a single-qubit state and ideal single-qubit measurement are

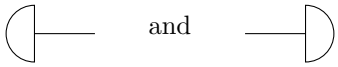

(10.18)

The horizontal lines represent single unencoded qubits, and the ideal measurement outputs a classical bit.

Again, these pictures represent CP maps. A noisy preparation gadget is a CP map that takes no input and outputs a state in the Hilbert space of the QECC. A noisy measurement gadget is a CP map that takes a noisy codeword as input and outputs a classical bit.

For the fault-tolerant preparation gadgets, there is no input, so we don't need to precede them by filters.

Definition 10.13 (FT Preparation Error Propagation Property)**.** Suppose we have a preparation gadget associated with a QECC with distance $2t + 1$. The gadget satisfies the *FT Preparation Error Propagation Property*, abbreviated *PPP*, if, whenever $s \leq t$,

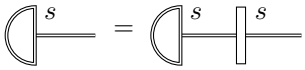

(10.19)

Definition 10.14 (Preparation Correctness Property)**.** Suppose we have a preparation gadget associated with a QECC with distance $2t+1$. The gadget satisfies the *FT Preparation Correctness Property*, abbreviated *PCP*, if, whenever $s \leq t$,

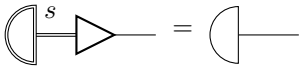

(10.20)

In other words, when $s \leq t$, a preparation gadget with s faults in it should output a state with no more than s errors in it, and the state should be an encoding of the correct state.

For the measurement gadget, we only have one property. We don't need to worry about error propagation through a measurement gadget because the output only involves classical information, which we are assuming is error-free.

Definition 10.15 (FT Measurement Correctness Property)**.** Suppose we have a measurement gadget associated with a QECC with distance $2t + 1$. The gadget satisfies the *FT Measurement Correctness Property*, abbreviated *MCP*, if, whenever $r + s \leq t$,

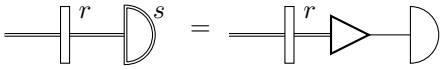

(10.21)

That is, if the initial state has no more than r errors, and there are not too many errors in the measurement gadget, the classical outcome of the measurement should be the same as if we did an ideal measurement on the decoded state.

10.2.4 Fault-Tolerant Error Correction Properties

Fault-tolerant error correction gadgets are a bit different from gadgets associated with locations. For other gadgets, we are concerned that error propagation is not too severe, but error correction gadgets are supposed to actually *reduce* the number of errors in the state. Of course, if there are faults in the error correction gadget itself, they may introduce more errors that must be corrected in a later error correction gadget.

Definition 10.16. A fault-tolerant error correction gadget (which I will usually abbreviate FTEC in the future) is represented by the following picture:

(10.22)

The horizontal lines represent blocks of the QECC.

As usual, we can interpret this picture as a CP map for any particular realization of the noisy circuit. Error correction gadgets invariably involve adding extra ancilla qubits and produce syndrome information. The syndrome information may either be in the form of classical bits or as extra qubits, and is usually discarded at the end of the gadget.

Definition 10.17 (FT Error Correction Recovery Property)**.** Suppose we have an error correction gadget associated with a QECC with distance $2t + 1$. The gadget satisfies the *FT Error Correction Recovery Property*, abbreviated *ECRP*, if, whenever $s \leq t$,

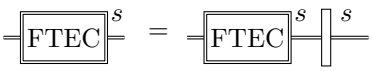

(10.23)

Note that the ECRP does not involve a filter on the input state. This is important: We want our FTEC gadgets to return us to a codeword (or a codeword with s errors when there are s faults in the FTEC gadget) no matter how many errors there are to start with. Otherwise, if we ever accumulate too many errors in a block, the rest of the circuit is a loss. When there are more than t errors in a block, we may not be able to decode correctly, but at least we'd like the remaining gadgets after the FTEC to do the right thing, even if it's on the wrong logical operator. That localizes the logical error to a small number of gadgets. In particular, when we prove the threshold theorem, we'll use concatenated codes to get more and more accuracy, but that won't work if sub-blocks of the code aren't brought back to *some* codeword, even if it is not the correct one.

Definition 10.18 (FT Error Correction Correctness Property)**.** Suppose we have an error correction gadget associated with a QECC with distance $2t + 1$. The gadget satisfies the *FT Error Correction Correctness Property*, abbreviated *ECCP*, if, whenever $r + s \leq t$,

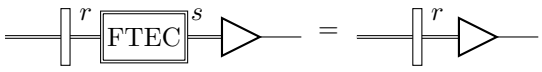

(10.24)

This property says that when the total number of errors (input errors plus faults in the gadget) is at most t, the encoded state does not change during an FTEC gadget.

10.2.5 Fault Tolerance Properties for Different Error Models

In the basic model for fault tolerance, we allow the faults in a gadget to be general CP maps, but ones which are independent between different locations. However, if you look at the definitions of the fault tolerance properties given in this section, you'll see that all of them are linear equations. That means that a version of theorem 2.4 applies in this case as well:

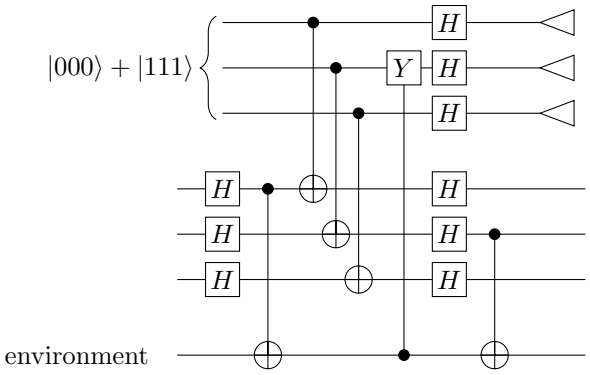

Figure 10.3: An example of a gadget interacting with a persistent environment on a fault path of size 3.

Theorem 10.1. *Consider a realization C_1 of a noisy gadget circuit with a fault path of size s, and suppose that the location of each fault is replaced by a linear Hilbert space operator (e.g., specific Kraus operators of the CP maps). Let C_2 be C_1 with one particular faulty location L replaced by a different linear Hilbert space operator. Suppose the operator for L in C_1 is E and the operator for L in C_2 is F, and let C_3 be the circuit realization C_1 with L replaced by $\alpha E + \beta F$, for any complex numbers α and β. If the gadget satisfies the relevant fault tolerance properties for realizations C_1 and C_2, then it also satisfies them for C_3.*

As a consequence of this, we need not check the fault tolerance properties for arbitrary CP maps inserted for faults. It is sufficient to check them for a basis of errors. In particular, Pauli errors suffice.

Corollary 10.2. *If a gadget satisfies the relevant fault tolerance properties when arbitrary Pauli errors are inserted for all faults, then it satisfies the fault tolerance properties when arbitrary CP maps are inserted for faults.*

Recall that a Pauli error model means that the location acts correctly and then afterwards there is a Pauli error, so when I say a "Pauli error is inserted" at a location, I mean that it is inserted after the correct action of the location (unless it is a measurement location, in which case the error flips the outcome of the measurement). This corollary is very convenient, since it is much easier to check the properties for just Pauli errors than for general CP maps.

The logic behind theorem 10.1 has a more far-reaching consequence than just convenience. We could also take the superposition when we change the faults in multiple locations, and the result would still work. This is not necessary in a basic model for fault tolerance, but it allows us to talk about certain correlations between errors, and will actually be needed for proving the threshold theorem. Indeed, once we have checked the fault tolerance properties for Pauli errors, we know they hold under the most general error that can happen to a circuit with faults in those s specific locations.

Theorem 10.3. *Consider a realization of a gadget with a particular fault path S, $|S| = s$. Suppose a gadget satisfies the relevant fault tolerance properties when arbitrary Pauli errors are inserted at the locations of S. Then it also satisfies the fault tolerance properties when subjected to a persistent environment which starts in an arbitrary state (possibly even one entangled with the qubits involved in the gadget), and interacts with the locations of S through arbitrary unitaries, as illustrated in figure 10.3.*

This picture allows for arbitrary dynamics within the environment, since the unitaries implementing the self-interaction can be absorbed into the unitaries interacting the system and environment.

We haven't even defined the fault tolerance properties in this case, but it is straightforward to do so by extending the pictures to include the environment and then tracing over it at the end of each picture. We don't put a restriction on the initial state of the environment, but consider it as extra input qubits for the circuit. For instance, see figure 10.4. The resulting equations are again equalities of CP maps; indeed, since

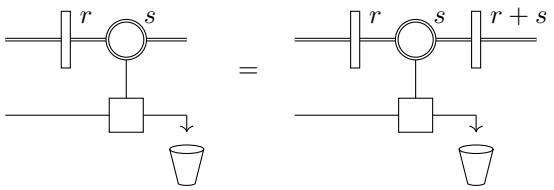

Figure 10.4: The one-block GPP with an environment. The s locations of the fault path within the gate gadget are arbitrary interactions with the environment register (bottom line), and the left-hand side and right-hand side have the same interactions.

the interactions with the environment are unitary, we can consider the picture to represent a linear operation on the Hilbert space. The gadget may involve measurement, so to make a linear Hilbert space operator, we purify each measurement, replacing the classical computations afterwards with quantum gates (with no additional faults). The filters that appear in the pictures are projections, so the operators we get will not be unitary.

Because we don't care what happens to the environment, we need not compare the environment on the LHS of each equation with the environment on the RHS of each equation. Indeed, in the various correctness properties, the environment on the LHS interacts with the faults in the gadget, whereas there *are* no faults on the RHS. The final state of the environment therefore differs for the LHS and RHS of the correctness properties.

Proof. Let us label the interactions between the environment and the faulty locations in the circuit as $U_1, \ldots, U_s$, and say that the ith faulty location L_i involves g_i qubits. We can write

$$U_i = \sum_{P \in \hat{\mathsf{P}}_{g_i}} P \otimes V_{i,P}, \tag{10.25}$$

where $V_{i,P}$ acts on the environment qubits. Since U_i is unitary,

$$\sum_{P,Q \in \hat{\mathsf{P}}_{g_i}} PQ \otimes V_{i,P}^\dagger V_{i,Q} = I \otimes I, \tag{10.26}$$

which means

$$\sum_{P \in \hat{\mathsf{P}}_{g_i}} V_{i,P}^\dagger V_{i,P} = I \tag{10.27}$$

$$\sum_{P \in \hat{\mathsf{P}}_{g_i}} V_{i,P}^\dagger V_{i,PQ} = 0 \quad \forall Q \in \hat{\mathsf{P}}_{g_i} \setminus \{I\} \tag{10.28}$$

Let M be the operator corresponding to a picture involving the environment, with interactions U_i in place. Let $M_{\{P_i\}}$ be the operator corresponding to the same picture, but where U_i is replaced by $P_i \otimes V_{i,P_i}$. Then

$$M = \sum M_{\{P_i\}}. \tag{10.29}$$

That is, the operator corresponding to the picture with unitary interactions with an environment can be written as the sum of operators corresponding to different Pauli fault paths.

In the FT error propagation properties and the FT error correction recovery property, both sides of the equation involve the same set of faults in the system. By the hypothesis, the LHS and RHS match when we substitute Pauli errors, resulting in pictures $M_{\{P_i\}}$. Therefore, the sums M match term by term, so the totals match as well.

For the various FT correctness properties, let $M = \sum M_{\{P_i\}}$ be the LHS of the equation. The LHS with Pauli errors in the faulty locations and V_{i,P_i} in the corresponding environment locations matches the RHS side picture, which is a tensor product between the system qubits and the environment (still with V_{i,P_i} acting in appropriate places). The total LHS M is therefore equal to the RHS picture tensored with a sum of the V_{i,P_i}s acting on the environment.

The only question is whether the trace over the environment gives a different value for the LHS and RHS. We can calculate this by looking at what happens to the environment's trace for each faulty location L_i. The environment undergoes

$$\sum_{P \in \hat{\mathsf{P}}_{g_i}} V_{i,P} \tag{10.30}$$

at interaction location i, and its trace becomes

$$\operatorname{tr} \rho \left(\sum_{P,Q \in \hat{\mathsf{P}}_{g_i}} V_{i,P}^\dagger V_{i,Q} \right) = \operatorname{tr} \rho \tag{10.31}$$

by equations (10.27) and (10.28). □

As a consequence of theorem 10.3, once we fix the locations of the faults in a circuit, anything, including horrible correlated errors, can happen at the faulty locations, and the fault tolerance properties will still pull us through, allowing things to work correctly. However, the theorem does *not* immediately allow us to generalize the independent stochastic error model to arbitrary correlated models. We'll want to calculate the probability of having a logical error, and that involves summing over multiple fault paths. The probability of having a particular fault path is not even well-defined in more general error models, so we'll need to be careful.

10.3 Statement of the Threshold Theorem for the Basic Model

The main goal of part II is to prove the threshold theorem. This is one of the key results in the theory of quantum information. If it were not true, it would probably be impossible to build big quantum computers. The threshold theorem sets a definite goal for experimentalists hoping to build a scalable quantum computer: It says that if you can make the basic components of the computer good enough, and can make enough qubits, then that suffices, and error-correcting codes and fault-tolerant protocols exist that can take you the rest of the way. The point here is that "good enough" is a value independent of the algorithm you want to run, so you don't need to continue to improve your experimental error rates to solve a new, bigger problem. (Of course, you may need more qubits to solve a bigger problem.)

Theorem 10.4 (Threshold Theorem for Basic Model of Fault Tolerance)**.** *Suppose a system satisfies a basic model for fault tolerance, with $p_P = p_G = p_S = p_M = p$. Then there exists a family of fault-tolerant protocols $\mathcal{F}_l$ and a threshold error rate p_T such that, if $p < p_T$, then for any ideal quantum circuit C which starts with preparation locations and ends with measurement locations, and any $\epsilon > 0$, there exists an l such that the output distribution of $\widetilde{FT_l(C)}$, the noisy fault-tolerant simulation of C by $\mathcal{F}_l$, has statistical distance at most ϵ from the output of C. When C has T locations, then $FT_l(C)$ has $O(T \operatorname{polylog}(T/\epsilon))$ locations (i.e., the circuit size overhead is $O(\operatorname{polylog}(T/\epsilon))$.*

In other words, if the physical error rates for all locations are below the magical threshold error value p_T, there exists a fault-tolerant protocol that makes the logical error rate on the complete circuit as small as we like. Note that we actually need a *family* of FT protocols to make this work — as the circuit gets bigger, or the logical error rate we'd like to achieve gets smaller, than we need to work harder at getting rid of errors, which means more overhead and a more involved FT protocol. The nice thing about the threshold theorem is that the extra work needed scales reasonably, only as a polynomial in the log of T/ϵ. Scaling up to a really really big quantum computer is a lot of work even for an ideal circuit, but adding fault-tolerance

to the circuit does not require much more effort than it does to add fault-tolerance to a merely big quantum computer.

Unfortunately, while the asymptotic scaling for large T/ϵ is good, the actual amount of overhead needed is still pretty large. The problem is that the constants hidden by big-O notation are significant. Even relatively efficient fault-tolerant protocols have a space overhead of hundreds, thousands, or even tens of thousands of physical qubits per logical qubit, and many are much worse than that. While it's not mentioned explicitly in the theorem, the overhead is also dependent on p/p_T, so it helps to get the physical error rates down as much as possible, but even then the costs are high. One approach is to abandon the notion of a family of protocols with a threshold, and just pick a specific FT protocol that works for the size of the circuit you are interested in. By carefully choosing a protocol, you may be able to get the overhead down, although with existing protocols, it is still likely be at least a few dozen physical qubits per logical qubit. And of course, there may exist fault-tolerant protocols with much lower overhead than any we know of today.

The threshold theorem is proven using concatenated codes, introduced in section 9.1. The basic idea is straightforward: Given a fault-tolerant protocol $\mathcal{F}$, we can take any circuit and produce the fault-tolerant simulation $FT(C)$ of that circuit. Provided the error rate p per location is small enough, the logical error rate for the FT simulation should be less than the physical error rate, and we have improved matters by using the fault-tolerant simulation. Then we do it again, and take the FT simulation of the simulation, i.e., $FT(FT(C))$. That improves the error rate some more. With multiple iterations, we can drive the error rate down very rapidly. The family of fault-tolerant protocols $\mathcal{F}_l$ that we need for the threshold theorem is then the fault-tolerant protocol $\mathcal{F}$ concatenated l times. The result is really an FT protocol that uses an l-level concatenated code. I will explain how to make this intuitive argument precise in chapter 14. The main challenge is to properly define and determine the "logical error rate" for a fault-tolerant simulation.

Topological codes, discussed in chapter 17, can also be used to get a threshold, as can families of low-density parity check codes (LDPC codes) with a constant rate. It may be other families of codes exist that can give a threshold. We sometimes talk about the threshold for a specific code family, and sometimes just about "the threshold" for fault tolerance. In the latter case, we are talking about the best (i.e., highest) threshold p_T optimized over all possible families of codes. In addition, different fault-tolerant protocols for the same code family can lead to substantially different "threshold" values, but the real threshold is defined using the best possible FT protocol.

The threshold theorem can be extended in various ways. One obvious way, still sticking to a basic model for fault tolerance, is to let the error rates for different types of locations be different. In that case, the threshold is no longer a single number, but a surface in the 4-dimensional space of error rates (p_P, p_G, p_S, p_M). The threshold surface separates the noiseless point $(0, 0, 0, 0)$ from the completely noisy point $(1, 1, 1, 1)$, and the extended theorem then says that we can achieve error rate ϵ for the outcome distribution for any point on the noiseless side of the surface with polylogarithmic overhead. It is also possible to go beyond a basic model by loosening or removing some of the assumptions. Not all of the assumptions can be relaxed; which ones can and which ones can't is discussed in chapter 15. Even when it is possible to derive a threshold with relaxed conditions, the actual numerical value of the threshold may decrease significantly, or the overhead may increase, or both. Building a fault-tolerant quantum computer will therefore likely involve making a number of trade-offs in order come up with an implementation for which the error rate is below the relevant threshold value.

10.4 Different Ways of Computing the Threshold and Overhead

Since the threshold error rate determines whether a given experimental implementation will or will not be useable for fault-tolerance, a great deal of effort has gone into determining the actual value of the threshold for various code families. Likewise, the overhead (of every kind) determines how many resources will be needed for a given computation, and has also been a subject of intense study. However, comparing threshold and overhead values you might find in the literature is not completely straightforward because of different techniques used to derive them. First all, remember that for a specific code family, it might be possible to come up with better FT gadgets that give a better threshold value or lower overhead. Secondly, to be

fair, you should only compare estimates derived using comparable techniques, since different techniques have different sources of inaccuracy.

An estimate of the threshold and overhead will generally involve some combination of rigorous proof, simplifying assumptions, and statistical sampling. Pretty much every approach uses some simplifying assumptions — indeed, by working with a basic model of fault tolerance, you are already making a number of simplifying assumptions — but some approaches go further. It is perhaps worth distinguishing between assumptions about the quantum computer (e.g., assuming an independent stochastic error model) and assumptions about the calculation (e.g., assuming that a particular type of state preparation gadget can be performed reliably under conditions of interest). The former type of assumption gives you a complete threshold estimate, albeit one that only applies under the given conditions.

Assumptions about the calculation are a bit more tricky to evaluate: Sometimes the assumption is a conservative one, in which an effect which may lower the threshold value is simplified to have the worst possible effect it can have. An approach which only uses conservative assumptions will give a threshold value that is definitely lower than the true value and an overhead that is higher than the true value by an unknown amount. The advantage of this is that we can be sure we have a lower bound on the threshold and an upper bound on the overhead. Sometimes the assumption is a reasonable approximation, in which case we may expect that the calculated threshold and overhead are roughly the same as it would be without the assumption, maybe slightly higher or lower. However, as long as the approximation hasn't been fully checked, there is a chance it is wrong, so we cannot have full confidence in any value derived with the assumption. Occasionally, the assumption is obviously an over-optimistic one, giving a significant *overestimate* of the threshold value. Optimistic assumptions are sometimes used to tease out how much of the threshold error rate comes from different effects, or to estimate upper bounds on thresholds for a code family. It is important not to think of thresholds calculated using optimistic assumptions as actual threshold values, since they don't provide any kind of guarantee for an experimentalist achieving that error rate.

One particularly widespread example of an optimistic assumption is a *phenomenological error model*. In a phenomenological error model, there is an error rate per physical qubit per time step (regardless of gates) and an error rate on each bit of the error syndrome that is measured. The phenomenological error model is a greatly simplfied model which still includes constantly occurring errors and imperfect error syndrome measurements. It is used to get a quick handle on the general performance of a QECC, syndrome extraction, and syndrome decoding method without having to design and analyze detailed fault-tolerant circuits. Usually this is done primarily to learn about the threshold and not for overhead. A threshold in a phenomenological model should *not* be confused with the threshold derived from a full circuit model; they are not at all comparable. It makes some sense to compare phenomenological thresholds for different FT protocols with each other, but even there, caution is needed, as the relationship between the phenomenological threshold and the circuit threshold can vary between codes and even between different FT protocols for the same code. For instance, the number of gates needed to extract a bit of the syndrome in a full circuit analysis can be greatly different between different protocols, but a phenomenological noise model completely ignores this important contribution to the threshold.

The next big distinction is between rigorous proofs, simulations of FT protocols using statistical sampling, and analytical estimates. Rigorous proofs use only conservative assumptions about the calculations and carefully justify any assumptions needed to be sure they actually are conservative. Consequently, a rigorous proof provides a lower bound on the threshold and upper bound on the overhead given the stated assumptions about the computer.

Simulations, in contrast, simulate a big chunk of a FT circuit on a classical computer and run it many times, randomly generating errors according to the appropriate error model and calculating the logical error rate for the run. Classical simulations of general quantum circuits are unlikely to be possible, but as you'll see, the main parts of many FT protocols are composed just of Clifford group gates, and simulating Clifford circuits with Pauli errors can be done efficiently using procedure 6.4. In some cases, additional properties of the FT circuit and QECCs used can lead to additional simplifications of the simulation. Simulations invariable require some assumptions which may lead to good approximations, but are not necessarily conservative ones. Consequently, a well-done simulation can give more accurate threshold and overhead estimates than a rigorous proof, but we can never be quite certain if the true values are higher or lower than the simulated

values.

An analytical estimate focuses on formulas for the performance of a fault-tolerant protocol. They may be derived in part from simplifying assumptions and may use empirical results from simulations to determine constants in the formulas. The purpose of an analytical estimate is clarify the role of certain parameters and to develop some insight into what changes when they are varied. For instance, you might approximate the logical error rate or overhead of a protocol as a function of p/p_T in order to understand what can be gained by improving the physical error rate p in the quantum computer.

Note that some proofs also use statistical methods as part of the threshold calculation. In this case, there is some statistical error, but the size of the error is controlled and known, so the technique comes with a guarantee that we cannot be much above the true threshold value, in contrast with simulations, which cannot have such a guarantee.

Another distinction between proofs and simulations comes in the error models used. Often, rigorous proofs use an adversarial error model within the basic model for fault tolerance. That is, they work with the worst possible error model consistent with a given value of the error rate p. Indeed, as we'll see in chapter 14, the threshold proof actually uses an even broader error model which involves some potential correlation between qubits. Simulations usually have to work with some particular Pauli error model. Frequently X, Y, and Z errors are given the same probability, so the error model is related to the depolarizing channel. Thus, proofs generally apply to a broader range of quantum computers than simulations.

There is often a difference of an order of magnitude or more between the rigorously proven value of the threshold for a given family of codes and that derived using simulations. For instance, the best known threshold value comes from Knill's technique of using concatenated error-detecting codes to prepare ancilla states (see section 16.1). Simulations of the technique suggest a threshold error rate of a few percent, say 3%, depending on the error model, whereas the best existing proof for this approach shows that the threshold is at least 10^{-3}, thirty times smaller. Most likely, the simulations are closer to the correct value, but as noted above, we cannot have full confidence that they are underestimates and not overestimates.

10.4.1 Tips For Comparatively Evaluating Fault-Tolerant Protocols

FT protocols are complicated things, with many different components. Moreover, the various different aspects of an FT protocol can interact in complicated and unexpected ways, so, for instance, a gate gadget or FTEC technique that works well for one protocol can be poorly suited for another protocol even if the QECC is the same. That makes it challenging to determine which of the many existing FT techniques is a good choice for a protocol you are designing.

Today, most comparative information about the relative strengths and weakness of different FT protocols comes from simulations. In the early days of fault-tolerant quantum computation, there were a number of unreliable simulations of the threshold. The methodology has improved, but if you are not careful, it is easy to find yourself making a misleading comparison. Here is a checklist to think about as you go about deciding between FT protocols.

- *There is no "best":* It's rare to have an FT technique which, in isolation, is uncategorically *better* than another. As I have already noted, the different components of an FT protocol interact, and so they need to be chosen to be well-suited to each other. If you go through a list and try to pick the "best" QECC, the "best" state preparation method, and so on, without seeing how they work together, you will not even end up with a functional protocol, and certainly not the "best" protocol that could be devised. Some techniques might be *usually* worse than others, but perhaps in the right context, they can be the optimal solution to some problem. I tend to view the array of FT techniques in the literature as a toolbox, and you want to pick a tool that is right for the job you are actually trying to do.

- *Check the assumptions:* Make sure to read carefully what assumptions and simplifications are made for the simulations (or proofs or analytic estimates) you are relying on for the comparison. Certainly, you should be careful about comparing a threshold estimated via simulation to one bounded below by a proof. Also, pay close attention to things like use of a phenomenological error model. In general,

you should be aware of what error model is being used in a simulation; a comparison between two simulations with different error models may be misleading.

- *Check which aspects of the protocol are included:* It has become common to cite threshold values based on simulations of a pure storage scenario, that is, one for which only a FTEC gadget is run repeatedly, and not any gate gadgets or even preparation or measurement gadgets. While this makes comparison between two such threshold values relatively straightforward, it can sometimes overestimate the threshold by an amount that may differ between protocols. Generally, simulating only storage is reasonable because FTEC consumes a large fraction of the error budget of an FT protocol, but sometimes there are additional reductions to the threshold that come from other gadgets. Overhead computations are sometimes for storage only and sometimes for full protocols. Be sure of which you are looking at, and only compare two overhead calculations if they are calculating the same thing. Also, be aware that different protocols for FTEC might constrain the rest of the protocol in ways that produce a very different overhead for the full protocol even when overhead for pure storage is similar.

- *Consider the tradeoffs:* Sometimes the tradeoffs between FT protocols are reasonably straightforward, such as one protocol with a higher threshold vs. a second with a lower overhead. But there are other properties which can also be important, including connectivity of the physical qubits (for instance, 2-dimensional nearest-neighbor gates vs. long-range gates), speed of the syndrome decoding algorithms, behavior under different error models, and more. In any given implementation, some of these properties may be more salient than others. A good understanding of the full range of properties of the FT protocols under consideration will help you choose one that is most appropriate for the specific implementation you have in mind (if any).

- *Compare the degree of optimization:* Finally, be aware that some protocols have been intensely studied and have undergone a high degree of optimization to improve performance in all aspects. By comparison, a newly proposed protocol may look inefficient or seem to have too many requirements. But that doesn't mean it is useless — it may be that with further study, or in conjunction with other new fault-tolerant tricks, the new protocol can become competitive with the old one. Again, keeping a large toolbox of FT techniques allows us to study different combinations which may allow apparently inferior approaches to shine.

Chapter 11

If Only It Were So Easy: Transversal Gates

This chapter and the next two chapters (chapters 12 and 13) will explain how to create gadgets that satisfy the fault-tolerance properties we defined in chapter 10. We'll start with the simplest case, that of transversal gates. You already saw an example of a transversal gate in section 10.1.3, so you know how straightforward they are. There's not much to be said about performing transversal gates, so in this chapter, I'll mostly focus on the question of figuring out which gates can be performed transversally for a given QECC.

Since transversal gates are so nice, we generally like to build FT protocols using codes for which many gadgets can be performed transversally. The 7-qubit code is particularly nice, as measurement and all Clifford group gates can be performed transversally. Sadly, to get a full universal set of gates, we need to add something non-transversal. This is not just a property of the 7-qubit code, but is true for any QECC. If it were not true, the theory of fault tolerance would be a lot simpler.

11.1 What is a Transversal Gate?

11.1.1 Definition of Transversal

Transversal gates are constructed so that they automatically satisfy the FT Gate Error Propagation Property. In particular, a transversal implementation of a gate gadget should never change the weight of a pre-existing error within a single block of the QECC. One way to achieve this is by just using single-qubit gates, but we can also talk about multiple-qubit transversal gates, using the following definition:

Definition 11.1. Let $\mathcal{F}$ be a quantum operation acting on a Hilbert space $\mathcal{H}_{2^n}^{\otimes m}$, interpreted as m blocks each consisting of n qubits. Then $\mathcal{F}$ is *transversal* if $\mathcal{F} = \bigotimes_{i=1}^{n} \mathcal{G}_i$, where $\mathcal{G}_i$ acts on the 2^m-dimensional Hilbert space composed of the ith qubit from each of the m blocks.

Of course, this definition can easily be extended to work for qudits as well as for qubits. Since we're interested in fault-tolerance, we invariably consider situations where each block of n qubits forms a QECC. Almost always, all m blocks are separate blocks of the same QECC. The operation $\mathcal{F}$ is frequently a unitary, but we don't require that, and occasionally we want to talk, for instance, about transversal measurements.

Often, all the $\mathcal{G}_i$ are the same gate, but I will not require that for the definition of transversal. If all $\mathcal{G}_i$ are equal to $\mathcal{G}$, I may describe the gate $\mathcal{F}$ as a *transversal* $\mathcal{G}$ to indicate its construction. (The phrase "bitwise $\mathcal{G}$" is also sometimes used.) Because it is the most common case, sometimes in the literature, you will find the notion of transversal gates restricted to having all $\mathcal{G}_i$ identical, but there is no real reason to do so.

A gate consisting of a tensor product of single-qubit gates certainly is transversal, with $m = 1$, but it is also possible to have transversal gates with $m > 1$. For instance, consider figure 11.1, illustrating the transversal CNOT on two blocks of 7 qubits each.

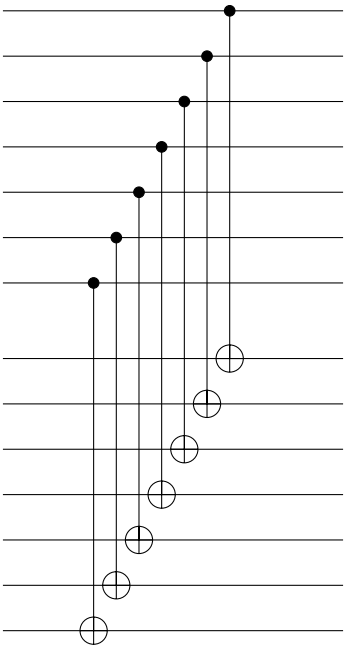

Figure 11.1: The transversal CNOT gate acting on two blocks of the 7-qubit code.

11.1.2 Transversal Gates Satisfy the FT Gate Properties

The point of this definition is that a transversal gate will always satisfy the GPP. The GCP requires a little more work, but actually, all the work just goes into checking that the transversal gate is in fact a gadget for the desired type of location — in other words, that it maps codewords correctly to codewords.

Proposition 11.1. *Suppose the circuit $\mathcal{F}$ is a gate gadget for the QECC Q and $\mathcal{F}$ is transversal. Then $\mathcal{F}$ satisfies the GPP and the GCP.*

Note that the definition of gadget actually requires that we specify a circuit, not just a quantum operation. This is an important distinction, since different circuits for the same quantum operation can produce different results in the presence of noise. In the case of the proposition, assume that the circuit implementing $\mathcal{F}$ is one that directly implements the decomposition required by the definition of transversal.

Proof. We will consider the case where $\mathcal{F} = U$ is unitary; non-unitary $\mathcal{F}$ can be handled by purification. Since U is transversal, $U = \bigotimes_{i=1}^{n} V_i$. Suppose $|\psi\rangle$ is the input to the gadget, and is a state on mn qubits which is produced by putting an r_a filter in front of the ath block of n qubits. Then $|\psi\rangle$ is a superposition of codewords with errors of weight at most r_a on block a,

$$|\psi\rangle = \sum_j E_j|\psi_j\rangle \quad (\mathrm{wt}\, E_j|_{\text{block } a} \leq r_a), \tag{11.1}$$

with $|\psi_j\rangle$ a possibly entangled state of valid codewords on all m blocks.

Suppose the faulty circuit for U has errors at s locations given by the fault path S. By corollary 10.2, it suffices to check the case where the errors are Pauli errors. Let $\mathcal{H}_i$ be the Hilbert space $\mathcal{H}_{2^m}$ composed of the ith qubits of all m blocks. Suppose the fault path performs U and then a Pauli error $\bigotimes_i F_i$, where F_i acts on $\mathcal{H}_i$. We can also assume E_j is a tensor product (by increasing the number of terms in the sum over j, if needed), and further write $E_j = \bigotimes_{i=1}^{n} E_{ij}$, where E_{ij} acts on $\mathcal{H}_i$. Then

$$\widetilde{U}|\psi\rangle = \sum_j \left(\bigotimes_i F_i\right)\left(\bigotimes_i V_i\right)\left(\bigotimes_i E_{ij}\right)|\psi_j\rangle = \sum_j \bigotimes_i \left[F_i\left(V_i E_{ij} V_i^\dagger\right)\right] U|\psi_j\rangle \tag{11.2}$$

Note that $V_i E_{ij} V_i^\dagger$ acts only on $\mathcal{H}_i$ always. If $E_{ij} = I$, then $V_i E_{ij} V_i^\dagger = I$, so the term $F_i \left(V_i E_{ij} V_i^\dagger \right)$ is not the identity only if either E_{ij} and F_i is not the identity.

Now, for any j, at most $\sum_{a=1}^m r_a$ of the E_{ij}s are not the identity, and the number of non-identity F_i terms is at most s, the size of the fault path. Thus, the maximal possible number of non-identity tensor factors in $F_i \left(V_i E_{ij} V_i^\dagger \right)$ is $s + \sum_{a=1}^m r_a$. That is,

$$\widetilde{U}|\psi\rangle = \sum_j G_j U |\psi_j\rangle, \tag{11.3}$$

where G_j is not the identity on at most $s + \sum_a r_a$ tensor factors $\mathcal{H}_i$. Since U is a gate gadget for the code and $|\psi_j\rangle$ is a valid codeword for each block, $U|\psi_j\rangle$ also consists of valid codewords for each block. Therefore, this state will pass a $\sum_a r_a + s$ filter on each n-qubit block, so the gadget satisfies the GPP.

For the GCP, we take equation (11.3) and apply an ideal decoder for the QECC to each n-qubit code block. G_j has weight $s + \sum_a r_a \leq t$ for each n-qubit code block, with t the number of errors the code corrects, so if $\mathcal{D}$ is the ideal decoder,

$$\mathcal{D}(G_j U |\psi_j\rangle) = U|\psi_j\rangle. \tag{11.4}$$

Now, E_j also has weight $\leq t$ for each n-qubit code block, so

$$\mathcal{D}(E_j|\psi_j\rangle) = |\psi_j\rangle, \tag{11.5}$$

and

$$\mathcal{D}(\widetilde{U} E_j |\psi_j\rangle) = U|\psi_j\rangle = U\mathcal{D}(E_j|\psi_j\rangle). \tag{11.6}$$

Thus, by linearity,

$$\mathcal{D}(\widetilde{U}|\psi\rangle) = U\mathcal{D}(|\psi\rangle), \tag{11.7}$$

which is the GCP. □

Of course, this proof is a long-winded way of saying something that is fairly obvious, which is that transversal gates can spread errors between blocks, but they cannot cause errors to propagate within a block of the code. Thus, the total number of errors in any single block of the output of a transversal gate is at most the total number of errors summed over all input blocks plus the total number of faulty locations in the circuit.

Note that the proof of the GPP does not make use of the constraint $\sum_a r_a + s \leq t$, so transversal gates actually satisfy a stronger version of the GPP.

One nice property of transversal gates is that a series of them can be strung together, and the result is another transversal gate.

Proposition 11.2. *The product of transversal gate gadgets is a transversal gate gadget.*

Proof. From the definition of transversal, it immediately follows that the product of two transversal gates is a transversal gate. The product of gadgets for locations L_1 and L_2 is also a gadget, for the circuit consisting of L_1 followed by L_2. □

In the standard fault-tolerant simulation, we put an error correction gadget after each gate gadget. However, the notion of what a fundamental gadget is can be relative. As a consequence of proposition 11.2, the composite gadget consisting of a product of some number of consecutive transversal gate gadgets also satisfies the GPP and GCP, so is also fault-tolerant. Therefore, we still get a valid fault-tolerant simulation if we only put a single error correction gadget after the whole composite gadget rather than after each of the gate gadgets making it up.

Of course, if we combine two m-block transversal gadgets that act on some different blocks, the result can be a gadget that acts on as many as $2m-1$ blocks (assuming the gadgets share at least one block). Even though transversal gates satisfy the GPP, each output block of the combined gadget may contain the errors combined from all the input blocks. This sets a real limit to how many transversal gate gadgets one can safely do in sequence before doing quantum error correction. Single-block transversal gadgets (composed of single-qubit gates) don't have this problem, although it's still true that faults in the physical gates making up a composite single-block transversal gadget will eventually add up.

11.2 Transversal Gates for Stabilizer Codes

So, transversal gate gadgets are automatically fault-tolerant. How do we determine, for a given code, what transversal gates are available? In general, this problem doesn't have a satisfactory known solution. A good first step is to ask, for a given QECC and a given transversal circuit, is it a valid gadget for some logical gate, or does it take some codewords to non-codewords? If it is a gate gadget, what is the logical gate? For a general circuit and QECC, we can answer the latter questions by applying the circuit to a set of basis states for the code and determining if we always get codewords. If we do, we can then compute the overall logical operation. This works, but takes exponential time in the number of qubits involved. For the special case of stabilizer codes and Clifford group circuits, we can do much better.

11.2.1 Transversal Paulis

Let's start with the easiest case, transversal gates made up of Pauli gates. In fact, we've already answered the question for this case: a Pauli P is a gate gadget for stabilizer code S iff $P \in \mathsf{N}(\mathsf{S})$. Furthermore, by theorem 3.11, P is a gate gadget for a logical Pauli gate location, and we can determine which one by looking at which coset in $\mathsf{N}(\mathsf{S})/\mathsf{S}$ contains P.

Note that all the Paulis in the same coset in $\mathsf{N}(\mathsf{S})/\mathsf{S}$ implement the same logical Pauli. All are transversal and therefore fault-tolerant. This makes it clear that FT gate gadgets are not unique. In this case, there are a total of 2^{n-k} perfectly good transversal implementations of the same gate gadget. However, from the point of view of fault tolerance, the different implementations are not completely equivalent. In particular, they involve different sets of physical locations, which can lead to different error rates and different kinds of errors. For instance, for the five-qubit code, $X \otimes X \otimes X \otimes X \otimes X$ and $I \otimes Y \otimes Y \otimes I \otimes X$ are both representatives of the $\overline{X}$ equivalence class. However, the first involves 5 X-gate locations, whereas the second involves only 3 gate locations (two Ys and one X) and 2 wait locations. If p_S is less than p_G, the second implementation is probably preferred. In other circumstances, the first implementation might be better, for instance if Y locations are noticeably more error-prone than X locations, or just because of its greater symmetry.

11.2.2 Clifford Gadgets Preserve the Stabilizer

Moving to more general Clifford group gates takes a little more work, but we've seen most of what to do in chapter 6. Under the action of physical Clifford group gate U, $M \in \mathsf{S}$ gets mapped to $UMU^\dagger$, and the stabilizer of the system afterwards is $U\mathsf{S}U^\dagger$. So when is a Clifford group circuit a valid gadget? Certainly, if $UMU^\dagger = M$ for all $M \in \mathsf{S}$, that means that the stabilizer post-operation is the same as the stabilizer before the circuit, which in turn means that the final state is still a codeword of the same code. However, this logic reveals that the condition $UMU^\dagger = M$ is too stringent. It is sufficient if the stabilizer group as a whole remains the same, and in particular, it is acceptable if conjugation by U permutes the elements of the stabilizer.

Conversely, if $U\mathsf{S}U^\dagger = \mathsf{T} \neq \mathsf{S}$, then U maps some codewords to non-codewords. Why is that? Well, the conjugation action by U is a group isomorphism. That means that not only do distinct Paulis remain distinct, but independent Paulis remain independent. In particular, that means that T has the same number of generators as S, and thus has a code space of the same dimension. Since U is unitary, the map from $\mathcal{T}(\mathsf{S})$ to $\mathcal{T}(\mathsf{T})$ is onto. But $\mathcal{T}(\mathsf{T}) \neq \mathcal{T}(\mathsf{S})$, so there is some $|\phi\rangle \in \mathcal{T}(\mathsf{T})$ which is not a codeword of S, and there is some $|\psi\rangle \in \mathcal{T}(\mathsf{S})$ such that $U|\psi\rangle = |\phi\rangle$.

Summing up, we find a straightforward condition for U to give a valid gate gadget:

Theorem 11.3. *Clifford group circuit U maps codewords of S to codewords of S iff $UMU^\dagger \in \mathsf{S}$ for all $M \in \mathsf{S}$.*

In other words, U is in the normalizer *in the Clifford group* of S. This generalizes the fact that Paulis give logical operations of the code space if they are in the Pauli group normalizer of S.

Checking all 2^{n-k} elements of the stabilizer could take a long time, but as usual, it is sufficient to check only generators, which is much quicker.

Corollary 11.4. *Clifford group circuit U maps codewords of S to codewords of S iff $UMU^\dagger \in \mathsf{S}$ for all generators M of S.*

This is true because conjugation is a group homomorphism, so the image of a product of generators is the product of the images, which is again in S.

Theorem 11.3 and corollary 11.4 hold for arbitrary Clifford group circuits, but for the purposes of fault-tolerance, we are most interested in transversal gates. Theorem 11.3 combined with proposition 11.1 tells us that if we have a transversal Clifford gate in the normalizer of S than we have a fault-tolerant gadget. For single-block transversal gates, that is straightforward enough, but you might wonder how exactly to apply these ideas to multiple-block transversal gates. In this case, we should apply theorem 11.3 to the stabilizer for multiple blocks of the code. For instance, a two-block transversal Clifford gate should preserve the stabilizer $\mathsf{S}^{\otimes 2} = \{M \otimes N | M, N \in \mathsf{S}\}$.

Let us illustrate by considering the 4-qubit code, as given in table 3.5. We will start with single-block transversal gates, implemented by a tensor product of single-qubit operations. The stabilizer of the 4-qubit code contains four elements, $\{I \otimes I \otimes I \otimes I, X \otimes X \otimes X \otimes X, Y \otimes Y \otimes Y \otimes Y, Z \otimes Z \otimes Z \otimes Z\}$. Conjugation can never mix I up with the other three Paulis, but we should consider permutations of the other elements of S.

Indeed, we can implement any permutation of the three non-identity Paulis in S. The trivial permutation can be achieved by the logical Paulis, and indeed, these are the only gates that will leave the stabilizer elements unchanged. Otherwise, we want to permute X, Y, and Z the same way on all four qubits. This can be achieved by performing the same single-qubit Clifford gate on all four qubits. For instance, transversal H (i.e., $H \otimes H \otimes H \otimes H$) will swap $X \otimes X \otimes X \otimes X$ with $Z \otimes Z \otimes Z \otimes Z$, and map $Y \otimes Y \otimes Y \otimes Y$ to itself. Note that H maps Y to $-Y$ on a single qubit, but when applied to all four qubits, the minus signs cancel out.

Since single-qubit Clifford group elements can perform any permutation of the single-qubit Paulis, we can achieve any possible permutation of the stabilizer by picking an appropriate single-qubit Clifford U and then performing the transversal U. We need to do the same permutation of X, Y, and Z on each qubit, but what happens to the phases of X, Y, and Z can be different on different qubits. The single-qubit Cliffords which change the phase of Paulis without otherwise permuting them are exactly the Pauli subgroup of C_1. Thus, the most general single-block transversal Clifford gadget for the four-qubit code can be written uniquely as PU, where $P \in \mathsf{N}(\mathsf{S})/\mathsf{S}$ and $U = V^{\otimes 4}$, with $V \in \check{\mathsf{C}}_1$ an arbitrary single-qubit Clifford group operation.

Now let us consider the two-block transversal Clifford gadgets. The stabilizer of two blocks of the code consists of 16 elements. It will perhaps be clearest if we group them in pairs consisting of the ith qubit of both blocks. Thus, for instance, two elements of $\mathsf{S}^{\otimes 2}$ would be $XI \otimes XI \otimes XI \otimes XI$ and $ZY \otimes ZY \otimes ZY \otimes ZY$. We can take the generators of $\mathsf{S}^{\otimes 2}$ to be

$$\{(XI)^{\otimes 4}, (ZI)^{\otimes 4}, (IX)^{\otimes 4}, (IZ)^{\otimes 4}\}. \tag{11.8}$$

Imagine we take a two-qubit Clifford gate and perform it transversally. For instance, what happens when we perform $\mathrm{CNOT}^{\otimes 4}$? The four generators become

$$\{(XX)^{\otimes 4}, (ZI)^{\otimes 4}, (IX)^{\otimes 4}, (ZZ)^{\otimes 4}\}. \tag{11.9}$$

But $(XX)^{\otimes 4} = (XI)^{\otimes 4}(IX)^{\otimes 4}$ and $(ZZ)^{\otimes 4} = (ZI)^{\otimes 4}(IZ)^{\otimes 4}$, so $\mathrm{CNOT}^{\otimes 4}$ is a valid transversal gadget.

Indeed, *any* transversal two-qubit Clifford group gate will give a valid gadget. If $U \in \mathsf{C}_2$, then $U^{\otimes 4}$ maps any Pauli of the form $P^{\otimes 4}$ to $Q^{\otimes 4}$, with $P, Q \in \mathsf{P}_2$. But $Q^{\otimes 4} \in \mathsf{S}^{\otimes 2}$, since Q can be written as a product of XI, ZI, IX, and IZ, and any phase will disappear when taken four times. The same argument applies to m-block Cliffords for arbitrary m: If $U \in \mathsf{C}_m$, then $U^{\otimes 4}$ is a valid transversal Clifford gate gadget. Indeed, by the same argument as in the single-block case, up to logical Paulis, these are the only valid transversal Clifford gadgets for the 4-qubit code.

11.2.3 Determining the Encoded Gate for a Clifford Gadget

So, now we know how to determine if a Clifford circuit is a gadget for the stabilizer code. But a gadget for what?

In chapter 6, you learned to characterize Clifford group gates by their action on Paulis. We can use the same concept to characterize logical Clifford gates. Since $\mathsf{N}(\mathsf{S})/\mathsf{S}$ is the logical Pauli group, the transformation performed on it by a Clifford gate will tell us what Clifford operation has been performed on the encoded state. (Of course, this only applies to Clifford circuits which are gadgets, since a circuit which is not will change S and therefore also not preserve $\mathsf{N}(\mathsf{S})/\mathsf{S}$.)

Let us illustrate the procedure by again considering the 4-qubit code. We know that any gate of the form $U^{\otimes 4}$ for $U \in \mathsf{C}_m$ is a transversal gadget. Suppose we do $H^{\otimes 4}$. It changes the logical Paulis as follows:

$$\overline{X}_1 = X \otimes X \otimes I \otimes I \to Z \otimes Z \otimes I \otimes I \tag{11.10}$$

$$\overline{X}_2 = X \otimes I \otimes X \otimes I \to Z \otimes I \otimes Z \otimes I \tag{11.11}$$

$$\overline{Z}_1 = I \otimes Z \otimes I \otimes Z \to I \otimes X \otimes I \otimes X \tag{11.12}$$

$$\overline{Z}_2 = I \otimes I \otimes Z \otimes Z \to I \otimes I \otimes X \otimes X \tag{11.13}$$

What we'd like to do is to write everything on the right-hand side as a product of logical Paulis in order to figure out what transformation is being performed. But, hold on a second: $Z \otimes Z \otimes I \otimes I$ can't possibly be written as a product of $I \otimes Z \otimes I \otimes Z$ and $I \otimes I \otimes Z \otimes Z$! What's wrong?

Don't panic. Remember that the logical Paulis are not unique. We've chosen particular representatives of cosets in $\mathsf{N}(\mathsf{S})/\mathsf{S}$, but other representatives are equally valid. What's happened here is that the transversal gate has changed, by itself, to a different representative of the coset. Yes, it's rude to make the change without telling us, but what can you do? Fault-tolerant gates do what they want and don't listen to complaints.

In this case, it's not too difficult to recover and figure out what is going on. We can immediately recognize $Z \otimes Z \otimes I \otimes I = (Z \otimes Z \otimes Z \otimes Z)(I \otimes I \otimes Z \otimes Z) = \overline{Z}_2$, and can similarly identify the other logical Paulis by multiplying them by stabilizer elements. Overall, we find the following transformation of the logical Paulis:

$$\overline{X}_1 \to \overline{Z}_2 \tag{11.14}$$

$$\overline{X}_2 \to \overline{Z}_1 \tag{11.15}$$

$$\overline{Z}_1 \to \overline{X}_2 \tag{11.16}$$

$$\overline{Z}_2 \to \overline{X}_1 \tag{11.17}$$

We can recognize this as a gate which swaps the two logical qubits and applies the Hadamard to both.

Notice that when the QECC encodes multiple qubits, as in the case of the 4-qubit code, even single-block transversal gates can do multiple-qubit *logical* gates. However, in the case of the 4-qubit code, not every logical two-qubit Clifford gate can be performed by transversal operations — there simply aren't enough of them.

11.3 Transversal Gates for the 7-Qubit Code

In section 11.2, we saw that the set of transversal gates for a stabilizer code is based on the set of symmetries of the stabilizer. The more symmetric the stabilizer, the more transversal gates are available. The 4-qubit code is pretty symmetric, but the 7-qubit code is more so, extending the symmetry to the logical Paulis as well as the stabilizer generators. Consequently, the 7-qubit code is particularly attractive based on the number of transversal gates it has available.

Looking at the stabilizer of the 7-qubit code and going through the same logic as for the 4-qubit code, we immediately see that for the 7-qubit code, it is also true that $U^{\otimes 7}$ is a valid m-block transversal gate gadget for any m-qubit Clifford U. All elements of the stabilizer for the 7-qubit code also have weight 4, so the phases will take care of themselves. Let's go through some examples to see what logical operations they perform.

First, Hadamard:

$$\overline{X} = X \otimes X \otimes X \otimes X \otimes X \otimes X \otimes X \to Z \otimes Z \otimes Z \otimes Z \otimes Z \otimes Z \otimes Z = \overline{Z} \tag{11.18}$$

$$\overline{Z} = Z \otimes Z \otimes Z \otimes Z \otimes Z \otimes Z \otimes Z \to X \otimes X \otimes X \otimes X \otimes X \otimes X \otimes X = \overline{X} \tag{11.19}$$

Thus, transversal Hadamard implements the logical Hadamard.

Next comes $R_{\pi/4}$:

$$\overline{X} = X \otimes X \otimes X \otimes X \otimes X \otimes X \otimes X \to Y \otimes Y \otimes Y \otimes Y \otimes Y \otimes Y \otimes Y \tag{11.20}$$

$$\overline{Z} = Z \otimes Z \otimes Z \otimes Z \otimes Z \otimes Z \otimes Z \to Z \otimes Z \otimes Z \otimes Z \otimes Z \otimes Z \otimes Z = \overline{Z} \tag{11.21}$$

We need to be careful with $Y^{\otimes 7}$. $Y = iXZ$, so

$$Y^{\otimes 7} = i^7 X^{\otimes 7} Z^{\otimes 7} = -i\overline{XZ} = -\overline{Y}. \tag{11.22}$$

Thus, the transversal $R_{\pi/4}$ does not do the logical $R_{\pi/4}$. Instead, we can identify the gate as $\overline{R_{\pi/4}}^\dagger = \overline{R_{-\pi/4}}$. This is an important example of a place where you need to be careful with phases or you get the wrong answer. If we want to do $\overline{R_{\pi/4}}$, we can instead do it using the transversal $R_{-\pi/4}$.

Next, let's try a two-block gate, the transversal CNOT:

$$\overline{X \otimes I} = (XI)^{\otimes 7} \to (XX)^{\otimes 7} = \overline{X \otimes X} \tag{11.23}$$

$$\overline{I \otimes X} = (IX)^{\otimes 7} \to (IX)^{\otimes 7} = \overline{I \otimes X} \tag{11.24}$$

$$\overline{Z \otimes I} = (ZI)^{\otimes 7} \to (ZI)^{\otimes 7} = \overline{Z \otimes I} \tag{11.25}$$

$$\overline{I \otimes Z} = (IZ)^{\otimes 7} \to (ZZ)^{\otimes 7} = \overline{Z \otimes Z}. \tag{11.26}$$

We can identify this as the logical CNOT between the qubits encoded in the two blocks of the code.

Now, H, $R_{\pi/4}$, and CNOT are generators of the Clifford group, and we have transversal implementations of all of them. That means we can implement the whole logical Clifford group on m blocks of the 7-qubit code just by doing transversal operations. The transversal U does not always give us the logical U — instead it gives us the complex conjugate U^* — but nevertheless, it is straightforward to perform any logical Clifford group operation for this code. This gives us high hopes for finding a fault-tolerant protocol for the 7-qubit code, and indeed this is a good start, but unfortunately, it gets harder from here. This is the full list of transversal gate gadgets for the 7-qubit code. To get a gate outside the Clifford group, we will need another construction, discussed in chapter 13.

11.4 Transversal Gates and Measurement for CSS Codes

The 7-qubit code is not bad, but there's a whole world of codes out there, so it's worth looking at a broader class of codes to see what we can say about transversal gates. One gate that plays a particularly big role in quantum computation is the CNOT gate, so it's convenient that the 7-qubit code allows a transversal implementation of it. What other codes have this property? It's not straightforward to make a completely general statement about transversal implementations of CNOT, but for the 7-qubit code, the gadget for CNOT is just transversal CNOT. Let's try to generalize that.

Take an arbitrary stabilizer code S, and consider two blocks of the code. Let's see what happens when we apply transversal CNOT. If $M \in \mathsf{S}$, then $M \otimes I \in \mathsf{S}^{\otimes 2}$. Suppose M has binary symplectic representation $(x_M|z_M)$; then transversal CNOT applied to $M \otimes I$ gives $(x_M x_M|z_M 0)$. For this to be in $\mathsf{S}^{\otimes 2}$, we need $(x_M|0) \in \mathsf{S}$. By the fact that S is a group, $(0|z_M)$ is also in S. By choosing generators appropriately, we can thus always have all generators of the form $(x_M|0)$ or $(0|z_M)$. That means it is a CSS code.

For a CSS code, we can always choose the logical X operators to be tensor products of X and I and the logical Z operators to be tensor products of Z and I. The choice of basis codewords given in section 5.1.3 has this property. In that case, we can see that transversal CNOT will perform logical CNOT between all corresponding pairs of encoded qubits. In other words, we find the following:

Theorem 11.5. *A stabilizer code* S *has a gadget consisting of transversal* CNOT *iff* S *is a CSS code. If so,* S *has a choice of logical operators for which the gadget simulates a location consisting of the tensor product of* CNOT*s from logical qubit* i *in the first block to logical qubit* i *in the second block, for all* i*.*

Theorem 11.5 makes CSS codes very attractive for fault tolerance. Just by choosing to work with a CSS code, we know for sure we have logical CNOT gates available, albeit performed together on all logical qubits in the block. It turns out that CSS codes always have another transversal gadget that is just as useful: measurement.

Recall from section 5.1.3 that we can write the basis codewords of a CSS code as

$$|u + {C_2}^\perp\rangle = \sum_{v \in {C_2}^\perp} |u + v\rangle. \tag{11.27}$$

The logical state encoded by this basis state is given by the coset of $C_1/{C_2}^\perp$ which u lies in. Thus, to measure the encoded data in the standard basis, it suffices to measure u up to an element of ${C_2}^\perp$. But we can achieve this by simply measuring transversally in the standard basis: When we do so, we get $u+v$, with v a random element of ${C_2}^\perp$. Thus, transversal standard basis measurement followed by classical decoding is a gadget for measurement of logical qubits in the standard basis. The classical decoding part to determine the coset of u is not implemented transversally, but in a basic error model, we assume that classical processing is completely reliable.

Proposition 11.1 only tells us transversal gate gadgets are fault tolerant, so we should also check that transversal measurement satisfies the MCP. In fact, for a general stabilizer code, transversal measurement is *not* fault-tolerant, although it does serve as a gadget for some codes. For instance, for the five-qubit code, transversal measurement of a perfect codeword will tell you the encoded state — consulting equations (3.11) and (3.12), we see that $|\overline{0}\rangle$ always gives an even parity string and $|\overline{1}\rangle$ always gives an odd parity string — but even a single bit flip error due to a faulty measurement location will cause us to get the wrong answer.

CSS codes, however, have the special property that transversal measurement is fault tolerant.

Theorem 11.6. *For any CSS code, transversal measurement followed by classical decoding is a fault-tolerant gadget implementing logical measurement of all encoded qubits.*

Proof. The theorem is true because the codewords are superpositions of states from a classical error-correcting code. That means a small number of errors in the classical output cannot confuse us between different logical codewords.

To prove the MCP formally, let us consider the output state of an r-filter

$$|\psi\rangle = \sum_j E_j |\psi_j\rangle \quad (\mathrm{wt}\, E_j \leq r). \tag{11.28}$$

Invoking corollary 10.2 again, we can assume the errors E_j are Pauli errors. Furthermore, we can assume that all E_j in the sum have distinct error syndromes: If the code is non-degenerate, this is automatically true. If the code is degenerate, since $\mathrm{wt}\, E_j \leq r \leq t$, degenerate errors will act the same on the codewords $|\psi_j\rangle$, and we can re-write the decomposition over j to have only one error of each syndrome.

Let us write $|\psi_j\rangle = \sum_u c_{ju} |\overline{u}\rangle$. Then the ideal decoder applied to equation (11.28) gives

$$\sum_{j,u} c_{ju} |u\rangle |\sigma(E_j)\rangle, \tag{11.29}$$

where the second tensor factor contains the syndrome bits. Since all $\sigma(E_j)$ are distinct, measurement of this state simply gives codeword u with probability $\sum_j |c_{ju}|^2$. This is the RHS of the MCP.

Now let us figure out what a faulty measurement gadget does to equation (11.28). We have

$$|\psi\rangle = \sum_u \left(\sum_j c_{ju} E_j \right) |\overline{u}\rangle. \tag{11.30}$$

The s faults in the transversal measurement have the effect of up to s additional bit-flip errors, which we can encapsulate as F, with $\mathrm{wt}\, F \leq s$. That gives us the state

$$F|\psi\rangle = \sum_u \left(\sum_j c_{ju} F E_j \right) |\overline{u}\rangle, \tag{11.31}$$

on which we perform perfect single-qubit measurement. Notice that $\mathrm{wt}(FE_j) \leq r + s \leq t$. Let's go even further and expand $|\overline{u}\rangle = \sum_{v \in {C_2}^\perp} |u + v\rangle$. Then

$$F|\psi\rangle = \sum_{u \in C_1/{C_2}^\perp} \sum_{v \in {C_2}^\perp} \left(\sum_j c_{ju} F E_j \right) |u + v\rangle. \tag{11.32}$$

Now, C_1 has distance d_1. If the CSS code is non-degenerate, $d_1 \geq 2t + 1$, and $FE_j|w\rangle$ is orthogonal to $FE_{j'}|w'\rangle$ for any $w \neq w' \in C_1$. When the code is degenerate, it is possible that $FE_j|w\rangle = \pm FE_{j'}|w'\rangle$ for some $w \neq w' \in C_1$. However, since the quantum code does have distance $2t + 1$, the only way this can happen is if $w + w' \in {C_2}^\perp$. Thus, if we want to calculate the probability of some output string x, at most one coset u can contribute. This means the classical decoding of x will be unambiguous, giving a unique coset u, which we can interpret as the measurement outcome.

It just remains for us to check that the probability of getting the outcome u is the same as in the ideal case. The probability of the measured string being x for that particular measurement error F is

$$|\langle x|F|\psi\rangle|^2 = \left| \langle x| \left(\sum_j c_{ju} F E_j \right) |\overline{u}\rangle \right|^2, \tag{11.33}$$

where u is the unique u consistent with x. The probability of outcome u is (11.33) summed over x:

$$\Pr(u) = \sum_x \sum_{j,j'} c_{ju} c^*_{j'u} \langle \overline{u}|E^\dagger_{j'} F^\dagger|x\rangle \langle x|FE_j|\overline{u}\rangle. \tag{11.34}$$

The sum over x is summed over all xs that have non-zero probability for u, so we can replace $\sum_x |x\rangle \langle x|$ with the identity. Then

$$\Pr(u) = \sum_{j,j'} c_{ju} c^*_{j'u} \langle \overline{u}|E^\dagger_{j'} E_j|\overline{u}\rangle. \tag{11.35}$$

But we have restricted the sum over j to have just a single E_j with each error syndrome. Therefore, the inner product gives 0 unless $j = j'$. Thus, $\Pr(u) = \sum_j |c_{ju}|^2$, as desired. □

It's also worth discussing briefly when a CSS code has additional transversal operations beyond CNOT (or product of CNOTs) and measurements. Thinking briefly about the structure of a CSS code, it's clear that transversal Hadamard is a gadget iff $C_1 = C_2$. The 7-qubit code has this property, as does the 4-qubit code. In general, we can form a CSS code with $C_1 = C_2$ whenever ${C_1}^\perp \subseteq C_1$. However, as in the case of the 4-qubit code, the action of the transversal Hadamard can be more than just Hadamard applied to all encoded qubits. Since transversal Hadamard changes Xs into Zs and vice-versa, it does perform the logical Hadamard on all qubits, but there may be some additional classical operation (such as SWAP or CNOT) interacting the encoded qubits within a single block.

To have transversal $R_{\pi/4}$ as a valid gadget for the code, we need further additional structure. $R_{\pi/4}$ maps X to Y, so the X generators of the code will get mapped to tensor products of Y and I, which must also be in the stabilizer. Furthermore, the product of an X generator M and $N = R^{\otimes n}_{\pi/4} M R^{\dagger \otimes n}_{\pi/4}$ must also be in the stabilizer. The product will be a tensor product of Z and I, in fact what would be obtained from M via a transversal Hadamard, but with an additional phase which depends on the weight of M. The phase is $i^{\mathrm{wt}\, M}$. Since the stabilizer must be Abelian, $\mathrm{wt}\, M$ must be even, or else M and N would not commute, but we can still get a phase of -1. In other words, to have transversal $R_{\pi/4}$ as a valid gadget, we must have $C_1 = C_2$ *and* the weight of every generator must be a multiple of 4 (the classical code ${C_1}^\perp$ is *doubly even*). However, even if ${C_1}^\perp$ is not doubly even, there is still a corresponding transversal gate, consisting of transversal $R_{\pi/4}$ followed by some phase flips to fix up the phase. The logical operation performed by the transversal $R_{\pi/4}$ (with or without bit flips) does not necessarily involve logical $R_{\pi/4}$s, however.

11.5 Other Topics Relating to Transversal Gates

11.5.1 Codes With Transversal $\pi/8$ Gates

All the examples we've seen so far of transversal gates are Clifford group gates, but naturally it's also possible to have codes with non-Clifford group transversal gates. Either the physical operations involved in the gate or the logical effect of the gadget — or most often, both — can be a non-Clifford unitary. However, stabilizer codes have a particular affinity for Clifford group gates because both are so closely connected with the Pauli group. For many stabilizer codes, all the transversal gates are Clifford group gates. Nevertheless, a few examples are known of stabilizer codes with non-Clifford transversal gates. We don't currently have a systematic understanding of when this is possible and which gates can be done with which codes, but in this section I'll present one particular family of codes with a non-Clifford transversal gate. This will illustrate the principle, and the smallest code from this family will be of use in section 13.5.

The gate we'll be using is the transversal $\pi/8$ gate $R_{\pi/8}^{\otimes n}$. The $R_{\pi/8}$ gate on a single qubit (also called the T gate) produces a relative phase $e^{i\pi/4}$ between $|0\rangle$ and $|1\rangle$. Therefore, n of them applied to a basis state $|x\rangle$ with $\operatorname{wt} x = w$ produce a phase $e^{i\pi w/4}$ relative to the $|00\ldots0\rangle$ state. In particular, basis states whose weight is a multiple of 8 acquire no overall phase relative to the all-0's state.

Recall that the codewords of CSS codes are superpositions over cosets of some classical code. Suppose, therefore, that we consider a classical code ${C_2}^\perp$ whose codewords all have weights 0 mod 8. (Such a code is *quadruply even*.) The logical 0 of the corresponding CSS code is thus

$$|\overline{0}\rangle = \sum_{v \in {C_2}^\perp} |v\rangle, \tag{11.36}$$

which is a superposition of basis states with weight 0 mod 8. Therefore, $R_{\pi/8}^{\otimes n}|\overline{0}\rangle = e^{i\phi}|\overline{0}\rangle$. There is a global phase $e^{i\phi}$ with $\phi = -n\pi/8$ because of our definition of $R_{\pi/8}$, but the point is that $|\overline{0}\rangle$ is an eigenstate of the transversal $\pi/8$ gate. If we look at any other logical basis codeword

$$|u + {C_2}^\perp\rangle = \sum_{v \in {C_2}^\perp} |u + v\rangle, \tag{11.37}$$

we get a superposition of words of the form $u+v$, $v \in {C_2}^\perp$. Now, $\operatorname{wt}(u+v) = \operatorname{wt} u + \operatorname{wt} v - 2\operatorname{wt}(u \cdot v)$, since the coordinates where both u and v are 1 appear twice in $\operatorname{wt} u + \operatorname{wt} v$, but appear 0 times in $\operatorname{wt}(u+v)$. In order for all $u+v$ to have the same weight modulo 8 as we vary $v \in {C_2}^\perp$, we need that $2\operatorname{wt}(u \cdot v) = 0 \bmod 8$, or $\operatorname{wt}(u \cdot v) = 0 \bmod 4$.

That is, if we have a code C_2 such that all codewords in ${C_2}^\perp$ have weight 0 mod 8 and another code C_1 such that $\operatorname{wt}(u \cdot v) = 0 \bmod 4$ for all $u \in C_1$, $v \in {C_2}^\perp$, then for $u \in C_1$,

$$R_{\pi/8}^{\otimes n}|u + {C_2}^\perp\rangle = e^{i(\phi + \pi \operatorname{wt} u/4)}|u + {C_2}^\perp\rangle. \tag{11.38}$$

The transversal $\pi/8$ is thus a valid gadget for any CSS code formed from such a pair (C_1, C_2). The resulting logical gate is a diagonal gate. Its action on the logical basis state corresponding to $u \in C_1$ is to produce a phase $e^{i(\phi + \pi w/4)}$, where $w = \operatorname{wt} u$.

The smallest interesting distance 3 code for which this happens is the 15-qubit code with stabilizer given in table 11.1. C_1 is the $[15, 5, 8]$ punctured Reed-Muller code $\mathcal{R}(1,4)$ (i.e., $\mathcal{R}(1,4)$ with the last register deleted). ${C_2}^\perp$ is the even subcode, namely the set of codewords of C_1 with even weight, which is the punctured $\mathcal{R}(1,4)$ with the all 1's vector removed. The 15-qubit code is a $[[15, 1, 3]]$ code. Since $\mathcal{R}(1,4)$ is quadruply even, the codewords in C_1 have weight either 0 mod 8 or 7 mod 8, and ${C_2}^\perp$ is the set of codewords with weight 0 mod 8. This implies C_1 and C_2 have the right form, so the resulting CSS code also has the right form.

Indeed, we can see immediately that the $|\overline{0}\rangle$ state is a superposition of those codewords of C_1 with weight 0 mod 8 and the $|\overline{1}\rangle$ state is a superposition of the codewords of C_1 with weight 7 mod 8. Therefore, the transversal $\pi/8$ gate applied to $|\overline{a}\rangle$ gives a phase $e^{i\pi(1/8 - a/4)}$, which is the logical $-\pi/8$ gate $\overline{R_{-\pi/8}}$.

Z	Z	Z	Z	I	I	I	I	I	I	I	I	I	I	I
Z	Z	I	I	Z	Z	I	I	I	I	I	I	I	I	I
Z	I	Z	I	Z	I	Z	I	I	I	I	I	I	I	I
Z	Z	I	I	I	I	I	I	Z	Z	I	I	I	I	I
Z	I	Z	I	I	I	I	I	Z	I	Z	I	I	I	I
Z	I	I	I	Z	I	I	I	Z	I	I	I	Z	I	I
Z	Z	Z	Z	Z	Z	Z	Z	I	I	I	I	I	I	I
Z	Z	Z	Z	I	I	I	I	Z	Z	Z	Z	I	I	I
Z	Z	I	I	Z	Z	I	I	Z	Z	I	I	Z	Z	I
Z	I	Z	I	Z	I	Z	I	Z	I	Z	I	Z	I	Z
X	X	X	X	X	X	X	X	I	I	I	I	I	I	I
X	X	X	X	I	I	I	I	X	X	X	X	I	I	I
X	X	I	I	X	X	I	I	X	X	I	I	X	X	I
X	I	X	I	X	I	X	I	X	I	X	I	X	I	X

Table 11.1: The stabilizer for the 15-qubit code.

11.5.2 Transversal Gates Plus Permutations

Transversal gates are useful for fault-tolerance in part because they conjugate pre-existing errors into errors of the same weight. Phrased in terms of our pictorial language, they have the property

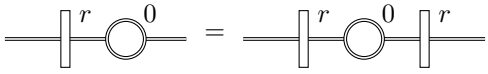

(11.39)

regardless of whether $r \leq t$ or $r > t$.

Transversal gates are not the only set of gates that behave this way. Another option is the set of gates which permute the qubits in the code but don't otherwise change their values. Under a permutation gate of this sort, an error on a single qubit just gets moved to a different qubit. You could think of this as propagation, since an existing error causes an error to appear on a new qubit, but in the process, the error is eliminated from the old qubit. Thus, property (11.39) is satisfied.

For some codes, it is possible to make interesting gates out of permutations. For instance, in the 4-qubit code, suppose we swap the second and third qubits. The stabilizer generators are left unchanged, but $\overline{X}_1 \leftrightarrow \overline{X}_2$ and $\overline{Z}_1 \leftrightarrow \overline{Z}_2$. $\mathrm{SWAP}_{2,3}$ is thus a gadget for the logical SWAP gate between the code's two encoded qubits.

However, permutation gates are not fault tolerant unless we are careful about the implementation. The permutation group can be generated by transpositions of pairs of elements, so it is sufficient to consider circuits where every gate is the SWAP gate. The problem is that a fault on a SWAP gate can cause both of the qubits involved in the gate to have errors. Therefore, instead of the GPP, we have

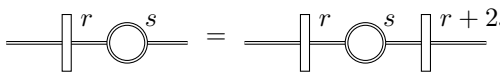

(11.40)

In order to get around this, we need to be careful how to implement the SWAP. The circuit given in figure 11.2 is one solution. To swap two data qubits, add a third ancilla qubit to act as an intermediary. By performing three SWAP gates as in the figure, the overall effect is to do a SWAP on the data qubits, but none of the three gates directly interacts the two data qubits. Thus, a single faulty gate can only cause an error on one of the data qubits. After the circuit is finished, the ancilla qubit can be discarded. Also note that the initial state of the ancilla qubit is irrelevant — the circuit works just as well no matter what it is. It is also OK to reuse the ancilla qubit many times in SWAPs like this.

The upshot is that a circuit of SWAP gates each implemented via the method of figure 11.2 is fault-tolerant, satisfying both the GPP and GCP. For some codes, this can significantly expand the set of available fault-tolerant gadgets. Another possibility is to consider gadgets built of a transversal gate followed by a

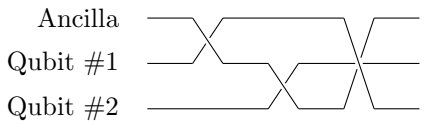

Figure 11.2: A circuit for swapping two physical qubits for which one fault only causes one error in the final state. The ancilla can be in any state.

fault-tolerant implementation of a permutation gate. The combination will be fault-tolerant as well. However, whereas any product of transversal gates remains fault tolerant, as does any product of permutation gates, the combination (transversal gate – permutation gate – transversal gate) is *not* in general fault tolerant. In particular, consider a case for which the transversal gates interact two different blocks of the code. A fault in the first transversal gate can create an error in qubit i of both blocks of the code. If the permutation gate treats the two blocks differently, it could move one of those errors to qubit $j \neq i$ on one block, and then the second transversal gate could propagate the error to qubit j on the other block, which would then have errors on the two qubits i and j even though there was only a single fault in the circuit. Therefore, if we want to combine transversal gates and permutations, we will need to periodically do error correction.

11.5.3 Transversal Gates Cannot Be Universal

For the 7-qubit code, transversal gate gadgets implement the full Clifford group. This is tantalizing — if we can just do one more transversal gate, by theorem 6.9, we get a universal set of gates. Unfortunately, for the 7-qubit code, there are no more transversal gates. The Clifford group by itself can be classically simulated, so we definitely need something more to achieve the full power of quantum computation. Perhaps there is another code which lets us do a universal set of gates transversally? Unfortunately, there is not:

Theorem 11.7 (Eastin-Knill)**.** *If Q is an $((n, K, d))_q$ QECC with $d \geq 2$, and G is the set of logical unitary gates that have transversal gadgets for Q, then G is a discrete group. In particular, G is not dense in $\mathsf{SU}(K)$.*

Theorem 11.7 tells us that transversal gate gadgets can never be enough to get a universal set of gates. We will always need to do something else; the most common source of something else is to add in magic states, which will be discussed in chapter 13.

Note that there does exist a classical code with a classically universal set of transversal gadgets: The repetition code. Any classical gate that we wish to perform on the encoded state of a repetition code can just be done by doing it separately on each copy.

The intuition behind this theorem is that if G is not discrete, it must have some non-trivial small unitaries in it. But there is no way the QECC can distinguish between a small transversal gate that is supposed to be a gadget and an error: As in theorem 1.1, the tensor product of unitaries very close to the identity is also very close to a one-qubit error channel, and with distance 2, the code should at least detect if not correct any one-qubit error channels. Presented with a gate gadget which is a small transversal gate, the code will treat it as an error and correct it, meaning the logical action of the gadget is the identity. Thus, any sufficiently small elements of G are trivial and G is discrete. To make this intuition precise, we should look at infinitesimal unitaries, which means dealing with the Lie algebra.

Proof. It is sufficient to consider single-block transversal gadgets. An m-block transversal gadget can be thought of as a single-block transversal gadget for the code $Q^{\otimes m}$, which can be interpreted as an $((n, K, d))_{q^m}$ code, with the ith register consisting of the ith registers of all m blocks.

Let $\tilde{G}$ be the set of transversal gates which are gadgets for the code. G is equal to $\tilde{G}/K$, with K the set of transversal implementations of the identity.

The proof will use a few facts about Lie groups and Lie algebras, which I will bring up as needed. The first observation is that $\tilde{G}$ is a topologically closed subgroup of the compact finite-dimensional Lie group $\mathsf{U}(q)^{\otimes n}$, and is therefore a Lie group itself. $\tilde{G}$ is a subgroup by proposition 11.2, and it is closed because it

is the intersection of the set of transversal gates $\mathsf{U}(q)^{\otimes n}$ and the set $\mathsf{U}(K) \otimes \mathsf{U}(q^n - K)$ of unitaries which preserve the code space, both of which are closed sets.

Since $\tilde{G}$ is a Lie group, it has a Lie algebra $\mathfrak{g}$ which is a subalgebra of the Lie algebra $\mathfrak{t}$ of $\mathsf{U}(q)^{\otimes n}$. $\mathfrak{t}$ is spanned by elements of the form iH, where H is a weight-1 Hermitian operator. Therefore, an arbitrary element iD of $\mathfrak{g}$ can be written as a sum of weight-1 operators. However, the code has distance at least 2, so it detects any single-register error. By theorem 2.4, D must therefore be a detectable error. That is, for any codeword $|\psi\rangle$, $D|\psi\rangle = \alpha|\psi\rangle + |\phi\rangle$, where $|\phi\rangle$ is orthogonal to the code space Q.

Now, a neighborhood of the identity in $\tilde{G}$ is generated from the Lie algebra by the exponential function, $U = e^{itD}$, $D \in \mathfrak{g}$.

$$U|\psi\rangle = e^{itD}|\psi\rangle = \sum_r \frac{(itD)^r}{r!}|\psi\rangle = |\psi\rangle + (itD)|\psi\rangle + O(t^2). \tag{11.41}$$

For any t, U is a logical operation on the code, so this sum is a codeword for all t and all $|\psi\rangle \in Q$. The only way this can be is if $D|\psi\rangle \in Q$. Combining with the error detection property, we find

$$D|\psi\rangle = \alpha_D|\psi\rangle \tag{11.42}$$

when $|\psi\rangle \in Q$ and $D \in \mathfrak{g}$. α_D can depend on D, but by the error correction conditions, it cannot depend on $|\psi\rangle$.

Therefore, given any element $U = e^{iD}$ in a neighborhood of the identity in $\tilde{G}$, we have

$$U|\psi\rangle = e^{iD}|\psi\rangle = e^{i\alpha_D}|\psi\rangle. \tag{11.43}$$

U performs the trivial logical gate, and the neighborhood of the identity lies within K.

The finite-dimensional Lie group $\tilde{G}$ is a union of a discrete set of connected components. The connected component containing the identity is generated by a neighborhood of the identity, and therefore the whole connected component of the identity lies within K. The other connected components are cosets of the identity component, so $G = \tilde{G}/K$ is a discrete group. □

Chapter 12

Who Corrects The Correctors?: Fault-Tolerant Error Correction And Measurement

In this chapter, I'll mostly discuss fault-tolerant error correction gadgets. An FTEC gadget invariably involves some ancilla qubits, which are used to measure the error syndrome without removing the state from its protective QECC. Since measurement is a big part of an FTEC gadget, the major methods of fault-tolerant error correction can also be modified to produce fault-tolerant measurement gadgets, so I'll talk about those too.

FTEC gadgets are much more complicated than transversal gate gadgets. Designing one is a special challenge. For other FT gadgets, you must simply be careful not to cause errors to propagate too badly and not cause too many new errors. An FTEC gadget, operating correctly, must be able to eliminate errors despite being imperfect itself. It's too much to hope for (and, indeed, impossible to achieve) that the FTEC gadget will necessarily output a perfect codeword, since there's always the possibility of faults at the very end of the procedure, but in a well-designed FTEC gadget, any errors dating from before the beginning of the gadget will be corrected. Thus, an FTEC gadget may not be able to correct *itself*, but it at least corrects for the previous EC gadget as well as any gate or other gadgets that may have occurred in between.

12.1 Fault Tolerant Pauli Measurement for Stabilizer Codes

For a stabilizer code, error correction consists of measuring the eigenvalue of all generators of the stabilizer. One approach to doing this is to measure the eigenvalues one-by-one and then put them together to form the complete error syndrome. This approach is not the only option, but it is conceptually the most straightforward, so I'll start with it. Indeed, I'll go right ahead and discuss how to fault-tolerantly measure any single Pauli operator, whether in the stabilizer or the normalizer, for a general stabilizer code.

Unfortunately, while the basic idea of the technique is simple, there are a lot of annoying details needed to make it work right. That means this section and the next can get a bit involved at times. If you're not *really* into the details, you may want to read the basic idea of cat state measurement and Shor EC and skim through the rest of sections 12.1 and 12.2.

12.1.1 Non-Fault-Tolerant Measurement of Paulis

Let's start by talking about something we passed over in chapter 3, how to measure the eigenvalue of an arbitrary Pauli operator. We want this for error correction, to measure the eigenvalues of stabilizer elements, and we want to be able to measure eigenvalues of logical Pauli operators, for instance at the end of the computation. It may not be immediately apparent how to do either, even when we don't have to

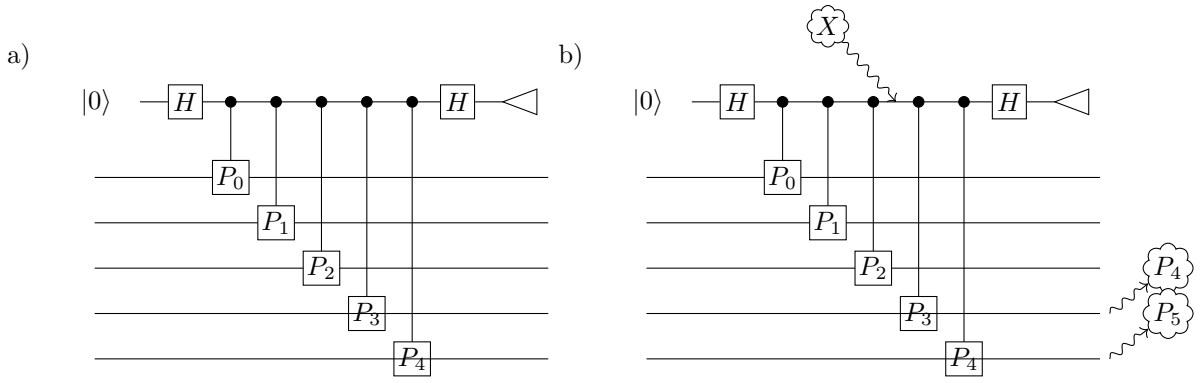

Figure 12.1: a) A non-fault-tolerant measurement procedure for eigenvalues of a Pauli operator $P_1 \otimes P_2 \otimes P_3 \otimes P_4 \otimes P_5$, b) A single fault can lead to multiple output errors.

worry about fault tolerance. In any case, the construction serves as a good starting point for building a fault-tolerant measurement procedure.

The solution is illustrated in figure 12.1a. To make the procedure useful for error correction, we'd like to do a non-destructive measurement, leaving the data unchanged except for projecting on the eigenstate of the Pauli P; assume the phase of P is such that the eigenvalues are ± 1. Therefore we'll need an ancilla, and since the classical output is just one bit, a single ancilla qubit will suffice. Suppose we perform a controlled-P with the ancilla as control and the data qubits as target. If the data began in a $+1$ eigenstate of P, then whether the ancilla is $|0\rangle$ or $|1\rangle$, nothing happens. If the data began in a -1 eigenstate of P, then when the ancilla is $|0\rangle$, again nothing happens, but if the ancilla is $|1\rangle$, the state acquires an overall sign of -1. When the ancilla starts as $|+\rangle = |0\rangle + |1\rangle$, the state of the ancilla after the controlled-P gate is $|0\rangle + (-1)^b|1\rangle$, where b is the eigenvalue of P for the data. Then a Hadamard transform on the ancilla maps $|0\rangle + (-1)^b|1\rangle \mapsto |b\rangle$, and measuring the ancilla qubit gives us the answer. If the data began in a superposition of eigenvalues, it collapses to an eigenstate with eigenvalue $(-1)^b$.

In the non-fault-tolerant scenario, this works well, but it fails miserably as part of an FT gadget. For one thing, it clearly fails the MCP. For instance, if there is an error in the ancilla qubit during the final measurement, the classical outcome can be wrong, no matter how good the QECC used for the data is. Furthermore, if this Pauli measurement is part of an EC gadget, it will likely also cause the gadget to fail the ECRP. The problem is that we are using a single qubit to control multiple qubits within the same block of the code. Thus, a single fault can cause multiple errors in the outgoing state. There's no measurement propagation property, since the standard measurement gadget is a destructive measurement, but if we made a gadget for non-destructive measurement, and tried to do it via the method discussed above, the measurement propagation property would fail as well.

Let's see precisely what goes wrong. An example is shown in figure 12.1b. If the initial state of the ancilla suffers a bit flip, that does nothing — $X|+\rangle = |+\rangle$. However, if the ancilla undergoes a bit flip halfway through the controlled-P gate, we have a problem. The $|0\rangle$ branch and the $|1\rangle$ branch switch, so the data qubits involved in gates after the bit flip get their Pauli operations when they're not supposed to, and *don't* get Paulis when they are supposed to. Thus, a single faulty gate can cause multiple data errors, even if the fault doesn't directly affect the data block. If an event like this happens near the end of an EC gadget, the state won't pass a 1-filter at this point. Even if it's in the beginning or middle of an EC gadget, if the code only corrects 1 error, it isn't strong enough to function properly after getting so many errors affecting the same code block.

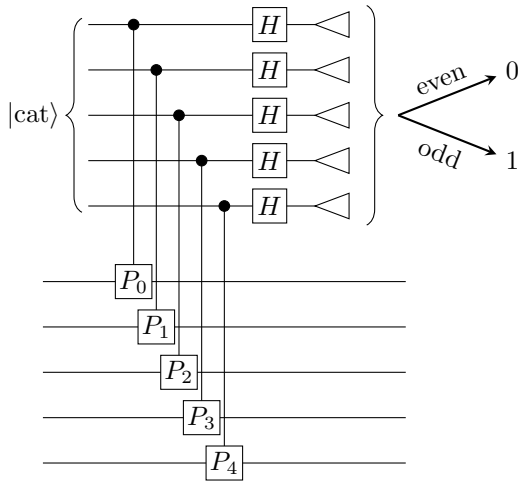

Figure 12.2: Measurement of a Pauli operator $P_1 \otimes P_2 \otimes P_3 \otimes P_4 \otimes P_5$ using a cat state.

12.1.2 Single Measurement Attempt Through Cat States

To solve this problem, let's take inspiration from transversal gates. The problem of having a single error in the ancilla propagate to multiple qubits is precisely the same error propagation issue we worried about before, so we should somehow make the controlled-P gate into a transversal gate. This means increasing the size of the ancilla to involve $m = \operatorname{wt} P$ qubits. Then we'll have one ancilla qubit for each single-qubit Pauli gate making up P, and each ancilla qubit interacts with only one qubit in the data block. That limits error propagation, just as for transversal gate gadgets.

What state should the ancilla be in? We want a coherent superposition between two cases: one where we do nothing to any of the data qubits, and one where we perform P on all m of the relevant data qubits. Thus, the ancilla should be $|00\ldots0\rangle + |11\ldots1\rangle$. In the general quantum information literature, this state is sometimes called the m-qubit GHZ state, but in the literature on fault tolerance, it is usually known as a *cat state*. Like Schrödinger's Cat, the cat state is in a macroscopic superposition, in this case between the all 0s and all 1s states.

After performing the transversal P, we have $|0\ldots0\rangle + (-1)^b|1\ldots1\rangle$ when the eigenvalue of P is b. We could determine b by disentangling the cat state and measuring $|0\ldots0\rangle + |1\ldots1\rangle$ vs. $|0\ldots0\rangle - |1\ldots1\rangle$ vs. everything else, but it turns out there is an easier way. Perform the Hadamard transform on each qubit of the cat state. Then

$$H^{\otimes m}(|0\ldots0\rangle + (-1)^b|1\ldots1\rangle) = \sum_x \left[1 + (-1)^{b+x\cdot(1,\ldots,1)}\right]|x\rangle \tag{12.1}$$

$$= \sum_x \left[1 + (-1)^{b+\operatorname{wt} x}\right]|x\rangle \tag{12.2}$$

$$= \begin{cases} \sum_{\operatorname{wt} x \text{ even}} |x\rangle & b = 0 \\ \sum_{\operatorname{wt} x \text{ odd}} |x\rangle & b = 1 \end{cases} \tag{12.3}$$

After the Hadamard transform, we can then measure every qubit and look at the weight of the resulting string. The parity of the weight is equal to b. The procedure is summarized in figure 12.2.

If we assume the cat state is provided to us with no errors, this circuit solves the issue of error propagation. A single fault in it can certainly only produce one error in the data block. If we define a picture for the

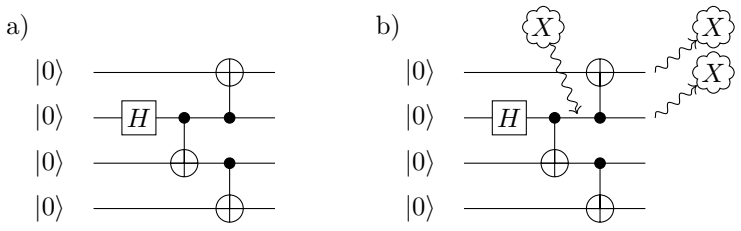

Figure 12.3: a) A non-fault-tolerant circuit to construct a 4-qubit cat state. b) The effect of an error on this construction.

gadget of "non-destructive cat-state measurement"

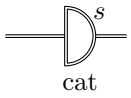

(12.4)

which gives a classical bit as output and has the data block persist, then we have shown that

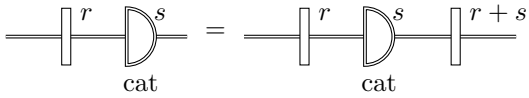

(12.5)

assuming a perfect cat state is provided to us.

Of course, the procedure still fails the MCP. A single bit flip error in the final measurement of the ancilla will give the wrong output value, as will a phase error earlier in the circuit. While we've made progress, we still have two problems to take care of: How can we create a cat state reliably, and how can we make the output bit more robust?

12.1.3 Constructing Cat States

First, let's think about how to make the cat state. There are lots of simple circuits to make cat states, such as the one in figure 12.3a.

Unfortunately, they all share a common structure: Put one qubit in the state $|+\rangle$ and start the others as $|0\rangle$. Then do a bunch of CNOTs in order to entangle all the qubits.

The problem is that this is not transversal at all. Again, a bit flip error in the middle, as in figure 12.3b, can produce multiple bit flips in the output, giving us a state such as $|0011\rangle+|1100\rangle$ instead of $|0000\rangle+|1111\rangle$. If you use the erroneous cat state in the measurement circuit of figure 12.2, the data block will inherit the errors on the cat state, leading to multiple errors in the data block, all from a single fault during the construction of the cat state. That is not acceptable.

One solution is to build the cat state as in figure 12.3a, but then check it before using it. How can we check it? Well, the cat state is kind of a repetition code — all qubits are supposed to be the same in the standard basis. We can check that by looking at pairs of qubits and seeing if they are the same or different. (But remember, we don't want to collapse the superposition, so we should only measure the parity, not whether they are 0 or 1.) We've already discussed how to do that in chapter 2; just use an ancilla qubit and two CNOTs, as in figure 12.4.

If we do this on enough pairs of qubits, any single fault in the circuit originally constructing the cat state (figure 12.3a) will be picked up by the checks. If we are using a code that corrects more errors, we can do additional checking to take care of up to s faults. If the checks reveal a serious problem, we can discard the state and start over. If you find that wasteful, you may prefer to do extra checks and instead try to correct the cat state. Either way works.

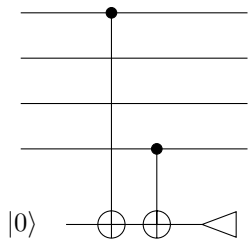

Figure 12.4: Checking a cat state to see if the first and last qubits are the same or different.

But hold on! Circuit figure 12.4 is non-transversal itself. Couldn't a single error in it cause two errors in the final cat state?

Surprisingly, no. To understand this, we have to look carefully at the types of errors and how they propagate. As usual, it is sufficient to consider Pauli errors. Now, on the cat state, a single Z error on any qubit gives us $|0\ldots0\rangle - |1\ldots1\rangle$. Two Z errors on different qubits gives us $|0\ldots0\rangle + |1\ldots1\rangle$, which is the correct state again. In general, an odd number of Z errors gives us the same state as just one Z error and an even number of Z errors is the same as no Z errors. That is, for the cat state, it's only possible to have a single Z error! (A more pessimistic point of view is that a single Z error is already enough to completely ruin the cat state, so having more can't make things worse.) A Y error we can think of as an X error plus a Z error, so we don't have to worry about it separately here.

Now, multiple X errors are definitely a possibility, and something we need to avoid. But the circuit from figure 12.4 can only cause one X error in the cat state if there is a single faulty location. We'll detect a single pre-existing X error with the check, so we're not so worried about propagation of pre-existing X errors. Looking at figure 12.4, we don't have anything to worry about anyway, since X can propagate in the first CNOT from the cat state into the check qubit, but then in the second CNOT, it doesn't propagate back into a second cat state qubit. (X only propagates from control to target in a CNOT gate.) A fault in the second CNOT can never cause more than one fault in the cat state. So that leaves a fault in the $|0\rangle$ check qubit preparation location or a fault in the first CNOT. But since CNOT only propagates phase errors from the check qubit into the cat state, either of these faults can only produce a phase error in the second cat state qubit. The worst case then seems to be a fault in the first CNOT that produces a bit flip error in the first cat state qubit and a phase error in the check qubit, which then propagates into a phase error in the second cat state qubit. This would seem to lead to a bit flip error in one cat state qubit and a phase error in a second cat state qubit, for a total of two errors from one fault. However, Z errors on different qubits act the same way on the cat state — they are degenerate — so $X \otimes Z$ on the cat state can be rewritten as $-iY \otimes I$, which is a one-qubit error.

There is one other issue we need to be careful about with the check qubits. A single bit flip error on the check qubit, whether coming from the preparation of the check qubit or due to a fault on one of the CNOT gates, can lead to the wrong outcome of the check qubit. This doesn't directly lead to a problem in the cat state, but as part of a gadget where multiple errors are a possibility, an incorrect check qubit could combine with other faults to lead us to the wrong decision as the whether to keep the cat state or not. This can be avoided by repeating the checks extra times, meaning more erroneous check qubits are required to trick us.

Taking all this into account, we can now say

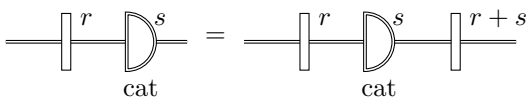

(12.6)

without assuming a perfect cat state is provided. We'll build our own.

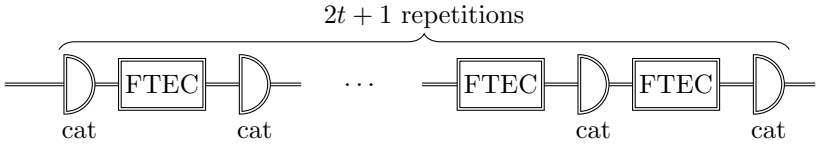

Figure 12.5: Fault-tolerant cat state measurement, including repetition and interspersed error correction steps.

12.1.4 Repeating the Measurement

Of course, it's still true that a single error in the cat state will cause the measurement to give the wrong result. The solution is to repeat the measurement using a new cat state. One fault somewhere in the circuit can cause an error only in one cat state, so if the number of repetitions we use is sufficiently larger than the number of faults we need to worry about, we should be able to deduce the correct outcome.

That's the principle, anyway. To actually make a FT measurement gadget this way requires a more careful analysis and an additional modification. As long as the errors in the circuit only affect the cat state, simple repetition is enough, but if there are also errors in the codeword we are measuring, we get more problems.

To see why, consider a codeword of the five-qubit code with a single physical bit flip error on qubit i, $X_i|\overline{\psi}\rangle$. Suppose we wish to measure the logical $\overline{Z}$ on this state. A representative of $\overline{Z}$ for the five-qubit code is $Z \otimes Z \otimes Z \otimes Z \otimes Z$, so we might hope it is sufficient to use the above cat state measurement procedure to measure its eigenvalue. However, X_i anticommutes with this representative of $\overline{Z}$, so the eigenvalue of $X_i|\overline{\psi}\rangle$ for $Z^{\otimes 5}$ is the opposite of the eigenvalue of $|\psi\rangle$ for Z. Note that X_i commutes with other representatives of the same logical Pauli $\overline{Z}$; this is another example where choice of apparently equivalent representatives of logical Pauli operators produces fault-tolerant protocols with potentially different properties. More generally, if the physical error E undergone by the codeword anticommutes with the Pauli P which we are measuring, cat state measurement will give the wrong answer, no matter how many times we repeat it.

In order to solve this problem, clearly we should do error correction just before beginning the cat state measurement procedure. We haven't discussed how to do error correction yet, but we will shortly. Any method of FT error correction will work, but out of the methods discussed in this chapter, the Steane and Knill error correction techniques have associated measurement techniques, and it makes more sense to use the matching measurement techniques since they have the same advantages and disadvantages as the EC gadgets. The cat state measurement technique is thus best paired with Shor error correction, which I'll discuss in section 12.2.

However, one property all FTEC gadgets have in common is that they only guarantee correcting errors on the input state. It is always possible that an error late in the FTEC gadget will leave a residual error at the end of the gadget. Therefore, EC just before cat state measurement is not sufficient to be sure that there are no physical errors around. Furthermore, a fault during a single cat state measurement procedure can produce an error in the data — we have gone to great effort to ensure that one fault just produces a single-qubit error, but we can't rule out errors altogether. That would have the effect of making all future cat state measurement repetitions wrong too if the error anticommutes with P. The current repetition may or may not be wrong, depending on the exact nature of the fault.

In order to handle these problems, we'll need to do error correction not just at the beginning of the measurement gadget, but after each repetition of the cat state measurement. We don't actually need to include an EC gadget at the beginning of the measurement gadget at all, since our standard FT simulation (definition 10.6) already puts an EC between every adjacent pair of gadgets. Putting another one right at the start of the measurement gadget would thus be redundant. The overall measurement gadget thus looks like figure 12.5.

Note that the EC steps included inside the cat state measurement gadget are constructed exactly like the standard EC gadgets discussed later in this chapter, but they are considered part of the measurement

gadget as a whole rather than as separate error correction gadgets. They are *sub-gadgets*, if you like, of the bigger FT measurement gadget.

12.1.5 Cat State Measurement Satisfies the FT Measurement Property

Now to prove that this procedure taken as a whole actually works, giving a measurement gadget that satisfies the MCP.

Theorem 12.1. *For a code that corrects t errors, the cat state measurement gadget consisting of $2t+1$ repetitions of single-cat state measurements interspersed by FTEC steps satisfies that MCP. The classical measurement outcome is taken by choosing the majority measurement outcome among the repetitions.*

Proof. We have constructed the single-copy cat state measurement procedure so that

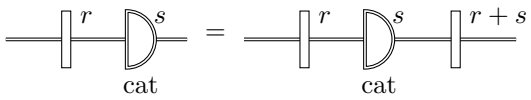

(12.7)

Furthermore, if there are no errors in the incoming state and the single-copy cat state measurement circuit has no faults (including during the construction of the cat state), then the outcome is correct:

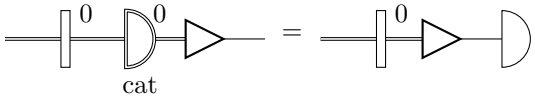

(12.8)

The picture assumes a non-destructive ideal measurement, since the cat state measurement procedure is non-destructive, and equality includes having the same classical bits for the measurement outcome.

We need one more property of the single-copy cat state measurement. It is a non-destructive procedure, and the output state does not have too many new errors (maximum equal to the number of faults). We'd like to say that the encoded state doesn't change under this procedure, except for being decohered in the basis being measured. If the whole procedure has no incoming errors and no faults, we've already included this effect in equation (12.8), but when there are errors or faults, we want a weaker property where the encoded state is correct, but the measurement result may not be. We can codify this using the pictures

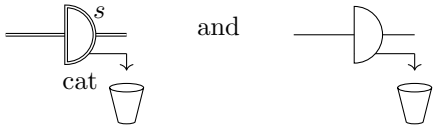

(12.9)

to represent measuring non-destructively (using the cat-state measurement gadget and ideal measurement, respectively) and discarding the classical outcome but keeping the quantum state.

Lemma 12.2. *Single-copy cat state measurement satisfies*

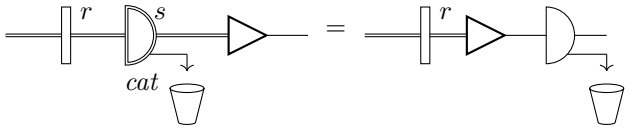

(12.10)

if $r + s \leq t$.

Proof of lemma. To prove equation (12.10), consider an input state

$$|\psi\rangle = \sum_j E_j|\psi_j\rangle = \sum_{j,a} c_{ja} E_j|\overline{a}\rangle, \tag{12.11}$$

where $|\overline{a}\rangle$ are encoded basis states for an eigenbasis of the Pauli P being measured, and we may assume E_j are Paulis with weight $\leq r$ because of the r-filter. As in the proof of theorem 11.6, we can assume there is only one E_j for each error syndrome of the code.

Because of the procedure checking the cat state, if there are at most s_c faults in the circuit constructing and checking the cat state, the cat state used in the main part of the procedure can be written $F(|0\ldots0\rangle + |1\ldots1\rangle)$, with $\operatorname{wt} F \leq s_c$. The part of the procedure involving controlled-Paulis from the cat state to the data has s_g faults, with $s_c + s_g \leq s$, and assume we can write the new errors as $G_c \otimes G_d \in \mathsf{P}_{n+m}$, occurring after the gate. Subscripts c and d indicate the parts acting on cat state and data, respectively. We have $\operatorname{wt} G_c \leq s_g$ and $\operatorname{wt} G_d \leq s_g$.

Now, E_j can propagate into the cat state and F propagates into the data block. Therefore, after the interaction, the data has error $H_{dj} = G_d F' E_j$ and the cat state has error $H_{cj} = G_c E'_j F$. Here F' is the effect of propagating F into the data and E'_j is the effect of propagating E_j into the cat state. Note that the interaction gates are controlled-Pauli gates, which leave a single-qubit error the same on the original qubit, but may add a Pauli on the other qubit involved in the gate. The only really important points are that

$$\operatorname{wt} H_{dj} \leq \operatorname{wt} G_d + \operatorname{wt} F' + \operatorname{wt} E_j \leq s_g + s_c + r \leq r + s \leq t \tag{12.12}$$

and that H_{dj} and H_{cj} are Paulis.

Now suppose we trace over the cat state and apply an ideal decoder to the data block. The ideal decoder measures the error syndrome of H_{dj}, so different values of the error syndrome get decohered. Since the error syndrome $\sigma(H_{dj}) = \sigma(G_d F') + \sigma(E_j)$, all E_j have different error syndromes, and G_d and F' don't depend on j, it follows that all different H_{dj} have different error syndromes too. Thus, we can treat the output state as a mixture over different js. In particular, we can analyze each j separately.

For a specific j, H_{cj} is a fixed Pauli. When the encoded basis state $|\overline{a}\rangle$ has eigenvalue b for P, the cat state, with errors, is $H_{cj}\left(|0\ldots0\rangle + (-1)^b|1\ldots1\rangle\right)$. Since H_{cj} is unitary, for fixed j, the states $|\overline{a}\rangle$ with eigenvalue $+1$ have an orthogonal cat state value to the basis states with eigenvalue -1. Thus, tracing over the cat state has the effect of decohering the system according to the eigenvalues of P. The output of the left hand side is thus

$$\sum_j |\psi_{j+}\rangle\langle\psi_{j+}| + |\psi_{j-}\rangle\langle\psi_{j-}|, \tag{12.13}$$

where $|\psi_{j\pm}\rangle = \sum_a c_{ja}|a\rangle$, with the sum taken over a with eigenvalue ±1.

The right hand side does the same thing: The ideal decoder immediately decoheres j, and then the ideal decoherence step decoheres the $+1$ eigenvalues from the -1 eigenvalues. □

Since we use fault-tolerant EC steps in the gadget, they satisfy the ECRP and ECCP. Therefore, if we have a sequence of adjacent EC steps and cat state measurement with no faults, the measurement outcome of that cat state measurement will be correct for the encoded state exiting the EC step, regardless of the number of errors going into the EC step:

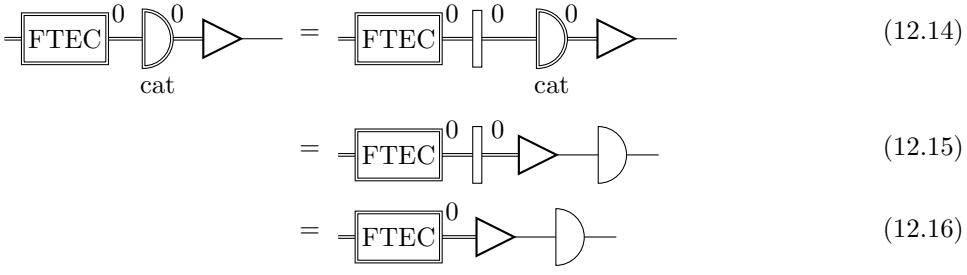

(12.14)

(12.15)

(12.16)

We use the ECRP in the first line to add a 0-filter and again in the last line to remove the 0-filter, and use equation (12.8) to get the second line.

Now suppose we have a state which passes an r-filter initially and subject it to a circuit with s_i faults in cat state measurement repetition i ($i = 0, \ldots, 2t$) and s'_i faults in EC step i ($i = 1, \ldots, 2t$). EC step i occurs between measurement repetition $i-1$ and i. The total number of errors plus faults is $r + \sum_i s_i + \sum_j s'_j \leq t$.

I claim that the state after cat state measurement repetition i passes an r_i-filter, with $r_i = s_i + s'_i$: Let $s'_0 = r$. The case $i = 0$ follows directly from equation (12.7). For repetition i, we have

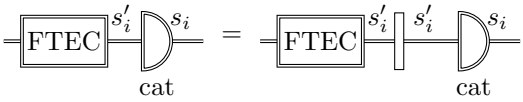

(12.17)

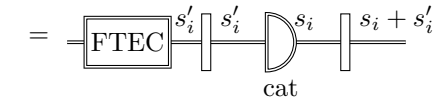

(12.18)

using the ECRP in the first line and equation (12.7) in the second.

After all repetitions of the cat state measurement gadget are completed, we discard the residual quantum state and keep only the majority classical result. Suppose, however, we didn't throw away the state, but instead performed an ideal decoder on it. Then the LHS of the MCP would look like

(12.19)

Let us look at the last repetition of the measurement. By equation (12.18), we can insert a r_{2t-1} filter before the last EC step, and by the ECRP, we can insert a s'_{2t}-filter after the last EC step. We have for the LHS of the MCP (focusing on the last repetition)

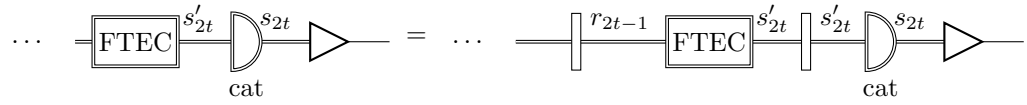

(12.20)

If $r_{2t} = s'_{2t} + s_{2t} = 0$, we can apply equation (12.8) to move the ideal decoder left past the cat state measurement, getting an ideal measurement instead:

(12.21)

If $r_{2t} > 0$, we cannot do this, but it is still true that $r_{2t} \leq t$, so we can apply equation (12.10) to move the ideal decoder left. Instead of getting an ideal measurement, we get an ideal decoherence, and must discard the classical measurement result to get equality:

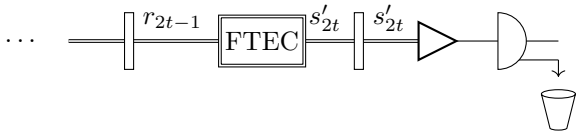

(12.22)

Of course, in the real system, we don't know which case we have; this is just a formal approach to help us understand the effect of the faulty measurement gadget.

The point is, in either case, we are left with the combination

(12.23)

followed by an ideal measurement. If $r_{2t} = 0$, the classical measurement outcome is correct, whereas if $r_{2t} > 0$, the classical measurement outcome might be incorrect. We can further process (12.23) using the FTEC properties. First use the ECRP to remove the s'_{2t}-filter, then use the ECCP, with the condition that

$r_{2t-1} + s'_{2t} \leq t$, to move the ideal decoder further left:

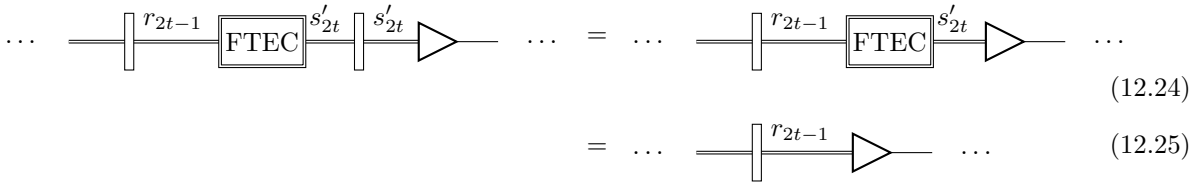

(12.24)

(12.25)

Now we can remove the r_{2t-1}-filter using equation (12.18) again, and we now have the $(2t-1)$st repetition of the single-copy cat state measurement followed by an ideal decoder. We can follow the same procedure to move the ideal decoder left again, past the EC step and cat state measurement, leaving the ideal decoder after the $(2t-2)$th repetition. We keep on doing this until the ideal decoder is just after the first repetition:

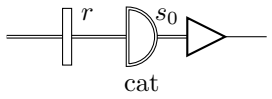

(12.26)

We then apply equation (12.8) or equation (12.10) one last time to move the ideal decoder to just after the r-filter.

We are left with an r-filter, followed by an ideal decoder, followed by a sequence of measurement steps, in some of which we keep the measurement result and in others of which we discard the measurement result. In particular, we had to discard all the measurement results corresponding to repetitions with faults, and keep the measurement results corresponding to repetitions with no fault in either the EC step or cat state measurement step. In the real measurement gadget, we don't know which ones to keep and which ones to throw away, so instead we just get a sequence of ideal measurement steps, but with *some of the classical results being possibly wrong*. Notice that, since each cat state measurement is for the same Pauli P, at least all the correct measurement results are the same.

Since $\sum_{i=0}^{2t} r_i \leq t$, at least $t+1$ of the r_i must be 0. Thus, out of the $2t+1$ classical measurement results, at least $t+1$ of them are correct. Therefore, taking the majority gives the correct measurement outcome, and we can conclude

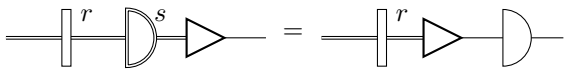

(12.27)

leaving the same residual quantum state on the left and the right. Therefore, the LHS and RHS are also the same if we throw away the quantum state, which means we no longer need the ideal decoder on the LHS. That gives us the MCP. □

12.2 Shor Error Correction

12.2.1 The Challenge for Shor EC Construction

Cat state measurement gives us an FT measurement gadget valid for any stabilizer code, but only if we already have an FTEC gadget for the code. So we should figure out an error correction gadget, don't you think?

Luckily, we can build one using the same basic component of cat state measurement. This technique was invented by Peter Shor, so is known as Shor error correction.

The basic idea is simple: We use cat state measurement to measure the eigenvalue of each generator of the stabilizer in sequence. Put these together, and we have the error syndrome as a classical bit string. Then we do classical processing to figure out what error corresponds to that error syndrome, and correct the appropriate qubit(s) of the code. There may be some error syndromes that correspond to no errors of weight $\leq t$. Nevertheless, we'll assign some error to each such error syndrome; that way, if a rare error occurs that happens to have one of the extra error syndromes, we won't be totally lost.

We've constructed the cat state measurement so that we don't get too many extra errors appearing in the data during the syndrome measurement — no more than the number of faults. However, that's not good enough for the ECRP; we need to get rid of all the pre-existing errors too. Furthermore, we still have the problem that a single error during a cat state measurement can give us the wrong result. While we don't care about the value of syndrome *per se* — we discard it after the EC gadget is done — we are going to try to correct a qubit based on the syndrome, and if we have the wrong syndrome, we will incorrect the state rather than correcting it.

For instance, consider the five-qubit code, table 3.2. Suppose the true error is Y_3, which has syndrome 1110. A single fault during the cat state measurement for the first syndrome bit could instead give us syndrome 0110, which corresponds to the error X_4. Instead of removing the error, we add one.

This may not worry you, since the ECCP only insists that the EC gadget behave correctly when $r+s \leq 1$, and a pre-existing Y error plus a fault during the measurement gives $r+s=2$. However, imagine that there are no errors on the incoming state ($r=0$), but a single fault occurs on the controlled-Z gate between qubit 3 of the cat state and qubit 3 of the data block during the cat state measurement for the first syndrome bit. Since the location is a two-qubit gate, a fault can produce errors on both qubits involved in the block. For instance, it could produce a Y error on the data qubit and a Z error on the cat state qubit. With just a single fault, this will cause both the error on the state to be Y_3, as above, and the first bit of the syndrome measurement to be wrong. Thus, we have a mistaken notion that the error is X_4 and perform the appropriate correction, giving us an output state with two errors on it. Even an ideal decoder won't get it right at this point.

Actually, the situation is even worse than that. Imagine that instead of having the fault at the beginning of the syndrome measurement process, we had it in the middle. Initially, there is no error, but then, perhaps after successfully measuring the first two bits of the error syndrome (and getting 00, since there is as yet no error), the error Z_2 occurs. Suppose we then measure the next two syndrome bits correctly too, getting 01. We then put this together to find the syndrome 0001, which corresponds to error X_1. The error syndrome *changes* in the middle of error correction, causing us to get a hybrid syndrome, which corresponds to a totally different error. Again, a single fault causes us to end up with two errors in the code block.

12.2.2 Repeated Syndrome Measurement

The solution, as with the cat state measurement gadget, is to repeat the syndrome measurement multiple times. That might make you nervous, since before we needed to use EC steps between each repetition. However, the situation is a bit different here. Before, there was a true measurement outcome (once the state collapses), and we need the gadget to output the correct classical bit. Each attempt at a cat state measurement tells us something about the encoded state, but also something about the error on the state, which is extraneous information for a measurement gadget.

Here, we *want* to learn about the error. We don't care what the original syndrome is, only a syndrome that tells us what the pre-existing errors were. If it also tells us about some errors that have subsequently occurred during error correction, so much the better. The main thing to avoid, as we saw with the examples, is the case where the syndrome is simply wrong, and is telling us about errors that *didn't* occur.

We need to be careful in how we do the repetition, though. Suppose we were to say, OK, I need to repeat each syndrome bit so that I can rely on it. I'll repeat the first syndrome bit measurement three times, then I'll do the second syndrome bit measurement three times, and so on, as in figure 12.6. If we were to do that, we'll avoid the problem from the first example. The repetition of each measurement will ensure that we get the right value for the first syndrome bit, giving us the right overall syndrome for this case. This recipe for repetition won't help us with the second example, however. In that example, all four syndrome bits were correct when they were measured, it's just that the syndrome changed while we were measuring it.

Instead, we should measure all bits of the syndrome, and then repeat, as in figure 12.7. It's still possible that the syndrome could change in the middle of a measurement, but at least then the next time we measure the syndrome, it will be correct (assuming there are no new faults).

How many times do we need to repeat the measurement? To get the ECCP and ECRP, we need to consider cases in which there are up to t faults in the circuit. If we ever get $t+1$ syndrome measurements

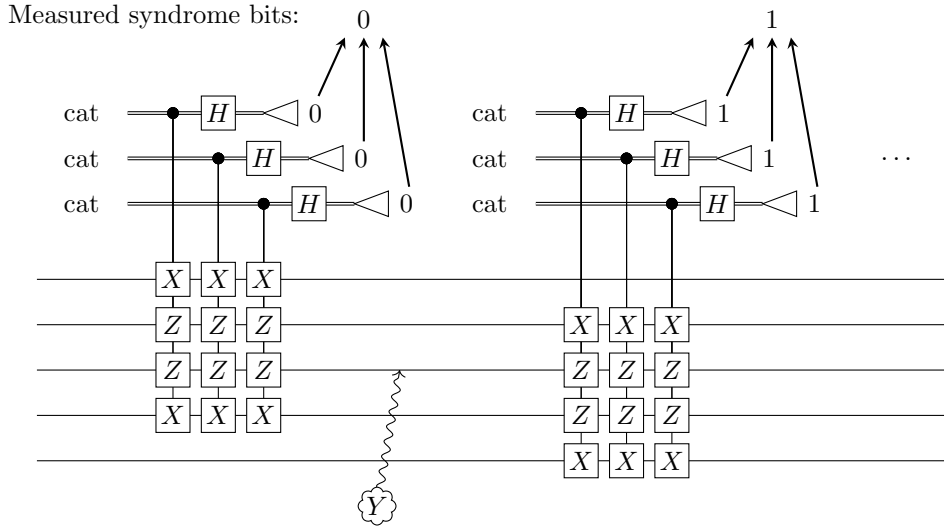

Figure 12.6: Repeating measurement of syndrome bits one-by-one for the five-qubit code. Because Y_3 occurs only after all repetitions of the first syndrome bit measurement are complete, the observed syndrome is 0110, which corresponds instead to X_4, instead of the correct syndrome 1110.

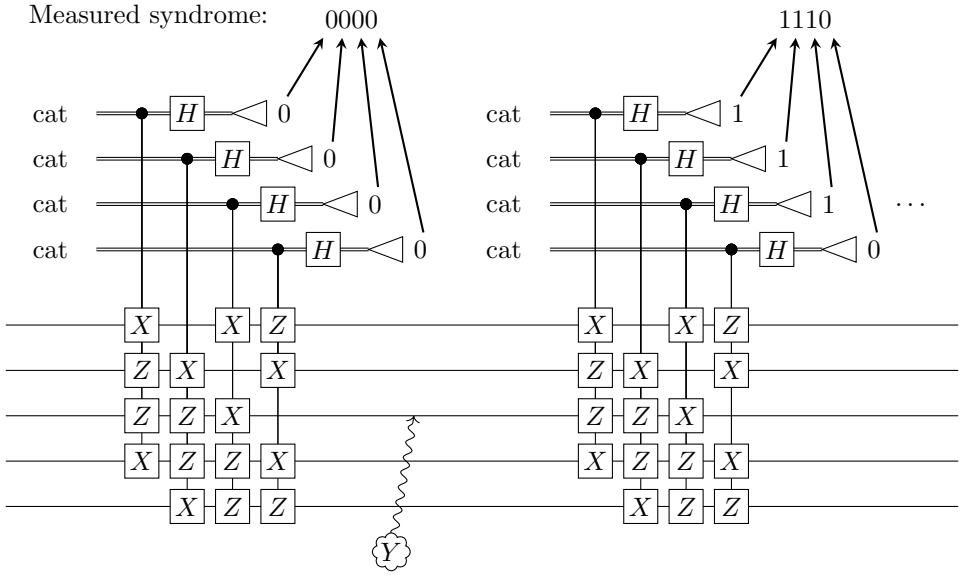

Figure 12.7: Measuring the full syndrome and then repeating for the five-qubit code. When the Y_3 error occurs after the first syndrome measurement, the second and future syndrome measurements give the correct syndrome 1110.

in a row that are all the same, we thus know they must be correct, since at least one of those measurements occurred with no faults. Indeed, even if not all the syndrome measurements that agree are consecutive, we can be sure one of them was correct. It may not correspond to the *current* syndrome, but at least it corresponded to the correct syndrome at some point, and that will actually be enough to give us both the ECCP and the ECRP. The ECRP, for instance, insists that we correct all the errors that were in the state going into the EC gadget, but doesn't insist that we correct errors due to faults during the gadget.

Unfortunately, since there are 2^{n-k} possible values of the syndrome, it is not enough to repeat $2t+1$ times and take the majority, as we did for the measurement gadget. There might not *be* a majority. In particular, the syndrome can change over the course of the process, so even though a majority of the measurements have to be correct, the syndromes produced by the correct measurements could differ.

For simplicity, I'll use the rule "repeat many times and then look for a sequence of $t+1$ consecutive syndrome measurements that all agree." If there is more than one such sequence, take the last one (since it will give the most up-to-date value of the syndrome). How many repetitions do we need to ensure that we get a sequence all the same? Well, we could get a sequence of t that agree (without faults), followed by one that disagrees (due to a fault). Then we could get another sequence of t that agree, followed by one that disagrees, and so on. To get each one that disagrees, we need a fault, and there are a maximum of t faults in the circuit. Therefore, we could use up $t(t+1)$ repetitions without ever getting a sequence of t in a row that all agree. However, if then do $t+1$ further repetitions, there can be no more faults in the circuit, and all the last $t+1$ repetitions will agree. Therefore, $(t+1)^2$ repetitions is sufficient.

In the case where we don't have any string of $t+1$ consecutive syndrome measurements that agree, take the longest string (and latest, if there is a tie), and use that. This can only occur if there are more than t faults in the circuit, but it makes sure we have a well-defined protocol in all cases.

Certainly, using different rules to determine the syndrome, we could significantly reduce the number of repetitions needed. Indeed, we might even hope to track changes to the syndrome as new faults occur, which could allow us to deduce the current syndrome rather rapidly. However, it is difficult to analyze such strategies in the completely general case, so I'll stick with the simple rule given above.

12.2.3 Shor EC Satisfies the FT EC Properties

Theorem 12.3. *The Shor EC gadget satisfies the ECRP and ECCP.*

Proof. As usual, we can assume all faults cause Pauli errors and the errors on the input state are Pauli errors. By linearity, we don't need to consider a superposition of input states with different errors; it will be sufficient to just look at a single Pauli error and show that we can correct that.

From equation (12.7), we know that each single cat state measurement can add only as many errors as the total number of faults in the circuit. Thus, if the input state passes an r-filter, and the circuit has s faults, then at all times, the data state will pass an $(r+s)$-filter. However, this is not quite sufficient, since we'd also like to know the error on the state doesn't radically change, which would invalidate any earlier attempt we made at learning the error syndrome. We'd also like to be able to say something about the case when the measurement has no errors. Equation (12.8) is also insufficient, since to do error correction, we need to consider the case where the state being measured has errors on it.

Claim 12.4. *Suppose $|\psi\rangle$ is a codeword of S, $E \in \mathsf{P}_n$, and $E|\psi\rangle$ is given as input to a single cat state measurement of $M \in \mathsf{S}$. If the measurement circuit has 0 faults, then the output state is $E|\psi\rangle$ and the classical measurement outcome is $c(E, M)$. If the measurement circuit has $s \leq t$ faults, then the output state is $FE|\psi\rangle$, with $F \in \mathsf{P}_n$, $\operatorname{wt} F \leq s$.*

Proof of claim. The 0-fault part of the claim can be easily checked directly from the description of cat state measurement. For the s-fault part of the claim, consider applying equations (12.7) and (12.10) to the code obtained from S by applying the Pauli E. (The code $E\mathsf{S}E^\dagger$ has the same distance as S.) □

First, we'll prove the ECRP. As discussed above, if we have an s-fault Shor EC gadget with $s \leq t$, then there must be a sequence of $t+1$ consecutive syndrome extraction steps (each consisting of $n-k$ cat state

measurements of the syndrome bits) for which all extracted syndromes agree, and furthermore, at least one of the syndrome extraction steps has no faults.

Consider the last sequence of $t+1$ indentical syndromes and the last faultless syndrome extraction step in the sequence, and suppose the error entering that step is E. Then, according to claim 12.4, the syndrome deduced by the measurements is indeed $\sigma(E)$. According to the rule used above for determining the syndrome in Shor EC, $\sigma(E)$ is thus chosen as the "correct" error syndrome deduced by the gadget. The state exiting the last cat state measurement in the faultless syndrome extraction is $E|\psi\rangle$. Then we can apply claim 12.4 repeatedly to deduce that the state after the last cat state measurement in the whole gadget is $FE|\psi\rangle$. The additional error F has weight equal to at most the total number of faults in the circuit after the faultless syndrome extraction we identified, so $\operatorname{wt} F \leq s$.

If the final Pauli correction step has no faults, the final output state of the gadget will be $E'FE|\psi\rangle = \pm F(E'E)|\psi\rangle$, where E' is an error with the same error syndrome as E. We have not put any constraint on $\operatorname{wt} E$, so it is certainly quite possible that $E' \neq E$. However, we do know that $E'E \in \mathsf{N}(\mathsf{S})$ since they have the same error syndrome. Thus, $(E'E)|\psi\rangle$ is also a valid codeword, and the state passes an s-filter, as desired for the ECRP.

When the final Pauli correction step does have faults, the output state of the gadget will have additional errors. However, the Pauli correction is done transversally (though it is not a gadget!), so any faults in the correction can only cause errors on the individual qubits affected by the locations with the faults. That is, the output state will instead be $GE'FE|\psi\rangle = \pm(GF)(E'E)|\psi\rangle$, with $\operatorname{wt} G$ at most the number of faults in the Pauli correction step. Since $\operatorname{wt}(GF)$ is less than the total number of faults in the gadget, the final state does still pass an s-filter.

For the ECCP, a slightly modified version of the above argument works. Now we restrict the input state to have at most r errors. Assume the input state is $E_0|\psi\rangle$, with $|\psi\rangle$ a codeword and $\operatorname{wt} E_0 \leq r$. Again we identify a faultless syndrome extraction step in the sequence of $t+1$ steps used to deduce the error syndrome. Applying claim 12.4 to all the cat state measurements before the syndrome extraction step of interest, we find the error entering that syndrome extraction step is $E_1E_0|\psi\rangle$, with $\operatorname{wt} E_1$ at most equal to the number of faults before the chosen step. Let $E = E_1E_0$. Applying the 0-fault part of claim 12.4, the syndrome deduced by the faultless syndrome extraction step is $\sigma(E)$ and the state exiting the step is $E|\psi\rangle$. Then we apply claim 12.4 to all the cat step measurement steps after the chosen syndrome extraction, ending up with the state $FE|\psi\rangle$. As before, the final Pauli correction leaves us with the state $GE'FE|\psi\rangle = \pm(GF)(E'E)|\psi\rangle$. From above, we know that $\operatorname{wt}(GF) \leq s \leq t$.

In this case, we also have a bound on $\operatorname{wt} E$: We know $\operatorname{wt} E_0 \leq r$, and $\operatorname{wt} E_1 \leq s$, since E_1 comes from faults in cat state measurements during the gadget. Thus, $\operatorname{wt} E \leq r + s \leq t$. Since the code corrects t errors and $\sigma(E)$ is a syndrome which includes errors of weight $\leq t$, it must be that $E'E \in \mathsf{S}$. (It's still possible that $E' \neq E$ if the code is degenerate.) Therefore, the output of the gadget is the state $\pm(GF)|\psi\rangle$. Since $\operatorname{wt}(FG) \leq t$, the ideal decoder can correct this error, so the LHS of the ECCP gives output $\pm|\psi\rangle$.

The RHS of the ECCP has the ideal decoder acting on the state $E_0|\psi\rangle$, with $\operatorname{wt} E_0 \leq r \leq t$. The ideal decoder can correct E_0, giving the output $|\psi\rangle$. The LHS and the RHS could differ by a global phase which depends on E and F but not on $|\psi\rangle$. The pictures represent equality as CP maps, so the global phase does not matter. Therefore, we have proven the ECCP for Shor EC. □

You might be a bit worried by the global phase appearing at the end of the proof. If the errors are indeed pure Pauli errors, the phase is indeed a global phase, and everything is fine. But what if we have a superposition of Pauli errors instead? Since the phase depends on the exact errors and fault path, it seems like this might produce a relative phase rather than a global phase. However, it turns out everything is still OK.

Let's carefully think through the proof of the ECCP with superpositions of errors. We have a syndrome measurement procedure that determines the syndrome is $\sigma(E)$. That means that, even if the error at the point of syndrome extraction is actually a superposition of different errors, the syndrome extraction itself will decohere the errors (as we saw in section 2.4) to produce a superposition over only Pauli errors that share the same syndrome. Since $r + s \leq t$, all the Paulis in the superposition will have weight less than t and those with the same syndrome can differ only by elements of the stabilizer. That is, $E = E'' \sum_\alpha c_\alpha M_\alpha$,

where $E'' \in \mathsf{P}_n$ and $M_\alpha \in \mathsf{S}$. Then

$$E|\psi\rangle = E'' \sum_\alpha c_\alpha M_\alpha |\psi\rangle = E''|\psi\rangle \tag{12.28}$$

up to normalization.

The correction E' is always a Pauli (for a stabilizer code, which is assumed for Shor EC) since we are choosing it based on the measured syndrome. However, F, caused by faults after the successful syndrome measurement, and G, caused by faults in the final Pauli correction, could be superpositions of Paulis. The state of the LHS of the ECCP just before the ideal decoder is

$$GE'FE|\psi\rangle = GF'|\psi\rangle, \tag{12.29}$$

where F' is the same superposition of Paulis as F, but with some signs changed due to commuting E' through. GF' might be a different error than GF in more significant ways than a global phase, but both are t-qubit errors and so the ideal decoder will correct either just as well. Thus, the final state of the LHS of the ECCP is indeed $|\psi\rangle$ up to global phase and perhaps normalization, so the ECCP holds even for superpositions of Pauli errors.

12.3 Steane Error Correction and Measurement

With all the issues about repeating syndrome measurements and verifying cat states, Shor EC gets to be pretty complicated. Perhaps more importantly, it involves a lot of locations. Lots of locations means lots of opportunities for errors, which eventually will translate into a lousy threshold. We'd therefore like to reduce the number of locations in an error correction gadget. Unfortunately, error correction for quantum codes seems to be a pretty complicated thing, so there's a limit to how simple we can make the error correction gadget.

There's another trick we can play. Not all faults are equally bad. What we'd like to avoid is a build-up of errors in a single data block. Locations that include physical qubits from the code block are therefore inherently dangerous. Even the best fault-tolerant techniques won't usually be able to tolerate more than t faults directly affecting the data qubits.

On the other hand, errors in the ancilla are only bad if they propagate into the data or cause us to make a wrong choice (for instance, concluding the wrong error syndrome). We've already seen the trick of checking our cat state ancillas before using them, and other ancillas can be checked too. If we're careful about it, we can create a circuit that will satisfy the FT conditions even when there are many more than t faults, provided most of the faults are in the part of the circuit creating ancillas. Why can we check ancillas but not the data qubits? The reason is that we know the precise ancilla state that we are trying to create, but the state of the logical qubits somewhere in the middle of a long computation is unknown, and moreover, any single logical qubit is likely to be entangled with many other logical qubits.

Consequently, we can benefit by shifting a lot of the work we do during error correction into creating an ancilla. Steane EC (again named after its inventor) uses more complicated ancillas than Shor EC, but involves much simpler interaction between the data and the ancilla.

12.3.1 Steane EC

Steane error correction is available for CSS codes. The basic idea is to take advantage of the fact that transversal CNOT performs the logical $\overline{\text{CNOT}}$ for any CSS code.

How can that help us do error correction? Consider the circuit of figure 12.8a. The ancilla is in the state $|\overline{+}\rangle = |\overline{0}\rangle + |\overline{1}\rangle$, encoded in the same CSS code as the data. The transversal CNOT from the data block to the ancilla block performs $\overline{\text{CNOT}}$ on the logical state, but $\text{CNOT}|\psi\rangle|+\rangle = |\psi\rangle|+\rangle$, regardless of $|\psi\rangle$. The operation is therefore trivial if we only focus on the encoded states. Still, the transversal CNOT does do something: It propagates errors. In particular, if there are bit flip errors in the data block, they propagate to the same locations in the ancilla block.

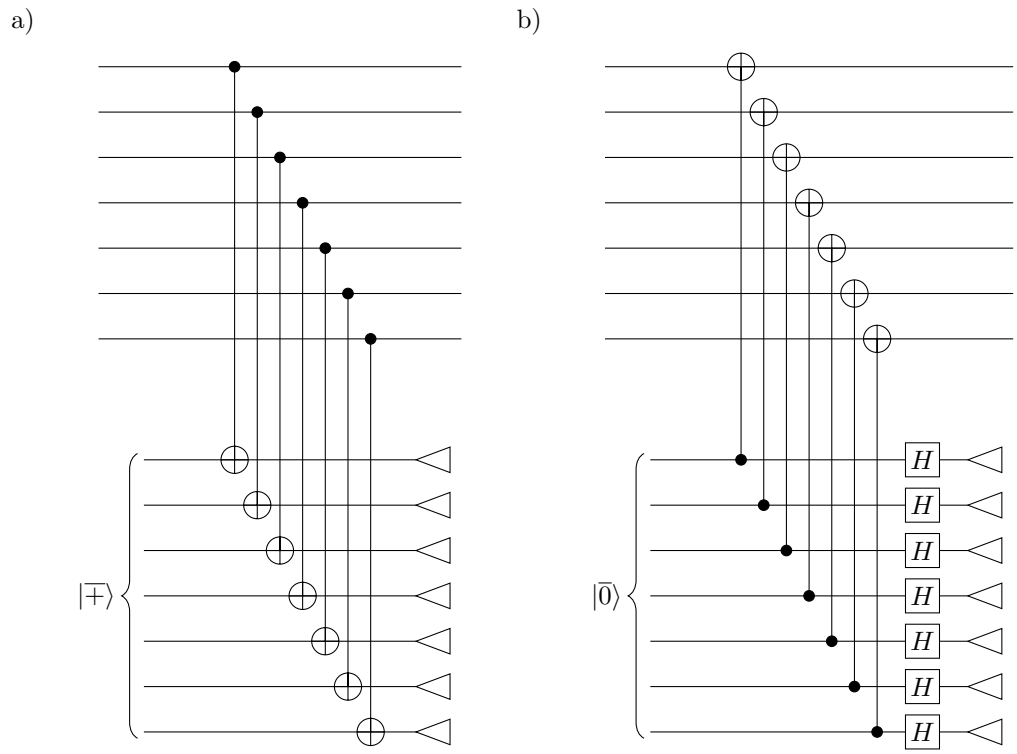

Figure 12.8: a) The Steane method of bit flip error correction for the 7-qubit code, b) The Steane method of phase error correction for the 7-qubit code

We saw in section 11.4 that transversal measurement followed by classical decoding performs logical measurement for a CSS code. Since the ancilla encodes the state $|+\rangle$, logical measurement just gives a random outcome. In this case, however, we're interested in another aspect of the decoding, namely the classical error correction. Recall that transversally measuring a codeword of a CSS code gives a classical codeword, chosen randomly from the appropriate coset of $C_1/{C_2}^\perp$. In this case, the coset is also random, so in the absence of errors, we would get a uniformly random codeword of C_1.

When the state being measured has bit flip errors in it, instead of a codeword of C_1, we get a codeword of C_1 with some errors in it. If the measurement itself has no faults and the original quantum state has the bit flip error $(e|0)$ (written in binary symplectic notation), then the classical codeword resulting has the error e. Thus, calculating the classical error syndrome will tell us the bit flip part of the error syndrome for the CSS code. If there are faults in the measurement, a few additional classical bits may end up flipped, specifically those corresponding to the qubits affected by the faults. The classical error will thus include the quantum bit flip error plus a small number of additional bit flips.

Of course, what we are actually measuring is the bit flip error on the *ancilla*. Any bit flips present in the data have propagated to the ancilla, but there might also have been bit flips already present in the ancilla block. The circuit of figure 12.8a taken as a whole thus measures the error syndrome of an error $e + f + g$, where $(e|0)$ is the bit flip part of the error initially on the data block, $(f|0)$ is the bit flip error on the ancilla block entering the circuit, and $(g|0)$ are errors due to faults in the measurement step. Still, this tells us something about bit flips on the data block, so we can use it for error correction.

Of course, as we discussed in section 10.1.2, error propagation works both ways. While the bit flip errors from the data block are getting copied into the ancilla block, where they can be measured, any phase errors in the ancilla block simultaneously jump onto the data block. This is analogous to what happens in cat state measurement, where errors in the cat state construction can propagate into the data.

For these two reasons, we'll have to be careful how we build the ancilla state. If it has too many bit flip errors, the syndrome we deduce will be badly wrong, and if it has too many phase errors, the data block will inherit them and may end up wrecked, with too many phase errors to be fixed by error correction.

We also need a way to measure the phase errors in the data block. We can do that as in figure 12.8b, using the ancilla $|\overline{0}\rangle$ (encoded in a block of the same code) plus transversal CNOT with the ancilla as control and the data as target. Then phase errors flow from the data into the ancilla; of course, bit flip errors now propagate from ancilla into data. Since we want to identify the phase error syndrome, we should perform a transversal Hadamard, switching C_1 with C_2 and X errors with Z errors. Now when we measure transversally, we get a random codeword of C_2 with errors in the locations of the phase errors in the ancilla. Thus, we learn $e' + f' + g'$, where $(0|e')$ is the phase error in the data block, $(0|f')$ is the phase error in the ancilla, and $(0|g')$ are phase errors in the measurements. And of course, while we do this, any bit flip errors in the ancilla block will propagate into the data block.

A full Steane EC gadget consists of both bit flip syndrome measurement and phase error syndrome measurement, followed by a Pauli correction step. The process is summarized in figure 12.9. The figure has bit flip error correction before phase error correction, but the procedure is also fault-tolerant when they are done in the reverse order. In theorem 12.5 I'll prove the ECRP, which says that the state at the end of the gadget has no more than s errors when there are s faults in the gadget. The order of error correction steps doesn't affect this, but it does mean that the *type* of errors at the end of the gadget is more likely to be the type corresponding to the first type of error correction you choose to do, simply because there's more time (i.e., more locations) since the error correction was performed, giving more opportunity for new errors of that type. On the other hand, if there are more errors of one type than another in the state entering the FTEC gadget, doing that type of error correction first makes it more likely that we'll be able to correct the state even if $r + s > t$: we may get lucky and be able to correct the pre-existing error before new errors occur due to faults in the gadget.

There's something clearly missing in my description of Steane EC: How do we make the ancilla states and ensure they do not have too many errors? That is the complicated part of Steane EC. However, it is a complication that we would have to face anyway: In order to have a full FT protocol, we need preparation gadgets that create at least one type of encoded state, such as a $|\overline{0}\rangle$. This is precisely the ancilla state we need to do Steane phase error correction. For Steane bit flip error correction, we also need a $|\overline{+}\rangle$ state. That

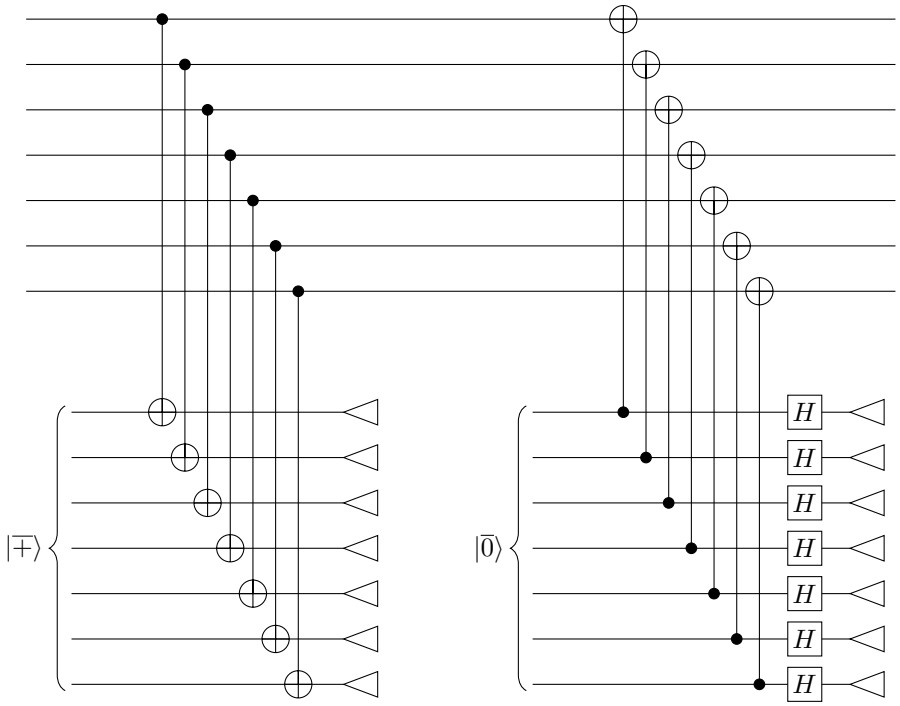

Figure 12.9: Steane error correction as a whole, excluding the final Pauli correction

will require a slightly different protocol, but one that uses the same ideas. We'll discuss how to make both of these states in chapter 13.

12.3.2 Steane Measurement

For CSS codes, we already have a destructive measurement gadget, namely transversal measurement. However, it is helpful sometimes to also have a non-destructive measurement gadget, and the ideas of Steane EC can be easily adapted to provide one. A non-destructive measurement gadget is fault-tolerant if it satisfies a slightly modified version of the MCP with a qubit output:

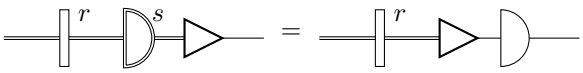

(12.30)

It also must satisfy a *measurement propagation property* (or MPP):

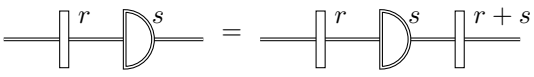

(12.31)

Both properties hold when $r + s \leq t$.

The procedure is almost obvious — perform a logical CNOT from the data block to an ancilla block in the state $|\overline{0}\rangle$, then measure the ancilla block transversally. The procedure is pictured in figure 12.10.

The main reason to mention this procedure is to point out the similarities to the bit flip part of Steane EC, figure 12.8a. Indeed, the *only* difference is that we use $|\overline{0}\rangle$ for the ancilla instead of $|\overline{+}\rangle$. This means instead of getting a completely random classical codeword (perhaps with errors), we get a codeword (with errors) chosen randomly from some coset $C_1/{C_2}^{\perp}$. Which coset we get tells us the result of the measurement.

Also note that the Steane measurement procedure combines non-destructive measurement with bit flip error correction. When we just think of it as a measurement gadget, we ignore the extra syndrome information

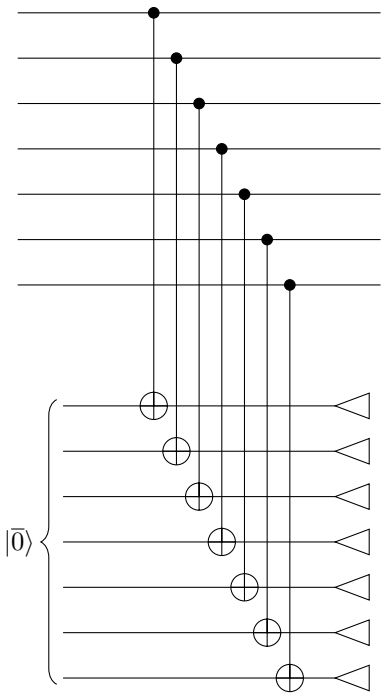

Figure 12.10: Steane measurement for the 7-qubit code

produced by decoding the classical codeword. But that information is there, and is useful just as in Steane EC. In the right context, it is helpful to both measure the state and correct any bit flip errors we might find.

12.3.3 Do We Need to Repeat Steane EC and Measurement?

For Steane measurement, no repetition is needed. It's just built up of two steps: transversal gate, followed by transversal measurement. The creation of the ancilla state is not transversal, but we're assuming we use a protocol from chapter 13 that is fault tolerant. All steps by themselves are fault tolerant, so together they should be fault tolerant too. (Actually, you shouldn't take that for granted; there are cases where it's not true. This time it works, however.) The result is reliable even if we don't repeat it. In particular, ancilla errors are taken care of along with errors from the data block. Both are handled by a classical error correction step which follows the transversal measurement.

As I've described Steane EC, we also don't repeat the syndrome measurement for that either. Can that be correct? After all, it's still true that errors in the ancilla can cause us to deduce the wrong syndrome. Surely we still have to worry about that.

It turns out, though, that we don't. The extra errors caused by the ancilla or measurement errors are additive: We can describe the final classical error as $e + f + g$, where e is the actual bit flip or phase error in the data block and f and g are ancilla and measurement errors. The measured error thus corresponds to the true error plus some additional errors. If we try to correct the error by doing the Pauli $(e + f + g|0)$ (for a bit flip error), then we are left with bit flip error $(f + g|0)$. Among other things, this means that a single-qubit error in the ancilla can only produce a single-qubit error in the final state. This is in contrast to Shor EC, where a single ancilla error changing one bit of the error syndrome could totally change the error we deduce.

Another important aspect of Steane EC is that the errors in the data are detected by looking at an ancilla qubit which corresponds to the location of the error in the data block. Recall that in Shor EC, it was possible that a single fault in a controlled-Pauli location could produce an error in the data block and also cause an

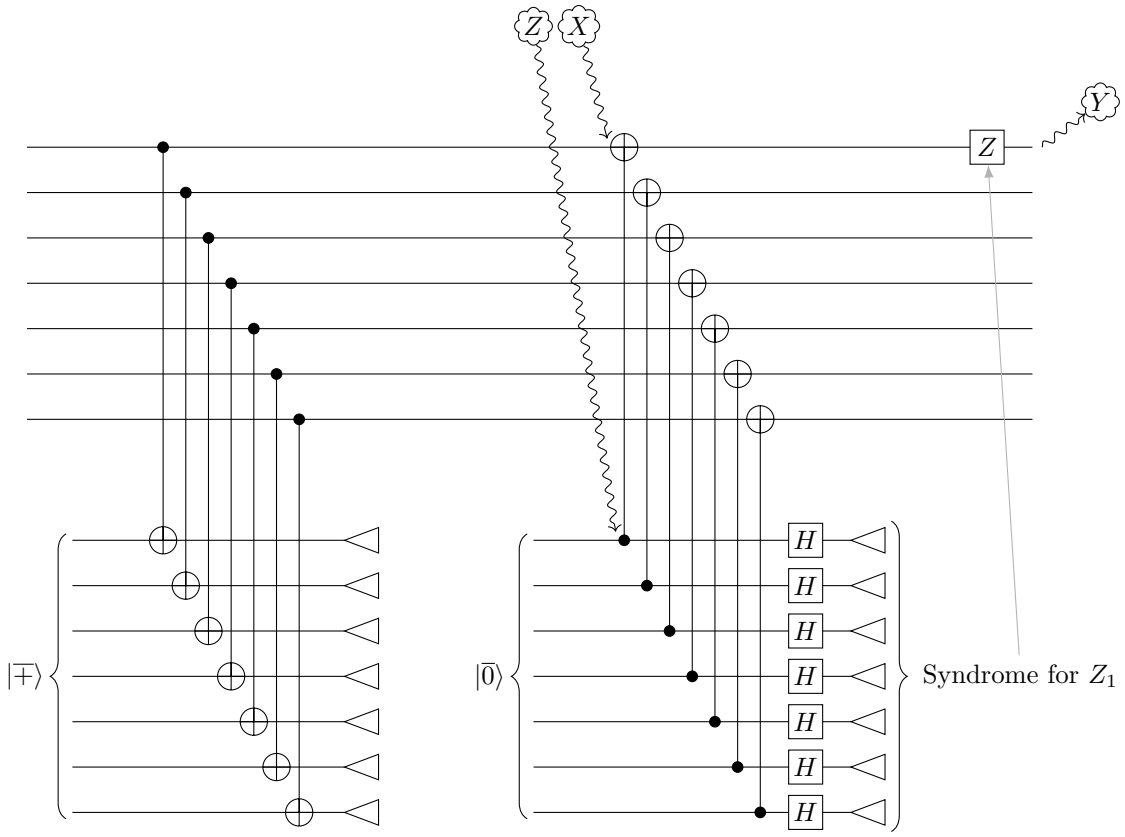

Figure 12.11: Steane error correction with a fault in one of the CNOT gates. The gate fault causes a Z error in the first ancilla qubit, which produces an error syndrome corresponding to a Z error in the first data qubit. The corresponding "correction" combines with an X error in the first data qubit caused by the same gate fault to produce an overall Y error on the first qubit; but it is still a single-qubit error.

error in the ancilla which changed the measured syndrome. For Steane EC, this can still happen, but only in a very restricted way: The ancilla error caused by such a fault can only change the syndrome in such a way as to add or remove an error on the same qubit involved in the two-qubit location, as in figure 12.11. (This is presuming the total number of faults in the circuit is less than t.)

The upshot is that we don't have the same problems that made it mandatory to repeat syndrome measurements in Shor EC. Of course, by not repeating, we do make it easier for errors in the ancilla to end up in the data. No matter what we do, in Steane EC, phase errors from the ancilla will propagate into the data during bit flip correction, but if we don't repeat the syndrome measurement, bit flip errors in the ancilla will also end up in the data, as in figure 12.12. Without repeating the measurement, there is no way to distinguish them from bit flip errors in the data, so our attempt at correcting them will actually add them as errors to the data block. That's not a huge problem; they will be corrected in the next EC gadget.

If you prefer to repeat the syndrome measurement for Steane EC, that's fine. It's a trade-off, however. By repeating, you will have more confidence in the syndrome you deduce, and ancilla errors will be less likely to end up in the data block. However, you also increase the overhead, and in the process add more opportunity for errors to build up and overwhelm your error correction capability.

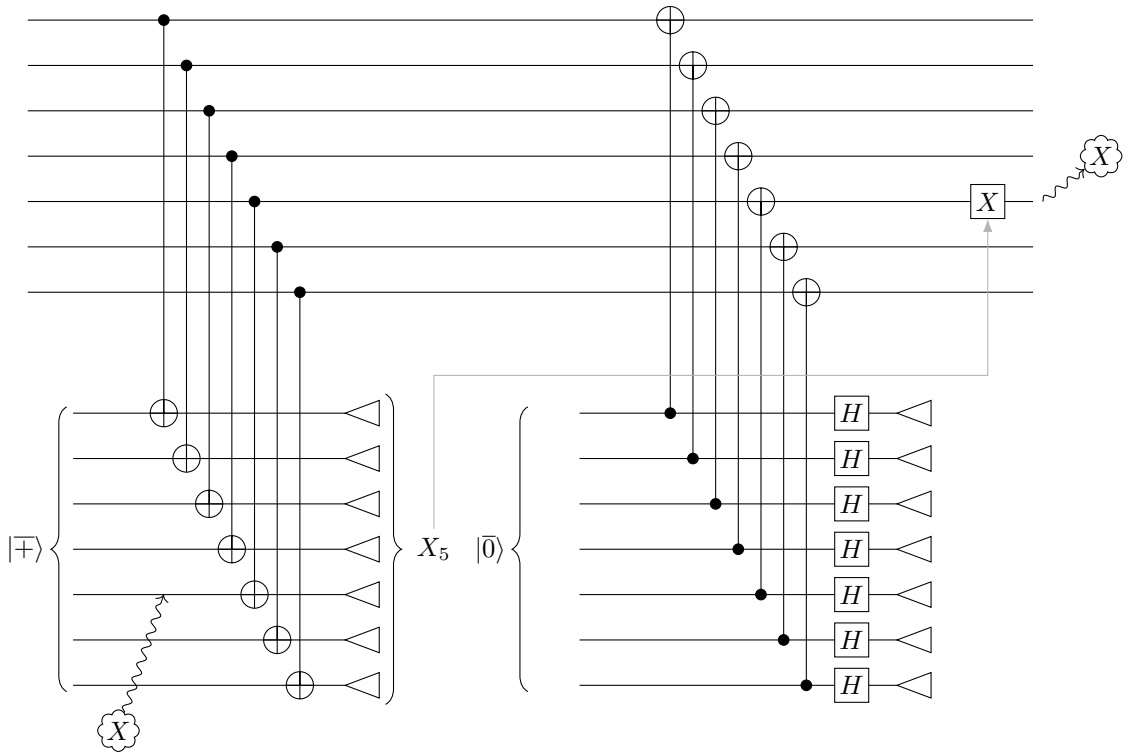

Figure 12.12: If Steane error correction is not repeated, an ancilla error will be incorrectly interpreted as a data error that needs to be corrected.

12.3.4 Steane EC and Measurement Satisfy the FT Properties

Theorem 12.5. *Steane EC satisfies the ECRP and ECCP. Steane non-destructive measurement satisfies the non-destructive version of the MCP and the non-destructive measurement propagation property.*

Proof. Proving Steane measurement satisfies the two non-destructive measurement properties is not hard: Steane measurement is made of three steps, $|\overline{0}\rangle$ FT state preparation, transversal CNOT, and transversal (destructive) measurement. All three of these steps are FT gadgets in their own right, so we can apply the FT properties of the sub-gadgets in order to prove the FT properties for Steane measurement.

To be more explicit: First, apply the PPP and the GPP to put filters after the first two subgadgets:

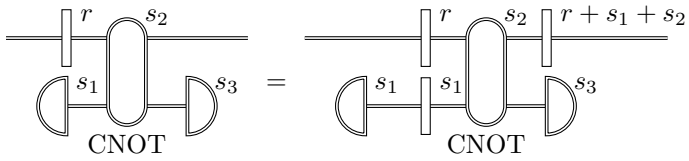

(12.32)

(Note that we can use the GPP to put just a filter on the first block and not on the second, see exercise **??**.) Then by using the PPP again to remove the s_1-filter, we have already proven the measurement propagation property, since $s = s_1 + s_2 + s_3 \geq s_1 + s_2$.

For the MCP, we do the same thing to a circuit with an ideal decoder and then use the destructive measurement MCP to replace the measurement subgadget with an ideal decoder. We can do this since $(r + s_1 + s_2) + s_3 = r + s \leq t$ by hypothesis. We find

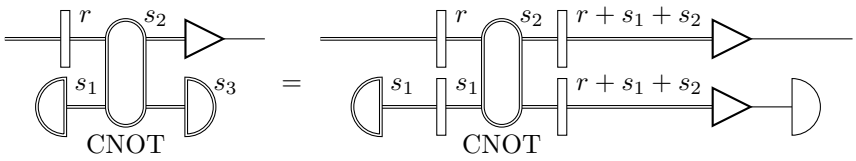

(12.33)

We can then remove the $(r + s_1 + s_2)$-filters using the GPP and apply the GCP to move the ideal decoders to before the gate gadget:

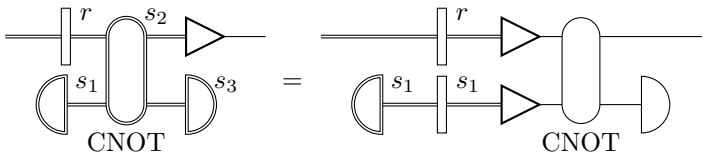

(12.34)

Then use the PPP to remove the s_1-filter after the ancilla preparation and the PCP to turn it into an ideal preparation:

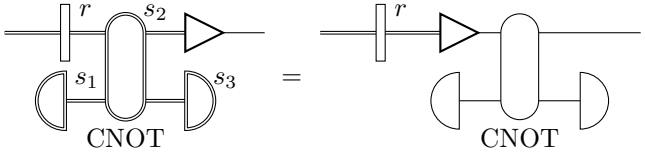

(12.35)

The RHS takes the state that passes through the r-filter, decodes it, and does a perfect CNOT to a perfect $|0\rangle$ and measures the ancilla. This implements an ideal non-destructive measurement, proving the MCP.

Steane EC requires a more careful treatment. We'll prove fault-tolerance for the version of Steane EC with phase error correction first, but the proof is essentially identical when bit flip error correction is first. As usual, we'll assume the input state has a Pauli error and that all faults in the gadget also cause Pauli errors.

It will be most convenient to represent the errors in binary symplectic form. We'll name the errors from the various parts of the circuit as described in table 12.1. Depending on the detailed implementation, there

	new data	new ancilla	total data	total ancilla
Input error	$(e_x\|e_z)$		$(e_x\|e_z)$	
Phase prep.		$(a_x\|a_z)$	$(e_x\|e_z)$	$(a_x\|a_z)$
Ph. CNOT	$(c_x\|c_z)$	$(c'_x\|c'_z)$	$(e_x + a_x + c_x\|e_z + c_z)$ $= (D_x\|D_z)$	$(a_x + c'_x\|a_z + e_z + c'_z)$
Phase meas.		$(f_x\|f_z)$	$(D_x\|D_z)$	$(a_z + e_z + c'_z + f_x\|a_x + c'_x + f_z)$
Bit flip prep.		$(b_x\|b_z)$	$(D_x\|D_z)$	$(b_x\|b_z)$
B.f. CNOT	$(d_x\|d_z)$	$(d'_x\|d'_z)$	$(D_x + d_x\|D_z + b_z + d_z)$	$(b_x + D_x + d'_x\|b_z + d'_z)$
B.f. meas.		$(g_x\|g_z)$	$(D_x + d_x\|D_z + b_z + d_z)$	$(b_x + D_x + d'_x + g_x\|b_z + d'_z + g_z)$

Table 12.1: Symbols for errors in the various parts of Steane EC in the data block and ancilla blocks. The ancilla column is for the ancilla block used for the type of errors being corrected at the moment. "New" indicates new errors caused at the end of that part, and "total" indicates the overall error at the end of that part due to error propagation. Error means error relative to the ideal starting codeword.

may be wait steps on the data block after the CNOT steps; for the purposes of this calculation, errors due to the wait locations can be absorbed into the errors due to the CNOTs. Similarly, the errors due to the Hadamards needed for the phase measurement can be absorbed into the measurement locations.

Based on this calculation, we see that the phase error syndrome we will see in this circuit is $a_z+e_z+c'_z+f_x$ and the bit flip error syndrome we see is $b_x + e_x + a_x + c_x + d'_x + g_x$. However, as discussed before, we may not be able to exactly deduce these errors. Instead, we'll decide the error is $(s_x|s_z)$, a Pauli with the same error syndrome as the actual measured error

$$P = (b_x + e_x + a_x + c_x + d'_x + g_x|a_z + e_z + c'_z + f_x) \tag{12.36}$$

Since their syndromes are the same, we know

$$M = (b_x + e_x + a_x + c_x + d'_x + g_x + s_x|a_z + e_z + c'_z + f_x + s_z) \in \mathsf{N}(\mathsf{S}). \tag{12.37}$$

At this point, the actual error is

$$Q = (e_x + a_x + c_x + d_x|e_z + c_z + b_z + d_z) \tag{12.38}$$

Now, when we make the correction in the final step of the gadget, there may be an additional error $(h_x|h_z)$. Therefore, at the end of the gadget, the overall error, taking into account the correction $(s_x|s_z)$ performed, is

$$(e_x + a_x + c_x + d_x + s_x + h_x|e_z + c_z + b_z + d_z + s_z + h_z). \tag{12.39}$$

Now, multiplying by an error in the normalizer leaves us with a codeword, so we can conclude that the final state is a quantum codeword with error

$$E = (d_x + b_x + d'_x + g_x + h_x|c_z + b_z + d_z + a_z + c'_z + f_z + h_z). \tag{12.40}$$

This seems more complicated. However, we have designed each part (state preparation, CNOTs, measurement) of the Steane EC gadget to itself be fault-tolerant. Therefore, the number of new errors in a block due to any part cannot be greater than the number of faults in that part. Furthermore, for the CNOT steps, the errors in the data block and ancilla block must be on corresponding qubits; i.e., $\mathrm{wt}(0|c_z + c'_z)$ must be at most the number of faults in the phase CNOT step and $\mathrm{wt}(d_x + d'_x|d_z)$ must be at most the number of faults in the bit flip CNOT step. In all, we can conclude that if there s faults in the circuit, any sum of errors excluding e_x and e_z must have weight at most s. In particular, $\mathrm{wt}\, E \leq s \leq t$. Therefore, the ECRP is satisfied.

For the ECCP, we assume the input state passes an r-filter, so $\mathrm{wt}(e_x|e_z) \leq r$. Then, using the same logic as the previous paragraph, we conclude from equation (12.36) that $\mathrm{wt}\, P \leq r + s \leq t$. If the code is non-degenerate, then there is just one error of weight $\leq t$ with a given error syndrome, so $(s_x|s_z) = P$. If

the code is degenerate, there might be more than one error with the same syndrome as P, but regardless, it will be the case that $M \in \mathsf{S}$ (whereas before we could only say that M is in the normalizer). Therefore, we conclude that if the initial state is $(e_x|e_z)|\overline{\psi}\rangle$, then the final state is $E|\overline{\psi}\rangle$, with E given by equation (12.40). Since the error has weight at most t, the ideal decoder will correctly decode it to $|\psi\rangle$, which is the same as what the ideal decoder gets from the initial state. □

Notice that in the final error equation (12.40), we can see that the phase error has more contributions to it than the bit flip error rate. This is because we did phase error correction first, and as a result the phase error rate leaving the gadget is higher than the bit flip error rate.

12.4 Knill Error Correction and Measurement

So, Steane EC replaces the multiple rounds of repetition and numerous two-qubit gates needed for Shor EC with simply two CNOTs per physical data qubit, but at the cost of using encoded $|\overline{0}\rangle$ and $|\overline{+}\rangle$ states as ancillas instead of the simpler cat states. Steane EC trades off ancilla complexity for minimal direct disturbance of the data block. Can we go further in this direction, and reduce to a single CNOT gate per data qubit?

We'd also like to overcome one of the limitations of Steane EC. In particular, we'd like an FT error correction method that is as efficient as Steane EC but works for all stabilizer codes, not just CSS codes.

Knill EC achieves both of these goals. The basic idea is to combine teleportation of the logical state with error correction. Teleportation here is used simply as a trick to perform error correction. We don't actually intend to move the quantum state to a different location, so in this case Alice and Bob will be right next to each other in the same quantum computer. Of course, if you want to move the data and perform error correction at the same time, you could do that too.

12.4.1 Knill EC

Knill error correction for an arbitrary stabilizer code is shown in figure 12.13. The ancilla used for Knill EC is a logical Bell state, encoded in two blocks of the same code as the data.[1] Then we perform a transversal Bell measurement between the data block and the first ancilla block.

Note, in particular, that the encoded Bell state $|\overline{00}\rangle + |\overline{11}\rangle$ is different from n two-qubit Bell states $(|00\rangle + |11\rangle)^{\otimes n}$. Thus, even though Knill EC involves a transversal Bell measurement between the data block and the first ancilla block, it is *not* the same as teleporting each individual qubit. Instead, the Bell measurements have the effect of gathering information which lets us deduce the error syndrome.

As with Steane EC, I won't discuss yet how to create the needed ancilla state. That will be deferred until chapter 13. For now, just assume that the ancilla preparation procedure somehow satisfies the PPP and PCP.

What happens when we perform transversal Bell measurement using half of a logical Bell state? We can best understand this by breaking up the transversal Bell measurement into two steps: a transversal CNOT followed by transversal Pauli measurement (in the X basis for the data block and the Z basis for the ancilla block). Assume for the moment the CNOT and measurement are done without any faults. We'll allow errors in the ancilla state and data state before the CNOT, but only up to a total of t errors between them.

Consider an arbitrary Pauli P acting on the data block, and the same Pauli, but with possibly a different sign, acting on the first block of the ancilla. We are mostly interested in cases where $P \in \mathsf{N}(\mathsf{S})$ or $P \in \mathsf{S}$. We can write

$$(-1)^{b_i} P = i^{P_X \cdot P_Z} (-1)^{b_i} P_X P_Z, \tag{12.41}$$

where P_X is a tensor product of X's and I's, P_Z is a tensor product of Z's and I's, and $P_X \cdot P_Z$ is shorthand for "the number of qubits where both P_X and P_Z are non-trivial" (the power of i comes from the Y operators in P). The factor of $(-1)^{b_i}$ indicates the sign of the Pauli on the data block ($i = 0$) or ancilla block

[1] Actually, the second block doesn't need to be in the same code. If it is encoded in a different code, then Knill EC combines error correction with a code conversion gadget changing the way the data is encoded.

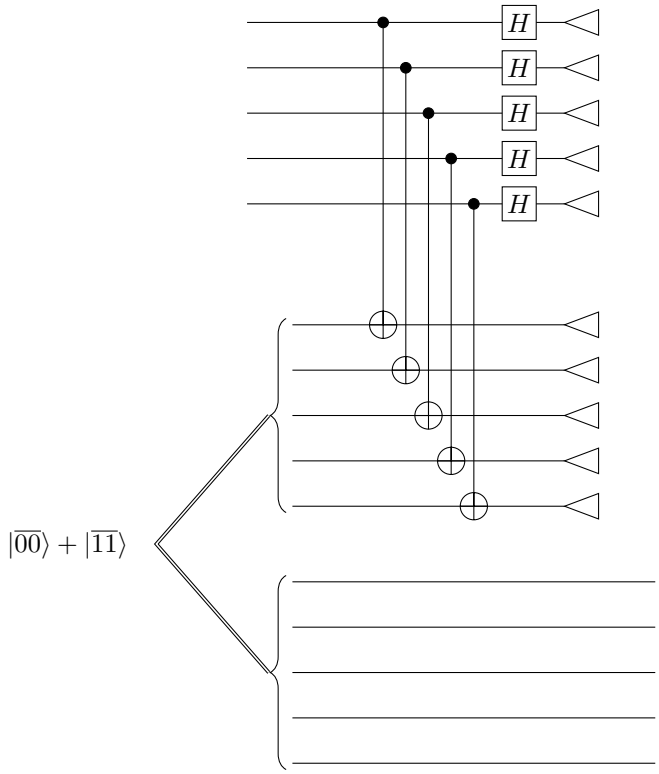

Figure 12.13: Knill error correction for the 5-qubit code; it works the same way for any stabilizer code, just with a different number of qubits. The transversal Bell measurement between the data block and first ancilla block is not the same as a logical Bell measurement, although it can be used to deduce the outcome of the logical Bell measurement.

($i = 1$). Unfortunately, in this argument, we care a lot about the phases, so working in the binary symplectic formalism is out.

The effect of the CNOT in figure 12.13 is to map

$$(-1)^{b_0} P \otimes I \to i^{P_X \cdot P_Z} (-1)^{b_0} P_X P_Z \otimes P_X \tag{12.42}$$

$$(-1)^{b_1} I \otimes P \to i^{P_X \cdot P_Z} (-1)^{b_1} P_Z \otimes P_X P_Z. \tag{12.43}$$

Notice that

$$(-1)^{b_0+b_1} P \otimes P \to (-1)^{b_0+b_1+c(P_X,P_Z)} P_X \otimes P_Z \tag{12.44}$$

because $c(P_X, P_Z) = P_X \cdot P_Z \bmod 2$. In other words, the tensor product $P \otimes P$ becomes a tensor product of X's on the data block and Z's on the ancilla block. Therefore, the subsequent measurement of X on each physical data qubit and Z on each physical qubit in the first ancilla block lets us deduce the eigenvalue of this operator. Since $c(P_X, P_Z)$ is known, we then learn $b_0 + b_1$.

This observation is very helpful, since we can apply it to *any* Pauli P. When P is a generator of the stabilizer, we can deduce the corresponding bit of the error syndrome, only we don't learn the syndrome of just the data block, but rather the sum $s_0 + s_1$, where s_0 is the syndrome of data block and s_1 is the error syndrome of the first ancilla block. This is no different than what happened for Shor or Steane EC: In Shor EC, errors in the cat state could cause errors in the syndrome we deduce, and in Steane EC, as in Knill EC, the syndrome we measure is also the sum of the syndrome in the data block with a syndrome derived from errors of the same type in the ancilla.

We can also apply the observation to measure logical Paulis. Indeed, from our measurement results we can deduce the eigenvalues of both $\overline{X}_i \otimes \overline{X}_i$ and $\overline{Z}_i \otimes \overline{Z}_i$ for every logical qubit i. That is, in addition to error correction, we can perform the logical Bell measurement. With that in hand, since the ancilla is part of an encoded Bell state, we can perform teleportation of the logical state.

However, we need to be careful about interpreting the outcome of the logical Bell measurement. First of all, I'm still just considering the case where there are no faults in the CNOT or measurement. Even so, remember that pre-existing errors in the data block or ancilla block can change the eigenvalue of $\overline{Q} \otimes \overline{Q}$ without actually changing the codeword one would deduce using an ideal decoder. Suppose we have E on the data block and F on the first ancilla block, both Paulis, satisfying $\operatorname{wt} E + \operatorname{wt} F \leq t$. Then if $(-1)^b$ is the correct eigenvalue of $\overline{Q} \otimes \overline{Q}$, meaning the value we'd get after doing ideal error correction, we instead measure $(-1)^{b'}$, where $b' = b + c(E, \overline{Q}) + c(F, \overline{Q})$.

Luckily, the same set of measurements that let us deduce b' also told us the error syndrome. The only problem is that they didn't tell us the error syndromes of E and F separately, but the sum of the error syndromes $\sigma(E) + \sigma(F) = \sigma(EF)$ (by proposition 3.7). Since $\operatorname{wt}(EF) \leq \operatorname{wt} E + \operatorname{wt} F \leq t$, from $\sigma(EF)$, we deduce an error $G = EFM$, with $M \in \mathsf{S}$.

Now, again using proposition 3.7, we find

$$c(E, \overline{Q}) + c(F, \overline{Q}) = c(EF, \overline{Q}) \tag{12.45}$$

$$= c(G, \overline{Q}) + c(M, \overline{Q}). \tag{12.46}$$

But $\overline{Q}$ is a logical operator, in $\mathsf{N}(\mathsf{S})$, so $c(M, \overline{Q}) = 0$. Thus, once we deduce G, we can deduce the correct eigenvalue $(-1)^b$ of $\overline{Q} \otimes \overline{Q}$, and therefore get the correct outcome for the logical Bell measurement.

Now let's consider what happens when there are faults in the CNOTs and measurements. As usual, we can assume the faults cause Pauli errors. The basic model for fault tolerance says that a fault on a CNOT location causes errors after the end of the CNOT, though of course we must allow the possibility that one faulty CNOT location could produce a one-qubit error in both the data and ancilla blocks. We can assume the errors in the measurement locations occur *before* the measurements, and therefore we can combine the errors from the CNOTs and measurements into a Pauli error E' on the data block and an error F' on the ancilla block. It may be that $\operatorname{wt} E' + \operatorname{wt} F'$ is greater than the number of faults, since a fault in a single CNOT location contributes to both, but it is true that $\operatorname{wt}(E'F')$ is at most equal to the number of faults in CNOT and measurement locations.

Since the data qubits are about to be measured in the X basis, a bit flip error has no effect. A phase or Y error on a data qubit will reverse the measurement outcome on that qubit. Therefore, we might as well assume E' is composed of only Z errors. Similarly, we can assume F' consists only of X errors, since the ancilla qubits are measured in the Z basis.

Now let's look at the effect of the additional errors on the measurement outcomes. When we measure the error syndrome of $M \otimes M \in \mathsf{S} \otimes \mathsf{S}$, the outcome is only affected if E' acts on qubits where M has an X or Y, or if F' acts on qubits where M has a Y or Z. In fact, the overall effect is to change the parity of the outcome by the parity of the number of qubits that meet this condition. In other words, the outcome of the measurement of $M \otimes M$ is changed by exactly $c(E'F', M)$. Running this over all generators in the stabilizer, we find that instead of the syndrome $\sigma(EF)$, we end up measuring the syndrome $\sigma(EFE'F')$.

Now, if the input data state passes an r-filter, the ancilla preparation has s_1 faults, and the CNOT and measurements combined have s_2 faults, then $\mathrm{wt}(EFE'F') \leq r + s_1 + s_2$. When this is less than t, we can deduce an error G' with the syndrome $\sigma(EFE'F')$. G' will only differ from $EFE'F'$ by an element of the stabilizer. Since E' and F' have the same effect on the logical operators $\overline{P} \otimes \overline{P}$ that they did on the stabilizer elements, that means we again end up deducing the correct value for the Bell measurement outcome.

Note that the physical qubits that exit Knill EC are brand new qubits, produced for the ancilla. There may be errors in them, but they are fresh errors arising from the ancilla preparation, and the errors are unrelated to whatever errors were in the data before. Furthermore, the only information that is directly used to complete the teleportation is the result of the logical Bell measurement. The error syndrome of the data is discarded. Still, we can't simply ignore the error syndrome: As discussed above, it is instrumental to determining correctly the outcome of the logical Bell measurement.

12.4.2 Knill Measurement

Essentially the same procedure can be used to measure the logical state directly. As we discussed in section 12.4.1, the transversal CNOT between two blocks of a general stabilizer code followed by transversal measurement of X on the first block and Z on the second block lets us deduce the sum of the error syndromes for the two blocks as well as the outcome of a logical Bell measurement on the two blocks. If the measurement we want to do *is* a logical Bell measurement, that's all we need.

Suppose, though, we want to measure a more standard single-block operator, such as $\overline{Z}$ for all encoded qubits in a block. We can use the same procedure as Knill EC, but with a $|\overline{0}\rangle$ ancilla instead of an encoded Bell state. Figure 12.14 is an example. As with Knill EC, we deduce the error G (which, in the absence of additional faults, is actually the product of the errors on the data and ancilla, up to a stabilizer element), and use it to deduce the outcome of a logical Bell measurement between the data block and the ancilla block. However, out of the logical Bell measurement, we're only really interested in the eigenvalue of $\overline{Z} \otimes \overline{Z}$. Since the logical state of the ancilla is $+1$ eigenstate of $I \otimes \overline{Z}$, the eigenvalue of $\overline{Z} \otimes \overline{Z}$ is the same as the eigenvalue of $\overline{Z} \otimes I$, which is what we're actually only really interested in. Because the original ancilla state is $|\overline{0}\rangle$, the eigenvalue of $\overline{X} \otimes \overline{X}$ is always completely random; it tells us nothing about the data. And that's all there is to Knill measurement.

12.4.3 Knill EC and Measurement Satisfy the FT Properties

Theorem 12.6. *Knill EC satisfies the ECRP and ECCP. Knill measurement satisfies the MCP.*

Proof. We already did most of the work proving that the Knill EC gadget is fault-tolerant in section 12.4.1. As usual, we can assume faults cause Pauli errors, and we will assume the input state also has a Pauli error on it.

As in section 12.4.1, we assume the ancilla preparation has s_1 faults, leading to error F on the first ancilla block and H on the second ancilla block, with $\mathrm{wt}\, F, \mathrm{wt}\, H \leq s_1$ by the PPP. We assume there are a total of s_2 faults on the CNOT and measurement steps (split up into s_2' on the CNOT, and s_2'' and s_2''' on the measurements), producing errors E' on the data block and F' on the first ancilla block, with $\mathrm{wt}(E'F') \leq s_2$. There are also s_3 faults on the logical Pauli correction step to end the teleportation and

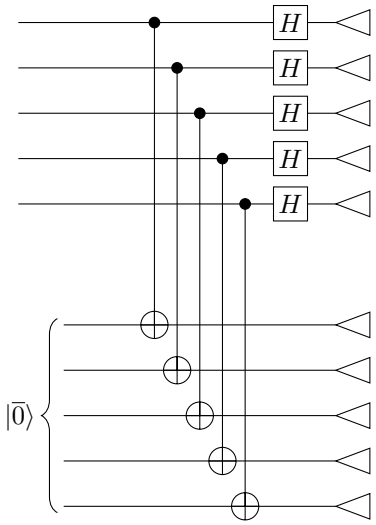

Figure 12.14: Knill measurement for the 5-qubit code. It may look almost the same as Steane measurement (figure 12.10), but the classical decoding (not shown) is different.

on any wait steps used for the second ancilla block, producing error H' on the second ancilla block, with $\mathrm{wt}\, H' \leq s_3$. $s_1 + s_2 + s_3 = s$, the total number of faults in the gadget.

For the ECCP, the input state Pauli error E has $\mathrm{wt}\, E \leq r$ so it passes the r-filter. We assume $r + s \leq t$. The argument in section 12.4.1 shows that, with this bound on the number of errors, the CNOT plus measurement plus classical processing steps give the same outcome as would an ideal Bell measurement applied to the state produced by the ideal decoder. In terms of pictures

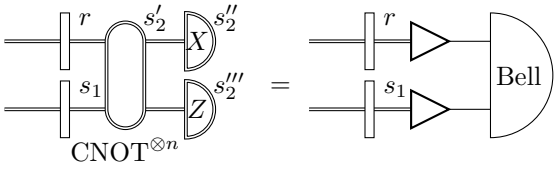

(12.47)

In particular, we can use the PPP to put an s_1-filter on each ancilla block after the ancilla preparation step, then use the above equation to replace the transversal Bell measurement with an ideal decoder followed by ideal Bell measurement. For the second ancilla block, the only operation after ancilla preparation is the logical Pauli (plus waiting), which is done transversally. We can thus use the GCP to push an ideal decoder on the output block back before the logical Pauli and remove the s_1-filters with the PPP. We find

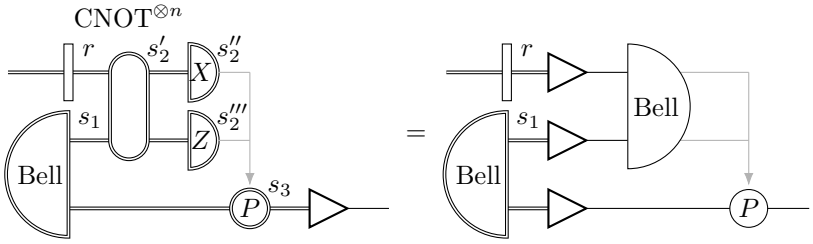

(12.48)

Then using the PCP, we can replace the state preparation gadget and ideal decoders with an ideal Bell state preparation. The RHS then consists of decoding the data block, followed by putting it through an ideal teleportation procedure. In other words, we have proven the ECCP.

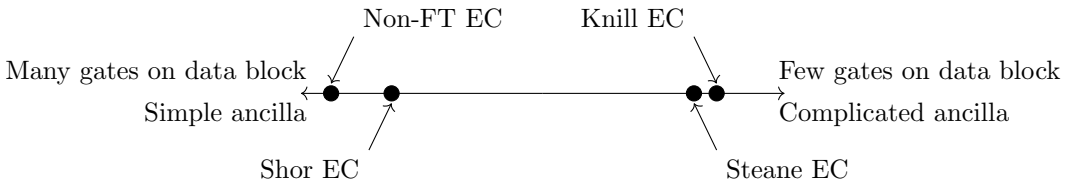

Figure 12.15: The spectrum of different error correction gadgets. Non-fault-tolerant EC has the same number of gates touching the data block as Shor EC but is more vulnerable to error propagation.

For the ECRP, we don't put any constraint on the input error, but the argument is nonetheless much simpler. The PPP tells us that we can put an s_1-filter after the ancilla preparation, and then the GCP applied to transversal gates tells us we can put an $(s_1 + s_3)$-filter after the logical Pauli step. Thus, the output state passes an s-filter, as demanded by the ECRP.

For Knill measurement, the MCP uses the same argument as the ECCP. The ancilla preparation is now of a $|\overline{0}\rangle$ state instead of a logical Bell measurement, but if the preparation procedure has at most s_1 faults, we can still use the PPP to put an s_1-filter after it. Then, using equation (12.47), we replace the transversal Bell measurement by ideal decoders and a logical Bell measurement, and use the PCP to replace the faulty ancilla preparation procedure with an ideal $|0\rangle$ state preparation. The RHS then consists of decoding the data, then doing an ideal Bell measurement between the data qubit(s) and a $|0\rangle$ state, which lets us deduce the outcome of a Z measurement on the decoded qubit. This is precisely what we want for the MCP. □

12.5 Efficiency of FTEC Protocols

12.5.1 Comparison of Shor, Steane, and Knill EC

Which FTEC gadget should you choose as part of an FT protocol? In this section, I'll compare the advantages and disadvantages of the three methods of fault-tolerant error correction to help you pick. Obviously, if you're using a non-CSS code, Steane EC is off the table, but even then there is a still a choice between Shor and Knill EC. What's more, most work on fault tolerance does use CSS codes, because they are easy to derive from classical codes and have transversal CNOT and measurement gadgets, so frequently all three protocols are possibilities. The best choice will depend both on what QECC you're using for the protocol and on various physical properties of the quantum computer implementation you may be using. So far, I've only discussed the basic model for fault tolerance, which corresponds to one particular choice of those physical properties. The alternate assumptions should probably be comprehensible now, but if you prefer, you could hold off reading this section until you've gone through chapter 15, which discusses variations on the basic model.

Basically, the three protocols lie on an axis from simple ancillas/many gates on data to complicated ancillas/few gates on data, as in figure 12.15. Shor EC is on the simple ancilla end of the axis and Knill EC is on the complicated ancilla end, with Steane EC in the middle (though not too far, perhaps, from Knill EC). There are other "Shor-like" EC methods that use even fewer qubits. In a system where you can't, for whatever reason (perhaps due to lack of sufficient extra qubits), deal with complicated ancillas, FTEC protocols on the simpler end of the axis are needed. In most other cases, it is better to have a gadget where fewer gates are performed on the data, since that will lead to lower logical error rates. This suggests using Steane or Knill EC.

The previous paragraph is conditional, however, on whether you can reliably prepare the ancillas needed. You might think Shor EC has an advantage here, since the cat state ancillas are so simple, but it is not so straightforward. Recall that a single phase error in a cat state results in the measurement giving the wrong outcome. When the cat state gets large, the probability of having a phase error somewhere in the cat state becomes high. Roughly speaking, if there is a p probability of phase error per qubit, an m-qubit cat state

has a probability $(1-p)^m$ of having no phase error on any qubit. When $mp \approx 1$, the measurement outcome is nearly uniformly random, unrelated to the actual syndrome bit being measured. Of course, we repeat the measurement result, which exponentially reduces the chance of reaching a wrong final conclusion about the syndrome, but if we are in the regime $mp \gtrsim 1$, many repetitions are needed to overcome the high noise rate. This makes Shor EC extremely unappealing for most large codes.

This issue is inherently less of a problem for Steane and Knill EC, where the ancillas are states encoded in blocks of the same QECC used for the main protocol, which is presumably capable of correcting a certain number of errors. The cat state is relatively robust against single bit flip errors, which may propagate to single-qubit errors in the data but otherwise are not too harmful, but can be completely destroyed by a single phase error. In contrast, a real QECC can correct single bit flip or phase errors; only if the total number of errors is large is there a serious problem. When the block size is big, creating the requisite encoded ancilla states can be challenging nonetheless; see section 13.1 for details. To deal with faults in a large quantum computation, we will need big codes to suppress the logical error rates sufficiently to complete the computation reliably. Thus, even Steane and Knill EC can be an issue unless we have a family of codes that allows us to make larger and larger ancilla blocks. Indeed, this is important in any case, since we need to be able to make $|\overline{0}\rangle$ states for preparation gadgets.

One thing to notice is that the size of the cat states for Shor EC depends on the weight of the stabilizer generators rather than the total number of qubits in the block. Therefore, a code with many physical qubits, but for which all stabilizer generators have low weight (an "LDPC", or *low-density parity check* code), still has very simple cat states. For most large codes, the problems of large cat states make Steane and Knill EC definitely better than Shor EC, but for LDPC codes, Shor EC can be better. For instance, in chapter 17, we'll see a family of LDPC codes known as *surface codes*. Frequently people using surface codes don't even bother with Shor EC, instead using the non-FT measurement technique of section 12.1.1 instead. They're willing to put up with the fact that one fault can cause multiple errors in order to have the even simpler one-qubit ancilla used in non-FT measurement instead of the four-qubit cat states they would need for Shor EC. Other LDPC codes can be appealing candidates for real systems as well, so that makes Shor EC and other small-ancilla techniques useful.

For non-LDPC code families, though, Steane and Knill EC seem better than Shor EC. But which of Steane and Knill EC should we choose? Their threshold performance is probably pretty similar, though as of this writing that hasn't been studied very systematically. The advantage of Steane EC is that the ancillas needed for it are exactly the same as those needed for a preparation gadget, whereas making the two-block entangled states for Knill EC can sometimes create an extra challenge. On the other hand, we'll see in chapter 13 that many gates can be performed via teleportation through an appropriate ancilla. Knill EC can be easily combined with this construction, producing a gadget that does error correction and a gate all at once. This is a useful way to save resources.

Another nice advantage of Knill EC is that the data ends up on brand new qubits. Many systems suffer erasure errors that take the physical qubits out of the standard two-dimensional Hilbert space, for instance though loss of photons or transitioning to additional energy levels in the system. Knill EC automatically returns the qubits to the computational Hilbert space every time it is performed. Knill EC can also be useful in shunting the data away from physical qubits which have an usually high error rate, perhaps due to a manufacturing defect or some nearby noise source.

12.5.2 The Pauli Frame

In this chapter, I've described the FTEC protocols in two steps: Measure the syndrome, then correct the errors. (In the case of Knill EC, the last step is instead "finish the logical teleportation.") The second step is straightforward, but it still involves some single-qubit gates, and therefore an opportunity for faults to occur. It turns out, though, that it is usually not necessary to do those quantum gates at all. Instead, it is sufficient to keep track of the information classically.

Imagine a Pauli error E with weight $\leq t$ occurs in the data, and then we do an EC gadget without faults. The syndrome measurement part of the EC gadget will tell us what E is, possibly up to an element of the stabilizer if the code is degenerate. Suppose we don't correct E, but simply make a note of it. If we are

working with a stabilizer code S, the subspace $E\mathcal{T}(\mathsf{S})$ is also a QECC. It is even a stabilizer code, and its stabilizer is $E\mathsf{S}E^\dagger$, which is just S again, but with different signs for the generators. It's an error-correcting code that has essentially all the same properties as S did. We can think of the EC gadget without correction as a combined gadget for error correction and code conversion. The final code, however, is chosen randomly. By making note of the error E, we can keep track of what the code is. The side classical information about E is known as the *Pauli frame*. Note that each block of the code has its own Pauli frame.

One difference between S and $\mathsf{T} = E\mathsf{S}E^\dagger$ is that they may have slightly different fault-tolerant gates. However, since the two codes differ only by a Pauli, the gates will be quite similar. We could simply modify any gates we want to perform to take account of the new code. As long as we are doing Clifford group gates, we don't even need to do that: A Clifford group gate will change the Pauli error E into a different Pauli error F in a known way. All we have to do is update the Pauli frame, replacing E with F.

We can keep doing Clifford group gates like this indefinitely. Of course, new errors are occurring, but so are new error correction steps. The EC gadgets contain further syndrome measurements, which let us update the Pauli frame to take the new errors into account. At each EC step, we choose a low-weight error relative to the Pauli frame entering the gadget rather than the Pauli frame at the beginning of the computation: When errors are rare, it is unlikely the Pauli frame changes too quickly, but given enough time, the accumulated error rate can be arbitrarily large. This means that after a while, the Pauli frame may be an element of $\mathsf{N}(\mathsf{S})$, a logical operator. That's OK — what it means is that we've gotten back to the original code, but in a twisted way. The basis states have changed, but since we know how they've changed, we can adapt without much difficulty.

Non-Clifford group gates present more of a quandary. A transversal implementation of a non-Clifford group gate could modify the pre-existing error E to be some non-Pauli error (and always will for at least some Paulis E). The only way to deal with that is by using a different FT implementation of the gate gadget that's modified for the current Pauli frame. A lot of the time, though, we are implementing non-Clifford group gates via some circuit construction involving a logical measurement, as discussed in chapter 13. In that case, it's important to implement the logical measurement step relative to the current Pauli frame. For instance, if we are using the five-qubit code and the Pauli frame is $I \otimes Y \otimes Y \otimes I \otimes X$, the current code has a logical bit flip relative to the original code, so we should interpret measurement outcome of 0 as 1 and 1 as 0. After the non-Clifford group gate gadget is complete, we resume tracking the Pauli frame as usual.

The benefit of keeping track of the Pauli frame classically is small. It saves us one single-block transversal Pauli gate per block per FTEC gadget. Two-qubit transversal gates, measurements, state preparation, and particularly repetitions of the syndrome measurement consume many more resources, so the fraction of locations saved by calculating the Pauli frame classically is small. Nevertheless, every little bit helps, so we might as well do it.

Chapter 13

Any Sufficiently Advanced Fault-Tolerant Protocol is Indistinguishable from Magic States: State Preparation And Its Applications

There are some big loose ends left over from previous chapters. For one thing, I still haven't told you how to make the state preparation gadgets at the beginning of a fault-tolerant computation. Chapter 12 introduced the Steane and Knill EC methods but only if you already know how to do state preparation. Clearly it's time to discuss that.

At some point, we also need to discuss how to create a universal set of gates, since we saw in chapter 11 that transversal gates are insufficient. A chapter on state preparation might seem a strange place to do that, but it turns out that, for certain gates, the difficult part of the implementation can be encapsulated in particular quantum states. It's a bit like magic: Drink the potion and poof! You're a frog. (Of course, we're considering *unitary* transformations, so there must also be an inverse potion that turns a frog into a human.) Like a magic potion, a magic state is consumed when used. Unlike a magic potion, there's actually a scientific explanation for how the protocol works, which of course I'll discuss. That makes it technology, and an advanced technology at that, because it's the last component needed to give us a complete fault-tolerant protocol.

13.1 Preparation of Encoded Stabilizer States

In this section, I'll explain how to fault-tolerantly prepare stabilizer states encoded in stabilizer codes. That gives us a number of fault-tolerant preparation gadgets, for instance for $|\overline{0}\rangle$, as well as the ability to create the ancillas for Steane and Knill EC.

The states we're creating for now are all stabilizer states. Sometimes it's helpful to just lump together the stabilizer for the logical state with the stabilizer for the QECC, giving us just a single stabilizer with n generators on n qubits. Sometimes, it's instead better to think separately about the stabilizer of the code and the stabilizer of the encoded state. For instance, when defining fault tolerance for a state preparation gadget, we refer to the distance of the code, not the distance of the overall stabilizer state.

The first step to a fault-tolerant gadget for stabilizer states is generally to do a non-fault-tolerant encoding circuit to create the state. Chapter 6 explained how to make such circuits. (This is one of those places where

it is helpful to lump the stabilizers together.) If there are no faults in the encoding circuit, we get the state we'd like to have. However, because the encoding circuit inevitably contains many non-transversal gates, a single fault during the encoding circuit can cause multiple errors in the state produced. Therefore, we'll need to figure out a way to verify and/or correct the states created this way.

13.1.1 Preparation Using Shor EC

The first and most general way to verify the prepared state is using Shor error correction. In particular, after preparing the desired state non-fault-tolerantly, we perform Shor EC to measure the generators of the full stabilizer, including both the generators for the code and logical stabilizer state being prepared. This is essential, since we want to check two things: that the state is close to a valid codeword (PPP), and that the logical state is the *correct* logical state (PCP). This procedure works for an arbitrary stabilizer state.

Theorem 13.1. *State preparation via Shor EC verification satisfies the PPP and the PCP.*

Proof. Both the PPP and the PCP follow from the ECRP for Shor EC. Measuring the generators of the QECC ensures that s faults in the EC circuit lead to an output state which passes an s-filter for the code, no matter how many faults there were in the non-fault-tolerant encoding circuit at the beginning of the gadget. The one thing to check here is that performing a few additional cat state measurements for the stabilizer of the logical state does not mess up the ECRP for the QECC. It doesn't.

That takes care of the PPP. Furthermore, the ECRP for the combined stabilizer says that when there are s faults in the EC step, the output state passes an s-filter for the combined stabilizer, meaning the output state is in the space spanned by the ideal output state with s-qubit errors on it. An ideal decoder applied to such a state will give the ideal output state, since $s \leq t$. That gives us the PCP. □

A variety of simplifications are possible, some of them contradictory. One possibility is to skip the original non-fault-tolerant encoding circuit. We still need to perform the Shor EC step (after all, we need to do *something*), but we can do it on an arbitrary input state, perhaps the $|00\ldots0\rangle$ state or a randomly chosen state. Remember, measuring the error syndrome collapses the state to a subspace compatible with that syndrome, and since we're measuring a stabilizer with n generators, there is only a 1-dimensional subspace compatible with a given syndrome — a single state. Once we know the error syndrome (determined via the usual Shor method of repeating the measurement), we know the state, and can correct it to the right encoded state by a Pauli operation. Yes, fault-tolerant error correction is so powerful that it can literally make an encoded state out of random junk.

A different simplification is to simply verify that the original preparation circuit is correct rather than trying to correct the state produced. If the preparation fails, we simply discard the whole state and try again. We are thus using the Shor EC method for error detection rather than error correction. One advantage of doing so is that we need not repeat the syndrome measurement as often: If we simply repeat the syndrome measurement t times, discarding the state if any measured syndrome is non-trivial, that is sufficient. This will often lead to discarding perfectly good states when a small number of syndrome measurements fail, but that's an acceptable price, provided we do not falsely accept an incorrect state. There is only a single state that has trivial syndrome, so it is sufficient to verify that the syndrome truly is 0.

In order for an erroneous state to slip past our procedure, there needs to be an fault in the original encoding circuit, plus a fault in each of the t syndrome extractions, for a total of $t+1$ faults, which is more than we allow. Any fewer faults means that either the original encoding circuit is correct or at least one of the syndrome measurements is correct. When the true syndrome is nonzero, a correct syndrome measurement will always detect that and cause us to discard the state. If the original circuit is correct, the state going into the error detection step is perfect, but of course faults during the error detection step can introduce errors. However, by equation (12.7), we know that each fault during a cat state measurement can introduce at most one additional single-qubit error into the system being measured. Therefore, s faults during the verification procedure result in a state that passes an s-filter relative to the true state, as desired.

Besides the need for fewer repetitions of the syndrome measurement, this simplification is more sensitive to errors and thus likely to produce a state that has fewer errors in it than one produced via a full error

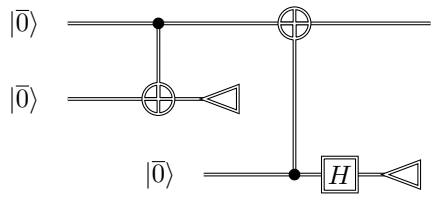

Figure 13.1: Using Steane error correction and measurement to verify an encoded $|\overline{0}\rangle$ state.

correction step. This is because error detection can detect up to $2t$ errors when the code has distance $d = 2t + 1$ whereas error correction can only reliably handle t. Of course, there are still combinations of $t + 1$ faults that can fool us, as discussed above, but they are rare since they require the false syndromes to exactly cancel the true errors present.

The disadvantage of error detection is straightforward: Whenever the procedure detects an error, we have to start over. This may require many repetitions before we succeed in preparing a state we trust enough to use. For maximum efficiency, we probably want to try many preparations in parallel, throwing out the ones that fail and switching the ones that succeed to where they are needed. That way, we don't lose any time waiting for the preparation, but we do need extra qubits. If there are at most t faults in the gadget as a whole, we may need to prepare as many as $t+1$ copies of the state in order to get one that passes the check.

Note also that these two simplifications are not completely compatible, but with some adaptation of the error detection, they can be made to work together. If we skip the original encoding circuit *and* only do error detection, then the chance of getting a zero syndrome (no error) is exponentially small. Instead, we should loosen the error detection to allow a non-zero syndrome, provided the syndrome is repeated consistently. However, if we only repeat the syndrome measurement t times, it is certainly possible that t faults could make us think we got the same syndrome each time even though all of them are wrong. If we want to combine the two simplifications, we should repeat the syndrome measurement $t+1$ times and keep the state only if all $t + 1$ syndromes are in agreement. That guarantees at least one of them is correct and ensures that we are no more than t errors away from the right state. Another way of thinking about this particular combination is that the first error syndrome extraction is a non-fault-tolerant encoding protocol, and then the t subsequent repetitions are error detection steps.

13.1.2 Preparation of CSS Codewords

CSS codewords are particularly favorable for fault tolerance because they allow transversal CNOT and measurement. These properties also give us more options for checking correctness. I will describe one such option now.

Just as we can verify stabilizer states encoded in general stabilizer codes using Shor EC, we can verify states encoded in CSS codes using Steane error correction. However, there is a significant complication: Shor EC measures the syndrome using cat state ancillas, which can be prepared as described in section 12.1.3. Steane EC uses $|\overline{0}\rangle$ and $|\overline{+}\rangle$ states encoded in the same QECC. Therefore, if we want to verify a $|\overline{0}\rangle$ using Steane EC, we need additional encoded states, which must in turn be verified somehow. We could use Shor EC to verify them, as discussed in section 13.1.1, but if we're going to do that, we might as well just verify the state being prepared directly with Shor EC and cut out some extra steps. However, by looking closely at the structure of the overall preparation procedure, we can see that the ancillas used for verification need not be checked as closely as those used in a regular Steane EC step.

First let us consider what Steane EC looks like when applied to a single state rather than a code. Normally Steane EC calls for encoded $|\overline{0}\rangle$ and $|\overline{+}\rangle$ ancillas, but such things don't exist for a single state. Instead, it suffices to do both phase and bit flip verification using ancillas which are the same as the state being verified, as in figure 13.1. Essentially, we just compare the state we want to keep with the two ancillas to make sure they are identical.

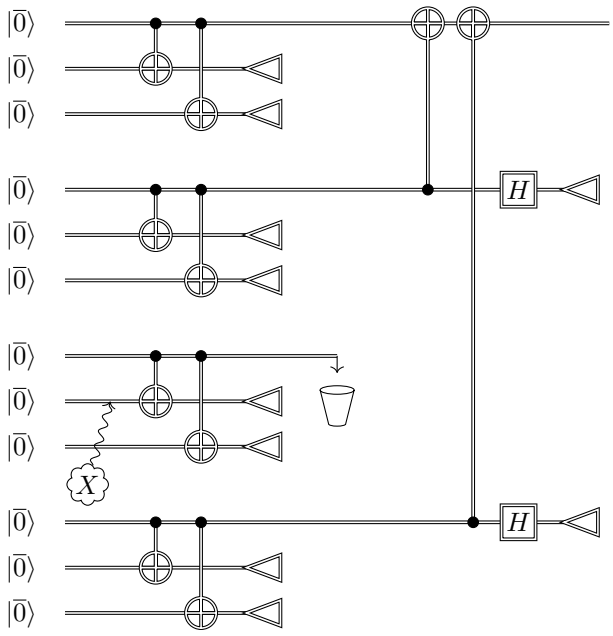

Figure 13.2: Hierarchical verification of CSS codewords when $t = 2$ and the circuit has 1 fault.

However, a straightforward verification procedure like this may not be sufficient. If we produce the three $|\overline{0}\rangle$ states in figure 13.1 using a non-fault-tolerant encoding circuit, then a single fault in one of the encoding circuits can cause multiple errors in the state entering the verification. Depending what kind of errors they are and which encoding circuit has the fault, that may be OK — the comparison might catch the errors. However, multiple phase errors in the last ancilla state can propagate into the state being prepared without being checked. Furthermore, if *two* of the encoding circuits each have a single fault, multiple errors of either type could slip through the verification unnoticed.

In order to solve this problem, we will need to perform more extensive verification. We can arrange a two-level verification of the states. First, prepare many copies of the desired ancilla state with non-fault-tolerant circuits and divide them up into groups of $t + 1$ states. Compare the states in each group for phase errors. If there are at most t faults in the encoding circuits for a group, then any phase errors will be detected; in this case, discard the states in that group. Keep one ancilla state from each group which does not detect phase errors. Next, compare $t + 1$ of the surviving states for bit flip errors, as depicted in figure 13.2. An error during encoding of a single state in the first phase could cause multiple bit flip errors, which would then propagate into the state being kept. However, in order for the multiple bit flip errors to survive the second round of checking, all $t + 1$ states which survive the first round would need errors, which would require $t + 1$ faults in the overall circuit. Therefore, when there are at most t faults in the entire preparation and verification circuit, the only cause of errors in the output state are faults during the verification procedure, which only affect single qubits as per theorem 12.5. This hierarchical procedure can be viewed as a *distillation* process through which a number of low-quality (i.e., noisy) ancilla states are distilled down into one or a small number of high-quality purer ancillas.

By taking advantage of the structure of the code and perhaps using other tricks, the complexity of this procedure may in some cases be reduced considerably. Without any optimization, though, this two-level Steane EC verification procedure, which uses at least $(t + 1)^2$ ancillas, is worse than the general Shor EC verification procedure, which needs only t syndrome repetitions.

An example of an optimized $|\overline{0}\rangle$ state preparation gadget for the 7-qubit code appears in figure 13.3. Notice that in this optimized gadget, we don't bother to check the phase. We can get away with this because

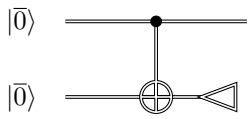

Figure 13.3: An optimized verification procedure for an encoded $|\overline{0}\rangle$ state of the 7-qubit code.

the 7-qubit code is built from the classical 7-bit Hamming code, which is perfect. Therefore, every phase error syndrome corresponds to a single-qubit phase error, and because we are preparing the encoded $|0\rangle$ state, there is no logical phase error. No matter what happens in the circuit, the output state will pass a 1-filter for phase errors, since every state does. If there is a fault causing bit flip errors in one of the two non-FT preparation circuits in figure 13.3, the check will catch it. Therefore, the only way to get bit flip errors in the output state when there is one fault in the circuit is to have a fault during the verification procedure. This part is transversal, so any fault will cause the final state to pass a 1-filter relative to both the seven-qubit code and the $|\overline{0}\rangle$ state we are trying to create. Thus, figure 13.3 gives an FT preparation gadget.

As with the Shor EC verification procedure, the Steane EC method can be adapted to correct errors on the state being prepared rather than simply post-selecting for the case where no errors are detected. This requires additional ancillas in order to repeat the syndrome measurement enough to have confidence in the answer. The considerations are similar to those for Shor EC, discussed in section 12.2.2.

13.1.3 Preparation of Ancillas for Steane and Knill Error Correction

One important application of these state preparation procedures is to produce the ancillas needed to perform Steane and Knill error correction. For Steane error correction, the process is straightforward: We need $|\overline{0}\rangle$ and $|\overline{+}\rangle$, and these can be directly created by either of the above protocols. (Steane EC is only used for CSS codes, so the second procedure is fine.)

The ancilla for Knill error correction is not too much harder. For a CSS code, we can just create two encoded blocks in the state $|\overline{+}\rangle \otimes |\overline{0}\rangle$, and then perform transversal CNOT between them to create the logical Bell state. For a non-CSS stabilizer code, we need to be a little more clever. The trick is to think of the two blocks together as a single bigger stabilizer state (which of course they are). Then we can perform the Shor EC verification procedure to verify the stabilizer of the full state, which is generated by $\mathsf{S} \otimes I$, $I \otimes \mathsf{S}$, $\overline{X} \otimes \overline{X}$, and $\overline{Z} \otimes \overline{Z}$.

13.2 Gate Teleportation

Now we'll get started on figuring out how to get a universal set of gates. To do so, it's best to first step away from the framework of fault tolerance. Instead, let's try to figure out how to build circuits performing non-Clifford group gates, without any concern about whether the construction is fault tolerant or not. Assume we have the ability to perform Clifford group gates and Pauli measurements, and, since this is the chapter on state preparation, the ability to prepare an arbitrary state of our choice.

13.2.1 Gate Teleportation Construction

One thing we can do with the available tools is teleport a quantum state; this requires a Bell measurement, an EPR pair, and a Pauli operator (with classical control). Suppose we want to perform a gate U (which might be a Clifford group gate or a non-Clifford group gate) on a state $|\psi\rangle$. One way to do this, as in the left part of figure 13.4, is to teleport $|\psi\rangle$ through an EPR pair from Alice to Bob, and then have Bob perform U. As usual in teleportation, Alice does a Bell measurement and sends the resulting two classical bits to Bob, who performs the Pauli corresponding to the value of the the classical bits. Then he finishes off with

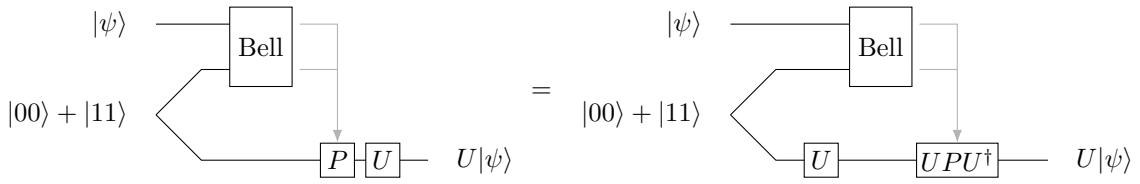

Figure 13.4: Performing a quantum gate U with quantum teleportation.

U. You might think this is perverse, and of course you'd be right: We've reduced the task of performing U to teleporting and then performing U. That is not a simplification. Just bear with me for a moment.

Now suppose Bob is an impatient sort, and he wants to perform U right away, before he's heard from Alice. He can do that, of course, but now when he does get the classical bits from Alice, he should undo U, do the appropriate Pauli, and then re-do U. In other words, if Alice's message indicates that he is supposed to perform P, he should instead do $UPU^\dagger$, as shown on the right side of figure 13.4.

Believe it or not, this is actually progress: Bob's impatience means that he performs the gate U on a fixed state $|00\rangle + |11\rangle$, regardless of Alice's state $|\psi\rangle$. That means we've converted the task of performing U into three steps:

Protocol 13.1 (Gate Teleportation)**.**

1. Create $(I \otimes U)(|00\rangle + |11\rangle)$ shared between Alice and Bob.
2. Alice performs a Bell measurement and sends the results to Bob.
3. Bob performs $UPU^\dagger$ when Alice's classical bits correspond to Pauli P.

Step 2 is no problem — it only involves CNOT, H, and Z measurements. Step 1 could be very difficult, but it is clearly a state preparation task. Let's assume for the moment that this state is given to us. We'll discuss how to create such states in sections 13.4 and 13.5.

Then there's step 3. For general U, the gate $UPU^\dagger$ could be a pretty complicated thing. There's no reason to assume it will be any easier to do than U. But for certain special U, the conjugated Pauli always is simpler that U.

For instance, if $U \in \mathsf{C}_1$, then $UPU^\dagger \in \mathsf{P}_1$, and Bob only needs to perform a Pauli at step 3. It turns out that there are a number of gates U with the property that whenever $P \in \mathsf{P}_n$, then $UPU^\dagger \in \mathsf{C}_n$: These gates conjugate Pauli operations into Clifford group gates.

This gate teleportation construction therefore is a way to bootstrap from simpler operations to more complicated ones. If Alice and Bob can requisition whatever ancilla states they need, then they can use the gate teleportation construction to build up more and more complicated gates. Given Pauli gates, they can perform Clifford gates, and given Clifford group gates, they can perform any gate with the property $UPU^\dagger \in \mathsf{C}_n$.

Of course, the use of Alice and Bob is only for illustrative purposes. Teleportation is generally thought of as a communication protocol, so normally Alice and Bob are far apart. In this case, we're using teleportation to perform gates, which is an interesting thing to do even if Alice and Bob are right next to each other, for instance adjacent qubits in a quantum computer. (Or, given the main point of this book, adjacent *logical* qubits in a quantum computer.)

Also worth pointing out is that, while protocol 13.1 is described explicitly for a single-qubit gate U, that is not at all necessary. An n-qubit gate can be done in the same way just using the state $(I \otimes U)(|00\rangle + |11\rangle)^{\otimes n}$ instead of the 1-qubit version. In step 2 Alice teleports all her qubits, and in step 3, the Paulis run over n-qubit Paulis. It all works just the same as the single-qubit case.

The state $(I \otimes U)(|00\rangle + |11\rangle)$ is known as a *magic state*. Protocol 13.1 is an example of a class of protocols called *magic state injection*, whereby a magic state is used to perform a non-Clifford group unitary on some data qubits using only Clifford group gates and Pauli measurements. The term "magic state" is

used somewhat loosely to mean one of three things: It could be a state like this that can be used directly for magic state injection. It could be a state (pure or mixed) that can be further processed by Clifford group operations, at which point it could then be used to perform a non-Clifford group gate. The term is also sometimes used to refer to any non-stabilizer pure state.

One somewhat peculiar feature of this construction is that the qubit that comes out of it is in a different location from the qubit that goes in. There's nothing really wrong with that, but you might find it a bit surprising that to perform a unitary gate we end up transferring the data to a different qubit.

13.2.2 $\mathcal{C}_k$ Gates

So, what gates have the property we need to make protocol 13.1 work?

Definition 13.1. Let $\mathcal{C}_1 = \mathsf{P}_n$ and let

$$\mathcal{C}_k = \left\{U \in \mathsf{U}(2^n) \,|\, UPU^\dagger \in \mathcal{C}_{k-1} \forall P \in \mathsf{P}_n\right\}. \tag{13.1}$$

The collection of the sets $\{\mathcal{C}_k\}$ is known as the *Clifford hierarchy.*

The number of qubits n is implicit in this notation, but $\mathcal{C}_k$ can also refer to the union of $\mathcal{C}_k$ over all values of n. The sets $\mathcal{C}_k$ are defined recursively. $\mathcal{C}_1$ is the Pauli group, $\mathcal{C}_2$ is the Clifford group C_n, and $\mathcal{C}_3$ is the set of gates we're now interested in. The higher values of $\mathcal{C}_k$ are potentially interesting too: If we can perform arbitrary $\mathcal{C}_3$ gates, then we can use gate teleportation to directly perform $\mathcal{C}_4$ gates, which then lets us perform $\mathcal{C}_5$ gates, and so on.

Let's look at some examples. The first example is $R_{\pi/8}$:

$$R_{\pi/8} X R_{\pi/8}^\dagger = X R_{\pi/4}^\dagger \tag{13.2}$$

$$R_{\pi/8} Z R_{\pi/8}^\dagger = Z. \tag{13.3}$$

$R_{\pi/4} \in \mathsf{C}_1 = \mathcal{C}_2$, so equations (13.2) and (13.3) imply that $R_{\pi/8} \in \mathcal{C}_3$. Note that for $\mathcal{C}_3$, we don't need to check Y, since the image of Y under conjugation is the product of the images of X and Z, and $\mathcal{C}_2$ is a group. For higher $\mathcal{C}_k$, you may also need to check the image of Y, since $\mathcal{C}_k$ is not closed under multiplication for $k \geq 3$.

Another gate in $\mathcal{C}_3$ is the Toffoli gate Tof:

$$\mathrm{Tof}(X \otimes I \otimes I)\mathrm{Tof} = X_1 \mathrm{CNOT}_{2,3} \tag{13.4}$$

$$\mathrm{Tof}(I \otimes X \otimes I)\mathrm{Tof} = \mathrm{CNOT}_{1,3} X_2 \tag{13.5}$$

$$\mathrm{Tof}(I \otimes I \otimes X)\mathrm{Tof} = X_3 \tag{13.6}$$

$$\mathrm{Tof}(Z \otimes I \otimes I)\mathrm{Tof} = Z_1 \tag{13.7}$$

$$\mathrm{Tof}(I \otimes Z \otimes I)\mathrm{Tof} = Z_2 \tag{13.8}$$

$$\mathrm{Tof}(I \otimes I \otimes Z)\mathrm{Tof} = (\mathrm{C-Z})_{1,2} Z_3 \tag{13.9}$$

This is why the universal gate sets $\langle \mathsf{C}_n, R_{\pi/8}\rangle$ and $\langle \mathsf{C}_n, \mathrm{Tof}\rangle$ are particularly interesting for fault tolerance: They each consist of the Clifford group plus a single $\mathcal{C}_3$ gate, which can be implemented via gate teleportation.

What about phase rotation by other angles?

$$R_\theta X R_\theta^\dagger = X R_{2\theta}^\dagger \tag{13.10}$$

$$R_\theta Z R_\theta^\dagger = Z. \tag{13.11}$$

Now, $R_{2\theta} \in \mathcal{C}_2$ iff $2\theta = m\pi/4$ for some integer m, so $R_\theta \in \mathcal{C}_3$ iff $\theta = m\pi/8$ for integer m. By induction, we immediately find that $R_{m\pi/2^k} \in \mathcal{C}_k \setminus \mathcal{C}_{k-1}$ when m is an odd integer, and that $R_\theta \notin \mathcal{C}_k$ for any k if $\theta \neq m\pi/2^k$ for some integers k and m. Thus, we see that every $\mathcal{C}_k$ contains some elements that are not in

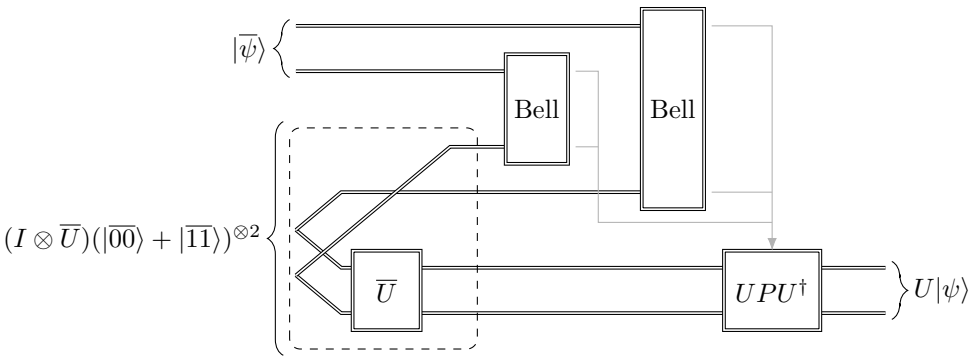

Figure 13.5: Gadget for implementing a two-block logical gate through gate teleportation.

$\mathcal{C}_{k-1}$, and that there are some unitaries that are not in any $\mathcal{C}_k$. This means that there are some gates we won't be able to produce exactly through a chained teleportation circuit.

But maybe $\mathcal{C}_k$ is dense in $\mathsf{U}(2^n)$ for large enough k? No. In fact, for fixed k and n, $\mathcal{C}_k/\{e^{i\phi}I\}$ (which is $\mathcal{C}_k$ with global phases removed) must be finite. This can be easily seen by induction: $\mathcal{C}_{k-1}/\{e^{i\phi}I\}$ is finite, and a unitary can be uniquely determined by the image of the Paulis under conjugation. If $UPU^\dagger = e^{i\phi}V$ for Pauli P, there are only two possible values for ϕ because $(e^{i\phi}V)^2 = I$. ($P^2 = I$, and group identities are preserved under conjugation.) Therefore, there are only a finite number of possible images of a Pauli P in $\mathcal{C}_{k-1}$, and thus only a finite number of maps from P_n to $\mathcal{C}_{k-1}$.

This means that direct constructions via teleportation are not enough. In order to get a universal set of gates, we can construct a $\mathcal{C}_3$ gate such as $R_{\pi/8}$ via teleportation, but then we will need to multiply gates together to get good approximations of arbitrary unitary transformations.

13.2.3 Universal Fault Tolerance

Now we are ready to put together these ideas to see how to make fault-tolerant gadgets for a universal set of gates, given access to the right kind of ancillas. First, note that, using the tools we've already discussed, we can perform Clifford group gates for any stabilizer code:

Theorem 13.2. *For any Clifford group gate $U \in \mathsf{C}_n$ and any stabilizer code, there exists a fault-tolerant gate gadget for U.*

Proof. The protocol will consist of implementing protocol 13.1 for the encoded qubits of the code.

For step 1, we must create the state $(I \otimes \overline{U})(|\overline{00}\rangle + |\overline{11}\rangle)$. The first qubit of the pair is encoded in one block of the code, and the second qubit is encoded in a second block. If the code encodes k qubits, first imbed U in a 2^k-dimensional Hilbert space via tensoring with the identity on other qubits. That means we want k encoded EPR pairs, of which one has $\overline{U}$ applied on Bob's side. If U is intended to interact qubits encoded in m separate blocks of the code, the state to construct will consist of $2m$ code blocks, as in figure 13.5.

Because $U \in \mathsf{C}_n$, the state we want to create is an encoded stabilizer state, which is a stabilizer state in its own right. Therefore, the Shor EC preparation technique of section 13.1.1 can be used to create this state.

For step 2, we must perform a logical Bell measurement between the data block and the ancilla block created in step 1. The logical Bell measurement consists of Pauli measurements, so could be done via a sequence of cat state measurements (section 12.1). However, it is much more efficient to simply perform transversal Bell measurements. This has the effect of combining Knill error correction (section 12.4) with gate teleportation. In particular, by appropriate classical post-processing, we can extract the outcome of the logical Bell measurement from the outcomes of the transversal Bell measurements. We deduce a Pauli P.

Finally, in step 3, we must perform $\overline{UPU^\dagger}$. But since $U \in \mathsf{C}_n$, $UPU^\dagger$ is a Pauli and the logical version of it is a Pauli as well. This can just be performed transversally.

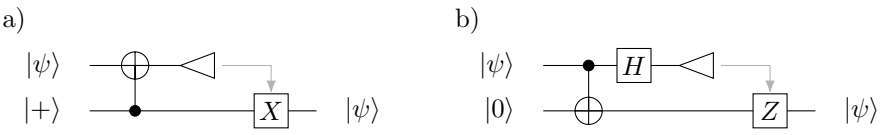

Figure 13.6: Two versions of one-bit teleportation.

Each of the three steps is performed via fault-tolerant gadgets, so it straightforward to check that the overall procedure satisfies the GPP and GCP. □

But the Clifford group is not universal, so we'll need more gates. By theorem 6.9, any gate added to the Clifford group will give us a dense subgroup of $\mathsf{SU}(2^n)$. In particular, we can pick a $\mathcal{C}_3$ gate such as $R_{\pi/8}$ or Tof. Then we can use the teleportation construction to perform the $\mathcal{C}_3$ gate fault-tolerantly.

Theorem 13.3. *There exists a fault-tolerant protocol for any stabilizer code.*

Proof. By theorem 13.1, we have a FT $|\overline{0}\rangle$ preparation gadget. By theorem 12.1 or theorem 12.6, we have FT measurement gadgets. By theorem 12.3 or theorem 12.6, we have FT error correction gadgets. The FT storage gadget consists of transversal wait locations. By theorem 13.2, we have FT gate gadgets for all Clifford group gates. Therefore, all we need to construct a full fault-tolerant protocol is a FT gate gadget for a non-Clifford group gate.

We will use gate teleportation, protocol 13.1, for some gate U in $\mathcal{C}_3 \backslash \mathcal{C}_2$. For step 1, we invoke lemma 13.5, which will be discussed in section 13.4. The upshot is that we have a construction that creates the desired state $(I \otimes U)(|\overline{00}\rangle + |\overline{11}\rangle)$ and satisfies the PCP and the PPP. For step 2, we perform the logical Bell measurement via cat state measurement or Knill measurement. The procedure satisfies the MCP. For step 3, we must perform $\overline{UPU^\dagger}$ for some Pauli P. Since $U \in \mathcal{C}_3$, $UPU^\dagger \in \mathsf{C}_n$, which means we can implement it fault-tolerantly as per theorem 13.2. Putting together three fault-tolerant gadgets once again implies that the full gadget satisfies the GPP and the GCP. □

13.3 Compressed Gate Teleportation

Protocol 13.1 is very useful, but the ancilla is a bit awkward. Even for a single-qubit gate, the construction demands a two-qubit ancilla, and an n-qubit gate needs a $2n$-qubit ancilla. For certain gates, we can reduce the size of the construction and use a smaller ancilla.

13.3.1 One-Bit Teleportation

The first step is to notice that there are protocols very similar to teleportation that work with a CNOT, a single-qubit measurement, and a single-qubit ancilla rather than a Bell measurement and a two-qubit ancilla. Two such protocols are shown in figure 13.6. Other variations are possible using other two-qubit gates.

These constructions presume the ability to perform a CNOT between Alice and Bob. This is not usually possible in a communications scenario where Alice and Bob are separated, but is well-suited for applications to fault tolerance. After the CNOT, Alice measures a single qubit, and therefore only gets one classical bit to send to Bob. If the bit value is 0, Bob need do nothing to his qubit. If the classical bit is 1, Bob performs the Pauli indicated in the figure. Straightforward computation shows that these circuits have the desired effect.

13.3.2 $\pi/8$ Compressed Gate Teleportation Construction

Now, how can we use these smaller teleportation-like circuits to perform gates? There is a significant complication over protocol 13.1. Before, Bob's post-teleportation gate could easily be moved before the Bell

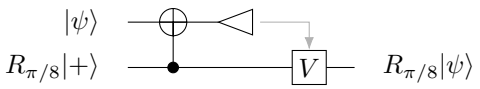

Figure 13.7: A smaller circuit for gate teleportation with the $\pi/8$ phase rotation. Here, $V = R_{\pi/8}XR_{-\pi/8}$.

measurement, since the output qubit is unaffected by the Bell measurement. That is no longer true. Instead, we should restrict our attention to performing gates that commute with the CNOT (or at any rate, have some simple commutation relationship with it). For instance, if we use the circuit of figure 13.6a, where the control qubit of the CNOT is the ancilla qubit, then we can commute past it any diagonal gate, such as the $R_{\pi/8}$. The resulting circuit is pictured in figure 13.7. The magic state in this case is

$$R_{\pi/8}|+\rangle = e^{-i\pi/8}|0\rangle + e^{i\pi/8}|1\rangle. \tag{13.12}$$

Since $R_{\pi/8}XR_{\pi/8}^\dagger = XR_{\pi/4}^\dagger$, whenever Alice gets 1 as her measurement outcome, to complete the construction, Bob must perform $R_{-\pi/4}$ followed by X on his qubit.

13.4 Clifford Eigenstate Preparation by Measurement

There's still one piece missing from the universal gate construction: How to build the magic states. There are two known methods for building magic states. One is quite general and conceptually straightforward, but rather ugly and inefficient in practice. It is built around the cat state measurement procedure we discussed in section 12.1. The second method, magic state distillation, is simple and elegant, but with more subtle conceptual underpinnings. Furthermore, so far it only works with certain magic states. We'll discuss magic state distillation in section 13.5.

For this section, we'll ignore most properties of the magic states we'd like to build. The only thing we need to know is that the magic states we care about have a "stabilizer" made up not of Pauli operators, but of Clifford group operators. Why is that? Well, the magic states for a $\mathcal{C}_3$ gate U are of the form $U|\psi\rangle$ or $(I \otimes U)|\psi\rangle$, where $|\psi\rangle$ is some stabilizer state.

Proposition 13.4. *Let $|\phi\rangle = U|\psi\rangle$, where $U \in \mathcal{C}_k$ and $|\psi\rangle$ is a stabilizer state with stabilizer S. Then $|\phi\rangle$ is the $+1$ eigenstate of $V = UMU^\dagger$ when $M \in \mathsf{S}$. $V \in \mathcal{C}_{k-1}$. Furthermore, $|\phi\rangle$ is the only state (up to global phase) that is a $+1$ eigenstate of all operators of this form.*

Proof. Since $M|\psi\rangle = |\psi\rangle$,

$$V|\phi\rangle = VU|\psi\rangle = UM|\psi\rangle = U|\psi\rangle = |\phi\rangle. \tag{13.13}$$

The fact that $V \in \mathcal{C}_{k-1}$ follows immediately from the definition of $\mathcal{C}_k$.

To show uniqueness, note that the projector on the subspace of $+1$ eigenstates of all V is

$$\Pi = \prod_V \frac{1}{2}(I + V). \tag{13.14}$$

Since a $+1$ eigenstate of V and V' is a $+1$ eigenstate of the product, we have

$$\frac{1}{8}(I+V)(I+V')(I+VV') = \frac{1}{4}(I+V)(I+V'). \tag{13.15}$$

In other words, we can eliminate the redundant Vs from the expression for Π. Furthermore, $(UMU^\dagger)(UNU^\dagger) =$

$UMNU^\dagger$, so the independent Vs can be considered to come from a generating set $\{M_1, \ldots, M_n\}$ for S. Thus,

$$\Pi = \frac{1}{2^n}\prod_{i=1}^{n}(I + UM_iU^\dagger) \tag{13.16}$$

$$= \frac{1}{2^n}U\left[\prod_{i=1}^{n}(I + M_i)\right]U^\dagger \tag{13.17}$$

$$= U\Pi_{\mathsf{S}}U^\dagger, \tag{13.18}$$

where Π_{S} is the projector on the code subspace of S, i.e., $|\psi\rangle$. The unitary conjugation of a rank-one projector is again a rank-one projector, so $|\phi\rangle$ is unique. □

As a result of proposition 13.4, the magic states we need to create $\mathcal{C}_3$ gates can be uniquely defined as $+1$ eigenstates of a list of Clifford group operators. For instance, the magic state $R_{\pi/8}|+\rangle$ is the unique $+1$ eigenstate of $XR^\dagger_{\pi/4}$. To verify that we have the magic state, it therefore suffices to measure these Clifford group operators. This can be done fault-tolerantly using techniques we already know. Actually, we can go further and deterministically prepare the states. By "deterministically," I mean that we will always get a state output; no post-selection is needed. Naturally, if there are too many faults in the circuit, we might prepare the wrong state.

Lemma 13.5. *Let $|\psi\rangle$ be any state which is uniquely defined by being an eigenstate of Clifford group operators $U_1, \ldots, U_n$. Let Q be a code for which there exists a fault-tolerant implementation of the full Clifford group. Then there exists a fault-tolerant state preparation gadget for $|\psi\rangle$ for the code Q. If $U_i = VP_iV^\dagger$, where the P_i's generate a stabilizer and $V \in C_3$, then the gadget can be done without post-selection.*

Proof. Let us for the moment assume that the fault-tolerant implementation of Cliffords is transversal. The lemma still holds for more general FT gate gadgets, but the procedure is more complicated.

In section 12.1, I presented the cat state procedure for measuring Paulis on arbitrary stabilizer codes. There is little about this procedure that is specific to Pauli operators. It can also be used to measure Clifford group operators, or really any other operation for which we have a transversal implementation on the code.

If the Clifford group operation U has eigenvalues ± 1, then no modification of the procedure is needed — simply substitute the transversal implementation of U for the transversal implementation of the Pauli. If U has other eigenvalues, a little more work is necessary.

First note that any $U \in \mathsf{C}_n$ has finite order r, since C_n is a finite group. (This also means that the eigenvalues of U are of the form $e^{2\pi ic/r}$ for integer c.) Next, observe that if the transversal implementation of U is $\bigotimes_a W_a$, then $\bigotimes_a W_a^b$ is a transversal implementation of U^b. We wish to perform gates interacting an r-dimensional unencoded qudit with a single physical qubit. The action of the gate is

$$C - W_a : |b\rangle \otimes |\psi\rangle \mapsto |b\rangle \otimes W_a^b|\psi\rangle. \tag{13.19}$$

In other words, it is a controlled-W_a gate. In a basic model for fault-tolerance, we are assuming a universal set of physical gates is available, so this gate is allowed (or at any rate, can be approximated with arbitrarily high precision). Therefore, we can modify the cat state measurement procedure in three ways:

1. Replace the qubit cat state with a qudit cat state $\sum_{b=1}^{r}|bb\ldots b\rangle$.
2. Instead of the controlled-Pauli gates, do the gate $C - W_a$ between the ath qudit of the qudit cat state and the ath qubit of the code.
3. Instead of measuring in the Hadamard basis, perform the transversal qudit inverse Fourier transform and measure.

If the logical codeword $|\phi\rangle$ is an eigenvalue of U with eigenvalue $e^{2\pi ic/r} = \omega^c$, the $C - W_a$'s transform the qudit cat state to $\sum_{b=1}^{r}\omega^{bc}|bb\ldots b\rangle$, which is an ω^c eigenstate of the qudit Pauli operator $X \otimes X \otimes \cdots \otimes X$.

The inverse Fourier transform gives us instead an ω^c eigenstate of $Z \otimes Z \otimes \cdots \otimes Z$, so if we measure the individual qudits and take the sum modulo r, we get out c. This is in the absence of faults, of course, but just as with cat state measurement, if we repeat the procedure enough, do all the necessary checking when building the cat state, and intersperse the measurements with error correction steps, we can indeed deduce c. This procedure constitutes a fault-tolerant measurement gadget for U, with the same proof as the one showing cat state measurement of Paulis is fault tolerant.

Therefore, given a code with transversal implementation of all Clifford group elements, such as the 7-qubit code, we can fault-tolerantly measure the eigenvalue of any Clifford group operators. To create an encoded Clifford eigenstate, we can thus create it with a non-fault-tolerant circuit, then sequentially perform fault-tolerant cat state measurements of U_i. If any of the eigenvalues is wrong, discard the state. Otherwise keep it. Since the $|\overline{\psi}\rangle$ state is the only codeword with all the correct eigenvalues, a state that is kept must be correct, up to a possible t-qubit error, unless there are more than t faults during the measurement.

When $|\psi\rangle = V|\xi\rangle$ for some stabilizer state $|\xi\rangle$, $V \in \mathcal{C}_3$ (an equivalent property to the condition in the last sentence of the theorem's statement), we can improve this procedure by fixing up the state even if the eigenvalues are wrong. Think about the original stabilizer state $|\xi\rangle$, which has stabilizer S generated by $\{P_i\}$. Suppose we were to take some other state and measure the eigenvalues of all P_i. Depending on the state's overlap with $|\xi\rangle$, there is a chance we would get all the right eigenvalues, in which case the state would actually be projected on $|\xi\rangle$. If we don't get the right eigenvalues, we could form an error syndrome s by noting which generators have the wrong eigenvalue, and we would instead have the state $|\xi(s)\rangle$. Choose some Pauli $Q(s)$ which has error syndrome s for S. Then $Q(s)|\xi(s)\rangle = |\xi\rangle$, since $Q(s)$ changes all the eigenvalues to the correct ones, and $|\xi\rangle$ is the only state with those eigenvalues.

Let $|\psi(s)\rangle = V|\xi(s)\rangle$. Then $|\psi(s)\rangle$ and $|\psi\rangle$ have the same eigenvalue for $U_i = VP_iV^\dagger$ iff the ith bit of s is 0. (Note that when $U_i = VP_iV^\dagger$, U_i has the same eigenvalues as P_i.) Therefore, if we measure the eigenvalues of all U_i's, we can again form an error syndrome s, which implies that the post-measurement state is projected onto $|\psi(s)\rangle$. Furthermore, $U(s) = VQ(s)V^\dagger$ has the effect of changing $|\psi(s)\rangle$ to $|\psi\rangle$. Since $V \in \mathcal{C}_3$, $U(s) \in \mathsf{C}_n$. The following procedure will thus fault-tolerantly create the desired state $|\overline{\psi}\rangle$:

1. Encode $|\overline{\psi}\rangle$ non-fault-tolerantly
2. Measure $\overline{U}_i$ for all i using cat state measurement
3. Determine the error syndrome s
4. Perform $\overline{U(s)}$ fault-tolerantly

Finally, let me say a few words about the case when we have a fault tolerant but not transversal procedure to implement arbitrary Clifford group gates. The difficulty in the above procedure comes in how to do the Clifford measurement. If the gadget involves only unitary gates and perhaps some scratch ancilla qubits, it is not hard to modify the procedure, at least for Clifford gates with eigenvalues ± 1 (which is the most interesting case). We can assume without loss of generality that all ancilla qubits are reset to their initial values at the end of the gadget. To do the measurement, simply use a cat state with one qubit per gate in the implementation of the Clifford U being measured, and perform the fault-tolerant implementation of U with each gate being controlled by a different cat state qubit. Verifying the cat state first ensures that bit flip errors in it are effectively uncorrelated, so a single fault in the cat state preparation can only propagate errors into the data block via a single gate. This is the same effect as having a fault in that gate. Therefore the procedure is fault tolerant.

When we wish to measure more general Clifford gates with other eigenvalues, a similar procedure will work, but we need to perform up to U^{r-1}. This means a circuit potentially $r-1$ times larger, so we should pick the cat state to be correspondingly large. Once more, let us make it a qudit cat state using dimension r qudits. If the circuit for U involves m gates, we use a cat state with rm qudits. The first m qudits in the cat state will perform the first power of U, the second m perform the second power, and so on. In particular, for a qudit in the jth block of m qudits in the cat state, perform a controlled gate operation (for the appropriate gate in the FT gadget for U) which activates the gate only if the cat state qudit is $\geq j$. This ensures that

if the cat state qudits are all a, the circuit for U is performed a times, leading to a conditional $\overline{U}^a$ logical gate, just as for tranversal gates.

If the procedure for U involves measurements and classical processing, we first modify the circuit to be purely unitary. This can be done replacing each measurement with a CNOT to an ancilla qubit. We would also like to replace the classical circuitry with corresponding quantum gates, but there is a complication. In a basic model for fault tolerance, classical gates are assumed to be perfect but quantum gates are not, so blindly replacing classical gates with quantum ones leads to new opportunities for errors. The solution is turn the classical circuit into a classical fault-tolerant circuit, and then replace those gates with quantum ones. The details are discussed in section 15.3. □

The procedure described above for magic state preparation starts with a non-fault-tolerant encoding circuit for the magic state, but that is not really necessary. *Any* encoded state could be the starting point. The fault-tolerant Clifford measurements will project on the state $|\overline{\psi(s)}\rangle$, which can then be corrected to $|\overline{\psi}\rangle$ as discussed above. The advantage of starting with a different encoded state, such as a stabilizer state, is that it can often be prepared fault-tolerantly via a simpler procedure. This segments the whole gadget into smaller gadgets, each of which is fault tolerant, and can thus potentially reduce the vulnerability to errors.

If you look closely at the proof of lemma 13.5, you'll see that it doesn't depend very much on having Clifford group operators. We can fault-tolerantly measure the eigenvalue of any unitary operator U with finite order provided we have a fault-tolerant implementation of U, and can thus create any state which can be uniquely characterized by its eigenvalues for such a set of unitaries.

13.5 Magic State Distillation

The method of magic state preparation discussed in section 13.4 is rather awkward. For codes with big block sizes, it is especially undesirable, since it involves cat states as large as the code block. Another class of techniques, known as *magic state distillation* protocols, is generally preferable for large codes.

Magic state distillation is a procedure that takes as input some number of imperfect magic states and, through a sequence of Clifford group operations and Pauli measurements, produces a smaller number of better magic states. Usually these procedures are designed for a simplified scenario where Clifford group operations and Pauli measurements are perfect, with no faults, and no non-Clifford gate gadgets are allowed. Some sort of magic state preparation gadget is available, but it does have faults. If the error rate on the magic state preparation gadget is not too high, the effect of magic state distillation is to produce a magic state with a lower error rate than could be made using the original gadget.

Typically, these procedures are described for unencoded states. In reality, though, we would want to apply them for encoded magic states. The assumption, therefore, is that we work with a code which has a large error-correcting capability and a good set of gadgets for arbitrary Clifford group gates and Pauli measurements. Under these conditions, it is not a bad approximation to assume that the Clifford group gates and Pauli measurements cannot have errors. In reality, of course, there will be faults during the circuit, but the GPP and GCP ensure that the overall circuit remains fault tolerant. We may want to perform error correction along the way for additional robustness.

The theory of magic state distillation protocols is still under active development, and as of this writing, there is no real systematic understanding of the range of possible distillation procedures. The contents of this section should therefore be viewed mostly as examples of the types of protocols we know about.

13.5.1 State Distillation Via Transversal Non-Clifford Gates

The first class of protocol takes advantage of a QECC with a non-Clifford transversal gate. For instance, we could use the 15-qubit code discussed in section 11.5.1, which has a transversal $\pi/8$ gate. Note that the use of the 15-qubit code is completely independent of the QECC used for fault tolerance, which can be a totally different code. As mentioned above, I will describe the protocol for unencoded magic states, so only the 15-qubit code will make an appearance at first. At the end of this section, I will be more explicit about how one combines the distillation protocol with encoded operations.

For the $\pi/8$ gate, the relevant magic state is $R_{\pi/8}|+\rangle$. One magic state of this form lets us perform one $R_{\pi/8}$ gate using the circuit in figure 13.7, which involves only Clifford group gates and Pauli measurements. Now suppose we wanted to create a magic state encoded in the 15-qubit code. We can create the $|\overline{+}\rangle$ state for the 15-qubit code using only Clifford group gates. Then we would have to perform a logical $\overline{R_{\pi/8}}$ gate.

A transversal $\pi/8$ applied to the code does the logical $-\pi/8$ rotation, which is close. If we then follow it by a $\pi/4$ rotation $\overline{R_{\pi/4}}$, we will get the right result. The logical $\pi/4$ gate can be performed on the 15-qubit code using transversal $-\pi/4$ gates. (You can check this.) Therefore, the only non-Clifford component we need is the transversal $\pi/8$ gate. By the rules of magic state distillation, we don't have the ability to do such a thing directly.

That is where the noisy magic states come in. Suppose we take 15 low-quality $R_{\pi/8}|+\rangle$ states, and use the compressed gate teleportation technique to perform 15 single-qubit $R_{\pi/8}$ gates, comprising the transversal $\pi/8$ rotation we need. If all the magic states we used were perfect, the result would be the perfect logical $\overline{R_{\pi/8}}|\overline{+}\rangle$ state. If r of the magic states are wrong, however, we instead get a state with errors on it. An error in a magic state causes the gate performed to be something other than the correct $\pi/8$ rotation. However, since the teleportation circuit for a single magic state only touches a single qubit of the 15-qubit code, r incorrect magic states can only produce errors on r qubits of the 15-qubit code. The 15-qubit code has distance 3, so if $r = 1$, we can perform error correction — which only uses Clifford group gates and Pauli measurements — and end up with a perfect encoded magic state.

Actually, since this is a state preparation procedure, we're happy to use post-selection if it lets us tolerate more error. Instead of error correction, we could use error detection, since the 15-qubit code can detect up to 2 errors. If we detect an error in the code, throw away the whole thing and start again using new magic states. If $r \leq 2$, we end up with a perfect encoded magic state. Admittedly, if $r \geq 3$, it's possible an error will slip by and give us a bad magic state, but if the probability of a single magic state being bad is p and errors on different magic states are independent, the probability of having $r \geq 3$ is $O(p^3)$, which for small p is much better.

Of course, we don't really want a magic state encoded in the 15-qubit code, we want an unencoded magic state (or rather, one encoded in the QECC we're using for fault tolerance, but leave that be for now). The 15-qubit code is a stabilizer code, though, so we can decode it using a Clifford group circuit, leaving an unencoded magic state with the same error rate as the encoded one produced after error detection. In summary, we have the following procedure:

Protocol 13.2.

1. Begin with 15 $R_{\pi/8}|+\rangle$ magic states, possibly with some errors.
2. Create $|\overline{+}\rangle$ for the 15-qubit code using a Clifford group encoding circuit.
3. Use compressed gate teleportation with the magic states to perform a transversal $R_{\pi/8}$ gate on the 15-qubit code block.
4. Perform a transversal $R_{-\pi/4}$ gate on the code.
5. Perform error detection for the 15-qubit code. If any errors are detected, throw it out and restart the protocol.
6. Decode the 15-qubit code.

When the input of the protocol is 15 magic states which have independent errors with probability p per state, the output of the protocol is an improved magic state with error probability $O(p^3)$.

In the literature, you will often see magic state distillation protocol protocols with a more compact form:

Protocol 13.3.

1. Begin with 15 $R_{\pi/8}|+\rangle$ magic states, possibly with some errors.
2. On the 15 magic states, measure the error syndrome of the 15-qubit code. If the syndrome is non-zero, throw out all the qubits and restart the protocol.

3. Decode the 15-qubit code, keeping only the decoded qubit.

4. Perform $R_{\pi/4}$ on the remaining qubit.

This is a closely related procedure, and works for much the same reason. Since the transversal $R_{\pi/8}$ is a valid gadget for the 15-qubit code, it commutes with the projector Π_{15} on the code:

$$R_{\pi/8}^{\otimes 15}\Pi_{15} = \Pi_{15}R_{\pi/8}^{\otimes 15}. \tag{13.20}$$

The effect of step 2, measuring the syndrome and then discarding if it is non-trivial, is to perform Π_{15}. Therefore, after step 2, in the absence of errors, we have the state

$$\Pi_{15}\left(R_{\pi/8}|+\rangle\right)^{\otimes 15} = R_{\pi/8}^{\otimes 15}\Pi_{15}|+\rangle^{\otimes 15}. \tag{13.21}$$

But $\Pi_{15}|+\rangle^{\otimes 15} = |\overline{+}\rangle$ (up to normalization). This need not be true for a general stabilizer code, but it is true for a CSS code using the standard basis codewords. Therefore, after step 2 of the protocol, we have the state

$$R_{\pi/8}^{\otimes 15}|\overline{+}\rangle = \overline{R_{-\pi/8}}|\overline{+}\rangle, \tag{13.22}$$

and the remaining two steps leave us with the desired magic state.

When some of the initial magic states have errors in them, we rely on the QECC projection to alert us to their presence. The magic state lives in a two-dimensional Hilbert space, which can be spanned by $R_{\pi/8}|+\rangle$ and $R_{\pi/8}|-\rangle = R_{\pi/8}Z|+\rangle$, so let's assume that the error Z_e on the initial set of 15 magic states is a tensor product of Z's and I's. Then

$$\Pi_{15}R_{\pi/8}^{\otimes 15}Z_e|+\rangle^{\otimes 15} = R_{\pi/8}^{\otimes 15}\Pi_{15}Z_e|+\rangle^{\otimes 15}. \tag{13.23}$$

We can break up Π_{15} into a product $\Pi_{15} = \Pi_{15,X}\Pi_{15,Z}$, with $\Pi_{15,X}$ consisting of the sum over X generators and $\Pi_{15,Z}$ the sum over Z generators. Now, $\Pi_{15,Z}$ commutes with Z_e, so we have

$$\Pi_{15}R_{\pi/8}^{\otimes 15}Z_e|+\rangle^{\otimes 15} = R_{\pi/8}^{\otimes 15}\Pi_{15,X}Z_e\Pi_{15,Z}|+\rangle^{\otimes 15}. \tag{13.24}$$

What is $\Pi_{15,Z}|+\rangle^{\otimes 15}$? Well, $|+\rangle$ is a $+1$ eigenstate of X, so the tensor product of $|+\rangle$ states will be an eigenstate of any X generator of the code as well. Thus, $\Pi_{15,X}|+\rangle^{\otimes 15} = |+\rangle^{\otimes 15}$, so

$$\Pi_{15,Z}|+\rangle^{\otimes 15} = \Pi_{15,Z}\Pi_{15,X}|+\rangle^{\otimes 15} = |\overline{+}\rangle, \tag{13.25}$$

and

$$\Pi_{15}R_{\pi/8}^{\otimes 15}Z_e|+\rangle^{\otimes 15} = R_{\pi/8}^{\otimes 15}\Pi_{15,X}Z_e|\overline{+}\rangle. \tag{13.26}$$

On the RHS, we have a situation where the phase errors Z_e afflict a codeword of the 15-qubit code, and then we detect phase errors. Since the code has distance 3, it can detect two errors, so if there are phase errors on one or two qubits, the projection $\Pi_{15,X}$ annihilates the state. Once again, the probability of magic state errors surviving the distillation procedure is reduced from p to $O(p^3)$.

One notable difference between the protocols as written is that in the second version, there is a good chance that the state will be rejected for failing the $\Pi_{15,Z}$ projection even if all the magic states are perfect. This drawback can be easily eliminated: Since the ability of the code to correct bit flip errors is never actually used to eliminate errors — it was sufficient to detect phase errors — we can keep the state regardless of the result of measuring the Z generators. However, we will in general need to do some additional Clifford group gates in order to end up with the right state.

You remember, I hope, that the purpose of all this was to provide a fault-tolerant magic state preparation gadget. So, how do these protocols look when we make them fault tolerant?

Protocol 13.4.

1. Create 15 $\overline{R_{\pi/8}}|\overline{+}\rangle$ encoded magic states using non-fault-tolerant circuits. The states are encoded in the QECC Q used for fault tolerance.

2. Perform fault-tolerant error correction on the magic states.

3. Create the state $|\overline{+}\rangle$ encoded in a concatenated code with the 15-qubit code as the inner code, and Q as the outer code. (I.e., each qubit of the 15-qubit code is encoded in Q.) Since the $|+\rangle$ state encoded in the 15-qubit code is a stabilizer state, the desired state is a stabilizer state encoded in Q, and should thus be created using one of the methods for fault-tolerantly preparing encoded stabilizer states discussed in section 13.1.

4. Use compressed gate teleportation with the encoded magic states to perform an $\overline{R_{\pi/8}}$ gate on each of the blocks of Q comprising the 15-qubit code. This step involves Clifford group gates and Pauli measurements, which should be implemented using the appropriate fault-tolerant gadgets for Q.

5. Perform an $\overline{R_{-\pi/4}}$ gate on each of the blocks of Q comprising the 15-qubit code. This is a Clifford group gate, and should be implemented using the relevant fault-tolerant gadget for Q.

6. Measure the generators of the 15-qubit code on the concatenated code block. This should be done using procedures that are fault-tolerant for the code Q, but need not be fault-tolerant for the 15-qubit code. If any errors are detected, throw the whole block out and restart the protocol.

7. Decode the 15-qubit code.

8. If more error tolerance is needed, take the surviving magic states (still encoded in Q) and repeat the protocol starting from step 3, as many times as is needed.

All the steps except for step 1 are built out of fault-tolerant gadgets for Q. Therefore, one fault (or two, if the code can correct 2 errors) anywhere in steps 2 or later still has the protocol satisfy the PPP and PCP. If there are one or two faults in step 1, only one or two magic states are bad, and the distillation procedure will detect the error. With one fault in the magic state preparation and one fault later in the circuit, the PPP and PCP are also satisfied (see exercise **??**).

If the code Q has larger distance, we may want to repeat the magic state distillation procedure more than once to tolerate more errors in the initial magic states. Magic state distillation can be used as an iterative procedure: Use the outputs of one round of magic state distillation as inputs to a second round. If the initial states have error rate p, the first round gives us states with error rate $O(p^3)$, and two rounds give us states with error rate $O(p^9)$, detecting up to eight erroneous magic states in the initial pool of 15^2 magic states. (The two-round procedure only fails if there are at least three first-round states that are wrong, and each of those can only happen if there are three faults in the corresponding part of the circuit.) If that's not good enough, you can feed the states surviving the second round into a third round, then a fourth round, for however many rounds you need. Assuming the Clifford group operations really are perfect, we will rapidly converge to pure 200-proof magic states.

13.5.2 Twirling of Magic States

In analyzing the 15-qubit code, we considered a stochastic Pauli error model for the initial magic states — with probability $1 - p$ the state is perfect, and with probability p there is a Z error on it. When dealing with circuits containing only Clifford group gates, sticking with a Pauli error model is a self-consistent thing to do: If the original fault causes a Pauli error, later Clifford group gates may change the type of Pauli, but it will still be a Pauli error. However, to create a magic state, we need to stick in one or more non-Clifford group gates somewhere, which creates the potential for trouble, since a pre-existing Pauli error could become a non-Pauli error.

For distillation of $R_{\pi/8}|+\rangle$ by the 15-qubit code, we are on pretty safe ground considering only Pauli errors. Theorem 2.4 ensures that the 15-qubit code can correct or detect superpositions of Pauli errors as well, so the protocol will still work, but as we widen the class of magic state distillation procedures we consider, there is a possibility that something will go wrong.

We'd like to compare the probability of error after a round of distillation with the probability before. This only makes sense at all if the error model is a stochastic one, and even then is a bit tricky for a general

stochastic error model, since some of the "errors" could be represented by Kraus operators which are close to the identity but not equal to it. (This could happen before the distillation, but is much more likely to happen afterwards.) Treating such a Kraus operator as a big error on a par with X or Z won't really do the protocol justice.

One solution is to simply use fidelity to the correct state as the measure of success. This is well-defined always and correctly quantifies the power of the protocol. However, within the magic state model of faulty magic states plus perfect Clifford operations, there is another way to ensure that all errors are handled clearly, and it also simplifies the analysis of the protocol.

Theorem 13.6. *Let $\{|\psi_i\rangle\}$ be a basis for a Hilbert space $\mathcal{H}$, and let $\{U_a\}$ be a set of Clifford group operations on $\mathcal{H}$. Suppose $U_a|\psi_i\rangle = \lambda_{ai}|\psi_i\rangle$, and let $v_i = (\lambda_{ai})$ be the vector of eigenvalues for $|\psi_i\rangle$. Assume $v_i \neq v_j$ for $i \neq j$, so each $|\psi_i\rangle$ is uniquely determined by its eigenvalues for $\{U_i\}$. Let the order of U_a be m_a (i.e., $U_a^{m_a} = I$).*

Suppose we take some (possibly mixed) state ρ in $\mathcal{H}$, and for each a, perform $U_a^{r_a}$, where r_a is a random integer from $[0, m_a - 1]$. This procedure converts ρ into a mixture $\rho' = \sum_i p_i|\psi_i\rangle\langle\psi_i|$, with $p_i = \langle\psi_i|\rho|\psi_i\rangle$.

This procedure is an example of *twirling*. In general, twirling involves averaging over some group of operations in order to simplify the form of the noise. This particular example says that we can twirl noisy Clifford eigenstates to produce a stochastic noise model where the true state is a mixture of Clifford eigenstates with different eigenvalues. For instance, the magic state $R_{\pi/8}|+\rangle$ is a $+1$ eigenstate of $U = XR_{\pi/4}^\dagger$, so by performing U with probability $1/2$, we produce a mixture of the ± 1 eigenstates of U, namely $R_{\pi/8}|\pm\rangle$.

It's worth noting that implicit in theorem 13.6 is that the operations U_a all commute with each other, since they share an eigenbasis. Therefore, the order that we perform them in doesn't matter, and the procedure described is equivalent to choosing a random element of the group generated by the $\{U_a\}$.

Proof. Let us write ρ in the specified basis:

$$\rho = \sum_{ij} \rho_{ij}|\psi_i\rangle\langle\psi_j|. \tag{13.27}$$

The effect of performing $U_a^{r_a}$ is to give us $U_a^{r_a}\rho U_a^{-r_a}$. Averaging over r_a, we see the state is

$$\sum_{ij} \rho_{ij} \left[\frac{1}{m_a}\sum_{r_a=0}^{m_a-1} \lambda_{ai}^{r_a}(\lambda_{aj}^*)^{r_a}\right] |\psi_i\rangle\langle\psi_j|. \tag{13.28}$$

Now, U_a has order m_a, so λ_{ai} and λ_{aj} are m_a-th roots of unity. Thus, if $\lambda_{ai} \neq \lambda_{aj}$, then the sum

$$\frac{1}{m_a}\sum_{r_a=0}^{m_a-1} (\lambda_{ai}\lambda_{aj}^*)^{r_a} = 0. \tag{13.29}$$

When $\lambda_{ai} = \lambda_{aj}$,

$$\frac{1}{m_a}\sum_{r_a=0}^{m_a-1} (\lambda_{ai}\lambda_{aj}^*)^{r_a} = 1, \tag{13.30}$$

since $|\lambda_{ai}|^2 = 1$. The effect of averaging over powers of one U_a is thus to make a block-diagonal matrix with blocks corresponding to the eigenspaces of U_a. Within an eigenspace, the entries of the matrix do not change.

Since $|\psi_i\rangle$ and $|\psi_j\rangle$ have different eigenvalues for at least one Clifford U_a, averaging over powers of all of the U_b eliminates the off-diagonal elements, leaving ρ' of the form claimed. The remaining diagonal elements $\rho'_{ii} = \rho_{ii} = \langle\psi_i|\rho|\psi_i\rangle$. □

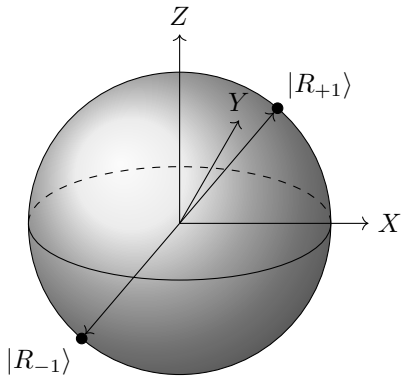

Figure 13.8: $|R_{+1}\rangle$ and $|R_{-1}\rangle$ states in the Bloch sphere.

13.5.3 Other Magic State Distillation Procedures

There are other classes of magic state distillation procedures that don't derive from transversal non-Clifford gates. One common feature of the known procedures is that they distill eigenstates of Clifford group operators using codes which have those Clifford group operations as transversal gates. However, there are additional factors in play. The fact that the code can correct errors does not necessarily play a role, and there may be different mechanisms at work in different protocols.

An example of a protocol falling in this class uses the 5-qubit code to distill the state $|R\rangle = \cos\beta|0\rangle + e^{i\pi/4}\sin\beta|1\rangle$, with β given by $\cos(2\beta) = 1/\sqrt{3}$. $|R\rangle$ is an eigenstate of the Clifford group gate R which maps $X \mapsto Z \mapsto Y \mapsto X$ under conjugation. As we saw in exercise **??**, transversal R is a gadget for the 5-qubit code. $|R\rangle$ is the state in the center of the first octant of the Bloch sphere, as depicted in figure 13.8.

The $|R\rangle$ state is a magic state only in the more general sense of the term. There is no known general procedure such as protocol 13.1 for directly using $|R\rangle$ to perform a unitary gate. Instead, there is a probabilistic procedure using additional Clifford group gates and Pauli measurements to convert $|R\rangle$ to another state which can in turn be used to perform a unitary non-Clifford group gate (though not, interestingly, a $\mathcal{C}_3$ gate). I won't go into the details of the additional processing. They are not complicated but are a bit ad hoc.

The distillation procedure itself is similar to the briefer version of the 15-qubit protocol:

Protocol 13.5.

1. Begin with 5 $|R\rangle$ magic states, possibly with some errors.
2. Twirl in the R eigenbasis by performing I, R, or R^2 each with probability 1/3.
3. On the 5 magic states, measure the error syndrome of the 5-qubit code. If the syndrome is non-zero, throw out all the qubits and restart the protocol.
4. Decode the 5-qubit code, keeping only the decoded qubit.
5. Perform YH on the remaining qubit.

In order to understand protocol 13.5, we should first consider the eigenstates and eigenvalues of R. $|R_{+1}\rangle \equiv |R\rangle$ is one eigenstate. The other eigenstate is the state $|R_{-1}\rangle$ on the opposite pole of the Bloch sphere (see figure 13.8). The eigenvalues of $|R_{+1}\rangle$ and $|R_{-1}\rangle$ for R are ... well, actually there is an ambiguity in the eigenvalues. In section 6.1.4, we saw how to find the matrix representation of a Clifford group operation given its conjugation action on Paulis. However, the matrix is only determined up to a global phase. Normally, that's not a problem, but of course the global phase affects the actual eigenvalues.

For the purposes of the analysis of protocol 13.5, we will choose a global phase for R such that the eigenvalues are

$$R|R_a\rangle = e^{i\pi a/3}|R_a\rangle. \tag{13.31}$$

The matrix corresponding to this choice of global phase is

$$\frac{e^{i\pi/4}}{\sqrt{2}}\begin{pmatrix}1 & 1\\ i & -i\end{pmatrix}. \tag{13.32}$$

The transversal R applied to the 5-qubit code performs a logical $\overline{R}$, but it might be a realization of $\overline{R}$ with a different global phase. Normally, again, this doesn't matter, but we need to be careful since we want to reason about eigenvalues.

Let's put that off for a moment, and plow ahead to figure out the effect of the projection on the code space on some possible input states. The twirling step and theorem 13.6 ensure that we can consider the noisy magic state to be a mixture of $|R_{+1}\rangle$ and $|R_{-1}\rangle$. Via a simple calculation or simply looking at figure 13.8, you can see that

$$|R_{\pm 1}\rangle\langle R_{\pm 1}| = \frac{1}{2}\left[1 \pm \frac{1}{\sqrt{3}}(X+Y+Z)\right], \tag{13.33}$$

so the tensor product of five copies is

$$(|R_{\pm 1}\rangle\langle R_{\pm 1}|)^{\otimes 5} = \frac{1}{2^5}\sum_{P\in\hat{\mathsf{P}}_5}\left(\pm 1/\sqrt{3}\right)^{\mathrm{wt}\,P} P. \tag{13.34}$$

Now, the projector on the 5-qubit code is

$$\Pi_5 = \frac{1}{2^4}\sum_{M\in\mathsf{S}} M, \tag{13.35}$$

where S is the stabilizer of the 5-qubit code, so

$$\mathrm{tr}\left[(|R_{\pm 1}\rangle\langle R_{\pm 1}|)^{\otimes 5}\Pi_5\right] = \frac{1}{2^4}\sum_{M\in\mathsf{S}}\left(\pm 1/\sqrt{3}\right)^{\mathrm{wt}\,M}\mathrm{phase}(M). \tag{13.36}$$

Here, phase(M) means the phase which appears for M in S (i.e., if $M = -X\otimes X\otimes X\otimes X \in \mathsf{S}$, then phase$(M) = -1$). However, for the 5-qubit code, all elements of the stabilizer appear with overall phase $+1$. We can therefore identify the projection of magic states on the code in terms of the weight enumerator, introduced in section 7.4.1:

$$\mathrm{tr}\left[(|R_{\pm 1}\rangle\langle R_{\pm 1}|)^{\otimes 5}\Pi_5\right] = \frac{1}{16}A\left(\pm 1/\sqrt{3}\right). \tag{13.37}$$

For the five-qubit code, $A(x) = 1 + 15x^4$, giving us $1/6$ for both tensor products.

In particular, both $\Pi_5|R_{+1}\rangle^{\otimes 5}$ and $\Pi_5|R_{-1}\rangle^{\otimes 5}$ are non-zero, and that will let us identify the global phase for the logical $\overline{R}$ gate. I claim $\Pi_5|R_{\pm 1}\rangle^{\otimes 5}$ are the eigenstates of $\overline{R}$. Let $\overline{R} = e^{i\phi}R^{\otimes 5}$. Since $R^{\otimes 5}$ is a valid gadget for the 5-qubit code, $R^{\otimes 5}$ maps the code subspace into itself, meaning Π_5 and $R^{\otimes 5}$ commute. Thus,

$$\overline{R}\Pi_5|R_{\pm 1}\rangle^{\otimes 5} = e^{i\phi}R^{\otimes 5}\Pi_5|R_{\pm 1}\rangle^{\otimes 5} \tag{13.38}$$

$$= e^{i\phi}\Pi_5 R^{\otimes 5}|R_{\pm 1}\rangle^{\otimes 5} \tag{13.39}$$

$$= e^{i\phi}e^{\pm 5i\pi/3}\Pi_5|R_{\pm 1}\rangle^{\otimes 5}. \tag{13.40}$$

Therefore, $\Pi_5|R_{\pm 1}\rangle^{\otimes 5}$ is an eigenvector of $\overline{R}$ with eigenvalue $e^{i(\phi\mp\pi/3)}$. The only way for this to match the correct eigenvalues for $\overline{R}$ is to let $\phi = 0$. We thus find that

$$|\overline{R}_{\mp 1}\rangle = \sqrt{6}\Pi_5|R_{\pm 1}\rangle^{\otimes 5}. \tag{13.41}$$

This tells us that if we put in 5 perfect magic states $|R_{+1}\rangle$, then with probability 1/6 the state is accepted, in which case after decoding the 5-qubit code we have the state $|R_{-1}\rangle$. YH will then map this back to the desired state $|R_{+1}\rangle$. On the other hand, suppose one of the five magic states is wrong, so we have $|R'\rangle$, a tensor product of 4 $|R_{+1}\rangle$ states and one $|R_{-1}\rangle$ state (in some order). We can repeat the above calculation, and find

$$\overline{R}\Pi_5|R'\rangle = e^{i\pi}\Pi_5|R'\rangle. \tag{13.42}$$

But -1 is not an eigenvalue of $\overline{R}$, so the only way this can be true is if $\Pi_5|R'\rangle = 0$. If we put in 3 $|R_{+1}\rangle$ states and 2 $|R_{-1}\rangle$ states, the projection is non-zero again.

This means that in order for the decoded magic state to be wrong, there must have been at least 2 errors on the magic states fed into the protocol. When there is only one error, the state is always rejected by the projection onto the code space. In particular, when the error rate per magic state is p, the error rate after the protocol will be $O(p^2)$. If this is not good enough, the procedure can be applied iteratively, as with the 15-qubit code distillation protocol, to decrease the error rate as much as desired.

Chapter 14

If It's Worth Doing, It's Worth Overdoing: The Threshold Theorem

It's taken a while, but finally we have all the pieces for a complete fault-tolerant protocol. But there's something important missing — we haven't shown that a fault-tolerant protocol gives us a more reliable answer than a non-fault-tolerant protocol. That's what I'll cover in this chapter: The proof that the logical error rate for a fault-tolerant simulation is lower than the error rate for an unencoded circuit. The proof requires some more formal stuff to make precise what that statement means, but it uses the same basic tools of gadgets and ideal decoders that you should hopefully be familiar with by now.

And since doing a fault-tolerant simulation of a noisy circuit gives an improvement, doing an FT simulation of a simulation is even better. If two levels of simulation are good, three levels of simulation must be even better, and four levels better yet. Binging on fault tolerance[1] leads us to the idea of concatenated fault-tolerant protocols and the threshold theorem: If the physical error rate per location is low enough, arbitrarily long quantum computation is possible.

14.1 Adversarial Errors

In chapter 10, I introduced the independent stochastic error model, which is a natural starting point for discussions of fault tolerance. Unfortunately, the "independent" part of the model is not sufficiently general to prove the threshold theorem. The basic problem is that when we have a fault-tolerant protocol, the correct description of the error model on the logical qubits is not independent, even when the underlying physical error model is an independent stochastic model.

The solution is to prove the threshold theorem using a more general error model, the adversarial stochastic error model. An independent stochastic error model is a specific type of adversarial error model, so our final result will also apply for systems with independent noise.

14.1.1 The Adversarial Local Stochastic Error Model

To motivate the definition of adversarial noise, first consider an independent stochastic error model, with error rate p_L for location L. Consider a set S of locations. What is the probability that the fault path realized in a run of the circuit has a fault on every location in S? Why, it is just $\prod_{L \in S} p_L$. The probability decreases exponentially with the number of locations in S. For adversarial noise, we'd like to keep this property and discard another property of independent noise, namely that the *type* of error is independent between faulty locations.

[1] Don't actually do this: While too much fault tolerance won't make you sick, it will waste resources you probably want to use to make a bigger logical circuit.

Definition 14.1. Given a circuit C, an *adversarial local stochastic error model* on C is a circuit $\widetilde{C}$ which is a mixture over realizations of C with different fault paths. In a given realization of C with fault path Φ, locations outside Φ perform the correct action for the given location, and locations in Φ are replaced by arbitrary interactions (not necessarily a tensor product between faulty locations) with a persistent environment which begins the computation in a standard state such as $|0\dots0\rangle$. Fault path Φ occurs with probability p_Φ, such that the following property holds: For each location L, there exists an *error rate* (or *error probability*) p_L such that, if S is any set of locations, then $\sum_{\Phi|S\subseteq\Phi} p_\Phi \leq \prod_{L\in S} p_L$.

In other words, there is some error probability associated with each location, and the total probability of error on some set of locations is at most the product over the error rates of those locations. In the case where all p_L are equal to p, the probability that the fault path includes the set S is at most $p^{|S|}$, with $|S|$ the number of locations in S. The noise model doesn't make any restriction on whether there are other faulty locations outside S or not. There could be all sorts of horrible correlations between errors at different locations, provided the probability of having many errors decays in the right way as a function of the number of errors. The "local" in the name doesn't refer to any geometric property of where qubits or errors are located; it refers to errors acting on only a few qubits at a time.

One way to think about an adversarial local stochastic error model is to imagine laying out the ideal circuit C, and then for each location L, choose it to be possibly faulty with probability p_L, choosing independently for each location. Then an enemy (the eponymous *adversary* of the error model), determined to foil your computation whenever possible, gets to control the possibly faulty locations. The adversary can choose to do whatever she likes on those faulty locations, interacting them with each other or an environment as she wishes. She can even let a faulty location act correctly if that is in her best interest — and sometimes it is! The only thing she cannot do is change the locations that were not selected as potentially faulty. Those locations do the right thing, as specified by C.

In practice, we use the adversarial local stochastic error model to represent situations where there is no actual adversary, but where we simply do not know — or don't want to keep track of — precisely what happens when there is an error. You could think of this as an error model being run by an adversary who has some additional limitations (besides the restriction on which locations she can attack), or one that is simply not intelligent enough to pick the worst possible choice for us.

Frequently, either the word *local* or the word *adversarial* is omitted from the name of error model: *adversarial stochastic errors* or *local stochastic errors*. The latter choice is more common in the literature, but is a little confusing since one might incorrectly think "local" means the errors are physically close to each other. I will use "adversarial stochastic errors" instead. I have no intention of using the full name of the error model: It is long enough even shortened,

14.1.2 What Is and Is Not Included in the Adversarial Error Model

As noted above, independent stochastic noise is included in the adversarial error model, but so are many more things. For instance, if the error model has an error on each location with probability p, but either all faulty locations have X errors or all faulty locations have Z errors (each with probability $1/2$), that is an adversarial noise model but not an independent one, since there is a strong correlation between the type of errors on different locations.

Perhaps less clear is that even when the probability of having an error is correlated between locations, the error model may still qualify as an adversarial stochastic model. For instance, suppose the qubits are laid out on a grid in two or three dimensions and gates are only performed between nearest-neighbor qubits. Imagine an error model where the locations involving adjacent pairs of qubits fail with probability p, and disjoint pairs of locations fail independently. For an error model of this type, the probability that a single location will fail is about Dp, where D is the number of adjacent locations to the one under consideration. The probability that a specific pair of adjacent locations will fail is about $p + (Dp)^2$.

At this point, it may seem like this is not an adversarial stochastic error model, since the probability of two locations failing is not $O(p^2)$. However, no one said that the error rate p_L had to be equal to Dp, the probability of a single location failing; it can be larger. Note that the probability of $s = 2r$ locations

failing is $O(p^r)$, which is the desired exponential decay. Therefore, if we pick p_L to be about $\sqrt{2p}$, provided that is still less than 1, we see that the error model qualifies: The probability of a single location failing is $Dp \leq \sqrt{2p}$ (for small enough p), the probability of two locations failing is about $p + (Dp)^2 \leq (\sqrt{2p})^2 = 2p$, and the probability of s locations failing is about $p^{s/2} \leq (\sqrt{2p})^s$. Similarly, an error model which has correlated errors affecting sets of t errors at a time with probability p is an adversarial stochastic error model with $p_L = O(p^{1/t})$. Naturally, this is a bit inefficient as a way of bounding the errors, since frequently the probability of a specific set of locations having errors is much less than the bound, but the adversarial error model has the advantage of including a wide variety of different types of correlated models using a single argument.

However, don't get the idea that the adversarial error model applies to everything. For instance, an error model that has some very small (but constant) probability that all the qubits in the computer experience an X error is not an adversarial stochastic error model. We shouldn't expect to be able to correct an error affecting all the qubits in the computer and indeed we can't. Another more significant defect of the error model is that it only deals with stochastic noise: The non-faulty locations are perfect even though the faulty locations can be arbitrary. For instance, this doesn't include a systematic error in which every unitary gate in C is over-rotated by some small angle $\delta\theta$. It also doesn't include even perfectly independent noise where each gate location is replaced by a quantum channel that is very close to the correct action U of the location, unless every channel is of the form $\rho \mapsto (1-p)U\rho U^\dagger + p\mathcal{E}(\rho)$. These last two non-stochastic error models are very natural. Luckily, the threshold theorem *does* apply to them. We won't cover them in this chapter, but we'll return to the topic in section 15.8.

Of course, when I say that a particular error model is not an adversarial stochastic error model, that is not strictly mathematically true. You *could* write these examples — or any other error model — as adversarial stochastic ones by taking $p_L = 1$ for all locations. What I really mean is that it would be foolish to think of them as adversarial stochastic error models, because doing so would require us to take p_L to be large even though the actual error is small, causing us to vastly overestimate the prevalence of errors in the circuit.

14.2 Good and Bad Extended Rectangles

Now let's start on the task of proving that fault-tolerant circuits tolerate faults. We don't want to have to look at a huge circuit all at once, so the first task is to chop it up into manageable pieces called *extended rectangles*.

14.2.1 Definition of an Extended Rectangle

Definition 14.2. Let C be a circuit with fault-tolerant simulation $FT(C)$. Then an *extended rectangle* of $FT(C)$ consists of the locations comprising one of:

- A gate or wait gadget and all error correction gadgets immediately before and immediately after it
- A preparation gadget and the error correction gadget(s) immediately after it
- A measurement gadget and the error correction gadget(s) immediately before it

The phrase "extended rectangle" can be abbreviated *exRec*. An extended rectangle can be labeled by a location L in C, the location for which the corresponding gadget in $FT(C)$ appears in the exRec. We thus may speak of *gate exRecs*, *wait exRecs*, *preparation exRecs*, or *measurement exRecs*. Any EC gadget in the exRec before the gadget for L is known as a *leading EC gadget*, and any EC gadget after the gadget for L is a *trailing EC gadget*.

A *rectangle* is defined similarly, but omits the leading EC gadget(s) in the exRec.

An example of extended rectangles is shown in figure 14.1. An extended rectangle for a two-qubit gate location must include both EC gadgets before the gate gadget and both EC gadgets after the gate. Note that extended rectangles overlap: Two consecutive gates in C give rise to a pair of exRecs that overlap,

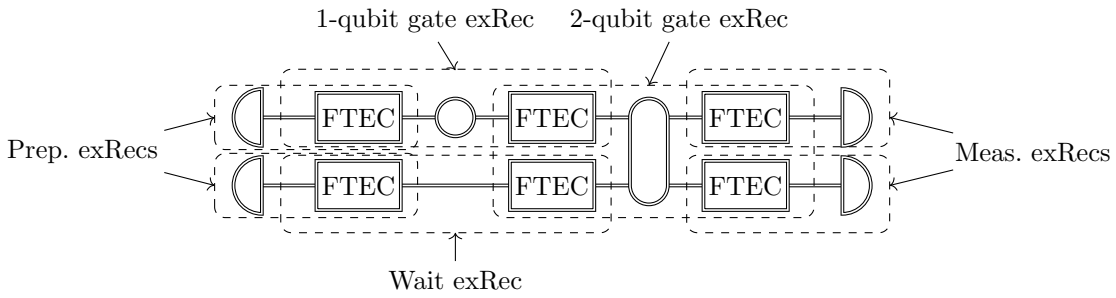

Figure 14.1: An example of a circuit with extended rectangles marked.

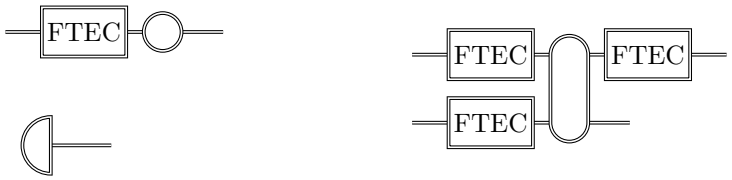

Figure 14.2: Examples of truncated extended rectangles.

sharing one or more EC gadgets. The trailing EC gadget for the earlier location is the leading EC gadget for the later location.

ExRecs are "extended" because they include EC gadgets both before and after the gate. Rectangles are perhaps a more natural notion than exRecs, since $FT(C)$ can be broken up uniquely into non-overlapping rectangles, but it turns out that analyzing individual rectangles in isolation doesn't suffice to understand the circuit's fault tolerance properties, for reasons I will explain in section 14.3. Therefore, the proofs in this chapter will use extended rectangles and not rectangles.

The last combination one might consider is an EC gadget followed by a gate, wait, or measurement gadget. This combination is needed in the proof:

Definition 14.3. A *truncated extended rectangle* is an extended rectangle with one or more trailing EC gadgets removed.

Note that a truncated exRec for a 2-qubit gate location could have a single trailing EC gadget or none at all.

14.2.2 Definition of Good and Bad Extended Rectangles

Given a fault path, some exRecs will have many faults and some will have few or none. Clearly, we expect extended rectangles with sufficiently few errors to behave like the corresponding ideal location and ones with many faults to create logical errors. Therefore, let's classify exRecs as "good" or "bad" depending on how many faults are in them:

Definition 14.4. Let Q be a QECC correcting t errors, let C be a circuit, and let $FT(C)$ be a fault-tolerant simulation of C using a fault-tolerant protocol for the code Q. Fix a particular realization of $FT(C)$ with a particular fault path Φ. An exRec in $FT(C)$ is *bad* for Φ if the exRec contains $t+1$ or more faults in Φ. The exRec is *good* for Φ if it contains t or fewer faults in Φ. A truncated exRec can be classified as good or bad in the same way, counting only those locations actually present in the truncated exRec, and not locations in the omitted EC gadgets.

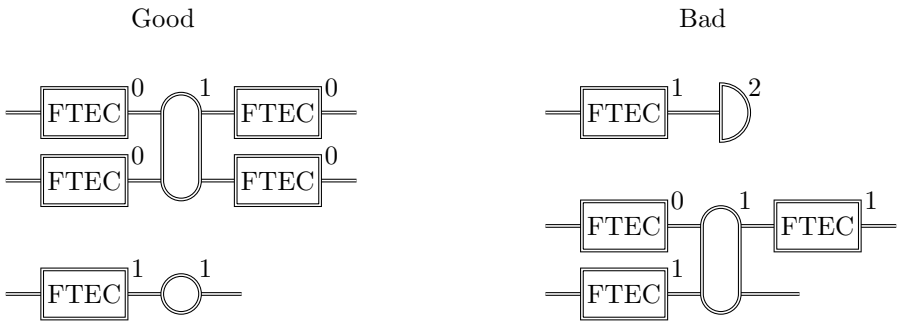

Figure 14.3: Examples of good and bad exRecs and truncated exRecs for a code with $t = 2$.

Thus, it is possible for a truncated exRec to be good even though the exRec it is contained in is bad. This can happen in a number of ways. For instance, there could be t faults in the truncated exRec and one more error in a trailing EC gadget. When the EC gadget is included in the exRec, there are $t + 1$ faults in total, making the exRec bad, but when it is not included, there are only t faults.

Note that when we say an exRec is good or bad, we are really talking about a property of a particular fault path. A different fault path has a different set of good and bad exRecs. Frequently, though, I will imagine a situation where the fault path is fixed and therefore does not need to be explicitly mentioned.

14.3 Correctness

The next step is to show that good exRecs actually behave correctly. But what does it mean for an exRec to be correct?

14.3.1 Definition of a Correct Rectangle or Circuit

To define correctness formally, we go back to the pictures I introduced to describe fault-tolerant properties back in chapter 10. It's most straightforward to define correctness for a rectangle rather than an extended rectangle. We can use the ideal decoder to talk about the state encoded at any given time, and a rectangle is correct if the encoded state evolves under the gadget in the way specified for the corresponding location in the ideal circuit.

Definition 14.5. Let L be a location in a circuit C, and suppose we have some realization of $FT(C)$ with a particular fault path Φ.

- If L is a one-block gate gadget, the rectangle for L is *correct* if

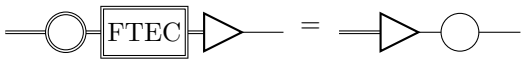

(14.1)

- If L is a two-block gate gadget, the rectangle for L is *correct* if

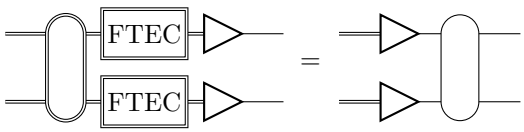

(14.2)

  and similarly for multiblock gate gadgets.

- If L is a preparation location,

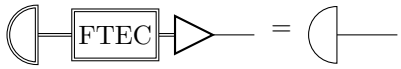

(14.3)

- If L is a measurement location,

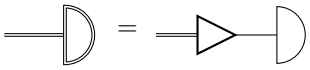

(14.4)

We say an exRec is correct if the rectangle contained in it is correct. If a rectangle or exRec is not correct, it is *incorrect*.

For a measurement location, note that a rectangle consists just of the measurement gadget, since there is no EC step after measurement.

The correctness property for gate gadgets lets us move ideal decoders to the left through an exRec to produce ideal gates. For a preparation location, moving the ideal decoder to the left gets us to the start of the circuit, so correctness for a preparation location lets us get rid of an ideal decoder. Similarly, correctness for a measurement location lets us create an ideal decoder.

Notice that the definition of correctness improves on the various fault-tolerant properties in that it uses only ideal decoders and not filters. This lets us consider the correctness of a rectangle or an exRec in isolation without having to worry too much about how many errors are carried over from the previous part of the circuit. As with "good" and "bad", however, the terms "correct" and "incorrect" only apply to an exRec for a particular fault path Φ, but whereas "good" and "bad" only depend on the locations of the faults in Φ, "correct" and "incorrect" may also depend on the types of errors produced by the specific faults.

For truncated rectangles or exRecs, the definition is essentially the same. A truncated rectangle may just be a single gate gadget, although a truncated multi-block rectangle could have some trailing EC steps remaining. There is no truncated measurement exRec, since the measurement exRec does not have a trailing EC to remove.

Definition 14.6. A truncated rectangle is correct if:

- When L is a one-block gate gadget,

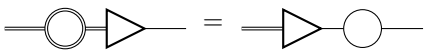

(14.5)

- When L is a two-block gate gadget,

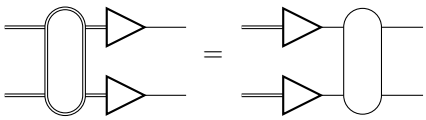

(14.6)

or

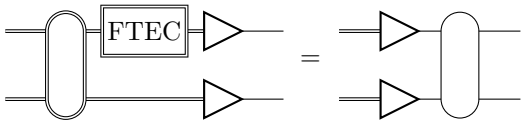

(14.7)

and similarly for multi-block gate gadgets.

- If L is a preparation location,

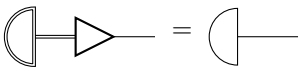

(14.8)

A truncated exRec is correct if the truncated rectangle contained in it is correct. A truncated rectangle or exRec is incorrect if it is not correct.

14.3.2 Good Extended Rectangles Are Correct

Comparing the notions of "good" and "correct", we see that they are somewhat complementary: A rectangle is good if it doesn't have too many faults, which is easy to check by looking at the fault path, and a rectangle is correct if it behaves in the way it is supposed to.

We'd like to say that a good rectangle is correct, so that when the density of faults is low, the circuit behaves correctly. However, if we look at just a single rectangle and see that it is good, we still don't have enough information to say that it is correct. For instance, suppose that we have a code with distance 3, such as the 7-qubit code, and the fault path before the rectangle implies that the state at that point has one error (which could be formalized by saying it passes a 1-filter but not a 0-filter). Further suppose there is one fault in the rectangle. The rectangle is good, but depending on the exact nature of the fault, it could produce a new single-qubit error which combines with the pre-existing single-qubit error to give a state which will be decoded to the incorrect state.

To be even more concrete, imagine we have a wait rectangle for the 7-qubit code and the pre-existing error is X_5, a bit flip on qubit 5. Before the rectangle, an ideal decoder applied to the state will correct the bit flip error, producing some logical state, say $|0\rangle$. Then suppose during the wait step, which occurs before the EC gadget in the rectangle, there is a fault which produces an additional X_7 error on the state. The state of the system at that point is then $X_5X_7|\overline{0}\rangle$. But for the 7-qubit code, $X_5X_7 = X_6\overline{X}$, so the state could also be written as $X_6|\overline{1}\rangle$. The EC step has no faults, so it will correct any errors present in the system, but it will do so acting under the assumption that there is at most one error. Therefore, it will "correct" the state to $|\overline{1}\rangle$. The ideal decoder applied after the rectangle therefore gives $|1\rangle$, meaning correctness fails for this fault path. On the other hand, if there were no pre-existing error, the state after the wait step would be $X_7|\overline{0}\rangle$, and the EC step would correct that to $|\overline{0}\rangle$. Whether or not this rectangle is correct depends on what errors are in the fault path outside the rectangle.

This problem can be solved by working with *extended* rectangles instead. The leading EC in an extended rectangle ensures that there cannot be too many errors in the state entering the main gadget of the exRec. We have the following result:

Theorem 14.1. *If an extended rectangle is good, then it is correct. If a truncated extended rectangle is good, it is correct.*

Proof. I will prove this for a single-block gate exRec. The cases of multi-block gate exRecs, measurement exRecs, and preparation exRecs are all extremely similar.

The exRec is good, so there are at most t faults in the whole exRec. We break that down into s_1 faults in the leading EC, s_2 faults in the gate gadget, and s_3 faults in the trailing EC, $s_1 + s_2 + s_3 \leq t$.

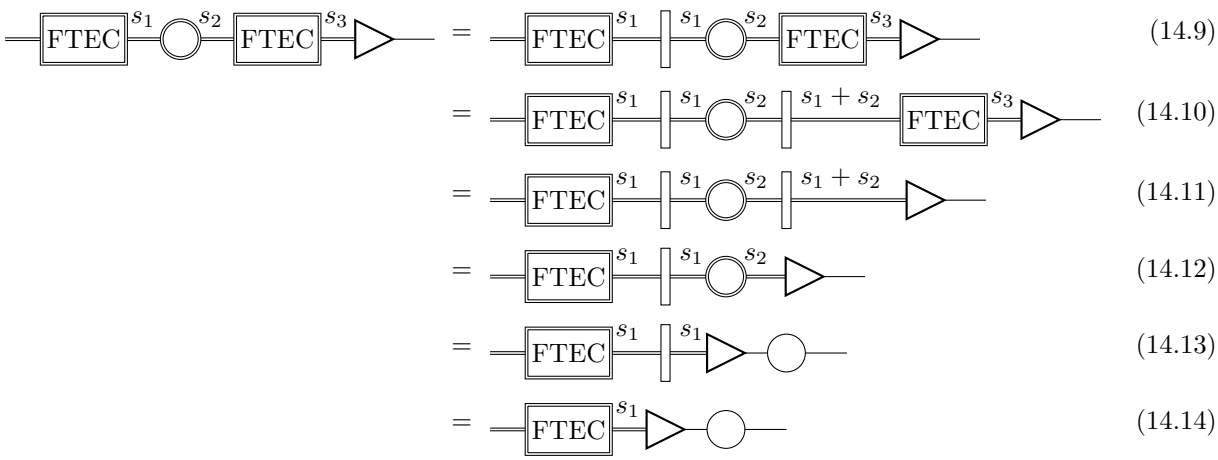

In the first line, we use the ECRP, which we can do because $s_1 \leq t$. To get the second, we use the GPP, which is allowed because $s_1 + s_2 \leq t$. The third uses the ECCP and the fact that $s_1 + s_2 + s_3 \leq t$. To get

the fourth line, we use the GPP in reverse. For line 5, use the GCP, and then use the ECRP in reverse to get rid of the remaining filter for line 6. This shows that the exRec is correct.

For truncated exRecs, you could go through a similar argument to directly show that truncated good exRecs are correct. However, we can save time by observing that

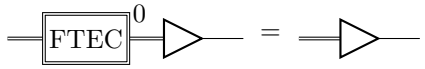

(14.15)

so we can transform a truncated exRec followed by an ideal decoder into a regular untruncated exRec with 0 faults in the trailing EC(s). Then correctness for a good truncated exRec follows from correctness for a good untruncated exRec. □

Note that by theorem 10.3, theorem 14.1 holds not only when faults produce Pauli errors, but for arbitrary faults, including those chosen by an adversary as in the adversarial stochastic model. Only the fault path needs to be known in order to determine whether an exRec is good or bad.

14.3.3 Benign and Malignant Sets of Errors

While being good is sufficient for an exRec to be correct, it is not necessary. There are many situations where a fault path may lead to an exRec that has more faults than allowed for a good exRec, but the exRec is nonetheless correct. Sometimes this happens because of a cancellation between the particular errors occurring at the locations in the fault path. However, in an adversarial error model, we assume the adversary can pick the errors in such a way as to avoid cancellations, even turning off one or more faults if necessary. Still, in most exRecs, there are still many possible sets of locations which cannot cause the exRec to be incorrect no matter which particular set of errors the adversary selects. This is known as a *benign* set of locations.

Definition 14.7. Consider a single exRec in an arbitrary fault-tolerant circuit simulation, and let S be a set of locations in the exRec. If the exRec is correct given any fault path Φ that exactly agrees with S in the exRec (but may include additional locations outside the exRec) and any choice of errors on the locations in Φ, then S is *benign*. If there exists a fault path Φ and a choice of errors on Φ such that the exRec is not correct for that choice of errors, then S is *malignant*.

Note that for a set of locations to be malignant, it only needs the exRec to be incorrect for some choice of errors at those locations and outside the exRec; it may be that most choices are fine, but since we are currently working with an adversarial error model, we must assume that the adversary is going to choose the particular types of errors that cause us the most problems.

Based on this definition, theorem 14.1 can be rephrased as saying that any set of $\leq t$ locations in an exRec is benign.

For proving the existence of a threshold for fault-tolerance, it sufficient to think about good and bad extended rectangles. However, considering benign and malignant sets of errors lets you prove a significantly better lower bound on the threshold. It can be difficult to classify by hand sets of locations as benign or malignant, but it is not too hard to count using a computer, at least approximately, the number of malignant sets of locations of a given cardinality.

When determining whether a given set is malignant or benign, it suffices to consider only Pauli errors. (Although you must consider *all* possible arrangements of Pauli errors on those locations, including the identity on some locations.) If the set is benign for Pauli errors, the same arguments as for theorem 10.3 then show that the set is benign for general errors, including when the adversary interacts faulty locations with a persistent ancilla that may even begin the circuit entangled with the input state to the exRec.

14.3.4 Simulation with Only Correct Extended Rectangles

When we have a sequence of correct exRecs, the correctness property ensures that we can put them together into a circuit which also behaves correctly.

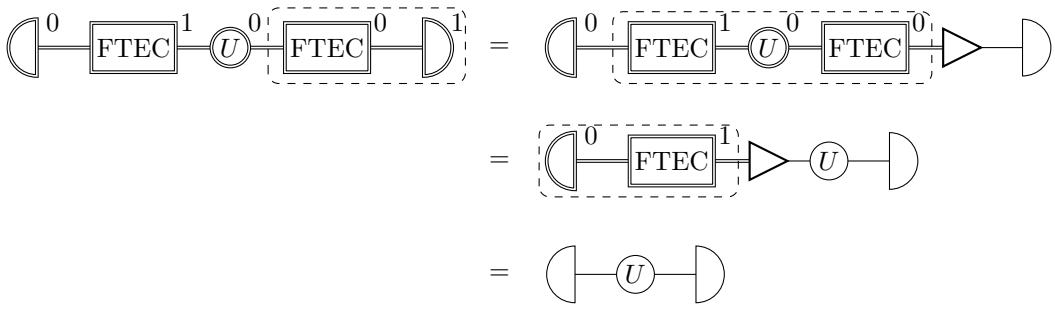

Figure 14.4: Applying the correctness properties to prove that a fault-tolerant circuit with good exRecs is equivalent to an ideal circuit. In this example, $t = 1$, so all exRecs are good. At each step, the next exRec to apply correctness to is indicated by a box.

Theorem 14.2. *Let C be a circuit starting with state preparation locations and ending with measurement locations, and let $FT(C)$ be the fault-tolerant simulation of C. Suppose for a particular fault path Φ that all the exRecs in $FT(C)$ are good (or that the fault path restricted to each exRec gives a benign set of locations). Then the output distribution of $FT(C)$ for any adversarial choice of noise for Φ is identical to the output distribution of C with ideal gates.*

Proof. The proof can be done using our graphical notation. All exRecs are good, so by theorem 14.1, all exRecs are correct. Consider first the measurement exRecs throughout C. By correctness for measurement exRecs,

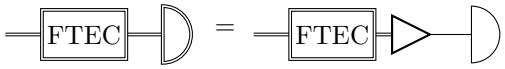

(14.16)

We can therefore replace each noisy FT measurement gadget in $FT(C)$ by an ideal decoder followed by ideal measurement.

Next, we can use induction to replace the gate gadgets by ideal gates. Suppose C has depth d. The measurement gadgets in the last temporal layer of $FT(C)$ have been replaced by ideal decoders followed by ideal measurements, so the gate exRecs in layer $d-1$ are all followed by ideal decoders. Therefore, we can apply correctness for a gate exRec to all gate exRecs in layer $d-1$ to replace

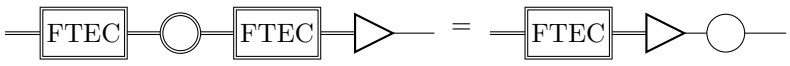

(14.17)

and similarly for multiple-block gate exRecs.

Now all the exRecs in layer $d-2$ have ideal decoders after them. In the rth step, the exRecs in layer $d-r$ are followed by ideal decoders, and we can use the correctness property to push the ideal decoder before each layer $d-r$ gate rectangle, replacing the rectangle by an ideal gate corresponding to the gate gadget in $FT(C)$. The ideal gate is thus precisely the gate in the corresponding location of C.

Eventually, we have converted all gate exRecs into ideal gates, and the only gadgets remaining in the circuit are preparation gadgets followed by EC gadgets, and all the EC gadgets are followed by ideal decoders. That is, we have preparation exRecs followed by ideal decoders. Using correctness for a preparation exRec,

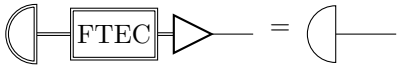

(14.18)

we replace each preparation exRec with the corresponding ideal preparation location. The result of all these manipulations is the desired circuit C.

An example of this procedure for a small circuit is given in figure 14.4. □

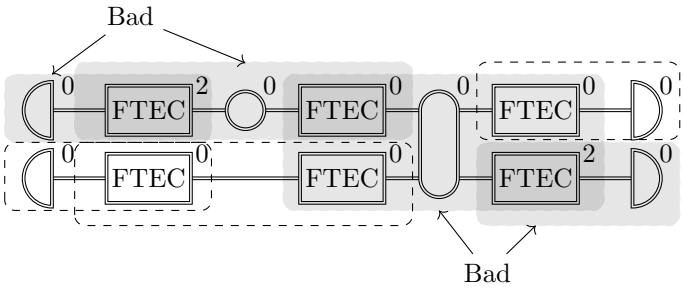

Figure 14.5: An example where 4 faults cause 4 bad exRecs when $t = 1$. Bad exRecs are shaded.

14.4 Incorrectness: Simulations With a Bad Extended Rectangle

14.4.1 The Problem of Simulations With Bad Extended Rectangles

Of course, if we are performing the fault-tolerant simulation of a large circuit, there is little chance that we will get a fault path for which every extended rectangle is good. We'll also need some way to deal with bad extended rectangles.

Based on the previous section, we know we can replace a good extended rectangle by an ideal gate (or whatever location is appropriate to the exRec). Naturally, we'd like to replace each bad extended rectangle by a noisy gate. We'd want to look at the actual set of errors occurring in the exRec in a particular realization of the noisy circuit, and replace the exRec by the corresponding unencoded location but with an appropriate error. Then, we'd like to say that an adversarial stochastic noise model acting on the physical locations for the fault-tolerant simulation of C is equivalent to another adversarial stochastic noise model acting directly on the locations of C, but with a lower error rate. Actually, we'd really prefer to do it with independent stochastic noise, but we'll settle for adversarial stochastic noise.

The first problem we face in doing this is that correlations between bad extended rectangles are too strong. A schematic example of the difficulty is shown in figure 14.5. Since the trailing EC of one exRec is the leading EC of the subsequent exRec, a single fault during an EC step contributes to the possibility of two extended rectangles being bad. This can lead to situations, as in figure 14.5, where $m(t+1)$ faults cause as many as $2m$ bad exRecs, whereas if the extended rectangles were non-overlapping, the same number of faults could cause at most m bad exRecs. Consequently, if we were to simply replace the rectangle in each bad exRec with a faulty unencoded location, we would find that the probability of a particular set of r simulated locations being faulty is $O(p^{r(t+1)/2})$. In the case of $t = 1$, this is just the same p^r scaling we get from implementing a faulty circuit without fault tolerance, and for larger t, it is still not nearly as good as the scaling we expect to get from a code correcting many errors.

To deal with this, we need to get rid of the overlaps between bad exRecs. If we replace the complete exRec with a faulty location rather than just the "rectangle" part of it, we can then excise the shared EC(s) from the previous exRec(s). We've already taken their faults into account, so we don't need to consider them again. This leads to truncated exRecs. The details of how to decide which exRecs are truncated and which aren't will be discussed in section 14.6.

Unfortunately, there's another problem: A noisy exRec doesn't correspond to a particular unencoded faulty location. That sounds crazy, I know. Surely the only alternative to having a perfect gate is having a noisy gate, right? Indeed it is. The problem is that by looking at just one noisy exRec, you can't deduce precisely *what* noise occurs on the logical state of the code. In general, the logical error corresponding to a bad exRec depends not just on the fault path within the exRec, but also on the error syndrome of the state entering the exRec.

As an example, consider a wait exRec for the 7-qubit code using Steane error correction, as in figure 14.6. Suppose the gate gadget before this exRec had a fault in it, so that the state entering the leading EC step of the wait exRec has an error E in it. We'd like to replace the whole exRec with an ideal decoder followed

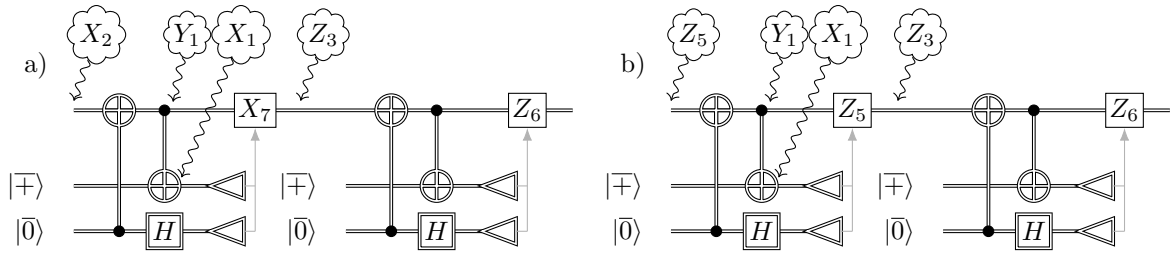

Figure 14.6: An example of how different errors outside an exRec can combine with faults inside a bad exRec to produce different logical errors.

by a faulty wait location. Suppose that the state we get from applying an ideal decoder to the input state is $|\psi\rangle$, meaning that the actual state entering the exRec is $E|\overline{\psi}\rangle$. Further suppose that we consider a fault path with two faults in the exRec, making it a bad exRec. One is in the CNOT interacting the first data qubit with the first ancilla qubit in the bit flip error correction step of the leading EC; that fault produces an error Y on the first data qubit after the CNOT, and a corresponding error on the ancilla qubit so that the bit flip part of the new error shows up in the error syndrome. The second fault causes an Z_3 error during the transversal wait gadget.

Let's consider different possibilities for the pre-existing error E and determine what the state is if we perform ideal decoding after the exRec. If E is an X_2 error, then the pre-existing error and the X_1 error due to the fault in the EC step combine, and the bit flip correction step mistakenly believes the syndrome to be due to a X_7 error. In addition, we have the new Z error due to the fault in the wait step. Therefore, after the initial EC step, the state is $Y_1X_2X_7|\overline{\psi}\rangle = -iZ_1\overline{X}|\overline{\psi}\rangle$. The Z_3 error in the wait step then combines with the Z_1 error so that the phase error correction step of the trailing EC step believes the phase error to be Z_6. Therefore the state of the block at the end of the exRec is $-iZ_1Z_3Z_6\overline{X}|\overline{\psi}\rangle = \overline{Y}|\overline{\psi}\rangle$. To simulate this properly, if we replace the full exRec by an ideal decoder followed by a faulty wait step, the logical wait step should therefore have a Y error.

On the other hand, imagine $E = Z_5$. Then the phase error correction step of the leading EC step eliminates it, and the bit flip error correction step eliminates the X part of the fault Y_1. Therefore the state exiting the leading EC step is $iZ_1|\overline{\psi}\rangle$. The phase error during the wait gadget combines with Z_1 to make a two-qubit phase error which, as before, is mistaken for a Z_6 error in the trailing EC. The final state of the exRec is thus $\overline{Z}|\overline{\psi}\rangle$. To simulate this situation properly, the decoded faulty wait step should have a Z error. As you can see, the error being simulated here depends on the error coming into the exRec. We'd like to be able to analyze the exRec by only considering what is going on inside it, but apparently we also need to consider faults outside the exRec.

Note that if we only push the ideal decoder through the rectangle part of the exRec, then this particular example doesn't cause trouble, since in both cases, we can accurately simulate the circuit by having a logical wait step with a Z error relative to the state that comes out of the leading EC step, and we can deduce that by only looking at faults within the exRec (although not just the faults within the rectangle). However, in other situations, possibly involving some extra faults, we can still have the problem (although not, as it happens, for Steane EC; see exercise **??**). Moreover, as I noted above, this strategy runs into the problem that pushing the ideal decoder back only to the leading exRec allows overly strong correlations between bad exRecs.

14.4.2 The *-Decoder

To solve this problem, we need a way to keep track of the essential information from other exRecs that is needed to determine what fault we should use to replace a particular realization of a bad exRec. We don't need full information about what faults occurred where in the rest of the circuit; the quantum state entering the exRec is enough. The quantum state can be written as superposition over Pauli errors of things of the

form $E|\overline{\psi}\rangle$, where E is a Pauli error and $|\overline{\psi}\rangle$ is a valid codeword. The ideal decoder applied to this state extracts $|\psi\rangle$, but discards information about the error. As we saw above, this is a problem because we need to know what E is in order to determine the correct fault for the logical location simulated by the exRec.

Therefore, we introduce a new object, the $*$-decoder. It works just like an ideal decoder, but instead of throwing away the syndrome information, it keeps it. I will draw the $*$-decoder this way:

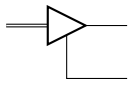

(14.19)

When applied to a state $E|\overline{\psi}\rangle$, the upper output line holds the decoded state $|\psi\rangle$, and the lower output line holds the syndrome information $\sigma(E)$. The $*$-decoder can be chosen to be unitary, which ensures that no information is lost. It is just the purification of the regular ideal decoder, which can be easily recovered from the $*$-decoder by simply discarding the second output register:

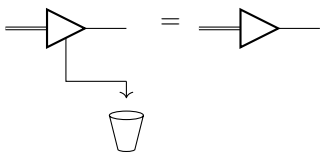

(14.20)

We can define correctness for the $*$-decoder similarly to correctness for the regular ideal decoder. The only complication is that we must specify what happens to the syndrome information when we shift the $*$-decoder forward. However, for correctness we don't need a strong requirement; anything that happens to the syndrome register is acceptable, as long as it doesn't interact with the decoded state:

Definition 14.8. The rectangle corresponding to a single-block gate location L is *correct for $*$-decoding* if

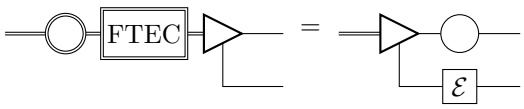

(14.21)

where $\mathcal{E}$ can be any map applied to the syndrome register, including an interaction with a persistent memory held by the adversary. $\mathcal{E}$ will generally depend on the precise faults occurring in the noisy gate gadget. Correctness for $*$-decoding is defined similarly for a multi-block gate rectangle. Preparation and measurement rectangles are correct for $*$-decoding if:

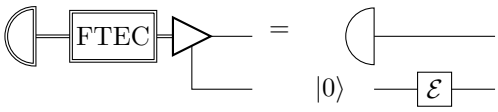

(14.22)

or

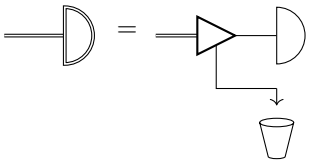

(14.23)

An exRec is correct for $*$-decoding if the rectangle contained within it is correct. To get the definition of correctness for $*$-decoding for a truncated extended rectangle, simply remove the FT EC step(s) from the definition for an untruncated exRec.

The syndrome register does change when we shift the $*$-decoder leftwards in the definition of correctness. The type of error changes due to conjugation by any gates, some errors are corrected in the EC steps, and new errors may be added due to faults in the rectangle. Precisely how the syndrome is altered is not important for the proof of the threshold theorem, but if you're interested, it can be determined exactly by

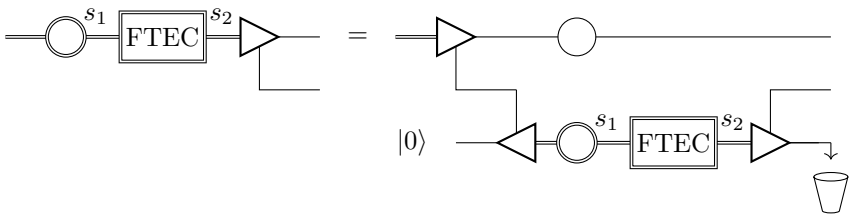

Figure 14.7: A combination of gadgets which produces the correct change in the syndrome information during a correct rectangle. The left-pointing triangle is a $*$-*encoder*, the inverse of the $*$-decoder, encoding a logical qubit into a codeword with errors determined by the syndrome (which enter and exit from the top of the $*$-encoder and $*$-decoder on the bottom line).

encoding some dummy data using the syndrome information and subjecting it to the same noise as in the original gate gadget. The procedure is illustrated in figure 14.7.

If an exRec is correct for $*$-decoding, we can simply discard the syndrome information on both sides of the equality, which means that it is also correct for regular ideal decoders. However, at first glance, it may not be clear if correctness for $*$-decoding is a strictly stronger property than regular correctness. In fact, though, they are completely equivalent:

Proposition 14.3. *If a rectangle, exRec, or truncated exRec is correct, then it is correct for $*$-decoding.*

Proof. As a starting point, use the relationship between ideal decoders and $*$-decoders to replace the decoders in the definition of correctness with $*$-decoders. For instance, for a single-block rectangle, we get

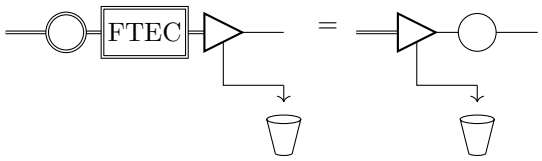

(14.24)

This statement is an equality of completely positive maps (for a particular Pauli fault path), and holds for all input data states, including states that are entangled with some reference system. Let us take a maximally entangled input state between the code block and a reference system. The terms in this entangled state run over all possible syndromes and all possible logical states of the code block.

With this input, we can write the output state of the LHS as $\mathrm{tr}_S \rho_L$ and the output state of the RHS as $\mathrm{tr}_S \rho_R$, where S is the syndrome register and ρ_L and ρ_R are joint states of the reference system, the data register, and the syndrome register. In fact, $\mathrm{tr}_S \rho_L$ and $\mathrm{tr}_S \rho_R$ are the states to which the LHS and RHS maps correspond to under the Choi-Jamiolkowski isomorphism. The equation tells us that $\mathrm{tr}_S \rho_L = \mathrm{tr}_S \rho_R$.

Now purify ρ_L and ρ_R to $|\psi_L\rangle$ and $|\psi_R\rangle$. We may assume that that the extra register A needed is held by the adversary. Since $\mathrm{tr}_{AS} |\psi_L\rangle \langle\psi_L| = \mathrm{tr}_{AS} |\psi_R\rangle \langle\psi_R|$, there is a unitary map U acting on AS such that

$$U|\psi_R\rangle = |\psi_L\rangle. \tag{14.25}$$

But $|\psi_L\rangle$ and $U|\psi_R\rangle$ are the Choi-Jamiolkowski states corresponding to purified versions of the LHS and RHS of the definition of correctness for $*$-decoding. Therefore the maps are equal as well. □

Corollary 14.4. *If an extended rectangle or truncated extended rectangle is good, it is correct for $*$-decoding.*

14.4.3 Simulation of a Single Bad Extended Rectangle

Using the $*$-decoder, we can then replace a bad extended rectangle with a noisy decoded state, provided we let the noise possibly depend on the syndrome information from the input state:

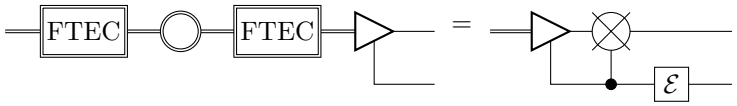

(14.26)

The noisy gate on the right hand side can be determined explicitly. Let U be the $*$-decoder, which is unitary, and E be the overall action of the full bad exRec (-[FT EC]-[FT Gate]-[FT EC]-), with a particular fault path and choice of errors for that fault path. $U^\dagger$ is a $*$-encoder, which takes a logical state $|\psi\rangle$ plus an error syndrome s and creates an encoded state $F|\overline{\psi}\rangle$ such that F is a correctable error with $\sigma(F) = s$. Since $UU^\dagger = I$, we have

$$EU = UU^\dagger EU. \tag{14.27}$$

We thus recognize the noisy decoded gate location above as $U^\dagger EU$. As desired, this depends only on the fault path inside the exRec.

We can replace a bad truncated exRec in the same way. Naturally, E now includes the overall action of the truncated exRec rather than the full exRec. The procedure is otherwise identical.

The procedures for bad preparation and measurement exRecs are similar, just lacking the leading or trailing EC gadgets, respectively.

14.5 Probability of Having a Bad Rectangle

14.5.1 Basic Calculation of the Probability of Being Bad

Given a circuit broken up into good and bad extended rectangles, we now have an idea how to determine the behavior of each of those exRecs. The next step is to figure out the probability over fault paths of a particular set of good and bad extended rectangles. We'll start by calculating the probability of a single isolated exRec being bad. Actually, we'll just upper bound the probability of having a bad exRec — the adversarial stochastic noise model doesn't let us do more than that, since it only sets an upper bound on the probability of error on a set of locations.

The formula is not difficult. An exRec is bad if there are $t+1$ or more faults in it. Consider a particular set S of $t+1$ locations. The definition of adversarial stochastic noise tells us the probability of having faults on all the locations in S is at most $\prod_{L\in S} p_L$. Applying a union bound, we sum over all sets S of size $t+1$ to find:

$$\text{Prob(bad)} \leq \sum_{|S|=t+1} \prod_{L\in S} p_L. \tag{14.28}$$

Note that we don't need to sum over sets of $t+2$ or more locations — any such set certainly includes a set S of $t+1$ locations, and the bound on the probability of faults at S includes all fault paths that have faults at S, including those that also have other faults in the same exRec. Of course, using the union bound means we overcount, since a set of size $t+2$, for instance, includes $t+2$ different sets of size $t+1$, all of which are separately included in the sum. Compensating to subtract off the overcounting would be difficult, however, as the definition of adversarial stochastic noise doesn't give us a lower bound on the probability of the sets of size $t+2$.

In the special case where $p_L = p$ for all locations L, the formula simplifies even more. We simply get

$$\text{Prob(bad)} \leq \binom{A}{t+1} p^{t+1}, \tag{14.29}$$

where A is the total number of locations in the exRec.

It's also worth considering how to modify the formula if you are willing to count malignant sets rather than just considering bad exRecs. In that case, we should sum over sets S of locations, restricting attention

to malignant S. We need only consider *minimal* malignant sets, i.e., those malignant sets S such that no proper subset of S is malignant. Note that if S is malignant than any set containing S is also malignant, since the adversary can, if necessary, just choose to turn off faults outside S by choosing the identity "error" for those locations. Thus we necessarily have overcounting, as we did for bad exRecs, but once again we can safely set an upper bound by simply summing over minimal sets. We find

$$\text{Prob(malignant)} \leq \sum_{\text{minimal malignant } S} \prod_{L \in S} p_L, \tag{14.30}$$

or

$$\text{Prob(malignant)} \leq \sum_{r=t+1}^{A} M_r p^r \tag{14.31}$$

in the case where the error probabilities for all locations are the same. Here, M_r is the number of minimal malignant sets in the exRec containing exactly r locations.

Frequently it is inconvenient to count *all* malignant sets of arbitrary size, so we may want to cut off the sum at some value of r. To do this, we must make a conservative estimate of the number of minimal malignant sets of larger size. One straightforward way to do that would be to simply count all sets of size greater than the cutoff as malignant sets. For instance, we could count malignant sets of size $t+1$ and assume all sets of size $t+2$ are malignant. Then we would get

$$\text{Prob(malignant)} \leq M_{t+1} p^{t+1} + \binom{A}{t+2} p^{t+2}. \tag{14.32}$$

This a serious overcounting of the minimal malignant sets of size $t+2$; for instance, it includes many sets which have a subset of size $t+1$ which is malignant and therefore are already counted. However, threshold error rates tend to be low enough that the probability of a bad exRec is often dominated by the lowest-order one or two terms ($t+1$ and maybe $t+2$ errors), so overcounting the higher-order malignant sets does not matter very much.

14.5.2 Probability for Post-Selected Ancilla Preparation

One special case that is worth considering separately is what happens when we use ancilla preparation techniques that involve post-selection, as did many of the methods introduced in chapter 13. It's not enough to just count the number (and perhaps type) of locations in a single attempt to create the ancilla, since post-selection can distort probabilities. We need to be a bit more careful.

Let us assume throughout this section that the ancilla preparation gadget always succeeds when there are no faults in it. Note, however, that some magic state distillation protocols do not have this property.

Consider the bigger picture. When I say "prepare the ancilla via post-selection," what I really mean is that you should make many parallel attempts to create the ancilla. Some of them will succeed, hopefully (meaning the state passes the post-selection test, whether or not it is actually correct), and other attempts may fail. Impose some ordering of the ancilla creation attempts and use the first one that succeeds for the main exRec. If all the attempts fail, use one in the main exRec anyway — say, the ancilla produced by the last attempt. Naturally, if we have to resort to this option, the ancilla has a good chance of being wrong, but if we make enough attempts, the situation is unlikely to arise in the first place.

We can analyze this overall ancilla preparation protocol by including all the ancilla creation attempts inside the same exRec. To make sure that a good exRec is correct, we need to be sure that least one of the ancilla attempts succeeds when there are at most t errors in the exRec. $t+1$ attempts to create the ancilla are sufficient since then at least one try will have no faults.

The drawback of doing this when we count only the probability of an exRec being good or bad is that by repeating the ancilla preparation step many times, most likely making many more attempts than are needed, we greatly increase the number of locations in the exRec. Since the probability of a bad exRec goes as $\binom{A}{t+1} = \Theta(A^{t+1})$, this leads to an unpleasant explosion in our upper bound on the probability of an exRec being bad. We'd like to find a better bound.

One solution is to count all the malignant sets properly. Imagine a fault path in which the first ancilla preparation attempt has no faults, but there are $t+1$ or more errors scattered throughout the other preparation attempts. Such a path is certainly benign, since we use the ancilla created in the first attempt, making irrelevant what happens in the other attempts. Still, with so many locations altogether, an exact counting of the malignant sets might be difficult.

We can make a good approximation, however, by considering the structure of the overall ancilla preparation protocol. Each attempt at creating an ancilla is fault-tolerant. In particular, if there are t or fewer faults in the circuit for one attempt, then either the state produced by that try is rejected or it is correct (i.e., satisfies the PCP and PPP). Furthermore, all of the attempts to produce the ancilla use the same circuit, so the same patterns of faults cause the same problems in the different tries.

Imagine a simplified procedure where the ancilla created in attempt j is used in the main part of the exRec regardless of which attempts succeed or fail. We shall say that a fault path is *malignant for ancilla j* if there is a choice of errors by the adversary consistent with this fault path such that the simplified exRec using ancilla j is incorrect *and* ancilla j is accepted for that choice of errors. (Note that the ancilla might or might not be responsible for the exRec's failure to be correct.) Let P be the total probability of having a fault path which is malignant for ancilla 1; since all ancilla attempts are the same, P is also the probability of having a fault path which is malignant for ancilla j for any j.

In the real ancilla preparation protocol, only the first accepted ancilla is used. The adversary can choose the nature of the errors, but can only cause an attempt to fail if there is at least one error in the attempt. Therefore, in order for a fault path to be malignant for the exRec, it needs to be malignant for ancilla j (for some j) *and* there needs to be at least one fault in each attempt up to j. (It is possible, though, for a fault path to have this form and yet not be malignant, as there might be some locations in the ancilla preparation step that cannot lead to the ancilla being rejected.)

The probability of having at least one fault in a single attempt is at most $Q = \sum_L p_L$, where the sum is taken over the locations in a single try at creating an ancilla. The total probability of a malignant fault path is then at most

$$\text{Prob(malignant)} \leq P + QP + Q^2P + \ldots \leq \frac{P}{1-Q}. \tag{14.33}$$

(This is assuming $Q < 1$.) Therefore, we can bound the probability of incorrectness by calculating the probability of getting a malignant set using just a single attempt at creating the ancilla and then correcting by dividing by a bound $1 - Q$ on the probability of acceptance. In other words, we need to compute the conditional probability of being malignant, conditioned on accepting the ancilla.

In the special case where all locations have the same error rate p, $Q = Bp$ (with B the number of locations in a single ancilla creation attempt) and $P \leq \sum_{r=t+1}^{A} M_r p^r$, as above. If there are multiple ancillas created via post-selection in the same exRec, we need to divide by $1 - Q$ for each separate ancilla used. There could be multiple different values of Q involved if the ancillas used are different or are created in different ways.

14.5.3 Example: Probability of Incorrectness for the 7-Qubit Code

To see how these ideas work in practice, let's go through the calculation of the probability of incorrectness for single exRecs with the 7-qubit code.

There are 6 types of location and 6 types of exRec for the 7-qubit code: $|0\rangle$ preparation locations (physical error rate p_P), Z measurement locations (error rate p_M), wait locations (error rate p_S), single-qubit Clifford group gate locations (error rate p_G), CNOT locations (error rate p_{CNOT}), and $\pi/8$ gate locations (error rate p_{NC}). You could add additional types of locations, such as X measurement locations, or could split up single-qubit Clifford group gates into H locations, $R_{\pi/4}$ locations, and Pauli locations, but this set of 6 is universal and covers the essential variety of exRecs.

One component shared by all of these types of exRecs is the fault-tolerant error correction gadget. Indeed, most of the locations for most of these exRecs come from FT EC steps. Let us therefore start by counting the number and types of locations in an FT EC gadget. We'll use the circuit described in figure 12.9 except that we will do the phase error correction first so that the data block doesn't have to wait for the Hadamard gates. The $|\overline{0}\rangle$ ancillas used are created via the circuit of figure 14.8a and checked as in figure 13.3: we make

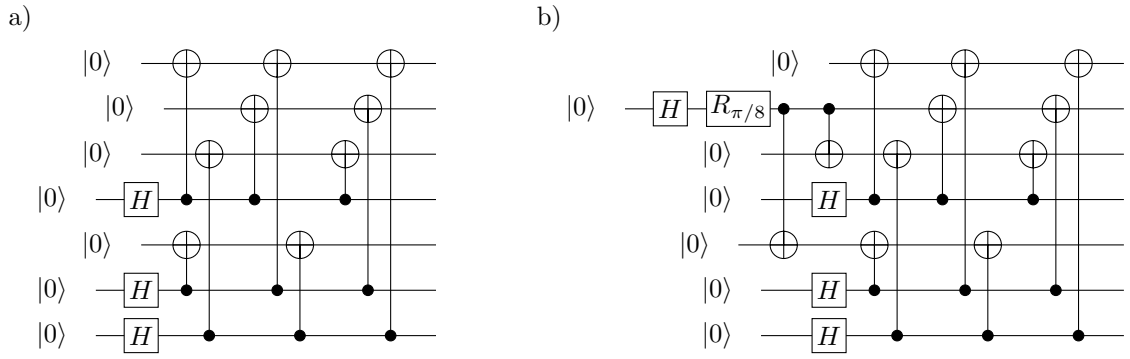

Figure 14.8: Non-fault-tolerant circuits for creating an a) $|\overline{0}\rangle$ state and b) $R_{\pi/8}|+\rangle$ state for the 7-qubit code designed to minimize waiting times.

two $|\overline{0}\rangle$ states and check them against each other, post-selecting on detecting no errors. The $|\overline{+}\rangle$ ancillas are created by making a $|\overline{0}\rangle$ and performing the transversal Hadamard gate.

In a single EC gadget, we can count a total of 4 non-FT $|\overline{0}\rangle$ encoding circuits, 2 transversal Hadamards (containing 14 single-qubit Clifford group gates in total), 3 transversal wait steps (consisting of 21 wait locations), 1 Pauli correction (7 locations, including zero to two single-qubit Pauli operations, the remainder being wait locations), 4 transversal measurements (28 measurement locations), and 4 transversal CNOTs (28 CNOT locations). There are two ancilla post-selections. Each non-FT $|\overline{0}\rangle$ encoding circuit consists of 9 CNOTs, 3 Hadamards, 2 waits, and 7 $|0\rangle$ preparation locations. The error rate for a gate location should be at least as bad as the error rate for a wait location, so we can take the worst-case number of Pauli operations as two. Therefore, the EC gadget consists of 182 locations, broken down as:

- 28 single-qubit Clifford group gates
- 34 wait locations
- 28 $|0\rangle$ preparations
- 28 measurements
- 64 CNOTs

The post-selected ancilla preparation consists of two non-FT $|0\rangle$ preparations plus a transversal CNOT (7 locations) and one transversal measurement (7 measurement locations and 7 wait locations). The total probability of having a fault in one ancilla preparation step is at most

$$Q = 6p_G + 11p_S + 14p_P + 7p_M + 25p_{\text{CNOT}}, \tag{14.34}$$

or $Q = 63p$ when all error rates are the same. We need to divide by $(1-Q)^2$ for each EC gadget in the exRec to correct for post-selection.

A single-qubit Clifford gate exRec just consists of two FT EC gadgets and a transversal Clifford gate, so there are a total of 371 locations:

- 63 single-qubit Clifford group gates
- 68 wait locations
- 56 $|0\rangle$ preparations
- 56 measurements

- 128 CNOTs

The probability of a single-qubit Clifford group gate exRec being bad is thus

$$\text{Prob(single-qubit Clifford gate exRec bad)} \leq \frac{68635p^2}{(1-63p)^4}, \tag{14.35}$$

or

$$\begin{aligned}\text{Prob(bad)} \leq & \frac{1}{(1-Q)^4}\left(1953p_G^2 + 4284p_Gp_S + 3528p_Gp_P + 3528p_Gp_M + 8064p_Gp_{\text{CNOT}} + 2278p_S^2 + \right. \\ & + 3808p_Sp_P + 3808p_Sp_M + 8704p_Sp_{\text{CNOT}} + 1540p_P^2 + 3136p_Pp_M + 7168p_Pp_{\text{CNOT}} + \\ & \left. + 1540p_M^2 + 7168p_Mp_{\text{CNOT}} + 8128p_{\text{CNOT}}^2\right).\end{aligned} \tag{14.36}$$

As you can see, keeping track of separate error rates for all these different types of locations becomes rather tedious. For the rest of this calculation, I'll therefore assume the simpler case where all error rates are equal to p.

The wait exRec is very similar. Instead of a transversal gate gadget, it uses a transversal wait gadget. Therefore, the total number of locations is the same, but there are 56 single-qubit Clifford group gates and 75 wait locations in the gadget instead. The total probability of a wait location being bad is also

$$\text{Prob(wait exRec bad)} \leq \frac{68635p^2}{(1-63p)^4}. \tag{14.37}$$

The measurement exRec is actually simpler. It consists of just one EC step followed by a transversal measurement. It therefore consists of just 189 locations, comprised of

- 28 single-qubit Clifford group gates
- 34 wait locations
- 28 $|0\rangle$ preparations
- 35 measurements
- 64 CNOTs

The probability of it being bad is

$$\text{Prob(measurement exRec bad)} \leq \frac{17766p^2}{(1-63p)^2}. \tag{14.38}$$

A preparation exRec also involves only one EC step. The preparation part itself can use the same procedure from figure 13.3 as used in the EC steps, including the same post-selection. The whole exRec thus consists of 245 locations:

- 34 single-qubit Clifford group gates
- 45 wait locations
- 42 $|0\rangle$ preparations
- 35 measurements
- 89 CNOTs

There is one additional post-selection, so we must divide by $(1-Q)^3$ rather than $(1-Q)^2$. The overall probability of being bad is

$$\text{Prob(preparation exRec bad)} \leq \frac{29890p^2}{(1-63p)^3}. \tag{14.39}$$

The CNOT exRec is bigger, but not significantly more complicated. There are 4 EC steps, two for each block, plus a transversal CNOT with 7 locations. The total number of locations is 735:

- 112 single-qubit Clifford group gates
- 136 wait locations
- 112 $|0\rangle$ preparations
- 112 measurements
- 263 CNOTs

The total probability of being bad is

$$\text{Prob(CNOT exRec bad)} \leq \frac{269745p^2}{(1-63p)^8} \tag{14.40}$$

The last kind of exRec is the most complicated: The $\pi/8$ gate exRec. First we have to make the magic state, test it, and then inject the $\pi/8$ gate into the computation. To test it, we will use the cat state measurement procedure described in section 13.4. Then we inject it with the circuit of figure 13.7.

The first thing to do is make a non-fault-tolerant $\overline{R_{\pi/8}|\mp\rangle}$ state, as in figure 14.8. This involves 11 CNOTs, 4 Hadamards, 1 $R_{\pi/8}$, 3 waits, and 7 $|0\rangle$ preparation locations. Next, we do the cat state measurement. The first step of cat state measurement is to perform a full EC step: The cat state measurement will check if the logical state is correct, but recall that it can give the wrong answer if there is an error on even a single physical qubit in the incoming state. In particular, we are concerned here that a single fault in the $\overline{R_{\pi/8}|\mp\rangle}$ encoding circuit will produce both the wrong logical state and a single-qubit error that causes the cat state measurement to give the wrong answer, incorrectly allowing the state to pass.

The next step is to create and verify a cat state and use it to measure the eigenvalue of $U = R_{\pi/8}XR_{\pi/8}^\dagger$ on the logical state. We can do this via physical controlled-U gates from the cat state qubits to the ancilla block physical qubits. These are gates which are not in our gate set, so we break them down into $R_{\pi/8}^\dagger = R_{\pi/8}R_{-\pi/4}$, followed by CNOT, followed by $R_{\pi/8}$. The cat state can be checked using a single extra ancilla qubit to make sure that a single fault doesn't produce two bit flip errors in it. The full cat state creation and $\overline{U}$ measurement is shown in figure 14.9. Overall, the cat state measurement has 15 CNOT gates, 15 single-qubit Clifford group gates (8 Hadamards and 7 $R_{-\pi/4}$ gates), 14 $R_{\pi/8}$ gates, 12 wait steps, 8 $|0\rangle$ state preparations, and 8 measurements.

Altogether, the $\overline{R_{\pi/8}|\mp\rangle}$ preparation and checking (including the EC step) involves a total of

- 47 single-qubit Clifford group gates
- 15 $R_{\pi/8}$ gates
- 49 wait locations
- 43 $|0\rangle$ preparations
- 36 measurements
- 90 CNOT gates

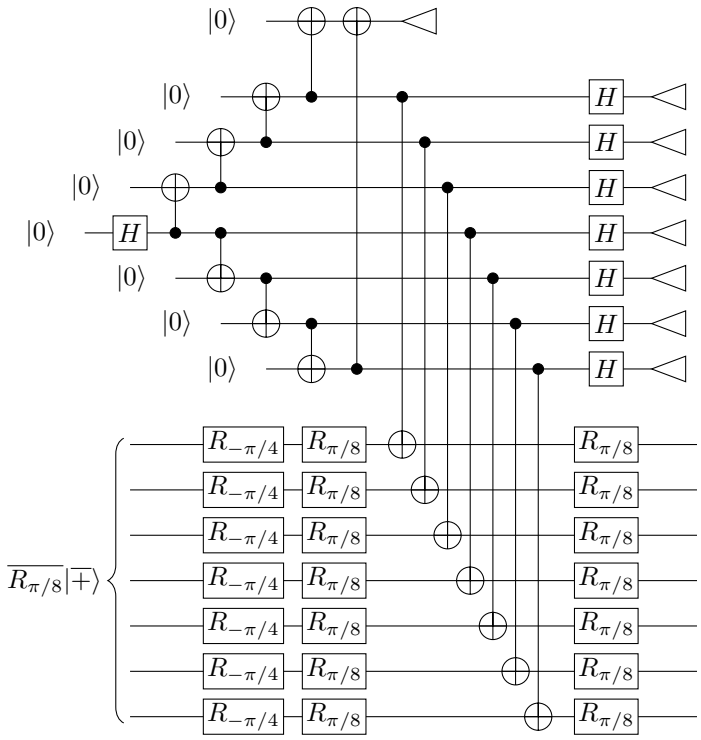

Figure 14.9: Testing a $\overline{R_{\pi/8}}|\overline{+}\rangle$ state via cat state measurement. An EC step (not shown) precedes this circuit.

This is a total of 282 locations. We will post-select on the cat state passing verification and the $\overline{R_{\pi/8}}|\overline{+}\rangle$ passing the cat state measurement, as well as the ancillas in the included EC step. The magic state injection contains a transversal CNOT, a transversal measurement, a wait step for one block, and potentially a transversal U (which is a Clifford group gate). Each of these involves 7 locations, and the whole $\pi/8$ exRec has an additional 2 EC steps.

The $\pi/8$ gate exRec therefore has a total of

- 110 single-qubit Clifford group gates
- 15 $R_{\pi/8}$ gates
- 124 wait locations
- 99 $|0\rangle$ preparations
- 99 measurements
- 225 CNOT gates

This is a total of 672 locations, and we are post-selecting on the $\overline{R_{\pi/8}}|\overline{+}\rangle$ preparation as well as the preparation of the ancillas in the two main EC steps. Thus, the probability that a $\pi/8$ exRec is bad is

$$\text{Prob}(\pi/8 \text{ exRec bad}) \leq \frac{225456p^2}{(1-63p)^4(1-282p)}. \tag{14.41}$$

14.6 Level Reduction

The next step is to put all of this together. We've talked about what to do with a single exRec, whether it is good or bad. We now need to figure out what to do when we have a full circuit.

14.6.1 Truncation

Given a particular fault-path for a fault-tolerant simulation of circuit C, we can look at each exRec to decide whether it is good or bad. At first sight, this seems straightforward, but on closer examination, there is a complication. The naïve approach would be to look at each exRec in isolation and determine whether it is good or bad based on that. However, before deciding if an exRec is good or bad, we should first figure out whether it is truncated or not, and that depends on the other exRecs around it. Remember, we want to avoid a situation where a small number of failures in a single EC step can make both of the exRecs sharing that EC step fail. We'd like to assign the EC step to just one of these two exRecs — we'll choose the later one — so that the other exRec has a chance to be good. Or at least, if it's bad, it's bad for completely different reasons that have nothing to do with the shared FTEC gadget.

If the exRecs immediately after the exRec under consideration are good, correctness will let us move ideal decoders (or $*$-decoders) from the end of the subsequent exRecs to just after the trailing FTEC gadgets for the current exRec. Therefore, we can leave the exRec untruncated. However, if one of the exRecs following the current exRec is bad, we want to truncate the EC step shared with the bad exRec.

Therefore, we can use the following procedure to determine truncation and decide which exRecs are good and bad:

Procedure 14.1.

1. Initialize $s = T$, where T is the number of layers (time steps) in the circuit C we are simulating.
2. Given a fault-tolerant simulation $FT(C)$ of C and a fault-path Φ for $FT(C)$, look at the exRecs simulating locations in time step s of C. Determine if each such exRec is good or bad by counting the number of faults in it. (Alternatively: determine whether the fault path in it is benign or malignant.)

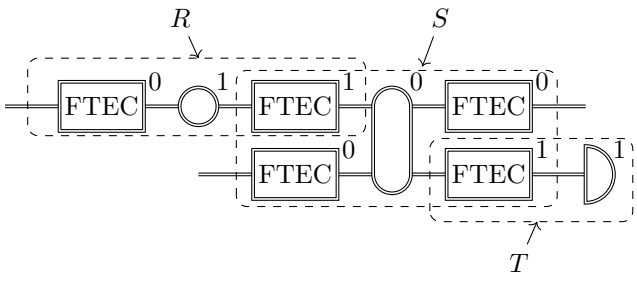

Figure 14.10: Three exRecs for a code where $t = 1$. Each of the three exRecs has 2 faults, but only two are bad due to the truncation rules: T is bad, so S is truncated, which means S is good. That means R is untruncated, so R is bad.

3. $s \mapsto s - 1$. If $t = 0$, end.

4. For each exRec simulating a location in time step s of C, look at the exRec or exRecs immediately after it in the circuit (namely, those at time $s + 1$ and sharing a FTEC gadget with it). If one or more of these exRecs is bad (has a malignant fault path), truncate the current time s exRec by removing the trailing FTEC gadget or gadgets shared with the bad (malignant) exRecs.

5. Return to step 2, evaluating truncated exRecs according to the usual definitions.

In other words, we start at the end and work our way backward, determining truncation and badness together. As an example, consider figure 14.10 for an FT protocol involving a code correcting 1 error. Because T is the last exRec, it is bad. However, that means that exRec S is truncated. Now it only has 1 fault in it, so it is *not* bad, even though S untruncated would be bad. But since S is good, that means that R is not truncated and is therefore bad.

14.6.2 Level Reduction Theorem

Combining the results of sections 14.3 and 14.4.3 with procedure 14.1, we now know what to do with a fault-tolerant circuit experiencing a particular fault path:

Lemma 14.5. *Let C be a circuit starting with state preparation locations and ending with measurements, and let $FT(C)$ be a fault-tolerant simulation of C. Suppose $FT(C)$ experiences a fault path Φ with particular errors assigned at fault locations. Use procedure 14.1 to truncate the extended rectangles and determine whether each is good or bad. Then the output of $FT(C)$ has the same distribution as the output of C, where each location L of C which corresponds to a bad exRec of $FT(C)$ is replaced by a noisy location, as described in section 14.4.3.*

Proof. The proof follows that of theorem 14.2. The differences are that we use $*$-decoders everywhere, that some exRecs are truncated, and that some exRecs are bad. Only the last issue causes a meaningful change in the proof, and it is only a small change.

As before, we begin by replacing good measurement exRecs according to the rule for correctness with $*$-decoders. A bad measurement exRec is replaced with a $*$-decoder followed by a noisy measurement on the decoded state, as per section 14.4.3. Then we work our backwards through the circuit, replacing good exRecs using the rules for correctness and bad exRecs as in section 14.4.3. Every time we replace a bad exRec, the preceding exRec(s) are truncated. The resulting truncation is consistent with procedure 14.1. Once we have replaced all the gate and wait exRecs, the only remaining exRecs are preparation exRecs, each of which is followed by a $*$-decoder. Using correctness for preparation exRecs, we replace the good preparation exRecs by unencoded ideal preparation locations. The bad preparation exRecs are replaced by

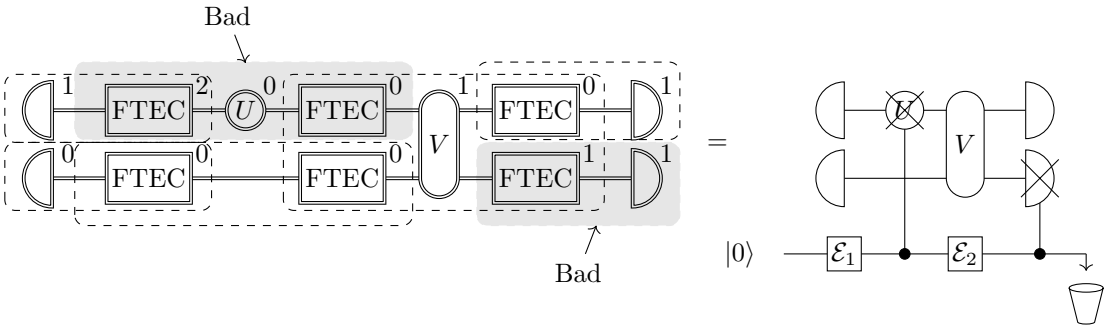

Figure 14.11: An example of translating a fault path on a noisy fault-tolerant simulation into a noisy circuit. In this example, $t = 1$. Because of truncation, only two exRecs (shaded) are bad. They are replaced by noisy locations. The other exRecs are replaced by ideal locations.

noisy preparation locations. Either way, the $*$-decoders are eliminated, leaving us with the circuit C, but with locations corresponding to bad exRecs replaced with noisy locations. □

This lemma tells us what to do for a fixed fault path. An example of the procedure is given in figure 14.11. To understand the behavior given a distribution over fault paths, we simply need to consider the probability of having different kinds of fault paths.

Up until now, the analysis has not depended at all on the precise code used in the FT protocol. However, when we move a $*$-decoder through a bad exRec, if the QECC encodes multiple qubits per block, the noisy location that results affects all of the qubits encoded in the block. If those qubits were part of separate locations in the original unencoded circuit, then those locations have potentially correlated errors in them. There are a few possible ways to handle this, but the most straightforward is to simply rule it out as an issue for now by restricting attention to QECCs with only one logical qubit per block.

Theorem 14.6 (Level Reduction)**.** *Let C be a circuit starting with state preparation locations and ending with measurements, and let $FT(C)$ be a fault-tolerant simulation of C using a QECC that encodes one qubit per block. Suppose $FT(C)$ is subjected to an adversarial stochastic error model with error probabilities p_M for locations $M \in FT(C)$. Then the noisy realization $\widetilde{FT(C)}$ of $FT(C)$ is equivalent to a noisy realization $\widetilde{C}$ of C undergoing an adversarial stochastic error model, with error probabilities p'_L for $L \in C$ bounded by*

$$p'_L \leq \sum_{\text{minimal malignant } S} \prod_{M \in S} p_M, \tag{14.42}$$

where the sum is taken over minimal malignant sets S for the exRec corresponding to L.

Proof. Consider a set of T of locations of the circuit C. We need to bound the probability of having a fault path for $FT(C)$ which is malignant for all of the exRecs corresponding to locations of T. For our purposes, we can equally well consider T to be a set of exRecs in $FT(C)$.

Let Φ be a fault path which is malignant for all exRecs in T. Then any exRec immediately before an exRec in T is truncated for Φ, in accordance with procedure 14.1. There may be additional exRecs truncated for Φ as well since Φ might be malignant for additional exRecs. I will refer to the locations before the ones in T as "known to be truncated."

In order for Φ to qualify as malignant for all exRecs in T, the locations $\Phi \cap R_L$ must form a malignant set for each $L \in T$, where R_L is the set of locations for the exRec corresponding to L. If L is known to be truncated, then R_L contains the locations in the appropriately truncated version of the exRec; otherwise, R_L contains all locations in the exRec.

For each $L \in T$, fix a fault path Ω_L which is contained in R_L and is malignant for the exRec corresponding to L. Let

$$\Phi = \bigcup_{L \in T} \Omega_L. \tag{14.43}$$

Note that because of the truncation rules, $\Omega_L \cap \Omega_{L'} = \emptyset$ if $L \neq L'$. Since the noise model for $\widetilde{FT(C)}$ is an adversarial stochastic one, the total probability of having a fault path Φ' such that $\Phi \subseteq \Phi'$ is at most

$$P_\Phi = \sum_{\Phi' \supseteq \Phi} p_{\Phi'} \leq \prod_{L \in T} \prod_{M \in \Omega_L} p_M. \tag{14.44}$$

Note that for some of the fault paths Φ' that appear in the sum, the exRec corresponding to $L \in T$ might not actually be malignant. This can occur if the fault path is malignant for an exRec for a location L' immediately after L and $L' \notin T$. Then the exRec for L is actually truncated for Φ' even though it is not truncated for Φ, which means that the fault path restricted to the correctly truncated exRec for Φ' might be smaller and potentially benign. That's OK, though. That just means that we will overestimate the probability of error by including some fault paths that don't cause a problem.

Now let us upper bound the total probability that every exRec in T is malignant. Any such fault path Φ' must contain a fault path constructed as in equation (14.43). The sum over $p_{\Phi'}$ can therefore be bounded above by a sum $\sum P_\Phi$, with Φ as in equation (14.43). We can sum over Φ by summing over all possible malignant fault paths Ω_L for all $L \in T$, but actually it is sufficient to just sum over minimal malignant Ω_L, since taking $\Omega_L \subseteq \Omega'_L$ implies that the resulting $\Phi \subseteq \Phi'$, and therefore Φ' is already included in the sum for P_Φ. Then

$$\sum_{\Phi'} p_{\Phi'} \leq \sum_{\Phi} P_\Phi \leq \sum_{\{\text{minimal malignant } \Omega_L, L \in T\}} \prod_{L \in T} \prod_{M \in \Omega_L} p_M \tag{14.45}$$

$$= \prod_{L \in T} \sum_{\text{minimal malignant } \Omega_L} \prod_{M \in \Omega_L} p_M \tag{14.46}$$

$$= \prod_{L \in T} p'_L, \tag{14.47}$$

where

$$p'_L = \sum_{\text{minimal malignant } \Omega_L} \prod_{M \in \Omega_L} p_M. \tag{14.48}$$

This differs from the desired result in just one respect, although the notation does not make the difference completely evident. The desired result sums over fault paths which are malignant for the untruncated exRec corresponding to L, whereas equation (14.48) sums over a truncated exRec if L is known to be truncated. This is not a problem, however, since any set which is malignant for the truncated exRec is also malignant for the untruncated exRec, so equation (14.48) is a tighter bound than is needed for equation (14.42). □

The level reduction theorem tells us that a noisy fault-tolerant circuit is equivalent to a noisy unencoded circuit with a new, hopefully reduced error rate. We still have adversarial stochastic noise, and the simulated circuit has an error rate p'_L for location L.

By approximating and assuming that the error rates p for all locations are the same, and that any set of size $t+1$ or greater is malignant (meaning we count simply bad exRecs rather than malignant sets), and assuming for simplicity that there is no post-selection, we find

$$p'_L \leq \binom{A_L}{t+1} p^{t+1}, \tag{14.49}$$

as in section 14.5, where A_L is the number of locations in the exRec for L. We see that if

$$\binom{A}{t+1} p^{t+1} \leq p, \tag{14.50}$$

where A is the size of the largest exRec, then the error rate per location has decreased in the simulated noisy circuit compared to the error rate per location in the original error model.

14.6.3 Why We Consider Adversarial Errors

At this point, it is worth pausing briefly to understand why we needed to consider adversarial errors. Certainly, the level reduction theorem would have worked just as well if $\widetilde{FT(C)}$ underwent independent stochastic noise rather than adversarial stochastic noise, since independent stochastic noise is a special case of adversarial stochastic noise. However, that would not change the conclusion: the noise model for the noisy simulated circuit $\widetilde{C}$ would still have been an adversarial stochastic one.

There are two reasons for this. The first is because the presence of errors in adjacent exRecs is not independent. If the second exRec is bad, then the first exRec must get truncated, which *reduces* the probability of the first exRec also being bad, since a truncated exRec is smaller and has fewer locations. That is, error probability is *anti-correlated* between adjacent exRecs. This is a failure of independent stochastic noise, though perhaps not one that bothers you very much. A second failure might be more worrying: the *type* of errors that occur on adjacent bad exRecs can be correlated as well. This is because the type of error given by the procedure in section 14.4.3 is conditioned on the error syndrome register, which persists between adjacent bad exRecs. Therefore errors on them can be entangled or otherwise potentially problematic, and certainly are not independent. This means that, like it or not, once we deal with fault-tolerant simulations, independent stochastic errors are not sufficient.

14.7 Concatenation and the Threshold Theorem

We've seen that it is possible to improve the effective error rate by using a fault-tolerant simulation of a circuit. For instance, by using a code to correct 1 error, we can change the logical error rate from p per location to $O(p^2)$ per location. If we're doing a long calculation, however, that might not be good enough. After about $1/p^2$ steps, it's likely that the logical circuit will suffer a fault, which means that any computation longer than that is likely to get the wrong answer.

We'll need to do better than a distance 3. How much better can the logical error rate get? Using the simplified formula,

$$p'_L \leq \binom{A_L}{t+1} p^{t+1}, \tag{14.51}$$

we see that we can get high powers of p, and therefore great reductions in the error rate, by working with codes which correct many errors. However, bigger codes also mean bigger exRecs, so A increases as well. Counting malignant sets of locations improves the bound on the logical error rate, but doesn't change the basic conclusion: To reliably simulate larger and larger circuits, we'll need a family of codes that correct more and more errors, but we can't just pick any family. We must find a family of codes where the number of malignant sets does not increase too rapidly with the size of the codes.

14.7.1 Concatenation of Simulation Circuits

A natural family of codes to use is concatenated codes. If we can encode an arbitrary circuit C in a fault-tolerant simulation $FT(C)$ and reduce the logical error rate, then surely we can perform a simulation of the simulation, $FT(FT(C))$, and make the logical error rate even smaller. And if that's not good enough, we can keep on adding levels of simulation as long as necessary to make the error rate as small as we like.

That intuition is completely correct. I've now introduced all the formalism necessary to make the previous paragraph rigorous and quickly prove the resulting threshold theorem.

The resulting protocol is a fault-tolerant protocol for a concatenated code, as discussed in section 9.1. The protocol itself has a self-similar structure much like the code being used and is illustrated in figure 14.12. For instance, to perform a logical gate gadget on a level k qubit, we need to perform a series of gate gadgets on level $k-1$ qubits, interspersed with fault-tolerant error correction steps on level $k-1$ qubits. Each of the gate gadgets and EC steps for level $k-1$ qubits is in turn made up of a number of gadgets for level $k-2$ qubits, and so on.

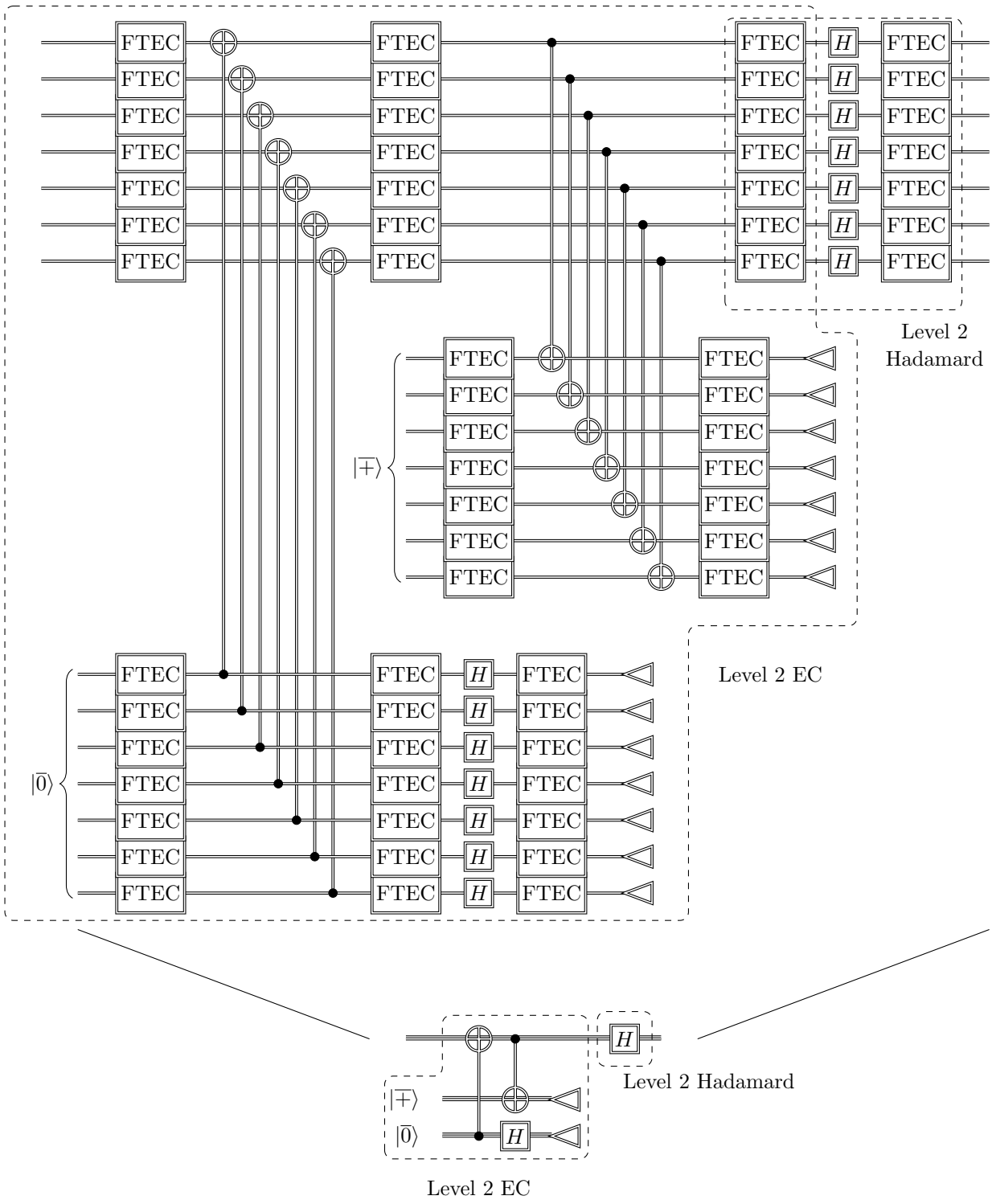

Figure 14.12: A portion of a 2-level concatenated fault-tolerant protocol for the concatenated 7-qubit code. Each level 1 qubit in the top part of the figure consists of 7 level 0 (physical) qubits, each level 1 transversal gadget consists of 7 level 0 locations, and each level 1 FT EC gadget consists of another Steane EC step made up of level 0 locations.

Definition 14.9. Let $C_0 \equiv C$ be a circuit, and let $C_k = FT(C_{k-1})$. Consider C_l, the *level l fault-tolerant simulation of C*. The physical locations of C_l are the *level 0 locations* of the circuit. The gadgets simulating the physical locations of the circuit C_k in the recursive definition of C_l are the *level $l-k$ locations* and the *level $l-k$ fault-tolerant error correction gadgets* for C_l.

The logic behind these definitions is that the gadgets for C_k, when realized in C_l, are simulated via $l-k$ levels of encoding, and perform operations which act on level $l-k$ qubits.

14.7.2 The Threshold Theorem

Now let us prove theorem 10.4. Let me remind you of the precise statement:

Theorem 10.4 (Threshold Theorem for Basic Model of Fault Tolerance)**.** *Suppose a system satisfies a basic model for fault tolerance, with $p_P = p_G = p_S = p_M = p$. Then there exists a family of fault-tolerant protocols $\mathcal{F}_l$ and a threshold error rate p_T such that, if $p < p_T$, then for any ideal quantum circuit C which starts with preparation locations and ends with measurement locations, and any $\epsilon > 0$, there exists an l such that the output distribution of $FT_l(C)$, the fault-tolerant simulation of C by $\mathcal{F}_l$, has statistical distance at most ϵ from the output of C. When C has T locations, then $FT_l(C)$ has $O(T \operatorname{polylog}(T/\epsilon))$ locations (i.e., the circuit size overhead is $O(\operatorname{polylog}(T/\epsilon))$.*

Based on the previous discussion, we can immediately identify $FT_l(C)$ as C_l. Recall that back in chapter 10, we were using a basic model of fault tolerance, which assumes independent stochastic noise. Our proof will work just as well for adversarial stochastic noise.

Proof. Let us determine the logical error rate for C_l, the level l fault-tolerant simulation of C. Let us assume for simplicity that no post-selection is needed in the fault-tolerant simulation, and that the code used at each level encodes only one qubit per block and has distance 3. Fault-tolerant protocols exist with these properties, so this assumption is sufficient to prove the theorem. For instance, we may use the 7-qubit code.

Since $C_l = FT(C_{l-1})$, by theorem 14.6, if C_l undergoes adversarial stochastic noise with error rate $p_0 = p$ per physical location, $\widetilde{C_l}$ is equivalent to $\widetilde{C_{l-1}}$ undergoing adversarial stochastic noise with an error rate p_1 per location, with

$$p_1 \leq \binom{A}{2} p_0^2, \tag{14.52}$$

where A is the number of locations in the largest exRec in the fault-tolerant protocol. But, again applying theorem 14.6, $\widetilde{C_{l-1}}$ undergoing adversarial stochastic noise with error rate p_1 per location is equivalent to $\widetilde{C_{l-2}}$ with adversarial stochastic noise and an error rate

$$p_2 \leq \binom{A}{2} p_1^2. \tag{14.53}$$

Let $p_j = p_T(p_{j-1}/p_T)^2$, with

$$p_T = 1/\binom{A}{2}. \tag{14.54}$$

By induction, we see that $\widetilde{C_l}$ with adversarial stochastic noise and error rate p_0 is equivalent to $\widetilde{C_{l-j}}$ with adversarial stochastic noise and error rate p_j. In particular, $\widetilde{C_l}$ is equivalent to $\widetilde{C_0} = \widetilde{C}$ with error rate p_l.

Notice that

$$\frac{p_l}{p_T} = \left(\frac{p_{l-1}}{p_T}\right)^2 = \left(\frac{p_{l-2}}{p_T}\right)^4 = \left(\frac{p_{l-3}}{p_T}\right)^8 = \dots \tag{14.55}$$

$$= \left(\frac{p_{l-j}}{p_T}\right)^{2^j} \tag{14.56}$$

$$= \left(\frac{p_0}{p_T}\right)^{2^l}. \tag{14.57}$$

The logical error rate decreases as the *double exponential* of the number of levels if $p_0 < p_T$.

Our goal for the fault-tolerant computation is for the outcome distribution to have statistical distance at most ϵ from the correct distribution for a circuit with T locations. Let us therefore choose l sufficiently large so that $p_l \leq \epsilon/T$. That is, we should choose

$$l = \left\lceil \log\left(\frac{\log(Tp_T/\epsilon)}{\log(p_T/p)}\right)\right\rceil. \tag{14.58}$$

Given this, the total probability of having a faulty level l location in the circuit is $P \leq Tp_l \leq \epsilon$. If the correct outcome distribution is D, the true distribution of outcomes is thus $(1-P)D + PD'$ for some D'. The statistical distance between this and D is

$$\frac{1}{2}\sum_x |D_x - [(1-P)D_x + PD'_x]| = \frac{1}{2}\sum_x P|D_x - D'_x| \leq P \leq \epsilon, \tag{14.59}$$

as desired.

Now let us bound the circuit size overhead needed for this simulation. $C_k = FT(C_{k-1})$, so each location in C_{k-1} is replaced by a fault-tolerant gadget, and between each pair of gadgets is an FT EC step. If we choose B to be the total number of locations in the largest rectangle (not exRec), then we can safely bound the number of locations in C_k by B times the number of locations in C_{k-1}. (Note that $B \leq A$, since every rectangle is contained in an exRec.) Therefore, the size of C_l is at most $B^l T$, where T is the number of locations in C_0.

This is an exponential cost with the number of levels of concatenation. That sounds bad, but remember, the error decreases doubly-exponentially with the number of levels. Compared to a double exponential, a single exponential is nothing. In particular, we find that the total number of locations in C_l is at most

$$TB^l \leq BTB^{\log[\log(Tp_T/\epsilon)/\log(p_T/p)]} = O\left(T\left[\frac{\log(Tp_T/\epsilon)}{\log(p_T/p)}\right]^{\log B}\right). \tag{14.60}$$

p_T and B are constants depending on the fault-tolerant protocol. If we consider p to be a constant as well, we recover the desired form for the overhead $O(\text{polylog}(T/\epsilon))$.

If desired, you can separately count the space overhead needed by letting B' be the number of qubits needed for a single gate gadget plus EC step. The formula is otherwise the same. □

When $p > p_T$, the proof above suggests that the logical error rate actually *increases* as a double exponential as we add levels of concatenation. This happens because when the error rate is too high, the extra locations introduced by the fault-tolerant simulation offer too many new opportunities for errors, and errors occur in the fault-tolerant circuit faster than they can be corrected by the EC steps. Adding more levels of concatenation rapidly makes the problem worse.

We can think of error rate in a concatenated fault-tolerant protocol as a flow diagram, with a vector at a point p pointing towards the error rate for an FT circuit with physical error rate p. The threshold is an unstable fixed point for this flow diagram. Points below the threshold will flow towards the stable fixed point at $p = 0$, while points above the threshold flow towards the stable fixed point at $p = 1$. Essentially, the threshold marks a *phase transition* between a phase where long quantum computations are possible and a computationally weaker phase where quantum information can last only a short time before being destroyed by noise. The threshold is not a phase transition in precisely a conventional condensed matter sense, since this is a dynamical system with active error correction occurring frequently, but it does have many of the qualitative behaviors normally seen in a phase transition.

The proof of theorem 10.4 suggests that the threshold value is $p_T = 1/\binom{A}{2}$, but of course, that was based on the crudest method of bounding the error rate from section 14.5. We can potentially do much better by doing a careful counting of malignant sets:

Theorem 14.7. *In theorem 10.4, let the family of protocols $\mathcal{F}_l$ be l levels of concatenation of the fault-tolerant protocol $\mathcal{F}$. Then the threshold value p_T can be taken to be the supremum over $p < 1$ such that*

$$p > \sum_{r=t+1}^{A} M_r p^r \tag{14.61}$$

for all exRecs, where A is the number of locations in an exRec and M_r is the number of minimal malignant sets of r locations contained in the exRec. The values A and M_r should be taken for the type of exRec that gives the smallest solution p_T.

The proof just duplicates the proof above for theorem 10.4, but uses the formula for the probability of an incorrect exRec in terms of malignant sets instead of counting all sets of t locations. Solutions to equation (14.61) are fixed points in the flow diagram for a particular type of exRec, and the smallest positive solution is an unstable fixed point, as discussed above. We take the type of exRec that gives the smallest solution because then for all other exRecs, the error rate is definitely below the unstable fixed point, so the errors will flow towards 0. We know there always is at least one unstable fixed point between 0 and 1 provided we use a QECC that corrects at least one error, because if we count all sets of size $t + 1$ as malignant, as in the simplified formula, we are overestimating the error rate, and yet there always is a fixed point solution for the simplified formula.

14.7.3 The Significance of the Threshold Theorem

I am tempted to say that it is impossible to overstate the importance of the threshold theorem, but that would be overstating the importance of the theorem. Let me instead just say that it would be *difficult* to overstate its importance.

The threshold theorem says that, if the error rate per location is sufficiently low, then arbitrarily long quantum computation is possible. It is an important theoretical result, saying that there is no barrier, in principle, to building arbitrarily long quantum computations. It is also an important practical result for experimentalists, since it sets them a definite goal: If an experimentalist can satisfy all the assumptions of the basic model of fault tolerance and have error rates per location less than the threshold value, and can build many qubits with that same error rate, then the system can be used as a reliable quantum computer. As we'll see in chapter 15, the assumptions built into the basic model can be relaxed substantially without eliminating the threshold, although in some cases there is a cost in the form of reducing the numerical value of the threshold. Consequently, it seems extremely likely that the threshold theorem applies to real world quantum computers as well as to the simplified theoretical constructs we've been discussing so far.

Without the threshold theorem, it would probably be impossible to build a large quantum computer. A weaker version of fault tolerance might suffice, but building a larger computer would require both more qubits and also more accurate gates. Most systems seem to have a fundamental limit on how accurate they can be, since there are noise sources that cannot be completely eliminated, so very likely in the absence of a threshold theorem, there would be an upper limit to the length of any quantum computation.

The existence of quantum computation presents a profound challenge to the strong Church-Turing thesis, one of the pillars of theoretical computer science. The strong Church-Turing thesis says that all physically reasonable models of computation are equivalent, up to polynomial slowdowns or speedups. Quantum computers appear to violate that, but without a threshold theorem, quantum computation would not be physically plausible. The threshold theorem forces us to confront the apparent computational speed-ups provided by quantum mechanics as a real thing, and not just some peculiar hypothetical model.

Similarly, the threshold theorem, and more generally quantum error correction, offers a challenge to previous physical intuition. We are used to quantum mechanics being confined to very small objects and short times. Larger objects decohere rapidly and become classical. A fault-tolerant quantum computer, in contrast, can maintain arbitrarily large and complicated quantum states for arbitrarily long times. A quantum computer functioning below the threshold is somehow in a fundamentally different phase of matter than normal materials, a phase with macroscopic quantum phenomena. Superconductivity, superfluidity, and

the like are frequently referred to as macroscopic quantum states, but a fault-tolerant quantum computer is even more quantum.

When first presented with the idea of a large quantum computer, many physicists and computer scientists have the reaction "there must be something wrong with that." Most often the first candidate for "something wrong" is that errors in the implementation will get in the way. The threshold theorem answers that objection. When confronted with it, some quantum computation skeptics reluctantly accept that quantum computers are a theoretically viable possibility. Others turn to the hope that quantum mechanics will somehow turn out to be wrong in a way that causes quantum computation to fail, or to attempts to find holes in the theory of fault tolerance. In any case, it is not possible to sensibly discuss the viability of quantum computation without understanding the threshold theorem.

14.7.4 The Numerical Value of the Threshold

Turning to a more practical question, let us consider the numerical value of the threshold. It is a useful thing to know, to give experimentalists something to shoot for, and to evaluate how difficult it will be to get there. The same techniques that proved the existence of the threshold can give us useful insight into its value.

Before discussing the numerical value of the threshold, let me be more precise about what I mean when I say "threshold."

Definition 14.10. Suppose you have a family $\mathcal{F}_l$ of fault-tolerant protocols, such that, if $p < p_T$, arbitrarily long quantum computations are possible using an appropriate member of $\mathcal{F}_l$ with only polylogarithmic overhead, as in theorem 10.4. The largest value of p_T for which this statement is true is the *threshold for* $\mathcal{F}_l$. Given a QECC Q, consider all possible fault-tolerant protocols $\mathcal{F}$ using Q, and the families $\mathcal{F}_l$ formed by concatenating $\mathcal{F}$ l times. The best achievable threshold for such a family $\mathcal{F}_l$ is also known as the *threshold for* Q. The *threshold for fault-tolerant quantum computation*, or just the *threshold* for short, is the supremum over all codes Q of the threshold for Q.

Thus, the threshold for fault-tolerant quantum computation is independent of a specific choice of code or fault-tolerant protocol. By considering specific protocols or specific codes and finding a value p_T such that the threshold condition holds, all we can ever achieve is to find a *lower bound* on the threshold. No matter how clever you are in coming up with a code or fault-tolerant protocol, it may be that there is a better code or protocol out there yet to be discovered. By the same token, when we perform a calculation for a specific code with a specific fault-tolerant protocol, that only sets a lower bound on the threshold for that code. It may be that a more clever protocol will achieve a higher threshold. Furthermore, the techniques discussed in this chapter for proving the existence of thresholds also only give you lower bounds. It may be that you can improve (i.e. raise) the lower bound using a more careful analysis of the same family of protocols, for instance by counting malignant sets instead of just all sets of $t + 1$ locations in an exRec.

It is also possible to set upper bounds on the threshold, but probably the existing upper bounds are not very tight. I'll discuss upper bounds on the threshold in section 16.4.

Strictly speaking, the threshold also depends on the nature of the error model and allowed circuit properties. By default, when I speak of a threshold without any additional qualification, I will usually mean the threshold for a basic model of fault tolerance, using the worst possible error model consistent with a single error rate $p = p_P = p_G = p_S = p_M$. We usually set lower bounds on this by using the adversarial stochastic noise model. When I want to talk about the threshold for another error model or using other assumptions about the circuits allowed for the protocol, I will qualify the statement and talk about, for instance, the threshold for depolarizing noise, or the threshold in two dimensions. In the midst of an extended discussion of a threshold with some such qualification, I may talk about just the "threshold," but hopefully it will be clear from context that I haven't changed topics to discuss the threshold for a basic model of fault tolerance instead.

Based on the calculations in section 14.5, we can immediately calculate a lower bound on the threshold

Levels	Max. Length	Overhead (Loc.)
0	3.7×10^3	1
1	3.7×10^4	492
2	3.7×10^6	242,064
3	3.7×10^{10}	1.2×10^8
4	3.7×10^{18}	5.9×10^{10}
5	3.7×10^{34}	2.9×10^{13}

Table 14.1: The circuit size overhead and maximum length of a computation given a certain number of levels of concatenation of the 7-qubit code. These calculations use $p_T = 2.7 \times 10^{-5}$, $p/p_T = 0.1$, $\epsilon = 0.01$.

for the 7-qubit code. The CNOT exRec is the biggest exRec for the protocol we were using, and we saw that

$$\text{Prob(CNOT exRec bad)} \leq \frac{269745p^2}{(1-63p)^8}. \tag{14.62}$$

(The $\pi/8$ exRec has a different, possibly worse, post-selection formula for the denominator, but a lower constant in the numerator, so comes out to be a less stringent bound.) We want to know the value of p such that the RHS is equal to p. Since $Cp^2/(1-63p)^8 \geq Cp^2$, we know the fixed point occurs for $p < 1/C < 10^{-5}$. Therefore,we can bound the fixed point:

$$p = \frac{269745p^2}{(1-63p)^8} < 272000p^2, \tag{14.63}$$

so $p_T > 3.6 \times 10^{-6}$. Of course, this is just a very rough bound. By doing some small additional optimizations on the circuits and more importantly by counting malignant sets carefully, we find the threshold for the 7-qubit code is at least $p_T \geq 2.7 \times 10^{-5}$, almost an order of magnitude better.

However, the 7-qubit code doesn't have the best threshold. The best known lower bound on the threshold as of this writing comes from a family of protocols due to Knill which uses concatenated error-detecting codes to do extensive verification of ancillas before they are used in the main part of the computation. I will discuss this protocol a bit more in section 16.1. The proven threshold for Knill's scheme is above 10^{-3}, one error per one thousand locations, but simulations suggest the actual threshold for Knill's scheme is much higher: in a basic model of fault tolerance with depolarizing noise and CNOT gate error rate p_{CNOT} slightly higher than the error rates p_G, p_P, p_M for one-qubit gates, state preparation, and measurement, the threshold is at least 3% and probably higher, perhaps as high as 5%. Knill's protocol is not very practical, as the overhead is ridiculously large (a factor of billions or more at error rates above 1%). A much more practical choice is the surface code, which we will discuss in chapter 17, and simulations suggest that the threshold for surface codes is about 0.7%.

14.7.5 The Overhead Required by the Threshold Theorem

Equation (14.60) tells us the overhead needed for a fault-tolerant circuit using concatenated codes. Asymptotically, for large T, this is very good scaling. However, for computations of realistic size, the need for at least a few levels of concatenation can make the overhead rather large.

For the case of the 7-qubit code, let us work out the actual overhead needed. In terms of locations, the largest rectangle is actually the $R_{\pi/8}$ rectangle since the CNOT rectangle (not exRec) has only two EC steps. Using the numbers from section 14.5.3 adjusted for a rectangle rather than an exRec, we find that the $\pi/8$ rectangle has $B = 492$ locations in total.

Suppose we have a physical error rate $p = 0.1p_T$, and let us insist on a failure rate $\epsilon = 0.01$. Then we can calculate the maximum allowed T for a given number of levels of concatenation. Let us use the optimized threshold value $p_T = 2.7 \times 10^{-5}$. The results are given in table 14.1.

You can see the polylogarithmic scaling start to kick in after 3 or 4 levels of concatenation. Because the physical error rate is quite low in this scenario, we can do fairly long calculations (with over three

thousand locations) without error correction. However, remember that this is the number of *locations* in the circuit, not necessarily gates. A calculation lasting 100 time steps on 40 qubits will be too many locations (although the failure rate ϵ is still only about 0.011). With 2 levels of concatenation, we can do much longer computations, containing over a million locations. Three levels allows more than 30 billion locations, which should handle all but the most demanding computations, and four levels of concatenation should be enough for any computation we can seriously imagine doing. However, by the time we've reached 3 levels of concatenation, the number of physical locations needed for each logical location is over 100 million, so a long computation with 10^9 logical locations requires a daunting 10^{17} physical locations.

However, bear in mind the threshold theorem is primarily a feasibility result. It says that long reliable computations are possible in principle, and only provides a lower bound on the performance of fault-tolerant protocols. In practice, we now know fault-tolerant protocols (for instance based on the surface code, chapter 17) which have much lower overheads in addition to much higher thresholds.

14.7.6 Threshold Surfaces and Pseudothresholds

The statement of the threshold theorem and the subsequent discussion assumed that all error rates were the same. What happens in the more realistic situation where different types of locations have different error rates? It no longer makes sense to talk about *the* value of the threshold. We'll need to specify conditions for all of the different error rates, and there could be a trade-off where we allow one type of location to have a larger error rate in exchange for a smaller error rate for another type of location. We end up with a *threshold surface* in the parameter space. As before, we can discuss threshold surfaces for a specific family of concatenated codes or for all possible families of codes. If the vector of error rates lies inside the threshold surface, arbitrarily long quantum computation is possible via fault tolerance. If the vector lies outside of the threshold surface, attempting a fault-tolerant protocol will hurt more than it helps.

To see how this works, we can perform an analysis similar to that in the proof of theorem 10.4. The only difference is that instead of having a single error rate p_l for each level, we have a different error rate for each type of location that we track. These error rates can be related by coupled recurrence relations derived as before.

For example, let us consider the concatenated 7-qubit code. For simplicity, we will consider circuits with only Clifford group gates, and lump together the error rates for one-qubit gate locations, wait locations, preparation locations, and measurement locations. The CNOT error rate we will track separately. At level l, we thus have two error rates $p_{G,l}$ and $p_{\mathrm{CNOT},l}$. Based on the calculations in section 14.5.3, we see that the CNOT exRec contains 263 CNOT locations and 472 single-qubit locations. The largest one-qubit exRec is a gate exRec, which contains 128 CNOT locations and 243 single-qubit locations. Therefore,

$$\begin{aligned} p_{G,l} =& \frac{1}{(1-Q_l)^4}(29403p_{G,l-1}^2 + 31104p_{G,l-1}p_{\mathrm{CNOT},l-1} + 8128p_{\mathrm{CNOT},l-1}^2) \\ p_{\mathrm{CNOT},l} =& \frac{1}{(1-Q_l)^8}(111156p_{G,l-1}^2 + 124136p_{G,l-1}p_{\mathrm{CNOT},l-1} + 34453p_{\mathrm{CNOT},l-1}^2) \\ Q_l =& 38p_{G,l-1} + 25p_{\mathrm{CNOT},l-1}. \end{aligned} \tag{14.64}$$

If the physical error rates are $(p_{G,0}, p_{\mathrm{CNOT},0})$, using these recurrence relations, we can track the pair of error rates as a function of l. For some starting values, the error rates will eventually decrease and both head towards 0. For other starting values, they will both head towards 1. The boundary between these two regions is the threshold surface, and is plotted in figure 14.13.

You might think that, since the CNOT exRec is the largest, given the physical error rates $(p_{G,0}, p_{\mathrm{CNOT},0})$, it is sufficient to check that $p_{\mathrm{CNOT},1} < p_{\mathrm{CNOT},0}$ to verify that we are inside the threshold surface. That is not the case, however.

To see what can go wrong, imagine an extreme case where $p_{G,0} = 0$. Then we have that

$$p_{\mathrm{CNOT},1} = \frac{1}{(1-25p_{\mathrm{CNOT},0})^8} 34453 p_{\mathrm{CNOT},0}^2, \tag{14.65}$$

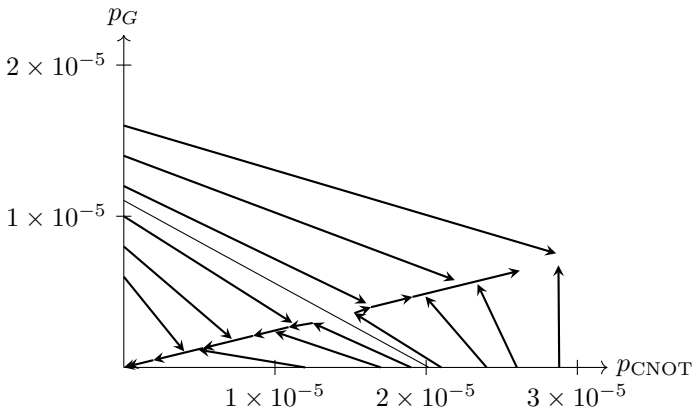

Figure 14.13: Plot of the threshold surface for Clifford gates and CNOT gates for the 7-qubit code derived using equation (14.64). The arrows indicate the effect of the recursion relations at various points inside and outside the threshold surface.

so $p_{\text{CNOT},1} < p_{\text{CNOT},0}$ when $p_{\text{CNOT},0} < 2.88 \times 10^{-5}$. But $(0, 2.88 \times 10^{-5})$ is actually outside the threshold surface! 2.88×10^{-5} is a CNOT *pseudothreshold*, not an actual threshold.

The problem is that, while the CNOT error rate goes down from level 0 to level 1, the single-qubit error rate increases from 0 to something significant:

$$p_{G,1} = \frac{1}{(1 - 25p_{\text{CNOT},0})^4} 8128 p_{\text{CNOT},l-1}^2 \approx 6.76 \times 10^{-6}. \tag{14.66}$$

When we calculate the level 2 error rates, we must take this into account. We find

$$p_{G,2} = 1.41 \times 10^{-5} \tag{14.67}$$

$$p_{\text{CNOT},2} = 5.77 \times 10^{-5}. \tag{14.68}$$

As you see, both error rates increase going from level 1 to level 2. The recurrence relations are monotonic in the error rates, so once all error rates increase when adding a level, they will continue to get worse and worse as we add more and more levels. In particular, we know that $(0, 2.88 \times 10^{-5})$ is outside the threshold surface. Or at least, it is outside the surface calculated using these particular formulas. It is quite likely that a more careful calculation counting malignant sets would give a different result.

The point, however, is this: When dealing separately with error rates for different types of locations, it is possible that some error rates will go up and some go down when you add a level of concatenation. When this happens, you need to look at more levels to figure out if you are inside or outside the threshold surface. Only once all error rates are moving the same direction can you reach a firm conclusion. Even for fault-tolerant protocols not based on concatenation, it is quite common for the protocol to improve the logical CNOT error rate but make single-qubit error rates worse, for example, and it is not immediately clear if this constitutes an actual improvement or not without a more careful analysis.

Because it is difficult to plot and completely study threshold surfaces, frequently a further simplification of error rates is made. For instance, a common choice is to assume that storage errors are less likely than other kinds of errors, so perhaps one assumes that $p_P = p_G = p_M = p$, and that $p_S = p/10$. In this case, the threshold once again becomes a single number, expressed as a bound on p. The other considerations of this section apply in full. In particular you cannot assume that the level 1 error rates satisfy the same relationship as the level 0 physical error rates!

Chapter 15

Now Hold On Just a Second: Assumptions Re-Examined

OK, we've proven the threshold theorem. This shows that arbitrarily large quantum computers can in principle be built. There is obviously a lot of theoretical and experimental work left to do, optimizing the value of the threshold, reducing the overhead needed, and of course actually *building* a device with low enough error rates and sufficiently many qubits to run a fault-tolerant protocol. But at least we can rest easy that the main question of principle has been resolved, and that if society is willing to devote enough time and money to the task, someday we will be able to build large quantum computers.

Not so fast! The threshold theorem we proved was for a basic model of fault tolerance, which is a theoretically tractable construct that is simplified in various ways to make it easier to analyze than a real system. Many of the assumptions built into the basic model will be violated in a real system. (Although exactly *which* assumptions are violated may vary considerably depending on the physics of the implementation.)

In this chapter, I'll discuss the assumptions which may be violated, and examine which of them are truly necessary for a threshold theorem to hold. As you'll see, we can substantially relax the assumptions of the basic model and still have a threshold. We do need a few assumptions, some of which are violated in some specific systems, but the prerequisites for a threshold are loose enough that it seems likely that a fault-tolerant quantum computer really ought to be possible, provided we use the right type of system to build it.

15.1 Solovay-Kitaev Theorem

15.1.1 Different Universal Gate Sets

The first concern is what gates are available to our circuits. All of the gadgets in the protocol are written in terms of some universal set of gates. For instance, the fault-tolerant protocols we have described for stabilizer codes use only physical Clifford group gates and C_3 gates, and usually just one kind of C_3 gate, such as $R_{\pi/8}$. But what if our physical machine doesn't naturally perform these gates, but instead uses some other universal gate set? Since the actual gate set is universal, we can certainly rewrite the gates used in the fault-tolerant protocol in terms of the implementation's natural gate set, but there will be a cost in overhead and reduced tolerance to error (since we need more physical gates to produce the same number of logical gates). Will that cost destroy or substantially weaken the threshold theorem?

There are actually two issues. Not only do we need to build the physical gates used in the fault-tolerant protocol out of the gates directly available in the physical realization of the computer, but we also need to convert from the set of logical gates that can be directly produced by the fault-tolerant protocol to the logical gates used in the algorithm being performed.

Let us first consider the physical gates. Suppose that the available physical gates are $\{U_i\}$ and the ones

needed for the fault-tolerant protocol are $\{V_j\}$. Let us first consider the case where we can exactly realize the V_js in terms of the U_is. We can then write

$$V_j = \prod_{i=1}^{m_j} U_{a_{ij}} \tag{15.1}$$

for some sequence $\{a_{ij}|i = 1, \ldots, m_j\}$ of length m_j. The gate U_i has an error rate p_{U_i}. By the union bound, the error rate for V_j is therefore

$$p_{V_j} \leq \sum_{i=1}^{m_j} p_{U_{a_{ij}}}. \tag{15.2}$$

This is true even for adversarial stochastic errors. In the special case where $p_{U_i} = p$, $p_{V_j} = m_j p$. Thus, there is a blow-up in the error rate for the gates used in the fault-tolerant protocol. The value of the threshold could therefore decrease by a factor of as much as $\max_j m_j$. That is undesirable, particularly if m_j can be large, but at least it leaves the threshold theorem in place.

When the V_js cannot be written exactly as a product of U_is, or even if it is just very costly to do so, we instead should approximate the V_js. We again get equations like equation (15.1), but now instead of having V_j on the left, we have V_j', with $\|V_j' - V_j\| < \delta$. δ then acts like an additional error rate on top of the p_{V_j} that we calculated above. If δ is a constant as a function of the size of the computation, which can be achieved with a constant value for each m_j, the total error rate remains constant. This is important, because we don't want the per-gate error rates to increase as the computation gets bigger. If the error rate stays the same, we can bundle the gate approximation error in with all the other sources of error and correct them together with the same QECC.

There is a catch, however: we have left the basic model of fault-tolerance. The difference between V_j' and V_j cannot be written in terms of a stochastic error model, not even an adversarial one, unless $p = 1$: Every time we try to do V_j, we will instead do the unitary V_j' or have an error in one of the U_i used to produce V_j'. However, since V_j and V_j' are close to each other, the operation is not *very* wrong, so 100% error rate would be a horrible overestimate. The correct way to handle this type of error is as a coherent error, which we will treat in section 15.8. The overall result is that, as in the exact case, the threshold still exists, but is lower.

Now for the logical gates. A fault-tolerant protocol includes gadgets for a universal set of logical gates, but frequently, as in the example of the 7-qubit code or other stabilizer codes, it is a *finite* set. The basic model assumes that the logical circuit we are trying to simulate has already been written in terms of the logical gates used. If it's not, we need to convert the logical circuit to use the same universal set that is produced by the fault-tolerant protocol, and again there is an extra overhead to doing so. Does that undermine the threshold?

If we can exactly realize the gates in the simulated circuit C using the gates with fault-tolerant gadgets, there is no problem. If it takes up to m fault-tolerant gates to write each circuit gate, the total number of locations T could increase to mT. Since the number of levels l of concatenation needed scales as $\log \log T$, this means that l stays the same or at most increases by 1 unless m is particularly large. This increases the overhead slightly, but doesn't fundamentally alter the theorem.

If the gates in C can only be approximated using the gates for which we have fault-tolerant gadgets, more care is needed. Each time we approximate a gate, that is another source of error. Since this is an approximation of *logical* gates, the error is a logical error which cannot easily be dealt with via more error correction. Instead, we need to make sure that when we approximate gates, the approximation is good enough that over the course of the whole computation, the total error is still manageable.

To be precise, the original circuit C has T locations, and our goal is to get an output state which has statistical distance at most ϵ from the correct distribution D. We approximate each gate in C to accuracy δ (in ∞-norm) using at most m_δ fault-tolerant gadgets, so we have a fault-tolerant circuit with $\leq m_\delta T$ logical locations. Greater accuracy δ might require a larger number m_δ of fault-tolerant gadgets, which in turn contributes to a greater logical error rate, so we must choose δ to balance these concerns. (See appendix **??** for a discussion of distance measures. Note that the choice to use statistical distance and ∞-norm don't

really matter here — the same type of arguments apply to any reasonable choice of distances assuming all the gate sets involved act on a constant number of logical qubits.)

Each of the $m_\delta T$ locations has a logical error rate p_l, as in the proof of theorem 10.4, and there is an additional source of error δ for each of the T locations in C because our approximation is imperfect. With probability at most $p_l m_\delta T$, there is a logical error in one or more of the fault-tolerant gadgets in the simulation, giving us an incorrect distribution D'. Otherwise, we get the distribution D'' produced by performing C but with the approximate gates instead of the true gates. Each approximate gate is at most δ away from the true gate, so the total distance of the final state of the approximate circuit is at most δT. Therefore, the output distribution $p_l m_\delta T D' + (1 - p_l m_\delta T) D''$ has statistical distance at most $p_l m_\delta T + \delta T$ from the ideal distribution D. In order for this to be below the target error rate ϵ, it is sufficient to pick l and δ such that $\delta < \epsilon/(2T)$ and $p_l < \epsilon/(2m_\delta T)$.

In particular, we need an approximation that improves linearly with the length of the computation we are doing. A better approximation generally needs more gates, so m_δ must increase with T. That increases the overhead in two ways: First, directly, since the number of fault-tolerant gadgets used is proportional to m_δ, and second, indirectly, by setting a more stringent requirement on p_l. Referring to theorem 10.4, we see that the overhead acquires an extra factor of $m_\delta \operatorname{polylog} m_\delta$. We therefore need to be careful of how m_δ scales with T, since a poor scaling rate could completely undermine the threshold theorem.

15.1.2 Statement of the Solovay-Kitaev Theorem

Luckily, the scaling is not bad.

Theorem 15.1 (Solovay-Kitaev)**.** *Let $\mathcal{S} = \{U_i\}$ be a finite universal set of gates for $\mathsf{SU}(D)$, closed under inverses (i.e., $U \in \mathcal{S}$ iff $U^\dagger \in \mathcal{S}$). Then for any $U \in \mathsf{SU}(D)$ and any $\delta > 0$, there exists a finite sequence $a_1, \ldots, a_m$ such that*

$$\|U - \prod_{i=1}^{m} U_{a_i}\| < \delta, \tag{15.3}$$

and $m = O(\text{polylog}(1/\delta))$. Furthermore, a sequence $a_1, \ldots, a_m$ satisfying these conditions can be found via a classical algorithm running for time $O(\text{polylog}(1/\delta))$.

The Solovay-Kitaev theorem says that all universal sets of gates are equivalent up to polylogarithmic overhead. In it, D, the Hilbert space dimension, is fixed. Most of the time, we are interested in $D = 2^2$ or $D = 2^3$ (when the universal set of gates includes two- or three-qubit gates, respectively), so taking D constant is perfectly reasonable. If D starts to get larger, $D = 2^n$, the scaling is not as good: m increases exponentially with n. This is inevitable: For fixed ϵ, the number of unitaries in $\mathsf{SU}(2^n)$ which are distance ϵ from each other is exponential in D, so $\text{poly}(D)$ gates ($= \exp O(n)$ gates) from a finite set will certainly be needed to cover all of them.

Of course, for many specific $\mathcal{S}$ and U, even better approximations are possible. For instance, for the gate set that shows up most often in fault-tolerant protocols, a tighter result is possible:

Theorem 15.2. *Let $\mathcal{S} = \hat{\mathsf{C}}_1 \cup \{R_{\pi/8}\}$ and $D = 2$. Then for any $U \in \mathsf{SU}(2)$, $\delta > 0$, there exists a circuit of size $O(\log 1/\delta)$ realizing U' such that $\|U' - U\| < \delta$. Furthermore, the circuit can be found classically in time $O(\text{polylog}(1/\delta))$.*

That is, any single-qubit gate can be approximated to accuracy δ using just $\log 1/\delta$ Clifford gates and $R_{\pi/8}$ gates. This is the optimal asymptotic scaling possible, which can be shown by a counting argument: You need at least this many gates so that every point in $\mathsf{SU}(D)$ is in a ball of radius δ from the exactly achievable gates. The gate set $\mathcal{S}$ was chosen because of its convenience for fault tolerance, but the fact that this optimal asymptotic approximation is possible is an extremely nice additional property of $\mathcal{S}$ that is not shared by all approximately universal gate sets.

In order to approximate a 2- or 3-qubit gate U using Clifford gates and $R_{\pi/8}$ gates, we can first write U exactly as a product of a constant number m of CNOT gates and single-qubit gates, since the set $\{\text{CNOT}, \text{single-qubit unitaries}\}$ is an exactly universal gate set. Then we can approximate the single-qubit

gates to accuracy δ/m using theorem 15.2, giving us an $O(\log 1/\delta)$-size circuit approximating U to accuracy δ. For multi-qubit gates, this strategy doesn't give the optimal approximation, but the scaling in δ is still better than that provided by the Solovay-Kitaev theorem.

As a consequence of theorems 15.1 and 15.2, the threshold theorem does not need be qualitatively changed when the circuit C involves gates outside of the universal set used for fault tolerance. Since $m_\delta = O(\text{polylog}(1/\delta)) = O(\text{polylog}(T/\epsilon))$, the overhead due to the Solovay-Kitaev theorem is comparable to the overhead from the threshold theorem. Combining them, we simply get a higher degree polynomial in the logarithm. This means that once T is very large, making it even larger does not substantially increase the overhead. As before, though, nice asymptotic behavior does not mean it isn't painful dealing with the constant factors. Even mediocre approximations using the Solovay-Kitaev theorem can take many gates, so it is very helpful to develop shortcuts for the specific gates used in C.

15.2 Short-Range Gates

The next assumption I'll examine is not part of the basic model per se, but was implicit in all of the fault-tolerant gadget constructions I showed you. Specifically, in designing gadgets, I assumed we could do CNOT gates between any pair of qubits, no matter where they are in the computer. In many systems, however, qubits only interact locally, and it is only possible to do CNOT or other two-qubit gates between qubits that are physically near each other. In the extreme case, only gates between nearest-neighbor particles are allowed. Is there still a threshold under these circumstances?

15.2.1 SWAP Gates in a Fault-Tolerant Circuit

Putting fault-tolerance aside for a moment, one way to convert a general circuit C to one using only nearest-neighbor gates is by using the SWAP gate, which exchanges two qubits. With a series of SWAP gates, we can move a qubit between any two locations in the quantum computer (assuming the geometry is connected).

Proposition 15.3. *For any circuit C, there exists a circuit C' with the same output as C such that C' uses only nearest-neighbor qubits when the qubits are arranged on some sort of regular D-dimensional structure (most often a square grid). When C has n qubits and T locations, the number of locations in C' is at most $O(n^3T)$.*

Proof. We can build C' by replacing each gate in C by a subroutine. Whenever C calls for a two-qubit gate U between qubits i and j, the subroutine begins with a series of SWAP gates that move qubit j to a location next to i and then finishes by performing U between i and the new location of j. If there are n qubits in the computer, C' has at most $n-1$ times as many gates as C (even in 1 dimension, $n-2$ SWAPs suffices to move a qubit from one end of the line to a spot next to the far end, plus the gate U). However, the procedure could potentially spoil the parallelism of C. It may not be possible to simultaneously move all of the qubits that need to interact in a given time step to where they need to go. Therefore, the depth of C could blow up by a factor of up to $\frac{n}{2}(n-1) = O(n^2)$. That would cause the total number of locations in C to increase by a factor of $O(n^3)$. □

When we want to make a fault-tolerant circuit using only nearest-neighbor gates, the first thing to do is make sure the logical circuit uses only nearest-neighbor gates, as in proposition 15.3. SWAP is a Clifford group gate and has an obvious transversal implementation for any code (not only a stabilizer code) encoding one qubit per block: Swap all the qubits of the first block with all the qubits of the second block. That is, the transversal SWAP always performs the logical SWAP as well.

However, this is not sufficient. The fault-tolerant gadget constructions from prior chapters might (and generally do) involve gates which interact qubits which might not be nearest neighbors. That's not obviously a problem. Perhaps we can simply take the circuit for a fault-tolerant gadget and simply convert it into one that uses only nearest-neighbor gates with proposition 15.3. Indeed, this gives us a gadget with the same purpose as the original one.

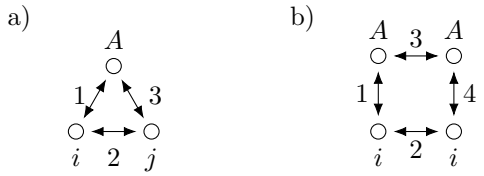

Figure 15.1: Two possible arrangements of qubits that use nearest-neighbor gates and ancillas (A) to perform a SWAP which is safe for fault tolerance between data qubits i and j. The arrows indicate a physical SWAP between the two indicated positions in numerical order.

However, it is not generally a fault-tolerant gadget. The problem is that the SWAP gates used to move qubits around are not transversal ones. This means that if a SWAP location has a fault, it could potentially cause errors in two qubits in the same block. This means the gadget will probably violate the relevant FT conditions.

Normally, there is a second problem with non-transversal gates, namely error propagation, but it is not an issue for SWAP gates. An ideal SWAP gate interacting qubits i and j does indeed cause errors which begin in qubit i to propagate to qubit j, but in the process, those errors depart qubit i. That is, SWAP not only swaps the data stored in two qubits, it also swaps the errors. Therefore, the picture

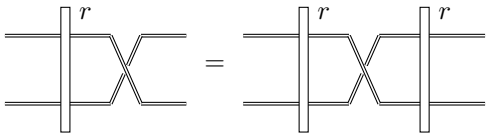

(15.4)

holds, whereas the corresponding statement is not true of the CNOT gate.

Using this fact, we can come up with a non-transversal but "safe" implementation of the SWAP gate that can be used to be move qubits in a fault-tolerant gadget in such a way that the resulting gadget is also fault-tolerant. We discussed this before, in chapter 11, and the circuit is pictured in figure 11.2. It uses one ancilla qubit A and proceeds via 3 physical SWAP gates. To swap data qubits i and j, first SWAP i with A. Then SWAP A (in its new location) with j. Finally SWAP A with i again. Then j ends up in the location originally containing i and i ends up in the location where j began. The ancilla qubit A ends up back where it started. Note that the value of the ancilla is irrelevant; the circuit works the same way regardless of the state of the ancilla. Each of the three SWAP gates interacts A with one of the data qubits, so a single fault during this circuit can create correlated errors in A and one of the two data qubits. But since ideal SWAPs only move errors around and cannot change the weight of a pre-existing error, the data error caused by a single fault cannot spread to the other data qubit by the end of the SWAP circuit. Of course, if there are two faults during the circuit, that could cause both qubits to fail, but two faults can always cause two qubits to fail, so that won't violate the definition of fault-tolerance.

In order to do this SWAP circuit using only nearest-neighbor gates, we need the two data qubits and the ancilla qubit to be arranged in a triangle, as in figure 15.1a. If the geometry of qubits in the computer is a square lattice, or some other arrangement that lacks triangles, we can still do it by adding one or more extra ancilla qubits, as in figure 15.1b. This necessitates one or more extra SWAPs to move the qubits where they're needed, but doesn't significantly change the analysis.

Another option for moving qubits around is to generate entangled ancilla pairs $|00\rangle + |11\rangle$ between the two locations and then teleport qubits around or do remote CNOT gates. Doing this requires a sequence of entanglement swapping operations in between, and over longer distances, entanglement distillation (section 18.2) will be needed as well to keep the error rate in the entangled pairs under control. Thus, there will be significant extra space overhead from this option, but most of the work can be done in parallel, meaning a minimal time overhead. Qubit routing via entangled pairs is a good option when the cost of extra qubits is not too high and fast measurement and classical communication is available.

15.2.2 Architecture of a Local Fault-Tolerant Quantum Computer

How do we use this idea to create a fault-tolerant quantum computer using only local gates? Since the number of locations in the local version of a circuit can depend on the number of qubits involved in the circuit, we need to be a bit careful to make sure that the overhead and error rates of a local fault-tolerant circuit don't blow up as the ideal circuit gets very large.

The main variable to keep in mind is the spatial dimension of the computer. In order to take advantage of the fault-tolerance-safe SWAP circuit in figure 11.2, we need to have qubits arranged in at least two dimensions. This can certainly be satisfied in a computer with qubits arrayed in a two-dimensional lattice, but it is also enough to have a one-dimensional system with two parallel lines of qubits. Ideally the two lines would be offset by half a lattice site in order to get the triangles as in figure 15.1a.

The next consideration is the QECC used. In the case of a concatenated code, we can consider just a single level of the code and find a local fault-tolerant protocol for that. First we convert the logical circuit C which wish to implement to one which involves only local gates arranged in the correct number of dimensions. Then we store each block of the QECC with all the ancillas needed to perform a complete set of fault-tolerant gadgets. This includes all the qubits needed to prepare any ancillas. If we attempt ancilla preparation many times in parallel and post-select to keep only one attempt, we also store locally all the qubits needed for the all the simultaneous preparation attempts. The total number of ancilla qubits depends on the protocol, but importantly, it does not depend on the size of the logical circuit C. Therefore, there the total number of qubits needed for all possible gadgets involving two adjacent logical qubits is a constant N. In order to perform one of these gadgets, the maximum distance any qubit needs to travel is N (in one dimension) or about $\sqrt{N}$ (in two dimensions). We can use safe SWAP gates to convert the usual set of fault-tolerant gadgets into fault-tolerant gadgets using only nearest-neighbor gates. The maximum size of any gadget is polynomial in N, independent of the size of C.

By concatenating the local protocol for a single level of the code, we get another local protocol for multiple levels. The overall effect in two dimensions is pictured in figure 15.2. The architecture of the computer becomes self-similar. Local blocks of some size R store a single block of the QECC with one level of encoding and all the ancillas needed for level one fault-tolerant gadgets. Within a larger region of size R^2, some of the local blocks combine to form a qubit encoded with two levels of concatenation, while others combine to form the ancillas needed for level two fault-tolerant gadgets. Then a region of size R^3 contains everything necessary for gadgets with three levels of concatenation, and so on.

When applied to a two-dimensional computer, the concatenated protocol remains two-dimensional. Since the one-dimensional protocol required two lines of qubits, straightforward concatenation with l levels produces a linear computer which is 2^l qubits thick. With a little thought, we can reduce this to a line two qubits thick. One way to do so is to imagine that instead of nearest-neighbor gates, we have next-to-nearest neighbor gates. Then we could make a protocol which works on a single line of qubits by alternating data qubits with ancilla qubits and using the safe SWAP (figure 11.2) to move qubits around. With a series of safe SWAPs, we can add a fault-tolerant gadget for next-to-nearest-neighbor SWAP at one level of encoding. Concatenating the next-to-nearest-neighbor protocol results in a one-dimensional computer, still using just a single line of qubits. Going back to nearest-neighbor gates, we can implement the physical next-to-nearest-neighbor SWAP via SWAPs involving a second line of qubits. The resulting architecture is shown in figure 15.3.

In fact, it is possible to do even better and make a fault-tolerant quantum computer with nearest-neighbor gates and a single line of qubits. To do so, we give up on the safe SWAP concept and simply accept that a single faulty SWAP gate can create two errors in a block. We'll need to be able to correct both of those errors, which means we need to concatenate a QECC that corrects two errors per block (i.e., a distance 5 code). Other than that, there is no further complication. Concatenating such a protocol again gives you a threshold. However, rigorously proving that this works requires the concept of gadgets with a *spread*, which I'll discuss in section 16.3.

Figure 15.2: Cartoon of the arrangement of a two-dimensional fault-tolerant quantum computer using concatenated codes. The small shaded rectangles mark out level-1 blocks, including the level-1 encoding and all ancillas needed for fault-tolerant error correction, logical state preparation, logical measurement, and logical gates. (This is a cartoon because the real number of qubits needed is much larger.) The medium-sized, dashed, lightly-shaded rectangles indicate level-2 blocks, including the level-2 code and all necessary level-2 ancillas. The level-2 code and ancillas are made up of level-1 blocks. The large rectangle indicates a level-3 block.

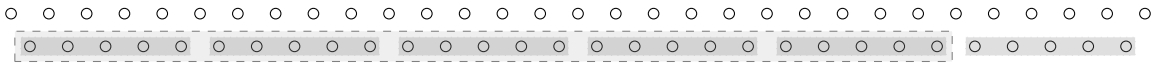

Figure 15.3: A cartoon of the arrangement of a one-dimensional fault-tolerant protocol using 2 lines of qubits. The top line are ancillas used only for level-1 SWAP gates. In the bottom line, the small shaded rectangles indicate level-1 blocks and all relevant ancillas. The larger dashed, lightly shaded rectangle is a level-2 block.

15.2.3 Effect of Short-Range Gates on the Threshold

Because the constructions above all use concatenation to make families of fault-tolerant protocols with nearest-neighbor gates in one or two dimensions, they all have thresholds. This shows that thresholds exist even when only local gates are allowed. Unfortunately, the conversion to nearest-neighbor gates necessarily adds overhead. More locations means more opportunities for faults and lower thresholds.

The concatenated 7-qubit code has been a favorite subject for threshold studies in various settings, and in particular, thresholds have been proven for optimized concatenated 7-qubit codes in both one and two dimensions. Recall that with no geometric constraint, the threshold for the 7-qubit code is provably at least 2.7×10^{-5} when the physical error rates for all locations are equal. For the same context in two dimensions, the threshold is at least 1.1×10^{-5}. When the storage error rate is 1/10 the error rate for other locations, the threshold in two dimensions is at least 1.8×10^{-5}. In one dimension, the threshold hasn't been calculated when all error rates are equal, but when the storage error rate is 1/10 of the error rate for other locations, the threshold is at least 2×10^{-6}.[1] These numbers are all proofs, so the actual thresholds are higher.

Naturally, other fault-tolerant protocols which use only nearest-neighbor gates are possible. Some codes are more naturally suited to being implemented in two dimensions. (Sadly, few codes are well-suited for one dimension.) In chapter 17, I'll discuss surface codes, which are defined using a two-dimensional geometry and give the best known thresholds in that context. The threshold for fault-tolerant computation with surface codes has been largely determined via simulations, some of which report threshold estimates close to 1%.

In short, while working with nearest-neighbor gates does come with a cost to the threshold, it is a manageable cost. In two dimensions, the threshold only seems to decrease by a factor of 2 or 3 at worst. Working in one dimension is more costly, incurring at least an order of magnitude reduction in the threshold even when two lines of qubits are available.

15.3 Slow Measurement or No Intermediate Measurement

Another implicit assumption in the fault-tolerant protocols I've described is that there is such a thing as a measurement location that can be performed whenever you want. Certainly, you must be able to measure qubits at the end of the computation, otherwise there's no way to learn the answer of the computation. However, in some physical systems, you may *only* be able to measure at the end. This may be because the only way to reliably measure the system is to do something to all of it at once, for instance, to couple the whole computer strongly to a measurement device. Alternatively, it may just be that measurement is very slow compared to a single unitary gate. This is a common situation: Normally, we want to do quantum computation in systems with weak coupling to the environment, but measurement requires a coupling to the environment, or at least the part of the environment containing the experimenter. Another scenario is for measurement to be reasonably fast, but the quantum gates operate on such a short time scale that classical processing of the measurement results takes an appreciable number of time steps for the quantum computer.

Slow measurements present a potentially serious problem for a fault-tolerant circuit. Our fault-tolerant error correction gadgets and non-transversal gate gadgets (usually magic state injection) make heavy use of measurements followed by classical processing. If the qubits which don't get measured have to wait around a long time during the measurement and/or classical processing, storage errors can accumulate. If the waiting time is a constant, independent of system size, there will still be a threshold, but it might be much lower. The case where we must wait until the end of the computation to do measurements is even worse. We'll need some way to do error correction and non-transversal gates without measurements, or we won't even have a full fault-tolerant protocol, let alone a threshold.

15.3.1 Replacing Classical Processing With Quantum Circuits

In a non-fault-tolerant quantum computation, there is no real need to have measurements in the middle of the circuit, even though it might be sometimes convenient to think about the algorithm as calling for a

[1] This is for a computer composed of two lines of qubits, as discussed above.

measurement at certain points along the way. A quantum computer can do anything a classical reversible computer can do, which in turn can do anything a classical irreversible computer can do, with some slight overhead. If the algorithm calls for a measurement followed by a classical computation, with the output of the classical computation determining what happens next in the quantum circuit, all of that can be replicated exactly using a quantum circuit. Any measurements can be safely delayed until the end of the computation, with minimal change in the resources (space and time) required. Note that some alternatives to the circuit model, most notably measurement-based quantum computation (see chapter 20), *do* require measurements during the computation in order to make up for a lack of universal unitary quantum control in the system. Once we have universal gate sets, however, measurement is only needed at the end of the computation. Even then, it is really only needed because we insist the outcome of the computation be transformed into a classical value so that we can tell our friends, write papers about it, or simply store it in our limited classical brains.

We'd like to follow the same strategy for a fault-tolerant circuit: replace classical computations with quantum ones. However, there's a complication. In the basic model of fault tolerance, classical gates are perfect whereas quantum ones are not. We need to make important decisions that can affect the logical state of the computer based on the outcome of the classical computations, and a single mistake can ruin the data. Therefore, to be safe, we must replace classical circuits with fault-tolerant quantum circuits.

But that seems circular. In order to have a fault-tolerant protocol without measurements, we must replace the measurement locations and subsequent classical processing in all gadgets with fault-tolerant quantum circuits, but general fault-tolerant quantum circuits require FT EC gadgets, state preparation gadgets, and magic state injection protocols, which in turn use measurements, which must be replaced .... The way out of the loop is to notice that we don't replace classical processing with a completely general quantum circuit, only with a quantum circuit to manipulate classical data. In particular, we don't care about phase errors on the classical data, so it's enough to use a *classical* error-correcting code and fault-tolerant protocol for this part of the circuit.

The natural fault-tolerant classical protocol uses the repetition code. It is simple yet effective: Perform three (or more) copies of the computation and periodically compare the current states of the copies, taking the majority for any bit where they disagree. All classical gates can be performed transversally on the repetition code, so we have a classically universal gate set. Fault-tolerant classical error correction is a bit more complicated, but still much simpler than fault-tolerant quantum error correction. We don't have to worry about phase errors, and bit flip errors can only propagate from control to target in a CNOT, so we don't have to use cat states or any other special structured ancillas. We do need to be a little bit careful about Toffoli gates or the like; while errors can't propagate from the target into the two control bits, a fault in the gate itself could produce errors in both control bits, so we should make sure that either the two control bits are in separate blocks of a repetition code or copy one of the control bits to an additional ancilla qubit. We don't even need to worry about uncomputing any scratch qubits, since the usual quantum concern is that unerased scratch qubits will decohere the quantum computer, and we don't care about decohering the classical bits. The bottom line is we only need to bring in a few ancilla bits, calculate the error syndrome in them, and then correct the state. You may have worked out the details as exercise **??**.

Depending on the fault-tolerant measurement gadget we are replacing, there may be a delicate moment converting from one classical code encoding the measurement outcomes to the repetition code used for classical fault tolerance. The other potentially tricky step is when we want to apply the classical result to determine something in the quantum circuit.

In Shor EC or Shor measurement, we repeat each one-bit measurement multiple times to make it reliable. This is already a repetition code, which is a good start. We can perform these protocols as normal, except that whenever the standard circuit calls for a measurement location, we do nothing except to start considering that bit as a classical bit. For Shor measurement, we then get a repetition code encoding the measurement outcome and can proceed using a regular classical fault-tolerant circuit. In Shor EC, however, the standard procedure (described in section 12.2.2) determines the consensus syndrome in a way that depends on the order of the measurement outcomes rather than the simple majority. In order to compute the consensus syndrome requires non-transversal gates. The way to do this safely is to introduce rs extra bits (plus any needed scratch bits) and use them to compute the r-bit syndrome s times, each time starting from the bits

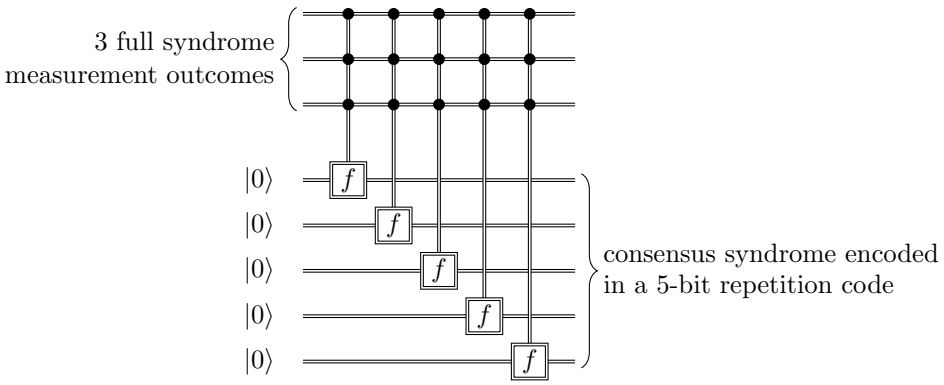

Figure 15.4: Converting outcomes of repeated syndrome measurement into a repetition code. Each doubled line represents a full r-bit syndrome value and the function f determines which syndrome to use, for instance using the procedure discussed in section 12.2.2. The computation of f may use additional scratch bits not shown.

produced by the measurement locations, or rather those locations that would have been measurements if we allowed them. Once we've done this, we are left with a code using s repetitions, and we can consider the majority value of those repetitions to be the canonical one. A single fault in one calculation of the consensus syndrome can result in a wrong value, but to get many wrong values requires either faults in many of the syndrome calculations or multiple faults in the stored "measurement outcome" bits, enough to cause Shor EC to fail. From this point, we can treat the rest of the syndrome extraction procedure using standard repetition code fault tolerance techniques.

For Steane or Knill EC, the measurement outcomes form (possibly noisy) codewords of some classical error-correcting code, generally not the repetition code. We wish to convert this to a repetition code using s copies. As with Shor EC or measurement, we can simply remove the measurement locations and instead begin treating the qubits classically. Then to convert to a repetition code, we can perform the full syndrome decoding procedure s times, each time starting from the same set of "measurement outcome" bits but storing the result in a different ancilla register. Again, a fault during a single syndrome decoding circuit can cause one of the outcomes to be wrong, but many faults are needed to get many wrong outcomes. An alternative procedure is to copy all "measurement outcome" bits s times and then perform a classical fault-tolerant implementation of the decoding circuit. Steane or Knill measurement work the same way: The classical decoding procedure first corrects errors on the classical codeword, then deduces the logical bit value. To make this fault-tolerant, just repeat the whole procedure s times.

Finally, we must understand how to use bits stored in a classical repetition code to safely control quantum gates. If we're in the middle of an error correction gadget, we may want to use the classical syndrome information to perform a Pauli operation, correcting the error. If we're preparing an ancilla, we may wish to use the testing data we've gathered to reject the ancilla and pick another one in its place, which involves a series of SWAP gates on ancilla blocks. If we're doing a magic state injection gadget for a C_3 gate, we need to perform some Clifford group operation conditioned on the classical measurement outcome. In all of these cases, depending on the code, we may only be doing a transversal quantum gate, but we want the decision of *which* gate to do to depend on the classical register.

To do this safely, it's best if the classical repetition code uses as many copies as there are qubits in the QECC block we are controlling. Hopefully, we planned ahead so that this is true. Otherwise, we can increase the number of copies by calculating the majority value of the classical repetition code enough times to create the extra bits. (It's not safe to simply duplicate one of the bits in the repetition code, since if that bit happens to be wrong, we'll get multiple wrong bits in the enlarged code.) Once we have the right number of classical bits, we can use each one of them to control one qubit in the QECC. Since the classical bits are in a repetition code, they are supposed to be the same, so in the absence of errors, we perform the correct

transversal gate on the data block(s). If there is one fault in the classical circuit, there might be one wrong control bit, but that means only one qubit in each block suffers by having the wrong physical gate applied. This is acceptable, since a single fault in that gate location could produce a similar result.

For many of the applications described above, we can combine the "convert to repetition code" and "control qubits" steps to simplify the overall procedure. For instance, when we are doing error correction, we don't need to calculate the full description of the error n times for a QECC using n qubits. To fix the first qubit of the code, all we need to know is if the error is on the first qubit, and if so, whether it is an X, Y, or Z error. This comes to only 2 bits of information. Similarly for the other qubits. Therefore, we need only $2n$ ancilla bits, and we can make a slightly different calculation for each pair. Since the n corresponding bits are no longer supposed to be identical, taking the majority value for classical error correction is no longer possible. That's not a serious problem: the syndrome decoding circuit is of a fixed size, and once we correct the quantum error, we no longer care about the value of the syndrome. We can just skip error correction of the classical register. The resulting streamlined circuit is shown in figure 15.5 for the 7-qubit code.

Of course, as you can see, replacing the classical syndrome computations with quantum circuits entails a significant increase in overhead. For a single gadget, the increase is just a constant factor, so there is still a threshold, but it might be substantially lower. As it happens, however, it appears to make minimal difference for the 7-qubit code. The threshold for classical computation is quite high, much higher than the threshold for the 7-qubit code. Also, the classical computations needed for the 7-qubit code are fairly simple. The combination means that the classical subroutines in gadgets for the 7-qubit code are a rather robust part of those gadgets, and most small malignant sets of locations don't involve them. For other more sophisticated codes, however, the threshold is higher and the amount of classical computation needed for syndrome decoding can be substantially larger, so there might be a great cost to performing a fault-tolerant protocol for one of these codes when measurement is not available. As of this writing, the question has not been carefully studied, however.

15.3.2 Delayed Measurements

When measurements are possible during the computation, but are slow, one option is to simply eliminate intermediate measurements as discussed above. Given the consequent increase in overhead and perhaps reduction of the threshold value, it's worth exploring alternatives. If possible, we'd like to go ahead and start each measurement, but to put off doing anything about the results until much later, once there's been enough time to complete the measurement.

It turns out that this is, in fact, possible. As we saw in section 12.5.2, we don't actually need to literally correct errors each time we do an EC gadget. We can get the same benefit by classically keeping track of the Pauli frame. As long as we do only transversal Clifford gates, this is enough. Fault-tolerant error correction circuits consist only of Clifford group gates, so if we use a code which, like the 7-qubit code, allows the full Clifford group to be implemented transversally, and wish to simulate an ideal circuit containing only Clifford group gates, we can do the whole computation without ever needing to do a quantum gate conditioned on a classical measurement outcome. (We will also need to forgo ancilla preparation techniques that rely on post-selection, instead using ones which determine the location of any error on the ancilla.) This works whether we are using just a single level of the code or many levels of a concatenated code.

Such a circuit is perfectly suited for slow measurements. We perform the usual measurements as part of each FT EC gadget, but continue on with the circuit without waiting for the result. By the time the measurement is complete, we've done many more quantum gates, so our information about the Pauli frame is always delayed relative to the current state of the circuit. Note, though, that the delay is constant, based on the duration of a measurement, and doesn't get longer as the computation proceeds: The measurement from the next EC gadget takes just as long as the previous one, so it is done shortly after the previous one. At the end of the computation, we make a measurement, wait as long as needed for the result, and combine that result with the Pauli frame, which is now fully up-to-date as well, to learn the outcome of the circuit.

When we wish to simulate a circuit involving non-Clifford group gates, things are a bit more complicated. In order to do magic state distillation or injection, we need measurements, and we need to do Clifford group gates which depend on the measurement outcome. We can't simply proceed with the computation without

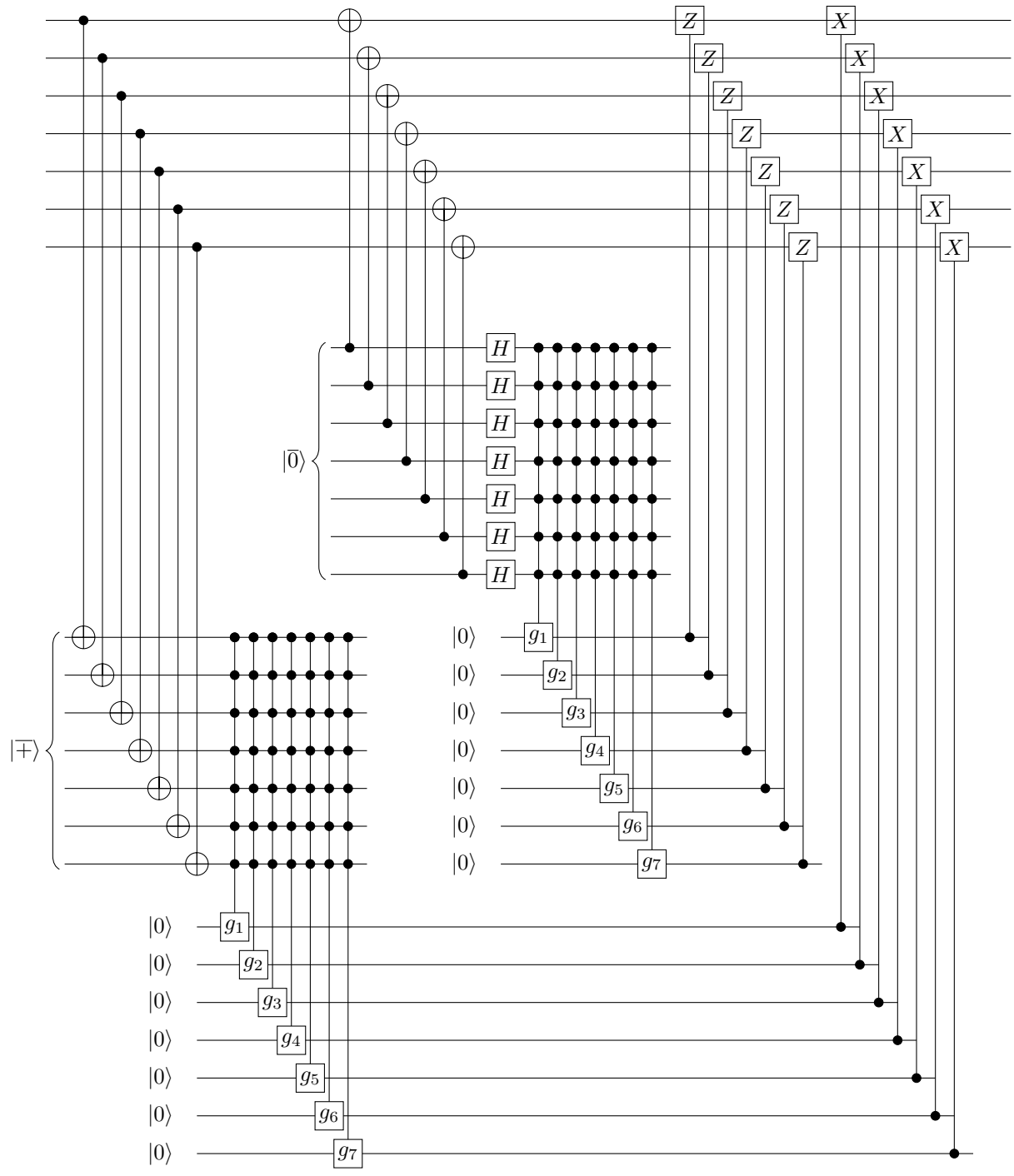

Figure 15.5: Steane error correction for the 7-qubit code, with the syndrome decoding performed using classical repetition codes. The function g_i is the syndrome decoding algorithm for the 7-bit classical Hamming code to determine if there is an error on the ith bit. The computation of g_i may use additional scratch bits not shown.

knowing the result of the measurement as well as the current Pauli frame, which influences the interpretation of the measurement. That means that to complete a magic state injection protocol, we need to wait for the time needed to do a measurement.

In the strictly self-similar concatenation protocol discussed in chapter 14, we did logical non-Clifford group gates at level l by making magic states encoded at level l, which was done using level $l-1$ non-Clifford group gates. Those used level $l-1$ magic states and level $l-2$ non-Clifford group gates, and so on down to level 1 magic states. Waiting a long time for a level l measurement is not a big deal, since the l-level code has a very low logical error rate. But if we have to ultimately build this up out of level 1 non-Clifford group gates, we have a problem. At level 1, we can't afford to wait very long, since the level 1 error rate is relatively large.

The solution is to skip all of the intermediate levels and go right ahead with level l magic states and non-Clifford gates. The main observation is that it is perfectly possible to create a noisy level l magic state using just a single physical non-Clifford group gate and a whole bunch of gates that are from the Clifford group. One way to do this is completely straightforward: Make an unencoded magic state, then encode it (in a non-fault-tolerant way) using one level of the code. We now have a slightly noisy level 1 magic state. Then take the level 1 magic state and encode each of its physical qubits with another level of the code, again using non-fault-tolerant circuits. Stop and do error correction for this level 2 magic state. The second level of encoding could introduce errors, but a single fault will only affect one level 1 block, and will be fixed by the level 2 error correction. (Well, we don't actually *fix* the errors but instead keep track of them in a Pauli frame.) Therefore, the logical error rate of the level 2 magic state, while higher than the level 1 magic state we had earlier, is not too much higher, and certainly not twice as large. Continue adding more levels of encoding, stopping to do error correction after each one. At each level, the additional logical error rate decreases, and the accumulated error through the whole encoding converges. Therefore, we end up with a level l magic state with a constant total logical error rate.

We can make many such level l magic states. The error rate for each one is much higher than we would tolerate for a level l gate on the data, but is below the threshold for magic state distillation. Indeed, this is just what magic state distillation is good at. The level l error rate for Clifford group gates is negligible, so we can rapidly reduce the logical error rate for the magic states. This does require measurement, but it is level l measurement, so we are willing to wait for the outcome. Then we do the magic state injection gadget. That again requires measurement, but once again, with l levels of encoding, we are willing to wait.

Actually, this description is not quite right. The problem is that if we wait to do magic state injection until we have all the measurement outcomes for the error corrections during magic state preparation and the measurements during magic state distillation, there will be new errors occurring while we wait. Of course, they are correctable errors since we have a high level of encoding. To deal with the new errors, we continue doing error correction while we are waiting ... but if we wait for the outcomes of *those* error corrections, then there will be more errors, and so on. We could end up waiting forever.

We might need to wait for the magic state distillation to conclude (depending on how useful a magic state that fails distillation is), but luckily, we don't need to wait for all the error correction measurements to come in to start the magic state injection procedure. We do need to know their outcomes to finish the conditional operation in magic state injection, since the Pauli frame will contribute to the calculation of the logical measurement outcome, but critically, we only need to know the error syndromes of EC steps up to the time of the measurement for magic state injection. Any new errors that occur after that point don't contribute to the logical measurement outcome. We still need to do error correction and collect error syndromes to add to the Pauli frame, but they won't be relevant until the *next* magic state injection. So if we do the measurement part of the magic state injection as soon as we have a good magic state to use, we can then afford to wait for the measurement outcome before performing the conditional operation. We thus have a fault-tolerant gadget with slow measurements.

15.4 Fresh Ancilla Qubits

Just as it may be the case that measurement can only be performed at the end of the computation, it may be that state preparation can only be performed at the beginning of the computation. For instance, in some physical implementations, preparation takes a long time or can only be done globally, on the whole computer at once. In that case, it is not valid to assume that we can prepare a new ancilla qubit whenever we need to.

If we have the ability to perform non-destructive measurement and to condition operations on classical information during a computation, we can also reset qubits by measuring and flipping a $|1\rangle$ qubit into a $|0\rangle$ qubit. This resetting can be used to refresh any needed ancillas. But we've seen that measurement is not critical to a threshold, so what if we don't have either measurement or state preparation in the middle of the computation?

If there is no way to generate fresh qubits while a computation is ongoing, then instead, at the beginning of the computation, we must determine how many ancilla qubits we will need to complete the computation and prepare all of them together. If sometime in the middle of the computation, we need an ancilla qubit for error correction or another purpose, we take an ancilla from the stockpile and use it. Unfortunately, these ancillas are no longer fresh; they have been sitting around for a long time, potentially accumulating errors during that time. Is there something we can do to keep ancillas from going stale before they are used? If not, we won't have a threshold.

15.4.1 Thermodynamic Analysis of Error Correction and Fault Tolerance

One way to understand this issue is to think about error correction and fault tolerance from a thermodynamic point of view. Our goal is to keep the data block relatively free of errors. Its entropy is low, so we can think of it as having a low temperature. If the data block is then put through a noisy channel, errors occur and the entropy rises; the system heats up. The purpose of error correction is to remove errors and cool the system back down again. The way we do this is to bring in cold ancilla qubits and interact them with the data to determine the error syndrome. Since the error was random, the ancilla qubits heat up in the process because they now record a random value, the error syndrome. Based on the error syndrome, we correct the data qubits, cooling them back down again. In other words, we have pumped the entropy due to the errors from the data block into the ancilla qubits. Fault-tolerant error correction protocols act as a refrigerator, continuously cooling down a system.

The nature of the ancillas used matters a lot. If the error correction procedure were ideal and the ancillas being used were perfect, the protocol would remove almost all of the errors (although any error sufficiently large to change the logical state would remain), so the data block would be cooled nearly to absolute zero. Actually, if you model the system with a Hamiltonian whose ground space is the whole code space, it would be at absolute zero, since the degeneracy of the ground space would produce a system with residual entropy at zero temperature. However, in order to achieve this, it is essential that not just the gates but also the ancillas being used are perfect. In a realistically noisy fault-tolerant protocol, errors in the ancilla qubits can feed back into the data, as we saw in chapter 12. Ancillas which have a low level of errors are cold, but not at zero temperature, and the data block can only be cooled down at most to the temperature of the ancillas being used.

If ancillas can only be prepared at the beginning of the computation and heat up like everything else in the computer, it is clear that we are in trouble. As the computation proceeds, the available ancillas become hotter and hotter, and we cannot hope to cool the data block down below the temperature of the ancillas. A system interacting only with another hotter bath will eventually heat up to the temperature of the bath. It is just a matter of time. The question, then, is how *much* time it takes before the system equilibrates with the bath. If it is a very long time (for instance, exponential in the system size), then fault tolerance is possible. If it is a short time, then fault tolerance will be severely limited at best.

This thermodynamic picture is more than just an analogy. Real experiments in quantum computation are often done at cryogenic temperatures, and heat leaking in from the outside world, directly or indirectly, is an actual source of noise. Cryogenic systems need continued cooling or they will heat up, and fault-tolerant quantum error correction is indeed one way of literally refrigerating the system of interest. However, quantum

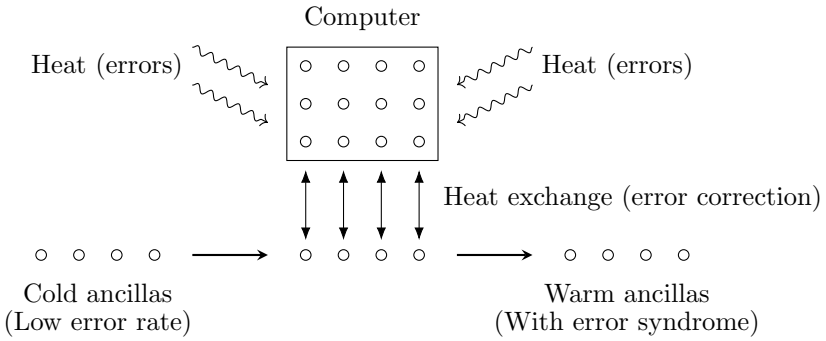

Figure 15.6: The thermodynamic picture of QECCs

error correction is more than just another method of cooling. The logical state we want to preserve is not in general a thermal state. Even if the system Hamiltonian is degenerate, there may be errors such as dephasing which don't change the energy (and thus don't heat the system) but still need to be avoided.

Note also that very little about this situation is uniquely quantum. Most of the same considerations apply to classical computers. Standard classical computers generate a lot of their own heat due to the irreversibility of the computation; but this is actually a form of error correction, with bits encoded in many redundant electrons which are forced into "0" and "1" states. Keeping the processors cool is a significant architectural concern with the design of classical computers as well.

15.4.2 A Case Where Fresh Ancilla Qubits Are Necessary

To see a concrete case where fault tolerant quantum computation is essentially impossible without fresh ancillas, let us consider a greatly simplified model. Assume that at each time step, we can perform any unitary we want, interacting as many qubits as we want, but then afterwards, each qubit undergoes the depolarizing channel (1.20) with some fixed error probability p. The "no fresh ancillas" assumption is present in this model with the requirement that at each time step, we perform a *unitary* map. The model allows arbitrary unitaries, which is very generous compared to the usual basic model of fault tolerance, which allows only one gate per qubit per time step. Thus, an impossibility result in the simplified model also applies to the basic model of fault tolerance when the noise is depolarizing.

Theorem 15.4. *In a closed quantum system of n qubits that undergoes depolarizing noise on each qubit with fixed error probability p at each time step, the system becomes exponentially close to the maximally mixed density matrix as a function of time.*

As a consequence of this theorem, any computation in such a system that runs for a time longer than $O(\log n)$ will give an input which is very close to completely random. This doesn't necessarily mean that a quantum computer with no fresh ancilla qubits is useless — it seems likely that there are interesting quantum algorithms which can be run in parallel in logarithmic time and yet beat any polynomial-time classical algorithm. Indeed, Shor's factoring algorithm is an example. What it does show is that no threshold theorem is possible for a closed system: A sufficiently large noisy quantum circuit will necessarily give a different result than the ideal version of the circuit (unless the ideal circuit was also supposed to produce a totally random output, I suppose).

Proof. We will track the entropy of the system going from time step t to time step $t+1$. Let $1, 2, 3, \ldots, n$ be the qubits in the computer after the unitary at time t but before the noise, and let $1', 2', 3', \ldots, n'$ be the qubits after the noise from time t and before the unitary for time step $t+1$. Then

$$S(1, 2, 3, \ldots, n) = \sum_{i=1}^{n} S(i|i+1, i+2, \ldots, n) \tag{15.5}$$

and

$$S(1', 2', 3', \ldots, n') = \sum_{i=1}^{n} S(i'|(i+1)', (i+2)', \ldots, n'). \tag{15.6}$$

$S(A|B) = S(AB) - S(B)$ is the conditional entropy of two subsystems A and B. In this case, we sum over the conditional entropies of qubit i or i', conditioned on the qubits later in the computer. But

$$S(i'|(i+1)', (i+2)', \ldots, n') \geq S(i'|i+1, i+2, \ldots, n). \tag{15.7}$$

By $S(i'|i+1, i+2, \ldots, n)$, I mean the conditional entropy taken for the density matrix in which the unitary at time $t+1$ has been done and qubit i has undergone the depolarizing noise, but qubits $i+1$ through n have not been depolarized. This equation can be proven by purifying the action of the depolarizing channel on qubits $i+1, \ldots, n$ and then tracing out the purifying system — the unitary interaction with the environment does not change the conditional entropy, and dropping the purifying system can only increase the conditional entropy.

Therefore,

$$\begin{aligned} S(1', 2', 3', \ldots, n') &\geq \sum_{i=1}^{n} S(i'|i+1, i+2, \ldots, n) && (15.8)\\ &\geq \sum_{i=1}^{n} \left[(1-4p/3)S(i|i+1, i+2, \ldots, n) + (4p/3)S(\tfrac{1}{2}I|i+1, i+2, \ldots n)\right] && (15.9)\\ &= (1-4p/3)S(1, 2, 3, \ldots, n) + 4pn/3. && (15.10) \end{aligned}$$

To get the second line, I used the decomposition of the depolarizing channel $\mathcal{D}_p(\rho) = (1-4p/3)\rho + (4p/3)\frac{1}{2}I$ and the concavity of the entropy (which also applies to the conditional entropy). Consequently,

$$n - S(1', 2', 3', \ldots, n') \leq (1-4p/3)[n - S(1, 2, 3, \ldots, n)]. \tag{15.11}$$

The entropy of the system approaches the maximal value n exponentially with time. The only state with maximal entropy is the completely mixed state, so we have the desired result. □

15.4.3 Other Error Models

For channels other than the depolarizing channel, other behaviors are possible. A trivial case is if the channel is actually a fixed unitary. The channel does not add any entropy, and in principle can be completely reversed by the inverse. No further error correction is needed in this case, so arbitrarily long computations are possible. A more interesting case is for a non-unital noise channel, such as the amplitude damping channel. The amplitude damping channel drives qubits towards the $|0\rangle$ state. But this is a cooling process! Given enough time, qubits will relax to an entropy-free state. This means that even though our control is only unitary, we can subvert the noise process to provide fresh ancillas. We prepare ancillas at the beginning of the computation, then use them for error correction. The used ancillas will contain a lot of entropy, so we let them sit for a while. They eventually relax back to the ground state, making them once more suitable for use. For a weak enough amplitude damping channel, a threshold theorem is once again possible.

It turns out that a similar statement can be made for any non-unital error model, but the proof is a bit more complicated. A quantum channel is *non-unital* if it takes the maximally mixed state to a state that is not maximally mixed. The amplitude damping channel is one such channel, but there are many others. One property of non-unital channels (at least when acting on qubits) is that it can be arranged that if the channel is repeatedly applied to the qubit (which corresponds to letting the qubit sit for a very long time), the state of the qubit will approach exponentially close to some fixed point. For the amplitude damping channel, the fixed point is the state $|0\rangle$, but for other non-unital channels, it can be any non-maximally mixed state.

This means that an ancilla qubit left sitting around for a long time will eventually get close to the fixed point. Ancillas prepared at the beginning of the computation may heat up over time, but at least they will

not become completely randomized, so they still have some value. Furthermore, used ancillas also relax to the fixed point; if the fixed point has less entropy than the ancilla does just after error correction, the channel will cool down used ancillas, just as did the amplitude damping channel. If the fixed point is sufficiently close to pure, the entropy in a qubit at the fixed point just acts like a small preparation error rate p_P. If this error rate is below the threshold, we can simply treat it as a source of preparation errors and go through the usual threshold argument.

Even if the fixed point has a significant amount of entropy (but not maximal), there is a trick which enables us to squeeze out some useful ancillas. Our control of the system is limited to unitary operations, which leave the total entropy of a system unchanged. However, nothing says that unitaries can't *move* entropy within the system. There is a technique known as *algorithmic cooling* which uses unitary operators to rearrange the entropy in a system, shuffling most of it into a smaller number of qubits and producing a few nearly pure qubits in the process. A few qubits are cooled down, and in the process, the remaining ones are heated up. Algorithmic cooling only works if we start with a non-maximally mixed state; if the entropy of the system is already maximal (infinite temperature), there is nowhere to push the entropy. Algorithmic cooling is a form of data compression, which also takes entropy (in the form of many possible messages) and rearranges it into a smaller number of qubits. However, in data compression, we are mostly interested in the qubits in the final state which contain lots of entropy, whereas in algorithmic cooling, we are primarily interested in the remaining qubits from which entropy has been removed.

Thus, to reset ancillas after they are used in error correction, we can let them sit for a while, until they reach the fixed point of the channel. Then we perform algorithmic cooling and extract out a few cold ancillas to use again in error correction. The remaining ancilla qubits heat up in the process, but we can once more let them sit and they will again approach the channel's fixed point. This procedure allows us to prove that for an independent error model with *any* non-unital channel on each qubit, a threshold theorem holds; I will omit the full analysis. Notably, this means that even if qubits equilibrate to a bath which is very hot (but finite temperature), a threshold still exists provided that the coupling between the system and bath is sufficiently weak so that the channel in one time step is below the threshold. The temperature of the bath will surely affect the threshold, though: the hotter the bath, the more work we need to do (using more ancilla qubits) to perform algorithmic cooling, and new errors during the algorithmic cooling procedure will ruin it. Precisely how much lower the threshold must be is at present unknown.

Finally, there is an interesting intermediate case with channels such as the dephasing channel. The dephasing channel will leave unchanged a classical basis state $|0\rangle$ or $|1\rangle$, or a mixture of such states, but will cause superpositions to decohere. If we prepare ancillas at the beginning of the computation in the state $|0\rangle$, they will stay there unchanged until we need them. Therefore, in this case it is acceptable to have no fresh ancillas. However, with dephasing noise, there is no way to reset used ancillas. For a computation of length T using n qubits, we will need a total of $O(nT)$ ancillas, and we must have them all from the start. We get a weakened threshold theorem, which says that for weak dephasing noise below the threshold, arbitrarily long quantum computation is possible, but with an overhead that is *polynomial* in the size of the logical circuit rather than polylogarithmic. It is possible to prove that polynomial overhead is the best possible for this situation (dephasing-type channel with no fresh ancillas).

Pure perfect dephasing noise is not at all generic, any more than perfectly unitary noise is. While dephasing noise is an important phenomenon in real systems, and is often the dominant error process, there is always some other source of noise, even if it is much smaller. When dealing with a large quantum computer, we may want to do millions or billions of logical gates, so even small error processes can be important. Thus, realistically, we are either likely to be in a situation like the depolarizing channel, where ancilla qubits will heat up over time, or like a non-unital channel, where we can arrange that ancilla qubits cool down over time. Depending on which sort of noise is present, a threshold may or may not be possible without fresh ancillas.

15.5 Parallelism and Timing

Now let's move from worrying about the timing of measurements to worrying about the timing of gates. We explicitly assumed, as part of the basic model of fault tolerance, that gates could be performed in parallel, but there was the additional implicit assumption that all gates take the same time, so there can only be one gate per qubit per time step. In this section, I'll examine these assumptions and a few other questions relating to gate timing.

15.5.1 The Need for Parallelism

To have a threshold, it is essential to do parallel gates, at least when the storage error rate p_S is non-zero. The reason is simple: Suppose we have a very large quantum computer containing many qubits, but lack the ability to do parallel gates. Even if all we want to do is to safely store these qubits in a noisy environment, we'll need to do something to correct the errors. Correcting errors on qubit 1 requires at least one gate involving qubit 1, and correcting errors on qubit 2 involves at least one gate on qubit 2, and so forth. If we can only do one gate involving c qubits at a time, we can only touch c qubits in each time step. Even if one gate suffices to correct all of those c qubits, we'll still need $\lceil n/c \rceil$ time steps to correct all of the qubits. By the time we get to the last set of qubits, they'll have accumulated storage errors over a very long time; the probability of not having a fault during the waiting period is $(1 - p_S)^{\lceil n/c \rceil}$. As n gets large, this goes to 0. In particular, the probability of error will go above the limit of the code's error correction capability, so the information stored in the qubit will be irreversibly lost.

Now, the basic model for fault tolerance assumes *maximal* parallelism — we can do gates on all qubits simultaneously, as long as no qubit is involved in two different gates. A lower degree of parallelism is also acceptable. It just means that qubits have to wait around some time between gates. For instance, if we can only do gates on one-third of the qubits at a time, we can compensate by putting up to two wait locations before each gate. This alters effective error rates, of course. The storage error rate would triple $p_S \mapsto 3p_S$, and the gate error rate would increase $p_G \mapsto p_G + 2p_S$. Note that the effective physical error rates change, but the logical error rates at level 1 and higher are still determined from the physical error rates by the usual formulas. If the storage error rate is low, it is not too costly to have a lower degree of parallelism, but if the storage error rate is high, the threshold might get lowered significantly. Nevertheless, we still *have* a threshold, provided we have the ability to perform gates on a constant fraction of the qubits in the computer, independent of the size of the computer.

Fault-tolerant protocols lend themselves well to parallelization. Transversal gates are naturally parallel, and even the non-transversal gadgets (including error correction and magic state injection) tend to have a number of transversal components. Thus, in a system capable of maximal parallelism, most qubits are doing something during almost every time step. We can therefore expect that the actual cost of less-than-maximal parallelism is going to be close to the upper bound noted above.

15.5.2 Synchronization of Gates

The next question is what happens when the notion of "time step" is not well-defined because different gates take different amounts of time. The simplest thing to do in such a case is take a time step to be the length of the longest gate (frequently, but not always, the CNOT gate). If the protocol calls for a shorter gate, do it and then wait for the remaining time until the next time step begins. Naturally, this makes the shorter gates a little more noisy since there are more storage errors occurring while they wait for the slower gates to finish, but it doesn't fundamentally alter the model. There is still a threshold, we just need to phrase it in terms of the error rates per time step.

When some gates are shorter than others, it is tempting to just jump ahead to the next gate as soon as we finish the previous one. The risk in doing so is that our qubits will get out of sync. Suppose CNOT gates are slower than H gates, and the idealized version of the circuit has a H on qubit A and a CNOT from qubit B to qubit C for step 1, then a CNOT from qubit A to qubit B for step 2. We can't start the CNOT for step 2 until the CNOT at time 1 is finished, even though qubit A is ready quickly. When it's just a delay due to

one slow gate, this is a minor problem, but if some qubits experience many more slow gates than others, the time difference could get to be quite large. A long wait time allows storage errors to accumulate, so we may have to do error correction on the qubits that are waiting in order to keep them safe. All in all, it is best to avoid this by keeping the gates synchronized. If all qubits are doing short gates at the same time, we can safely move on to the next step quickly, but otherwise, we should move at the pace of the slowest gates.

Another potential cause of synchronization problems comes from fault-tolerant gadgets that take a variable amount of time. For instance, in Shor error correction, one might decide that the number of repetitions of the syndrome measurement should depend on the outcomes. If the initial few measurements show a zero syndrome, you might decide to stop early and not repeat the measurement any more. If the first few measurements disagree on the error, you might want to measure a few extra times to be sure. When looking at the fault-tolerant gadget in isolation, that is OK, the gadget may still satisfy the ECCP and ECRP, but when you look at the circuit as a whole, you'll see that such a procedure is likely to cause synchronization issues. Some blocks of the code will experience fault paths which lead to a short EC gadget, but other blocks will take longer to complete the gadget. In order to properly account for errors in this situation, you must include the wait locations that must be inserted for the quick instantiations of the gadget as they wait for the slower gadgets to catch up. For this reason, the procedure I gave in section 12.2.2 uses a fixed number of repetitions, regardless of the outcomes.

Another example of variable-length gadgets is state preparation. When you test ancilla states and use post-selection to decide which ones to keep, you might want to make different attempts at creating the ancilla state sequential rather than in parallel, in order to reduce the total number of qubits needed at any given time. The difficulty, once again, is that other states being prepared at the same time will take different amounts of time, meaning some of them will have to wait a while before the next step of the computation.

If the storage error rate is low and the cost of qubits or the gate error rate is high, it might still be worth using tricks like these. Just remember to properly account for the cost of waiting when analyzing the system.

15.5.3 Pipelining of Ancillas

This discussion brings up another issue that I've alluded to before: when to prepare ancillas. Fault-tolerant protocols call for a lot of multiple-qubit entangled ancilla states, frequently some state encoded in a block of the QECC being used. If we prepare ancillas too early, they will have to wait around until they are needed, and will accumulate errors while waiting. If we wait until the last minute to prepare ancillas, just before they are needed, then the data qubits have to wait around for the ancillas, leading to more errors on the data qubits.

This is another advantage of standardizing the duration of fault-tolerant gadgets. Then we know exactly when each ancilla will be needed, and we know exactly how long it takes to create the ancilla. We can therefore begin preparing it at precisely the right time so that it will be ready just as it is needed.

Note that preparing ancillas usually takes significantly longer than the parts of the gadget that directly interact with the data block. For instance, Steane EC needs two time steps to perform CNOTs to and from the data block, plus time for a measurement location and Pauli correction step if we don't want to separately track the Pauli frame, a maximum of 4 time steps. Preparing the ancillas, however, requires 5 time steps for the initial encoding, plus a few more to test the ancilla before it is used. Therefore, if we want it to be ready just in time to be used, we need to start making it before the beginning of the *previous* EC gadget. At that time, we'll also be finishing off the preparation of the ancillas for that earlier EC gadget. If there's a $\pi/8$ logical gate sometime soon, we may also be preparing a magic state. In other words, ancilla preparation tends to *overlap*. Since the same types of ancillas are needed over and over again, and the ancillas are needed at staggered times, it is natural to design the computer to pipeline ancilla preparation. Perhaps one location in the computer specializes in encoding the QECC, and then it passes the ancilla blocks to the next location over, which tests ancillas against each other.

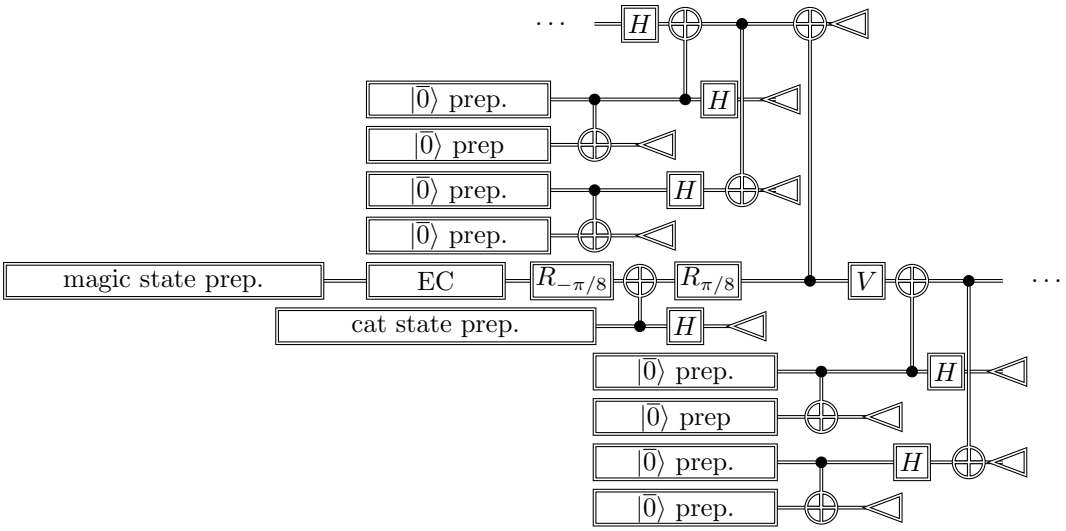

Figure 15.7: A segment of a circuit with ancilla preparation pipelined for an $\overline{H}$, $\overline{R_{\pi/8}}$, and two EC steps. Each of these preparations is done in parallel with 2 copies (not shown) in case one fails post-selection. The EC during magic state preparation requires its own ancillas (not shown). The size of the rectangles for state preparations represents the actual time needed for the non-fault-tolerant preparation circuit.

15.6 Leakage Errors

Now let's move to considering the assumptions about the types of errors allowed. With the basic model of fault tolerance, we said that for each location L, there is no error with probability $1-p$, and with probability p, the location does not implement the desired unitary but instead applies some other CPTP map to the qubit(s) involved in the location. This is not the most general error that can happen. I mean, certainly, the assumption that there is no error at all with probability $1-p$ is not completely general, but even in the case when there is an error, the basic model didn't allow the most general sort of error. The catch is the requirement in definition 10.2 that the error has "the same input and output Hilbert space dimensions as L." It doesn't make sense to allow a different input Hilbert space than L, but it is quite sensible to allow a different output Hilbert space than L.

If the output state is not in the usual computational Hilbert space of the qubit(s) involved in L, the error is an erasure error, or possibly a superposition of an erasure error and some more mundane sort of error that preserves the Hilbert space. Erasure errors are in some sense less serious than other kinds of errors, since a QECC with distance d can correct up to $d-1$ erasure errors but only $\lfloor (d-1)/2 \rfloor$ general errors. In the context of fault tolerance, however, erasure errors that leave the computational Hilbert space (in this context known as *leakage errors*) can present a potentially serious problem. We don't know what happens to qubits outside the usual computational Hilbert space when we perform a gate on them, even if the gate operates as designed. Furthermore, a steady stream of leakage errors could, if we don't counter it somehow, leave us with no valid qubits on which to perform the fault-tolerant protocol.

15.6.1 Leakage Detection

The first defense against leakage is to have some way of detecting it. The details of how to do so will depend on the nature of the leakage and the physical system in which the qubits are implemented.

One category of leakage is when the physical system acting as the qubit is gone. For instance, a qubit stored in the polarization of a photon is susceptible to leakage due to loss of the photon through absorption into a material or escape from the optical fiber, optical cavity, or whatever other device is used to store the

photon. Since the qubit is gone, attempting a gate after a leakage error of this type often produces no result at all (the identity on any other qubits involved in the gate), depending on the details of the implementation. In any case, there is usually a unique state resulting from the leakage, so fault-free gates always produce the same effect, which will be different from the effect of the gate when the qubit has not leaked. Therefore, a small circuit can usually detect the leakage. Once we know the qubit has leaked, we must replace it with a new qubit. This qubit will not necessarily be in the same state as the old qubit, but at this point we can treat it as a conventional erasure error: The data has undergone an error, but we know which qubit was affected.

A second category of leakage occurs when the physical system ends up in a different internal state than those usually used for computation. As an example, consider a qubit stored in the energy level of an electron of a trapped ion. The electron has many possible energy levels beyond the two acting as $|0\rangle$ and $|1\rangle$, so a faulty location in the circuit may cause the electron to end up in one of those other levels. Gates will usually do something when presented with a leakage of this type; however, since there are many possible erroneous internal states, it may not be possible to definitely predict how the leaked qubit will behave. Thus, it is more difficult to identify that the leakage occurred. However, it may be more straightforward to correct a leakage error of this type than it would be for outright loss of the qubit, since all that is needed is to move it back to the intended subspace.

Sometimes, leakage comes with an obvious signature. For instance, an electron in the wrong state may spontaneously emit a photon of a particular wavelength. By monitoring the system for photons of that frequency, we can detect the leakage and counter it, either by rotating the system back into the correct Hilbert space or by simply replacing the qubit with a new one. Either way, we know the qubit that suffered the leakage error, and returning it to the computational Hilbert space turns it into an erasure error.

Occasionally, a leaked qubit might return to the computational Hilbert space by itself. For instance, the electronic energy level in which the qubit ends up as a result of the noise might be very unstable, so the system might rapidly decay down to the ground state, which is used as $|0\rangle$. In that case, the leakage error acts like a regular error (amplitude damping in this example), and doesn't need to be treated separately. We still can treat it as an erasure error if we manage to identify the location of the error, for instance by detecting the photon emitted when the electron decays.

15.6.2 Knill EC and Leakage Recovery

The next strategy is to simply replace qubits with fresh ones whether or not they are known to have leaked. If qubits are constantly being replaced, leakage is automatically contained. Any gates involving a leaked qubit before it is replaced may still be wrong, but that is no worse than the error propagation that could occur from a regular error. One disadvantage of constantly replacing qubits is that it may lead to a potentially higher overhead. A more serious disadvantage is that it forgoes the opportunity to identify the leakage. The replaced qubit must be still be corrected, but without knowledge of where the leakage occurred, it is corrected as a general error rather than an erasure error.

Knill error correction provides this service for free. The qubits that come out of a Knill EC step are physically different qubits from the qubits that entered it. If a qubit in the data block leaks before the start of Knill EC, the leakage will show up in the measurement step of the EC gadget. Depending on the nature of the leakage and the measurement, it may show up as a general error or as a erasure error. For instance, a missing photon will produce neither a $|0\rangle$ or a $|1\rangle$ outcome in the measurement, so it can be easily identified. Based on this, we can correct errors normally, possibly taking advantage of any extra information we have about the erasure. The data block post-EC was originally part of a logical EPR pair created for the Knill EC gadget. Of course, it could have leakage errors of its own, but those errors are *independent* of the errors in the original data block. That is, Knill EC has the effect of restoring qubits to the computational Hilbert space, though naturally they immediately start to leak out again.

Gates performed by teleportation have the same property: The qubits that come out of the gadget are physically distinct from the qubits that enter the gadget. As a consequence, gate teleportation automatically restores qubits to the computational Hilbert space.

If these gadgets are somehow not appropriate to the specific fault-tolerant protocol you are running, it's

still possible to make use of the basic idea. By frequently teleporting qubits, you replace the original qubits with new ones, which restores them to the computational Hilbert space.

Also note that replacing qubits frequently is not incompatible with attempting other forms of monitoring for leakage errors. We can keep watch for tell-tale emitted photons at the same time as using Knill EC. The monitoring then gives us a chance to treat an error as an erasure error, allowing more efficient error correction.

15.7 Biased Errors

The basic error model assumes we have no information ahead of time about what *type* of errors to expect, other than that they are stochastic. Erasure errors offer one way for us to get more information, but there are others. Realistically, we probably will know a lot about the types of errors that occur in our machine. For instance, dephasing and amplitude damping are two common real-world types of error, and both families are much more restricted than general stochastic errors. It is possible to design quantum error-correcting codes that are more efficient for these restricted channels than for general errors of weight t, so it makes sense that we should also see improvements in the threshold when we restrict the error model. If the errors are *biased* — some types of errors are more common than others — we want to use a code that is better at correcting the common errors than the uncommon ones.

Naturally, any fault-tolerant protocol designed for adversarial errors will continue to work for a specific error model, such as a depolarizing channel or a biased Pauli channel. Analysis of existing protocols for a depolarizing channel produces a higher threshold (albeit not by much, perhaps a factor of 2–4) than for adversarial error models. It's not clear whether this is due to overly conservative assumptions in the adversarial model or if the depolarizing channel is simply not the most dangerous type of error. Beyond improving the analysis, if we can figure out how to build a fault-tolerant protocol designed for a specific error model, we would hope to raise the threshold even further.

15.7.1 Bias-Preserving Gates

While there are ways to design QECCs for particular error models, it is not totally straightforward — the stabilizer formalism is only really suited for Pauli channels, although it can sometimes provide insight for other sorts of channels. Even for Pauli channels, the only case that is really straightforward is when phase errors and bit flip errors are independent, with one being more common than the other. Then a CSS code is suitable, using codes C_1 and C_2 with different distances. For more complicated channels, good codes can sometimes be determined numerically or through some ad hoc tricks, but there is no reliable general methodology. (Of course, there is no general methodology for finding the best codes with a given distance, either.)

Unfortunately, tailoring fault-tolerant protocols for particular error models is much harder than doing it for quantum error-correcting codes. The problem is that in a fault-tolerant protocol, errors don't stay put. They move around, and more importantly for current purposes, they change their nature.

For instance, suppose a qubit experiences biased Pauli noise with Z much more common than X. Naturally, this suggests we should use a code that is much better at correcting phase errors than bit flip errors. But suppose we then perform a physical Hadamard transform on one or more qubits of the code. The Hadamard switches X and Z errors, so now X errors are much more common than Z errors on the rotated qubits. Not for long, though: Any new errors that occur still come from the same Pauli channel, so new errors will be predominantly Z errors. If we were to switch to a code that corrects mostly bit flips after the Hadamard, it will not be good at correcting new errors, but a code that corrects mostly phase errors will not be good at correcting the errors that propagated through the H. Gates in a fault-tolerant circuit tend to mix up the types of error, washing out differences in their relative frequency.

Even gates which don't change the type of errors under conjugation can still cause a problem. For instance, the CNOT propagates a Z error into either one or two Z errors, depending if it is on the control or the target qubit. Therefore, a phase error before the CNOT stays a phase error, and naturally a phase error

after the CNOT is a phase error as well. But what about a phase error *during* the CNOT? Gates cannot be performed instantaneously; instead they result from a process which takes some finite time. For instance, CNOT could be performed by turning on the Hamiltonian $\mathcal{H} = \frac{1}{2}(I+Z)\otimes I + \frac{1}{2}(I-Z)\otimes X = \text{CNOT}$ for a time $\pi/2$. (Actually this does iCNOT, which is the same up to a global phase.) Notice that an X appears in the Hamiltonian. Suppose a Z error occurs on the second qubit at time $\pi/4$, and assume the error itself takes negligible time. Then the actual unitary which is performed is

$$e^{-i\pi/4\mathcal{H}}(I\otimes Z)e^{+i\pi/4\mathcal{H}}\text{CNOT} = \frac{1}{2}(I - i\text{CNOT})(I\otimes Z)(I + i\text{CNOT})\text{CNOT} \tag{15.12}$$

$$= \frac{1}{2}[I\otimes Z - 2(I-Z)\otimes Y + Z\otimes Z]\text{CNOT}. \tag{15.13}$$

Thus, the second qubit could have either a Y or a Z error on it relative to the correct value when the faulty gate is completed. If we do CNOTs on a code that only corrects phase errors in conditions with only dephasing noise, we will be unpleasantly surprised to find that other sorts of error appear during the process.

For qubits, this is an unavoidable problem with CNOT gates. Interestingly, there exist bias-preserving implementations of the CNOT gate if your full physical state space is an infinite-dimensional Hilbert space, such as an electromagnetic field mode, out of which you use an appropriately-encoded two-dimensional computational subspace to act as the "physical" qubit of your quantum computer. (The scare quotes around "physical" are there because this encoding of a qubit in a continuous-variable system is itself a QECC, and the overall encoding is the continuous-variable code concatenated with a qubit code correcting phase errors.) The idea is to implement CNOT with a rotation through the extra degrees of freedom in a continous-variable system in such a way that the dominant source of errors in the system result in qubit phase errors, whether they occur before, during, or after the CNOT. Of course, this approach doesn't solve the problem with Hadamard or other gates that alter the error bias under conjugation.

When a bias-preserving CNOT gate is not available (or the analog for other error models), we should restrict attention to gates which can be implemented using Hamiltonians that commute with the error model. When the Hamiltonian commutes with the error, it doesn't matter when the error occurs relative to the gate, so this condition guarantees the gate will preserve the bias. In the case of pure phase errors, that means using diagonal Hamiltonians, such as two-qubit $Z\otimes Z$ interactions.

Another concern is what happens to errors of the type your code does not specialize in. Because any fault-tolerant protocol involves more locations than the circuit being simulated, there are also more opportunities for something to go wrong. While one type of noise may be much larger than the others, there will always be some contribution from a wide variety of noise sources, and using a fault-tolerant protocol will effectively amplify the error rate for any type of error it does not correct.

15.7.2 Fault Tolerance for Dominant Phase Errors

Despite these obstacles, for the simple case of dephasing, more specialized fault-tolerant protocols can be designed to take advantage of the restricted error model. Great care is needed, and the improvement gained over more general methods of fault tolerance is modest, but there *is* an improvement.

Naturally, for a pure dephasing channel, you want to use a phase correcting code. The 3-qubit code from section 2.2.3 or the obvious generalization to more qubits are good choices. Another good choice is the $XZZX$ code, suitably rotated, which is a relative of the surface codes we will discuss in chapter 17. The trick is then to build the main gadgets of the protocol using only bias-preserving gates, as well as preparation of $|+\rangle$ and X measurements. Diagonal gates commute with Z errors, so cannot ever change a Z error into an X or a Y. The only possible error on $|+\rangle$ is a Z error, since X does nothing even if we somehow manage to cause an X error, and similarly only a Z error changes the outcome of an X measurement. If we are in a system with a bias-preserving physical CNOT gate, we can use that as well. Even without a physical CNOT gate, we have enough tools to build gadgets for the logical $\overline{\text{CNOT}}$ gate and logical preparations and measurements in the $\overline{X}$ and $\overline{Z}$ bases, as well as an error correction gadget. From this point, magic state distillation can complete the universal set of logical gates.

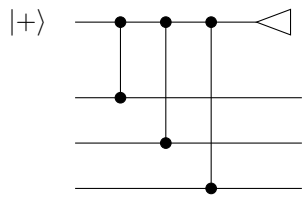

Figure 15.8: Logical X measurement for the 3-qubit phase repetition code

The gadgets for logical $\overline{Z}$ basis preparation and measurement are straightforward: simply perform transversal $|+\rangle$ preparation or transversal X measurement, respectively. In this context, we can consider a gadget to be fault-tolerant if it uses only phase-error-friendly locations and satisfies the usual fault-tolerant properties, but for numbers of phase errors instead of numbers of general Pauli errors. See section 16.3 for a more general discussion of what it means to be fault-tolerant beyond the usual definitions.

To measure in the logical $\overline{X}$ basis, we need ancillas. The logical $\overline{X}$ operator for this code is $Z \otimes Z \otimes Z$. We can measure this with a single ancilla qubit by performing three $\mathrm{C}-\mathrm{Z}$ gates between the three qubits of the code and the ancilla, which should start in the state $|+\rangle$. Then measure the ancilla in the X basis for the answer. Of course, using one ancilla qubit is not fault tolerant, but we can repeat the procedure for greater certainty. The whole circuit is shown in figure 15.8. Note that we don't need to worry about error propagation from the ancilla into multiple qubits of the code: There are only phase errors, which cannot propagate through a $\mathrm{C}-\mathrm{Z}$ gate. We can similarly measure tensor products of logical $\overline{X}$ on multiple blocks, e.g., $\overline{X} \otimes \overline{X}$ or $\overline{X} \otimes \overline{X} \otimes \overline{X}$.

The measurement gadget is non-destructive, so we can make a $|\overline{+}\rangle$ state by preparing a $|\overline{0}\rangle$ and making a logical $\overline{X}$ measurement. If we get the $+1$ outcome, we have the desired $|\overline{+}\rangle$ state; otherwise, we are left with an $|\overline{-}\rangle$ state. We could just discard a $|\overline{-}\rangle$ outcome and try again, but the procedure is a bit more efficient if instead we keep track of the fact that the state has a $\overline{Z}$ relative to the correct state. That is, update the Pauli frame (as in section 12.5.2) of the logical state to account for the preparation. Note that directly performing an actual $\overline{Z}$ gate on the state would be a bit tricky, since $\overline{Z} = X \otimes I \otimes I$, which is not diagonal, and therefore runs the risk of producing non-phase errors if a fault occurs during the gate. However, updating the Pauli frame is just a conceptual trick. It happens instantaneously and perfectly, so there is no need to worry about faults during the update. In principle, we do need to worry about error propagation, but a Pauli update simply adds a global phase to existing Pauli errors.

The error correction gadget uses a variant of Knill EC. Normally Knill EC is based on regular teleportation, using two ancilla blocks and a Bell measurement. For a phase-error-correcting code, we can instead use one of the one-bit teleportation circuits from figure 13.6. One ancilla block is sufficient because the syndrome only needs to specify the phase errors in the code, whereas a regular QECC needs a big enough ancilla for both bit and phase flip errors. If we don't have a bias-preserving CNOT gate, we can substitute measurements. If the ancilla starts as $|\overline{0}\rangle$, then we non-destructively measure $\overline{X} \otimes \overline{X}$, and finish by measuring the original data block with a transversal X measurement, which includes the $\overline{Z}$ measurement but also determines the error syndrome. The $\mathrm{C}-\mathrm{Z}$ gates in the $\overline{X} \otimes \overline{X}$ measurement commute with any Z errors in the state, so the transversal X measurement will pick up any pre-existing or new Z errors, but only ones in the data block. You can check that a logical $\overline{X} \otimes \overline{X}$ followed by $\overline{Z}$ does in fact perform a one-bit teleportation in the absence of faults. Each of the two measurements has two outcomes, and each outcome can result in a different logical state. The four possible results correspond to the original logical state with one of the four Paulis I, $\overline{X}$, $\overline{Y}$, $\overline{Z}$ on it. Once again, absorb the logical Pauli into the Pauli frame.

A logical $\overline{\mathrm{CNOT}}$ can be performed by a transversal CNOT in the opposite direction. If we don't have bias-preserving physical CNOT gates, we have to work harder, but a $\overline{\mathrm{CNOT}}$ gadget can also be performed using an appropriate sequence of measurements, as given in figure 15.9. Let us analyze the unencoded version of this circuit using the techniques from section 6.2. (This is precisely the type of application those techniques are meant for.) We start with two data qubits A and B and two ancilla qubits 1 and 2. The

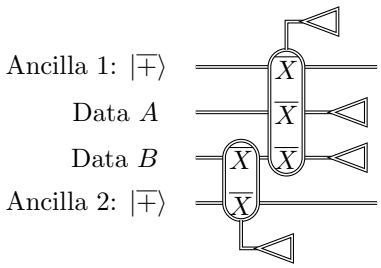

Figure 15.9: CNOT gadget for a phase-correcting code. The ovals represent non-destructive measurements.

stabilizer initially is $\langle Z_1, Z_2\rangle$, and the generators of the logical Pauli group are

$$\overline{X}_A = X_A \tag{15.14}$$
$$\overline{Z}_A = Z_A \tag{15.15}$$
$$\overline{X}_B = X_B \tag{15.16}$$
$$\overline{Z}_B = Z_B. \tag{15.17}$$

If the first measurement, of $X_B \otimes X_2$, has outcome -1, we can restore it to the same state as the $+1$ outcome by performing Z_B. (This can be done by absorbing the Z_B into the Pauli frame.) Afterwards, we have a stabilizer $\langle Z_1, X_B \otimes X_2\rangle$ and logical Paulis

$$\overline{X}_A = X_A \tag{15.18}$$
$$\overline{Z}_A = Z_A \tag{15.19}$$
$$\overline{X}_B = X_B \tag{15.20}$$
$$\overline{Z}_B = Z_B \otimes Z_2. \tag{15.21}$$

The next measurement is of $X_A \otimes X_B \otimes X_1$, and we can ensure the outcome of $+1$ by absorbing Z_1 into the Pauli frame if needed. The stabilizer after the measurement is $\langle X_A \otimes X_B \otimes X_1, X_B \otimes X_2\rangle$ and the logical Paulis are

$$\overline{X}_A = X_A \tag{15.22}$$
$$\overline{Z}_A = Z_A \otimes Z_1 \tag{15.23}$$
$$\overline{X}_B = X_B \tag{15.24}$$
$$\overline{Z}_B = Z_B \otimes Z_1 \otimes Z_2. \tag{15.25}$$

Finally, we measure Z_A and Z_B. In case of a -1 outcome of Z_A, we add X_1 to the Pauli frame. If exactly one of the two outcomes is -1, add (in addition to X_1, if appropriate) X_2. Once we have done this, the stabilizer of the final state is $\langle Z_A, Z_B\rangle$, indicating the data has been moved to the ancilla qubits. The logical operators are

$$\overline{X}_A = X_1 \otimes X_2 \tag{15.26}$$
$$\overline{Z}_A = Z_1 \otimes I_2 \tag{15.27}$$
$$\overline{X}_B = I_1 \otimes X_2 \tag{15.28}$$
$$\overline{Z}_B = Z_1 \otimes Z_2. \tag{15.29}$$

That is, we have done the CNOT on qubits A and B while transferring them to qubits 1 and 2.

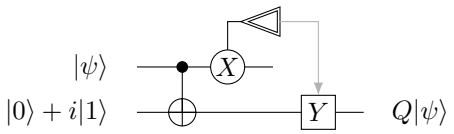

Figure 15.10: Compressed teleportation circuit for Q gate

The magic states for the $R_{\pi/4}$ and $R_{\pi/8}$ gates are $|0\rangle + i|1\rangle$ and $|0\rangle + e^{i\pi/4}|1\rangle$, respectively. They can be distilled using the 7-qubit code and 15-qubit code, respectively. See section 13.5 for an analysis of the 15-qubit code. Distillation of $|0\rangle + i|1\rangle$ using the 7-qubit code is very similar, using the fact that the transversal $R_{\pi/4}$ does a logical $\overline{R_{-\pi/4}}$. Both of these codes are CSS codes and can be encoded using only CNOTs plus $|0\rangle$ and $|+\rangle$ preparation. They can be decoded using only CNOTs; the syndrome measurement then requires both X and Z measurements. The $R_{\pi/4}$ and $R_{\pi/8}$ gates can be performed using the appropriate compressed gate teleportation circuits, as discussed in section 13.3.

This is not yet a universal of gates, since we don't have the full Clifford group. It can be completed with one more Clifford group gate, such as Q, a single-qubit gate which maps $Y \leftrightarrow Z$. Q can be performed using $|0\rangle + i|1\rangle$ preparation, CNOT, Y (which can be abosrbed into the Pauli frame), and X measurement using the circuit in figure 15.10.

That gives us a complete fault-tolerant protocol when the only errors are phase errors. In a more realistic situation where phase errors are dominant, but other types of errors exist too, we can concatenate a phase-error-correcting code with another more general QECC or use a code like the $XZZX$ code which is capable of correcting all kinds of Pauli errors to some degree. Because we are giving most of our attention to phase error correction and adding extra locations to compensate from the restriction to bias-preserving gates, such a protocol will not be nearly as good at correcting bit flip errors as a protocol which treats phase and bit flip errors more symmetrically. Therefore, this protocol is only helpful if the physical phase error rate is much higher than the rate of other sorts of errors.

Since there are two different error rates we care about, instead of a threshold value, there is a threshold surface in the space of phase and non-phase error rates. We can get an idea of its shape by studying specific points. For instance, suppose we concatenate the phase-correcting code with Knill's high-threshold post-selection based protocol (see section 16.1) and we don't have bias-preserving CNOT gates. Then, when the phase error rate is 2.5×10^{-3} and the non-phase error rate is 2.5×10^{-7}, the system is provably inside the threshold surface. A better decoding algorithm for the concatenated code allows this to be increased to 3.5×10^{-3} rate of phase errors and 3.5×10^{-7} for non-phase errors. Compare this to a proven threshold of at least 10^{-3} for stochastic noise with an unspecified bias. By taking advantage of the bias in the error rates, we can get an improvement in the threshold, albeit a modest one.

Based on simulations (and using a slightly different error model), when phase errors are 100 times more likely than bit flip errors, the $XZZX$ code can achieve an improvement of above a factor of 1.5 over the standard surface code approach, or a factor of about 2 improvement using the bias-preserving CNOT gate. This puts the threshold for the $XZZX$ code at about 2% in this model.

15.8 Error Independence and Non-Markovian Errors

In the previous section, we discussed errors that are more restricted than the errors in a basic model of fault tolerance. Now it's time to consider errors which are more general. This means errors which are correlated between locations and coherent errors that cannot be adequately described by a stochastic error model. Correlations could be between errors in different locations at the same time, or between locations at different times but possibly in the same physical position. The latter could be a consequence of manufacturing defects in a small fraction of the physical qubits, causing locations involving them to be frequently faulty. Correlations in time could also be the result of interaction with a non-Markovian environment, one which has a memory. With a non-Markovian environment, errors at one time can be influenced by the state of the

computer at a previous time.

15.8.1 Correlated Errors

First, let's take the simplest case, correlations between errors in locations at the same time. Furthermore, for the analysis, let's assume that we have a stochastic error model. The adversarial stochastic model already allows correlations between the types of errors at different locations, but we want to consider potentially more general correlated error models.

Certainly, we can't expect to handle completely arbitrary correlations. For instance, with some very small probability p_{meteor}, there is a chance a meteor strikes the quantum computer, completely destroying all the qubits. A more realistic example with a similar effect is a power failure. No amount of error correction will take care of that. Generally, the probability of extreme failures like this is small enough that we ignore it. If you are really concerned, however, you could disperse the qubits in the quantum computer to a number of distant locations, using entanglement to connect them up. That way, even a meteor can only destroy a small fraction of the qubits in the computer.

The more normal versions of correlated errors affect only a small number of qubits at once. For instance, suppose the computer has an error source that, with probability p_2, causes a pair of qubits to both have errors at the same time. If the affected qubits are involved in separate locations, both locations are faulty. This sort of error arises naturally from two-body interactions between qubits.

Whether this error source is a serious problem or not depends on what pairs of qubits are eligible to fail simultaneously. If every pair of qubits in the computer can fail independently with the same probability p_2, then the total probability that qubit i is involved in some pair with an error is $1-(1-p_2)^{n-1}$ when there are n qubits in total. That is, when $np_2 \approx 1$, the probability of an error involving qubit i is very large, and it continues to increase with n. When the error rate per qubit is large, well above the threshold, fault tolerance fails. Even if there is no other source of error, the adversarial stochastic model fails to capture this error model for large n unless you set $p \approx 1$.

Luckily, in more realistic situations, qubits which are close together are more likely to have simultaneous errors than qubits which are far apart. Suppose that the probability of a correlated error affecting qubits i and j simultaneously is p_2/r_{ij}^{α}, where r_{ij} is the distance between qubits i and j and $\alpha > 0$ is some exponent describing how quickly the interaction between qubits drops off with distance. For instance, a Coulomb interaction between charges might have $\alpha = 2$, whereas a dipole-dipole interaction might be $\alpha = 6$. (Both those examples would not give stochastic errors, but hopefully you get the idea.) If the qubits are arranged in D spatial dimensions then there are $O(r^{D-1})$ qubits at a distance r from a specific qubit i and the maximum distance is $n^{1/D}$. Thus, the total rate of errors involving qubit i is

$$O\left(\int_1^{n^{1/D}} p r^{D-1-\alpha} dr\right) = \begin{cases} O\left(\frac{p}{D-\alpha}(n^{1-\alpha/D}-1)\right) & D \neq \alpha \\ O\left(p \log n\right) & D = \alpha \end{cases} \tag{15.30}$$

If $D \geq \alpha$, there is a problem still, since there are too many close qubits: the probability of having an error that affects any single qubit diverges as the computer gets large (which really means it approaches 1). This means that for a big quantum computer with such errors, even one time step is enough to completely destroy any stored information.

If $D < \alpha$, however, the error rate per qubit converges. In this case, unlike in section 15.2, being in a lower dimension is good. Assuming the errors on distinct pairs of qubits are uncorrelated, we can then consider the error model to be an adversarial stochastic error model as follows: Consider any set of s locations. If the total probability of having qubit i fail is at most P (including the probability that it is part of a two-qubit fault), then you can show (exercise **??**) that the probability of having faults on all s locations in the set is at most $(1+P)(2P)^{s/2}$ when s is even and $P(2P)^{(s-1)/2}$ when s is odd. We can thus consider this as an adversarial stochastic error model with error probability $p = \sqrt{2P(1+P)}$. Unfortunately, that could lead to a rather low bound on the threshold. For instance, if we need $p < 10^{-3}$ to be below the threshold, then we need roughly $P < 5 \times 10^{-7}$.

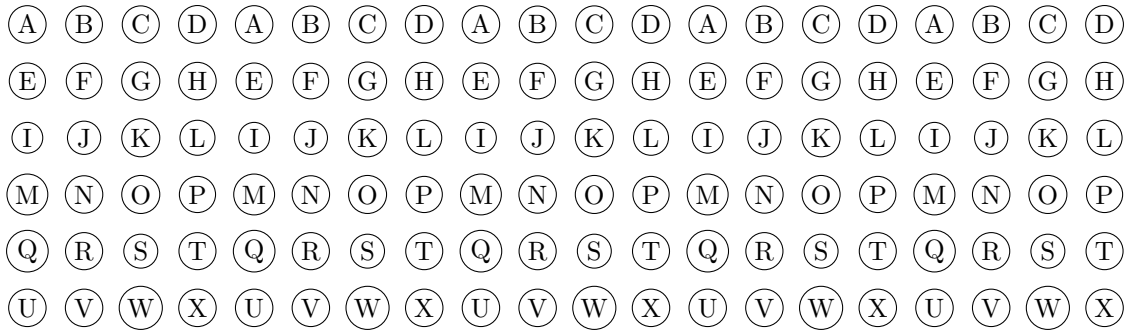

Figure 15.11: An example architecture where qubits in a single block of the QECC are stored far from each other. Qubits labelled by the same letter are part of the same block of the code.

Other options for deriving a better value for the threshold under these conditions haven't been studied carefully. It may make sense in this case to concatenate a code that corrects multiple errors rather than a distance 3 code. There is some evidence that the surface codes discussed in chapter 17 don't have too much more trouble with correlated error pairs that are close together than they do with independent errors. And even for a concatenated distance 3 code, the bound derived in this way from theorem 10.4 might be very poor. Only certain pairs of locations will fail in a correlated way, and a clever design for the fault-tolerant circuit can take advantage of that. For instance, it is probably a good idea to store the qubits in a given block far apart so that it is unlikely they will fail simultaneously. We need to create encoded blocks for preparation gadgets or to use as ancillas, and those will probably need to be made when the qubits are close together, but once the block is encoded, we can separate the qubits and then check the block as in section 13.1. When measurement and classical computation is freely available, the checking can probably be done with only transversal quantum gates.

The recommendation that qubits in the same block should be far apart may seem to contradict the architecture recommendations from section 15.2, where I suggested that the qubits in a block be stored locally along with all the ancilla qubits needed. That perception is correct, there really is a tension between the two suggestions. How it should be resolved depends on the relative importance of communication costs vs. correlated local errors. If communication between distant qubits is cheap, but correlated errors between nearby qubits are common, the qubits in a block should be far apart. If correlated errors are not very important, but communication is expensive, the qubits in the block should be close together. When both are important, it is best to find an appropriate middle ground, or to find a different solution to one or both problems.

15.8.2 Handling Coherent Errors

The next variation of error model to consider is when errors are not stochastic. We'll start by considering the case where errors on different locations are independent, but they are not stochastic. Recall that an independent (but not stochastic) error model associates a quantum channel with each location in the noisy circuit, with no further constraint on the form of the channels. We can no longer talk about the error probability for a location, but there is a natural sense in which we can say that the error rate is low. Specifically, we can compare the ideal operation $\mathcal{O}_L$ associated with location L to the actual channel $\mathcal{E}_L$ performed at L by the noisy circuit, and the error rate ϵ_L of L is low if the distance between the two channels is small:

$$\|\mathcal{O}_L - \mathcal{E}_L\|_\diamond < \epsilon_L. \tag{15.31}$$

The general independent error model incorporates a wider range of realistic channels than the independent stochastic model. For instance, amplitude damping on each qubit is an independent error model but not a stochastic one. Another good example is systematic over-rotation or under-rotation. Imagine that every time

we try to perform a gate e^{-itH}, we instead perform $e^{-i(t+\delta)H}$ for some fixed small δ, or even a δ that varies in some deterministic way from gate to gate. The actual effect of a location with over- or under-rotation is a unitary transformation, it is just not quite the right one. Therefore, the error model is not stochastic, but it is independent, and the error rate is low:

$$\|e^{-itH} - e^{-i(t+\delta)H}\|_\diamond = \|I - e^{-i\delta H}\|_\diamond \leq O(\delta\|H\|). \tag{15.32}$$

(However, if δ is a random variable equally likely to be positive and negative, then the average over δ turns this quantum channel back into a stochastic error.) An error model performing coherent rotations like this is potentially worrisome, because there is the possibility of constructive interference between the errors acting on different locations.

Nevertheless, the threshold theorem can be extended to apply to all independent error models. Theorem 1.1 doesn't quite apply, since it is designed for single qubits and some locations involve 2 or more qubits. More importantly, we need a bit more information than is provided by theorem 1.1 about which sets of qubits the errors act on. Still, the philosophy behind theorem 1.1 is very much in force. The independent error model with small coherent errors can be well approximated by an error model with large errors on a limited number of qubits and perfect gates elsewhere. I won't go through the whole argument and will be a bit sloppy about the details, since the result will be subsumed by theorem 15.5, but I hope you get the idea nevertheless.

In this case, one straightforward thing to do is to purify each quantum channel by adding environment qubits. Since the error model is independent, each location has a separate set of environment qubits. Let U_L be a purification of the ideal location and V_L be a purification of the actual noisy location. We can always choose the purifications so that

$$\|U_L - V_L\| < \epsilon, \tag{15.33}$$

where ϵ is some straightforward function of $\max_L \epsilon_L$. To be consistent, we purify all measurement locations as well and perform the classical processing of measurement results using idealized noiseless quantum gates.

The overall effect of the noisy circuit $\widetilde{C}$ on the computer qubits plus environment qubits is $\prod_L V_L$, where the product is taken in the correct order for the locations in the circuit. This can be expanded in terms of Pauli fault paths on the computer qubits, since the set of all Pauli fault paths spans the full matrix algebra. Actually, what we want to do is sum over Pauli fault paths *relative to the ideal circuit* C:

$$\prod_L V_L = \sum_{\Phi=(\Omega,\{P_L\})} \epsilon_\Phi \prod_L P_L U_L, \tag{15.34}$$

where P_L is the Pauli associated with L if $L \in \Omega$, and $P_L = I$ otherwise. The state at the end of the computation is therefore a superposition over results obtained from various possible Pauli fault paths. We know from theorem 14.2 that a fault path Ω such that all exRecs are good leads to exactly the correct output state (once we have traced over ancillas and environment qubits). ϵ_Φ is the amplitude for Pauli fault path Φ, so the question we must answer is the value of ϵ_Φ for Pauli fault paths that result in bad exRecs. In the context of a concatenated code, we are worried about bad exRecs at the top level of concatenation.

Since U_L is close to V_L, we can set a bound on ϵ_Φ. For a 1-qubit gate, we write

$$V_L = (\epsilon_I I \otimes A_I + \epsilon_X X \otimes A_X + \epsilon_Y Y \otimes A_Y + \epsilon_Z Z \otimes A_Z)U_L, \tag{15.35}$$

with $\|(\epsilon_I - 1)I + \epsilon_X X + \epsilon_Y Y + \epsilon_Z Z\| < \epsilon$. X, Y, Z act on the computational qubit involved in the gate and A_P acts on the environment qubit(s) for the gate. We have chosen the ϵs to be non-negative and so that $\|A_P\| = 1$. It then follows that $|\epsilon_I - 1| < c\epsilon$ and

$$\epsilon_X + \epsilon_Y + \epsilon_Z < c\epsilon \tag{15.36}$$

for some constant c. We have a similar equation for multiple-qubit gates U_L. By unitarity of V_L, $|\epsilon_I|^2 A_I A_I^\dagger + |\epsilon_X|^2 A_X A_X^\dagger + |\epsilon_Y|^2 A_Y A_Y^\dagger + |\epsilon_Z|^2 A_Z A_Z^\dagger = 1$, so $\epsilon_I \leq 1$. Then for the Pauli fault path $\Phi = (\Omega, \{P_L\})$,

$$\epsilon_\Phi = \prod_L \epsilon_{P_L}. \tag{15.37}$$

To find the total amplitude for a fault path Ω, sum over all Pauli fault paths Φ consistent with it:

$$\epsilon_\Omega = \sum_{\Phi=(\Omega,\{P_L\})} \epsilon_\Phi = \left(\prod_{L\notin\Omega} \epsilon_I\right)\left[\prod_{L\in\Omega} (\epsilon_X + \epsilon_Y + \epsilon_Z)\right] < (c\epsilon)^{|\Omega|}. \tag{15.38}$$

If instead we are interested in calculating the total amplitude for a fault path within a given part of the circuit, we can simply ignore the locations outside that region. Since the purified faulty operation is unitary on the locations we ignore, it won't contribute to the total amplitude one way or another. In particular, the amplitude to have faults on some particular set of r locations, regardless of what happens at other locations, is at most $(c\epsilon)^r$. This is very similar to the condition for an adversarial stochastic model, but instead of a probability of error, we have a bound on the total amplitude of fault paths with this property.

Definition 15.1. Given a particular Pauli fault path Φ, by lemma 14.5, the behavior of the noisy fault-tolerant simulation $\widetilde{FT(C)}$ of the circuit with the fault path Φ is equivalent to a noisy version of C with faults on locations that correspond to the bad exRecs. That is, given a fault path Ω, we can define a *logical fault path* or *level* 1 *fault path* Ω_1 which is the set of locations corresponding to bad exRecs for the level 1 fault-tolerant simulation with the fault path Ω. The *level* l *fault path* Ω_l can be defined similarly as the set of locations corresponding to the bad exRecs for the level l fault-tolerant simulation.

We can bound the total amplitude for a particular level l fault path by adding up the amplitudes for all the level $l-1$ fault paths that would result in that level l fault path. The calculation is more subtle than that for the adversarial stochastic model because now we are bounding the sum of the amplitudes of a set of fault paths rather than the probability of the set (and recall that there are inevitable correlations at levels 1 and higher because of the overlapping exRecs). I will discuss how to do the sum in the proof of theorem 15.5. The upshot is that, just as before, there is a threshold value ϵ_T, and if $\epsilon < \epsilon_T$, then the total amplitude of "bad" fault paths (i.e., those for which the level l fault path Ω_l is non-trivial) goes to zero as a double exponential in the level. Thus, the final state of the circuit has very high fidelity to one which results from a circuit with only good level l exRecs, which in turn gives the correct answer.

15.8.3 Handling Non-Markovian Errors

Once we allow correlations in space or time, it becomes a bit more complicated to deal with coherent errors. The argument above depended on the fact that if we are interested in the error path in a particular region of the circuit, we can ignore stuff that happens in different regions of the circuit. That's no longer true with error correlations, since the conditional amplitude of an error elsewhere might be much higher than the unconditional error amplitude.

There's also the question of how to model correlated coherent errors. If we are only interested in correlations in space and not in time, we can just say the noisy circuit performs some quantum channel at each time step, although it's still not obvious how to say that the errors are "small" in such a model. When the environment has a persistent memory, CPTP maps no longer suffice, since the environment can generate entanglement between qubits at different times, or return a qubit that leaked away earlier, or any number of other things that cannot happen with CP maps. The most common way to model such systems is to write down a Hamiltonian interacting the system and the environment.

Definition 15.2. A *non-Markovian error model* is a Hamiltonian $\mathcal{H} = \mathcal{H}_S + \mathcal{H}_B + \mathcal{H}_{SB}$. $\mathcal{H}_S$ is the *system Hamiltonian*. It acts only on the qubits in the computer, including any ancilla qubits, and implements the ideal gates of the circuit being performed. Assume any measurements and classical computation have been implemented coherently with qubits, with noiseless qubits replacing classical bits. $\mathcal{H}_B$ is the *bath Hamiltonian*; it acts only on environment qubits and represents the internal dynamics of the bath. The bath does not need to be composed of qubits — it can be any quantum system. $\mathcal{H}_{SB}$ goes by many names, such as *noise Hamiltonian* or *system-bath Hamiltonian*. It represents the actual source of errors, and acts on both computer qubits and environment qubits. A *t-local non-Markovian error model* has $\mathcal{H}_{SB} = \sum_T \mathcal{H}_T$, where T runs over sets of up to t computer qubits, and $\mathcal{H}_T$ acts on qubits in T and any number of environment

qubits. The *noise strength* of a t-local non-Markovian error model is $\max_T \|\mathcal{H}_T\|_\infty$. All Hamiltonian terms may be time-varying.

For simplicity, I will use units of time so that one computational time step takes one unit of time and units of energy so that $\hbar = 1$.

The terms $\mathcal{H}_{SB}$ are supposed to contain all the error sources for the computation. This includes both interactions with the environment causing decoherence and errors in the implementations of gates. In the remainder of this section I will consider only 1-local non-Markovian error models. Note, though, that this doesn't quite subsume earlier error models, even the independent stochastic error model. In an independent stochastic error model, a faulty gate can produce errors on all the qubits involved in a gate. When $\mathcal{H}_{SB}$ involves only single-qubit terms, it can still generate two-qubit errors via interaction with terms in $\mathcal{H}_S$ used to perform two-qubit gates. However, not all possible errors on two qubits can be generated this way. In order to fully incorporate gate errors, we need to consider 2-local or 3-local non-Markovian error models when the circuit involves 2- or 3-qubit gates. Provided the multi-qubit terms in $\mathcal{H}_{SB}$ are restricted to just locations where gates are being performed, or if the strength of correlated errors on distant qubits drops sufficiently fast, as discussed in section 15.8.1, a version of theorem 15.5 still holds.

Theorem 15.5. *There exists a threshold value p_T such that if the noise strength of a 1-local non-Markovian error model is below p_T, then for arbitrary T, $\epsilon > 0$, there exists a fault-tolerant simulation of any circuit of size T which gives an output within statistical distance ϵ of the correct output distribution. The overhead for the fault-tolerant simulation is polylogarithmic in T/ϵ.*

Proof. First, we need to show that we can break the computation up into a sum over fault paths.

Lemma 15.6. *The overall time evolution of the system from initialization at time 0 to the end of the computation at time T can be written as*

$$U = \sum_{\Omega} W_\Omega, \tag{15.39}$$

where the sum is taken over fault paths Ω and W_Ω is an operator acting on the system and environment that performs the correct ideal operation at locations $L \notin \Omega$. If the noise strength is at most p, and the circuit uses gates acting on at most m qubits, then

$$\|W_\Omega\|_\infty \leq (mp)^{|\Omega|}. \tag{15.40}$$

Furthermore, let

$$E_\Omega = \sum_{\Xi \supseteq \Omega} W_\Xi \tag{15.41}$$

be the sum over all fault paths containing a given fault path Ω. Then

$$\|E_\Omega\|_\infty \leq (mp)^{|\Omega|} \tag{15.42}$$

as well.

W_Ω is the non-unitary, non-CPTP operator performing the action on the system when the fault path is exactly Ω, whereas E_Ω is the operator performing the action on the system when there are faults in the locations of Ω and arbitrary behavior elsewhere.

Proof of Lemma 15.6. The first step is sometimes referred to as "trotterization": We use the Trotter formula to break the time evolution up into very small time steps of size Δ.

$$U = \lim_{\Delta \to 0} \prod_{j=0}^{\lceil T/\Delta \rceil - 1} e^{-i\mathcal{H}_S(j\Delta)\Delta} e^{-i\mathcal{H}_B(j\Delta)\Delta} e^{-i\mathcal{H}_{SB}(j\Delta)\Delta}. \tag{15.43}$$

(If the Hamiltonian terms do not vary smoothly, this formula may need to be slightly adjusted, but it won't have a big impact on the argument except for complicating the notation.) U is the overall unitary evolution of system plus bath over the course of the computation, which lasts for a time T.

There are $1/\Delta$ small time steps for each computational time step, but not very much happens in each small time step. Let us expand

$$e^{-i\mathcal{H}_{SB}(j\Delta)\Delta} = I - i\Delta\mathcal{H}_{SB}(j\Delta) + O(\Delta^2) = I - i\Delta\sum_a \mathcal{H}_a(j\Delta) + O(\Delta^2). \tag{15.44}$$

Since we are taking the limit $\Delta \to 0$, the $O(\Delta^2)$ terms are negligible. The sum over a is taken over physical locations in the computer (not the bath), and the terms $\mathcal{H}_a$ are the terms in the expansion of $\mathcal{H}_{SB}$, which is 1-local. We get

$$U = \lim_{\Delta\to 0} \prod_{j=0}^{\lceil T/\Delta\rceil - 1} e^{-i\mathcal{H}_S(j\Delta)\Delta} e^{-i\mathcal{H}_B(j\Delta)\Delta} [I - i\Delta\sum_a \mathcal{H}_a(j\Delta)] \tag{15.45}$$

$$= \lim_{\Delta\to 0} \sum_{r=0}^{N\lceil T/\Delta\rceil} \sum_{\Phi=((j_0,a_0),(j_1,a_1),\ldots,(j_{r-1},a_{r-1}))} V_{\Phi,\Delta}. \tag{15.46}$$

We get the second line by distributing the product over the difference in brackets in the first line. In the inner sum, Φ runs over sets of pairs (j,a), with a a physical qubit and j a precise time (as a multiple of Δ) within the time step of the location. (j,a) is thus a more fine-grained location. We can assume the qubits are ordered in some way, that $a_k \le a_{k+1}$, and if $a_k = a_{k+1}$, then $j_k < j_{k+1}$. N is the total number of physical computation qubits and $V_{\Phi,\Delta}$ is

$$V_{\Phi,\Delta} = \prod_{j=0}^{\lceil T/\Delta\rceil - 1} e^{-i\mathcal{H}_S(j\Delta)\Delta} e^{-i\mathcal{H}_B(j\Delta)\Delta} O_{j,\Phi,\Delta} \tag{15.47}$$

$$O_{j,\Phi,\Delta} = \prod_{a|(j,a)\in\Phi} (-i\Delta\mathcal{H}_a(j\Delta)). \tag{15.48}$$

Φ is a sort of detailed fault path, indicating where $\mathcal{H}_{SB}$ acts in the small time steps. r is the number of errors — insertions of $\mathcal{H}_a$ for some a — that appear in Φ. Note that $V_{\emptyset,\Delta}$, for trivial Φ, is the tensor product of the correct time evolution for ideal gates with some bath evolution given by $\mathcal{H}_B$. However, $V_{\Phi,\Delta}$ is probably not unitary when Φ is non-trivial.

Let us bundle together all the detailed fault paths that have errors in the same locations, i.e., all the Φ that give rise to the same fault path Ω, in the usual sense of fault path. Let

$$W_{\Omega,\Delta} = \sum_{\Phi \text{ producing } \Omega} V_{\Phi,\Delta} \tag{15.49}$$

For each location $L \in \Omega$, we must include Φ which have one of the qubits involved in L appearing one or more times. We can organize this sum as follows: For each location $L \in \Omega$, choose a single time step j_L and qubit a_L such that $(j_L, a_L) \in L$. Let $\Phi' = \{(j_L, a_L) | L \in \Omega\}$ be the detailed fault path consisting of just these pairs. Let us say that $\Phi > \Phi'$ if $\Phi' \subseteq \Phi$ and if $(j,a) \in \Phi \cap L$ implies $(j_L, a_L) \in \Phi'$ and either $j \ge j_L$ or $j = j_L$ and $a \ge a_L$; that is, (j_L, a_L) is the earliest fine-grained location in Φ within the location L and Φ contains no locations other than those in Φ'. If the location is a multiple-qubit gate, we order j first by time and then by qubit within the location. Then

$$W_{\Omega,\Delta} = \sum_{\Phi'} \sum_{\Phi > \Phi'} V_{\Phi,\Delta}. \tag{15.50}$$

But the sum over $\Phi > \Phi'$ means that within any location, we are summing over both I and $-i\Delta\mathcal{H}_{SB}$ for every time step within the location after (j_L, L), and thus get $e^{-i\mathcal{H}_{SB}\Delta}$. Thus,

$$W_{\Omega,\Delta} = \sum_{\Phi'} \prod_{j=0}^{\lceil T/\Delta\rceil - 1} \left[e^{-i\mathcal{H}_S(j\Delta)\Delta} e^{-i\mathcal{H}_B(j\Delta)\Delta} O_{j,\Phi',\Delta} \prod_a e^{-i\mathcal{H}_a(j\Delta)\Delta} \right], \tag{15.51}$$

where the product over a is over qubits for which $(j,a) \in L$, $(j_L, a_L) \in \Phi'$ and $j_L < j$. The point of this expansion is that we are identifying the first faulty fine-grained location within every location in Ω and then ignoring all later faults within the same location, since the location has already failed.

The exponentials in equation (15.51) are all unitary, and therefore have norm 1. Thus,

$$\|W_{\Omega,\Delta}\|_\infty \leq \sum_{\Phi'} \prod_{j=0}^{\lceil T/\Delta\rceil - 1} \|O_{j,\Phi',\Delta}\|_\infty \tag{15.52}$$

$$= \sum_{\Phi'} \Delta^{|\Phi'|} \prod_{(j,a)\in\Phi'} \|\mathcal{H}_a(j\Delta)\|_\infty. \tag{15.53}$$

Now, $\|\mathcal{H}_a\|_\infty \leq p$ for all a, and $|\Phi'| = |\Omega|$ since each location in Ω has exactly one fine-grained location in Φ'. For an m-qubit location L, there are at most $m\lceil 1/\Delta\rceil$ possible values of (j_L, a_L), so the total number of terms in the sum over Φ' is at most $(m\lceil 1/\Delta\rceil)^{|\Omega|} = m^{|\Omega|}\Delta^{-|\Omega|}(1 + O(\Delta))$. Thus,

$$\|W_{\Omega,\Delta}\|_\infty \leq (mp)^{|\Omega|}(1 + O(\Delta)). \tag{15.54}$$

Let $W_\Omega = \lim_{\Delta\to 0} W_{\Omega,\Delta}$, and we find that $\|W_\Omega\|_\infty \leq (mp)^{|\Omega|}$.

Notice that for locations outside Ω, W doesn't involve any insertions of $\mathcal{H}_{SB}$. $\mathcal{H}_S$ commutes with $\mathcal{H}_B$, since the former acts only on the system and the latter only on the bath. Furthermore, at a fixed time, $\mathcal{H}_S$ can be written as a sum of terms $\mathcal{H}_{S,L}$ acting on different locations, and those terms all commute as well. Therefore, for any location L with no insertions of $\mathcal{H}_{SB}$, W contains a factor

$$\prod_j e^{-i\mathcal{H}_{S,L}(j\Delta)\Delta} \to U_L, \tag{15.55}$$

the correct ideal unitary for that location.

Now consider E_Ω. We can bound the norm of it in much the same way as we did for W_Ω. Let $E_{\Omega,\Delta} = \sum_{\Xi\supseteq\Omega} W_{\Xi,\Delta}$, so $E_\Omega = \lim_{\Delta\to 0} E_{\Omega,\Delta}$. Then

$$E_{\Omega,\Delta} = \sum_{\Xi\supseteq\Omega} \sum_{\Phi' \text{ for } \Xi} \sum_{\Phi > \Phi'} V_{\Phi,\Delta} \tag{15.56}$$

$$= \sum_{\Phi' \text{ for } \Omega} \sum_{\Phi''\rhd\Phi'} V_{\Phi'',\Delta}. \tag{15.57}$$

For the inner sum over Φ'' in the second line, we say $\Phi'' \rhd \Phi'$ if $\Phi' \subseteq \Phi''$ and if, whenever $(j,a) \in \Phi'' \cap L$ and $(j_L, a_L) \in \Phi'$, then either $j \geq j_L$ or $j = j_L$ and $a \geq a_L$. That is, Φ'' contains locations other than those in Φ', but if a location in Φ'' is also in Φ', then the time of Φ' is earlier.

This means we end up summing over I and $-i\Delta\mathcal{H}_a$ not just for the time steps after a fine-grained location in Φ', but also for all locations $L \notin \Omega$. Thus,

$$\sum_{\Phi''\rhd\Phi'} V_{\Phi'',\Delta} = \prod_{j=0}^{\lceil T/\Delta\rceil - 1} e^{-i\mathcal{H}_S(j\Delta)\Delta} e^{-i\mathcal{H}_B(j\Delta)\Delta} O_{j,\Phi',\Delta} \prod_a e^{-i\mathcal{H}_a(j\Delta)\Delta}, \tag{15.58}$$

where the product over a is now over qubits for which either the location L containing (j,a) is not in Ω or $L \in \Phi'$ and $j_L < j$. The remainder of the calculation for E_Ω is identical to that for W_Ω, so we get the same bound. □

For any fault path Ω, use procedure 14.1 to assign truncation and determine whether each exRec is good or bad. We'd like to bound $\|\sum W_\Omega\|_\infty$ summed over any fault paths Ω that lead to bad exRecs at the top level of concatenation.

A natural way to derive such a bound would be to bound $\|W_\Omega\|_\infty$ over individual fault paths and then sum over fault paths. The problem with this plan is that it is doomed to failure: $\|\sum W_\Omega\|_\infty$ can be potentially be quite large as the system gets big because the amplitude to *not* have an error in a single location can be greater than 1. Amplitudes are not probabilities and the different fault paths need not be orthogonal, so there is potentially coherence between fault paths with and without errors, which is why the amplitude can be greater than 1. Another way of thinking about this is that because errors can add coherently, adding more fault paths to the sum can *reduce* the norm of the sum. With stochastic noise, we could safely overestimate the set of malignant fault paths, since extra fault paths only increased the probability, but doing that with coherent noise could lead to a false sense of security.

The solution is to work not with W_Ω but E_Ω, which is much better behaved. In particular, we can break the computation down level-by-level using a level reduction theorem:

Lemma 15.7. *Suppose we have a purely unitary computation U simulated by a unitary fault-tolerant protocol $FT(U)$ using a QECC correcting t errors, and the simulation undergoes a non-Markovian noise model which, when purified, can be written as*

$$\widetilde{FT(U)} = \sum_\Omega W_\Omega, \tag{15.59}$$

where the sum is taken over fault paths Ω and W_Ω is an operator acting on the system and environment that performs the correct ideal operation for $FT(U)$ at locations $L \notin \Omega$. Let

$$E_\Omega = \sum_{\Xi \supseteq \Omega} W_\Xi. \tag{15.60}$$

and suppose

$$\|E_\Omega\|_\infty \leq p^{|\Omega|}. \tag{15.61}$$

Then there exists $\widetilde{U}$ (a faulty realization of U) and classical map f taking basis states of the output qubits of $FT(U)$ to basis states of the output qubits of U such that

$$|\langle y|\widetilde{U}|0\rangle|^2 = \sum_{x|f(x)=y} |\langle x|\widetilde{FT(U)}|0\rangle|^2 \tag{15.62}$$

and

$$\widetilde{U} = \sum_\Omega W'_\Omega, \tag{15.63}$$

where the sum is taken over fault paths Ω and W'_Ω is an operator acting on the system and environment that performs the correct ideal operation for U at locations $L \notin \Omega$.

Moreover, if

$$E'_\Omega = \sum_{\Xi \supseteq \Omega} W'_\Xi, \tag{15.64}$$

then

$$\|E'_\Omega\|_\infty \leq (p')^{|\Omega|} \tag{15.65}$$

with

$$p' \leq \binom{A}{t+1} (2ep)^{t+1}. \tag{15.66}$$

Let me clarify a bit what the unitary circuit and purification are doing here. An arbitrary quantum circuit can be turned into a unitary one by replacing any mid-circuit measurement and subsequent classical computation with quantum processing. We do that here, using CNOTs to ancilla qubits which are never reused to decohere measured qubits and quantum gates to perform any classical circuit. Because we are

only studying the unitary circuit part, we assume the computation starts with the state immediately after preparation of $|0\rangle$ states and ends immediately before measurement of the output qubits of the circuit. This is a fairly standard quantum computation trick. The part that needs clarification here is what happens with the purification when we have a noisy realization of the circuit. The assumption is that any imperfections in the state preparation are absorbed into an initial error just after the $|0\rangle$ preparation, which are still perfect. Any qubits prepared after the start of the circuit are instead prepared at the beginning and wait, error-free, until the point at which they are actually invoked in the original non-unitary circuit. Measurements, mid-circuit or at the end, have their errors absorbed into the CNOT gate used to decohere the qubits, and the terminal measurements used to get classical output bits are assumed to be perfect. Any classical processing in the middle is assumed to be perfect as well even though it is being implemented using qubits.

The reason we can get away with assuming all of these modifications have no faults is that they are not real modifications. They are conceptual modifications to enable us to analyze the system as a unitary process rather than a more complicated CPTP map. Thus, we don't have to worry about the issues arising in sections 15.3 and 15.4.

Proof of Lemma 15.7. We can define:

$$W'_\Omega = \mathcal{D} \circ \sum_{\Phi|\Phi\mapsto\Omega} W_\Phi, \tag{15.67}$$

where $\mathcal{D}$ is the ideal $*$-decoder and notation $\Phi \mapsto \Omega$ means Φ is malignant for exactly the exRecs (no more, no less) corresponding to Ω in $FT(U)$. The map f is given by the fact that we have a simulation of U, so there must be a way of classically decoding the outputs of $FT(U)$ to give the outputs of U. Lemma 14.5 (at least the proof of that lemma) shows that W'_Ω has the desired property that it acts perfectly on locations not in Ω and that the decoded output distribution is the same. So all we need to do is to bound $\|E'_\Omega\|_\infty$.

Let C be a subcircuit (i.e., a set of locations in the circuit) and

$$V_{C,\Phi} = \sum_{\Omega|\Omega\cap C=\Phi} W_\Omega. \tag{15.68}$$

Note that a fault path is also a set of locations, but we are thinking of C as a set of locations that might or might not have faults, whereas we generally think of a fault path as a set of locations that do have faults. Then $V_{C,\Phi}$ is the sum over fault paths that have faults within C exactly at the locations of Φ, but outside C can have faults anywhere.

We can write E'_Ω in terms of $V_{C,\Phi}$ operators. Let C_Ω be the union of the exRecs in the simulation corresponding to the locations of Ω. Then

$$\begin{aligned}
E'_\Omega &= \sum_{\Xi\supseteq\Omega} W'_\Xi && (15.69)\\
&= \mathcal{D} \circ \sum_{\Xi\supseteq\Omega} \sum_{\Phi|\Phi\mapsto\Xi} W_\Phi && (15.70)\\
&= \mathcal{D} \circ \sum_{\Phi|\exists\Xi\supseteq\Omega,\Phi\mapsto\Xi} W_\Phi && (15.71)\\
&= \mathcal{D} \circ \sum_{\Phi|\Phi\cap C_\Omega\mapsto\Omega} W_\Phi && (15.72)\\
&= \mathcal{D} \circ \sum_{\Xi\subseteq C_\Omega|\Xi \text{ is malignant for the exRecs in } C_\Omega} V_{C_\Omega,\Xi}. && (15.73)
\end{aligned}$$

There are fewer terms in this sum than in the sum over W_Ξ. If we can bound $\|V_{C_\Omega,\Xi}\|_\infty$, then we can bound E'_Ω. The only assumption we have to help bound $\|V_{C_\Omega,\Xi}\|_\infty$ is that $\|E_\Omega\|_\infty \le p^{|\Omega|}$. We'd therefore like to write $V_{C,\Xi}$ as a sum over groups of fault paths E_Φ.

Claim 15.8. *Consider a subcircuit C and $\Xi \subseteq C$. Then*

$$V_{C,\Xi} = \sum_{s=0}^{|C|-|\Xi|} (-1)^s \sum_{\Phi \subseteq C | \Phi \cap \Xi = \emptyset,\ |\Phi| = s} E_{\Phi \cup \Xi}. \tag{15.74}$$

Proof of Claim. This is an inclusion-exclusion argument, meaning we overcount and then subtract off the extras. But actually we overcount the things to subtract off and so have to add some back, and so on.

We can imagine expanding $E_{\Phi\cup\Xi}$ on the RHS of equation (15.74) into V's. We have that, for $\Upsilon \subseteq C$,

$$E_\Upsilon = \sum_{\Pi \supseteq \Upsilon} W_\Pi \tag{15.75}$$

$$= \sum_{\Lambda_1 | \Upsilon \subseteq \Lambda_1 \subseteq C} \sum_{\Lambda_2 \cap C = \emptyset} W_{\Lambda_1 \cup \Lambda_2} \tag{15.76}$$

$$= \sum_{\Lambda_1 | \Upsilon \subseteq \Lambda_1 \subseteq C} V_{C,\Lambda_1}. \tag{15.77}$$

That is, we sum over all V_{C,Λ_1} for fault paths Λ_1 contained in C and containing Υ.

Let us consider the coefficient of $V_{C,\Phi\cup\Xi}$ on the RHS of equation (15.74) for a particular fault path $\Phi \cup \Xi$. If $\Phi = \emptyset$, the only contribution is from E_Ξ, which matches $V_{C,\Xi}$ on the LHS. Otherwise, if $|\Phi| = s > 0$, then $V_{C,\Phi\cup\Xi}$ shows up in $E_{\Phi'\cup\Xi}$ for any $\Phi' \subseteq \Phi$. There are $\binom{s}{j}$ subsets of Φ of size j, and those terms appear with a coefficient $(-1)^j$ in the sum. The total coefficient of $V_{C,\Phi\cup\Xi}$ on the RHS is thus

$$\sum_{j=0}^{s} \binom{s}{j} (-1)^j = 0. \tag{15.78}$$

This proves the claim. □

Putting this together, we have

$$E'_\Omega = \mathcal{D} \circ \sum_{\Xi \subseteq C_\Omega | \Xi \text{ is malignant for the exRecs in } C_\Omega} V_{C_\Omega,\Xi} \tag{15.79}$$

$$= \mathcal{D} \circ \sum_{\Xi \subseteq C_\Omega | \Xi \text{ is malignant for the exRecs in } C_\Omega} \sum_{s=0}^{|C_\Omega|-|\Xi|} (-1)^s \sum_{\Phi \subseteq C_\Omega | \Phi \cap \Xi = \emptyset,\ |\Phi| = s} E_{\Phi\cup\Xi} \tag{15.80}$$

$$= \mathcal{D} \circ \sum_{\Upsilon \subseteq C_\Omega | \Upsilon \text{ is malignant for the exRecs in } C_\Omega} c_\Upsilon E_\Upsilon. \tag{15.81}$$

In the last line, I have collected together all the times E_Υ appears in the sum. In the previous line, $\Upsilon = \Phi \cup \Xi$, so it is broken up into a malignant fault path Ξ on C and an additional fault path Φ of s extra locations. Of course, adding one or more faults to a malignant fault path produces another malignant fault path, so we get E_Υ once for each fault path $\Xi \subseteq \Upsilon$ which is malignant, and it appears with a coefficient $(-1)^{|\Upsilon|-|\Xi|}$. We therefore have

$$c_\Upsilon = \sum_{s'=0}^{|\Upsilon|} (-1)^{|\Upsilon|-s'} N_{s',\Upsilon}, \tag{15.82}$$

where $N_{s',\Upsilon}$ is the number of malignant fault paths of size s' which are subsets of Υ. Thus,

$$\|E'_\Omega\|_\infty \leq \sum_{\Upsilon \subseteq C_\Omega | \Upsilon \text{ is malignant for the exRecs in } C_\Omega} |c_\Upsilon| \|E_\Upsilon\|_\infty \tag{15.83}$$

$$\leq \sum_{\Upsilon \subseteq C_\Omega | \Upsilon \text{ is malignant for the exRecs in } C_\Omega} \sum_{s'=0}^{|\Upsilon|} N_{s',\Upsilon} p^{|\Upsilon|}. \tag{15.84}$$

Here, we have applied the lemma's assumption on a bound to $\|E_\Upsilon\|_\infty$.

This is substantial progress: Now we have a bound in terms of a sum of a positive quantity over malignant fault paths. That means it is safe to overestimate the number of malignant fault paths to get a bound.

Let M_s be the the number of malignant fault paths containing s physical locations for a single exRec, considering only the fault path within the exRec. If there are different kinds of exRecs, let M_s be the largest value over the possible kinds of exRecs. Then the number of fault paths contained in C_Ω with a total of s physical locations which are malignant for all r of the exRecs of C_Ω is bounded as

$$N_s \leq \sum_{s_1+s_2+\ldots s_r=s} \prod_{i=1}^{r} M_{s_i}. \tag{15.85}$$

It could be fewer, however, since some of the exRecs may be truncated and since not all exRecs may have the maximal value of M_{s_i}. Because we are considering only fault paths within C_Ω, we only truncate an exRec if one of the subsequent exRecs is also in C_Ω.

We can upper bound M_s by simply reverting to the simplest notion of bad exRecs. Then $M_s = 0$ for $s \leq t$ and $M_s \leq \binom{A}{s}$ for $s \geq t+1$, where A is the size of the largest exRec. (And $M_s = 0$ for $s > A$, since there are no fault paths of that size, malignant or benign.)

We can now finish bounding $\|E'_\Omega\|_\infty$ in the case where Ω has r locations (so C_Ω has r exRecs):

$$\|E'_\Omega\|_\infty \leq \sum_{s=0}^{\infty} N_s p^s \sum_{s'=t+1}^{s} \binom{s}{s'} \tag{15.86}$$

$$\leq \sum_{s=0}^{\infty} N_s p^s 2^s \tag{15.87}$$

$$\leq \sum_{s=0}^{\infty} \sum_{s_1+s_2+\ldots s_r=s} \prod_{i=1}^{r} M_{s_i} (2p)^{s_i} \tag{15.88}$$

$$\leq \left[\sum_{s=t+1}^{A} \binom{A}{s} (2p)^s \right]^r \tag{15.89}$$

$$\leq \left[\binom{A}{t+1} (2ep)^{t+1} \right]^r \tag{15.90}$$

The last line uses lemma 1.2; when we are below the threshold, $2p$ will always be small enough for it to apply. Thus, we can identify $p' = \binom{A}{t+1}(2ep)^{t+1}$.

□

Given lemmas 15.6 and 15.7, the threshold theorem for non-Markovian noise follows using the usual argument for the threshold. In particular, lemma 15.6 tells us that $\|E_\Omega\|_\infty \leq (mp)^{|\Omega|}$ when $\max_T \|\mathcal{H}_T\|_\infty < p$. If we have a computation encoded in an l-level concatenated fault-tolerant protocol, then lemma 15.7 tells us that it simulates an $(l-1)$-level concatenated fault-tolerant protocol with

$$\|E_\Omega\|_\infty \leq p_1^{|\Omega|}, \tag{15.91}$$

where

$$p_1/p_T = (mp/p_T)^{t+1}. \tag{15.92}$$

Here,

$$p_T = \frac{1}{2e\left[\binom{A}{t+1}2e\right]^{1/t}}. \tag{15.93}$$

Lemma 15.7 also tells us that the level-$(l-j+1)$ fault-tolerant protocol simulates a $(l-j)$-level fault-tolerant protocol with

$$\|E_\Omega\|_\infty \leq p_j^{|\Omega|}, \tag{15.94}$$

where

$$p_j/p_T = (p_{j-1}/p_T)^{t+1}. \tag{15.95}$$

We thus have that the level-l protocol simulates an unencoded circuit with

$$\|E_\Omega\|_\infty \leq \left[p_T(mp/p_T)^{(t+1)^l}\right]^{|\Omega|}. \tag{15.96}$$

In this simulated circuit, we can write $U = G + B$, with G the good fault path with no faults, and B a sum over fault paths with one or more faulty locations,

$$B = \sum_{\Omega||\Omega|\geq 1} W_\Omega. \tag{15.97}$$

We want to bound $\|B\|_\infty$. Applying claim 15.8 to the case where C is the full circuit, which has T locations, we have

$$\|B\|_\infty = \left\| \sum_{r=1}^{T} \sum_{\Omega||\Omega|=r} \sum_{s=0}^{T-r} (-1)^s \sum_{\Xi|\Omega\cap\Xi=\emptyset,|\Xi|=s} E_{\Omega\cup\Xi} \right\|_\infty \tag{15.98}$$

$$= \left\| \sum_{s'=1}^{T} \sum_{\Phi||\Phi|=s'} \sum_{r=1}^{s'} (-1)^{s'-r} \binom{s'}{r} E_\Phi \right\|_\infty \tag{15.99}$$

$$= \left\| \sum_{s'=1}^{T} \sum_{\Phi||\Phi|=s'} (-1)^{s'+1} E_\Phi \right\|_\infty \tag{15.100}$$

$$\leq \sum_{s'=1}^{T} \binom{T}{s'} \left[p_T(mp/p_T)^{(t+1)^l}\right]^{s'} \tag{15.101}$$

$$\leq Tep_T(mp/p_T)^{(t+1)^l}, \tag{15.102}$$

again applying lemma 1.2 in the last line. As with the threshold theorem for stochastic noise, if $p < 1/(mp_T)$, we can choose $l = O(\log\log(T/\epsilon))$ to ensure that $\|B\|_\infty < \epsilon/2$.

The trivial fault path G gives the correct logical output. If $|0\ldots0\rangle$ is initial state, $U|0\ldots0\rangle = |\psi_G\rangle + |\psi_B\rangle$ is the final state, with $|\psi_G\rangle = G|0\ldots0\rangle$, $|\psi_B\rangle = B|0\ldots0\rangle$. (Note that assuming the initial state $|0\ldots0\rangle$ does not exclude errors in preparation. We can model a potentially faulty preparation location as a one time step interaction with the bath acting on a perfect $|0\rangle$.)

We know that B, the sum of the potentially bad fault paths, has norm at most $\epsilon/2$. The statistical distance between the actual and ideal output distributions is given by at most the trace distance between $|\psi_G\rangle + |\psi_B\rangle$ and $1/N|\psi_G\rangle$, where $N = \||\psi_G\rangle\|$ is a normalization factor. The trace distance is

$$D = \|1/N^2|\psi_G\rangle\langle\psi_G| - (|\psi_G\rangle + |\psi_B\rangle)(\langle\psi_G| + \langle\psi_B|)\|_1 = 2\sqrt{1 - |1/N\langle\psi_G|(|\psi_G\rangle + |\psi_B\rangle)|^2}. \tag{15.103}$$

Since $\||\psi_G\rangle + |\psi_B\rangle\| = 1$, the trace distance is maximized when $|\psi_G\rangle$ and $|\psi_B\rangle$ are orthogonal, which gives $N^2 \geq 1 - (\epsilon/2)^2$, so

$$D \leq 2\sqrt{1 - N^2} \leq \epsilon. \tag{15.104}$$

□

15.8.4 Effect of Coherent Errors on the Threshold Value

When we specialize theorem 15.5 to distance 3 codes ($t = 1$) and 2-qubit gates ($m = 2$), we find the threshold value is

$$p_T = \frac{1}{4e^2\binom{A}{2}}. \tag{15.105}$$

Comparing to the threshold for stochastic noise from theorem 10.4, this is smaller by a factor $4e^2$. One factor of 2 is due to having only single-qubit noise in the non-Markovian error model we considered; if the error rate for stochastic noise is p per qubit, a two-qubit gate has error rate about $2p$. It thus seems like the threshold for non-Markovian noise is smaller than that for stochastic noise by a factor $2e^2 \approx 15$.

However, that perception is deceptive for two reasons. First, remember that these formulas just give lower bounds on the threshold. The true threshold might be much higher. Since the non-Markovian proof is more complex, it may well need more conservative assumptions, leading to a poorer threshold bound. Second, and more importantly, comparing these numbers directly is comparing apples and oranges. They are bounds on two different quantities and we can't expect to compare them directly.

In order to make a fair comparison, let us write a stochastic model using a system-bath Hamiltonian. There is not a unique way to do this, of course, but I'll write down a simple example in order to see how things work out. Let's assume that $\mathcal{H}_S$ and $\mathcal{H}_B$ act as delta functions at integral time steps, and at other times, $\mathcal{H}_{SB}$ is the only time evolution. Let $\mathcal{H}_{SB} = \sum_a \lambda Z_{Ea} \otimes P_a$. Z_{Ea} is Z acting on environment qubit a, while P_a acts on the corresponding computational qubit a. There is also an additional environment qutrit for a, which determines whether P is X, Y, or Z. Then at integer time values, $\mathcal{H}_B$ acts to randomize all the environment registers. The effect of this Hamiltonian is to select a random Pauli $P \in \{X, Y, Z\}$ for each time step and qubit, and do $e^{\pm i\lambda P}$ on that qubit, with + and − equally likely.

Averaging over the + and − yields an equal mixture of $e^{+i\lambda P}$ and $e^{-i\lambda P}$, which is equivalent to performing P with probability $\sin^2(\lambda) \approx \lambda^2$ (when λ is small) and I otherwise. Thus, with probability $1 - \lambda^2$, the qubit stays the same, and with probability λ^2, it undergoes a random Pauli. If the qutrit that determines the Pauli is uniformly random, the channel is a depolarizing channel, but by selecting other distributions for the qutrit, we could get any Pauli channel. For a location involving a two-qubit gate like the CNOT gate, the probability that either qubit has an error is about $p = 2\lambda^2$. By comparison, the noise strength for $\mathcal{H}_{SB}$ is $|\lambda|$.

Now let us compare the threshold we derive via the two versions of the threshold theorem. Theorem 15.5 says that we are below the threshold when

$$|\lambda| < \frac{1}{4e^2\binom{A}{2}}. \tag{15.106}$$

Theorem 10.4 says that we are below the threshold when

$$2\lambda^2 < \frac{1}{\binom{A}{2}}, \tag{15.107}$$

or

$$\lambda < \frac{1}{\sqrt{2\binom{A}{2}}}. \tag{15.108}$$

Thus, the non-Markovian threshold bound is worse not by a factor of $2e^2$, but by a factor of $2e^2\sqrt{2\binom{A}{2}}$ (or by the square of this, depending how you do the comparison). That's a very big difference. The underlying intuition here is that the threshold theorem for the basic model sets a bound on the *probability* of error, whereas the non-Markovian threshold theorem sets a bound on the *amplitude* of error, and the error probability is the square of the amplitude.

On the one hand, this is beneficial in that it means that the bound on $\|\mathcal{H}_{SB}\|$ is weak when the noise is stochastic. For instance, an error probability of 10^{-4}, comfortably below the threshold, corresponds to an error amplitude of around 1%, which seems very achievable. When the size of $\mathcal{H}_{SB}$ is the relevant experimental parameter, that makes things easier.

On the other, however, theorem 15.5 seems to be saying that we need a very low error probability when the noise is non-Markovian, or even coherent but non-stochastic. Instead of an error probability below 10^{-3}, we now need to achieve an error probability about 10^{-6}, which is much much harder.

But is it really true that the threshold for non-stochastic noise is so much worse than for stochastic noise, or is that just an artifact of the proof? Intuitively, we can understand why the difference might occur. A

series of T coherent errors that each alter the amplitude of the state by p could sum up to a total amplitude error of about Tp. Thus, in order to avoid a problem, we should set a bound on the amplitude error per location.

However, notice that in order for the different errors to produce a total amplitude error of Tp, they need to be coherent *with each other*. Each error has to alter the state in the same way and with the same phase, or the overall error will be much smaller. If the errors each have a random phase, the amplitude will accumulate as only $O(\sqrt{T})$. This is the same as the behavior of stochastic errors, so in this case, we expect the threshold should be a bound on the error probability. That means that errors, even coherent non-Markovian ones, caused by random factors in the environment probably have a threshold similar to that for stochastic noise.

It's much more plausible that systematic errors would produce the same effect every time. But note that it is not actually enough that each error has the same effect at the time it occurs. In order to add coherently, the error must have the same phase and be of the same type as the *current* error, which has been changed over time by the action of the fault-tolerant circuit. For instance, suppose there is an erroneous coherent rotation about the Z axis at time 0, then a perfect Hadamard gate, then another incorrect Z-axis rotation. The Hadamard converts the original Z-axis rotation into an X-axis rotation, so the overall error at this point is an X-axis rotation followed by a Z-axis rotation. Two Z-axis rotations have perfect constructive interference, but an X-axis rotation followed by one about the Z axis instead act at partial cross-purposes, resulting in a smaller overall error. Since the whole purpose of a fault-tolerant circuit is to do fault-tolerant gates, we are constantly going to be mixing up the types of errors, making it much harder for them to add coherently. An adversary could look at the circuit and perhaps figure out a way to change the type of error in just the right way to get them to add coherently, but it's unlikely that a blind natural environment could do this.

Indeed, it's actually *impossible* to get all of the errors to add coherently. Suppose we have two fault paths Φ and Ω that produce different error syndromes for some FTEC gadget. The syndrome measurement irrevocably decoheres these two fault paths, so we can never get interference between Φ and Ω. In order for Φ and Ω to add up coherently, they need to produce the same error syndrome for every FTEC gadget. This is hard to arrange. Typically only a few different fault paths will be able to constructively interfere, at best. Consequently, I expect that the threshold in practice to be maybe slightly smaller than the stochastic threshold, but not dramatically smaller, even when the true error model is systematic and coherent.

It's very difficult to take these considerations into account rigorously to develop an alternative proof with a better threshold for coherent or non-Markovian errors. Even a simulation is difficult, because the whole point is to properly keep track of quantum interference among the errors, which is hard to track classically. One solution that has been suggested is to simplify the analysis by physically performing a random Pauli operator on the state at each time step, and absorbing the operation into the Pauli frame to compensate. This is another example of twirling, which we saw in section 13.5 when talking about magic state distillation. If the Paulis are performed perfectly, the effect is to decohere the errors in the Pauli basis, modifying the channel to become a Pauli channel, which is covered by theorem 10.4. Realistically, we would need to take into account faults in the Pauli twirling, and those faults might not be stochastic, but it is plausible that the behavior will still be quite close to that of the stochastic channel resulting from perfect twirling.

15.8.5 Error Models Not Covered by the Existing Proofs

Theorem 15.5 is quite general, and covers sufficiently weak noise for a wide variety of error models. It can be extended even further, to include environments that interact with multiple computational qubits at once, provided the strength of the interactions decays fast enough with the distance between them (as in section 15.8.1). The big remaining gap is to handle systems where $\|\mathcal{H}_{SB}\|_\infty$ is large.

Naturally, the threshold theorem requires weak noise. We can't hope to prove the existence of a threshold for large noise strength and arbitrary Hamiltonians, but there are two general classes of systems for which $\|\mathcal{H}_{SB}\|$ is large but the noise is still weak. In general, we should expect that some sort of threshold will hold for any system where errors on each single qubit are rare, and errors on groups of r qubits decay exponentially with r, but to prove this requires some additional assumptions as to what "counts" as an error and what causes the errors.

One class is systems for which the interaction between the system and some state of the environment is strong, but the environment is rarely in the state that causes a problem. The somewhat silly example of a meteor striking the computer illustrates the principle. The large number of correlated errors caused by the meteor are not due to a fundamental many-body interaction in the meteor-qubit Hamiltonian, but rather are due to a strong interaction between the meteor and each individual qubit in the computer. When, as is almost always the case, the environment is in the $|\text{no meteor}\rangle$ state, the computer is fine, but on rare occasions, the environment enters the $|\text{meteor}\rangle$ state, and many qubits are affected. There are other more benign versions of this model, where a rare environmental excitation causes problems with a few qubits. Some such models actually fit naturally into theorem 10.4, but others do not. An example of one that might be realistic and potentially problematic is a drift in the calibration of control parameters. Because the control must be strongly coupled to the system in order to do gates, a change in the control parameters will have a big effect, and once the control parameters are far off the correct values, there will be frequent errors until the system is recalibrated. This particular problem can be dealt with by recalibrating sufficiently often to avoid the drift, or at least monitoring the system so that we are aware of the drift, but that requires additional action beyond the fault-tolerant protocol. Another error source of this class might be more troublesome if we don't know to look for it.

Another class of models with large $\|\mathcal{H}_{SB}\|_\infty$ includes systems where the part of the environment that interacts with the computer is infinite-dimensional. For instance, the spin-boson model is a standard model of decoherence where a single spin interacts with one or more harmonic oscillators. The spin here represents the computational qubit, and the oscillators form the environment. The qubit interacts more strongly with the higher-frequency modes of the oscillators, so the interaction Hamiltonian $\mathcal{H}_{SB}$ is unbounded. There are two issues with these systems. First, there is the possibility that some high-frequency modes get excited. Then there is a strong interaction with the computer, and we are potentially back in the situation discussed in the previous paragraph. However, it is physically sensible to consider a cold environment, in which case high-frequency modes are not excited, and even low-frequency modes are only weakly excited. In that case, we think the noise should be weak. Nevertheless, the Hamiltonian remains unbounded; the vacuum of the high-frequency modes still has an interaction with the system, and that messes up the argument. Presumably this is just a technical issue, but so far it has only been dealt with under some additional assumptions about the nature of the bath.

It will be difficult to find any sort of general proof appropriate for systems with the potential of strong interaction induced by rare states of the environment. While it's natural to assume an initial low-temperature state of the bath, entropy introduced into the system by faulty gates will find its way into the environment, heating it up. Furthermore, interaction between the environment and the computer may drive the bath out of thermal equilibrium. It's conceivable that energy could end up concentrated into a few modes, causing any qubits they interact with to fail at a much higher rate than we might expect based on the bath's initial state. In order to make a rigorous statement about the presence or absence of a threshold for such a system, we need to know a lot about the internal dynamics of the bath, and even then, given the interaction with the complicated time-varying system Hamiltonian that implements gates, it will be difficult to prove anything.

To be clear, there is no evidence that fault tolerance is impossible in such systems. In some cases, the bath states that cause problems won't be that unusual, and then errors will be relatively common. That, of course, is a problem. Since we are postulating a strong system-bath interaction, the errors, when they occur, might affect many qubits. That also is a potential problem, even if the errors are rare. However, both of these issues can be diagnosed without too much difficulty by putting the system through a battery of error testing.

Some people think that there are other scenarios that could produce low error rates in tests but nevertheless cause fault tolerance to fail. Frankly, I find those scenarios to be a bit far-fetched. They require a conspiracy on the part of nature to organize the environment in just such a way as to foil our computation without being obvious about it. It's logically possible, but that's more a statement about the limitations of what we can prove rather than a limitation on the ability of the system to perform quantum computation. And of course, there's also the logical possibility of fundamental many-particle interactions or a failure of quantum mechanics, either of which could potentially foil fault tolerance (though they don't *necessarily* do so). Either would be a big departure from physics as we know it, but the two scenarios can't be completely

Assumption	Required?	What happens to the threshold?
Specific universal gate set	No	Decreased by an $O(1)$ factor
Long-range gates	No	Decreased by an $O(1)$ factor
Fast measurements	No	Little change
Fresh ancilla qubits	Partially	Hot bath decreases threshold
Parallelism	Mostly	Tolerance of storage errors decreased with less parallelism
No leakage errors	No	Little change
Adversarial errors	No	No change or increased by an $O(1)$ factor
Uncorrelated errors	Partially	Decreased by one or more orders of magnitude
Stochastic errors	No	Little change or decreased by an $O(1)$ factor

Table 15.1: Summary of various assumptions going into the threshold theorem, whether they are necessary, and some speculation as to what happens to the threshold if the assumption is removed or relaxed.

ruled out. Ultimately, the question of whether a given system can be used to build a fault-tolerant quantum computer can only be definitively answered by experiment. And even experiment can't definitively answer the question of whether we can build a quantum computer that is *bigger* than the ones we currently have, whatever that may be when you read this.

Chapter 16

Now, What Did I Leave Out, Part Two?: Other Things You Should Know About Fault Tolerance

Part III

Miscellaneous Topics

Chapter 17

Donuts. Is There Anything They Can't Do?: Topological Codes

It's now time to talk about topological codes. We have seen a number of different codes with a variety of different properties, but one thing the codes we've discussed so far don't do very well is to fit nicely into two or even three dimensions. There's been no spatial relationship between the qubits in the codes we've presented, but of course in a real quantum computer, each qubit has to be somewhere. Some qubits are close to one another and some are far apart. If you just pick a random stabilizer code, it's unlikely that the generators involve only qubits that are near each other, which might make it difficult to physically measure the error syndrome. This depends on the precise capabilities of the physical system used to make the quantum computer, of course — in some quantum computers, it might be very easy for distant qubits to interact, perhaps via EPR pairs constantly being shared between different nodes in the computer. In others, however, qubits will happily talk to their neighbors but anything further away is too remote, and any messages have to be passed from qubit to qubit to qubit until they reach their destination.

As we saw in section 15.2, there is a threshold even for concatenated codes in 1 or 2 spatial dimensions. The low levels of the code are arranged to be close together, since error correction for them needs to be done very often. The generators for the higher levels of concatenation, however, consist of many qubits spread out over a wide area. Error correction at high levels is a rare event, so we are willing to absorb the cost of the needed communications, but still, it makes the system more expensive than we might like.

When geometry is important, it makes sense to concentrate on QECCs for which *every* stabilizer generator consists only of qubits which are close together, unlike for the concatenated codes. Surface codes are an example of codes that achieve this. Interestingly, they work by associating the logical qubits with topological properties of the surface on which the qubits are stored. In any QECC, the logical information is spread out over many qubits, but in a surface code the logical Pauli operators can be directly identified with non-contractible loops. You might say the surface codes act locally but store globally.

It turns out that topological codes have a lot of other interesting properties. They form simple examples of an exotic type of physical system called "topologically ordered systems." While a full discussion of topological order is beyond the scope of this book, some topologically ordered systems allow universal quantum computation just by moving around some particle-like excitations in the system. There is even some hope of finding naturally-occurring systems that behave this way and are thus naturally fault-tolerant. The more mundane surface codes discussed in this chapter are also good for fault tolerance and even have a pretty good threshold.

In order to have any logical qubits for a surface code, we need to place the qubits on a surface with non-trivial topology. The most theoretically straightforward way to do this is to use a torus, but it's also possible to use surfaces with carefully designed boundaries to define interesting codes which can more easily be laid flat. I'll start with the toric code, since it is the simplest example of a surface code. Studying it should give you a new appreciation for the power of donuts.

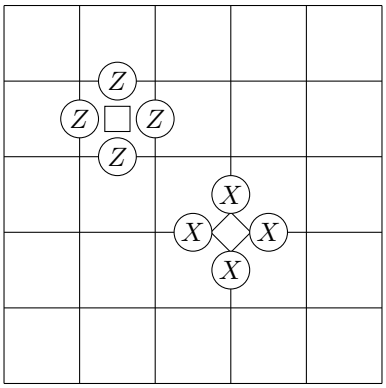

Figure 17.1: One Z_f (square) and one X_v (diamond) for the toric code

17.1 Toric Code and Surface Codes

17.1.1 Definition of the Toric Code

The toric code is a highly-degenerate CSS code. Typically it is defined via a square lattice on a torus, as shown in figure 17.1. The qubits are located on the edges on the graph. This is a torus because the top row and the bottom row of qubits are actually the same; we only separate them to make it look nice on the page. Similarly, the left column of qubits is the same as the right column. Thus, despite appearances, there are no outer edges to this graph — if you go off one end, you appear on the opposite one.

Each square f (a *face* of the graph, sometimes also called a *plaquette*) gives an element of the dual code ${C_1}^\perp$ and thus an element of the stabilizer

$$Z_f = \bigotimes_{i \in f} Z_i, \tag{17.1}$$

with the product taken over the four qubits i on the edges of f. Each vertex v (or *node* of the graph) defines an element of ${C_2}^\perp$, giving a stabilizer element

$$X_v = \bigotimes_{j \in v} X_j, \tag{17.2}$$

which is the product taken over the four qubits j in the *star* defined by v, which consists of the edges adjacent to v. (I will refer to both the star and the vertex itself as v.) It is purely a matter of convention whether the faces define the Z operators and the stars define the X operators or vice-versa, so you may encounter the opposite choice in the literature. The code has the same properties either way.

Notice that Z_f and X_v automatically commute. If the face f and the star v don't share any edges, then Z_f and X_v have support on disjoint sets of qubits and certainly commute. If v is a vertex on the face f, then there are exactly two edges shared between f and v, so again Z_f and X_v commute.

I was very careful not to call Z_f and X_v the generators of the stabilizer for the toric code (although I must confess I was tempted). This is because not all these operators are independent. Notice that if you take the product $Z_f Z_g$ for two adjacent faces f and g, the shared edge cancels out as shown in figure 17.2, and you get the product of Z's only around the border of the 2×1 region given by f and g. Similarly, if we take the product over all faces f, every edge appears twice in the product and we are left with nothing:

$$\prod_f Z_f = I. \tag{17.3}$$

Thus, one of the Z_f operators is dependent on the others. (Of course, we can choose which one we consider to be dependent — the faces are all equivalent.)

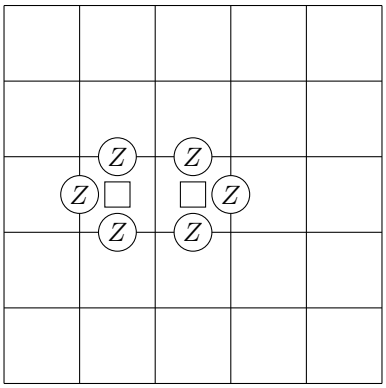

Figure 17.2: Product of two adjacent Z_f generators

If we take a product of Z_f's that does not include all of them, there will be at least one edge that is only included once (actually there will be at least four): Consider a face f that is not included in the product but that is adjacent to a face g that is included. The edge shared by f and g is just included once in the product. Thus the only way a non-trivial product of Z_f's can give the identity is if it is the product over all the faces, so there is only one Z_f that is dependent and the rest can all serve as generators of the stabilizer. Similarly, $\prod_v X_v = I$ and any smaller product is non-trivial, so all but one of the X_v operators is independent.

We can now compute the basic parameters of the code. If the torus is $L \times L$ in size, there are L vertical links in each column and L columns (recall that the right column is the same as the left column), for a total of L^2 vertical edges. There are also L^2 horizontal edges, so the number of qubits is $n = 2L^2$. There are also L^2 faces and L^2 vertices, so there are a total of $2L^2 - 2$ generators of the stabilizer (since one of each kind is redundant). Thus the number of logical qubits is $k = 2$.

17.1.2 Distance of the Toric Code

We can actually characterize all of the elements of the stabilizer and the logical Pauli operators in much more detail. Notice in figure 17.2 how the product of two adjacent Z_f operators consists of a tensor product of Z's in a closed loop. This generalizes quite easily:

Proposition 17.1. *Any product $\prod_{f \in \mathcal{F}} Z_f$ operators for the toric code is equal to the tensor product $M = \bigotimes_{i \in \mathcal{C}} Z_i$, where $\mathcal{C}$ is a set of closed loops.*

Proof. I will show that that the edges in $\mathcal{C}$ form curves that cannot end, and thus must form closed loops. Suppose Z_i appears in M. Then exactly one of the two faces adjacent to i is in $\mathcal{F}$. Suppose, without loss of generality, that the edge is horizontal and the adjacent face f which is in $\mathcal{F}$ is above the edge, as depicted in figure 17.3. Then there are four possibilities, depending on whether each of the two faces g and h to the right of the edge are in $\mathcal{F}$ or not: If neither of g or h is in $\mathcal{F}$ then $\mathcal{C}$ takes a left turn as it moves right from i. If g (which is adjacent to f) is in $\mathcal{F}$ but h is not, then $\mathcal{C}$ continues straight moving right from i. If both g and h are in $\mathcal{F}$, then $\mathcal{C}$ takes a right turn after i. Finally, if $h \in \mathcal{F}$ but $g \notin \mathcal{F}$, then two continuous curves bump up together and turn at the vertex right of i. In all cases, starting from i and going to the right, the curve $\mathcal{C}$ continues.

□

This sets a constraint on the form of elements of the stabilizer. However, it is not specific enough, since we can only guarantee that elements of that form are in the normalizer:

Proposition 17.2. *Any operator of the form $N = \bigotimes_{i \in \mathcal{C}} Z_i$, where $\mathcal{C}$ is a set of closed loops, is in $\mathsf{N}(\mathsf{S})$ for the toric code S.*

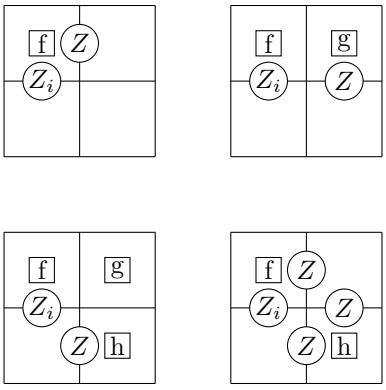

Figure 17.3: Four possible ways to continue an edge in M to the right

Proof. Suppose N has the form given. The curves comprising $\mathcal{C}$ do not end, so any star v contains 0, 2, or 4 edges in C. There are 0 edges if the curve does not pass through v, of course. If one curve enters v and leaves again, that gives 2 edges, and if two curves both enter and leave, as shown in the last part of figure 17.3, there are 4 edges in $v \cap \mathcal{C}$. In all cases, N commutes with X_v. This is true for arbitrary v so $N \in \mathsf{N}(\mathsf{S})$. □

The difference between the curves $\mathcal{C}$ that are in $\hat{\mathsf{N}}(\mathsf{S}) \setminus \hat{\mathsf{S}}$ and those that are in S can be understood through the notion of *homology*.

Definition 17.1. A set $\mathcal{C}$ of edges of a graph is a *cycle* if it consists of the product of closed loops, i.e., the paths in it never end. The *boundary map* ∂ is defined as a map that takes as input a set of faces $\mathcal{F}$ and gives as output the set of edges that border the region given by the union over $\mathcal{F}$. That is, $\partial(\mathcal{F})$ contains the edge i if and only if exactly one of the faces bordering i is in $\mathcal{F}$. A set $\mathcal{C}$ of edges is a *boundary* or an *exact cycle* if it is equal to the image $\partial(\mathcal{F})$ of some set $\mathcal{F}$ of faces. Let C_1 be the set of cycles of a graph, which is a subset of S_1, the set of all sets of edges. Let S_2 be the set of sets $\mathcal{F}$ of faces and let ∂S_2 be the set of boundaries. Note that by the same proof as proposition 17.1, $\partial S_2 \subseteq C_1$.

Define a notion of addition on S_2 and S_1 as follows: Let $\mathcal{F}, \mathcal{F}' \in S_2$. Then $\mathcal{F} \oplus \mathcal{F}'$ is the set of faces that is in either $\mathcal{F}$ or $\mathcal{F}'$ but not both, the XOR of $\mathcal{F}$ and $\mathcal{F}'$. Similarly, if $\mathcal{C}, \mathcal{C}' \in S_1$, $\mathcal{C} \oplus \mathcal{C}'$ is the XOR of $\mathcal{C}$ and $\mathcal{C}'$. S_2 and S_1 are Abelian groups with the group operation $\oplus$ and ∂ is a homomorphism. Define $H_1 = C_1/\partial S_2$. H_1 is the *first* $\mathbb{Z}_2$*-homology group* of the graph.

The elements of H_1 are sets of cycles up to equivalence of exact cycles. Definition 17.1 is an example of a general type of construction like this with a boundary map between sets of objects of different dimensions. There is also a set S_0 in this case, the set of vertices, and a natural boundary map ∂ from S_1 to S_0, with $C_1 = \ker \partial$. This is usually written as a sequence:

$$S_2 \xrightarrow{\partial} S_1 \xrightarrow{\partial} S_0. \tag{17.4}$$

When we have such a chain of maps and $\partial^2 = 0$ as in this case, the sequence is known as a *chain complex*, and it is possible to define *homology* as $\ker \partial / \operatorname{image} \partial$. That is, the elements of the homology group are sets of elements of $\ker \partial$, with each set (a *coset*) consisting of those elements of $\ker \partial$ that differ by elements of $\operatorname{image} \partial$ under $\oplus$. Definition 17.1 is the *first* homology group because it refers to objects of dimension 1 and it is $\mathbb{Z}_2$-homology because the addition we defined for S_1 and S_2 effectively makes them vector spaces over $\mathbb{Z}_2$.

The relevance of homology to the toric code is that proposition 17.1 tells us the Z elements of S consist of the boundaries for the graph and the Z elements of $\mathsf{N}(\mathsf{S})$ consist of the cycles. Thus, the logical Pauli $\overline{Z}$ operators are associated with the elements of H_1. Of course a homology class is not just a single cycle but a set of cycles equivalent up to addition by boundaries, just as a logical Pauli operator is not a single Pauli but a set of Paulis equivalent up to multiplication by elements of the stabilizer.

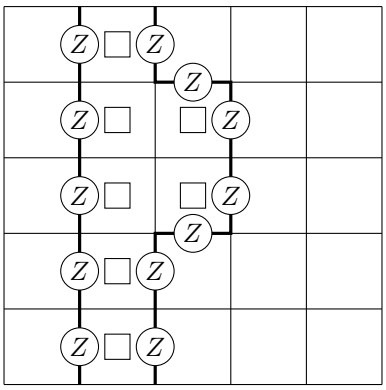

Figure 17.4: The product of two loops around the torus is the boundary of a set of faces.

For the torus, a loop is a boundary unless it stretches all the way around the torus in one direction or another. There are two different directions (horizontal and vertical in figure 17.1), which are associated to the logical operators $\overline{Z}_1$ and $\overline{Z}_2$. This matches the calculation from above, where we deduced that the toric code had two encoded qubits. Note that the non-trivial homology classes are only associated with loops that go *once* around the torus in a given direction. A loop that goes around twice, or the union of two loops that go around, is actually the boundary of a set of faces, as shown in figure 17.4.

The X elements of the stabilizer and the logical $\overline{X}$ operators can be understood through homology of the *dual graph*.

Definition 17.2. Let G be a graph on a surface with set of vertices $\mathcal{V}$, set of edges $\mathcal{E}$ and set of faces $\mathcal{F}$. The *dual graph* $G^\perp$ of G is the graph with set of vertices $\mathcal{F}$, set of edges $\mathcal{E}$ and set of faces $\mathcal{V}$. Each vertex of $G^\perp$ is a face of G and an edge connects two vertices of $G^\perp$ iff the two corresponding faces of G share an edge. G is sometimes referred to as the *primal* graph.

The dual graph for the square lattice on the torus is shown in figure 17.5. Note that the X elements of the stabilizer are associated to faces of the dual lattice in precisely the same way as Z elements were associated with faces of the primal lattice. That means we can reproduce the logic above and find that the X elements of the stabilizer are boundaries in the dual lattice and the logical $\overline{X}$ operators are the $\mathbb{Z}_2$-homology classes of the dual lattice. The cycles, boundaries, and homology for the dual lattice are also called the *cocycles*, *coboundaries*, and *cohomology* of the primal lattice.

We now have a complete characterization of the elements of S and of $\mathsf{N}(\mathsf{S})$. The elements of S are associated to cycles or cocycles that are contractible to a point. The elements of $\hat{\mathsf{N}}(\mathsf{S}) \setminus \hat{\mathsf{S}}$ are associated with loops in either the primal or dual lattice that go all the way around the torus, the non-contractible cycles and cocycles. Thus, the distance of this code is L, the size of the torus and the toric code is a $[[2L^2, 2, L]]$ code.

Note that if we take any product P of Z's, it can be represented as a set of curves (not necessarily closed curves) in the lattice. If Q has the same endpoints as P and can be distorted to P, as in the example shown in figure 17.6, then $Q = MP$, with $M \in \mathsf{S}$. This is true because the product PQ is an exact cycle, with the faces inside being those swept out as one is distorted into the other.

17.1.3 Defects in the Toric Code

Because the stabilizer generators for the toric code are geometrically local, the toric code can be realized as the ground (lowest energy) subspace of a geometrically local Hamiltonian, such as

$$H = \frac{1}{2}\sum_f (I - Z_f) + \frac{1}{2}\sum_v (I - X_v). \tag{17.5}$$

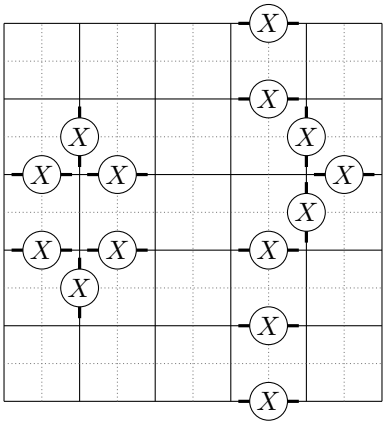

Figure 17.5: The dual graph for the square lattice is shown in dotted gray. An exact cocycle (left) and a cocycle that is not exact (right) are marked via edges on the primal lattice.

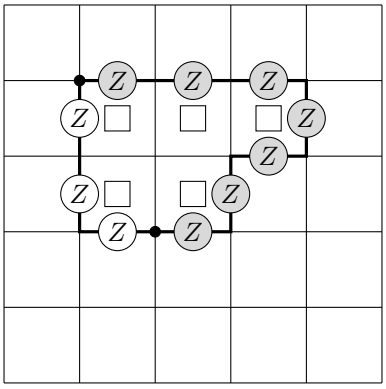

Figure 17.6: Two chains of Paulis P (unfilled) and Q (shaded) that have the same endpoints and can be distorted into each other. The product PQ is an exact cycle and $Q = MP$, with M the product of the marked Z_f operators.

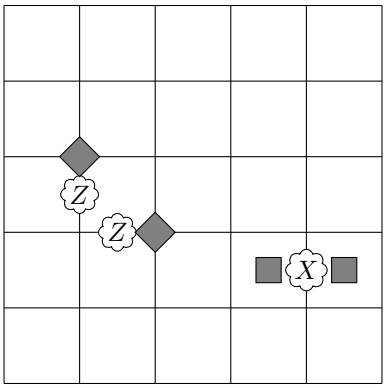

Figure 17.7: An example of the toric code with errors and corresponding defects marked (diamond for dual defect, square for primal defect). Z errors cause primal defects and X errors cause dual defects.

(See appendix A for a discussion of the physical meaning of Hamiltonians.) Notice that I have included the sum over all faces and vertices, not just those used as generators of S. Including all of the Z_f and X_v operators produces a Hamiltonian that is translation-invariant (unchanged by shifting coordinates by a lattice vector). If we were to omit the last Z_f and X_v operator from the sum, we would get a Hamiltonian that is physically slightly different even though the ground subspace would be the same, as we shall see in a moment.

The Hamiltonian given by equation (17.5) does actually have the toric code as the ground subspace. This is because each term $\frac{1}{2}(I - Z_f)$ or $\frac{1}{2}(I - X_v)$ has energy 0 for precisely the $+1$ eigenspace of Z_f or X_v and energy 1 for the -1 eigenspace of Z_f or X_v. All the terms commute, so the ground subspace is the joint $+1$ eigenspace — the code space $\mathcal{T}(\mathsf{S})$.

Because all the terms in the Hamiltonian commute, it is easy to diagonalize H to find the energy eigenstates. The eigenspaces of H are subspaces that have different error syndromes, and the energy of a subspace with a given error syndrome is equal to the number of Z_f and X_v operators that have eigenvalue -1. We can picture the error syndrome by marking the faces and vertices corresponding to Z_f and X_v elements which have eigenvalue -1. For instance, we might place a square in the middle of any face f for which Z_f has eigenvalue -1 and a diamond at any vertex v for X_v has eigenvalue -1, as shown in figure 17.7. Each mark represents a *defect*, a place where the toric code is not perfect. The diamonds are *primal* defects because they are on nodes of the primal graph and the squares are *dual* defects. They are also sometimes called *electric* and *magnetic* excitations because the relationship between them is reminiscent of that between electric charges and magnetic monopoles. Each defect configuration corresponds to an orthogonal 2-qubit subspace of the Hilbert space, and each is a separate QECC with the same basic properties (distance, size, etc.) as the toric code.

Note that a single-qubit Z error produces a pair of primal defects at adjacent vertices. A pair of Z errors on two adjacent edges of the lattice produces a pair of primal defects at a distance 2 apart. Indeed, if we have a state with a primal defect located on a vertex v, and a Z operator is performed on the edge connecting v with w, the resulting state has a primal defect at w and none at v. By performing a series of Z operators, we can move a primal defect along any path we like, as in figure 17.8. If two primal defects meet in this way, they annihilate, reducing the total number of defects in the system by 2. Similarly, a single-qubit X operator can create a pair of dual defects, move a dual defect between adjacent faces, or cause two adjacent dual defects to annihilate.

We can think of the defects as *quasiparticles*, localized excitations that behave somewhat like particles. In this case, the dynamics are governed by Pauli errors. X controls dual defects and Z controls primal defects. Y manipulates both at once.

Moving quasiparticles relates the code spaces corresponding to different defect configurations. If we move

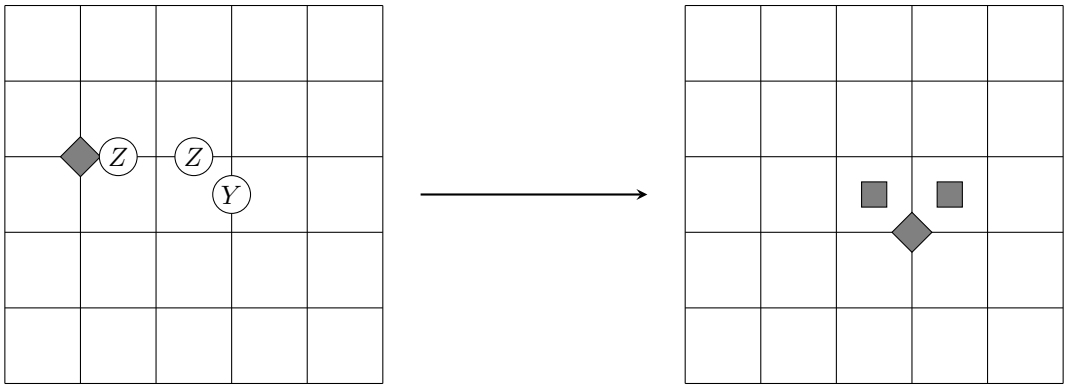

Figure 17.8: Moving defects using Pauli operators. In this example, the primal defect is moved 2 spaces right with Z operators and then a Y operator moves it down one spot while simultaneously creating two dual defects.

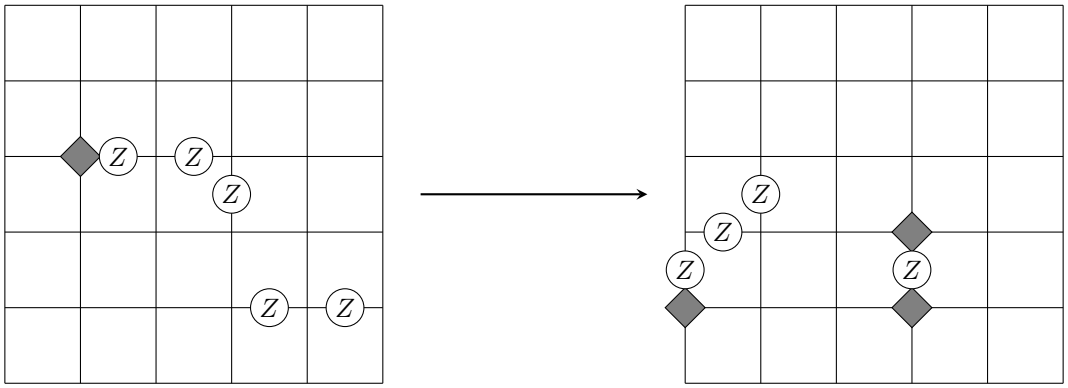

Figure 17.9: An example of performing a logical Pauli operation by moving a defect while creating a pair of defects, then moving one of the new defects and combining the old defect with the other new defect.

defects around but return them to their initial positions, or if we create pairs of defects and later annihilate an equal number of defects, we can return to the code space we started in. However, the encoded states may or may not be the same after moving the defects as they were before. If we move a defect around an non-contractible loop in the torus, that means we have performed a sequence of X or Z gates on a non-contractible loop. This is a logical Pauli operator $\overline{X}$ or $\overline{Z}$, so the encoded state has undergone a logical bit or phase flip. More subtlely, we don't have to move a single defect all the way around the torus. It is sufficient to move the defect a little bit, then create a new pair of defects, one of which annihilates with the original defect and the other of which moves the rest of the way around the torus back to the starting point of the original defect. You could have 2, 3, or more pair creation and annihilation events and still get a logical Pauli operator provided the overall effect is to perform a non-trivial loop.

The other interesting thing that can happen is that one defect can move around another. If a defect follows a closed loop which doesn't go all the way around the torus, it is an exact cycle, and we can write the loop as a product of stabilizer elements. Moving a primal defect around a loop gives us a product of Z_f operators and moving a dual defect gives a product of X_v operators. If there are no other defects inside the loop, the effect of the loop is just to return the encoded state to its original value. However, if a single dual defect is inside the loop traced out by a primal defect, then one of the stabilizer elements whose product produces the loop actually has value -1 rather than $+1$. Therefore, the encoded state gets a global phase

Imagine some pictures of donuts with one or more holes here.

Figure 17.10: Examples of manifolds.

of -1. Similarly if a dual defect moves around a primal defect. The phase is $+1$ if a defect moves around a defect of the same type as it or around an even number of defects of the other type.

Global phases have no physical significance, but the fact that they can appear for certain types of loops and not others makes the toric code a simple example of an *anyon* model. *Anyon* is a term for a quasiparticle for which interesting things may happen when you move one quasiparticle around another. The toric code is an abelian anyon model and therefore has little computational power, but there are also much more interesting and powerful systems of *nonabelian* anyons.

In the Hamiltonian equation (17.5), the total number of defects of each type must be even. This is despite the fact that any error syndrome is possible, including those of weight 1. The inclusion of the two extra (non-generator) stabilizer elements Z_f and X_v is responsible for the pairing of defects. If the Hamiltonian were the sum over only the generators of S, then unpaired defects would be possible — effectively the "missing" stabilizer elements create a vertex and face which can act as a sink or source of a single defect.

17.1.4 Surface Codes

If we really, truly want to create a system that realizes the toric code through the Hamiltonian equation (17.5), we are confronted with the awkward task of laying out qubits on the surface of a torus. It would be so much easier if we could have a system that lies flat on the table. Luckily, the toric code stabilizer and Hamiltonian can be adapted to work for any two-dimensional surface, flat or otherwise.

Given any two-dimensional surface Σ, choose a graph G and imbed G in Σ in such a way that edges do not intersect except at vertices (not all graphs can be imbedded in this way, only *planar* graphs). G has some set $\mathcal{V}$ of vertices, a set $\mathcal{E}$ of edges, and a set $\mathcal{F}$ of faces. We use the same definitions of the Hamiltonian, equation (17.5), and of the Z_f and X_v operators, equations (17.1) and (17.2), except that when we take the tensor product over all edges in a face or a star, there may be more or less than 4 of them. The Z_f and X_v commute still and thus define a stabilizer code. If the surface Σ is a manifold and the graph completely covers it, the logic in section 17.1.2 still applies, and the logical $\overline{X}$ and $\overline{Z}$ operators are associated with the homology and cohomology classes of Σ. Orientable 2-dimensional manifolds can be characterized by their *genus* — the number of holes. Basically, they are donuts with different numbers of holes. The number of logical qubits is equal to 2 times the genus and the distance is the length of the shortest non-trivial loop.

However, that doesn't help us make a system that can be flat in 2 dimensions. To do so, we need to consider surfaces with boundaries. We need two kinds of boundary: a smooth boundary and a rough boundary, shown in figure 17.11. At a smooth boundary, all of the edges connect back into the graph, so all vertices at the boundary have degree at least 2 (and generally 3 or more). At a rough boundary, there are edges that just kind of dangle out; i.e., a rough boundary consists of a contiguous group of vertices of degree 1. At a smooth boundary (or away from the boundaries), we define Z_f and X_v in the usual ways. At a rough boundary, we include additional Z_f operators of the form $Z \otimes Z \otimes Z$ for two adjacent dangling edges and the edge connecting them — effectively this produces additional partial "faces" at the boundary — but we do *not* include an operator X_v for the degree 1 vertices. See figure 17.11 for an example of this construction.

A Z error on one of the external dangling edges at a rough boundary produces just a single primal defect on the higher-degree interior vertex, and none on the degree 1 boundary vertex (which does not have an associated X_v). Thus, single primal defects can be created at a rough boundary or a primal defect can be moved to a rough boundary and disappear into it. At a smooth boundary, an X error on one of the external edges produces an unpaired dual defect on the face adjacent to the edge, so dual defects can appear or disappear at a smooth boundary. Dual defects at a rough boundary behave normally, as do primal defects at a smooth boundary.

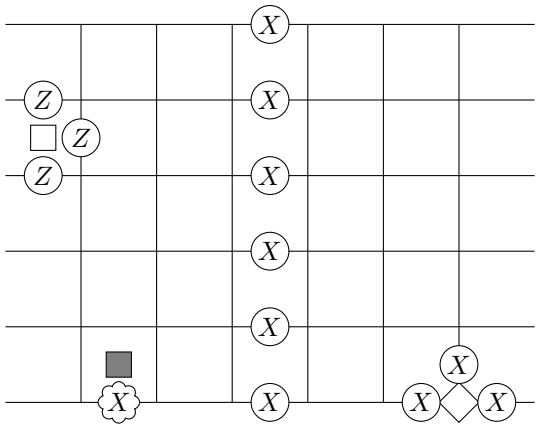

Figure 17.11: A surface code with two smooth and two rough boundaries has one logical qubit. Some stabilizer generators on the boundary are shown as well as a representative of the logical $\overline{X}$. The logical $\overline{Z}$ would be a horizontal line of Z's. An X error on smooth boundary produces a single dual defect.

The dual graph can be defined for a graph with boundaries in almost the same way as for the square lattice on a torus. In the dual graph, include vertices for the "missing" faces adjacent to smooth boundary faces and for partial faces at a rough boundary. Consequently, the dual of a smooth boundary is a rough boundary and vice-versa.

A Pauli which is a product of Z operators forming a curve which ends at rough boundaries will commute with the stabilizer, as will a Pauli made of X's which ends at smooth boundaries. As discussed in section 17.1.2, any two curves with the same endpoints that can be distorted to one another are equivalent up to elements of the stabilizer. Also, looking at the stabilizer elements at a rough boundary, we see that it is possible to multiply by a stabilizer element and distort a curve which is a product of Z elements and ends at a rough boundary to move the end of the curve one position over along the rough boundary. Thus, a Z curve which starts and ends at the same rough boundary can be distorted, via multiplication by stabilizer elements, into a closed curve, a cycle. Therefore, a product of Zs forms an element of $\hat{\mathsf{N}}(\mathsf{S}) \setminus \hat{\mathsf{S}}$ only if it performs a non-contractible loop or if it connects two distinct rough boundaries. Similarly, X operators can be shifted along smooth boundaries via multiplication by stabilizer elements, and such an operator is in $\hat{\mathsf{N}}(\mathsf{S}) \setminus \hat{\mathsf{S}}$ only if it is non-contractible, for instance if it connects different smooth boundaries.

Consequently, the distance of a surface code is equal to the size of the minimum non-contractible loop or the smallest distance between two boundaries of the same type (rough or smooth), whichever is smaller, and the logical Pauli operators are associated with paths which do those things. It is quite possible to have a surface code with an odd number of logical qubits — for instance, one — by taking advantage of boundaries, whereas a surface code on a manifold without boundary always has an even number of logical qubits. Figure 17.11 gives an example of a surface code with one logical qubit. The $\overline{X}$ operator is a product of X's forming a cochain (a path in the dual graph) between the two smooth boundaries, and the $\overline{Z}$ operator is a product of Z's forming a path connecting the two rough boundaries.

Another trick is to leave holes in the surface, as shown in figure 17.12. These are actual holes (at least in the part of the surface covered by qubits that form the code) rather than the handles of a higher-genus 2-manifold. This lets us have any number of logical qubits while still working with a surface that can be arranged in two spatial dimensions. Some of the holes consist of rough boundaries and some consist of smooth boundaries. There will then be some logical operators that stretch between the holes (or between one hole and the outer boundary of the system), and some logical operators that circle one or more holes. The distance of the code is then either the smallest distance between holes of the same type or between a hole and an outer boundary of the same type, or it is the circumference of the smallest hole.

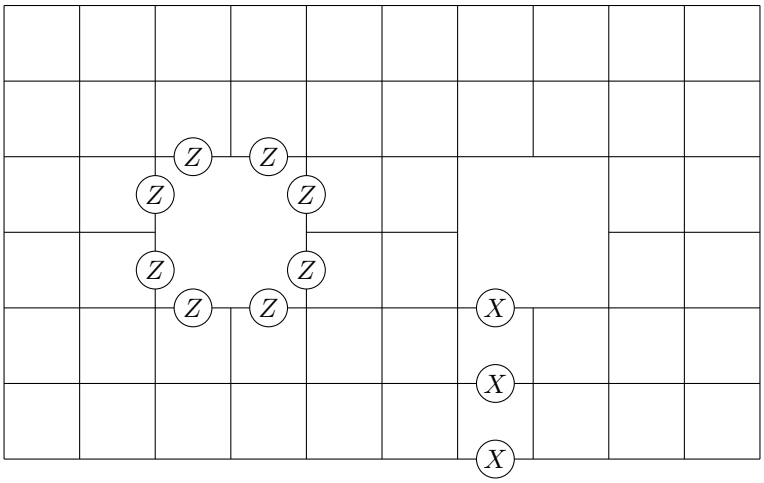

Figure 17.12: A surface code with two holes with smooth boundaries as well as smooth outer boundaries; it has two logical qubits. The logical $\overline{Z}_1$ and $\overline{X}_2$ are shown. The code pictured has distance 3.

17.2 Decoding of Surface Codes

One of the many nice features of surface codes is that they have efficient decoding algorithms that do quite well. By now, there are many known decoding algorithms and variations of decoding algorithms that can identify the error syndrome in polynomial time. There is still room for improvement in various aspects; building a fault-tolerant quantum computer is a demanding task, and we want to get every bit of performance out of the error correction while at the same time making sure that the classical computation being performed can keep up with the pace of error correction in a large quantum computer.

I will only present one algorithm here, the first one used for decoding of surface codes and the basis for many variations developed subsequently. It is based on a standard graph algorithm that works for any graph. The later improvements take advantage of properties of the restricted class of graphs that arise from surface code decoding problems to improve performance.

17.2.1 Decoding as a Matching Problem

Any error syndrome for a surface code corresponds to a configuration of primal and dual defects on the surface. In the case where the surface has no boundary, there is always an even number of each type of defect. One way of decoding is to pair up the defects and move them together using chains of X or Z operators. This corresponds to choosing some particular Pauli error consistent with the error syndrome. Of course, there are many possible errors which could result in a particular syndrome, and some of them differ by logical operators. If the true error is E and the guessed error is F, then the overall effect of error plus decoding is $EF \in \mathsf{N}(\mathsf{S})$, which means that it is the product of a cycle and a cocycle. As discussed above, EF is in the stabilizer iff it corresponds to a product of an *exact* cycle and an *exact* cocyle in the graph. If EF contains a non-trivial loop, then the decoding has failed.

It is enough to treat the X and Z errors independently by separately pairing up primal defects (the code C_2) and dual defects (the code C_1). That is, we look at the primal defects and find a *matching* — a set of pairs of primal defects such that each defect appears in exactly one pair. Then we choose a path connecting the primal defects within each pair, and the decoded error F will have a Z (or Y, if there is also an X error there) on every qubit that appears in the set of paths an odd number of times (so two overlapping paths will cancel on the overlap). The decoding algorithm should specify how to choose the paths, but typically will choose a path of minimal length (which might not be unique). Usually paths of similarly low weight will be equivalent up to stabilizer elements, but occasionally you might get two inequivalent paths of the same

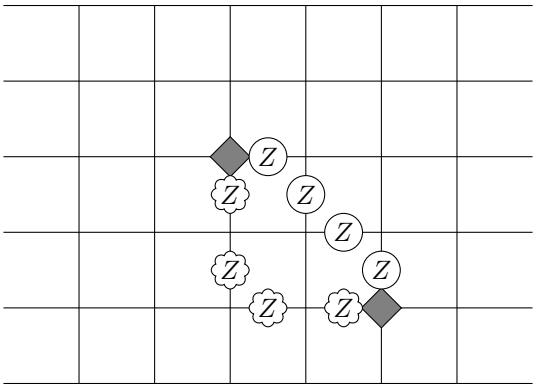

Figure 17.13: The true error E (wavy bubbles) may be different from the guessed error F, but as long as EF is in the stabilizer.

minimal length. We do the same thing in the dual lattice to match the dual defects, assigning an X error to each edge that appears in the dual paths an odd number of times.

Matching primal and dual defects independently might not be the best thing to do. For instance, if the code undergoes a depolarizing channel, X, Y, and Z Pauli errors are equally likely. Imagine we have a situation where there are two plausible inequivalent ways to pair up the primal defects but only one reasonable way to pair up the dual defects. However, in one pairing of primal defects, the Z errors are on different qubits than the X errors, whereas in the other pairing, many of the X and Z errors are on the same qubits, making Y errors. The second choice seems clearly better for the depolarizing channel (at least for small error probability), since it will result in a much lower total number of qubits with errors. The X and Z errors are correlated. However, ignoring the possibility of correlation still leaves us with a pretty good decoding algorithm.

Focusing, then, on the primal defects — the Z errors — we see that the weight of the Z Pauli error is the sum of the lengths of the chains connecting pairs of defects for the particular pairing we chose. All errors consistent with a given syndrome pair up the defects (they had to come from somewhere, after all), but some have additional loops of errors that don't help us pair up defects. Extra loops add to the weight of the error without gaining us anything in return, so we refuse to choose any set of paths that has extra loops associated with it. In the case that errors are independent between different qubits, the probability of having a particular error decreases exponentially with the weight of the error. Therefore, it makes sense to choose the error which has the smallest total weight since that is the likeliest single error that could have caused the observed error syndrome. It is actually possible to do better than that; really we should add the total probability of all errors in a particular coset of the stabilizer and choose the likeliest *coset* rather than the likeliest error. That is difficult to do, however, and choosing the lowest-weight error does pretty well, so we will stick with that for this book.

The problem of finding a minimum-weight pairing of defects can be solved by *Edmonds' maximum matching* algorithm. Maximum matching is an algorithm which, given a weighted graph, finds a way of partitioning the graph into pairs of adjacent vertices such that the sum of the weights of the edges between the members of each pair has the largest possible value. This is exactly what we need: consider the complete graph whose vertices are the primal defects. The weight of each edge connecting vertices v and w is $C - d(v, w)$, where $d(v, w)$ is the distance beween v and w, i.e., the length of the shortest chain connecting v and w, and $C \leq 2L$ is some constant greater than the largest distance between any pair of defects. We want *minus* the distance because Edmond's algorithm computes a matching which has the greatest sum of the weights, whereas we are actually interested in a matching which gives the smallest sum of the weights.

When doing decoding on a surface code with boundaries, primal defects can appear one at a time from a rough boundary and dual defects can appear one at a time from a smooth boundary. Defects can also appear in pairs in the interior of the code. Thus, we should try to match defects as before, but also allow

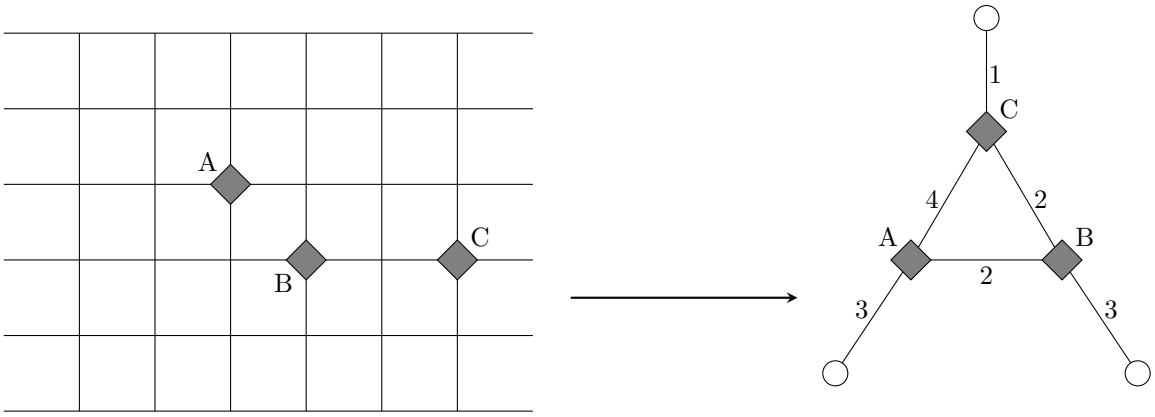

Figure 17.14: A configuration of defects and the corresponding weighted graph. Each edge represents a possible pairing of two nodes or a node with the closest rough boundary. The weights are the minimum number of single-qubit Pauli operators needed to move the nodes together or the node to the boundary.

for the possibility of matching defects to an appropriate type of boundary. We can do so by defining a more complicated graph. If the measured error syndrome has m primal defects, give the graph $2m$ nodes. Of these, m nodes correspond to the primal defects, and each defect has an additional node associated to it, which represents a "virtual defect" which could pair with the actual defect by sliding the defect to the closest rough boundary. All of the nodes corresponding to defects are connected to each other, again with a weight equal to C minus the distance between the nodes. Each node for a real defect is connected to the corresponding boundary node, and each boundary node is connected to only one defect node. The weight of an edge between a defect node and a boundary node is C minus the minimum distance between the defect and a rough boundary. Again, finding an optimal maximum matching on this graph corresponds to finding the lowest-weight product of Z errors that is consistent with the primal defect locations. An example of the graph obtained is shown in figure 17.14.

Edmonds' algorithm runs in polynomial time, but is not otherwise particularly fast. The best general version takes time $O(m^3)$ in the worst case when there are m defects. If the error probability per qubit is constant, then a constant fraction of the qubits will have defects, so $m = O(L^2)$, L the linear size (and thus distance) of the surface. Thus, the algorithm takes time $O(L^6)$, and even more when we need to do fault-tolerant decoding (see section 17.2.3). Using Edmonds' algorithm, syndrome decoding for a large surface code can take a long time. This is one of the motivations for finding other decoding algorithms for surface codes. (The other major one being the desire to correct higher error rates.)

17.2.2 Maximum Matching Algorithm

Before describing the maximum matching algorithm, let me review some terminology from graph theory.

Definition 17.3. A *graph* is a set $\mathcal{V} = \{v_i\}$ of *vertices* (also called *nodes*) and a set $\mathcal{E} = \{e_{ij}\}$ of *edges*, with edge e_{ij} connecting a pair of vertices v_i and v_j, with $v_i \neq v_j$ (I will not allow self-edges). Note that the numbering of the vertices and edges is arbitrary for our purposes, so long as it is consistent. A *weighted graph* is a graph $(\mathcal{V}, \mathcal{E})$ along with a list of numerical weights $W = \{w_{ij}\}$ associated to the edges. We can think of w_{ij} as the "value" of the edge e_{ij}. It will be sufficient for us to consider w_{ij} non-negative integers.

A *matching* in a graph $(\mathcal{V}, \mathcal{E})$ is a subset $\mathcal{M}$ of edges, $\mathcal{M} \subseteq \mathcal{E}$, with the property that no two edges in $\mathcal{M}$ share a vertex. A vertex v_i is *matched* with respect to matching $\mathcal{M}$ if $e_{ij} \in \mathcal{M}$ for some j; a vertex which is not matched is *unmatched*. The *weight* $\operatorname{wt}\mathcal{M}$ of a matching $\mathcal{M}$ is the total of the weights of the edges in the matching: $\operatorname{wt}\mathcal{M} = \sum_{e_{ij}\in\mathcal{M}} w_{ij}$. A *maximum-weight matching* is a matching with the maximum value of $\operatorname{wt}\mathcal{M}$ among all matchings in $(\mathcal{V}, \mathcal{E})$. (Note that a maximum-weight matching need not be unique.)

A *subgraph* $(\mathcal{V}', \mathcal{E}')$ of the graph $(\mathcal{V}, \mathcal{E})$ is a graph with $\mathcal{V}' \subseteq \mathcal{V}$, $\mathcal{E}' \subseteq \mathcal{E}$. Note that the subgraph is a graph in its own right, so the edges in $\mathcal{E}'$ must connect pairs of vertices in $\mathcal{V}'$. A matching $\mathcal{M}$ restricted to a subgraph $H = (\mathcal{V}', \mathcal{E}')$ is the matching $\mathcal{M} \cap \mathcal{E}'$, also written $\mathcal{M} \cap H$. A *path* is a graph with edges in a line: $\mathcal{V} = \{v_1, \ldots, v_n\}$, $\mathcal{E} = \{e_{12}, e_{23}, \ldots, e_{i,i+1}, \ldots, e_{n-1,n}\}$. The path connects the endpoints v_1 and v_n. A *cycle* is a graph with edges arranged in a circle: $\mathcal{V} = \{v_1, \ldots, v_n\}$, $\mathcal{E} = \{e_{12}, \ldots, e_{i,i+1}, \ldots, e_{n-1,n}, e_{n,1}\}$. Here, $n = |\mathcal{V}| = |\mathcal{E}|$ is the *length* of the cycle. A graph is *connected* if there is a path subgraph of edges connecting any two vertices in the graph. A *tree* is a connected graph which has no cycle as a subgraph.

Edmond's maximum-weight matching algorithm keeps track of five things at any given time: The current graph $G = (\mathcal{V}, \mathcal{E})$ and edge weights $W = \{w_{ij}\}$, a prospective (incomplete) matching $\mathcal{M}$ in the current graph, a list of non-negative weights $\{x_i\}$ of vertices in the graph, and a tree subgraph T of the current graph. The current graph will change over the course of the algorithm, so the algorithm also needs to keep track of how the graph has changed and the weights of vertices that may not be present in the current graph. The algorithm uses subroutines that change the various objects in memory in a particular set of ways, which I will define in more detail shortly:

1. The matching $\mathcal{M}$ can be reversed along an *augmenting path*.

2. The graph G can change by expanding or collapsing *blossoms*, which may also entail modifying the tree T.

3. The weights of vertices in the tree can be adjusted, some increasing and some decreasing.

4. The tree T can grow by adding an additional edge and vertex.

The vertex weights are essentially the solution to a dual linear programming problem; you can think of them as guides to how to choose the matching. We will want to choose $\mathcal{M}$ and $\{x_i\}$ so that

$$x_i + x_j = w_{ij} \tag{17.6}$$

for all $e_{ij} \in \mathcal{M}$. We will insist that this condition be satisfied at all times as we grow $\mathcal{M}$, and even for edges not in $\mathcal{M}$, the vertex weights will satisfy

$$x_i + x_j \geq w_{ij}. \tag{17.7}$$

An edge satisfying equation (17.6) is called a *tight* edge. We also want to end up with a matching and with vertex weights so that $x_i = 0$ if the vertex v_i is unmatched. This will only be true at the end of the algorithm, not in the middle.

The tree T will always have a very specific structure:

Definition 17.4. A *planted tree* T with *root* r for matching $\mathcal{M}$ in graph G is a tree subgraph of G which has the following properties:

1. The set of vertices of T is equal to the disjoint union of two sets $\mathcal{I}$ (the *inner vertices*) and $\mathcal{O}$ (the *outer vertices*).

2. Each edge of T connects an inner vertex and an outer vertex.

3. Each inner vertex is on exactly two edges of T.

4. r is an outer vertex of T.

5. Every vertex of T except for r is on an edge of $\mathcal{M}$.

6. If $e_{ij} \in \mathcal{M}$ and $v_i \in T$, then $v_j \in T$ and $e_{ij} \in T$ as well.

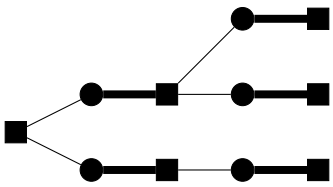

Figure 17.15: An example of a planted tree. Squares are outer vertices and circles are inner vertices. Thick lines are matched.

Thus, a planted tree consists of segments which are two edges long (with an inner vertex in the middle) followed potentially by branching at an outer vertex. An example is shown in figure 17.15. Note that working out from the root of the tree, we alternate between unmatched edges (i.e., edges not in $\mathcal{M}$) and matched edges, with each matched edge starting at an inner vertex and going to an outer vertex. The leaves of the tree (the nodes with only one edge) are always outer vertices.

The tree T which we work on during Edmond's algorithm will always be a planted tree. Furthermore, the tree will be chosen so that all edges e_{ij} in the tree are tight. We grow planted trees as an aid to increasing the size of the matching.

Definition 17.5. Given matching $\mathcal{M}$ and graph G, an *augmenting path* P is a path subgraph of G such that

1. One endpoint v_1 of P is unmatched for $\mathcal{M}$,
2. The other endpoint v_n is either unmatched for $\mathcal{M}$ or has $x_n = 0$, and
3. All other vertices of P are matched to each other with edges of P; i.e., $\{e_{23}, e_{45}, \ldots, e_{2j,2j+1}, \ldots\} \subseteq \mathcal{M}$. If v_n is matched, it is matched to v_{n-1}.

Note that the edges in an augmenting path alternate between unmatched and matched edges, starting with an unmatched edge. An augmenting path has an even number of vertices if v_n is unmatched and an odd number if $x_n = 0$.

Subroutine 17.1 (Reverse Augmenting Path)**.** Given G, $\mathcal{M}$, and augmenting path P in G, replace $\mathcal{M}$ with the matching $\mathcal{M}'$ as follows:

1. If $e_{ij} \in \mathcal{M}$ and e_{ij} is an edge of P, then $e_{ij} \notin \mathcal{M}'$.
2. If $e_{ij} \notin \mathcal{M}$ and e_{ij} is an edge of P, then $e_{ij} \in \mathcal{M}'$.
3. If e_{ij} is not an edge of P, $e_{ij} \in \mathcal{M}'$ iff $e_{ij} \in \mathcal{M}$.

That is, this subroutine switches the edges in P from matched to unmatched and vice-versa. After the reversal, the augmenting path still alternates between matched and unmatched edges, but now it starts with a matched edge rather than with an unmatched edge, as illustrated in figure 17.16.

If all the vertices in P are tight, then the weight of $\mathcal{M}$ restricted to P is just the sum of vertex weights except at the endpoints, $\operatorname{wt} \mathcal{M} \cap P = \sum_{i=2}^{n-1} x_i$. (If v_n is matched, $x_n = 0$, so it does not matter if we include it in the sum.) Similarly, $\operatorname{wt} \mathcal{M}' \cap P = \sum_{i=1}^{n} x_i$, the sum of vertex weights for all of P. Since the vertex weights are non-negative, $\operatorname{wt} \mathcal{M}' \geq \operatorname{wt} \mathcal{M}$; this motivates the name *augmenting path*. In fact, we will find augmenting paths for which $x_1 > 0$, so that $\operatorname{wt} \mathcal{M}' > \operatorname{wt} \mathcal{M}$.

Also note that we will only be looking for augmented paths in which all edges are tight, so that the new matching after reversal still has the property that all matched edges are tight.

Definition 17.6. A *blossom* B for matching $\mathcal{M}$ in graph G is a cycle subgraph of G which has odd length $2a + 1$ and contains a edges in $\mathcal{M}$.

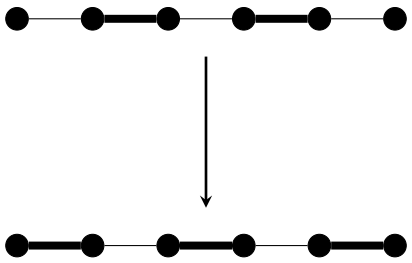

Figure 17.16: An example of reversing an augmented path. Matched edges are thick.

That is, a blossom has alternating edges matched and unmatched in $\mathcal{M}$ except at one vertex, which might be unmatched for $\mathcal{M}$ or might be matched to a vertex outside $\mathcal{M}$. We will restrict attention to blossoms for which all edges are tight.

Subroutine 17.2 (Collapse Blossom)**.** Given G, $\mathcal{M}$, T, W, $\{x_i\}$ and blossom B, replace $(G, \mathcal{M}, T, W, \{x_i\})$ with $(G', \mathcal{M}', T', W',$ and $\{x'_i\})$ as follows:

1. The vertices of G' consist of the vertices of G minus the vertices of B plus a new vertex v_b.
2. The edges of G' consist of all edges of G connecting two vertices not in B, plus a new set of edges as follows: If there exists an edge e_{ij} of G with $v_i \notin B$ and $v_j \in B$, G' contains an edge e_{ib} connecting v_i with v_b. Even if there are multiple such edges e_{ij} for a given $v_i \notin B$, there is only one edge e_{ib}.
3. $\mathcal{M}'$ contains all edges of $\mathcal{M}$ which connect vertices of G not in B, plus any edge e_{ib} for which $e_{ij} \in \mathcal{M}$, $v_j \in B$, $v_i \notin B$.
4. T' contains all vertices of T which are not in B and all edges of T connecting these vertices, plus v_b if T contains any vertex of B, and all edges e_{ib} for which $e_{ij} \in T$, $v_j \in B$, $v_i \notin B$.
5. The weight x'_b of the new vertex v_b is equal to $\min_{v_i \in B} x_i$. The weights of x'_i stay the same (equal to x_i) for $v_i \notin B$.
6. The weights w'_{ib} of the new edges e_{ib} are
$$w'_{ib} = w_{ij} - x_j + x'_b, \tag{17.8}$$
where e_{ib} is replacing the edge e_{ij} ($v_j \in B$). If there are multiple e_{ij} which get collapsed to e_{ib}, use the one which gives the lowest value for w'_{ib}. For all other edges e_{ij}, the weights are the same, $w'_{ij} = w_{ij}$.

Also record which vertices and edges of G are absorbed into v_b or replaced by e_{ib} and the weights of vertices that are removed. Also, for each edge e_{ij} that is removed and replaced by e_{ib}, record $\delta_{ij} = w_{ij} - w'_{ib}$, and for each edge e_{ij} between two vertices in B, remember w_{ij}. It is not necessary to keep track of those portions of $\mathcal{M}$ and T that are removed.

Note that since at most one vertex of a blossom can be matched outside the blossom, $\mathcal{M}'$ is still a matching. In principle, T' might not be a tree, but as it happens, the blossoms we choose to collapse will always result in T' being a tree. Also notice that if an edge e_{ij} containing vertex $v_j \in B$ and $v_i \notin B$ satisfies equation (17.6), then e_{ib} is also tight:

$$w'_{ib} = w_{ij} - x_j + x'_b = x_i + x_j - x_j + x'_b = x_i + x'_b. \tag{17.9}$$

Furthermore, if there are multiple tight edges e_{ij} corresponding to a single edge e_{ib}, they all give the same value of w'_{ib}. Conversely, if e_{ib} is tight, then there must be some tight edge e_{ij} which is replaced by e_{ib}. The blossom collapse procedure is illustrated in figure 17.17.

We also sometimes wish to expand a previously collapsed blossom. We will only do so when the vertex v_b to be expanded is an inner vertex of the planted tree T or when the tree is empty.

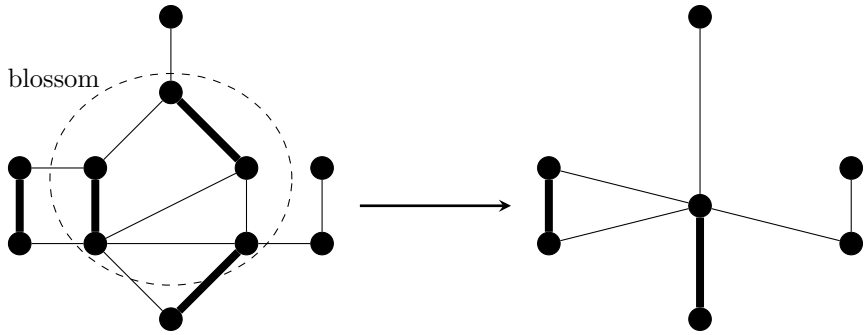

Figure 17.17: An example of collapsing a blossom. The thick lines are matched. The tree update and weight updated are omitted from the figure.

Subroutine 17.3 (Expand Blossom)**.** Given G, $\mathcal{M}$, T, W, $\{x_i\}$ and vertex v_b corresponding to previously collapsed blossom B, replace $(G, \mathcal{M}, T, W, \{x_i\})$ with $(G', \mathcal{M}', T', W',$ and $\{x'_i\})$ as follows:

1. The vertices of G' consist of the vertices of G minus v_b plus the vertices that were removed when B was collapsed to v_b.

2. The edges of G' consist of the edges of G minus the edges e_{ib} plus the edges that were removed when B was collapsed (i.e., edges connecting vertices of a B to each other and to vertices outside B).

3. The weights x'_i of the restored vertices are the same as they were before the blossom was collapsed. The weights of all other vertices stay the same.

4. The weights w'_{ij} of the restored edges e_{ij} for which $v_i \notin B$ and $v_j \in B$ are $w'_{ij} = w_{ib} + \delta_{ij}$. The weights of restored edges e_{ij} for which $v_i, v_j \in B$ are the same as before the blossom was collapsed. The weights of all other edges stay the same.

5. If v_b is unmatched in $\mathcal{M}$, then let v_j be a vertex of B with $x_j = \min_{v_i \in B} x_i$. The vertex v_j will also be unmatched in $\mathcal{M}'$, which is equal to $\mathcal{M}$ plus alternating edges around B to match all other vertices in B using edges of B.

6. If v_b is matched in $\mathcal{M}$ via edge e_{ib}, then $\mathcal{M}'$ is equal to $\mathcal{M}$ minus e_{ib} plus e_{ij} (for some e_{ij} which is replaced by e_{ib}) and alternating edges around the rest of B so that all vertices in B are matched using edges of B. If e_{ib} is tight, choose e_{ij} to be tight.

7. Since v_b is an inner vertex of T, only two edges e_{ib} and e_{jb} of T contain v_b. Both edges are tight; choose tight edges e_{ik} and e_{jl} which were absorbed into e_{ib} and e_{jb} respectively when the blossom was collapsed. (The edge e_{ik} should be the same as the edge e_{ik} chosen to be part of $\mathcal{M}'$.) There are two ways to go around the blossom to connect vertices v_k and v_l. Because B is an odd cycle, one direction will have an odd number of edges and one will have an even number of edges. Choose the direction with an even number of edges and make those edges and vertices part of T' along with e_{ik} and e_{jl}. The other edges and vertices of T' outside of B are the same as those of T.

By choosing the even length path within the blossom, we ensure that T' is also a planted tree.

When I talk about an edge e_{ij} that was "replaced by" or "aborbed into" e_{ib}, you need to take a slightly open-minded view of this. The issue is that the vertex v_i on the other end might have been absorbed into a blossom itself at some point after B was collapsed, in which case it is now part of a new node v_c. In this case, we do not actually use the original edge e_{ij}, but instead an edge e_{cj}. The weight adjustment for e_{cj} is still δ_{ij} since that only really depends on the blossom B.

Subroutine 17.4 (Weight Adjustment)**.** Given G, $\mathcal{M}$, T, W, and $\{x_i\}$, with $\mathcal{O}$ and $\mathcal{I}$ the sets of outer and inner vertices for T, respectively. Adjust the vertex weights to $\{x'_i\}$ for vertices in T as follows:

1. Let $\Delta_1 = \min_{v_i \in \mathcal{O}} x_i$, where $\mathcal{O}$ is the set of outer vertices for T.
2. Calculate
$$\Delta_2 = \min_{v_i \in \mathcal{O}} \min_{v_j | e_{ij} \text{ not tight}} (x_i + x_j - w_{ij}). \tag{17.10}$$
3. Let Δ_3 be the minimum value of $x_i - x_b$, where x_b is the weight of an inner vertex v_b which was produced by collapsing a blossom containing v_i, which had weight x_i.
4. Let $\Delta = \min(\Delta_1, \Delta_2, \Delta_3)$.
5. For each i with $v_i \in \mathcal{O}$, let $x'_i = x_i - \Delta$.
6. For each i with $v_i \in \mathcal{I}$, let $x'_i = x_i + \Delta$.
7. Return whether $\Delta = \Delta_1$, $\Delta = \Delta_2$, or $\Delta = \Delta_3$.

Note that since each edge in the planted tree T connects an inner vertex and an outer vertex, these edges remain tight. If $\Delta = \Delta_2$, some additional edges may become tight as a consequence of the weight adjustment subroutine, but since $\Delta \geq \Delta_2$, no edge will ever end up violating the condition $w_{ij} < x_i + x_j$. If $\Delta = \Delta_1$, then at least one vertex in T will have its weight adjusted to 0. If $\Delta = \Delta_3$, then the weight of at least one vertex in a collapsed blossom now matches the weight of the vertex that replaced the blossom.

The last subroutine is growing the tree, which is in fact the main loop of Edmond's algorithm. The idea of this subroutine is that either we can find a way to grow the tree having it remain a planted tree, or we will find conditions right to apply one of the other subroutines, which allow us to make progress on the matching.

Subroutine 17.5 (Grow Tree)**.** Given G, $\mathcal{M}$, T (with root r), W, and $\{x_i\}$, examine tight edges of G which are not edges of T, and consider only edges e_{ij} with one vertex v_i in $\mathcal{O} \subseteq T$. The other end of e_{ij} is v_j. Step through these edges until one of the following conditions is found:

1. If v_j is an unmatched node not in T, the path through T from r to v_i followed by e_{ij} is an augmenting path. Return the path and the message "augmenting path found."
2. If v_j is not in T and is matched through edge $e_{jk} \in \mathcal{M}$ connecting v_j and v_k, then add vertices v_j and v_k and edges e_{ij} and e_{jk} to T. v_j is now an inner vertex and v_k is an outer vertex. If $x_k = 0$, then the path from r to v_k through T is an augmenting path, so return the path and the message "augmenting path found." Otherwise return the message "tree grown."
3. If v_j is an outer vertex of T (possibly the root r), then e_{ij} is part of a blossom the rest of which is in T. Follow the paths from r to v_i and from r to v_j. At some outer vertex v_k these two paths will diverge, and the blossom B is the cycle formed by the paths v_k to v_i, e_{ij}, v_j to v_k. Return B and the message "blossom found."
4. Otherwise return the message "no growth possible."

Because we grow the tree by adding a pair of vertices, it remains a planted tree. Recall that we always have the property that all edges in T are tight, and this property is preserved if we grow the tree because we are only examining tight edges and matched edges are also tight.

Putting all of these subroutines together, we get the following algorithm:

Algorithm 17.6 (Edmonds' algorithm)**.**

1. Input is G and W. Initialize $\mathcal{M} = \emptyset$, $T = \emptyset$, $x_i = \lceil \max_{v_j} w_{ij}/2 \rceil$.
2. If there is an unmatched node $r = v_i$ with $x_i > 0$, let $T = \{r\}$. Otherwise we are finished: go to step 7.

3. Perform Grow Tree, subroutine 17.5, until it returns a message other than "tree grown."

4. If the message returned is "augmenting path found," do Reverse Augmenting Path, subroutine 17.1. Either there is now one more unmatched vertex with $x_i = 0$ or $|\mathcal{M}|$ has increased by 1. Reset $T = \emptyset$ and go to step 2.

5. If the message returned is "blossom found," do Collapse Blossom, subroutine 17.2. The blossom collapses to a node v_b which is an outer node of the updated tree T. Return to step 3.

6. If the message returned is "no growth possible," do Weight Adjustment, subroutine 17.4.

   (a) If it returns $\Delta = \Delta_1$, there is now one more outer node v_i with $x_i = 0$. If $v_i \neq r$, the root of the tree, then the path from r to v_i is an augmenting path. Perform Reverse Augmenting Path, subroutine 17.1. Afterwards, or if $v_i = r$, we have one additional unmatched vertex with $x_i = 0$. Reset $T = \emptyset$ and begin a new tree (step 2).

   (b) If Weight Adjustment returns $\Delta = \Delta_2$, there is a new tight edge connected to an outer vertex. Return to step 3.

   (c) Otherwise, Weight Adjustment returns $\Delta = \Delta_3$. Do Expand Blossom, subroutine 17.3. Return to step 3 and try to grow the tree again.

7. Expand all blossoms using Expand Blossom, subroutine 17.3. Since there may be nested blossoms, repeat the process until there are no remaining collapsed blossoms. Return $\mathcal{M}$, the desired matching.

The number of unmatched vertices never increases since all but one vertex in a blossom must be matched. The number of unmatched vertices with positive weight never increases either (although sometimes an unmatched vertex with 0 weight may become a matched vertex). We only abandon a tree if one of these two quantities actually decreases. Until then, we grow the tree steadily. Because blossoms only collapse to outer vertices of T and we only expand blossoms from inner vertices of T, the tree growth process always makes progress in the sense of adding new edges, although the actual size of the tree may shrink due to collapsing blossoms. Ultimately, all vertices will either be matched or have 0 weight. I omit the proof, but at this point, the matching $\mathcal{M}$ produced by expanding all blossoms is a maximum-weight matching.

17.2.3 Robust Syndrome Decoding

In section 17.3, I will discuss fault tolerance with surface codes. For surface codes, it is often sensible to use Shor error correction (or even a non-fault-tolerant error correction scheme), but that means there may be errors in individual syndrome bits. This means that some of the defects we see may not be real, and that there may be additional defects that are hidden by syndrome errors. We will need to repeat the syndrome measurement and deduce both the locations of the actual physical errors and the locations of syndrome bit errors. In section 12.2.2, I discussed one method of repetition applicable for Shor error correction — repeat until there are $t+1$ consecutive syndrome measurements that agree. However, for a large surface code, there will almost always be a new physical error somewhere in the system every time we measure the complete syndrome, so it is very unlikely we will actually get two consecutive identical syndromes, let alone $t + 1$ of them. We need a different approach.

Instead, we will repeat the syndrome measurement many times and try to deduce the location of syndrome errors from the way the measured syndrome changes over time. Any particular syndrome measurement can be phrased as a set of apparent defect locations. In the absence of syndrome errors, new pairs of defects can appear as new errors occur in the code block, or existing defects can move around or annihilate in pairs. When the error rate is low, all of these processes will be slow, so a defect that is present in a particular syndrome measurement is likely to be in the same location at the next syndrome measurement, or failing that at an adjacent location (where it may perhaps annihilate with another defect). In contrast, a false defect that appears because of an error in a syndrome measurement will probably not be present in the next syndrome measurement. In short, real errors are persistent and fake errors are not.

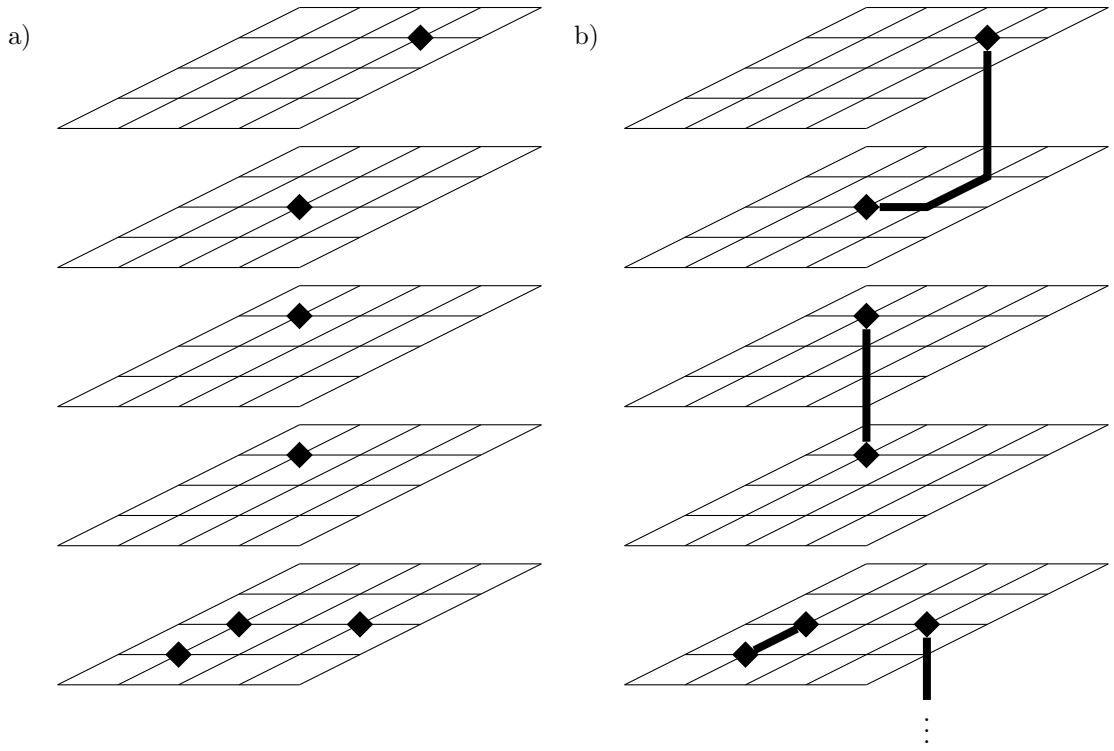

Figure 17.18: Matching defects to perform fault-tolerant decoding of the toric code. a) An example configuration of marked vertices where the measured eigenvalue of X_v changes in time. b) One way to pair these defects, with pairing marked by thick lines. Horizontal thick lines represent inferred qubit errors, whereas vertical thick lines represent inferred measurement errors. In this example, one defect is paired with the beginning edge, meaning that we have inferred a measurement error at time 1.

We can view this once again as a process of matching defects. Consider now a three-dimensional graph, the direct product $H = G \times [1, \ldots, T]$, with G the graph which defines the surface code we are using and $[1, \ldots, T]$ shorthand for a path graph with T vertices. Each of the points along the path represents a time at which we measure the error syndrome, and the graph contains a copy of G for each such time t. Corresponding points at adjacent times are connected. As before, we mark locations on the graph H and will use Edmond's algorithm to match them.

Not just the graph is different from the single syndrome measurement case: Instead of marking vertices in G that have primal defects (indicating violation of an X_v stabilizer generator), we mark vertices (v, t) in H where the eigenvalue of X_v *changes* between time $t-1$ and time t. At time $t = 1$, mark all vertices that have primal defects. If a small group of new real errors occurs at a particular time, it must correspond to a pair of new defects (or at any rate, a change in two adjacent X_v eigenvalues), meaning a pair of two marked vertices close together at the same time t. If a small number of syndrome errors occur at a particular location around the same time, they will produce a temporary in the syndrome, causing a defect to appear and then quickly disappear (or perhaps the other way around), so will correspond to two marked vertices at the same location and close in time. A particular guess as to a set of data errors and syndrome errors corresponds once again to a matching of the marked vertices in the graph, as shown in figure 17.18.

In particular, the marked vertices will again form pairs, with perhaps some marked vertices paired with the beginning and ending time boundaries because of syndrome errors at early or late times. A particular pairing of marked vertices corresponds to a choice of locations of real data errors and syndrome errors. This may not match the true locations of the errors, but as in the single syndrome-measurement case, the product

EF of the true error E and the candidate F for the error locations must consist of continuous paths that can only end on boundaries (spatial or temporal) of the graph.

The effect on the logical state of this choice of decoding depends on the topological properties of the paths in EF. Each "horizontal" link (i.e., corresponding to an edge in G at a fixed time t) corresponds to a physical Z performed on the code, either from an error that is not cancelled by a correction at that time or from a correction on a physical qubit that gets a correction at a given time but did not have an error then. If we ignore the "vertical" links in EF (i.e., those corresponding to edges in H between a particular vertex of G at different times) and accumulate all horizontal links, cancelling pairs in the same location, we end up with a set of paths on the original graph G. Note that it does not need to be a cycle — for instance, a pair of defects caused by a chain of 2 or more physical errors at the final time will potentially be paired with the final time boundary instead of each other, so errors occurring at late times may not be corrected.

We can decompose this set of paths into a cycle plus some additional paths. The extra paths correspond to errors not corrected by the decoding, and the cycle corresponds to errors where the decoding at least cancels out the error syndrome (even though the error does not match the decoding). If the cycle is an exact cycle, there is no logical error produced by the error/decoding sequence; if it is not an exact cycle, either because it has an odd number of paths that cross from one spatial boundary to another or because it contains a topologically non-trivial loop, then the decoding does have a logical error. Thus, the decoding can fail if EF contains topologically non-trivial loops or paths that cross between boundaries in a horizontal direction.

Decoding can also fail if we have paths in EF that cross between the starting time boundary and the ending one. Such a path need not produce a logical error directly. However, it *does* correspond to a failure to correct pre-existing errors in the system before the initial syndrome measurement. We need the error correction procedure to flush out pre-existing errors as well deal with new errors occurring during the syndrome measurement procedure itself, because otherwise the errors will accumulate between EC steps, eventually resulting in logical errors. As a concrete example, consider a case where there is a pre-existing error, either left over from the previous EC step or due to errors from gate gadgets between EC steps, that reaches about a third of the way across the surface. This is a correctable error, if we could make a perfect syndrome measurement. But suppose the imperfect EC gadget instead produces a chain in EF that reaches from one end of pre-existing error at the initial time to a location another third of the way around the surface at the final time. Something must also happen to the other end of the pre-existing error, so assume it is a chain that stretches from initial to final time in the same location. This configuration would again would lead to an error that, by itself, would be correctable through a perfect EC procedure. However, the combination of these two errors is an error that stretches two-thirds of the way across the surface and is no longer correctable. Essentially, vertical paths between time boundaries signal a failure of the ECRP. Or rather, it is a failure of a modified ECRP for this case, since the standard ECRP is written to apply to the case where we are trying to correct errors only up to half the distance of the code, and the typical case in a large surface code of n qubits will have $\Theta(n)$ errors even though the distance is only $O(\sqrt{n})$.

The upshot is that we want to choose an F such that EF is unlikely to have non-contractible horizontal or vertical paths. We want to solve this as a matching problem again, but we need to figure out what weights to use. It may be that syndrome measurement errors are more or less likely than physical data errors, so we don't want to just use the shortest paths in H. Instead, we want to weight horizontal and vertical edges differently.

Suppose there is a probability p per qubit per time step of a real data error and a probability q per time step of a syndrome error at each vertex, and further assume that these errors are independent. Then the probability of a particular set of a data errors and b syndrome errors over the course of T syndrome measurements is

$$\text{Prob} = p^a(1-p)^{nT-a}q^b(1-q)^{n'(T-1)-b} = \left(\frac{p}{1-p}\right)^a \left(\frac{q}{1-q}\right)^b p^{nT}q^{n'(T-1)}, \tag{17.11}$$

where n is the number of qubits in the code and n' is the number of vertices in the graph G (roughly $(n-k)/2$). Of course, in reality, the data errors and syndrome errors arise from the circuit used to measure the error syndrome and are not completely independent — for instance, a single fault can often cause one of

each — but treating them as independent will still lead to a reasonable decoding algorithm. (This, by the way, is an example of a *phenomenological error model*, which I previously discussed in section 10.4.)

The conclusion we can reach from equation (17.11) is that the probability of a particular set of errors is a constant times

$$p'^a q'^b = \exp(a \log p' + b \log q'), \tag{17.12}$$

with $p' = p/(1-p)$, $q' = q/(1-q)$. The error induces a particular matching of marked vertices of H. The ith pair is matched via a path containing a_i horizontal edges and b_i vertical edges, with $\sum_i a_i = a$, $\sum_i b_i = b$. If we weight the ith matched pair as $a_i \log p' + b_i \log q'$, then the total weight of the matching is $a \log p' + b \log q'$, which is the log of the error probability (up to a constant).

Consequently, we can use the following decoding algorithm: Create a graph whose vertices are the marked vertices of H as described above. The edge connecting a pair of vertices has weight equal to $C - \min |a \log p' + b \log q'|$, with the minimum taken over paths connecting the two vertices in H, a the number of spatial edges in a minimal path, b the number of temporal edges, and C a constant chosen to make the weights positive. Add extra boundary vertices for the boundaries of the surface and the starting and ending time, as discussed in section 17.2.1, with edge weights calculated based on paths from the vertex to the appropriate boundary. Perform Edmond's algorithm on this graph. The result gives a particular candidate of real data errors and syndrome errors, which by equation (17.11) corresponds to the most probable set of errors produced by the phenomenological error model.

17.3 Fault Tolerance with Surface Codes

Surface codes turn out to be quite good for fault-tolerant quantum computation, particularly if we are restricted to two or three dimensions. (If your quantum computer is one-dimensional ... well, then you'll have to keep looking for a better code.) Like concatenated codes, they have a threshold error rate below which arbitrarily long fault-tolerant quantum computations are possible, and simulations suggest the threshold error rate is quite high, around 6.7×10^{-3} in the basic model of fault tolerance with independent depolarizing errors and nearest-neighbor gates.

17.3.1 Transversal Gates and Error Correction for Surface Codes

We can use the methods introduced in part II to perform fault tolerance with the toric code or a surface code. This is not the most popular approach, but some aspects of these techniques might still be worthwhile.

First, which method of FT error correction should we use? Surface codes are CSS codes, so Shor, Steane, and Knill EC are all possibilities. As discussed in section 12.5, Steane and Knill EC are usually better for large codes. However, the one exception is for low-density parity check codes (LDPC codes), and surface codes are an example of this type of code — each stabilizer generator has low weight (4 or less). Thus Shor error correction only needs small cat states and is the most appealing possibility in this case, particularly given the robust decoding algorithm from section 17.2.3. Steane and Knill EC remain viable choices, but they require creating large surface code blocks to use as ancillas, making them less popular.

Actually, most commonly, people studying surface codes don't bother with any FT error correction method at all. Instead, they consider circuits where each stabilizer generator is measured by CNOTs to or from a single ancilla qubit, as in figure 12.1. How can they possibly get away with that? Remember, with such a circuit a single fault in the circuit can lead to errors on multiple qubits of the code block. However, because a single syndrome bit measurement only involves a few qubits around a single face or node (4 for a square lattice), the two-qubit correlated errors introduced this way will always be close together (meaning maximum matching will probably still pair the resulting defects correctly) and you can't get many-qubit correlated errors out of this circuit. By doing the CNOTs in order around the qubits involved in the generator, you can ensure that any correlated errors that arise will be in different directions on the lattice, further limiting the impact of the correlation. The code will be a little worse at correcting these correlated errors than the errors that arise from an FT syndrome measurement, but not too much worse, and because

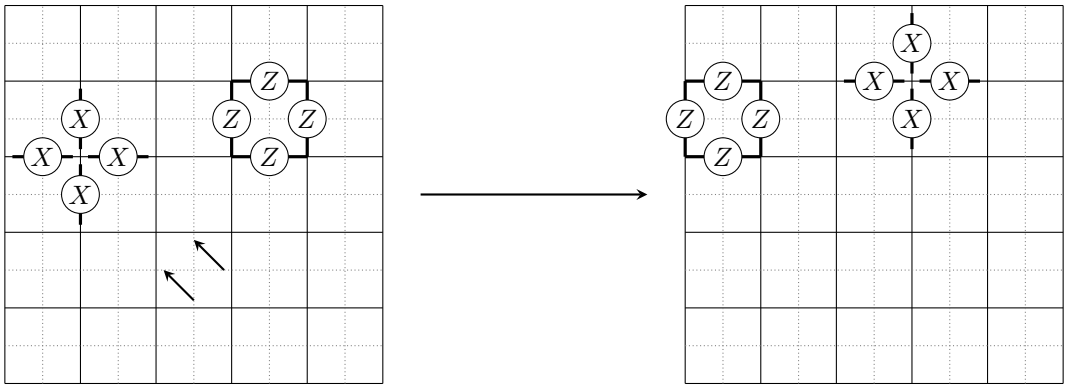

Figure 17.19: Transversal Hadamard plus permutating the qubits gives us a logical gate for the toric code. Each qubit is moved to the place above and to the left of it, and Hadamard is performed on all physical qubits. The X_v and Z_f operators switch roles under this transformation.

the non-FT circuit is simpler (fewer locations), the probability of *some* kind of error happening is lower. The overhead of the non-FT circuit is also lower.

A limited set of transversal gates is available for surface codes. They are CSS codes, so the transversal CNOT between two code blocks is a valid operation. It performs the logical $\overline{\text{CNOT}}$ between corresponding logical qubits of the two codes. Thus, the transversal CNOT between two copies of the toric code performs two logical $\overline{\text{CNOT}}$ gates in parallel. That's fine if there is only one encoded qubit per block, but it can be a bit inconvenient if there are many encoded qubits.

The two classical codes C_1 and C_2 used to construct a surface code are similar, but not identical. In particular, the transversal H is not a valid operation. It converts a Z_f operator into something of the form X_v but for the *dual graph*, and an X_v gets transformed to Z_f for the dual graph. For the toric code, we can compensate by taking advantage of symmetries of the torus. For instance, let us perform transversal Hadamard and then shift every qubit diagonally, moving a qubit on a horizontal edge to the vertical edge above and to the left, and a moving a qubit on a vertical edge to the horizontal edge above and to the left, as shown in figure 17.19. Now every stabilizer generator gets mapped to a stabilizer generator. The corresponding logical gate is $\overline{\text{SWAP}}_{1,2}(\overline{H}_1 \otimes \overline{H}_2)$ since the logical $\overline{X}_1$ is a vertical loop around the torus and $\overline{Z}_1$ is a horizontal loop, and vice-versa for $\overline{X}_2$ and $\overline{Z}_2$.

17.3.2 Creating and Measuring Logical Qubits

A new block of the surface code (of whatever shape and size) can be prepared using a variant of Shor state preparation, much as discussed in section 13.1.1. The logical state will be $|\overline{0}\rangle$ if there is one logical qubit and $|\overline{0\ldots0}\rangle$ if there are many. Begin with the $|0\ldots0\rangle$ state and measure the stabilizer generators for the surface code of interest, either using the Shor measurement procedure or just a non-fault-tolerant circuit, as discussed above. Note, though, that the starting state automatically satisfies the Z_f generators, at least in the absence of errors, so there is no need to measure those. We don't need to explicitly measure the logical operators $\overline{Z}$ either because they are also tensor products of Zs, and the initial state will automatically be in a $+1$ eigenstate of that (again, assuming no errors). That's good, because the $\overline{Z}$ is large and would be hard to measure.

We thus only need to measure the X_v generators. The initial measurement will reveal many many primal defects (on half the vertices on average). We pair them up somehow — it does not need to be an optimal pairing – and perform the appropriate correction, or just absorb the correction into the Pauli frame. We don't need to worry about a global phase error because we are making a $|\overline{0}\rangle$ state, so there is no $\overline{Z}$ error possible. Our goal here is to get rid of most of the defects, but there will still be a few primal defects left from syndrome bit measurement errors or from new data errors due to faults in the measurement circuit.

There will also be dual defects, of course, either from incorrectly prepared physical $|0\rangle$ qubits or from new errors introduced while measuring X_v. The point is that these residual defects will have low density, having been produced by (largely) uncorrelated local error processes, and in particular will be no more common than defects produced from a single syndrome measurement on an already-prepared surface code state.

Similarly, if we start with the $|+\ldots+\rangle$ state and measure all of the Z_f operators, we can prepare the logical $|\overline{+}\rangle$ state for all encoded qubits. Precisely the same analysis applies.

For the remainder of section 17.3, I will focus on a design composed of many rectangular patches of surface code, each with a square lattice, rough boundaries on two opposite sides, and smooth boundaries on the other two sides. A single such patch is one block of the surface code and encodes one logical qubit, with the logical $\overline{Z}$ operators associated to chains that stretch from one rough boundary to the other and logical $\overline{X}$ operators associated to cochains that stretch between the two smooth boundaries. The distance of the code is length of the shorter direction.

With such a design, it is easy to measure $\overline{X}$ or $\overline{Z}$ for a single logical qubit destructively (i.e., destroying the patch encoding that logical qubit). We can just use the standard CSS technique of measuring all physical qubits in the X or Z basis, respectively, and perform classical error correction to find the logical classical codeword. The classical error correction procedure we use is the same defect pairing algorithm as for full quantum error correction — because surface codes are highly degenerate, the two classical codes comprising the surface code have very low distance (just 4) as classical codes, but still are good at performing error correction in this context because of the degeneracy of errors.

17.3.3 Lattice Surgery

While transversal CNOT gates are a straightforward way of doing logical $\overline{\text{CNOT}}$ gates on two patches of surface code, there is a drawback to the transversal implementation: If the two patches are side-by-side in a 2-dimensional layout, the transversal CNOT requires long-range gates. In 3 dimensions, we can stack patches in the third dimension, allowing transversal CNOT to act on pairs of qubits for which the patches are close together, but not in two dimensions. It would be good to find an option for implementing $\overline{\text{CNOT}}$ between adjacent patches of surface code that use only short-range gates.

One class of techniques that have emerged as a relatively efficient way to do logical $\overline{\text{CNOT}}$ gates and other logical Clifford group gates is known as *lattice surgery*. There are two main primitive operations in lattice surgery, each with a few variations: lattice merging and lattice splitting.

Lattice surgery is an example of *code deformation*. In a fault-tolerant gadget involving code deformation, the QECC used to protect logical qubits is modified to create a sequence of other codes (usually related to the original one) before returning to the original code. By performing an appropriate sequence of alterations, the system returns to the original code space with the desired logical gate having been performed on the codewords.

Lattice surgery is an elective procedure which does not increase the lifespan of logical qubits, but does produce an improvement in the well-being of the logical qubits by helping them achieve their purpose of doing fault-tolerant quantum computations. Risks of the procedure include excessive defect production, but careful application of error correction during the surgery can minimize the chance of logical error. Code deformation is only temporary and should subside when the surgery is completed. On the plus side, lattice surgery can be performed without an M.D.

Lattice Merging

Suppose we have two adjacent patches of surface code with neighboring rough boundaries and we wish to merge them into a single larger patch. The rough edges have incomplete faces with only 3 edges. The difference between two small patches and one big patch is that the big patch has an extra fourth edge for all of those incomplete faces, shared between incomplete faces in the two adjacent rough edges. In the absence of errors, we could thus merge two patches by adding extra qubits in the $|0\rangle$ state for the shared fourth edges, as in figure 17.20a, and measuring the face operators Z_f and vertex operators X_v for the now complete faces and new vertices. Actually, we don't need to measure Z_f since the added qubits are Z eigenstates and the

incomplete faces already constrain the other three qubits on each face to be $Z \otimes Z \otimes Z$. Thus, the state is automatically a $+1$ eigenstate of Z_f. It is not automatically a $+1$ eigenstate of X_v, so we really do need to measure those.

If we measure the X_v operators along the merged boundary and happen to get all $+1$ eigenvalues, the resulting state is a single larger patch of surface code. Unfortunately, the chance of getting all $+1$ eigenstates is small, since each separate measurement we make has a 50% chance of giving $+1$ and a 50% chance of giving -1. That is, we will have defects on roughly half of the vertices on the merged edge. We can also view this as an alternative surface code where some X_v operators have eigenvalue $+1$ and some have eigenvalue -1.

Note, though, that not all the X_v operators along the merged edge are independent. They can't be — if the distance between smooth boundaries is L, we have added L extra qubits but $L+1$ X_v operators. The first L measurements are indeed independent and random, as we add $\pm X_v$ to the stabilizer and replace Z on one of the new qubits. The last one, though, is constrained. The product of all X_v operators on the merged boundary gives us two X cochains streching between the smooth boundaries, one to the left of the merge and one to the right of the merge. These we can identify as $\overline{X}_L$ and $\overline{X}_R$, the logical X operators on the left and right patches. Thus, the product of the X_v measurements (again, in the absence of error) is equal to $\overline{X}_L\overline{X}_R$. That means that the merge process acts as a logical measurement of $\overline{X}_L\overline{X}_R$.

If the measurement of $\overline{X}_L\overline{X}_R$ comes out as $+1$, that means that there are an even number of defects. We can pair up those defects and perform the corresponding Z operators to return to the standard surface code on the merged patch. We don't have to worry too much about how we pair them up (although since they are all on a line, there is an obvious way to pair them). The product of two different ways of pairing up the defects always corresponds to a topologically trivial loop and thus different pairings result in the same logical state.

If the measurement of $\overline{X}_L\overline{X}_R$ comes out as -1, that means that there are an odd number of defects. We can pair all but one of them, but the last one has to be paired with one of the remaining rough boundaries. However, one rough boundary is from the left patch and one is from the right patch. If we want to eliminate that defect by pairing it with a boundary, we need to make a decision whether to pair it with the left boundary using $\overline{Z}_L$ or with the right boundary using $\overline{Z}_R$. These are logically different states, differing by $\overline{Z}_L\overline{Z}_R$, which is the new logical $\overline{Z}$ operator after the merge.

This highlights an important feature of the lattice merging process: While there are two input qubits, there is only one output qubit. What happened to the missing qubit? Well, remember the lattice merge process involved measuring $\overline{X}_L\overline{X}_R$, a two-outcome measurement equivalent to measuring a single qubit, albeit in an entangled basis. The other qubit is the remaining logical qubit. The logical $\overline{Z}_L$ for the left qubit pre-merge doesn't commute with the measured operator, nor does the logical $\overline{Z}_R$ for the right qubit pre-merge, but the product $\overline{Z} = \overline{Z}_L\overline{Z}_R$ does, which is why that is the logical $\overline{Z}$ post-merge. The logical $\overline{X}_L$ and $\overline{X}_R$ do commute with the measurement, so they are still candidates for logical operators post-merge. If $\overline{X}_L\overline{X}_R$ has eigenvalue $+1$, then $\overline{X}_L = \overline{X}_R$, so it doesn't matter which one we pick. However, if $\overline{X}_L\overline{X}_R$ has eigenvalue -1, then $\overline{X}_L = -\overline{X}_R$, so there is an ambiguity — precisely the same ambiguity about whether we pair the extra defect with the left or right boundary. In practice, we generally resolve this ambiguity by using a merge only when one of the two patches is a known ancilla state, which, as we shall see shortly, gives a natural choice of which logical operator to use.

The analysis above assumes that there are no faults in the procedure. Of course, since the purpose of this lattice merge is to assist in fault-tolerant operations, that's a bad assumption. But if we follow the merge operation with a fault-tolerant error correction procedure for the merged patch, we can combine the defect matching from the merge with the 3D matching from fault-tolerant error correction. The number of defects in the initial merge is large, but the number of new defects created by data or syndrome errors at later stages of error correction is not large (at least, not large as a fraction of all locations in the error correction procedure), since the error rate is low. Thus, we would expect if the error correction procedure is working — and satisfies the appropriate ECRP-like property — that the defects created by the merge operation should also be properly paired. Note that we can't correctly identify the correct eigenvalue of $\overline{X}_L\overline{X}_R$ without the fault-tolerant error correction, since otherwise a single measurement error would change the eigenvalue of $\overline{X}_L\overline{X}_R$. The combination of merge followed by fault-tolerant error correction thus produces a fault-tolerant

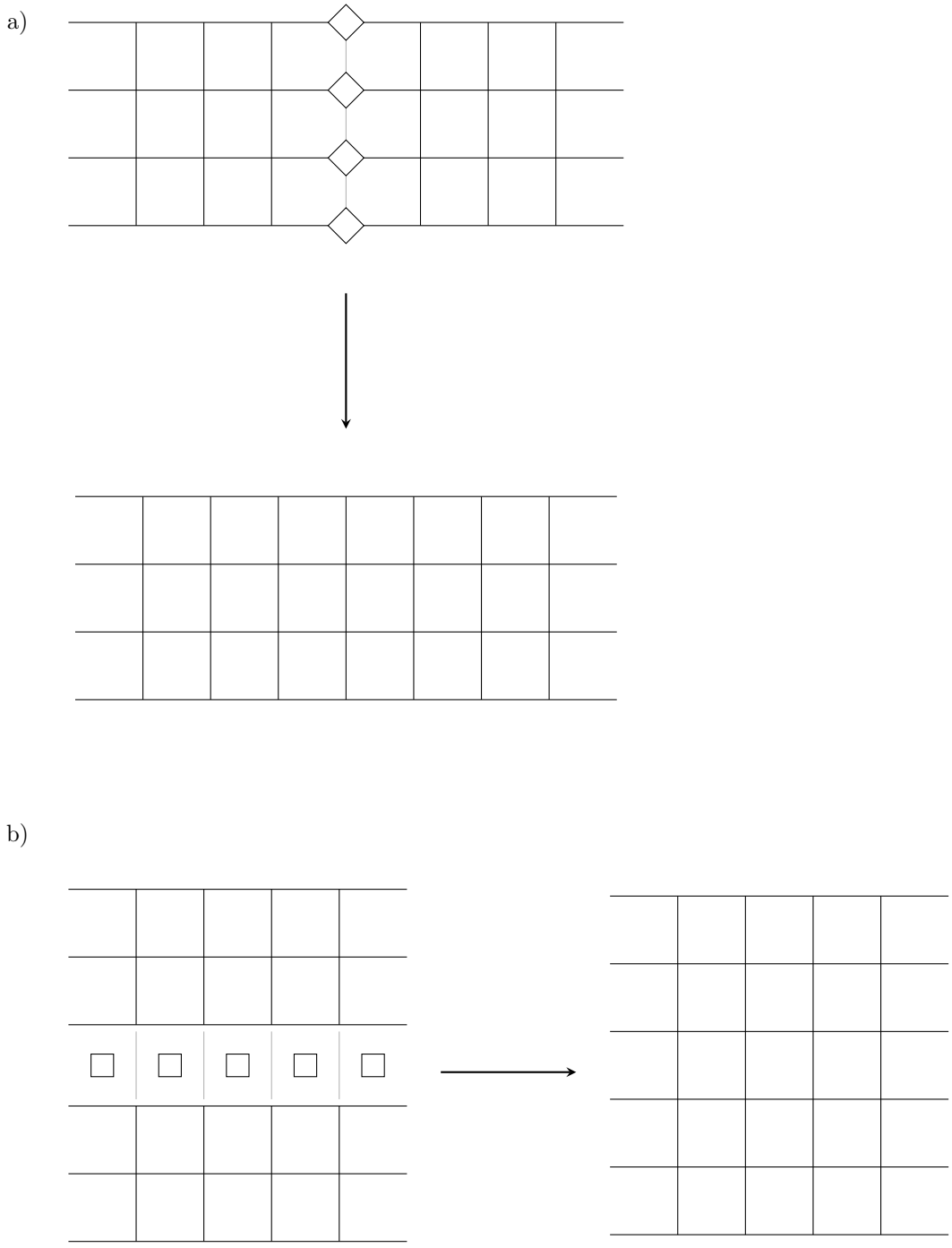

Figure 17.20: Merging two lattice patches along an a) rough edge or b) smooth edge

merge.

We can also merge two patches of surface code along a smooth boundary, as in figure 17.20b. Everything is the same but in the Hadamard basis: add $|+\rangle$ qubits between the two patches and measure the new Z_f operators created between the two surfaces, followed by a fault-tolerant error correction procedure. The smooth merge measures $\overline{Z}_L\overline{Z}_R$, and if the resulting eigenvalue is -1, there is an ambiguity as to whether to match the extra dual defect with the remaining smooth boundary on the left or right patch.

Lattice Splitting

We can also split a large patch of surface code into two smaller patches by splitting up the code. We can split to create either rough boundaries or a smooth boundaries. To split and create a pair of rough boundaries, we choose a line stretching between smooth boundaries to split on and measure Z on each of the qubits on the line, as in figure 17.21a. We then discard the measured qubits.

Before the split, the codeword was a $+1$ eigenstate of $Z \otimes Z \otimes Z \otimes Z$ for the faces along the splitting line, and post-split, the codewords are supposed to be $+1$ eigenstates of $Z \otimes Z \otimes Z$ for each of the incomplete faces on the new rough boundary. It will have the correct eigenvalue if the measured Z value on the discarded qubit from the face is $+1$, but if the measured Z has eigenvalue -1, then the incomplete face will have a defect. We will need to pair up the defects created this way, and, once again, we need to follow the basic split operation with a full fault-tolerant error correction cycle in order to deal with faults in the split.

Note that if a Z measurement gives an eigenvalue of -1, there are actually two defects: One in the corresponding incomplete face in the left patch and one in the corresponding incomplete face in the right patch. If we were to consider the Z measurement as an error on the original larger code block, the correct way to pair the defects would be to pair up these two defects. However, once we've done the split, we want to treat the two patches as separate code blocks, so we shouldn't pair between the two patches. Instead, we can pick a logically equivalent pairing that only matches defects within a single patch. For instance, if we have two pairs of defects and match the left side of the pairs and the right side of the pairs, that is topologically equivalent to matching the split-up pairs. If we decide to match a defect on the left to the top smooth boundary, we need to also match the corresponding defect on the right to the top smooth boundary of the right patch, and similarly for the bottom smooth boundaries. The correct matchings are illustrated in figure 17.22. Because of faults in the Z measurements and subsequent error correction step, it may not be possible to do exactly the same pairing on the left and right patches, but we should prioritize doing so as much as possible. When the error rate is low, we can usually succeed in doing so.

By measuring Z on the qubits on the splitting line, we have eliminated the X_v operators for vertices on that line (since they don't commute with single Zs). However, once again, if we are measuring L qubits, there are $L+1$ X_v operators, so there is still one residual extra operator in the stabilizer post-split, which is the product of all of the original X_v operators along the split line. Recall that this product doesn't actually involve any of the eliminated qubits (which is why it remains in the stabilizer), and is in fact equal to $\overline{X}_L\overline{X}_R$ post-split. Since we are starting with one logical qubit and ending with two logical qubits, it makes sense that there is an additional constraint on the logical states post-split, and this is it: The state, post-split, is a $+1$ eigenstate of $\overline{X}_L\overline{X}_R$.

We can also split to create a pair of smooth boundaries as in figure 17.21b. This involves measuring X along a co-chain stretching between rough boundaries to eliminate those qubits, followed by a full fault-tolerant error correction on the two new patches. We need to match the dual defects in the left patch the same way (as much as we can) as in the matching for the dual defects in the right patch. The resulting state, post-split, is a $+1$ eigenstate of $\overline{Z}_L\overline{Z}_R$.

17.3.4 Gates via Lattice Surgery

Given the two basic operations of lattice merging and lattice splitting, we can put together a universal set of gate gadgets by putting them together in a variety of different ways.

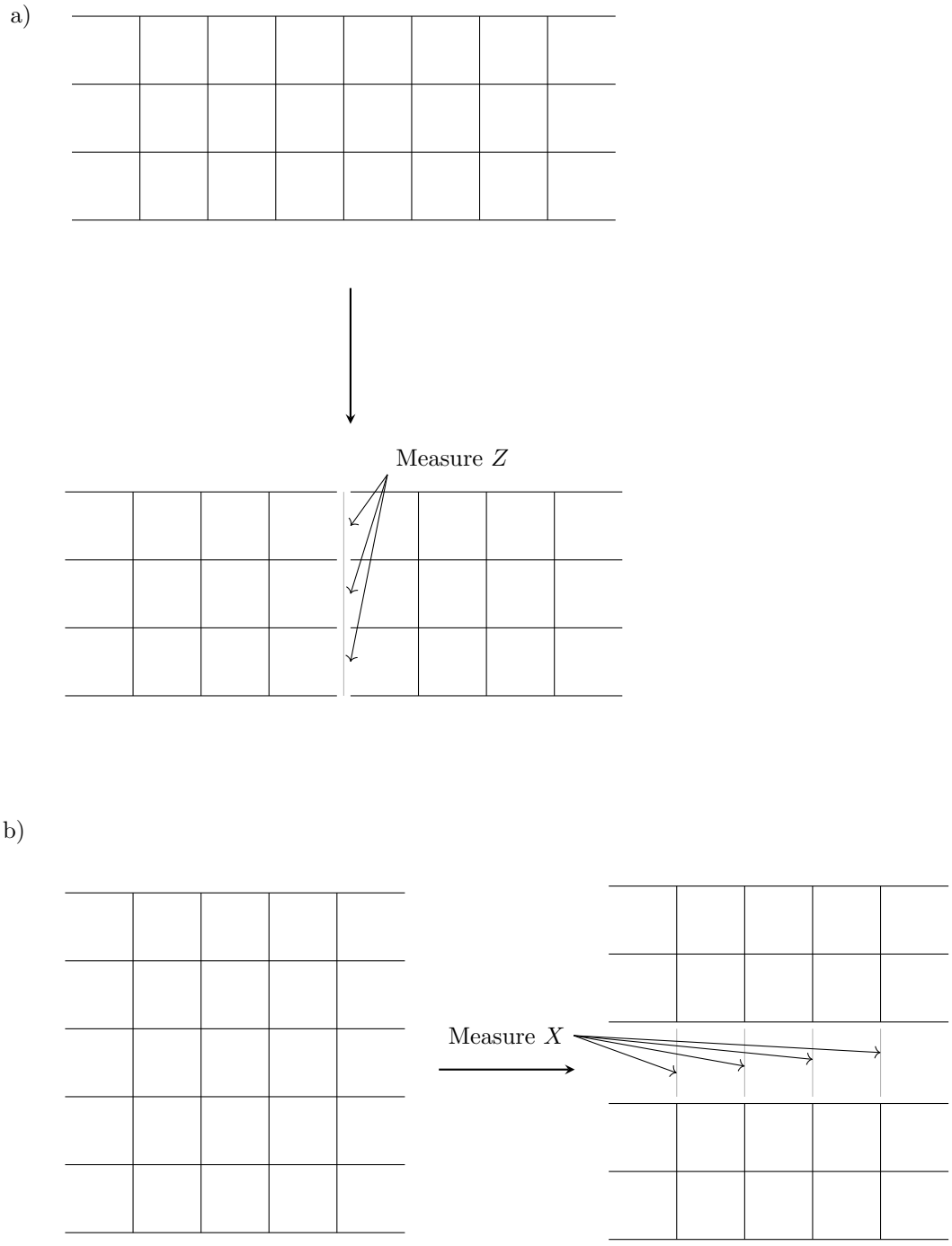

Figure 17.21: Splitting into two lattice patches while creating new a) rough edges or b) smooth edges

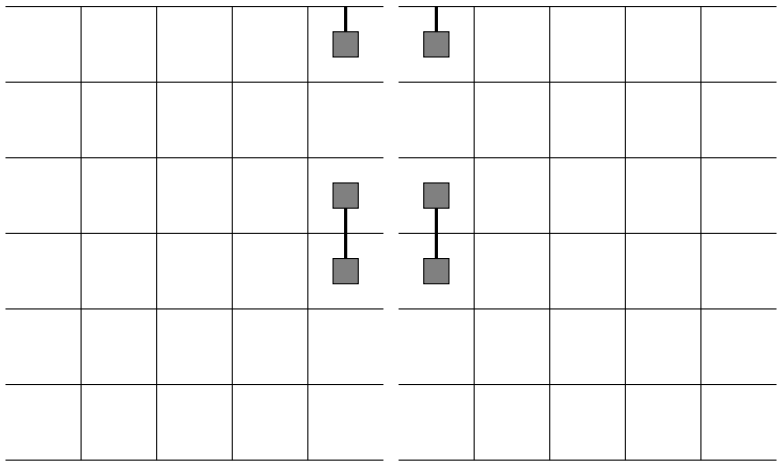

Figure 17.22: Pairing defects caused by a split creating rough edges.

CNOT via Lattice Surgery

The $\overline{\text{CNOT}}$ gate can be done through a pure sequence of lattice surgery operations. To see how, first note that CNOT can be done as a sequence of one- and two-qubit non-destructive measurements involving the control qubit C, the target qubit T, and an ancilla qubit A. The two-qubit non-destructive measurements can be implemented as a lattice merge followed by an immediate lattice split.

One sequence of measurements that works is to start the ancilla qubit in the state $|+\rangle$. Then measure $Z_C Z_A$ followed by a measurement of $X_T X_A$. Then conclude with a Z_A measurement. Supposing all three measurements both give us eigenvalue $+1$ (which can be guaranteed using the technique from chapter 6), the result is a CNOT gate from C to T. You can verify this using the Clifford simulation techniques in chapter 6.

The logical version of this using lattice surgery is to start with a $|\overline{+}\rangle$ ancilla patch and to do a smooth merge on the C block and the A block. Recall that this does the logical $\overline{Z}_C\overline{Z}_A$ measurement. As I promised, in this case, there is a natural way of resolving the ambiguity in how to match defects in case of a -1 result for the logical measurement — the ancilla starts in a $+1$ eigenstate of $\overline{X}_A$, so we should use that operation to pair the extra defect with the ancilla block's remaining smooth boundary, since doing so doesn't change the logical state (other than the change induced by the $\overline{Z}_C\overline{Z}_A$ measurement itself). We can then do a lattice split on the merged patch to recover the C and A blocks. The split allows the two patches to retain the $+1$ eigenvalue for $\overline{Z}_C\overline{Z}_A$. We can then do a rough merge and split on T and A to perform the $\overline{X}_T\overline{X}_A$ measurement. In this case, to switch from a -1 measurement result to a $+1$, we would need to perform $\overline{Z}_C\overline{Z}_A$, so we should resolve the possible defect pairing ambiguity by pairing the extra defect with the remaining rough boundary of A (doing $\overline{Z}_A$) *and* also perform $\overline{Z}_C$. Finally we can do a destructive measurement of A in the Z basis, and if the result is -1, perform $\overline{X}_T$. (The Clifford manipulation technique would tell us to perform $\overline{X}_T\overline{X}_A$ but actions on A are no longer relevant.) The procedure is picture in figure 17.23.

The natural architecture of such a lattice-surgery-based quantum computer compatible with this $\overline{\text{CNOT}}$ implementation is to have surface code patches in a checkerboard pattern. The black squares correspond to stored logical qubits and the white squares are for the ancilla qubits. We can then do $\overline{CNOT}$ gates between any pair of logical qubits that are diagonally adjacent. Suppose we choose to arrange all patches with the vertical boundaries as rough boundaries and the horizontal boundaries as smooth boundaries. Then if we wish to do $\overline{\text{CNOT}}$ with the control to the upper left and the target to the lower right, use the ancilla in the lower left, directly below the control patch. This means that the control and ancilla patches share a smooth boundary and the target and ancilla patches share a rough boundary, matching the needs of the $\overline{\text{CNOT}}$ implementation. To do a $\overline{\text{CNOT}}$ the other way, with the lower right patch as control and upper left patch

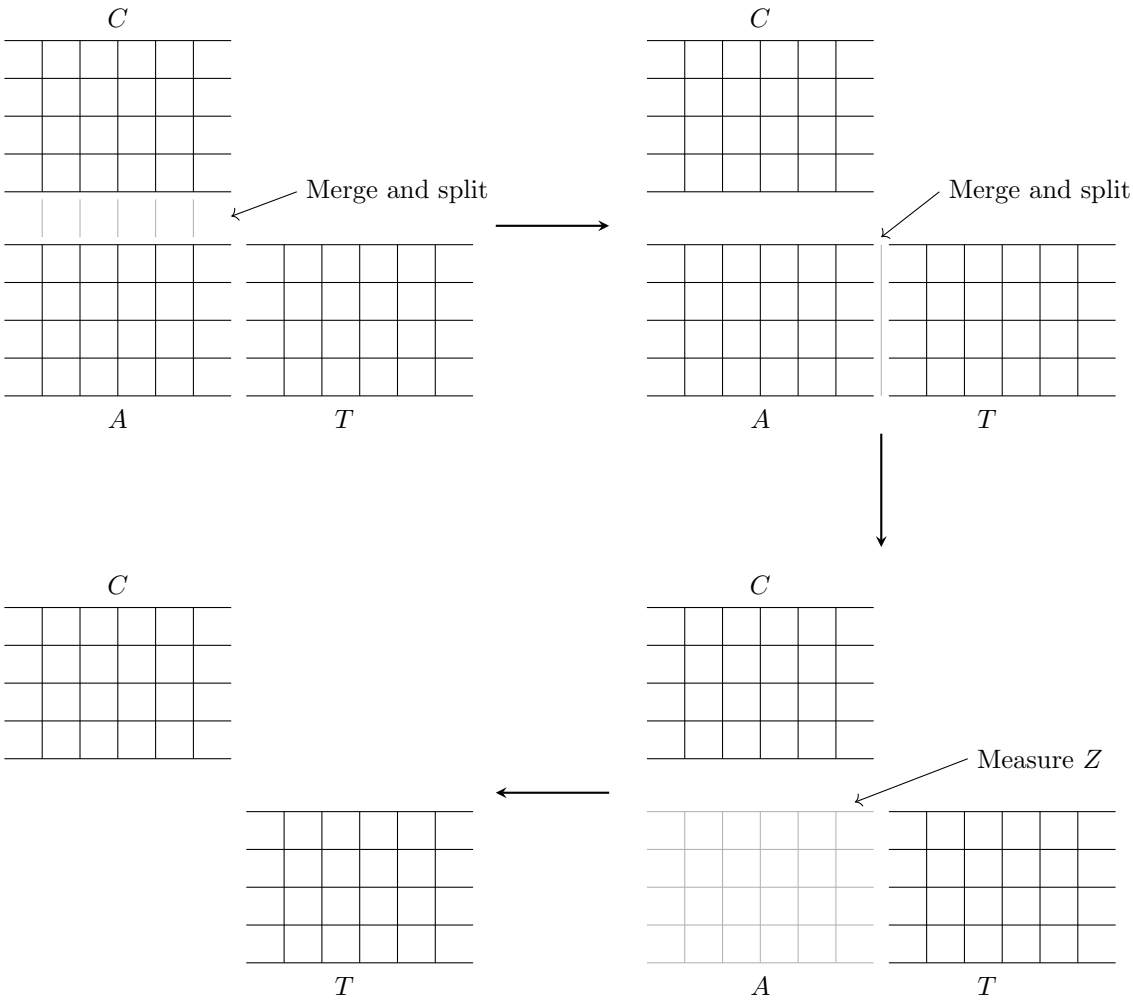

Figure 17.23: Performing a $\overline{\text{CNOT}}$ via lattice surgery between control logical qubit C and target logical qubit T. A is an ancilla patch initialized into the state $|\overline{+}\rangle$.

as target, use the ancilla in the upper right, above the control patch.

Moving and Rotating Surface Code Patches

Another useful thing to be able to do is swap a logical qubit stored in a surface code patch D with an adjacent ancilla patch A. If the two patches share a rough boundary, this can be done by initializing the ancilla into a $|\overline{0}\rangle$ state, merging the two patches, and then splitting them, resolving the ambiguity in the merge by pairing any extra defect with the ancilla boundary. This does the $\overline{X}_D\overline{X}_A$ measurement. We can then measure the ancilla in the Z basis to complete the move. If the two patches share a smooth boundary, we can do the move by starting with a $|\overline{+}\rangle$ ancilla and merging then splitting on the smooth boundary, again resolving the ambiguity by pairing any extra defect with the ancilla boundary. Then measure the ancilla in the X basis.

We can also rotate a surface code patch to switch the rough and smooth boundaries. The first step in doing so is to create an ancilla patch that has two *adjacent* rough boundaries and two adjacent smooth boundaries. Such a surface code has no logical qubits since any path that goes from rough boundary to

rough boundary is contractible, as is any path from smooth boundary to smooth boundary. If we merge this ancilla with the patch we wish to rotate along a rough boundary, there is no logical measurement since the merged edge does not stretch all the way across the boundary of the ancilla. However, there is still the possibility of an odd number of defects created, so we should match any extra defect to the remaining ancilla rough boundary so as not to change the logical qubit. We now have a larger patch which (going around the patch) has one short smooth edge, one long smooth edge, one short rough edge, and one long edge with one half smooth and one half rough. The smooth half of the second long edge is between the rough half and the short rough edge. This larger patch thus still has one logical qubit.

We can similarly attach ancilla patches to each of the other edges, in all cases adding ancillas with two adjacent rough boundaries and two adjacent smooth boundaries. The rough boundaries of the original patch merge with rough ancilla boundaries and the smooth boundaries merge with smooth ancilla boundaries. We orient the ancillas so that at all times, going around the full patch there is continuguous set of rough edges, then a continguous set of smooth edges, then a continguous set of rough edges, and finally another contiguous set of smooth edges. There is thus just one logical qubit at all times, provided we exercise sufficient caution around the corners. The process is illustrated in figure 17.24.

Next, we want to shrink the large cross-shaped patch resulting from the merge into a single patch of the original $L \times L$ size but rotated. We do this by splitting off each ancilla patch with the opposite kind of split we used to merge it. We are splitting off patches that have three boundaries of one kind and one of the other, so the split-off ancilla patches have no logical qubits and there is no constraint on the logical state imposed by the split. We are again careful to do the splits in such a way that there is only ever one logical qubit, as shown in figure 17.24. Also, note that the distance between non-adjacent rough boundaries or between non-adjacent smooth boundaries never shrinks below L. Once all ancillas have been split off, we are left with a patch of the original size encoding the original logical qubit, but rotated by 90°.

This rotation procedure can be considerably optimized and can be done with many fewer ancilla qubits. For instance, it is not necessary to merge in full-size ancillas if we are careful about how we split them off again to avoid having short chains or co-chains cross between boundaries of the same type.

Hadamard and Lattice Surgery

As we saw in section 17.3.1, the transversal Hadamard on a single surface code patch will perform the logical Hadamard, but it switches the primal and dual lattices. This has the effect of rotating the lattice so that now the vertical edges are smooth and the horizontal edges are rough. We can use the rotation procedure from above to fix this, restoring the original orientation.

Magic State Injection

Of course, this is not enough. CNOT and H are Clifford group operations, so are not universal by themselves. Indeed, they do not even generate the full Clifford group. We can also do logical Paulis, of course, since surface codes are stabilizer codes, but that doesn't help much. To get a universal set of gates, we will need a way to make magic states.

The general strategy we will use is the same as that discussed in chapter 13: use some non-fault-tolerant circuit to create a number of unreliable magic states and then use magic state distillation to produce a smaller number of more reliable magic states. We will use magic state constructions both for the $\overline{R_{\pi/4}}$ and the $\overline{R_{\pi/8}}$ gates. We already know how to inject $\overline{R_{\pi/8}}$ gates (figure 13.7). But how do we inject $\overline{R_{\pi/4}}$ gates?

Luckily, we don't have to think very hard to figure out how. The same tricks that let us do a fault-tolerant $\overline{R_{\pi/8}}$ can be adapted to do a fault-tolerant $\overline{R_{\pi/4}}$. The same logic from section 13.3 shows that figure 13.7 instead does an $R_{\pi/4}$ if we replace the ancilla state with $R_{\pi/4}|+\rangle$ (the $+1$ Y eigenstate) and replace the teleportation correction P' with $R_{\pi/4}PR_{-\pi/4}$. Since $R_{\pi/4}XR_{-\pi/4} = Y$, this is within our capabilities.

So can we implement these circuits? The $\overline{R_{\pi/4}}$ gate needs a $\overline{R_{\pi/4}}|\overline{+}\rangle = |\overline{0}\rangle + i|\overline{1}\rangle$ magic state (which is just a logical $\overline{Y}$ eigenstate), and the $\overline{R_{\pi/8}}$ gate uses a $\overline{R_{\pi/8}}|\overline{+}\rangle = |\overline{0}\rangle + e^{i\pi/4}|\overline{1}\rangle$ magic state, so we need to figure out how to make those magic states. We also need $\overline{\text{CNOT}}$ gates, which we have, and $\overline{Z}$ measurement, which we also have. The $\overline{R_{\pi/4}}$ magic state injection procedure might need a logical $\overline{Y}$ as a correction operation,

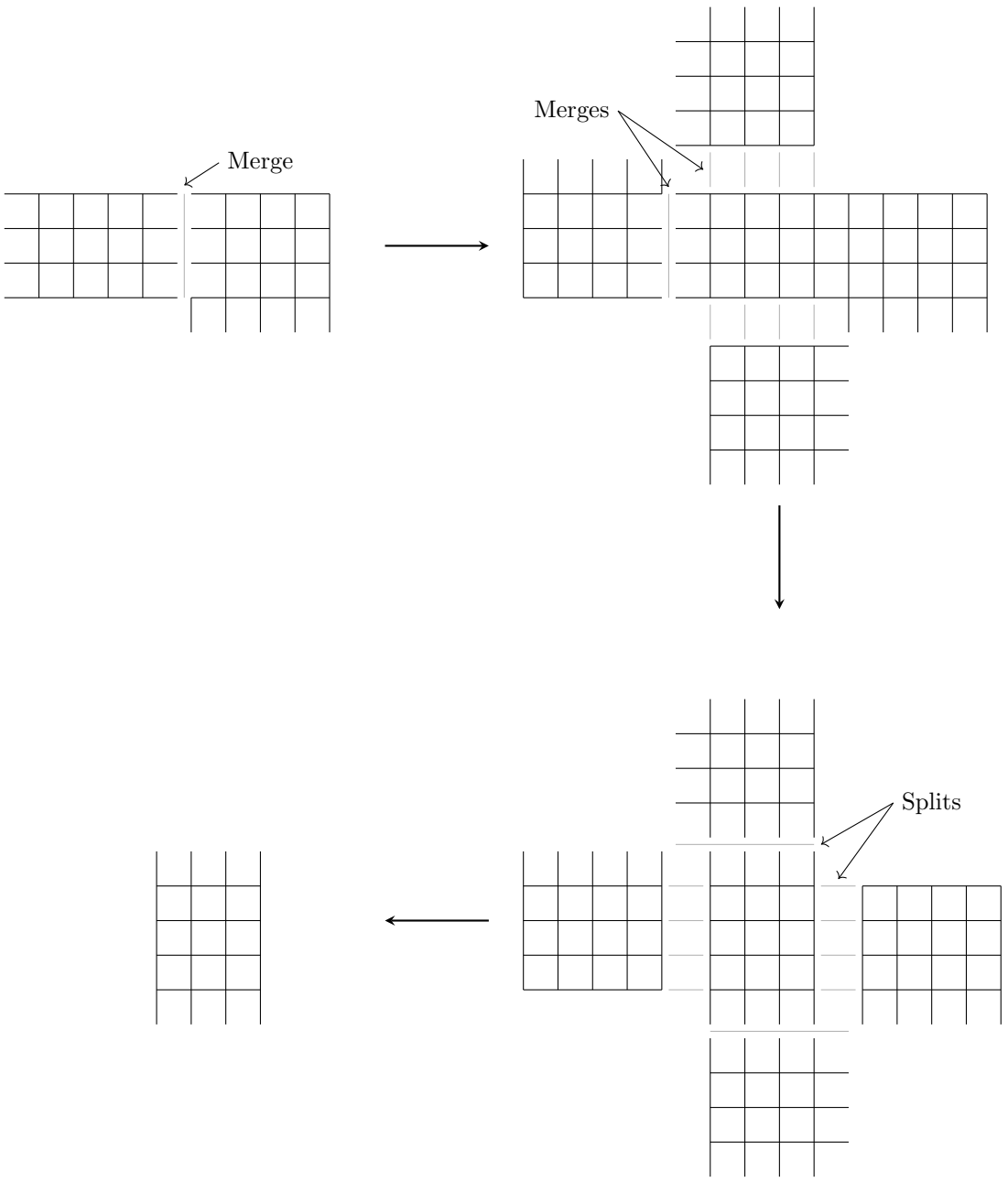

Figure 17.24: Rotating a surface code patch to change the orientation of the boundaries. Merge in 4 ancillas, each with 2 rough boundaries and 2 smooth boundaries, then split off the ancillas on the opposite type of boundary.

and we have that. The $\overline{R_{\pi/8}}$ magic state injection might need a logical $\overline{R_{\pi/4}}$ as a correction operation; and while we *don't* have that yet, we are working on it right now.

To make the unreliable magic states, the strategy is to start with a small surface code patch and then grow it. We can make a small (e.g., 3×3) patch of surface code encoding one of the two magic states using any appropriate non-FT circuit. Because the physical error rate is low, there is a reasonable chance of doing this successfully, although of course if there is a fault in the circuit, then the logical state might be wrong. Then we can merge this small patch of surface code with other patches using merge operations. If the additional patches are in the $|\overline{0}\rangle$ state, then we can resolve the merge ambiguity by pairing any extra defects with the boundaries of the new patches and the logical state remains the magic state we want. The merge procedure itself will have a logical error rate determined by the size of the small patch, but once the patch is grown by a merge, the logical error rate is much lower, exponentially small in the size of the current patch. The overall logical error rate is therefore just a constant times the physical error rate, the value of the constant depending on the details of the original encoding and merge procedures. If the final logical error rate is not too high, magic state distillation (section 13.5) will let us produce magic states with much lower logical error rates which we can then inject into the computation.

We already have a magic state distillation procedure for the $|\overline{0}\rangle + e^{i\pi/4}|\overline{+}\rangle$ magic state, but we also need a magic-state-distillation-like procedure to turn the unreliable Y eigenstates that we know how to make into more reliable ones. Following the logic of section 13.5, we can distill Y eigenstates using some code for which $R_{\pi/4}$ is a transversal gate. An example is the 7-qubit code. We can thus use protocol 13.3 to distill Y eigenstates, substituting the 7-qubit code for the 15-qubit code. In short, we can use the following procedure to perform $\overline{R_{\pi/4}}$:

Protocol 17.7.

1. Prepare a number of number of small patches in the state $|\overline{0}\rangle + i|\overline{1}\rangle$.
2. Grow them into full-size patches via lattice merge operations with $|\overline{0}\rangle$ states.
3. Perform state distillation as per protocol 13.3 using the 7-qubit code.
4. Use gate teleportation to perform the gate with the modified version of figure 13.7.

One point is worth noting. In section 13.5, we were assuming that we had available all Clifford group operations. That is no longer true. However, the 7-qubit code is a CSS code, so encoding or decoding the 7-qubit code or measuring its error syndrome can be done with only CNOT gates plus $|0\rangle$ and $|+\rangle$ preparation and X and Z basis measurements. These are all things we do have available using the techniques above.

This completes the universal set of fault-tolerant gates. We now have a full fault-tolerant protocol for surface codes.

17.3.5 Threshold with Surface Codes

While it's nice that we can put together reasonable fault-tolerant gadgets for the surface codes, there's not really much point unless we can actually make big surface codes and preserve a state encoded in one for a long time. By the fact that I went to all this bother describing the gadgets, you might deduce (correctly) that the family of surface codes has a threshold error rate below which arbitrarily long quantum computations are possible, just as in theorem 10.4.

I will show this in a simplified error model, the same phenomenological error model considered in section 17.2.3. To recap, at each time step, we do some set of locations perfectly. Then each data qubit experiences an error with error rate p per qubit. Each bit of the error syndrome (if we measured one at that time) experiences a bit flip error with error rate q. If we want to prove the surface code threshold for a standard error model, such as an adversarial stochastic error model, we need to take into account the actual errors in the gates and ancillas. We can derive q from the true error rate, but we also need to take into account the possibility that a single fault can result in both types of error. The numerical value of the thresholds derived this way will be less, but the basic conclusion — that there is a threshold — is unchanged.

Let us first focus on simply storing a qubit in a surface code with noisy syndrome measurements. As discussed in section 17.2.3, the probability of a particular set Φ of a data qubit errors and b syndrome bit errors is given by equation (17.11),

$$\text{Prob}(\Phi) = \left(\frac{p}{1-p}\right)^a \left(\frac{q}{1-q}\right)^b p^{nT} q^{n'(T-1)}. \tag{17.13}$$

We can think of each error as marking an edge in the 3-dimensional graph used in section 17.2.3. Data errors mark spatial edges and syndrome errors mark temporal edges.

When the error rate is low, the marked edges are rare, so the connected clusters of marked edges will be small. As the error rates p and q increase, though, the clusters become more common and get larger on average until at some point, they start to connect up with high probability. Indeed, when the error rates are high enough, with probability very close to 1, there will be some cluster of marked edges that stretches from one end of the graph to the other. The point where this happens is known as a *percolation transition*. Percolation is a very well-studied problem in graph theory. The case of perfect syndrome measurements ($q = 0$) turns out to be equivalent to a standard classical statistical mechanics model, the random-bond Ising model. However, we are more interested in the fault-tolerant case.

[A complete threshold proof will be added later.]

To determine the actual value of the threshold for surface codes, people have done many simulations. Usually they are done for a depolarizing channel. For the full fault-tolerant protocol using a circuit-level error model (i.e., with probably p of error per location, not the phenomenological model), the threshold error rate appears to be around 6.7×10^{-3}.

.

Chapter 18

They May Not Be Error Correction, But We Still Love Them: Other Methods Of Error Control

Chapter 19

Wholesale Error Correction: Channel Capacity

Chapter 20

It Certainly Helps If You Look At Things The Right Way: Graph States

Chapter 21

Uijt Dibqufs Jt B Tfdsfu: Quantum Error Correction and Quantum Cryptography

Part IV

Appendices

Appendix A

Quantum Computation

Appendix B

Group Theory

Appendix C

Finite Fields

Appendix D

Linear Algebra